

AA210A

COURSE READER

FUNDAMENTALS OF COMPRESSIBLE FLOW

by

Brian J. Cantwell

Department of Aeronautics and Astronautics
Stanford University, Stanford, California 94305

This AA210 course reader by Brian J. Cantwell is licensed under a Creative Commons Attribution-NonCommercial 4.0 International License.

<https://creativecommons.org/licenses/by-nc/4.0/>

January 25, 2022

Contents

| | | |
|----------|--|------------|
| 1 | Introduction to fluid flow | 1-1 |
| 1.1 | Introduction | 1-1 |
| 1.2 | Conservation of mass | 1-1 |
| 1.2.1 | Incompressible flow | 1-3 |
| 1.2.2 | Index notation and the Einstein convention | 1-4 |
| 1.3 | Particle paths, streamlines and streaklines in 2-D steady flow | 1-5 |
| 1.3.1 | Analysis of particle paths and streamlines | 1-8 |
| 1.3.2 | The integrating factor | 1-11 |
| 1.3.3 | Sample problem - the integrating factor and reconstruction of a function from its perfect differential | 1-13 |
| 1.3.4 | Incompressible flow in two dimensions | 1-14 |
| 1.3.5 | Compressible flow in two dimensions | 1-16 |
| 1.4 | Particle paths in three dimensions | 1-16 |
| 1.5 | The substantial derivative | 1-17 |
| 1.5.1 | Frames of reference | 1-18 |
| 1.6 | Momentum transport due to convection | 1-20 |
| 1.7 | Momentum transport due to molecular motion at microscopic scales | 1-23 |
| 1.7.1 | Pressure | 1-24 |
| 1.7.2 | Viscous friction - plane Couette flow | 1-24 |
| 1.7.3 | A question of signs | 1-26 |
| 1.7.4 | Newtonian fluids | 1-26 |
| 1.7.5 | Forces acting on a fluid element | 1-27 |
| 1.8 | Conservation of energy | 1-30 |
| 1.8.1 | Pressure and viscous stress work | 1-30 |
| 1.9 | Summary - the equations of motion | 1-35 |
| 1.10 | Problems | 1-36 |
| 2 | Thermodynamics of dilute gases | 2-1 |
| 2.1 | Introduction | 2-1 |
| 2.2 | Thermodynamics | 2-1 |

| | | |
|----------|--|------------|
| 2.2.1 | Temperature and the zeroth law | 2-1 |
| 2.2.2 | The first law | 2-2 |
| 2.2.3 | The second law | 2-4 |
| 2.3 | The Carnot cycle | 2-5 |
| 2.3.1 | The absolute scale of temperature | 2-8 |
| 2.4 | Enthalpy | 2-9 |
| 2.4.1 | Gibbs equation on a fluid element | 2-10 |
| 2.5 | Heat capacities | 2-12 |
| 2.6 | Ideal gases | 2-14 |
| 2.7 | Constant specific heat | 2-16 |
| 2.8 | The entropy of mixing | 2-18 |
| 2.8.1 | Sample problem - thermal mixing | 2-19 |
| 2.8.2 | Entropy change due to mixing of distinct gases | 2-20 |
| 2.8.3 | Gibbs paradox | 2-23 |
| 2.9 | Isentropic expansion | 2-24 |
| 2.9.1 | Blowdown of a pressure vessel | 2-24 |
| 2.9.2 | Work done by an expanding gas | 2-25 |
| 2.9.3 | Example - Helium gas gun | 2-27 |
| 2.9.4 | Entropy increase due to viscous friction | 2-29 |
| 2.10 | Some results from statistical mechanics | 2-29 |
| 2.10.1 | Diatomeric gases | 2-30 |
| 2.10.2 | Characteristic vibrational temperature | 2-31 |
| 2.11 | Enthalpy - diatomic gases | 2-31 |
| 2.12 | Speed of sound | 2-32 |
| 2.13 | Atmospheric models | 2-32 |
| 2.14 | The third law of thermodynamics | 2-35 |
| 2.15 | Problems | 2-36 |
| 3 | Control volumes, vector calculus | 3-1 |
| 3.1 | Control volume definition | 3-1 |
| 3.2 | Vector calculus | 3-2 |
| 3.2.1 | Useful vector identities | 3-5 |
| 3.3 | The Gauss theorem | 3-7 |
| 3.4 | Stokes' theorem | 3-7 |
| 3.5 | Problems | 3-9 |
| 4 | Kinematics of fluid motion | 4-1 |
| 4.1 | Elementary flow patterns | 4-1 |
| 4.1.1 | Linear flows | 4-1 |
| 4.1.2 | Linear flows in two dimensions | 4-4 |
| 4.1.3 | Linear flows in three dimensions | 4-6 |

| | | |
|----------|---|------------|
| 4.1.4 | Incompressible flow | 4-8 |
| 4.1.5 | Frames of reference | 4-10 |
| 4.2 | Rate-of-strain and rate-of-rotation tensors | 4-11 |
| 4.3 | Problems | 4-12 |
| 5 | The conservation equations | 5-1 |
| 5.1 | Leibniz' rule for differentiation of integrals | 5-1 |
| 5.1.1 | Differentiation under the integral sign | 5-1 |
| 5.1.2 | Extension to three dimensions | 5-3 |
| 5.2 | Conservation of mass | 5-5 |
| 5.3 | Conservation of momentum | 5-6 |
| 5.4 | Conservation of energy | 5-8 |
| 5.5 | Summary - differential form of the equations of motion | 5-10 |
| 5.6 | Integral form of the equations of motion | 5-11 |
| 5.6.1 | Integral equations on an Eulerian control volume | 5-11 |
| 5.6.2 | Mixed Eulerian-Lagrangian control volumes | 5-12 |
| 5.7 | Applications of control volume analysis | 5-13 |
| 5.7.1 | Example 1 - Solid body at rest in a steady flow | 5-13 |
| 5.7.2 | Example 2 - Channel flow with heat addition | 5-15 |
| 5.7.3 | Example 3 - Stationary flow about a rotating fan | 5-16 |
| 5.7.4 | Example 4 - Combined heat transfer and work | 5-18 |
| 5.8 | Stagnation enthalpy, temperature and pressure | 5-19 |
| 5.8.1 | Stagnation enthalpy of a fluid element | 5-19 |
| 5.8.2 | Blowdown from a pressure vessel revisited | 5-20 |
| 5.8.3 | Stagnation enthalpy and temperature in steady flow | 5-21 |
| 5.8.4 | Frames of reference | 5-23 |
| 5.8.5 | Stagnation pressure | 5-23 |
| 5.8.6 | Transforming P_t between fixed and moving frames | 5-25 |
| 5.9 | Problems | 5-25 |
| 6 | Several forms of the equations of motion | 6-1 |
| 6.1 | The Navier-Stokes equations | 6-1 |
| 6.1.1 | Incompressible Navier-Stokes equations | 6-2 |
| 6.2 | The momentum equation expressed in terms of vorticity | 6-2 |
| 6.3 | The momentum equation expressed in terms of the entropy and vorticity | 6-3 |
| 6.3.1 | Crocco's theorem | 6-4 |
| 6.3.2 | The energy equation for inviscid, non-heat conducting flow | 6-5 |
| 6.3.3 | Steady flow | 6-5 |
| 6.4 | Inviscid, irrotational, homentropic flow | 6-6 |
| 6.4.1 | Steady, inviscid, irrotational flow | 6-7 |
| 6.5 | The velocity potential | 6-8 |

| | | |
|----------|--|------------|
| 6.5.1 | Unsteady potential flow, the unsteady Bernoulli integral | 6-8 |
| 6.5.2 | Incompressible, irrotational flow | 6-11 |
| 6.6 | The vorticity equation | 6-11 |
| 6.7 | Fluid flow in three dimensions, the dual stream function | 6-13 |
| 6.8 | The vector potential | 6-15 |
| 6.8.1 | Selection of a Coulomb gauge | 6-15 |
| 6.9 | Incompressible flow with mass and vorticity sources | 6-16 |
| 6.10 | Turbulent flow | 6-17 |
| 6.10.1 | Turbulent, incompressible, isothermal flow | 6-20 |
| 6.11 | Problems | 6-21 |
| 7 | Entropy generation and transport | 7-1 |
| 7.1 | Convective form of the Gibbs equation | 7-1 |
| 7.2 | The kinetic energy equation | 7-2 |
| 7.3 | Internal energy | 7-3 |
| 7.3.1 | Viscous dissipation of kinetic energy | 7-4 |
| 7.4 | Entropy | 7-5 |
| 7.5 | Problems | 7-8 |
| 8 | Viscous flow along a wall | 8-1 |
| 8.1 | The no-slip condition | 8-1 |
| 8.2 | Equations of motion | 8-3 |
| 8.3 | Plane, compressible Couette flow | 8-4 |
| 8.3.1 | The energy integral in plane Couette flow | 8-6 |
| 8.3.2 | The adiabatic wall recovery temperature | 8-7 |
| 8.3.3 | Velocity distribution in Couette flow | 8-9 |
| 8.4 | The viscous boundary layer on a wall | 8-12 |
| 8.4.1 | Measures of boundary layer thickness | 8-17 |
| 8.5 | The Von Karman integral momentum equation | 8-18 |
| 8.6 | The laminar boundary layer in the limit $M^2 \rightarrow 0$ | 8-22 |
| 8.6.1 | The zero pressure gradient, incompressible boundary layer | 8-23 |
| 8.7 | The Falkner-Skan boundary layers | 8-27 |
| 8.7.1 | The case $\beta = -1$ | 8-32 |
| 8.7.2 | Falkner-Skan sink flow. | 8-33 |
| 8.8 | Thwaites' method for approximate calculation of laminar boundary layer characteristics | 8-37 |
| 8.8.1 | Example - free stream velocity from the potential flow over a circular cylinder. | 8-43 |
| 8.9 | Compressible laminar boundary layers | 8-46 |
| 8.9.1 | The energy integral for a compressible boundary layer with an adiabatic wall and $P_r = 1$ | 8-47 |

| | |
|--|-------------|
| 8.9.2 Non-adiabatic wall with $dP/dx = 0$ and $P_r = 1$ | 8-48 |
| 8.10 Mapping a compressible to an incompressible boundary layer | 8-49 |
| 8.11 Turbulent boundary layers | 8-62 |
| 8.11.1 The incompressible turbulent boundary layer velocity profile | 8-64 |
| 8.12 Transformation between flat plate and curved wall boundary layers | 8-69 |
| 8.13 Head's method for approximate calculation of turbulent boundary layer characteristics | 8-73 |
| 8.13.1 Head's method applied to the zero pressure gradient flat plate | 8-79 |
| 8.13.2 Head's method used to study the effect of Reynolds number on flow separation on a circular cylinder | 8-80 |
| 8.14 Problems | 8-83 |
| 9 Quasi-one-dimensional flow | 9-1 |
| 9.1 Control volume and integral conservation equations | 9-1 |
| 9.1.1 Conservation of mass | 9-2 |
| 9.1.2 Conservation of x -momentum | 9-3 |
| 9.1.3 Conservation of energy | 9-5 |
| 9.2 Area averaged flow | 9-5 |
| 9.2.1 The traction vector | 9-7 |
| 9.2.2 Example - steady, gravity-free, adiabatic flow of a compressible fluid in a channel | 9-11 |
| 9.3 Normal shock waves | 9-12 |
| 9.3.1 The Rankine-Hugoniot relations | 9-14 |
| 9.3.2 Shock property ratios in a calorically perfect ideal gas | 9-15 |
| 9.3.3 Stagnation pressure ratio across a normal shock wave | 9-18 |
| 9.3.4 Example - stagnation at a leading edge in supersonic flow | 9-20 |
| 9.4 Shock wave thickness | 9-24 |
| 9.5 Problems | 9-30 |
| 10 Gasdynamics of nozzle flow | 10-1 |
| 10.1 Area-Mach number function | 10-1 |
| 10.1.1 Mass conservation | 10-5 |
| 10.2 A simple convergent nozzle | 10-6 |
| 10.2.1 The phenomenon of choking | 10-8 |
| 10.3 The converging-diverging nozzle | 10-8 |
| 10.3.1 Case 1 - Isentropic subsonic flow in the nozzle | 10-9 |
| 10.3.2 Case 2 - Non-isentropic flow - shock in the nozzle | 10-10 |
| 10.3.3 Case 3 - Isentropic supersonic flow in the nozzle | 10-12 |
| 10.4 Examples | 10-14 |
| 10.4.1 Shock in a nozzle | 10-14 |
| 10.4.2 Cold gas thruster | 10-17 |

| | |
|--|-------------|
| 10.4.3 Gasdynamics of a double throat, starting and unstarting supersonic flow | 10-17 |
| 10.5 Problems | 10-21 |
| 11 Area change, wall friction and heat transfer | 11-1 |
| 11.1 Control volume | 11-1 |
| 11.2 Entropy and stagnation pressure | 11-2 |
| 11.3 Velocity, density, temperature and pressure | 11-4 |
| 11.4 The Mach number | 11-5 |
| 11.5 Mass flow, area-Mach-number function | 11-6 |
| 11.6 Integrated relations | 11-7 |
| 11.6.1 1-D, adiabatic, constant area flow with friction (Fanno line flow) | 11-7 |
| 11.6.2 Example - frictional flow in a long pipe | 11-8 |
| 11.6.3 Integrated relations - 1-D frictionless, constant area flow with heat transfer (Rayleigh line flow) | 11-11 |
| 11.6.4 Example - double throat with heat addition | 11-12 |
| 11.7 Detonations and deflagrations | 11-15 |
| 11.7.1 Example - detonation in a mixture of fluorine and hydrogen diluted by nitrogen. | 11-19 |
| 11.8 Problems | 11-20 |
| 12 Steady waves in compressible flow | 12-1 |
| 12.1 Oblique shock waves | 12-1 |
| 12.1.1 Exceptional relations | 12-4 |
| 12.1.2 Flow deflection versus shock angle | 12-5 |
| 12.2 Weak oblique waves | 12-7 |
| 12.3 The Prandtl-Meyer expansion | 12-10 |
| 12.3.1 Example - supersonic flow over a bump | 12-12 |
| 12.4 Problems | 12-13 |
| 13 Unsteady waves in compressible flow | 13-1 |
| 13.1 Governing equations | 13-1 |
| 13.2 The acoustic equations | 13-1 |
| 13.3 Propagation of acoustic waves in one space dimension | 13-4 |
| 13.4 Isentropic, finite amplitude waves | 13-7 |
| 13.5 Centered expansion wave | 13-10 |
| 13.6 Compression wave | 13-12 |
| 13.7 The shock tube | 13-13 |
| 13.7.1 Example - flow induced by the shock in a shock tube | 13-16 |
| 13.8 Problems | 13-19 |

| | |
|---|-------------|
| 14 Thin airfoil theory | 14-1 |
| 14.1 Compressible potential flow | 14-1 |
| 14.1.1 The full potential equation | 14-1 |
| 14.1.2 The nonlinear small disturbance approximation | 14-3 |
| 14.1.3 Linearized potential flow | 14-7 |
| 14.1.4 The pressure coefficient | 14-9 |
| 14.1.5 Drag coefficient of a thin symmetric airfoil | 14-11 |
| 14.1.6 Thin airfoil with lift and camber at a small angle of attack | 14-13 |
| 14.2 Similarity rules for high speed flight | 14-16 |
| 14.2.1 Subsonic flow $M_\infty < 1$ | 14-18 |
| 14.2.2 Supersonic similarity $M_\infty > 1$ | 14-23 |
| 14.2.3 Transonic similarity $M_\infty \approx 1$ | 14-23 |
| 14.3 Problems | 25 |
| A Some results from the kinetic theory of gases | A-1 |
| A.1 Distribution of molecular velocities in a gas | A-1 |
| A.1.1 The distribution derived from the barometric formula | A-1 |
| A.1.2 The Maxwell velocity distribution function | A-5 |
| A.2 Mean molecular velocity | A-7 |
| A.3 Distribution of molecular speeds | A-9 |
| A.4 Pressure | A-10 |
| A.4.1 Kinetic model of pressure | A-10 |
| A.4.2 Pressure directly from the Maxwellian pdf | A-12 |
| A.5 The mean free path | A-13 |
| A.6 Viscosity | A-14 |
| A.7 Heat conductivity | A-15 |
| A.8 Specific heats, the law of equipartition | A-16 |
| A.9 Diatomic gases | A-17 |
| A.9.1 Rotational degrees of freedom | A-17 |
| A.9.2 Why are only two rotational degrees of freedom excited? | A-20 |
| A.9.3 Vibrational degrees of freedom | A-22 |
| A.10 Energy levels in a box | A-25 |
| A.10.1 Counting energy states | A-28 |
| A.10.2 Entropy of a monatomic gas in terms of the number of states | A-30 |
| B Equations in cylindrical and spherical coords | B-1 |
| B.1 Coordinate systems | B-1 |
| B.1.1 Cylindrical coordinates | B-1 |
| B.1.2 Spherical polar coordinates | B-2 |
| B.2 Transformation of vector components | B-3 |
| B.2.1 Cylindrical coordinates | B-3 |

| | | |
|-------|--|------|
| B.2.2 | Spherical polar coordinates | B-4 |
| B.3 | Summary of differential operations | B-4 |
| B.3.1 | Cylindrical coordinates | B-4 |
| B.3.2 | Spherical polar coordinates | B-6 |
| B.4 | Continuity | B-7 |
| B.4.1 | Cylindrical coordinates | B-7 |
| B.4.2 | Spherical polar coordinates | B-8 |
| B.5 | Momentum | B-8 |
| B.5.1 | Cylindrical coordinates | B-8 |
| B.5.2 | Spherical polar coordinates | B-9 |
| B.6 | Energy equation | B-9 |
| B.6.1 | Cylindrical coordinates | B-10 |
| B.6.2 | Spherical polar coordinates | B-11 |
| B.7 | Components of the stress tensor | B-12 |
| B.7.1 | Cylindrical coordinates | B-12 |
| B.7.2 | Spherical polar coordinates | B-12 |
| B.8 | Energy dissipation function Φ | 13 |
| B.8.1 | Cylindrical coordinates | 13 |
| B.8.2 | Spherical polar coordinates | 13 |

Chapter 1

Introduction to fluid flow

1.1 Introduction

Compressible flows play a crucial role in a vast variety of natural phenomena and man-made systems. The life-cycles of stars, the creation of atmospheres, the sounds we hear, the vehicles we ride and the systems we build for generating energy and propulsion all depend in an important way on the mechanics and thermodynamics of compressible flow. The purpose of this course is to introduce students in Aeronautics and Astronautics to the fundamental principles of compressible flow with emphasis on the development of the equations of motion, as well as some of the analytical tools from calculus needed to solve practically important problems involving nozzles, channels and lifting bodies.

1.2 Conservation of mass

Mass is neither created nor destroyed. This basic principle of classical physics is one of the fundamental laws governing fluid motion and is a good departure point for our introductory discussion. Figure 1.1 below shows an infinitesimally small stationary, rectangular control volume $\Delta x \Delta y \Delta z$ through which a fluid is assumed to be moving. A control volume of this type, with its surface fixed in space, is called an Eulerian control volume. The fluid velocity vector has vector components $\bar{U} = (U, V, W)$ in the $\bar{x} = (x, y, z)$ directions and the fluid density is ρ . In a general, unsteady, compressible flow, all flow variables may depend on position and time. The law of conservation of mass over this control volume is stated

as

$$\left\{ \begin{array}{l} \text{rate of mass} \\ \text{accumulation} \\ \text{inside the control} \\ \text{volume} \end{array} \right\} = \left\{ \begin{array}{l} \text{rate of mass} \\ \text{flow} \\ \text{into the control} \\ \text{volume} \end{array} \right\} - \left\{ \begin{array}{l} \text{rate of mass} \\ \text{flow} \\ \text{out of the control} \\ \text{volume} \end{array} \right\}. \quad (1.1)$$

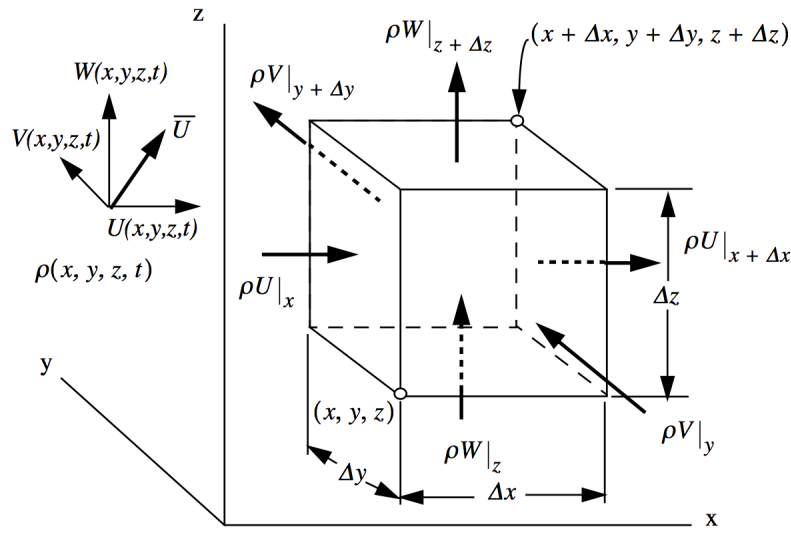


Figure 1.1: Fixed control volume in a moving fluid. The arrows denote fluxes of mass on the various faces of the control volume.

Consider a pair of faces perpendicular to the x -axis. The vector mass flux is $\rho \bar{U}$ with units $\text{mass}/(\text{area} \cdot \text{time})$. The rate of mass flow in through the face at x is the flux in the x -direction times the area $\rho U|_x \Delta y \Delta z$. The mass flow rate out through the face at $x + \Delta x$ is $\rho U|_{x+\Delta x} \Delta y \Delta z$. Similar expressions apply to the other two pairs of faces. The rate of mass accumulation inside the volume is $\Delta x \Delta y \Delta z (\partial \rho / \partial t)$ and this is equal to the sum of the mass fluxes over the six faces of the control volume. The mass balance (1.1) is expressed mathematically as

$$\begin{aligned} \Delta x \Delta y \Delta z \left(\frac{\partial \rho}{\partial t} \right) &= \Delta y \Delta z \rho U|_x - \Delta y \Delta z \rho U|_{x+\Delta x} + \\ &\Delta x \Delta z \rho V|_y - \Delta x \Delta z \rho V|_{y+\Delta y} + \Delta x \Delta y \rho W|_z - \Delta x \Delta y \rho W|_{z+\Delta z} \end{aligned} \quad (1.2)$$

which can be rearranged to read

$$\begin{aligned} \Delta x \Delta y \Delta z \left(\frac{\partial \rho}{\partial t} \right) + \Delta y \Delta z (\rho U|_{x+\Delta x} - \rho U|_x) + \\ \Delta x \Delta z (\rho V|_{y+\Delta y} - \rho V|_y) + \Delta x \Delta y (\rho W|_{z+\Delta z} - \rho W|_z) = 0 \end{aligned} . \quad (1.3)$$

Divide (1.3) through by the infinitesimal volume $\Delta x \Delta y \Delta z$.

$$\frac{\partial \rho}{\partial t} + \frac{\rho U|_{x+\Delta x} - \rho U|_x}{\Delta x} + \frac{\rho V|_{y+\Delta y} - \rho V|_y}{\Delta y} + \frac{\rho W|_{z+\Delta z} - \rho W|_z}{\Delta z} = 0 \quad (1.4)$$

Let $\Delta x \rightarrow 0, \Delta y \rightarrow 0, \Delta z \rightarrow 0$. In this limit (1.4) becomes

$$\frac{\partial \rho}{\partial t} + \frac{\partial \rho U}{\partial x} + \frac{\partial \rho V}{\partial y} + \frac{\partial \rho W}{\partial z} = 0. \quad (1.5)$$

Equation (1.5) is called the continuity equation and is the general partial differential equation for conservation of mass for any moving, continuous medium (continuum). The continuum might be a compressible gas, a liquid or a moving solid such as glacier ice or the rock crust of the Earth.

1.2.1 Incompressible flow

The compressibility of a medium becomes important when the speed of a body begins to approach the speed of sound in the medium. At speeds much lower than the speed of sound the disturbance created by a body pushing aside the fluid is too small to significantly change the thermal energy of the fluid and fluid behaves as if it is incompressible $\rho = constant$. In this limit (1.5) reduces to

$$\frac{\partial U}{\partial x} + \frac{\partial V}{\partial y} + \frac{\partial W}{\partial z} = 0. \quad (1.6)$$

Note that equation (1.6) applies to both steady and unsteady incompressible flow.

1.2.2 Index notation and the Einstein convention

For convenience, vector components are often written with subscripts. This is called *index notation* and one makes the following replacements.

$$\begin{aligned}(x, y, z) &\rightarrow (x_1, x_2, x_3) \\ (U, V, W) &\rightarrow (U_1, U_2, U_3)\end{aligned}\tag{1.7}$$

In index notation equation (1.5) is concisely written in the form

$$\frac{\partial \rho}{\partial t} + \sum_{i=1}^3 \frac{\partial (\rho U_i)}{\partial x_i} = 0\tag{1.8}$$

where the subscript refers to the *i*th vector component.

Vector calculus is an essential tool for developing the equations that govern compressible flow and summed products such as (1.8) arise often. Notice that the sum in (1.8) involves a repeated index. The theory of relativity is another area where such sums arise often and when Albert Einstein was developing the special and general theory he too recognized that such sums always involve an index that is repeated twice but never three times or more. In effect the presence of repeated indices implies a summation process and the summation symbol can be dropped. To save effort and space Einstein did just that and the understanding that a repeated index denotes a sum has been known as the Einstein convention ever since. Using the Einstein convention (1.8) becomes

$$\frac{\partial \rho}{\partial t} + \frac{\partial (\rho U_i)}{\partial x_i} = 0.\tag{1.9}$$

Remember, the rule of thumb is that a single index denotes a vector component and a repeated index represents a sum. Three or more indices the same means that there is a mistake in the equation somewhere! The upper limit of the sum is 1, 2 or 3 depending on the number of space dimensions in the problem. In the notation of vector calculus (1.9) is written

$$\frac{\partial \rho}{\partial t} + \nabla \cdot (\rho \bar{U}) = 0\tag{1.10}$$

and (1.6) is $\nabla \cdot \bar{U} = 0$. Vector notation has the advantage of being concise and independent of the choice of coordinates but is somewhat abstract. The main advantage of index notation is that it expresses precisely what differentiation and summation processes are

being done in a particular coordinate system. In Cartesian coordinates, the gradient vector operator is

$$\nabla \equiv \left(\frac{\partial}{\partial x}, \frac{\partial}{\partial y}, \frac{\partial}{\partial z} \right). \quad (1.11)$$

The continuity equation as well as the rest of the equations of fluid flow are presented in cylindrical and spherical polar coordinates in Appendix B.

1.3 Particle paths, streamlines and streaklines in 2-D steady flow

Let's begin with a study of fluid flow in two dimensions. Figure 1.2 shows the theoretically computed flow over a planar, lifting airfoil in steady, inviscid (non-viscous) flow. The theory used to determine the flow assumes that the flow is irrotational

$$\nabla \times \bar{U} = 0 \quad (1.12)$$

and that the flow speed is very low so that (1.6) holds.

$$\nabla \cdot \bar{U} = 0 \quad (1.13)$$

A vector field that satisfies (1.12) can always be represented as the gradient of a scalar potential function $\phi = \Phi(x, y)$ therefore

$$U = \nabla \Phi \quad (1.14)$$

or, in terms of components

$$(U, V) = \left(\frac{\partial \Phi}{\partial x}, \frac{\partial \Phi}{\partial y} \right) \quad (1.15)$$

When (1.14) is substituted into (1.13) the result is Laplace's equation.

$$\nabla \cdot \nabla \Phi = \nabla^2 \Phi = 0 \quad (1.16)$$

Figure 1.2 depicts the solution of equation (1.16) over the airfoil shown.

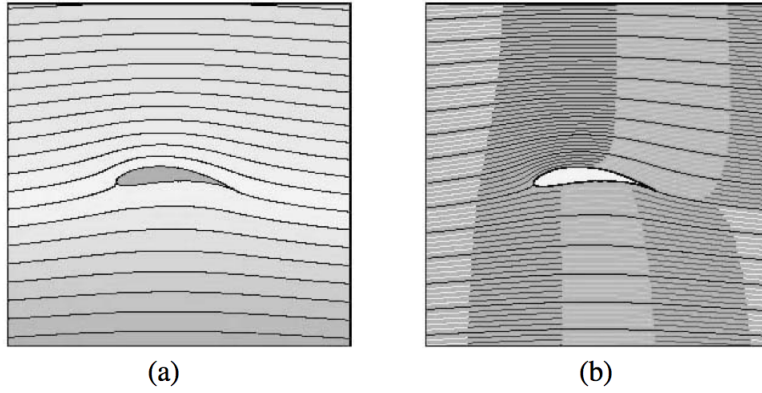


Figure 1.2: *Flow over a 2-D lifting wing, (a) streamlines, (b) streaklines.*

The boundary conditions on the airfoil are that the flow is allowed to slip tangent to the surface but cannot penetrate the surface and the flow is required to leave the sharp trailing edge of the airfoil smoothly. The latter requirement is the famous Kutta condition. In a real airfoil viscous friction prevents the flow from going around the sharp trailing edge. By enforcing the Kutta condition, the solution of (1.16) is able to mimic the effects of viscosity in real airfoils thus allowing the lift to be determined. Once the scalar potential is found the velocity field is generated using (1.14). The streamlines shown in Figure 1.2(a) are simply lines that are everywhere parallel to the velocity vector field.

A careful examination of the picture reveals quite a bit of information. First, note that the mass flow rate between any two streamlines is fixed (fluid cannot cross streamlines). As the streamlines approach the leading edge of the airfoil, the separation between lines increases indicating a deceleration of the fluid. Near the point of maximum wing thickness on the upper surface, the streamlines come closer together indicating a speed-up of the fluid to greater than the free stream speed. Below the airfoil the streamlines move apart indicating that the fluid slows down to less than the free stream speed. Downstream of the airfoil trailing edge the flow speed recovers to the free stream value. Notice that the largest velocity changes occur near the wing. In the upper and lower parts of the picture, far away from the wing, the flow is deflected upward by the wing but the distance between streamlines changes little and the corresponding flow speed change is relatively small.

Figure 1.2 (b) depicts streaklines in the flow over the airfoil. These are produced numerically the same way one would produce dye lines in a real flow. Fluid elements that pass through a given point upstream of the airfoil are marked forming a streak. In the figure, alternating bands of fluid are marked light and dark. The flow pattern produced by the streaklines is identical to the streamline pattern but there is one added piece of information. The streakline pattern depicts the time-integrated effect of the flow velocity on the

position of the fluid elements that constitute the streak.

One of the popular explanations of how an airfoil produces lift is that adjacent fluid elements on either side of the stagnation streamline ahead of the wing must meet at the trailing edge at the same time. The reasoning then goes as follows; since a particle that travels above the wing must travel farther than the one below, it must travel faster thus reducing the pressure over the wing and producing lift. Figure 1.2 (b) clearly shows that this explanation is completely erroneous. The fluid below the wing is substantially retarded compared to the fluid that passes above the wing.

The figures below show two more streamline examples in a slightly compressible situation with the effects of viscosity included. These are computations of the flow over a wing flap at a free stream speed of approximately 30 % of the speed of sound. The flow conditions are the same in both cases except that in the right-hand picture the trailing edge of the main wing (visible in the upper left corner of the picture) has attached to it a small vertical flap called a Gurney flap.

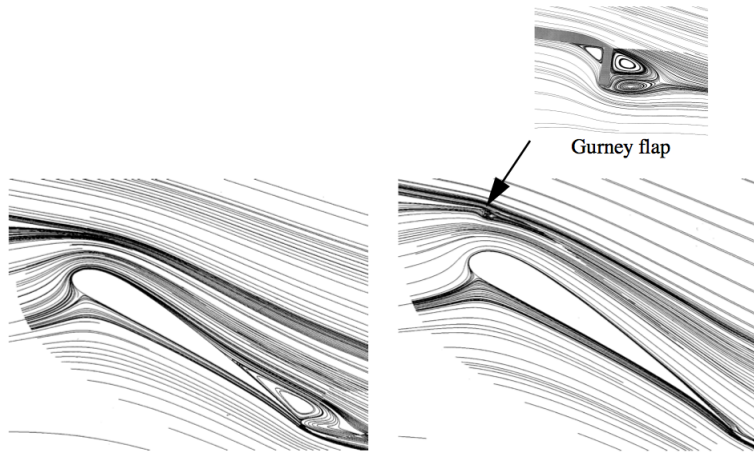


Figure 1.3: *Computed streamlines over a wing flap.*

The Gurney flap was developed by Dan Gurney in an effort to improve the speed of his new IRL race car prior to the start of the 1971 racing season in Phoenix. The car was disappointingly slow and after several days of testing, the driver Bobby Unser challenged Gurney to find a solution. Gurney decided to add a spoiler to the rear wing by riveting a length of aluminum right-angle to the trailing edge. When Unser tested the car it was just as slow as before and so everyone felt that the idea was a failure. Later Unser confided to Gurney that the reason the car was slow was that the down-force from the flap on the rear wheels was so large that the car was understeering badly. It was clear that with some adjustments to increase the down-force on the front wings the car could be made much

faster. For a while the Gurney team deflected questions with the fiction that the purpose of the flap was purely to increase the structural strength of the wing, but eventually the competition got wise and the Gurney flap was widely adopted.

While the Gurney flap increases both the lift and drag of a single wing the effect on a two-element airfoil is to cause the flow over the flap to reattach as shown in Figure 1.3 thereby increasing lift and reducing the overall drag of the wing-flap system. This allows the system to be effective at much higher flap angles. Figure 1.3 was produced using the computed velocity field. Once the velocity field is known, the user places computational particles at selected grid points and integrates the trajectory of the particles forward in time. The choice of initial points depends on the amount of detail one wants to visualize and this accounts for the uneven distribution of streamlines in these figures. The integration traces out the trajectories of the particles. Since the flow is steady, this process effectively traces out the streamlines. Changes in flow speed can be seen in terms of the convergence and divergence of streamlines, just as in the incompressible case, although the variation of fluid density over the field complicates this interpretation slightly. We shall return to this last point shortly.

1.3.1 Analysis of particle paths and streamlines

Let's learn how to analyze particle paths and streamlines theoretically. Figure 1.4 shows a typical trajectory in space of a fluid element moving under the action of a two-dimensional *steady* velocity field.

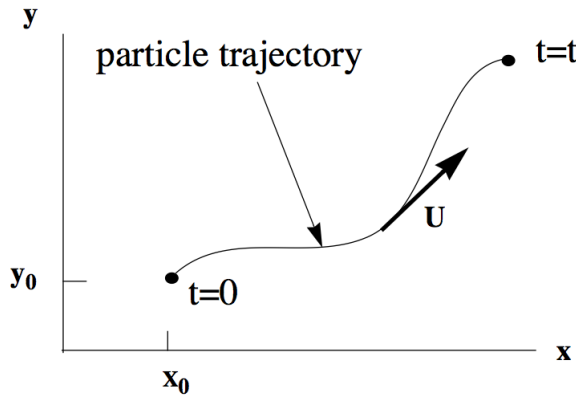


Figure 1.4: Particle trajectory in a 2-D steady flow field.

The equations that determine the trajectory are:

$$\begin{aligned}\frac{dx(t)}{dt} &= U(x(t), y(t)) \\ \frac{dy(t)}{dt} &= V(x(t), y(t))\end{aligned}\tag{1.17}$$

where U and V are the flow velocity components in the x and y directions respectively.

The velocity field is assumed to be a smooth function of position. Formally, these equations are solved by integrating the velocity field forward in time.

$$\begin{aligned}x(t) &= x_0 + \int_0^t U(x(t), y(t)) dt \\ y(t) &= y_0 + \int_0^t V(x(t), y(t)) dt\end{aligned}\tag{1.18}$$

The result is a set of parametric functions for the particle coordinates x and y in terms of the time, t , along a particle path.

$$\begin{aligned}x(t) &= F(x_0, y_0, t) \\ y(t) &= G(x_0, y_0, t)\end{aligned}\tag{1.19}$$

The solution of (1.17) can also be expressed as a family of lines derived by eliminating t between the functions F and G in (1.19).

$$\psi = \Psi(x, y)\tag{1.20}$$

This is essentially how the streamlines observed in Figure 1.2(a) and Figure 1.3 are generated. The value of a particular streamline is determined by the initial conditions.

$$\psi_0 = \Psi(x_0, y_0)\tag{1.21}$$

This is the situation depicted schematically in Figure 1.5 .

The streaklines in Figure 1.2(b) were generated by shading a segment of fluid elements that pass through an initial point (x_0, y_0) during a fixed interval in time. Selecting a vertical line of initial points well upstream of the airfoil leads to the bands shown in the figure.

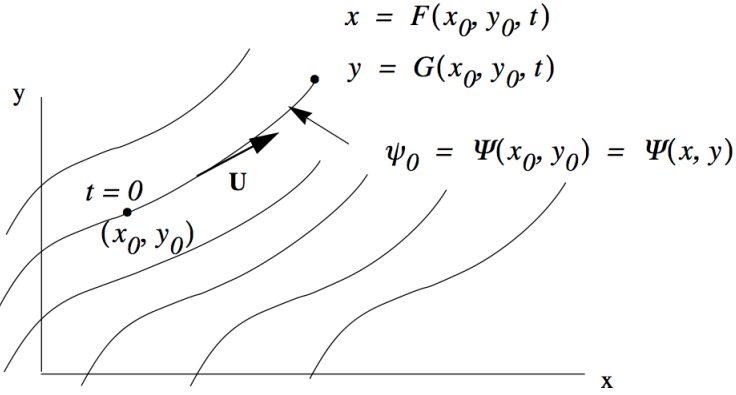


Figure 1.5: Streamlines in steady flow. The value of a particular streamline is determined by the coordinates of any point on the streamline.

The length of a segment is directly related to the velocity history of the fluid particles that make up the segment. The stream function can also be determined as the solution of the first order ordinary differential equation obtained by eliminating dt between the two particle path equations in (1.17).

$$\frac{dy}{dx} = \frac{V(x, y)}{U(x, y)} \quad (1.22)$$

The differential of $\Psi(x, y)$ is

$$d\Psi = \frac{\partial \Psi}{\partial x} dx + \frac{\partial \Psi}{\partial y} dy. \quad (1.23)$$

If we use (1.17) to replace the differentials dx and dy in (1.23) the result is

$$d\Psi = \left(U(x, y) \frac{\partial \Psi}{\partial x} + V(x, y) \frac{\partial \Psi}{\partial y} \right) dt. \quad (1.24)$$

On a line of constant $\psi = \psi_0$ the differential $d\Psi = 0$ and so for nonzero dt , the right hand side of (1.24) can be zero only if the expression in parentheses is zero. Thus the stream function, $\Psi(x, y)$, can be determined in two ways; either as the solution of a linear, first order PDE (1.25)

$$U \cdot \nabla \Psi = U(x, y) \frac{\partial \Psi}{\partial x} + V(x, y) \frac{\partial \Psi}{\partial y} = 0 \quad (1.25)$$

or as the solution of the ODE (1.22) which we can write in the form,

$$-V(x, y) dx + U(x, y) dy = 0. \quad (1.26)$$

Equation (1.25) is the mathematical expression of the statement that streamlines are parallel to the velocity vector field.

1.3.2 The integrating factor

On a line of constant $\psi = \psi_0$ the differential $d\psi = 0$ and

$$\frac{\partial \Psi}{\partial x} dx + \frac{\partial \Psi}{\partial y} dy = 0. \quad (1.27)$$

A very important question concerns the relationship between the differential expressions, (1.26) and (1.27). Are they the same? In particular, can (1.26) be regarded as a perfect differential? The test for a perfect differential is to compare cross derivatives. Equation (1.26) is a perfect differential if and only if,

$$-\frac{\partial V}{\partial y} = \frac{\partial U}{\partial x}. \quad (1.28)$$

If the integrability condition (1.28) is satisfied then there must exist some function $\Psi(x, y)$ such that $V = -\partial\Psi/\partial x$ and $U = -\partial\Psi/\partial y$ and the expression (1.26) can be equated to the differential of this function $d\psi$. In this case it is easy to solve for $\Psi(x, y)$ by direct integration of (1.26).

But for an arbitrary choice of the functions $U(x, y)$ and $V(x, y)$, the answer to the above question is in general no! In other words, for general V and U

$$\frac{V}{U} = -\frac{\partial\Psi/\partial x}{\partial\Psi/\partial y} \quad (1.29)$$

but

$$V \neq -\frac{\partial\Psi}{\partial x} \quad U \neq \frac{\partial\Psi}{\partial y}. \quad (1.30)$$

In order to convert equation (1.26) to a perfect differential it must be multiplied by an integrating factor. In general there is no systematic method for finding the integrating

factor and so the analytic solution of (1.26) for general functions U and V remains a difficult unsolved problem in mathematics. However we shall see later that in the case of fluid flow the integrating factor can be identified using the equation for conservation of mass.

It was shown by the German mathematician Johann Pfaff in the early 1800's that an integrating factor for the expression $-Vdx + Udy$ always exists. That is, for any choice of smooth functions U and V , there always exists a function $M(x, y)$ such that,

$$d\psi = -M(x, y)V(x, y)dx + M(x, y)U(x, y)dy \quad (1.31)$$

and the partial derivatives are

$$\begin{aligned} \frac{\partial \Psi}{\partial x} &= -M(x, y)V(x, y) \\ \frac{\partial \Psi}{\partial y} &= M(x, y)U(x, y) \end{aligned} \quad (1.32)$$

A differential expression like $-Vdx + Udy$ is often called a Pfaffian form. In the language of differential geometry it is called a differential 1-form. Pfaffian forms of higher dimension, say $Adx + Bdy + Cdz$ are often encountered in physics and with certain restrictions on $A(x, y, z)$, $B(x, y, z)$ and $C(x, y, z)$ an integrating factor can be found. But, the existence of the integrating factor is only assured unconditionally in two dimensions.

Pfaff's theorem can be understood by noting that the flow patterns formed by the vector field with local slope V/U and the flow pattern with slope $(MV)/(MU)$ are identical whereas the local flow speed differs by the scale factor $M(x, y)$. Since the solution of (1.17) clearly exists (we could just integrate the equations forward in time numerically) then the integrating factor must also exist.

Perfect differentials and integrating factors are generally covered in an upper level undergraduate course in calculus. Unfortunately the presentation is often cursory and tends to get passed over fairly quickly, often without making the deep connection that exists to the analysis of physical problems. In this chapter we see the connection between perfect differentials and the theory of fluid flow. In Chapter 2 we will find that the concept of a perfect differential is one of the fundamental building blocks needed to develop the laws of thermodynamics. The following sample problem is worked out in quite a bit of detail to help strengthen your understanding.

1.3.3 Sample problem - the integrating factor and reconstruction of a function from its perfect differential

Solve the first order ordinary differential equation

$$\frac{dy}{dx} = \frac{y}{x} H(xy) \quad (1.33)$$

where $H(x, y)$ is an arbitrary smooth function. Rearrange (1.33) to read

$$-yH(xy)dx + xdy = 0 \quad (1.34)$$

This differential expression fails the cross derivative test

$$\frac{\partial(-yH(xy))}{\partial y} \neq \frac{\partial(x)}{\partial x} \quad (1.35)$$

and is not a perfect differential. The integrating factor for (1.35) is known to be

$$M = \frac{1}{xy + xyH(xy)} \quad (1.36)$$

Multiplying (1.34) by (1.36) converts it to a perfect differential.

$$d\psi = -\frac{yH(xy)}{xy + xyH(xy)}dx + \frac{x}{xy + xyH(xy)}dy \quad (1.37)$$

We now know the partial derivatives of the solution.

$$\begin{aligned} \frac{\partial \Psi}{\partial x} &= -\frac{yH(xy)}{xy + xyH(xy)} \\ \frac{\partial \Psi}{\partial y} &= \frac{x}{xy + xyH(xy)} \end{aligned} \quad (1.38)$$

The expression (1.37) can now be integrated by integrating either partial derivative with the appropriate variable held fixed. Let's start by integrating the partial derivative with respect to y .

$$\psi = \int \frac{xdy}{xy + xyH(xy)} \Big|_{x-\text{constant}} + f(x) \quad (1.39)$$

Note that we have to include a constant of integration that can be at most a function of x . Let $\alpha = xy$. The solution can now be expressed as

$$\psi = \int \frac{d\alpha}{\alpha + \alpha H(\alpha)} + f(x) \quad (1.40)$$

Now differentiate (1.40) with respect to x and equate to the known partial derivative with respect to x in (1.38).

$$\begin{aligned} \frac{\partial}{\partial x} \left(\int \frac{d\alpha}{\alpha + \alpha H(xy)} + f(x) \right) &= \frac{y}{xy + xyH(xy)} + \frac{df}{dx} = \\ -\frac{yH(xy)}{xy + xyH(xy)} \rightarrow \frac{df}{dx} &= -\frac{1}{x} \rightarrow f = -\ln(x) \end{aligned} \quad (1.41)$$

This step allows us to determine $f(x)$. Finally the exact solution of (1.33) is

$$\psi = \int \frac{d\alpha}{\alpha + \alpha H(\alpha)} - \ln(x) \quad (1.42)$$

Note that we had to know the integrating factor in order to solve the problem. Sometimes what appears to be a trick will work. For example you can also get to the solution (1.42) by simply defining a new variable $\alpha = xy$. This allows (1.33) to be solved by separation of variables. All such tricks are equivalent to finding the integrating factor.

In the general case the required integrating factor is not known. For example the equation

$$\frac{dy}{dx} = \frac{xy + y + y^2}{2x^2 - xy} \quad (1.43)$$

comes up in the study of viscous boundary layer flow along a flat plate. We know an integrating factor exists but it has never been found. Fortunately when it comes to streamline patterns in two dimensions, conservation of mass can be used to determine the integrating factor.

1.3.4 Incompressible flow in two dimensions

The flow of an incompressible fluid in 2-D is constrained by the continuity equation (1.6)

that in two dimensions reduces to

$$\frac{\partial U}{\partial x} + \frac{\partial V}{\partial y} = 0 \quad (1.44)$$

This is exactly the condition (1.28) and so in this case the stream function and the velocity field are related by

$$U = \frac{\partial \Psi}{\partial y} \quad V = -\frac{\partial \Psi}{\partial x}. \quad (1.45)$$

So the 1-form, $-Vdx + Udy$ is guaranteed to be a perfect differential; The integrating factor is one. Therefore one can always write for 2-D incompressible flow

$$d\Psi = -Vdx + Udy. \quad (1.46)$$

If U and V are known functions, the stream function is determined analytically by integration of (1.46). In practice the easiest way to assign values to the streamlines is to integrate (1.46) beginning at some reference state well upstream of the airfoil where the velocity is uniform $(U, V) = (U_\infty, 0)$.

Incompressible irrotational flow in two dimensions

If the flow is incompressible and irrotational then the velocity field is described by both a stream function (1.45) and a potential function (1.15). The two functions are related by

$$\begin{aligned} \frac{\partial \Psi}{\partial y} &= \frac{\partial \Phi}{\partial x} \\ -\frac{\partial \Psi}{\partial x} &= \frac{\partial \Phi}{\partial y} \end{aligned} . \quad (1.47)$$

These are the well known Cauchy-Riemann equations from the theory of complex variables. Solutions of Laplace's equation (1.16) which is the equation of motion for this class of flows can be determined using the powerful methods of complex analysis. Interestingly, the flow can be solved just from the continuity equation (1.13) without the use of the equation for conservation of momentum. The irrotationality condition (1.12) essentially supplants the need for the momentum equation.

1.3.5 Compressible flow in two dimensions

The continuity equation for the steady flow of a compressible fluid in two dimensions is

$$\frac{\partial(\rho U)}{\partial x} + \frac{\partial(\rho V)}{\partial y} = 0. \quad (1.48)$$

In this case, the required integrating factor for (1.26) is the density $\rho(x, y)$ and we can write

$$d\psi = -\rho V dx + \rho U dy. \quad (1.49)$$

The stream function in a compressible flow is proportional to the mass flux with units *mass/(area – sec)* and the convergence and divergence of lines in the flow over the flap shown in Figure 1.2 is a reflection of variations in mass flux over different parts of the flow field.

1.4 Particle paths in three dimensions

Figure 1.6 shows the trajectory in space traced out by a particle under the action of a general three-dimensional, unsteady flow, $\bar{U}(\bar{x}, t)$.

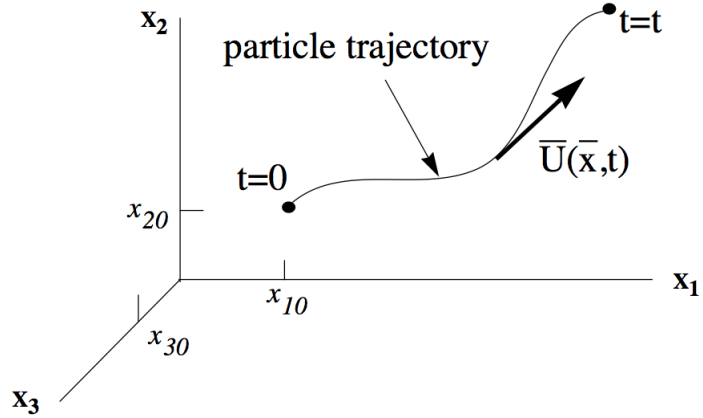


Figure 1.6: *Particle trajectory in three dimensions.*

Using index notation, the equations governing the motion of the particle are:

$$\frac{dx_i(t)}{dt} = U_i(x_1(t), x_2(t), x_3(t), t) \quad i = 1, 2, 3. \quad (1.50)$$

Formally, these equations are solved by integrating the velocity field.

$$x_i(t) = x_{i0} + \int_0^t U_i(x_1(t), x_2(t), x_3(t), t) dt \quad i = 1, 2, 3 \quad (1.51)$$

We shall return to the discussion of flow patterns in both 2 and 3 dimensions when we discuss the kinematics of flow fields in Chapter 4.

1.5 The substantial derivative

The acceleration of a particle is

$$\frac{d^2 x_i(t)}{dt^2} = \frac{d}{dt} U_i(x_1(t), x_2(t), x_3(t), t) = \frac{\partial U_i}{\partial t} + \frac{\partial U_i}{\partial x_k} \frac{dx_k}{dt}. \quad (1.52)$$

Remember, according to the Einstein convention, the repeated index denotes a sum over $k = 1, 2, 3$. Use (1.50) to replace dx_k/dt by U_k in (1.52). The result is called the substantial or material derivative and is usually denoted by $D() / Dt$.

$$\frac{D()}{Dt} = \frac{\partial()}{\partial t} + \bar{U} \cdot \nabla() \quad (1.53)$$

The substantial derivative of the velocity is

$$\frac{DU_i}{Dt} = \frac{\partial U_i}{\partial t} + U_k \frac{\partial U_i}{\partial x_k}. \quad (1.54)$$

The time derivative of any flow variable evaluated on a fluid element is given by a similar formula. For example the time rate of change of the density $\rho(x(t), y(t), z(t), t)$ of a given fluid particle is:

$$\frac{D\rho}{Dt} = \frac{\partial \rho}{\partial t} + U_k \frac{\partial \rho}{\partial x_k}. \quad (1.55)$$

The substantial derivative is the time derivative of some property of a fluid element referred to a fixed frame of reference within which the fluid element moves as shown in Figure 1.6.

1.5.1 Frames of reference

Occasionally it is necessary to transform variables between a fixed and moving set of coordinates as shown in Figure 1.7. The transformation of position and velocity is

$$\begin{aligned}x' &= x - X(t) \\y' &= y - Y(t) \\z' &= z - Z(t) \\U' &= U - \dot{X}(t) \\V' &= V - \dot{Y}(t) \\W' &= W - \dot{Z}(t).\end{aligned}\tag{1.56}$$

where $\bar{X} = (X(t), Y(t), Z(t))$ is the displacement of the moving frame in three coordinate directions and $d\bar{X}/dt = (\dot{X}(t), \dot{Y}(t), \dot{Z}(t))$ is the velocity of the frame. Note that in general, the frame may be accelerating.

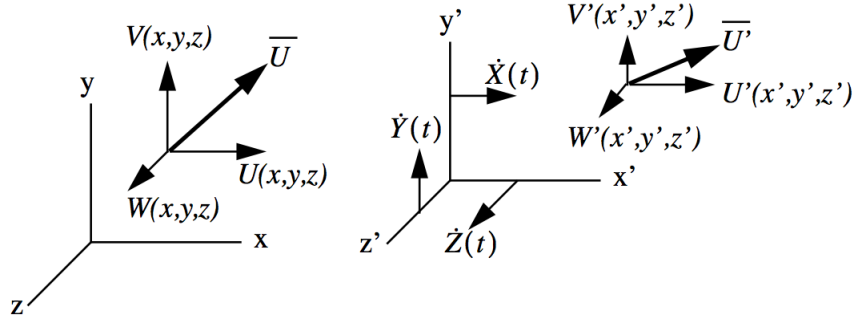


Figure 1.7: *Fixed and moving frames of reference.*

The substantial derivative of some property of a fluid element, (1.53), is sometimes referred to as the derivative moving with the fluid element. Do not interpret this as a transformation to a coordinate system that is attached to the fluid element. If for some reason it is actually desirable to make such a transformation the velocity of the particle in that frame is zero and the substantial derivative of the velocity is also zero. The substantial derivative of a variable such as the density of the particle at the origin of the moving coordinates is $D\rho/Dt = \partial\rho/\partial t$.

Both the momentum and kinetic energy of a fluid particle of mass m depend on the frame of reference. The momentum transforms linearly like the velocity.

$$m\bar{U}' = m\bar{U} - md\bar{X}/dt \quad (1.57)$$

The transformation of kinetic energy is a little more complex. In the two coordinate systems the definition of kinetic energy is the same,

$$\text{kinetic energy in moving coordinates} = \frac{1}{2}m(U'^2 + V'^2 + W'^2) \quad (1.58)$$

and

$$\text{kinetic energy in fixed coordinates} = \frac{1}{2}m(U^2 + V^2 + W^2). \quad (1.59)$$

The transformation of kinetic energy between frames is

$$\frac{1}{2}m(U'^2 + V'^2 + W'^2) = \frac{1}{2}m\left(\left(U - \dot{X}\right)^2 + \left(V - \dot{Y}\right)^2 + \left(W - \dot{Z}\right)^2\right) \quad (1.60)$$

which, when expanded to show the kinetic energies explicitly, becomes

$$\begin{aligned} \frac{1}{2}m(U'^2 + V'^2 + W'^2) &= \frac{1}{2}m(U^2 + V^2 + W^2) + \\ \frac{1}{2}m\dot{X}(X - 2U) + \frac{1}{2}m\dot{Y}(Y - 2V) + \frac{1}{2}m\dot{Z}(Z - 2W) \end{aligned} \quad (1.61)$$

or

$$k' = k + \frac{1}{2}m\dot{X}(X - 2U) + \frac{1}{2}m\dot{Y}(Y - 2V) + \frac{1}{2}m\dot{Z}(Z - 2W). \quad (1.62)$$

The transformation of kinetic energy depends nonlinearly on the velocity of the moving coordinate system. In contrast thermodynamic properties such as density, temperature and pressure are intrinsic properties of a given fluid element and so do not depend on the frame of reference.

1.6 Momentum transport due to convection

The law of conservation of momentum is stated as

$$\left\{ \begin{array}{l} \text{rate of momentum} \\ \text{accumulation inside} \\ \text{the control volume} \end{array} \right\} = \left\{ \begin{array}{l} \text{rate of} \\ \text{momentum} \\ \text{flow into} \\ \text{the control volume} \end{array} \right\} - \left\{ \begin{array}{l} \text{rate of} \\ \text{momentum} \\ \text{flow out of} \\ \text{the control volume} \end{array} \right\} + \left\{ \begin{array}{l} \text{sum of} \\ \text{forces acting} \\ \text{on the} \\ \text{control volume} \end{array} \right\}. \quad (1.63)$$

As a fluid moves it carries its momentum with it. This is called convective momentum transport. To study this kind of momentum transfer we use the same stationary control volume element $\Delta x \Delta y \Delta z$ that we used to develop the continuity equation. As before, the fluid velocity vector has components (U, V, W) in the (x, y, z) directions and the fluid density is ρ .

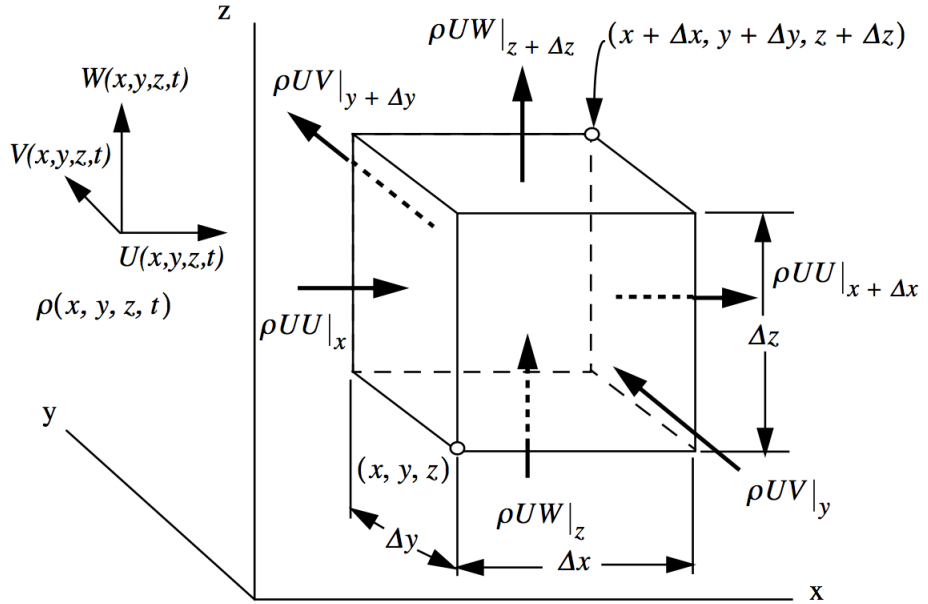


Figure 1.8: Fluxes of x -momentum through a fixed control volume. Arrows denote the velocity component carrying momentum into or out of the control volume.

Figure 1.8 shows the contribution to the x -momentum inside the control volume from the movement of fluid through all six faces of the control volume. Consider a pair of faces perpendicular to the x -axis. The flux of x -momentum is ρUU with units *momentum/(area-time)*. The rate at which the x -component of momentum enters the face at x is $\rho UU|_x \Delta y \Delta z$ and the rate at which it leaves through the face at $x + \Delta x$ is $\rho UU|_{x+\Delta x} \Delta y \Delta z$.

The rate at which the x -component of momentum enters the face at y is $\rho UV|_y \Delta x \Delta z$ and the rate at which it leaves through the face at $y + \Delta y$ is $\rho UV|_{y+\Delta y} \Delta x \Delta z$. To understand how fluid motion in the y -direction contributes to the rate of x -momentum transfer into or out of the control volume one can make the following interpretation of the momentum transfer.

$$\begin{aligned}\rho U &= \left\{ \begin{array}{l} x - \text{momentum} \\ \text{per unit volume} \end{array} \right\} \\ V|_y \Delta x \Delta z &= \left\{ \begin{array}{l} \text{volume of fluid per second} \\ \text{passing into the control volume through} \\ \text{the face normal to the } V - \text{velocity} \\ \text{component at position } y \end{array} \right\} \\ V|_{y+\Delta y} \Delta x \Delta z &= \left\{ \begin{array}{l} \text{volume of fluid per second} \\ \text{passing out of the control volume through} \\ \text{the face normal to the } V - \text{velocity} \\ \text{component at position } y + \Delta y \end{array} \right\}. \end{aligned} \quad (1.64)$$

Based on similar considerations, the rate at which the x -component of momentum enters the face at z is $\rho UW|_z \Delta x \Delta y$ and the rate at which it leaves through the face at $z + \Delta z$ is $\rho UW|_{z+\Delta z} \Delta x \Delta y$. The rate of x -component of momentum accumulation inside the control volume is $\Delta x \Delta y \Delta z (\partial \rho U / \partial t)$. For the x -component of momentum, the balance (1.63) is expressed mathematically as

$$\begin{aligned}\Delta x \Delta y \Delta z \left(\frac{\partial \rho U}{\partial t} \right) &= \Delta y \Delta z \rho UU|_x - \Delta y \Delta z \rho UU|_{x+\Delta x} + \\ \Delta x \Delta z \rho U V|_y - \Delta x \Delta z \rho U V|_{y+\Delta y} + \Delta x \Delta y \rho UW|_z - \Delta x \Delta y \rho UW|_{z+\Delta z} + \\ &\quad \{ \text{the sum of } x - \text{component forces acting on the system} \} \end{aligned} \quad (1.65)$$

which is rearranged to read

$$\begin{aligned} \Delta x \Delta y \Delta z \left(\frac{\partial \rho U}{\partial t} \right) + \Delta y \Delta z (\rho UU|_{x+\Delta x} - \rho UU|_x) + \\ \Delta x \Delta z (\rho U V|_{y+\Delta y} - \rho U V|_y) + \Delta x \Delta y (\rho UW|_{z+\Delta z} - \rho UW|_z) = \end{aligned} \quad (1.66)$$

{the sum of x-component forces acting on the system}.

Divide (1.66) through by the volume of the control element $\Delta x \Delta y \Delta z$.

$$\begin{aligned} \frac{\partial \rho U}{\partial t} + \frac{\rho UU|_{x+\Delta x} - \rho UU|_x}{\Delta x} + \frac{\rho U V|_{y+\Delta y} - \rho U V|_y}{\Delta y} + \frac{\rho UW|_{z+\Delta z} - \rho UW|_z}{\Delta z} = \\ \{ \text{the sum of } x-\text{component forces acting on the system per unit volume} \} \end{aligned} \quad (1.67)$$

Let $(\Delta x \rightarrow 0, \Delta y \rightarrow 0, \Delta z \rightarrow 0)$. In this limit (1.67) becomes

$$\frac{\partial \rho U}{\partial t} + \frac{\partial \rho UU}{\partial x} + \frac{\partial \rho UV}{\partial y} + \frac{\partial \rho UW}{\partial z} = \left\{ \begin{array}{l} \text{the sum of} \\ x-\text{component forces} \\ \text{per unit volume acting} \\ \text{on the control volume} \end{array} \right\}. \quad (1.68)$$

Similar equations describe conservation of momentum in the y and z directions.

$$\begin{aligned} \frac{\partial \rho V}{\partial t} + \frac{\partial \rho VU}{\partial x} + \frac{\partial \rho VV}{\partial y} + \frac{\partial \rho VW}{\partial z} = \left\{ \begin{array}{l} \text{the sum of} \\ y-\text{component forces} \\ \text{per unit volume acting} \\ \text{on the control volume} \end{array} \right\} \\ \frac{\partial \rho W}{\partial t} + \frac{\partial \rho WU}{\partial x} + \frac{\partial \rho WV}{\partial y} + \frac{\partial \rho WW}{\partial z} = \left\{ \begin{array}{l} \text{the sum of} \\ z-\text{component forces} \\ \text{per unit volume acting} \\ \text{on the control volume} \end{array} \right\} \end{aligned} \quad (1.69)$$

Equations (1.68) and (1.69) are the components of the vector partial differential equation that describes conservation of momentum for any moving continuum. In index notation,

equations (1.68) and (1.69) are concisely written in the form

$$\frac{\partial \rho U_i}{\partial t} + \frac{\partial (\rho U_i U_j)}{\partial x_j} = \left\{ \begin{array}{l} \text{the sum of} \\ \text{ith - component forces} \\ \text{per unit volume acting} \\ \text{on the control volume} \end{array} \right\} \quad i = 1, 2, 3 \quad (1.70)$$

where the subscript refers to the *i*th vector component and the sum is over the repeated index *j*. Since the repeated index is always summed it makes no difference what symbol is used and so it is called a dummy index. Rearrange (1.70) by carrying out the indicated differentiation.

$$\rho \frac{\partial U_i}{\partial t} + \rho U_j \frac{\partial (U_i)}{\partial x_j} + U_i \left(\frac{\partial \rho}{\partial t} + \frac{\partial (\rho U_j)}{\partial x_j} \right) = \left\{ \begin{array}{l} \text{the sum of} \\ \text{ith - component forces} \\ \text{per unit volume acting} \\ \text{on the control volume} \end{array} \right\} \quad i = 1, 2, 3 \quad (1.71)$$

The term in parentheses on the left hand side of (1.71) is zero by continuity and so the momentum equation becomes

$$\rho \frac{DU_i}{Dt} = \left\{ \begin{array}{l} \text{the sum of} \\ \text{ith - component forces} \\ \text{per unit volume acting} \\ \text{on the control volume} \end{array} \right\} \quad i = 1, 2, 3. \quad (1.72)$$

Equation (1.72) can be stated in words as follows.

$$\left\{ \begin{array}{l} \text{the rate of momentum change} \\ \text{of a fluid element} \end{array} \right\} = \left\{ \begin{array}{l} \text{the vector sum of} \\ \text{forces acting} \\ \text{on the fluid element} \end{array} \right\} \quad (1.73)$$

1.7 Momentum transport due to molecular motion at microscopic scales

Appendix A describes the molecular origin of two of the most basic forces that act on a fluid element; pressure and viscous friction. Although the derivations are restricted to

gases, both types of forces exist in all fluid motion and both arise from momentum transfer due to the motion and collisions of the molecules that make up the fluid. Molecules in the fluid move in random and chaotic ways and across any selected section of a surface within the fluid, there are molecules moving in both directions through the surface. The pressure and viscosity are defined through an average of the momentum transfer due to the collective motion of a very large set of molecules over a time scale that is short compared to the unsteady macroscopic motion of the fluid.

1.7.1 Pressure

Pressure forces arise from collisions between the molecules within the fluid and with whatever form of containment is used to hold or bound the fluid. In a fluid at rest, in the absence of gravitational forces, the pressure is uniform everywhere. When the fluid is set into motion the pressure becomes a scalar function of space and time. For example, variations in the pressure over a wing give rise to the lift of the wing. Pressure variations in the atmosphere are the primary driving forces behind wind patterns. The drag of a motor vehicle is primarily due to variations in the pressure field over the surface of the vehicle.

1.7.2 Viscous friction - plane Couette flow

All simple fluids exhibit resistance to flow due to the physical property of viscosity. The effects of viscosity are readily apparent in many everyday activities such as the spreading of honey on a piece of bread or the slow dripping of paint from a brush. Anyone who has purchased oil for their car knows that different grades of oil are characterized by different viscosities and that the viscosity depends on the oil temperature. The viscosity of air and other gases is less apparent but nonetheless just as real. The most important effect of viscosity on the motion of a fluid is that it causes the fluid to stick to the surface of a moving solid body, imposing the so-called no-slip condition on the velocity field at the surface. Even though the viscosity of air may be very small, viscous forces profoundly affect the flow and are critical to the generation of lift and drag by moving bodies.

To illustrate viscous friction, consider a fluid contained between two large parallel plates with area A as shown in Figure 1.9. The fluid is initially at rest. At $t = 0$ the upper plate is set into motion and, due to viscous forces, the adjacent fluid layers are dragged along with it. Eventually the velocity field reaches a steady state. If the speed of the upper plate is small compared to the speed of sound in the fluid, the final velocity profile is a straight line as shown. This is called plane Couette flow after Maurice Frederic Alfred Couette a Professor of Physics at the French University of Angers at the end of the nineteenth

century. Couette actually studied the flow between inner and outer concentric rotating cylinders with the goal of using his device to measure viscosity.

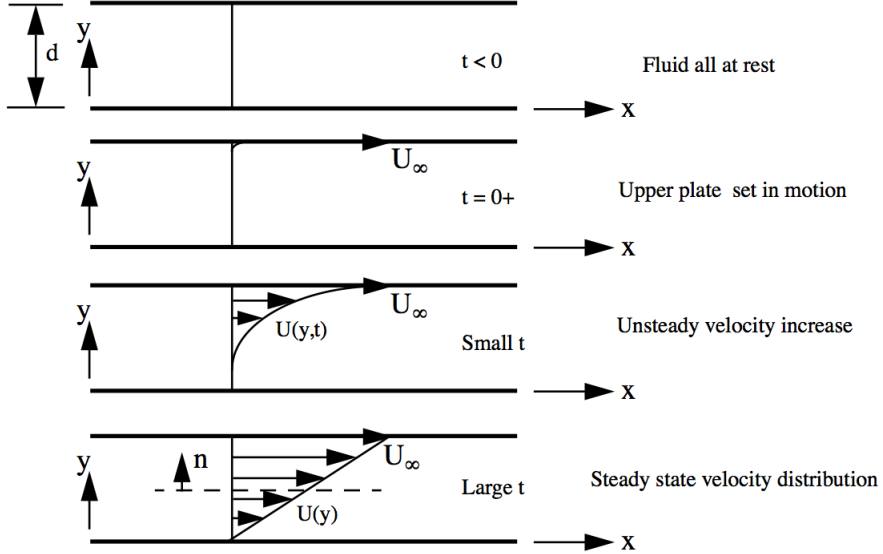


Figure 1.9: *Build-up to a steady laminar velocity profile for a viscous fluid contained between two parallel plates. At $t=0$ the upper plate is set into motion at a constant speed U_∞ .*

Once the flow reaches steady state a constant force F is required to maintain the motion of the upper plate. Provided the flow is laminar and the plate speed is not too large the force may be expressed as

$$\frac{F}{A} = \mu \frac{U_\infty}{d}. \quad (1.74)$$

The viscous stress on the plate *force/area* is proportional to the velocity gradient and the constant of proportionality is the viscosity of the fluid. Later we will generalize the notion of viscous stress to flow in three dimensions and so it is useful to write (1.74) in a somewhat more general form. The shear stress acting in the x direction exerted on a layer of fluid with an outward unit normal vector n in the positive y direction (as shown in Figure 1.9) is designated τ_{xy} . In terms of the velocity derivative (1.74) is written,

$$\tau_{xy} = \mu \frac{dU}{dy} \quad (1.75)$$

Equation (1.75) is called Newton's law of viscosity after Sir Isaac Newton who first proposed

it. In Chapter 8 we will consider the compressible case where the plate speed is not small and the steady-state velocity profile deviates from a straight line.

1.7.3 A question of signs

There is a subtle sign issue that comes up when one defines the viscous stress. In the discussion just above we have adopted the convention normally used in aeronautics that the stress is the force on a surface defined by its outward normal vector. In Figure 1.9 the outward normal on the lower surface is positive and the force is in the positive x-direction; on the upper surface the force is in the negative x-direction on a surface defined by an outward normal that points in the negative y-direction. Either way τ_{xy} is positive as indicated in (1.75).

But in certain fields such as chemical engineering a different interpretation of the stress is used. Here the stress is viewed as the transport of momentum in a certain direction. In this view the flow in Figure 1.9 would be interpreted as the transport of positive x-momentum in the negative y-direction and the expression in (1.75) would have a negative sign. If the general momentum conservation equation is developed with this interpretation of stress then another negative sign appears in front of the stress term. When the constitutive relation between stress and rate-of-strain is introduced both camps wind up solving the same system of equations, as they must.

1.7.4 Newtonian fluids

A fluid for which the viscous stress is linearly proportional to the velocity gradient is called Newtonian. Virtually all gases and most liquids are Newtonian. The few exceptions include polymers, pastes and slurries that exhibit non-Newtonian behavior where the stress depends nonlinearly on the rate of strain and may exhibit dependence on the total strain as in a solid. Some fluids are said to have memory where the stress can depend on the past history of the rate-of-strain. We will introduce the Newtonian stress-rate-of-strain relation in Chapter 5. For the present the stress is left in general terms. A truly exceptional case is liquid Helium that, when cooled below 2.3 K undergoes a transition to a strange macroscopic quantum state called Helium II. A sample of Helium below this temperature consists of two fluids that appear to co-exist. The normal fluid component exhibits viscosity whereas the superfluid component appears to flow without any viscous friction. In fact Helium II is an extraordinarily difficult fluid to contain since the superfluid component can pass through ultra-fine leaks in the dewar used to hold it. Exceptions to the no-slip condition occur in the flow of highly rarefied gases such as in the upper reaches of the atmosphere during re-entry of a spacecraft. When the density of the gas is extremely low the fluid can no longer be treated as a continuous medium. In this case the flow must be treated by

modeling the motion and collisions of individual molecules. Near a wall molecular collisions may not be perfectly specular and may on average exhibit a small difference between the velocity of the surface and the mean velocity of fluid particles near the surface. This is called the slip velocity and can become quite large as the density of the gas decreases to extremely low values.

1.7.5 Forces acting on a fluid element

At macroscopic scales the transport of momentum due to the net molecular motion of a very large number of molecules is equivalent to continuous pressure and viscous forces acting within the fluid. Figure 1.10 shows the contribution to the x -momentum inside our small control volume from the pressure and viscous stresses acting on the six faces of the control volume.

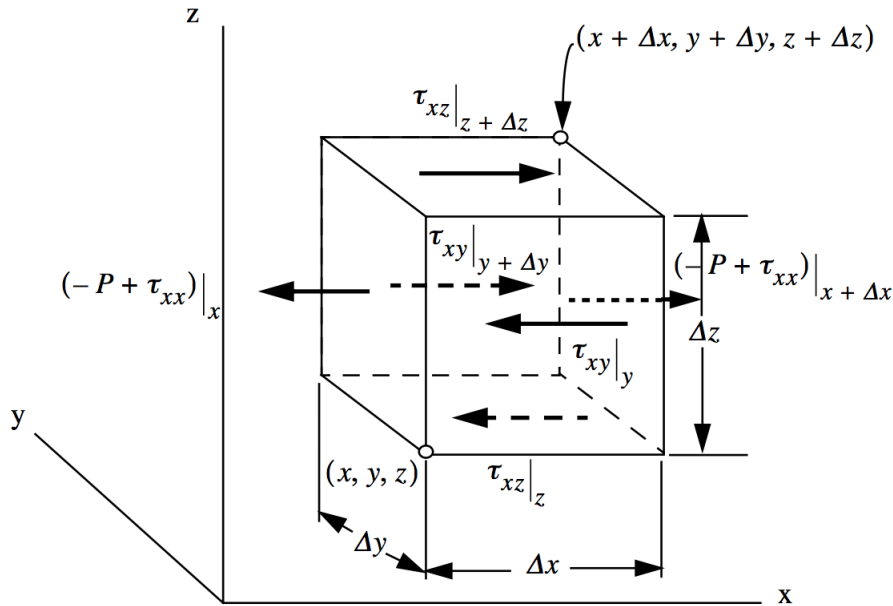


Figure 1.10: Pressure and viscous stresses acting in the x -direction.

Consider a pair of faces perpendicular to the x -axis in Figure 1.10. The force on the face at x with outward normal in the negative x -direction is $-(-P + \tau_{xx})|_x \Delta y \Delta z$ and the force on the face at $x+\Delta x$ with outward normal in the positive x -direction is $(-P + \tau_{xx})|_{x+\Delta x} \Delta y \Delta z$. The x -component of force on the face at y due to viscous stress is $-\tau_{xy}|_y \Delta x \Delta z$ and the x -component of force on the face at $y+\Delta y$ is $\tau_{xy}|_{y+\Delta y} \Delta x \Delta z$. Finally, the x -component of force on the face at z is $-\tau_{xz}|_z \Delta y \Delta z$ and the x -component of force on the face at $z+\Delta z$

is $\tau_{xz}|_{z+\Delta z} \Delta y \Delta z$. Note that the pressure is a scalar that acts normal to any surface in the fluid and therefore there is no component of the pressure acting in the x -direction on the faces perpendicular to the y and z directions. The pressure- viscous stress forces acting in all three directions on the control volume are

$$\begin{aligned} F_x &= \Delta y \Delta z ((-P + \tau_{xx})|_{x+\Delta x} - (-P + \tau_{xx})|_x) + \Delta x \Delta z (\tau_{xy}|_{y+\Delta y} - \tau_{xy}|_y) + \\ &\quad \Delta x \Delta y (\tau_{xz}|_{z+\Delta z} - \tau_{xz}|_z) \\ F_y &= \Delta y \Delta z (\tau_{xy}|_{x+\Delta x} - \tau_{xy}|_x) + \Delta x \Delta z ((-P + \tau_{yy})|_{y+\Delta y} - (-P + \tau_{yy})|_y) + \\ &\quad \Delta x \Delta y (\tau_{yz}|_{z+\Delta z} - \tau_{yz}|_z) \\ F_z &= \Delta y \Delta z (\tau_{xz}|_{x+\Delta x} - \tau_{xz}|_x) + \Delta x \Delta z (\tau_{yz}|_{y+\Delta y} - \tau_{yz}|_y) + \\ &\quad \Delta x \Delta y ((-P + \tau_{zz})|_{z+\Delta z} - (-P + \tau_{zz})|_z) \end{aligned} \quad (1.76)$$

With convection, pressure and viscous forces included, the x -component momentum balance over the control volume is, from (1.65)

$$\begin{aligned} \Delta x \Delta y \Delta z \left(\frac{\partial \rho U}{\partial t} \right) &= \Delta y \Delta z (\rho UU|_x - \rho UU|_{x+\Delta x}) + \\ \Delta x \Delta z (\rho U V|_y - \rho U V|_{y+\Delta y}) &+ \Delta x \Delta y (\rho UW|_z - \rho UW|_{z+\Delta z}) + \\ \Delta y \Delta z ((-P + \tau_{xx})|_{x+\Delta x} - (-P + \tau_{xx})|_x) &+ \\ \Delta x \Delta z (\tau_{xy}|_{y+\Delta y} - \tau_{xy}|_y) &+ \Delta x \Delta y (\tau_{xz}|_{z+\Delta z} - \tau_{xz}|_z) \end{aligned} \quad (1.77)$$

Divide (1.77) through by $\Delta x \Delta y \Delta z$ and move the convective, pressure and viscous stress terms to the left hand side. The result is

$$\begin{aligned} \frac{\partial \rho U}{\partial t} + \frac{\rho UU|_{x+\Delta x} - \rho UU|_x + (P - \tau_{xx})|_{x+\Delta x} - (P - \tau_{xx})|_x}{\Delta x} &+ \\ \frac{\rho U V|_{y+\Delta y} - \rho U V|_y - (\tau_{xy}|_{y+\Delta y} - \tau_{xy}|_y)}{\Delta y} &+ \frac{\rho UW|_{z+\Delta z} - \rho UW|_z - (\tau_{xz}|_{z+\Delta z} - \tau_{xz}|_z)}{\Delta z} = 0 \end{aligned} \quad (1.78)$$

Let $\Delta x \rightarrow 0, \Delta y \rightarrow 0, \Delta z \rightarrow 0$. In this limit (1.78) becomes

$$\frac{\partial \rho U}{\partial t} + \frac{\partial (\rho UU + P - \tau_{xx})}{\partial x} + \frac{\partial (\rho UV - \tau_{xy})}{\partial y} + \frac{\partial (\rho UW - \tau_{xz})}{\partial z} = 0. \quad (1.79)$$

The equations for conservation of momentum in the y and z directions are derived in a similar way using the expressions in (1.69) and (1.76).

$$\begin{aligned} \frac{\partial \rho V}{\partial t} + \frac{\partial (\rho VU - \tau_{xy})}{\partial x} + \frac{\partial (\rho VV + P - \tau_{yy})}{\partial y} + \frac{\partial (\rho VW - \tau_{yz})}{\partial z} &= 0 \\ \frac{\partial \rho W}{\partial t} + \frac{\partial (\rho WU - \tau_{xz})}{\partial x} + \frac{\partial (\rho WV - \tau_{yz})}{\partial y} + \frac{\partial (\rho WW + P - \tau_{zz})}{\partial z} &= 0 \end{aligned} \quad (1.80)$$

In index form, using the Einstein convention, the momentum conservation equation is

$$\frac{\partial \rho U_i}{\partial t} + \frac{\partial (\rho U_i U_j + P \delta_{ij} - \tau_{ij})}{\partial x_j} = 0 \quad i = 1, 2, 3. \quad (1.81)$$

The coordinate independent form of (1.81) is

$$\frac{\partial \rho \bar{U}}{\partial t} + \nabla \cdot (\rho \bar{U} \bar{U} + P \bar{I} - \bar{\tau}) = 0. \quad (1.82)$$

The tensor product of vectors that appears in (1.81), $\bar{U} \bar{U} = U_i U_j$, also called a dyadic product, is sometimes written $\bar{U} \otimes \bar{U}$. Fully written out, this product is

$$\bar{U} \bar{U} = \begin{bmatrix} UU & UV & UW \\ VU & VV & VW \\ WU & WV & WW \end{bmatrix}. \quad (1.83)$$

Note that the matrix (1.83) is symmetric and as we shall see in Chapter 5, so is the stress tensor τ_{ij} .

1.8 Conservation of energy

The law of conservation of energy is stated as

$$\left\{ \begin{array}{l} \text{rate of energy} \\ \text{accumulation} \\ \text{inside the control} \\ \text{volume} \end{array} \right\} = \left\{ \begin{array}{l} \text{rate of energy flow} \\ \text{into the} \\ \text{control volume} \\ \text{by convection} \end{array} \right\} - \left\{ \begin{array}{l} \text{rate of energy flow} \\ \text{out of the} \\ \text{control volume} \\ \text{by convection} \end{array} \right\} + \left\{ \begin{array}{l} \text{work done on the} \\ \text{control volume} \\ \text{by pressure and} \\ \text{viscous forces} \end{array} \right\} + \left\{ \begin{array}{l} \text{energy generation} \\ \text{due to sources inside} \\ \text{the control volume} \end{array} \right\} \quad . \quad (1.84)$$

The energy per unit mass of a moving continuum is $e + k$ where e is the internal energy per unit mass and

$$k = (1/2) (U^2 + V^2 + W^2) \quad (1.85)$$

is the kinetic energy per unit mass. The convection of energy into and out of the control volume is depicted in Figure 2.11.

1.8.1 Pressure and viscous stress work

The forces that act on the surface of a control volume do work on the fluid in the control volume and therefore contribute to the energy balance. The power (energy per second) put into the fluid within the control volume is given by the classical relation from mechanics

$$\text{Power input to the control volume} = \bar{F} \cdot \bar{U} \quad (1.86)$$

where \bar{U} is the flow velocity and \bar{F} is the net vector force on the control volume by pressure

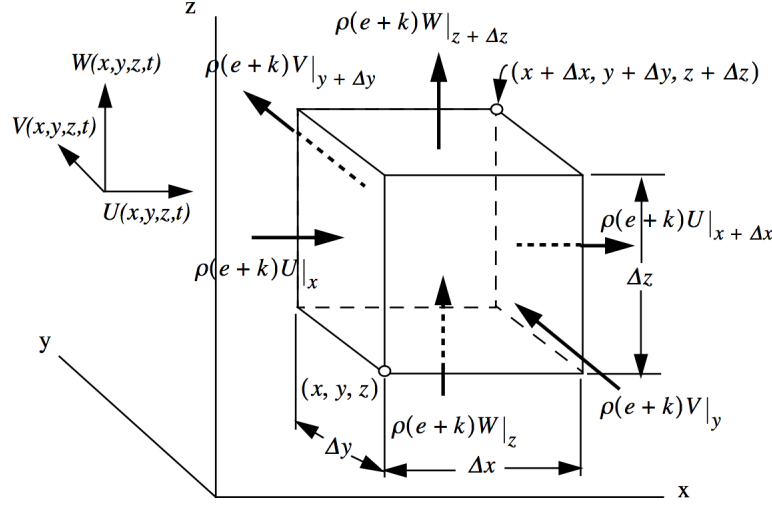


Figure 1.11: Convection of energy into and out of a control volume.

and viscous forces with components (1.76). Fully written out (1.86) is

$$\text{Power input to the control volume} = \bar{F} \cdot \bar{U} =$$

$$\begin{aligned}
 & \Delta y \Delta z \left\{ \left((-P + \tau_{xx})|_{x+\Delta x} - (-P + \tau_{xx})|_x \right) U + \right. \\
 & \quad \left. \left(\tau_{xy}|_{x+\Delta x} - \tau_{xy}|_x \right) V + \left(\tau_{xz}|_{x+\Delta x} - \tau_{xz}|_x \right) W \right\} + \\
 & \Delta x \Delta z \left\{ \left(\tau_{xy}|_{y+\Delta y} - \tau_{xy}|_y \right) U + \left((-P + \tau_{yy})|_{y+\Delta y} - (-P + \tau_{yy})|_y \right) V + \right. \\
 & \quad \left. \left(\tau_{yz}|_{y+\Delta y} - \tau_{yz}|_y \right) W \right\} + \\
 & \Delta x \Delta y \left\{ \left(\tau_{xz}|_{z+\Delta z} - \tau_{xz}|_z \right) U + \left(\tau_{yz}|_{z+\Delta z} - \tau_{yz}|_z \right) V + \right. \\
 & \quad \left. \left((-P + \tau_{zz})|_{z+\Delta z} - (-P + \tau_{zz})|_z \right) W \right\}.
 \end{aligned} \tag{1.87}$$

The right-hand-side of (1.87) can be parsed into a series of energy fluxes into and out of

the various faces of the control volume.

$$\text{Power input to the control volume} = \bar{F} \cdot \bar{U} =$$

$$\begin{aligned} & \Delta y \Delta z \left\{ \begin{array}{l} (-PU + \tau_{xx}U + \tau_{xy}V + \tau_{xz}W)|_{x+\Delta x} - \\ (-PU + \tau_{xx}U + \tau_{xy}V + \tau_{xz}W)|_x \end{array} \right\} + \\ & \Delta x \Delta z \left\{ \begin{array}{l} (-PV + \tau_{xy}U + \tau_{yy}V + \tau_{yz}W)|_{y+\Delta y} - \\ (-PV + \tau_{xy}U + \tau_{yy}V + \tau_{yz}W)|_y \end{array} \right\} + \\ & \Delta x \Delta y \left\{ \begin{array}{l} (-PW + \tau_{zx}U + \tau_{zy}V + \tau_{zz}W)|_{z+\Delta z} - \\ (-PW + \tau_{zx}U + \tau_{zy}V + \tau_{zz}W)|_z \end{array} \right\} \end{aligned} \quad (1.88)$$

The contribution of these fluxes to the energy balance over the control volume is illustrated in Figure 2.12.

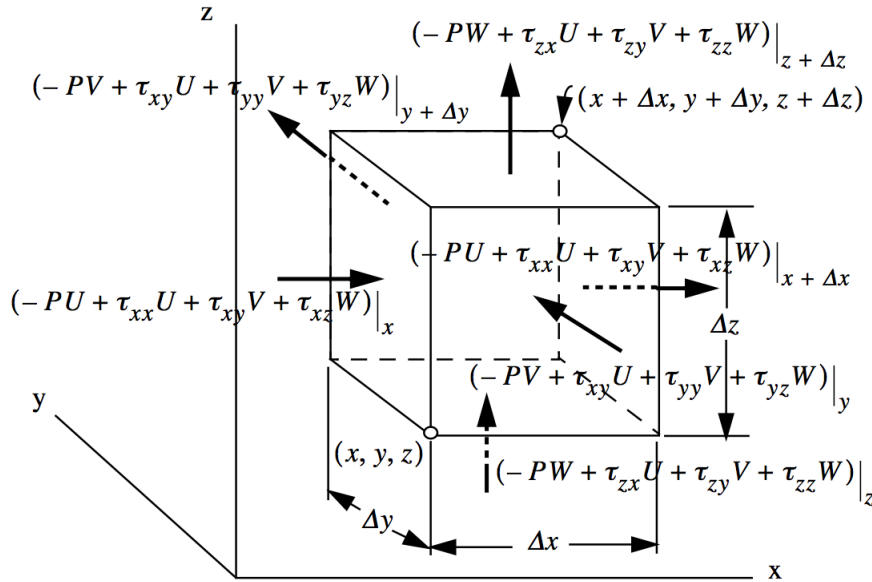


Figure 1.12: Energy fluxes due to the work done on the control volume by pressure and viscous forces.

In addition to the energy input due to work done by pressure and viscous forces one must also include the flux of heat Q into and out of the control volume due to thermal conduction. The rate of internal and kinetic energy accumulation inside the control volume is $\Delta x \Delta y \Delta z (\partial \rho (e + k) / \partial t)$. With all the various sources of energy taken into account, the

energy balance (1.84) is expressed mathematically as

$$\begin{aligned}
 & \Delta x \Delta y \Delta z \frac{\partial \rho (e + k)}{\partial t} = \\
 & \Delta y \Delta z (\rho (e + k) U|_x - \rho (e + k) U|_{x+\Delta x}) + \\
 & \Delta x \Delta z (\rho (e + k) V|_y - \rho (e + k) V|_{y+\Delta y}) + \\
 & \Delta x \Delta y (\rho (e + k) W|_z - \rho (e + k) W|_{z+\Delta z}) + \\
 & \Delta y \Delta z \left\{ \begin{array}{l} ((-P + \tau_{xx})|_{x+\Delta x} - (-P + \tau_{xx})|_x) U + \\ (\tau_{xy}|_{x+\Delta x} - \tau_{xy}|_x) V + (\tau_{xz}|_{x+\Delta x} - \tau_{xz}|_x) W \end{array} \right\} + \\
 & \Delta x \Delta z \left\{ \begin{array}{l} \left(\tau_{xy}|_{y+\Delta y} - \tau_{xy}|_y \right) U + \left((-P + \tau_{yy})|_{y+\Delta y} - (-P + \tau_{yy})|_y \right) V + \\ \left(\tau_{yz}|_{y+\Delta y} - \tau_{yz}|_y \right) W \end{array} \right\} + \quad (1.89) \\
 & \Delta x \Delta y \left\{ \begin{array}{l} (\tau_{xz}|_{z+\Delta z} - \tau_{xz}|_z) U + (\tau_{yz}|_{z+\Delta z} - \tau_{yz}|_z) V + \\ ((-P + \tau_{zz})|_{z+\Delta z} - (-P + \tau_{zz})|_z) W \end{array} \right\} + \\
 & \Delta y \Delta z (Q_x|_x - Q_x|_{x+\Delta x}) + \Delta x \Delta z (Q_y|_y - Q_y|_{y+\Delta y}) + \\
 & \Delta x \Delta y (Q_z|_z - Q_z|_{z+\Delta z}) + \\
 & \{ \text{power generation due to energy sources inside the control volume} \}.
 \end{aligned}$$

Divide (1.89) through by the infinitesimal volume $\Delta x \Delta y \Delta z$ and take the limit $\Delta x \rightarrow$

$0, \Delta y \rightarrow 0, \Delta z \rightarrow 0$. The conservation equation for the energy becomes

$$\begin{aligned} & \frac{\partial \rho(e+k)}{\partial t} + \\ & \frac{\partial (\rho(e+k)U + PU - \tau_{xx}U - \tau_{xy}V - \tau_{xz}W + Q_x)}{\partial x} + \\ & \frac{\partial (\rho(e+k)V + PV - \tau_{yx}U - \tau_{yy}V - \tau_{yz}W + Q_y)}{\partial y} + \\ & \frac{\partial (\rho(e+k)W + PW - \tau_{zx}U - \tau_{zy}V - \tau_{zz}W + Q_z)}{\partial z} = \\ & \{ \text{power generation due to energy sources inside the control volume} \} \end{aligned} . \quad (1.90)$$

In index form the energy conservation equation is

$$\frac{\partial \rho(e+k)}{\partial t} + \frac{\partial (\rho(e+k)U_j + PU_j - U_i\tau_{ij} + Q_j)}{\partial x_j} = \quad (1.91)$$

$\{ \text{power generation due to energy sources inside the control volume} \}$

and the coordinate independent form of (1.91) is

$$\frac{\partial \rho(e+k)}{\partial t} + \nabla \cdot (\rho(e+k)\bar{U} + P\bar{U} - \bar{\tau} \cdot \bar{U} + \bar{Q}) = \quad (1.92)$$

$\{ \text{power generation due to energy sources inside the control volume} \} .$

Power sources within the control volume can take on a wide variety of forms including chemical reactions, phase change, light absorption from an external source, nuclear reactions, etc.

1.9 Summary - the equations of motion

The combined conservation equations in Cartesian coordinates are

Conservation of mass

$$\frac{\partial \rho}{\partial t} + \frac{\partial \rho U}{\partial x} + \frac{\partial \rho V}{\partial y} + \frac{\partial \rho W}{\partial z} = 0$$

Conservation of momentum

$$\begin{aligned} \frac{\partial \rho U}{\partial t} + \frac{\partial (\rho UU + P - \tau_{xx})}{\partial x} + \frac{\partial (\rho UV - \tau_{xy})}{\partial y} + \frac{\partial (\rho UW - \tau_{xz})}{\partial z} &= 0 \\ \frac{\partial \rho V}{\partial t} + \frac{\partial (\rho VU - \tau_{xy})}{\partial x} + \frac{\partial (\rho VV + P - \tau_{yy})}{\partial y} + \frac{\partial (\rho VW - \tau_{yz})}{\partial z} &= 0 \\ \frac{\partial \rho W}{\partial t} + \frac{\partial (\rho WU - \tau_{xz})}{\partial x} + \frac{\partial (\rho WV - \tau_{yz})}{\partial y} + \frac{\partial (\rho WW + P - \tau_{zz})}{\partial z} &= 0 \end{aligned} \quad (1.93)$$

Conservation of energy

$$\begin{aligned} \frac{\partial \rho (e + k)}{\partial t} + \frac{\partial (\rho (e + k) U + PU - \tau_{xx}U - \tau_{xy}V - \tau_{xz}W + Q_x)}{\partial x} \\ \frac{\partial (\rho (e + k) V + PV - \tau_{yx}U - \tau_{yy}V - \tau_{yz}W + Q_y)}{\partial y} \\ \frac{\partial (\rho (e + k) W + PW - \tau_{zx}U - \tau_{zy}V - \tau_{zz}W + Q_z)}{\partial z} = \end{aligned}$$

$\{Power\ generation\ due\ to\ energy\ sources\ inside\ the\ control\ volume\}.$

See Appendix B for the equations of motion in cylindrical and spherical polar coordinates. In their current form (1.93) the equations cannot be solved until there is an additional equation that relates the viscous stresses to the velocity field. In Chapter 5 the general form of the Newtonian constitutive law (1.75) will be defined.

Also required is a way of relating the density and pressure that appear in the momentum equation to the internal energy that appears in the energy equation. This will come from thermodynamics and the definition of an equation of state. The heat flux in the energy equation will be related to the fluid temperature using Fick's law for linear heat conduction. Inclusion of these relations leads to a closed system of governing equations for viscous compressible flow where the number of equations is equal to the number of unknowns. Under certain flow assumptions that are of considerable aeronautical interest it will be possible to directly relate the density and pressure without having to know the temperature. In this case the momentum and mass conservation equations become a closed system that is sufficient to fully describe the flow. The two most common cases where this occurs are incompressible flow where the density is constant and isentropic compressible flow where the pressure is related to the density by a power law. Some of the tools of vector calculus will be established in Chapter 3. We will then return to the equations of motion in Chapter 5 and re-derive them using a much more general approach based on methods for differentiation of integrals over an arbitrarily shaped control volume.

1.10 Problems

Problem 1 - Show that the continuity equation can be expressed as

$$\frac{1}{\rho} \frac{D\rho}{Dt} + \frac{\partial U_j}{\partial x_j} = 0 \quad (1.94)$$

Problem 2 - Use direct measurements from the streamlines in Figure 2.13 to estimate the percent change from the free stream velocity at points A , B , C and D.

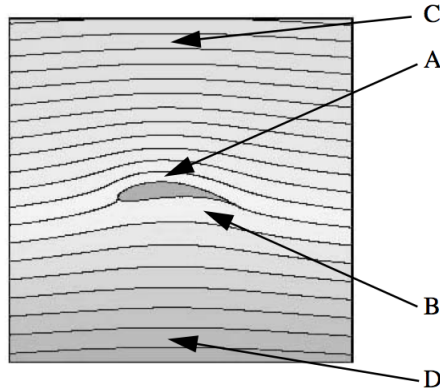


Figure 1.13: Streamlines about a wing in potential flow.

Problem 3 - The general, first order, linear ODE

$$\frac{dy}{dx} = -g(x)y + f(x) \quad (1.95)$$

can be written as the differential form

$$(g(x)y - f(x))dx + dy = 0 \quad (1.96)$$

Show that (1.96) can be converted to a perfect differential by multiplying by the integrating factor.

$$M = e^{\int g(x)dx} \quad (1.97)$$

Work out the solution of (1.95) in terms of integrals. What is the solution for the case $g = \sin(x)$, $f = \cos(x)$? Sketch the corresponding streamline pattern.

Problem 4 - Solve

$$y\frac{\partial\Psi}{\partial x} - \frac{x}{3}\frac{\partial\Psi}{\partial y} = 0. \quad (1.98)$$

Sketch the resulting streamline pattern.

Problem 5 - Show that the following expression is a perfect differential.

$$-\sin(x)\sin(y)dx + \cos(x)\cos(y)dy = 0 \quad (1.99)$$

Integrate (1.99) to determine the stream function and sketch the corresponding flow pattern. Work out the substantial derivatives of the velocity components and sketch the acceleration vector field.

Problem 6 - Determine the acceleration of a particle in the 1-D velocity field

$$\bar{U} = \left(k\frac{x}{t}, 0, 0\right) \quad (1.100)$$

where k is constant.

Problem 7 - In a fixed frame of reference a fluid element has the velocity components

$$(U, V, W) = (100, 60, 175) \text{ meters/sec.} \quad (1.101)$$

Suppose the same fluid element is observed in a frame of reference moving at

$$\dot{\bar{X}} = (25, 110, 90) \text{ meters/sec} \quad (1.102)$$

with respect to the fixed frame. Determine the velocity components measured by the observer in the moving frame. Determine the kinetic energy per unit mass in each frame.

Problem 8 - The stream function of a steady, 2-D compressible flow in a corner is shown in Figure 2.14.

$$\psi = \frac{xy}{1+x+y}$$

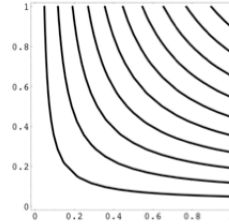


Figure 1.14: Streamlines for potential flow in a corner.

Determine plausible expressions for the velocity components and density field. Does a pressure field exist for this flow if it is assumed to be inviscid?

Problem 9 - The expansion into vacuum of a spherical cloud of a monatomic gas such as helium has a well-known exact solution of the equations for compressible isentropic flow. The velocity field is

$$U = \frac{xt}{t_0^2 + t^2} \quad V = \frac{yt}{t_0^2 + t^2} \quad W = \frac{zt}{t_0^2 + t^2}. \quad (1.103)$$

The density and pressure are

$$\begin{aligned} \frac{\rho}{\rho_0} &= \frac{t_0^3}{(t_0^2 + t^2)^{3/2}} \left(1 - \frac{t_0^2}{R_{initial}^2} \left(\frac{x^2 + y^2 + z^2}{t_0^2 + t^2} \right) \right)^{3/2} \\ \frac{P}{P_0} &= \left(\frac{\rho}{\rho_0} \right)^{5/3} \end{aligned} \quad (1.104)$$

where $R_{initial}$ is the initial radius of the cloud. This problem has served as a model of the expanding gas nebula from an exploding star.

- 1) Determine the particle paths $(x(t), y(t), z(t))$.

2) Work out the substantial derivative of the density $D\rho/Dt$.

Problem 10 - A moving fluid contains a passive non-diffusing scalar contaminant. Smoke in a wind tunnel would be a pretty good example of such a contaminant. Let the concentration of the contaminant be $C(x, y, z, t)$. The units of C are

$$\text{mass of contaminant}/\text{unit mass of fluid}. \quad (1.105)$$

Derive a conservation equation for C .

Problem 11 - Include the effects of gravity in the equations of motion (1.93). You can check your answer with the equations derived in Chapter 5.

Chapter 2

Thermodynamics of dilute gases

2.1 Introduction

The motion of a compressible fluid is directly affected by its thermodynamic state which is itself a consequence of the motion. For this reason, the powerful principles of thermodynamics embodied in the first and second law are a central part of the theory of compressible flow. Thermodynamics derives its power from the fact that the change in the state of a fluid is independent of the actual physical process by which the change is achieved. This enables the first and second laws to be combined to produce the famous Gibbs equation which is stated exclusively in terms of perfect differentials of the type that we studied in Chapter 1. The importance of this point cannot be overstated and the reduction of problems to integrable perfect differential form will be a recurring theme throughout the course.

2.2 Thermodynamics

Thermodynamics is the science that deals with the laws that govern the relationship between temperature and energy, the conversion of energy from one form to another especially heat, the direction of heat flow, and the degree to which the energy of a system is available to do useful work.

2.2.1 Temperature and the zeroth law

In his classic textbook *The Theory of Heat* (SpringerVerlag 1967) Richard Becker begins

with the following description of temperature.

"The concept of temperature is basic in thermodynamics. It originates from our sensations, warm and cold. The most salient physical property of temperature is its tendency to equalize. Two bodies in contact (thermal contact!) will eventually have the same temperature, independent of their physical properties and the special kind of contact. Just this property is used to bring a substance to a given temperature, namely, by surrounding it with a heat bath. Then, by definition, substance and heat bath have the same temperature. To measure the temperature one can employ any physical property which changes continuously and reproducibly with temperature such as volume, pressure, electrical resistivity, and many others. The temperature scale is fixed by convention."

In this description, Becker postulates an incomplete law of equilibrium whereby two systems placed in thermal contact will spontaneously change until the temperature of each system is the same. This is sometimes called the zeroth law of thermodynamics. James Clerk Maxwell (1831-1879), the famous British physicist, who published his own text entitled *Theory of Heat* in 1870, expressed the zeroth law as follows: "When each of two systems is equal in temperature to a third, the first two systems are equal in temperature to each other." A key concept implicit in the zeroth law is that the temperature characterizes the state of the system at any moment in time and is independent of the path used to bring the system to that state. Such a property of the system is called a variable of state.

2.2.2 The first law

During the latter part of the nineteenth century heat was finally recognized to be a form of energy. The first law of thermodynamics is essentially a statement of this equivalence. The first law is based on the observation that the internal energy E of an isolated system is conserved. An isolated system is one with no interaction with its surroundings. The internal energy is comprised of the total kinetic, rotational and vibrational energy of the atoms and molecules contained in the system. Chemical bond and nuclear binding energies must also be included if the system is undergoing a chemical or nuclear reaction.

The value of the internal energy can only be changed if the system ceases to be isolated. In this case E can change by the transfer of mass to or from the system, by the transfer of heat, and by work done on or by the system. For an adiabatic ($\delta Q = 0$), constant mass system, $dE = -\delta W$.

By convention, δQ is positive if heat is added to the system and negative if heat is removed. The work, δW is taken to be positive if work is done by the system on the surroundings and negative if work is done on the system by the surroundings.

Because energy cannot be created or destroyed the amount of heat transferred into a system

must equal the increase in internal energy of the system plus the work done by the system. For a nonadiabatic system of constant mass

$$\delta Q = dE + \delta W. \quad (2.1)$$

This statement, which is equivalent to a law of conservation of energy, is known as the first law of thermodynamics. In Equation (2.1) it is extremely important to distinguish between a small change in internal energy which is a state variable and therefore is expressed as a perfect differential d , and small amounts of heat added or work done that do not characterize the system per se but rather a particular interaction of the system with its surroundings. To avoid confusion, the latter small changes are denoted by a δ .

The internal energy of a system is determined by its temperature and volume. Any change in the internal energy of the system is equal to the difference between its initial and final values regardless of the path followed by the system between the two states. Consider the piston cylinder combination shown in Figure 2.1.

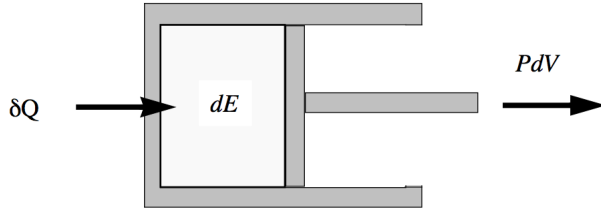


Figure 2.1: Exchange of heat and work for a system comprising a cylinder with a movable frictionless piston.

The cylinder contains some homogeneous material with a fixed chemical composition. An infinitesimal amount of heat, δQ is added to the system causing an infinitesimal change in internal energy and an infinitesimal amount of work δW to be done. The differential work done by the system on the surroundings is the conventional mechanical work done by a force acting over a distance and can be expressed in terms of the state variables pressure and volume. Thus

$$\delta W = Fdx = (F/A)d(Ax) = PdV. \quad (2.2)$$

where A is the cross sectional area of the piston and F is the force by the material inside the cylinder on the piston. The first law of thermodynamics now takes the following form.

$$\delta Q = dE + PdV \quad (2.3)$$

We will be dealing with open flows where the system is an infinitesimal fluid element. In this context it is convenient to work in terms of intensive variables by dividing through by the mass contained in the cylinder. The first law is then

$$\delta q = de + Pdv. \quad (2.4)$$

where δq is the heat exchanged per unit mass, e is the internal energy per unit mass and $v = 1/\rho$ is the volume per unit mass. As noted above, the δ symbol is used to denote that the differential 1-form on the right-hand-side of Equation (2.4) is not a perfect differential and in this form the first law is not particularly useful.

The first law, Equation (2.4), is only useful if we can determine an equation of state for the substance contained in the cylinder. The equation of state is a functional relationship between the internal energy per unit mass, specific volume and pressure, $P(e, v)$. For a general substance an accurate equation of state is not a particularly easy relationship to come by and so most applications tend to focus on approximations based on some sort of idealization. One of the simplest and most important cases is the equation of state for an ideal gas which is an excellent approximation for real gases over a wide range of conditions. We will study ideal gases shortly, but first let's see how the existence of an equation of state gives us a complete theory for the equilibrium states of the material contained in the cylinder shown in Figure 2.1.

2.2.3 The second law

Assuming an equation of state can be defined, the first law becomes,

$$\delta q = de + P(e, v) dv. \quad (2.5)$$

According to Pfaff's theorem, discussed in Chapter 1, the differential form on the right-hand-side of (2.5) must have an integrating factor which we write as $1/T(e, v)$. Multiplying the first law by the integrating factor turns it into a perfect differential.

$$\frac{\delta q}{T(e, v)} = \frac{de}{T(e, v)} + \frac{P(e, v)}{T(e, v)} dv = ds(e, v) \quad (2.6)$$

In effect, once one accepts the first law (2.5) and the existence of an equation of state, $P(e, v)$, then the existence of two new variables of state is implied. By Pfaff's theorem there exists an integrating factor which we take to be the inverse of the temperature postulated in the zeroth law, and there is an associated integral called the entropy (per unit mass) $s(e, v)$. In essence, the second law implies the existence of stable states of

equilibrium of a thermodynamic system. The final result is the famous Gibbs equation, usually written

$$Tds = de + Pdv. \quad (2.7)$$

This fundamental equation is the starting point for virtually all applications of thermodynamics. Gibbs equation describes states that are in local thermodynamic equilibrium i.e., states that can be reached through a sequence of reversible steps. Since (2.7) is a perfect differential we can conclude that the partial derivatives of the entropy are

$$\left. \frac{\partial s}{\partial e} \right|_{v=constant} = \frac{1}{T(e, v)} \quad \left. \frac{\partial s}{\partial v} \right|_{e=constant} = \frac{P(e, v)}{T(e, v)}. \quad (2.8)$$

The cross derivatives of the entropy are equal and so one can state that for any homogeneous material

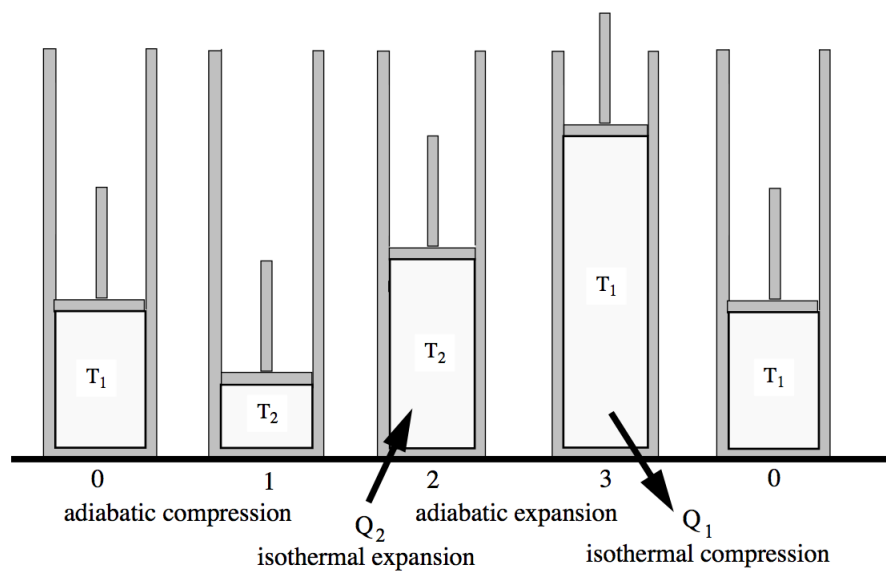
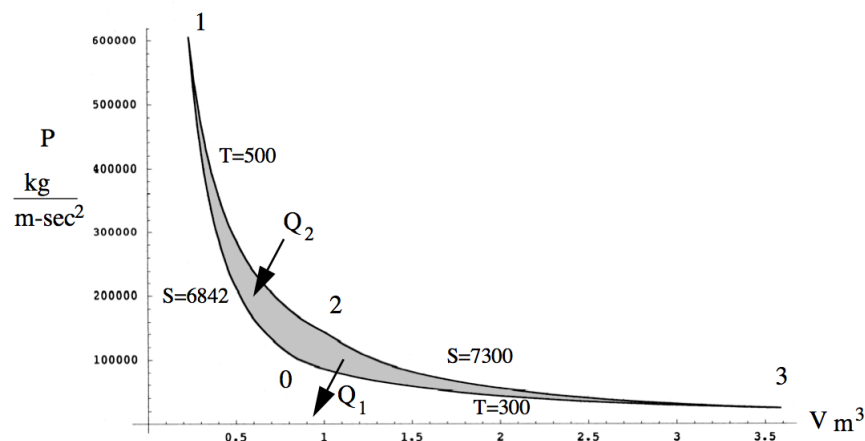
$$\frac{\partial^2 s}{\partial e \partial v} = \frac{\partial}{\partial v} \left(\frac{1}{T(e, v)} \right) = \frac{\partial}{\partial e} \left(\frac{P(e, v)}{T(e, v)} \right). \quad (2.9)$$

Note that the integrating factor (the inverse of the temperature) is not uniquely defined. In particular, there can be an arbitrary, constant scale factor since a constant times ds is still a perfect differential. This enables a temperature scale to be defined so that the integrating factor can be identified with the measured temperature of the system.

2.3 The Carnot cycle

Using the Second Law one can show that heat and work are not equivalent though each is a form of energy. All work can be converted to heat but not all heat can be converted to work. The Carnot cycle involving heat interaction at constant temperature is the most efficient thermodynamic cycle and can be used to illustrate this point. Consider the piston cylinder combination containing a fixed mass of a working fluid shown in Figure 2.2 and the sequence of piston strokes representing the four basic states in the Carnot cycle. In the ideal Carnot cycle the adiabatic compression and expansion strokes are carried out isentropically and the piston is frictionless.

A concrete example in the $P - V$ plane and $T - S$ plane is shown in Figure 2.3 and Figure 2.4. The working fluid is nitrogen cycling between the temperatures of 300 and 500 Kelvin with the compression stroke moving between one and six atmospheres. The entropy per unit mass of the compression leg comes from tabulated data for nitrogen computed from

Figure 2.2: *The Carnot cycle heat engine.*Figure 2.3: *P-V diagram of the Carnot cycle.*

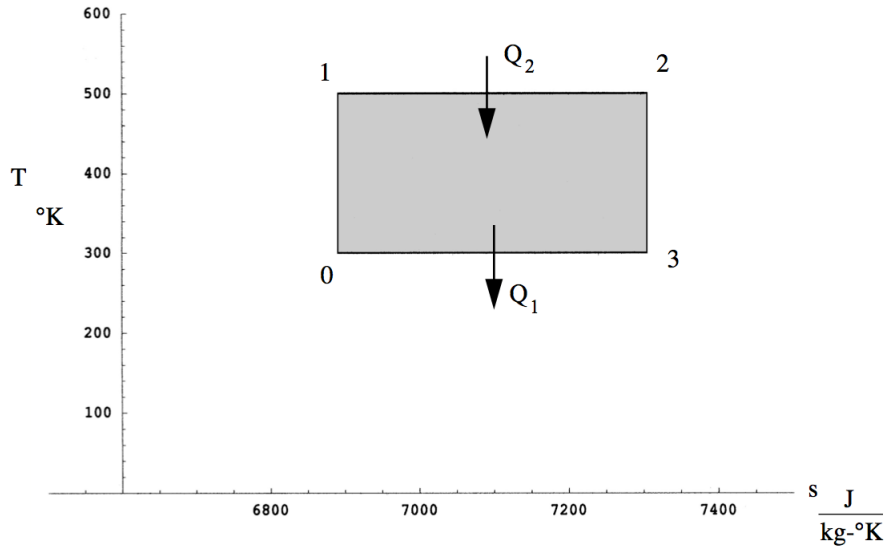


Figure 2.4: *T-S diagram of the Carnot cycle.*

Equation (2.120) at the end of this chapter. The entropy per unit mass of the expansion leg is specified to be $7300 \text{ J}/(\text{kg} \cdot \text{K})$. The thermodynamic efficiency of the cycle is

$$\eta = \frac{\text{work output by the system during the cycle}}{\text{heat added to the system during the cycle}} = \frac{W}{Q_2}. \quad (2.10)$$

According to the first law of thermodynamics

$$\delta Q = dE + \delta W. \quad (2.11)$$

Over the cycle the change in internal energy (which is a state variable) is zero and the work done is

$$W = Q_2 + Q_1. \quad (2.12)$$

where Q_1 is negative and so the efficiency is

$$\eta = 1 + \frac{Q_1}{Q_2}. \quad (2.13)$$

The change in entropy per unit mass over the cycle is also zero and so from the Second Law

$$\oint ds = \oint \frac{\delta Q}{T} = 0. \quad (2.14)$$

Since the temperature is constant during the heat interaction we can use this result to write

$$\frac{Q_1}{T_1} = -\frac{Q_2}{T_2}. \quad (2.15)$$

Thus the efficiency of the Carnot cycle is

$$\eta_C = 1 - \frac{T_1}{T_2} < 1. \quad (2.16)$$

For the example shown $\eta_C = 0.4$. At most only 40% of the heat added to the system can be converted to work. The maximum work that can be generated by a heat engine working between two finite temperatures is limited by the temperature ratio of the system and is always less than the heat put into the system.

2.3.1 The absolute scale of temperature

For any Carnot cycle, regardless of the working fluid

$$\frac{Q_1}{Q_2} = -\frac{T_1}{T_2}. \quad (2.17)$$

Equation (2.17) enables an absolute scale of temperature to be defined that only depends on the general properties of a Carnot cycle and is independent of the properties of any particular substance. As noted earlier the temperature, which is the integrating factor in the Gibbs equation (2.7), is only defined up to an arbitrary constant of proportionality. Similarly, any scale factor would divide out of (2.17) and so it has to be chosen by convention. The convention once used to define the Kelvin scale was to require that there be 100 degrees between the melting point of ice and the boiling point of water. Relatively recently there was an international agreement to define the ice point as exactly 273.15 K above absolute zero and allow the boiling point to be no longer fixed. As a result the boiling point of water at standard pressure is $273.15 + 99.61 = 372.76\text{ K}$ rather than 373.15 K . Note that the standard pressure is not one atmosphere at sea level, which is 101.325 kPa ,

but since 1982 has been defined by the International Union of Pure and Applied Chemistry (IUPAC) as 100 kPa.

Absolute temperature is generally measured in degrees Rankine or degrees Kelvin and the scale factor between the two is

$$T_{\text{Rankine}} = \left(\frac{9}{5}\right) T_{\text{Kelvin}}. \quad (2.18)$$

The usual Fahrenheit and Centigrade scales are related to the absolute scales by

$$\begin{aligned} T_{\text{Rankine}} &= T_{\text{Farenheit}} + 459.67 \\ T_{\text{Kelvin}} &= T_{\text{Centigrade}} + 273.15. \end{aligned} \quad (2.19)$$

2.4 Enthalpy

It is often useful to rearrange Gibbs' equation so as to exchange dependent and independent variables. This can be accomplished using the so-called *Legendre transformation*. In this approach, a new variable of state is defined called the enthalpy per unit mass.

$$h = e + Pv \quad (2.20)$$

In terms of this new variable of state, the Gibbs equation becomes

$$ds = \frac{dh}{T} - \frac{v}{T}dP. \quad (2.21)$$

Using this simple change of variables, the pressure has been converted from a dependent variable to an independent variable.

$$ds(h, P) = \frac{dh}{T(h, P)} - \frac{v(h, P)}{T(h, P)}dP \quad (2.22)$$

Note that $1/T$ is still the integrating factor. With enthalpy and pressure as the independent variables the partial derivatives of the entropy are

$$\left. \frac{\partial s}{\partial h} \right|_{P=\text{constant}} = \frac{1}{T(h, P)} \quad \left. \frac{\partial s}{\partial P} \right|_{h=\text{constant}} = -\frac{v(h, P)}{T(h, P)}. \quad (2.23)$$

and for any homogeneous material we can write

$$\frac{\partial^2 s}{\partial h \partial P} = \frac{\partial}{\partial P} \left(\frac{1}{T(h, P)} \right) = -\frac{\partial}{\partial h} \left(\frac{v(h, P)}{T(h, P)} \right). \quad (2.24)$$

It is relatively easy to re-express Gibbs' equation with any two variables selected to be independent by defining additional variables of state, the free energy $f = e - Ts$ and the free enthalpy $g = h - Ts$ (also called the Gibbs free energy). The Gibbs free energy is very useful in the analysis of systems of reacting gases. Using the Gibbs equation and an equation of state, any variable of state can be determined as a function of any two others. For example,

$$\begin{aligned} e &= \varphi(T, P)s = \varsigma(T, v) \\ g &= \xi(e, P)h = \phi(T, P) \\ s &= \theta(h, P)s = \beta(e, v). \end{aligned} \quad (2.25)$$

and so forth.

2.4.1 Gibbs equation on a fluid element

One of the interesting and highly useful consequences of (2.25) is that any differentiation operator acting on the entropy takes on the form of Gibbs equation. Let

$$s = s(h(x, y, z, t), P(x, y, z, t)). \quad (2.26)$$

Take the derivative of (2.26) with respect to time.

$$\frac{\partial s}{\partial t} = \frac{\partial s}{\partial h} \frac{\partial h}{\partial t} + \frac{\partial s}{\partial P} \frac{\partial P}{\partial t} \quad (2.27)$$

Use (2.23) to replace $\partial s/\partial h$ and $\partial s/\partial P$ in equation (2.27).

$$\frac{\partial s}{\partial t} = \frac{1}{T(h, P)} \frac{\partial h}{\partial t} - \frac{v(h, P)}{T(h, P)} \frac{\partial P}{\partial t} \quad (2.28)$$

This is essentially identical to Gibbs equation with the replacements

$$\begin{aligned} ds &\rightarrow \partial s / \partial t \\ dh &\rightarrow \partial h / \partial t \\ dP &\rightarrow \partial P / \partial t. \end{aligned} \tag{2.29}$$

Obviously, we could do this with any spatial derivative as well. For example

$$\begin{aligned} \frac{\partial s}{\partial x} &= \frac{1}{T(h, P)} \frac{\partial h}{\partial x} - \frac{v(h, P)}{T(h, P)} \frac{\partial P}{\partial x} \\ \frac{\partial s}{\partial y} &= \frac{1}{T(h, P)} \frac{\partial h}{\partial y} - \frac{v(h, P)}{T(h, P)} \frac{\partial P}{\partial y} \\ \frac{\partial s}{\partial z} &= \frac{1}{T(h, P)} \frac{\partial h}{\partial z} - \frac{v(h, P)}{T(h, P)} \frac{\partial P}{\partial z}. \end{aligned} \tag{2.30}$$

The three equations in (2.30) can be combined to form the gradient vector

$$\nabla s = \frac{\nabla h}{T} - \frac{v}{T} \nabla P \tag{2.31}$$

which is valid in steady or unsteady flow. All these results come from the functional form (2.26) in which the entropy depends on space and time *implicitly* through the functions $h(x, y, z, t)$ and $P(x, y, z, t)$. The entropy does not depend *explicitly* on x, y, z , or t . Take the substantial derivative, D/Dt , of the entropy. The result is

$$\frac{\partial s}{\partial t} + \bar{U} \cdot \nabla s = \frac{1}{T} \left(\frac{\partial h}{\partial t} + \bar{U} \cdot \nabla h \right) - \frac{v}{T} \left(\frac{\partial P}{\partial t} + \bar{U} \cdot \nabla P \right). \tag{2.32}$$

The result (2.32) shows how Gibbs equation enables a direct connection to be made between the thermodynamic state of a particular fluid element and the velocity field. One simply

replaces the differentials in the Gibbs equation with the substantial derivative.

$$\frac{Ds}{Dt} = \frac{1}{T} \frac{Dh}{Dt} - \frac{v}{T} \frac{DP}{Dt}$$

or

$$\frac{Ds}{Dt} = \frac{1}{T} \frac{De}{Dt} - \frac{P}{\rho^2 T} \frac{D\rho}{Dt} \quad (2.33)$$

Gibbs equation is the key to understanding the thermodynamic behavior of compressible fluid flow. Its usefulness arises from the fact that the equation is expressed in terms of perfect differentials and therefore correctly describes the evolution of thermodynamic variables over a selected fluid element without having to know the flow velocity explicitly. This point will be clarified as we work through the many applications to compressible flow described in the remainder of the text.

2.5 Heat capacities

Consider the fixed volume shown in Figure 2.5. An infinitesimal amount of heat per unit mass is added causing an infinitesimal rise in the temperature and internal energy of the material contained in the volume.

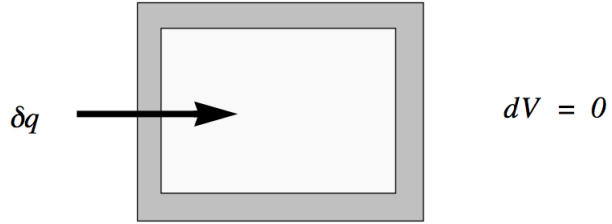
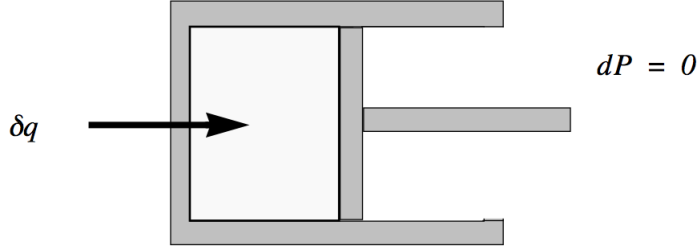


Figure 2.5: *Heat addition at constant volume.*

The heat capacity at constant volume is defined as

$$C_v = \left. \frac{\delta q}{dT} \right|_{v=const} = \left. \frac{de + Pdv}{dT} \right|_{v=const} = \left. \frac{\partial e}{\partial T} \right|_{v=const}. \quad (2.34)$$

Now consider the piston cylinder combination shown below.

Figure 2.6: *Heat addition at constant pressure.*

An infinitesimal amount of heat is added to the system causing an infinitesimal rise in temperature. There is an infinitesimal change in volume while the piston is withdrawn keeping the pressure constant. In this case the system does work on the outside world. The heat capacity at constant pressure is

$$C_p = \frac{\delta q}{dT} \Big|_{P=const} = \frac{dh - vdP}{dT} \Big|_{P=const} = \frac{\partial h}{\partial T} \Big|_{P=const}. \quad (2.35)$$

For a process at constant pressure the heat added is used to increase the temperature of the gas and do work on the surroundings. As a result more heat is required for a given change in the gas temperature and thus $C_p > C_v$. The enthalpy of a general substance can be expressed as

$$h(T, P) = \int C_p(T, P) dT + f(P) \quad (2.36)$$

where the pressure dependence needs to be determined by laboratory measurement. Heat capacities and enthalpies of various substances are generally tabulated purely as a functions of temperature by choosing a reference pressure of $P_{ref} = P^\circ = 10^5 N/m^2$ for the integration. This leads to the concept of a standard enthalpy, $h^\circ(T)$. The standard enthalpy can be expressed as

$$\begin{aligned} h^\circ(T) = & \int_0^{T_{fusion}} C_P^\circ dT + \Delta H_{fusion} + \\ & \int_{T_{fusion}}^{T_{vaporization}} C_P^\circ dT + \Delta H_{vaporization} + \int_{T_{vaporization}}^T C_P^\circ dT \end{aligned} \quad (2.37)$$

where the superscript \circ implies evaluation at the standard pressure. The heat capacity of almost all substances goes to zero rapidly as the temperature goes to zero and so the

integration in (2.37) beginning at absolute zero generally does not present a problem. We shall return to the question of evaluating the enthalpy shortly after we have had a chance to introduce the concept of an ideal gas.

2.6 Ideal gases

For an ideal gas, the equation of state is very simple.

$$P = \frac{nR_u T}{V} \quad (2.38)$$

where n is the number of moles of gas in the system with volume, V . The universal gas constant is

$$R_u = 8314.472 \text{ Joules/}(\text{kgmole} - \text{K}) . \quad (2.39)$$

It is actually more convenient for our purposes to use the gas law expressed in terms of the density

$$P = \rho RT \quad (2.40)$$

where

$$R = R_u/M_w \quad (2.41)$$

and M_w is the mean molecular weight of the gas. The physical model of the gas that underlies (2.38) assumes that the gas molecules have a negligible volume and that the potential energy associated with intermolecular forces is also negligible. This is called the dilute gas approximation and is an excellent model over the range of gas conditions covered in this text.

For gas mixtures the mean molecular weight is determined from a mass weighted average of the various constituents. For air

$$\begin{aligned} M_w|_{\text{air}} &= 28.9644 \text{ kilograms}/(\text{kg} - \text{mole}) \\ R &= 287.06 \text{ m}^2/(\text{sec}^2 - \text{K}) . \end{aligned} \quad (2.42)$$

The perfect gas equation of state actually implies that the internal energy per unit mass of a perfect gas can only depend on temperature, $e = e(T)$. Similarly the enthalpy of a perfect gas only depends on temperature

$$h(T) = e + P/\rho = e(T) + RT. \quad (2.43)$$

Since the internal energy and enthalpy only depend on temperature, the heat capacities also depend only on temperature, and we can express changes in the internal energy and enthalpy as

$$de = C_v(T) dT \quad dh = C_p(T) dT. \quad (2.44)$$

In this course we will deal entirely with ideal gases and so there is no need to distinguish between the standard enthalpy and the enthalpy and so there is no need to use the distinguishing character $^\circ$. We will use it in AA283 when we develop the theory of reacting gases.

Differentiate $RT = h(T) - e(T)$.

$$RdT = dh - de = (C_p - C_v) dT \quad (2.45)$$

The gas constant is equal to the difference between the heat capacities.

$$R = C_p - C_v \quad (2.46)$$

The heat capacities themselves are slowly increasing functions of temperature. But the gas constant is constant, as long as the molecular weight of the system doesn't change (there is no dissociation and no chemical reaction). Therefore the ratio of specific heats

$$\gamma = \frac{C_p}{C_v} \quad (2.47)$$

tends to decrease as the temperature of a gas increases. All gases can be liquefied and the highest temperature at which this can be accomplished is called the critical temperature T_c . The pressure and density at the point of liquefaction are called the critical pressure P_c and critical density ρ . The critical temperature and pressure are physical properties that depend on the details of the intermolecular forces for a particular gas. An equation of state that takes the volume of the gas molecules and intermolecular forces into account must

depend on two additional parameters besides the gas constant R . The simplest extension of the ideal gas law that achieves this is the famous van der Waals equation of state

$$P = \rho RT \left(\frac{1}{1 - b\rho} - \frac{a\rho}{RT} \right) \quad (2.48)$$

where

$$\frac{a}{b} = \frac{27}{8} RT_c \quad \frac{a}{b^2} = 27 P_c. \quad (2.49)$$

The van der Waals equation provides a somewhat useful approximation for gases near the critical point where the dilute gas approximation loses validity.

2.7 Constant specific heat

The heat capacities of monatomic gases are constant over a wide range of temperatures. For diatomic gases the heat capacities vary only a few percent between the temperatures of 200 K and 1200 K. For enthalpy changes in this range one often uses the approximation of a *calorically perfect gas* for which the heat capacities are assumed to be constant and

$$e_2 - e_1 = C_v (T_2 - T_1) \quad h_2 - h_1 = C_p (T_2 - T_1). \quad (2.50)$$

For constant specific heat the Gibbs equation becomes

$$\frac{ds}{C_v} = \frac{dT}{T} - (\gamma - 1) \frac{d\rho}{\rho} \quad (2.51)$$

which can be easily integrated.

Figure 2.7 shows a small parcel of gas moving along some complicated path between two points in a flow. The thermodynamic state of the gas particle at the two endpoints is determined by the Gibbs equation.

Integrating (2.51) between 1 and 2 gives an expression for the entropy of an ideal gas with constant specific heats.

$$\exp \left(\frac{s_2 - s_1}{C_v} \right) = \left(\frac{T_2}{T_1} \right) \left(\frac{\rho_2}{\rho_1} \right)^{-(\gamma-1)} \quad (2.52)$$

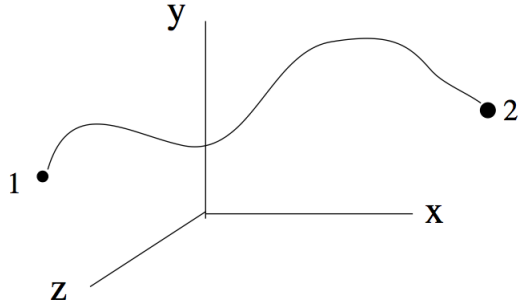


Figure 2.7: Conceptual path of a fluid element moving between two states.

We can express Gibbs equation in terms of the enthalpy instead of internal energy.

$$ds = \frac{dh}{T} - \frac{dP}{\rho T} = C_p \frac{dT}{T} - R \frac{dP}{P} \quad (2.53)$$

Integrate between states 1 and 2.

$$\exp\left(\frac{s_2 - s_1}{C_p}\right) = \left(\frac{T_2}{T_1}\right) \left(\frac{P_2}{P_1}\right)^{-\left(\frac{\gamma-1}{\gamma}\right)}. \quad (2.54)$$

If we eliminate the temperature in (2.54) using the ideal gas law the result is

$$\exp\left(\frac{s_2 - s_1}{C_v}\right) = \left(\frac{P_2}{P_1}\right) \left(\frac{\rho_2}{\rho_1}\right)^{-\gamma}. \quad (2.55)$$

In a process where the entropy is constant these relations become

$$\left(\frac{P_2}{P_1}\right) = \left(\frac{T_2}{T_1}\right)^{\frac{\gamma}{\gamma-1}} \quad \left(\frac{P_2}{P_1}\right) = \left(\frac{\rho_2}{\rho_1}\right)^\gamma \quad \left(\frac{\rho_2}{\rho_1}\right) = \left(\frac{T_2}{T_1}\right)^{\frac{1}{\gamma-1}}. \quad (2.56)$$

Lines of constant entropy in $P - T$ space are shown in Figure 2.8.

The relations in (2.56) are sometimes called the *isentropic chain*.

Note that when we expressed the internal energy and enthalpy for a calorically perfect gas in (2.50) we were careful to express only changes over a certain temperature range. There is a temptation to simply express the energy and enthalpy as $e = C_v T$ and $h = C_p T$. This is incorrect! The correct values require the full integration from absolute zero shown in

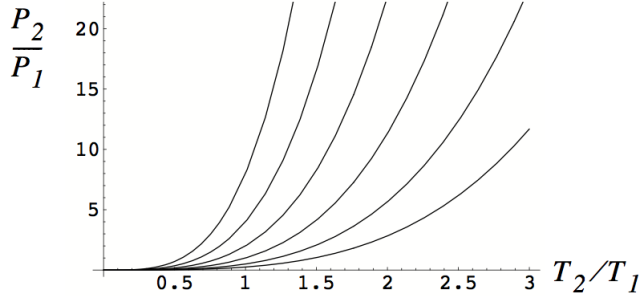


Figure 2.8: *Lines of constant entropy for a calorically perfect gas.*

(2.37). As it happens, the gases we deal with in this course, air, oxygen, nitrogen, hydrogen, etc, all condense at very low temperatures and so the contributions to the enthalpy from the condensed phase and phase change terms in (2.37) tend to be relatively small. This is also true for the monatomic gas Helium in spite of the fact that, unlike virtually all other substances, its heat capacity becomes very large in a narrow range of temperatures near absolute zero.

2.8 The entropy of mixing

The second law of thermodynamics goes beyond the description of changes that relate solely to equilibrium states of a system and quantifies the distinction between reversible and irreversible processes that a system may undergo. For *any* change of a system

$$\delta q \leq T ds \quad (2.57)$$

where ds is the change in entropy per unit mass. Substitute the first law into (2.57). For any change of a system

$$T ds \geq de + P dv. \quad (2.58)$$

Equation (2.58) is the basis of a complete theory for the equilibrium of a thermodynamic system. The incomplete notion of thermal equilibrium expressed by the zeroth law is only one facet of the vast range of phenomena covered by the second law (2.58).

2.8.1 Sample problem - thermal mixing

Equal volumes of an ideal gas are separated by an insulating partition inside an adiabatic container. The gases are at the same pressure but two different temperatures. Assume there are no body forces acting on the system (no gravitational effects).

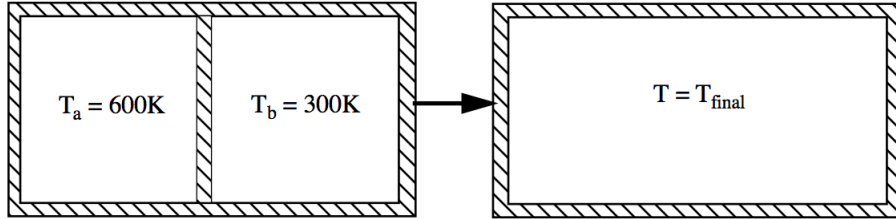


Figure 2.9: Thermal mixing of an ideal gas at two temperatures.

The partition is removed and the temperature of the system is allowed to come to equilibrium.

Part 1 - What is the final temperature of the system?

Energy is conserved and all the gas energy is in the form of internal energy.

$$E - E_{ref} = m_a C_v (T_a - T_{ref}) + m_b C_v (T_b - T_{ref}) = (m_a + m_b) C_v (T_{final} - T_{ref}) \quad (2.59)$$

Canceling the reference energies on both sides we can write

$$m_a C_v T_a + m_b C_v T_b = (m_a + m_b) C_v T_{final}. \quad (2.60)$$

The ideal gas law is

$$PV = m_a R T_a = m_b R T_b. \quad (2.61)$$

Rearrange (2.61) to read

$$\frac{m_b}{m_a} = \frac{T_a}{T_b}. \quad (2.62)$$

Solve (2.59) for T_{final} .

$$T_{final} = \frac{m_a T_a + m_b T_b}{(m_a + m_b)} = \frac{T_a + \left(\frac{m_b}{m_a}\right) T_b}{\left(1 + \frac{m_b}{m_a}\right)} = \frac{2T_a T_b}{T_a + T_b} = 400 K \quad (2.63)$$

Part 2 - What is the change in entropy per unit mass of the system? Express the result in dimensionless form.

The process takes place at constant pressure. In this case the entropy change per unit mass of the two gases is

$$\begin{aligned}\frac{s_{final} - s_a}{C_p} &= \ln\left(\frac{T_{final}}{T_a}\right) \\ \frac{s_{final} - s_b}{C_p} &= \ln\left(\frac{T_{final}}{T_b}\right).\end{aligned}\quad (2.64)$$

The entropy change per unit mass of the whole system is

$$\frac{s_{final} - s_{initial}}{C_p} = \frac{m_a \left(\frac{s_{final} - s_a}{C_p} \right) + m_b \left(\frac{s_{final} - s_b}{C_p} \right)}{m_a + m_b}. \quad (2.65)$$

This can be expressed in terms of the initial and final temperatures as

$$\begin{aligned}\frac{s_{final} - s_{initial}}{C_p} &= \frac{\ln\left(\frac{T_{final}}{T_a}\right) + \left(\frac{T_a}{T_b}\right) \ln\left(\frac{T_{final}}{T_b}\right)}{1 + \left(\frac{T_a}{T_b}\right)} = \frac{\ln\left(\frac{400}{600}\right) = 2 \ln\left(\frac{400}{300}\right)}{1 + (2)} = \\ \frac{s_{final} - s_{initial}}{C_p} &= \frac{-0.405465 + 2(0.28768)}{3} = 0.0566.\end{aligned}\quad (2.66)$$

The entropy of the system increases as the temperatures equalize.

2.8.2 Entropy change due to mixing of distinct gases

The second law states that the entropy change of an isolated system undergoing a change in state must be greater than or equal to zero. Generally, non-equilibrium processes involve some form of mixing such as in the thermal mixing problem just discussed. Consider two ideal gases at equal temperatures and pressures separated by a partition that is then removed as shown below.

For an ideal gas the Gibbs equation is

$$ds = C_p \frac{dT}{T} - R \frac{dP}{P}. \quad (2.67)$$

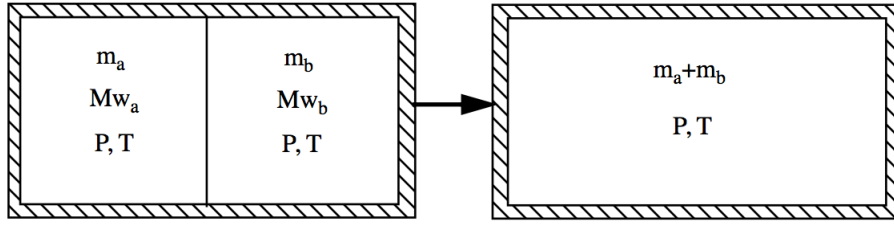


Figure 2.10: *Mixing of two ideal gases at constant pressure and temperature.*

The entropy per unit mass is determined by integrating the Gibbs equation.

$$s = \int C_p \frac{dT}{T} - R \ln(P) + \alpha \quad (2.68)$$

where \$\alpha\$ is a constant of integration. A fundamental question revolves around the evaluation of the entropy constant \$\alpha\$ for a given substance. This is addressed by the third law of thermodynamics discussed later. For the two gases shown in the figure

$$\begin{aligned} s_a &= \int C_{P_a} \frac{dT}{T} - \frac{R_u}{M_{wa}} \ln(P) + \alpha_a \\ s_b &= \int C_{P_b} \frac{dT}{T} - \frac{R_u}{M_{wb}} \ln(P) + \alpha_b. \end{aligned} \quad (2.69)$$

where \$M_{wa,b}\$ refers to the molecular weights of the two distinctly different gases. The entropy of the whole system is

$$S = m_a s_a + m_b s_b. \quad (2.70)$$

Define the mass fractions

$$\chi_a = \frac{m_a}{m_a + m_b}, \quad \chi_b = \frac{m_b}{m_a + m_b}. \quad (2.71)$$

The overall entropy per unit mass before mixing is

$$s_{before} = \frac{S_{before}}{m_a + m_b} = \chi_a s_a + \chi_b s_b. \quad (2.72)$$

Substitute (2.69).

$$s_{before} = \chi_a \left(\int C_{P_a} \frac{dT}{T} - \frac{R_u}{M_{wa}} \ln(P) + \alpha_a \right) + \chi_b \left(\int C_{P_b} \frac{dT}{T} - \frac{R_u}{M_{wb}} \ln(P) + \alpha_b \right) \quad (2.73)$$

After mixing each gas fills the whole volume V with the partial pressures given by

$$P_a = \frac{m_a}{V} \frac{R_u}{M_{wa}} T P_b = \frac{m_b}{V} \frac{R_u}{M_{wb}} T. \quad (2.74)$$

where

$$P = P_a + P_b. \quad (2.75)$$

The entropy of the mixed system is

$$s_{after} = \chi_a \left(\int C_{P_a} \frac{dT}{T} - \frac{R_u}{M_{wa}} \ln(P_a) + \alpha_a \right) + \chi_b \left(\int C_{P_b} \frac{dT}{T} - \frac{R_u}{M_{wb}} \ln(P_b) + \alpha_b \right). \quad (2.76)$$

Therefore the entropy change of the system is

$$s_{after} - s_{before} = \chi_a \frac{R_u}{M_{wa}} \ln\left(\frac{P}{P_a}\right) + \chi_b \frac{R_u}{M_{wb}} \ln\left(\frac{P}{P_a}\right) > 0. \quad (2.77)$$

The initially separated volumes were each in a state of local thermodynamic equilibrium. When the partition is removed the gases mix and until the mixing is complete the system is out of equilibrium. As expected the entropy increases. The nice feature of this example is that at every instant of the non-equilibrium process the pressure and temperature of the system are well defined. By the way it should be noted that as long as the gases in Figure 2.10 are dilute and the enthalpy and internal energy depend only on temperature then the mixing process depicted in Figure 2.10 occurs adiabatically without any change in enthalpy or internal energy. If the gases are very dense so that intermolecular forces contribute to the internal energy then the enthalpy and internal energy depend on the pressure and the mixing process may release heat. In this case heat must be removed through the wall to keep the gas at constant temperature. This is called the heat of mixing. Throughout this course we will only deal with dilute gases for which the heat of mixing is negligible.

2.8.3 Gibbs paradox

If the gases in Figure 2.10 are identical, then there is no diffusion and no entropy change occurs when the partition is removed. But the full amount of entropy change is produced as long as the gases are different in any way no matter how slight. If we imagine a limiting process where the gas properties are made to approach each other continuously the same finite amount of entropy is produced at each stage until the limit of identical gases when it suddenly vanishes. This unexpected result is called Gibbs paradox after J.W. Gibbs who first noticed it.

However the atomistic nature of matter precludes the sort of continuous limiting process envisioned. As long as the two gases are different by any sort of experimentally measurable property whatsoever, the full entropy change (2.77) is produced. This is true even if the two gases are chemically similar isotopes of the same element. For example, the inter-diffusion of ortho and para forms of hydrogen which differ only by the relative orientation of their nuclear and electronic spins would produce the same entropy increase. The entropy disappears only if the two molecules are identical.

A full understanding of this statement requires a combination of statistical thermodynamics and quantum mechanics. The founder of statistical mechanics is generally regarded to be Ludwig Boltzmann (1844-1906) an Austrian physicist who in 1877 established the relationship between entropy and the statistical model of molecular motion. Boltzmann is buried in the Central Cemetery in Vienna and on his grave marker is inscribed the equation

$$S = k \ln (W) \quad (2.78)$$

that is his most famous discovery.

Boltzmann showed that the entropy is equal to a fundamental constant k times the logarithm of W which is equal to the number of possible states of the thermodynamic system with energy, E . A state of the system is a particular set of values for the coordinates and velocities of each and every molecule in the system. Boltzmann's constant is essentially the universal gas constant per molecule

$$k = R_u/N \quad (2.79)$$

where N is Avagadro's number. For a monatomic ideal gas, statistical mechanics gives

$$W \approx V^{N_p} E^{\frac{3N_p}{2}} \quad (2.80)$$

where V is the volume and N_p is the number of atoms in the system. When (2.80) is substituted into (2.78) the result is

$$S \approx R_u \ln \left(V (C_v T)^{3/2} \right) \quad (2.81)$$

which is essentially the same expression that would be generated from Gibbs equation. See Appendix A for more detail.

When a volume of gas molecules is analyzed using quantum mechanics the energy of the system is recognized to be quantized and the statistical count of the number of possible states of the system is quite different depending on whether the individual molecules are the same or not. If the molecules are different the number of possible states for a given energy is much larger and this is the basis for the explanation of the Gibbs paradox.

2.9 Isentropic expansion

2.9.1 Blowdown of a pressure vessel

Shown in Figure 2.11 is the blowdown through a small hole of a calorically perfect gas from a large adiabatic pressure vessel at initial pressure P_i and temperature T_i to the surroundings at pressure P_a and temperature T_a . Determine the final temperature of the gas in the sphere.

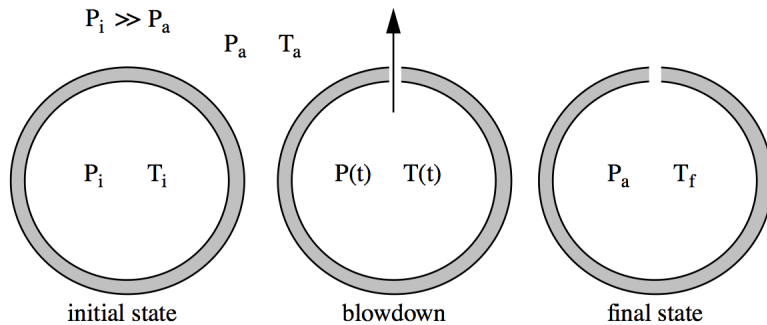


Figure 2.11: A spherical, thermally insulated pressure vessel exhausts to the surroundings through a small hole.

To determine the temperature imagine a parcel of gas that remains inside the sphere during the expansion process as shown in Figure 2.12. As long as the gas is not near the wall

where viscosity might play a role, the expansion of the gas parcel is nearly isentropic. The final temperature is

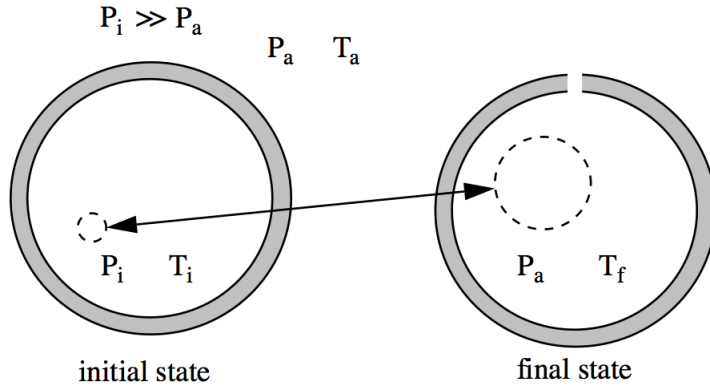


Figure 2.12: *Expansion of a parcel of gas as the pressure vessel exhausts to the surroundings.*

$$\frac{T_f}{T_i} = \left(\frac{P_a}{P_i} \right)^{\frac{\gamma-1}{\gamma}} \quad (2.82)$$

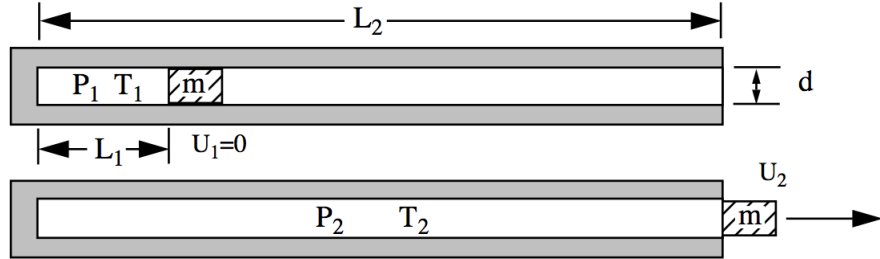
Determine the entropy change per unit mass during the process for the gas ejected to the surroundings. The ejected gas mixes with the infinite surroundings and comes to a final temperature and pressure, T_a and P_a . The entropy change is

$$\frac{s_f - s_i}{C_p} = \ln \left(\frac{T_a}{T_i} \right) - \left(\frac{\gamma - 1}{\gamma} \right) \ln \left(\frac{P_a}{P_i} \right) \quad (2.83)$$

Since the second term in (2.83) is clearly positive, the entropy change for the parcel is likely to be positive unless the ambient temperature is much lower than the initial temperature in the vessel.

2.9.2 Work done by an expanding gas

The gun tunnel is a system for studying the flow over a projectile at high speed in rarefied conditions typical of very high altitude flight. High pressure gas is used to accelerate the projectile down a gun barrel. The projectile exits into a large chamber at near vacuum pressure. The figure below depicts the situation.

Figure 2.13: *Projectile energized by an expanding gas.*

We wish to determine the kinetic energy of the projectile when it exits into the vacuum chamber. The work done by the gas on the projectile is equal to the kinetic energy of the projectile

$$W = \int_{L_1}^{L_2} P dV = \frac{1}{2} m U_2^2 \quad (2.84)$$

where the friction between the projectile and the gun barrel has been neglected as well as any work done against the small pressure in the vacuum chamber.

In order to solve this problem it is necessary to postulate a relationship between the gas pressure in the gun barrel and the volume. The simplest approach is to assume that the gas expands isentropically. In this case the pressure and density of the gas behind the projectile are related by

$$\frac{P}{P_1} = \left(\frac{\rho}{\rho_1} \right)^\gamma = \left(\frac{\frac{4m_{gas}}{\pi d^2 L}}{\frac{4m_{gas}}{\pi d^2 L_1}} \right) = \left(\frac{L_1}{L} \right)^\gamma \quad (2.85)$$

where \$m_{gas}\$ is the mass of the gas expanding behind the projectile. The work integral (2.84) becomes

$$\frac{1}{2} m U_2^2 = \left(\frac{\pi d^2}{4} \right) \int_{L_1}^{L_2} P_1 \left(\frac{L_1}{L} \right)^\gamma dL. \quad (2.86)$$

Carry out the integration

$$\frac{1}{2} m U_2^2 = \left(\frac{\pi d^2}{4} \right) \frac{P_1 L_1^\gamma}{1 - \gamma} (L_2^{1-\gamma} - L_1^{1-\gamma}) \quad (2.87)$$

or

$$\frac{1}{2}mU_2^2 = \left(\frac{\pi d^2 L_1}{4}\right) \frac{P_1}{\gamma - 1} \left(1 - \left(\frac{L_1}{L_2}\right)^{\gamma-1}\right). \quad (2.88)$$

The first term in brackets on the right side of (2.88) is the initial volume of gas

$$V_1 = \frac{\pi d^2 L_1}{4}. \quad (2.89)$$

Using (2.89) Equation (2.88) takes the form

$$\frac{1}{2}mU_2^2 = \frac{P_1 V_1}{\gamma - 1} \left(1 - \left(\frac{L_1}{L_2}\right)^{\gamma-1}\right). \quad (2.90)$$

Replace $P_1 V_1$ with $m_{gas}RT_1$ and recall that $R = C_p - C_v$ and $\gamma = C_p/C_v$. The kinetic energy of the projectile when it leaves the barrel is

$$\frac{1}{2}mU_2^2 = m_{gas}C_vT_1 \left(1 - \left(\frac{L_1}{L_2}\right)^{\gamma-1}\right). \quad (2.91)$$

Note that in the limit where the barrel of the gun is extremely long so that $L_1/L_2 \ll 1$ all of the gas thermal energy is converted to kinetic energy of the projectile.

2.9.3 Example - Helium gas gun

Suppose the tunnel is designed to use Helium as the working gas. The gas is introduced into the gun barrel and an electric arc discharge is used to heat the Helium to very high pressure and temperature. Let the initial gas pressure and temperature be $P_1 = 4 \times 10^8 N/m^2$ and $T_1 = 2000 K$. The initial length is $L_1 = 0.1 m$, the final length is $L_2 = 2.0 m$ and the barrel diameter is $d = 0.04 m$. The projectile mass is $0.1 kg$. Determine the exit velocity of the projectile. Compare the exit velocity with the speed of sound in the gas at the beginning and end of the expansion.

Solution: Helium is a monatomic gas with an atomic mass of 4.0026. The mass of Helium used to drive the projectile is determined from the ideal gas law

$$P_1 V_1 = m_{gas} \left(\frac{R_u T_1}{M_w}\right) \quad (2.92)$$

or

$$m_{gas} = \frac{P_1 V_1}{T_1} \left(\frac{M_w}{R_u} \right) = \frac{4 \times 10^8}{2000} \left(\frac{\pi (0.04)^2 (0.1)}{4} \right) \left(\frac{4.0026}{8314.472} \right) = 0.01208 \text{ kg.} \quad (2.93)$$

The velocity of the projectile at the exit of the barrel is

$$U_2 = \left(2 \left(\frac{0.01208}{0.1} \right) \left(\frac{3}{2} \right) \left(\frac{8314.472}{4.0026} \right) 2000 \left(1 - \left(\frac{0.1}{2} \right)^{2/3} \right) \right)^{1/2} = 1140.7 \text{ m/sec} \quad (2.94)$$

where the relation $C_v = (3/2)R$ has been used. Note that the final projectile speed is fairly small compared to the initial speed of sound in the gas

$$a_1 = \sqrt{\gamma R T_1} = 2631 \text{ m/sec.} \quad (2.95)$$

The temperature of the gas at the end of the expansion is determined using the isentropic relations (2.56).

$$T_2 = T_1 \left(\frac{L_1}{L_2} \right)^{\gamma-1} = 2000 \left(\frac{0.1}{2} \right)^{2/3} = 271 \text{ K} \quad (2.96)$$

The corresponding speed of sound is

$$a_2 = \sqrt{\gamma R T_2} = 968 \text{ m/sec.} \quad (2.97)$$

The main assumption used to solve this problem is embodied in the use of (2.85) to determine the pressure behind the projectile. This equation effectively neglects the motion of the gas and assumes that the pressure, temperature and density are uniform over the volume behind the projectile during the expansion. This is an excellent assumption if the expansion is slow but not so good if the expansion is fast. But fast compared to what? This is where the speed of sound calculation comes in. If the projectile speed is small compared to the sound speed, a , then the gas speed over the length of the barrel must also be small compared to a . In that limit the pressure variation is also small and the uniform property assumption works quite well. But notice that by the end of the expansion the speed of the projectile exceeds the speed of sound. A more accurate treatment of this problem requires a full analysis of the unsteady gas-dynamics of the flow.

2.9.4 Entropy increase due to viscous friction

In the gas gun example viscous friction is an important generator of entropy. The gas behind the projectile, away from the barrel wall is moving at very high speed but the gas near the wall is subject to the no slip condition. In the small gap between the projectile and the barrel the flow is similar to Couette flow considered in Chapter 8. Everywhere near the wall the flow is subject to very high shear rates leading to high viscous stresses.

So far we have seen how gradients in temperature and gas concentration lead to an increase in the entropy. In Chapter 7 we will show that flow kinetic energy dissipation due to viscous friction always leads to an increase in the entropy per unit mass. An accurate calculation of viscous effects in the gun tunnel problem requires a numerical analysis of the full viscous equations of motion and remains today a difficult research problem.

One of the most difficult challenges in the development of new power and propulsion systems is the accurate prediction of entropy changes in the system. Literally billions of dollars are spent by manufacturers in the pursuit of small reductions in the entropy generated in compressors and turbines and small excesses can spell the difference between success and failure of a new design.

2.10 Some results from statistical mechanics

A discussion of this topic can be found in Appendix A. Here we shall state the main results that will be used in our investigations of compressible flow. Classical statistical mechanics leads to a simple expression for C_p and C_v in terms of β , the number of degrees of freedom of the appropriate molecular model.

$$C_p = \left(\frac{\beta + 2}{2} \right) R \quad C_v = \frac{\beta}{2} R \quad \gamma = \frac{\beta + 2}{\beta} \quad (2.98)$$

For a mass point, m , with three translational degrees of freedom and no internal structure, $\beta = 3$. The law of equipartition of energy says that any term in the expression for the energy of the mass point that is quadratic in either the position or velocity contributes $(1/2) kT$ to the thermal energy of a large collection of such mass points. Thus the thermal energy (internal energy) per molecule of a gas composed of a large collection of mass points is

$$\tilde{e} = (3/2) kT \quad (2.99)$$

where k is Boltzmann's constant,

$$k = 1.3806505 \times 10^{-23} \text{ Joules/K.} \quad (2.100)$$

Over one mole of gas,

$$N\tilde{e} = (3/2) R_u T \quad (2.101)$$

where $R_u = Nk$ is the universal gas constant and N is Avogadro's number,

$$N = 6.0221415 \times 10^{26} \text{ molecules/kgmole.} \quad (2.102)$$

On a per unit mass of gas basis the internal energy is,

$$e = (3/2) RT. \quad (2.103)$$

This is a good model of monatomic gases such as Helium, Neon, Argon, etc. Over a very wide range of temperatures,

$$C_p = \frac{5}{2}R \quad C_v = \frac{3}{2}R \quad (2.104)$$

from near condensation to ionization.

2.10.1 Diatomic gases

At room temperature, diatomic molecules exhibit two additional rotational degrees of freedom and

$$C_p = \frac{7}{2}R \quad C_v = \frac{5}{2}R. \quad (2.105)$$

At very low temperatures, C_p can decrease below $(7/2)R$ because rotational degrees of freedom can freeze out; A phenomenon that can only be understood using quantum statistical mechanics. However, for N_2 and O_2 the theoretical transition temperature is in the neighborhood of 3 degrees Kelvin, well below the temperature at which both gases liquefy. For H_2 the transition temperature is about 90 K.

At high temperatures, C_p can increase above $(7/2)R$ because the atoms are not rigidly bound but can vibrate. This brings into play two additional vibrational degrees of freedom. At high temperatures the heat capacities approach

$$C_p = \frac{9}{2}R \quad C_v = \frac{7}{2}R. \quad (2.106)$$

2.10.2 Characteristic vibrational temperature

The determination of the temperature at which the specific heat changes from $(7/2)R$ to $(9/2)R$ is also beyond classical statistical mechanics but can be determined using quantum statistical mechanics. The specific heat of a diatomic gas from room temperature up to high combustion temperatures is accurately predicted from theory to be

$$\frac{C_p}{R} = \frac{7}{2} + \left\{ \frac{\frac{\theta_v}{2T}}{\sinh(\frac{\theta_v}{2T})} \right\}^2. \quad (2.107)$$

The characteristic vibrational temperatures for common diatomic gases are

$$\theta_v|_{O_2} = 2238 K \quad \theta_v|_{N_2} = 3354 K \quad \theta_v|_{H_2} = 6297 K. \quad (2.108)$$

The increasing values of θ_v with decreasing molecular weight reflect the increasing bond strength as the interatomic distance decreases.

2.11 Enthalpy - diatomic gases

The enthalpy of a diatomic gas is

$$h(T) - h(T_{ref}) = \int_{T_{ref}}^T C_p dT = R \int_{T_{ref}}^T \left(\frac{7}{2} + \left\{ \frac{\frac{\theta_v}{2T}}{\sinh(\frac{\theta_v}{2T})} \right\}^2 \right) dT. \quad (2.109)$$

This integrates to

$$\frac{h(T) - h(T_{ref})}{R\theta_v} = \frac{7}{2} \left(\frac{T - T_{ref}}{\theta_v} \right) + \frac{1}{e^{(\theta_v/T)} - 1} - \frac{1}{e^{(\theta_v/T_{ref})} - 1}. \quad (2.110)$$

The enthalpy is plotted below for $T_{ref} = 0$.

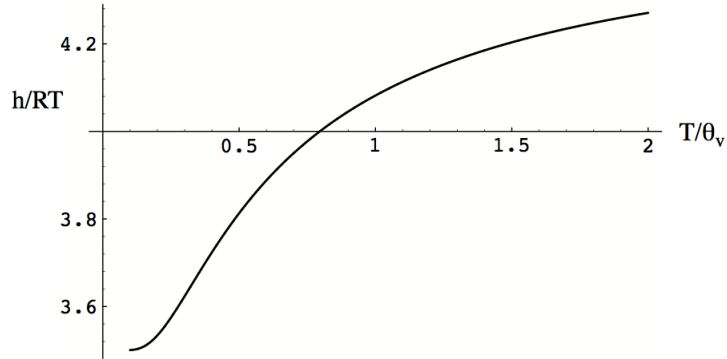


Figure 2.14: Enthalpy versus temperature for a diatomic gas.

2.12 Speed of sound

The speed of sound in a homogeneous medium is,

$$a^2 = \left(\frac{\partial P}{\partial \rho} \right)_{s=constant}. \quad (2.111)$$

For an ideal gas,

$$a^2 = \frac{\gamma P}{\rho} = \gamma R T. \quad (2.112)$$

For a flow at velocity U the Mach number is

$$M = \frac{U}{\sqrt{\gamma R T}}. \quad (2.113)$$

2.13 Atmospheric models

In a stable atmosphere where the fluid velocity is zero, the pressure force on a fluid element is balanced by the force of gravity

$$\nabla P = -\rho \nabla \Psi \quad (2.114)$$

where Ψ is the gravitational potential. Near the Earth's surface the variation of gravitational acceleration with height is relatively small and so we can write

$$\frac{dP}{dz} = -\rho g \quad (2.115)$$

where $g = 9.80665 \text{ m/sec}^2$ and z is the height above the ground.

In an atmosphere where the entropy is constant the pressure and density at a given height are related by

$$\frac{P}{P_0} = \left(\frac{\rho}{\rho_0} \right)^\gamma \quad (2.116)$$

where P_0 and ρ_0 are the pressure and density at ground level. Use (2.116) to replace the pressure in (2.115). The resulting equation can be integrated from the ground to a height z and the result is

$$\frac{\rho}{\rho_0} = \left(1 - (\gamma - 1) \frac{gz}{a_0^2} \right)^{\frac{1}{\gamma-1}}. \quad (2.117)$$

In this model the atmospheric density decreases algebraically with height and goes to zero (vacuum) when $gz/a_0^2 = 1/(\gamma - 1)$.

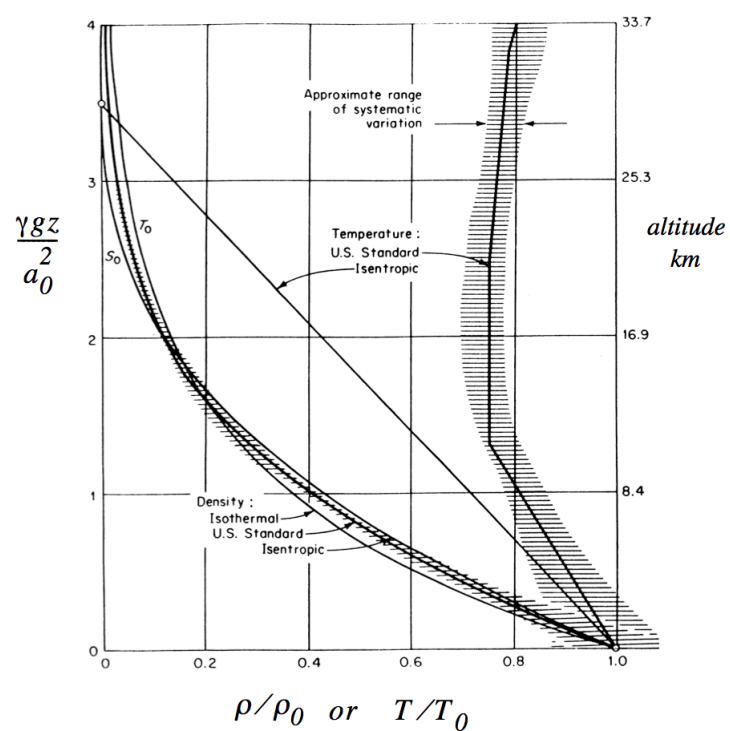
An alternative model that is more accurate in the upper atmosphere is to assume that the atmosphere is isothermal. In this case the pressure and density are related by the ideal gas law $P = \rho RT$ where the temperature is constant at the ground value $T = T_0$. In this case (2.115) integrates to

$$\frac{\rho}{\rho_0} = e^{-\left(\frac{\gamma g z}{a_0^2}\right)} \quad (2.118)$$

The length scale

$$H = \frac{a_0^2}{\gamma g} = \frac{RT_0}{g} \quad (2.119)$$

is called the scale height of the atmosphere. Roughly speaking it is the height where the gravitational potential energy of a fluid element is comparable to its thermal energy. For Air at 288.15 K the scale height is 8435 m .

Figure 2.15: *Density and temperature of the standard atmosphere.*

How accurate are these models? A comparison is shown in Figure 2.15. Note that the two models tend to bracket the actual behavior of the atmosphere. Below a scale height of one, the atmosphere is approximately isentropic and the temperature falls off almost linearly. Above a scale height of about 1.5 the temperature is almost constant.

2.14 The third law of thermodynamics

The first law is a statement of conservation of energy and shows that heat and work can be exchanged with one another. The second law restricts the possible occurrence of certain processes and can be utilized to predict the direction of a process. Moreover, the second law shows that no engine can be built that converts all the input heat energy to an equal amount of useful work. The first and second laws are well supported by a long history of agreement with experimental measurements in a vast variety of applications. The third law of thermodynamics is still a source of leading edge research in the thermodynamics of materials. It was first formulated by the German physicist Walther Hermann Nernst in 1906 whose work won him the Nobel prize for Chemistry in 1920. One statement of the Nernst theorem is that the entropy of a system at zero absolute temperature is a well-defined constant. Another statement is that the entropy of a pure perfect crystalline solid at absolute zero is zero.

The standard entropy of a gas at the standard pressure (10^5 N/m^2) is determined by integrating the Gibbs equation,

$$s^\circ(T) = \int_0^{T_{fusion}} C_P^\circ \frac{dT}{T} + \frac{\Delta H_{fusion}}{T_{fusion}} + \int_{T_{fusion}}^{T_{vaporization}} C_P^\circ \frac{dT}{T} + \frac{\Delta H_{vaporization}}{T_{vaporization}} + \int_{T_{vaporization}}^T C_P^\circ \frac{dT}{T}. \quad (2.120)$$

The heats of fusion and vaporization in (2.120) are at standard pressure. The third law of thermodynamics requires that the heat capacity $C_p \rightarrow 0$ as $T \rightarrow 0$ at a rate that is fast enough to insure convergence of the first integral in (2.120). Calorimetric measurements show that $C_p \approx T^3$ for nonmetals at very low temperatures. For metals C_p is proportional to T^3 at low temperatures but becomes proportional to T at extremely low temperatures. At very low temperature the atomic motion in a metallic crystal freezes out and the residual heat capacity comes from the motion of the conduction electrons in the metal.

Experimentally it does appear that the entropy at absolute zero approaches the same constant value for all pure substances. The third law codifies this result and sets $S(0) = 0$ for all pure elements and compounds in their most stable, perfect crystalline state at

absolute zero. So for example the entropy of water vapor at $125\text{ }^{\circ}\text{C}$ and one atmosphere would be calculated from heat capacity data as follows.

$$s^{\circ}(398.15) = \int_0^{273.15} C_P^{\circ} \frac{dT}{T} + \frac{\Delta H_{fusion}}{273.15} + \\ \int_{273.15}^{373.15} C_P^{\circ} \frac{dT}{T} + \frac{\Delta H_{vaporization}}{373.15} + \int_{373.15}^{398.15} C_P^{\circ} \frac{dT}{T} \quad (2.121)$$

This calculation assumes that the ice crystal is perfect. From a quantum mechanical viewpoint a perfect crystal at zero temperature would exist in only one (nonzero) energy state. The Boltzmann relation (2.78) would reduce to $S(0) = k \ln(1) = 0$ which is consistent with the Nernst theorem.

In a pure, perfect crystal there is no entropy of mixing but in a mixed crystal containing atomic or molecular species A and B there are different ways A and B can be arranged and so the entropy at absolute zero is not zero.

The entropy at absolute zero is called the residual entropy. There can be a significant residual entropy in a variety of common substances where imperfections can occur due to variations in the molecular orientation. Glasses (that are amorphous materials) and alloys (that are mixtures of metals) also have residual entropy. The determination of the residual entropy can be quite complex and is responsible for deviations between calculated and experimental values of the entropy.

Even in the case of a pure solid if the crystal is not perfect the entropy is nonzero. For example, the CO molecule has a small dipole moment and so there is a finite probability that, as it freezes, the molecules can align in the crystal as $\text{CO} - \text{OC} - \text{CO}$ instead of $\text{CO} - \text{CO} - \text{CO}$. A given crystal will contain a mixture of both types of alignment and so it is not perfect and the entropy at 0 K is not zero.

All these matters are the subject of ongoing research. In virtually all applications of thermodynamics to compressible flow the interesting result is based on changes in entropy associated with some process such as the mixing problem described earlier. Such changes are unaffected by possible errors in the entropy constant.

2.15 Problems

Problem 1 - Use the Gibbs equation to determine each of the following for an ideal

gas.

$$\begin{aligned} \left. \frac{\partial s(T, \rho)}{\partial T} \right|_{\rho=constant} & \quad \left. \frac{\partial s(T, \rho)}{\partial \rho} \right|_{T=constant} \\ \left. \frac{\partial s(T, P)}{\partial T} \right|_{P=constant} & \quad \left. \frac{\partial s(T, P)}{\partial P} \right|_{T=constant} \end{aligned} \quad (2.122)$$

Problem 2 - In Section 2 it was stated that the internal energy and enthalpy of an ideal gas depend only on temperature. Show that this is true. First show that for an ideal gas the Gibbs equation can be written in the form

$$ds(T, P) = \frac{1}{T}de(T, P) + \frac{R}{T}dT - \frac{v}{T}dP. \quad (2.123)$$

Work out the partial derivatives of the entropy, and show by the cross-derivative test that $\partial e(T, P) / \partial P = 0$.

Problem 3 - Use the Gibbs equation to show that for a general substance.

$$\left(\frac{\partial h}{\partial P} \right)_T = -T \frac{\partial v(T, P)}{\partial T} + v(T, P) \quad (2.124)$$

where $v(T, P)$ is the volume per unit mass.

Problem 4 - The temperature, entropy and pressure in a calorically perfect ideal gas moving in an unsteady, three-dimensional flow are related by the function

$$\exp \left(\frac{s - s_{ref}}{C_p} \right) = \left(\frac{T}{T_{ref}} \right) \left(\frac{P}{P_{ref}} \right)^{-\left(\frac{\gamma-1}{\gamma}\right)}. \quad (2.125)$$

Take the gradient of (2.125) and show directly that the flow satisfies

$$T \nabla s = \nabla h - \frac{\nabla P}{\rho}. \quad (2.126)$$

Problem 5 - Show that the internal energy of a van der Waals gas is of the form $e(T, v) = f(T) - a/v$.

Problem 6 - A heavy piston is dropped from the top of a long, insulated, vertical shaft containing air. The shaft above the piston is open to the atmosphere. Determine the

equilibrium height of the piston when it comes to rest. Feel free to introduce whatever data or assumptions you feel are required to solve the problem. Suppose you actually carried out this experiment. How do you think the measured height of the piston would compare with your model?

Problem 7 - In problem 6 what would be the equilibrium height if the gas in the shaft is helium.

Problem 8 - Consider the nearly isentropic flow of an ideal gas across a low pressure fan such as an aircraft propeller. Assume that the pressure change ΔP is small. Show that the corresponding density change is

$$\frac{\Delta\rho}{\rho_0} \approx \frac{1}{\gamma} \frac{\Delta P}{P_0} \quad (2.127)$$

where ρ_0 and P_0 are the undisturbed values ahead of the fan.

Problem 9 - Mars has an atmosphere that is about 96% Carbon Dioxide at a temperature of about 200 K . Determine the scale height of the atmosphere and compare it with Earth. The pressure at the surface of Mars is only about 1000 *Pascals*. Entry, descent and landing of spacecraft on Mars is considered to be in some ways more difficult than on Earth. Why do you think this is?

Problem 10 - Suppose you are driving and a child in the back seat is holding a helium filled balloon. You brake for a stoplight. In surprise, the child releases the balloon. The x-momentum equation governing the motion of the air in the car can be simplified to

$$\rho \frac{\partial U}{\partial t} = - \frac{\partial P}{\partial x}. \quad (2.128)$$

Use this result to show in which direction the balloon moves. What assumptions are needed to reduce the momentum equation to (2.128)? Compare this problem to the material developed in Section 2.13

Chapter 3

Control volumes, vector calculus

3.1 Control volume definition

The idea of the control volume is an extremely general concept used widely in fluid mechanics. In Chapter 1 we derived the equations for conservation of mass and momentum on a small cubic control volume fixed in space. In this chapter we will provide a general definition of the control volume and review some of the powerful mathematical tools of vector calculus used in conjunction with control volumes. This will enable us to re-derive in Chapter 5 the equations of motion on a general, arbitrarily moving, control volume suitable for a wide variety of applications.

The control volume $V(t)$ is a closed, simply connected region in space which may be finite or infinitesimal in size. The size and geometry of the volume is selected to provide a convenient imaginary vessel for systematically accounting for the fluxes of various flow quantities related to the conservation of mass, momentum and energy. Part or all of the surface of the control volume may be moving and the motion can be arbitrary as long as the control volume is not torn apart.

The surface $A(t)$ is the instantaneous surface of the control volume and dA is an infinitesimal surface element. The vector $n(t)$ is a unit vector normal to the surface pointing outward from the interior of the control volume.

Let $F(x_1, x_2, x_3)$ be any field variable. It could be a scalar or a component of a vector or tensor.

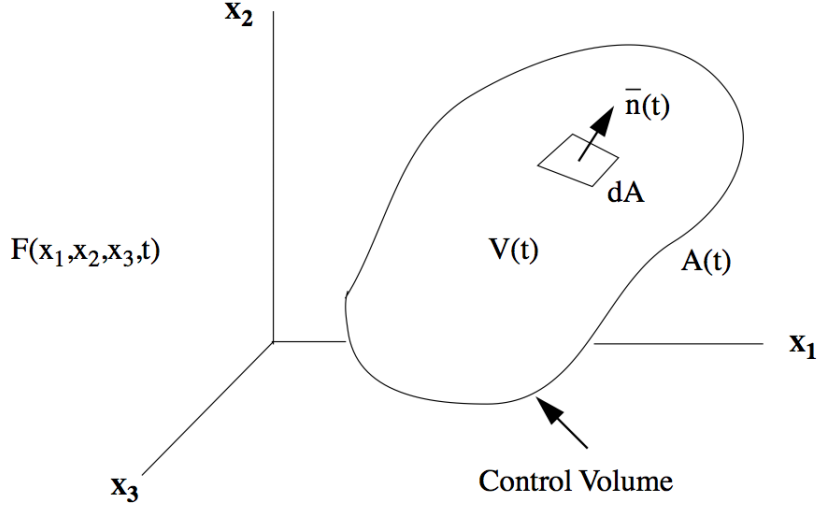


Figure 3.1: Simply connected control volume.

3.2 Vector calculus

The gradient operator is

$$\nabla \equiv \left(\frac{\partial}{\partial x}, \frac{\partial}{\partial y}, \frac{\partial}{\partial z} \right) = \frac{\partial}{\partial x_i} \quad (3.1)$$

where the subscript i on the right refers to the index of the vector component. As noted in Chapter 1 we will use this index notation to denote vectors and tensors throughout the text.

The gradient of a scalar function of space is written

$$\nabla F \equiv \left(\frac{\partial F}{\partial x}, \frac{\partial F}{\partial y}, \frac{\partial F}{\partial z} \right) = \frac{\partial F}{\partial x_i} \quad (3.2)$$

and the gradient of a vector function of space is

$$\nabla \bar{F} = \begin{pmatrix} \frac{\partial F_1}{\partial x_1} & \frac{\partial F_1}{\partial x_2} & \frac{\partial F_1}{\partial x_3} \\ \frac{\partial F_2}{\partial x_1} & \frac{\partial F_2}{\partial x_2} & \frac{\partial F_2}{\partial x_3} \\ \frac{\partial F_3}{\partial x_1} & \frac{\partial F_3}{\partial x_2} & \frac{\partial F_3}{\partial x_3} \end{pmatrix} = \frac{\partial F_i}{\partial x_j}. \quad (3.3)$$

The divergence of a vector is

$$\begin{aligned} \nabla \cdot \bar{F} = \text{trace}(\nabla \bar{F}) &= \sum_{i=1}^3 \sum_{j=1}^3 \delta_{ij} \frac{\partial F_i}{\partial x_j} = \delta_{ij} \frac{\partial F_i}{\partial x_j} = \\ &= \frac{\partial F_1}{\partial x_1} + \frac{\partial F_2}{\partial x_2} + \frac{\partial F_3}{\partial x_3} = \frac{\partial F_i}{\partial x_i} \end{aligned} \quad (3.4)$$

where the Kronecker unit tensor is defined as

$$\delta_{ij} = \begin{pmatrix} 1 & 0 & 0 \\ 0 & 1 & 0 \\ 0 & 0 & 1 \end{pmatrix}. \quad (3.5)$$

Equation (3.4) is the first time we have encountered a vector calculus relation involving two sets of repeated indices and the summation symbols have been included for clarity. For each index i there is a sum over j and the i 's are also summed. From here on we will use the Einstein convention and the summation symbols will be dropped. Note that multiplying by the Kronecker unit tensor and summing over both indices is equivalent to simply equating the two indices and summing as indicated in (3.4).

The dot (or inner) product of a vector and a tensor is

$$\bar{F} \cdot \nabla \bar{F} = F_j \frac{\partial F_i}{\partial x_j} = \begin{pmatrix} \frac{\partial F_1}{\partial x_1} & \frac{\partial F_1}{\partial x_2} & \frac{\partial F_1}{\partial x_3} \\ \frac{\partial F_2}{\partial x_1} & \frac{\partial F_2}{\partial x_2} & \frac{\partial F_2}{\partial x_3} \\ \frac{\partial F_3}{\partial x_1} & \frac{\partial F_3}{\partial x_2} & \frac{\partial F_3}{\partial x_3} \end{pmatrix} \begin{pmatrix} F_1 \\ F_2 \\ F_3 \end{pmatrix} = \begin{pmatrix} F_1 \frac{\partial F_1}{\partial x_1} + F_2 \frac{\partial F_1}{\partial x_2} + F_3 \frac{\partial F_1}{\partial x_3} \\ F_1 \frac{\partial F_2}{\partial x_1} + F_2 \frac{\partial F_2}{\partial x_2} + F_3 \frac{\partial F_2}{\partial x_3} \\ F_1 \frac{\partial F_3}{\partial x_1} + F_2 \frac{\partial F_3}{\partial x_2} + F_3 \frac{\partial F_3}{\partial x_3} \end{pmatrix}. \quad (3.6)$$

The curl of a vector is defined by the skew-symmetric operation

$$\nabla \times \bar{F} = \begin{vmatrix} \bar{e}_1 & \bar{e}_2 & \bar{e}_3 \\ \frac{\partial}{\partial x_1} & \frac{\partial}{\partial x_2} & \frac{\partial}{\partial x_3} \\ F_1 & F_2 & F_3 \end{vmatrix} = \left(\frac{\partial F_3}{\partial x_2} - \frac{\partial F_2}{\partial x_3} \right) \bar{e}_1 + \left(\frac{\partial F_1}{\partial x_3} - \frac{\partial F_3}{\partial x_1} \right) \bar{e}_2 + \left(\frac{\partial F_2}{\partial x_1} - \frac{\partial F_1}{\partial x_2} \right) \bar{e}_3 \quad (3.7)$$

or we can just write

$$\nabla \times \bar{F} = \left(\left(\frac{\partial F_3}{\partial x_2} - \frac{\partial F_2}{\partial x_3} \right), \left(\frac{\partial F_1}{\partial x_3} - \frac{\partial F_3}{\partial x_1} \right), \left(\frac{\partial F_2}{\partial x_1} - \frac{\partial F_1}{\partial x_2} \right) \right). \quad (3.8)$$

The quantities $(\bar{e}_1, \bar{e}_2, \bar{e}_3)$ are unit vectors in the three orthogonal coordinate directions. The curl can also be expressed using index notation

$$(\nabla \times \bar{F})_i = \varepsilon_{ijk} \frac{\partial F_k}{\partial x_j} \quad (3.9)$$

where the alternating unit tensor (also called the Levi-Civita tensor or the permutation tensor) is defined as follows.

$$\varepsilon_{ijk} = \begin{cases} 0, & \text{if any two indices are alike} \\ 1, & \text{ijk an even permutation } \{(1, 2, 3), (2, 3, 1), (3, 1, 2)\} \\ -1, & \text{ijk an odd permutation } \{(1, 3, 2), (3, 2, 1), (2, 1, 3)\} \end{cases} \quad (3.10)$$

The alternating unit tensor satisfies the following identities.

$$\begin{aligned}\delta_{ij}\varepsilon_{ijk} &= 0 \\ \varepsilon_{ipq}\varepsilon_{jpq} &= 2\delta_{ij} \\ \varepsilon_{ijk}\varepsilon_{ijk} &= 6 \\ \varepsilon_{ijk}\varepsilon_{pqr} &= \delta_{ip}\delta_{jq} - \delta_{iq}\delta_{jp}\end{aligned}\tag{3.11}$$

where δ_{ij} is the Kronecker unit tensor defined in (3.5)

3.2.1 Useful vector identities

Some useful vector identities involving first derivatives are as follows.

$$\begin{aligned}\nabla(\psi\phi) &= \psi\nabla\phi + \phi\nabla\psi \\ \nabla \cdot (\phi\bar{U}) &= \phi\nabla \cdot \bar{U} + \bar{U} \cdot \nabla\phi \\ \nabla \times (\phi\bar{U}) &= \phi\nabla \times \bar{U} + \nabla\phi \times \bar{U} \\ \nabla(\bar{U} \cdot \bar{V}) &= (\bar{U} \cdot \nabla)\bar{V} + (\bar{V} \cdot \nabla)\bar{U} + \bar{U} \times (\nabla \times \bar{V}) + \bar{V} \times (\nabla \times \bar{U}) \\ \nabla \cdot (\bar{U} \times \bar{V}) &= \bar{V} \cdot (\nabla \times \bar{U}) - \bar{U} \cdot (\nabla \times \bar{V}) \\ \nabla \times (\bar{U} \times \bar{V}) &= \bar{U}(\nabla \cdot \bar{V}) + (\bar{V} \cdot \nabla)\bar{U} - \bar{V}(\nabla \cdot \bar{U}) - (\bar{U} \cdot \nabla)\bar{V}\end{aligned}\tag{3.12}$$

Note that dot products involving the gradient operator are not always commutative. For example consider the difference between

$$\begin{aligned}\bar{U}(\nabla \cdot \bar{V}) &= U_j \frac{\partial V_i}{\partial x_i} = \\ \left(U_1 \left(\frac{\partial V_1}{\partial x_1} + \frac{\partial V_2}{\partial x_2} + \frac{\partial V_3}{\partial x_3} \right), U_2 \left(\frac{\partial V_1}{\partial x_1} + \frac{\partial V_2}{\partial x_2} + \frac{\partial V_3}{\partial x_3} \right), U_3 \left(\frac{\partial V_1}{\partial x_1} + \frac{\partial V_2}{\partial x_2} + \frac{\partial V_3}{\partial x_3} \right) \right)\end{aligned}\tag{3.13}$$

and

$$\begin{aligned} (\bar{V} \cdot \nabla) \bar{U} &= V_i \frac{\partial U_j}{\partial x_i} = \\ &\left(\left(V_1 \frac{\partial U_1}{\partial x_1} + V_2 \frac{\partial U_1}{\partial x_2} + V_3 \frac{\partial U_1}{\partial x_3} \right), \left(V_1 \frac{\partial U_2}{\partial x_1} + V_2 \frac{\partial U_2}{\partial x_2} + V_3 \frac{\partial U_2}{\partial x_3} \right), \left(V_1 \frac{\partial U_3}{\partial x_1} + V_2 \frac{\partial U_3}{\partial x_2} + V_3 \frac{\partial U_3}{\partial x_3} \right) \right) \end{aligned} \quad (3.14)$$

These two cases illustrate why the parentheses are needed and how useful the index notation can be in avoiding the kind of visual ambiguities that can arise in the use of vector notation.

Here are some more vector identities involving second derivatives

$$\begin{aligned} \nabla \cdot (\nabla F) &= \nabla^2 F \\ \nabla \cdot (\nabla \bar{F}) &= \nabla^2 \bar{F} \\ \nabla \cdot (\nabla \times \bar{F}) &= 0 \\ \nabla \times (\nabla \times \bar{F}) &= \nabla (\nabla \cdot \bar{F}) - \nabla^2 \bar{F} \end{aligned} \quad (3.15)$$

where the Laplacian is

$$\nabla^2 = \frac{\partial^2}{\partial x_1^2} + \frac{\partial^2}{\partial x_2^2} + \frac{\partial^2}{\partial x_3^2} = \frac{\partial^2}{\partial x_i \partial x_i}. \quad (3.16)$$

The Laplacian is a scalar operator. The Laplacian of a scalar is a scalar.

$$\nabla^2 F = \frac{\partial^2 F}{\partial x_i \partial x_i} \quad (3.17)$$

The Laplacian of a vector is a vector.

$$\nabla^2 \bar{F} = \frac{\partial^2 F_j}{\partial x_i \partial x_i} \quad (3.18)$$

Note that the index that is summed is a dummy index and any repeated symbol will do, for example

$$\frac{\partial^2 F_j}{\partial x_k \partial x_k} \quad (3.19)$$

has the same meaning as the right hand side of (3.18).

3.3 The Gauss theorem

Gauss's theorem can be used to convert a volume integral involving the gradient operator to a surface integral involving the outward unit normal. For example

$$\int_V \nabla F dV = \int_A F \bar{n} dA \quad (3.20)$$

where F is a scalar. Here is another example.

$$\int_V (\nabla \cdot \bar{F}) dV = \int_A \bar{F} \cdot \bar{n} dA \quad (3.21)$$

where F is a vector, and another

$$\int_V \frac{\partial F_{ij}}{\partial x_j} dV = \int_A F_{ij} n_j dA \quad (3.22)$$

where F_{ij} is a tensor. A volume integral involving the curl can be converted to a surface integral.

$$\int_V (\nabla \times \bar{F}) dV = \int_A \bar{n} \times \bar{F} dA \quad (3.23)$$

3.4 Stokes' theorem

Stokes' theorem can be used to convert a surface integral involving the curl of a vector to a line integral involving the unit tangent over the boundary of an unclosed control volume.

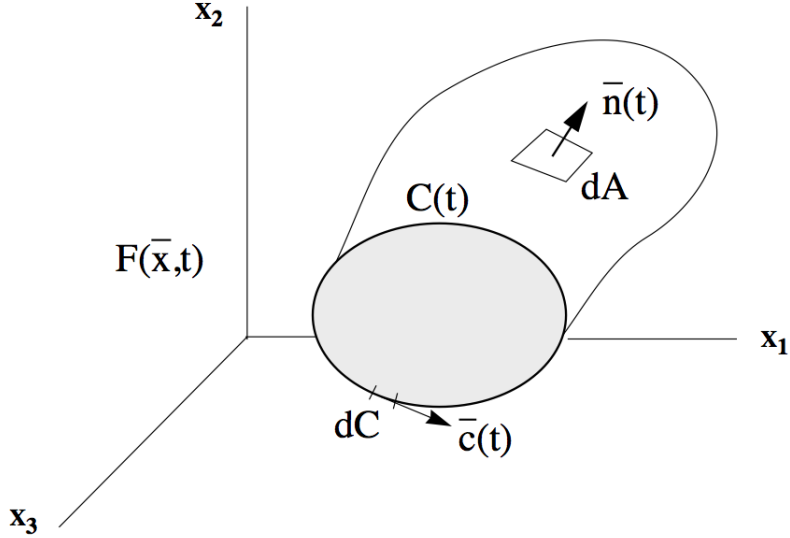


Figure 3.2: *Unclosed control volume used to define Stokes' theorem.*

Although we defined the control volume to be closed there are important instances when an unclosed control volume such as that depicted above (looking kind of like a wind sock!) can be useful.

The differential length dC is an infinitesimal line segment along the bounding curve $C(t)$ with unit tangent $c(t)$. Stokes theorem tells us that

$$\begin{aligned} \int_A (\nabla \times \bar{F}) \cdot \bar{n} dA &= \oint_C \bar{F} \cdot \bar{c} dC \\ \int_A \varepsilon_{ijk} \frac{\partial F_k}{\partial x_j} n_i dA &= \oint_C F_k c_k dC \end{aligned} \quad (3.24)$$

and

$$\int_A (\bar{n} \times \nabla F) dA = \oint_C F \bar{c} dC. \quad (3.25)$$

Gauss's theorem is used repeatedly in the derivation of the equations of motion. Stokes' theorem comes up in the theory of rotational flow particularly in the development of wing theory.

3.5 Problems

Problem 1 - Working in Cartesian coordinates and using index notation, prove each of the following the vector identities.

$$\nabla \cdot (\rho \bar{F}) = \bar{F} \cdot \nabla \rho + \rho \nabla \cdot \bar{F} \quad (3.26)$$

$$\nabla \times (\nabla \times \bar{F}) = \nabla (\nabla \cdot \bar{F}) - \nabla^2 \bar{F} \quad (3.27)$$

$$\bar{F} \cdot \nabla \bar{F} = (\nabla \times \bar{F}) \times \bar{F} + \nabla \left(\frac{\bar{F} \cdot \bar{F}}{2} \right) \quad (3.28)$$

Problem 2 - Let \bar{e}_i , \bar{e}_j and \bar{e}_k be the unit vectors in a right hand orthogonal coordinate system. Show that

$$\varepsilon_{ijk} = \bar{e}_i \cdot (\bar{e}_j \times \bar{e}_k). \quad (3.29)$$

Problem 3 - Demonstrate Stokes' theorem by integration of the curl of some smooth vector field variable over a square boundary.

Problem 4 - Find a unit vector normal to each of the following surfaces.

$$i) x + y + z = 2$$

$$ii) ax^2 + by^2 + cz^2 = 1 \quad (3.30)$$

$$iii) xyz = 1$$

Problem 5 - Show that the unit vector normal to the plane

$$ax + by + cz = d \quad (3.31)$$

has the components

$$\bar{n} = \left(\frac{a}{\sqrt{a^2 + b^2 + c^2}}, \frac{b}{\sqrt{a^2 + b^2 + c^2}}, \frac{c}{\sqrt{a^2 + b^2 + c^2}} \right). \quad (3.32)$$

Why doesn't \bar{n} depend on d ?

Problem 6 - Verify Gauss's theorem

$$\int_V (\nabla \cdot \bar{F}) dV = \int_A \bar{F} \cdot \bar{n} dA \quad (3.33)$$

in each of the following cases,

- i) $\bar{F} = (x, y, z)$ and V is a cube of side b aligned with the x, y, z axes,
- ii) $\bar{F} = \bar{n}_r r^2$ where n_r is a unit vector in the radial direction, V is a sphere of radius b surrounding the origin and $r^2 = x^2 + y^2 + z^2$.

Problem 7 - Verify Stokes' theorem

$$\int_A (\nabla \times \bar{F}) \cdot \bar{n} dV = \oint_C \bar{F} \cdot \bar{c} dC \quad (3.34)$$

where $\bar{F} = (x, y, z)$ and A is the surface of a cube of side b aligned with the x, y, z axes. The open face of the cube has an outward normal aligned with the positive x -axis.

Chapter 4

Kinematics of fluid motion

4.1 Elementary flow patterns

Recall the discussion of flow patterns in Chapter 1. The equations for particle paths in a three-dimensional, steady fluid flow are

$$\frac{dx}{dt} = U(\bar{x}) \quad \frac{dy}{dt} = V(\bar{x}) \quad \frac{dz}{dt} = W(\bar{x}). \quad (4.1)$$

Although the position of a particle depends on time as it moves with the flow, the flow pattern itself does not depend on time and the system (4.1) is said to be autonomous. Autonomous systems of differential equations arise in a vast variety of applications in mechanics, from the motions of the planets to the dynamics of pendulums to velocity vector fields in steady fluid flow. A great deal about the flow can be learned by plotting the velocity vector field $U_i(\bar{x})$. When the flow pattern is plotted one notices that among the most prominent features are stagnation points also known as critical points that occur where

$$U_i(\bar{x}_c) = 0. \quad (4.2)$$

Quite often the qualitative features of the flow can be almost completely described once the critical points of the flow field have been identified and classified.

4.1.1 Linear flows

If the $U_i(\bar{x})$ are analytic functions of \bar{x} ; The velocity field can be expanded in a Taylor

series about the critical point and the result can be used to gain valuable information about the geometry of the flow field. Retaining just the lowest order term in the expansion of $U_i(\bar{x})$ the result is a linear system of equations.

$$\frac{dx_i}{dt} = A_{ik}(x_k - x_{ck}) + O\left((x_k - x_{ck})^2\right) + \dots \quad (4.3)$$

The matrix A_{ik} is the gradient tensor of the velocity field evaluated at the critical point and \bar{x}_c is the position vector of the critical point.

$$A_{ik} = \left(\frac{\partial U_i}{\partial x_k} \right)_{\bar{x}=\bar{x}_c} \quad (4.4)$$

The solution of (4.3) with the higher order terms dropped is expressed in terms of exponential functions. Assume

$$(x_k - x_{ck}) = e_k \text{Exp}[\lambda t] \quad (4.5)$$

and substitute into (4.3).

$$\lambda e_i \text{Exp}[\lambda t] = A_{ik} e_k \text{Exp}[\lambda t]. \quad (4.6)$$

The solution for λ and e_k is determined by the matrix condition

$$(A_{ik} - \lambda \delta_{ik}) e_k = 0. \quad (4.7)$$

The problem is that, at first sight, (4.7) seems underdetermined since it is a set of n equations in $n+1$ unknowns, $(e_1, e_2, \dots, e_n, \lambda)$ where n is the number of dimensions of the problem. Nevertheless let's push on, and solve 4.7 in three dimensions. The system to be solved is

$$(A_{ik} - \lambda \delta_{ik}) e_k = \begin{pmatrix} (A_{11} - \lambda) e_1 + A_{12} e_2 + A_{13} e_3 \\ A_{21} e_1 + (A_{22} - \lambda) e_2 + A_{23} e_3 \\ A_{31} e_1 + A_{32} e_2 + (A_{33} - \lambda) e_3 \end{pmatrix} = \begin{pmatrix} 0 \\ 0 \\ 0 \end{pmatrix}. \quad (4.8)$$

Solve the first equation in (4.8) for e_1 in terms of e_2 and e_3 .

$$e_1 = \frac{-A_{12} e_2 - A_{13} e_3}{A_{11} - \lambda}. \quad (4.9)$$

Using (4.9), solve the second equation in (4.8) for e_2 in terms of e_3 .

$$e_2 = \frac{-A_{23}(A_{11} - \lambda) + A_{21}A_{13}}{(A_{11} - \lambda)(A_{22} - \lambda) - A_{21}A_{12}} e_3. \quad (4.10)$$

Substitute (4.9) and (4.10) into the third equation in (4.8). The result is

$$\begin{pmatrix} (A_{11} - \lambda)(A_{22} - \lambda)(A_{33} - \lambda) - \\ A_{21}A_{12}(A_{33} - \lambda) - A_{31}A_{13}(A_{22} - \lambda) - A_{32}A_{23}(A_{11} - \lambda) + \\ A_{31}A_{12}A_{23} + A_{32}A_{21}A_{13} \end{pmatrix} e_3 = 0 \quad (4.11)$$

The result (4.11) tells us that the matrix condition (4.7) can only be satisfied by specific values of the unknown exponent, λ , called eigenvalues that satisfy the expression in parentheses in (4.11) set to zero. The vector (e_1, e_2, e_3) corresponding to a given eigenvalue is called an eigenvector.

With a little rearrangement it can be shown that the expression in parentheses in (4.11) is just the determinant of $(A_{ik} - \lambda\delta_{ik})$ set to zero.

$$|A_{ik} - \lambda\delta_{ik}| = \begin{vmatrix} A_{11} - \lambda & A_{12} & A_{13} \\ A_{21} & A_{22} - \lambda & A_{23} \\ A_{31} & A_{32} & A_{33} - \lambda \end{vmatrix} = 0. \quad (4.12)$$

Equation (4.12) is a cubic equation for the eigenvalues.

$$\lambda^3 + P\lambda^2 + Q\lambda + R = 0 \quad (4.13)$$

called the characteristic equation. The coefficients of (4.13) are the invariants of A_{ik} , discussed further below.

The result (4.11) also tells us that the unknown eigenvector component, e_3 , is arbitrary. This is related to the scale invariance of the original system (4.3). So without loss of generality, let $e_3 = 1$. Often a different normalization is used such that the length of the eigenvector is one. From (4.9) and (4.10) the other eigenvector components are

$$e_2 = \frac{-A_{23}(A_{11} - \lambda) + A_{21}A_{13}}{(A_{11} - \lambda)(A_{22} - \lambda) - A_{21}A_{12}}. \quad (4.14)$$

$$e_1 = \frac{-A_{13}(A_{22} - \lambda) + A_{12}A_{23}}{(A_{11} - \lambda)(A_{22} - \lambda) - A_{21}A_{12}}. \quad (4.15)$$

Note that the denominator in (4.14) and (4.15) is the determinant of the upper left 2x2 matrix in (4.8) which could be zero in which case a different approach would be used

to determine the eigenvector. Indeed, a variety of special cases can occur and these are detailed in the paper, "*A general classification of three-dimensional flow fields*", by Chong, Perry and Cantwell, *Physics of Fluids A 2 (5) 1990*, included in the resources folder on my website.

Only a relatively small number of solution patterns are possible. These are determined by the invariants of A_{ik} . The invariants arise naturally as traces of various powers of A_{ik} . They are all derived as follows. Transform A_{nm}

$$B_{ik} = M_{in} A_{nm} \bar{M}_{mk} \quad (4.16)$$

where M is a non-singular matrix and \bar{M} is its inverse. Take the trace of (4.16). The dot (or inner) product of a vector and a tensor is

$$B_{ii} = M_{in} A_{nm} \bar{M}_{mi} = \bar{M}_{mi} M_{in} A_{nm} = \delta_{mn} A_{nm} = A_{mm}. \quad (4.17)$$

The trace is invariant under the affine transformation M_{ik} . One can think of the vector field U_i as if it is imbedded in an n -dimensional block of rubber. An affine transformation is one which stretches or distorts the rubber block without ripping it apart or reflecting it through itself. For traces of higher powers the proof of invariance is similar.

$$\begin{aligned} \text{tr}(B^\alpha) &= \\ M_{jn_1} A_{n_1 m_1} \bar{M}_{m_1 j_1} M_{j_1 n_2} A_{n_2 m_2} \bar{M}_{m_2 j_2} \cdots M_{j_{\alpha-1} n_\alpha} A_{n_\alpha m_\alpha} \bar{M}_{m_\alpha j} &= \quad (4.18) \\ &= \text{tr}(A^\alpha) \end{aligned}$$

The traces of all powers of the gradient tensor remain invariant under an affine transformation. Likewise any combination of the traces is invariant.

4.1.2 Linear flows in two dimensions

In two dimensions the eigenvalues of A_{ik} satisfy the quadratic

$$\lambda^2 + P\lambda + Q = 0 \quad (4.19)$$

where P and Q are the invariants

$$\begin{aligned} P &= -A_{ii} \\ Q &= \text{Det}(A_{ik}). \end{aligned} \tag{4.20}$$

The eigenvalues of A_{ik} are

$$\lambda = -\frac{P}{2} \pm \frac{1}{2}\sqrt{P^2 - 4Q} \tag{4.21}$$

and the character of the local flow is determined by the quadratic discriminant

$$D = Q - \frac{P^2}{4}. \tag{4.22}$$

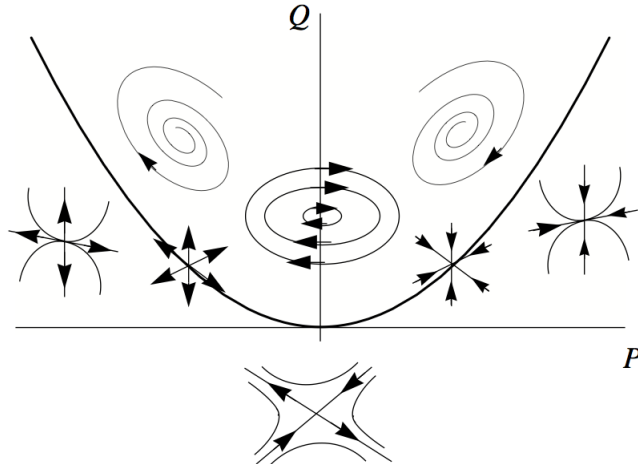


Figure 4.1: *Classification of linear flows in two dimensions*

The various possible flow patterns can be summarized on a cross-plot of the invariants as shown in Figure 4.1. If $D > 0$ the eigenvalues are complex and a spiraling motion can be expected in the neighborhood of the critical point. Depending on the sign of P the spiral may be stable or unstable (spiraling in or spiraling out). If $D < 0$ the eigenvalues are real and a predominantly straining flow can be expected. In this case the directionality of the local flow is defined by the two eigenvectors of A_{ik} . The case $P = 0$ corresponds to incompressible flow for which there are only two possible kinds of critical points, centers with $Q > 0$ and saddles with $Q < 0$. The line $Q = 0$ in Figure 4.1 corresponds to a

degenerate case where (4.19) reduces to $\lambda(\lambda + P) = 0$. In this instance the critical point becomes a line with trajectories converging from either side of the line.

4.1.3 Linear flows in three dimensions

In three dimensions the eigenvalues of A_{ik} satisfy the cubic

$$\lambda^3 + P\lambda^2 + Q\lambda + R = 0 \quad (4.23)$$

where the invariants are

$$\begin{aligned} P &= -\text{tr}[A_{ij}] = -A_{ii} \\ Q &= \frac{1}{2}(P^2 - \text{tr}[A_{ik}A_{kj}]) = \frac{1}{2}(P^2 - A_{ik}A_{ki}) \\ R &= \frac{1}{3}(-P^3 + 3PQ - A_{ik}A_{km}A_{mi}). \end{aligned} \quad (4.24)$$

Any cubic polynomial can be simplified as follows. Let

$$\lambda = \alpha - \frac{P}{3}. \quad (4.25)$$

Then α satisfies

$$\alpha^3 + \hat{Q}\alpha + \hat{R} = 0 \quad (4.26)$$

where

$$\begin{aligned} \hat{Q} &= Q - \frac{1}{3}P^2 \\ \hat{R} &= R - \frac{1}{3}PQ + \frac{2}{27}P^3. \end{aligned} \quad (4.27)$$

Let

$$\begin{aligned} a_1 &= \left(-\frac{\hat{R}}{2} + \frac{1}{3\sqrt{3}} \left(\hat{Q}^3 + \frac{27}{4} \hat{R}^2 \right)^{1/2} \right)^{1/3} \\ a_2 &= \left(-\frac{\hat{R}}{2} - \frac{1}{3\sqrt{3}} \left(\hat{Q}^3 + \frac{27}{4} \hat{R}^2 \right)^{1/2} \right)^{1/3}. \end{aligned} \quad (4.28)$$

The real solution of (4.26) is expressed as

$$\alpha_1 = a_1 + a_2 \quad (4.29)$$

and the complex (or remaining real) solutions are

$$\begin{aligned} \alpha_2 &= -\frac{1}{2} (a_1 + a_2) + \frac{i\sqrt{3}}{2} (a_1 - a_2) \\ \alpha_3 &= -\frac{1}{2} (a_1 + a_2) - \frac{i\sqrt{3}}{2} (a_1 - a_2). \end{aligned} \quad (4.30)$$

When (4.23) is solved for the eigenvalues one is led to the cubic discriminant

$$D = \frac{27}{4} R^2 + \left(P^3 - \frac{9}{2} PQ \right) R + Q^2 \left(Q - \frac{1}{4} P^2 \right). \quad (4.31)$$

The surface $D = 0$, is depicted in Figure 4.2.

To help visualize the surface in Figure 4.2 it is split down the middle on the plane $P = 0$ and the two parts are rotated apart to provide a better view. Note that (4.31) can be regarded as a quadratic in R and so the surface $D = 0$ is really composed of two roots for R that meet in a cusp. If $D > 0$ the point (P, Q, R) lies above the surface and there is one real eigenvalue and two complex conjugate eigenvalues. If $D < 0$ all three eigenvalues are real. The invariants can be expressed in terms of the eigenvalues as follows. If the eigenvalues are real

$$\begin{aligned} P &= -(\lambda_1 + \lambda_2 + \lambda_3) \\ Q &= \lambda_1 \lambda_2 + \lambda_1 \lambda_3 + \lambda_2 \lambda_3 \\ R &= -\lambda_1 \lambda_2 \lambda_3. \end{aligned} \quad (4.32)$$

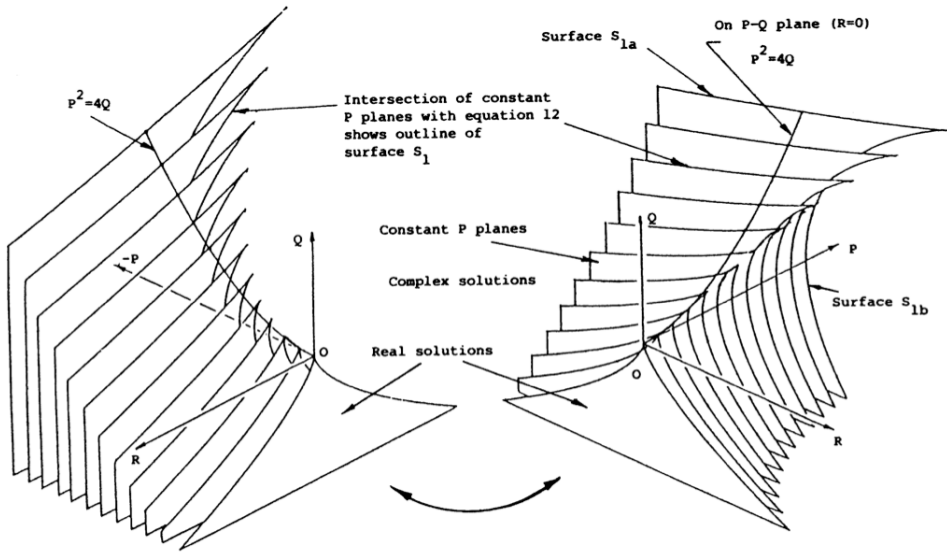


Figure 4.2: *The surface dividing real and complex eigenvalues in three dimensions.*

If the eigenvalues are complex

$$\begin{aligned} P &= -(2\sigma + b) \\ Q &= \sigma^2 + \omega^2 + 2\sigma b \\ R &= -b(\sigma^2 + \omega^2). \end{aligned} \tag{4.33}$$

The variable b is the real eigenvalue and σ and ω are the real and imaginary parts of the complex conjugate eigenvalues.

4.1.4 Incompressible flow

Flow patterns in incompressible flow are characterized by

$$\nabla \cdot \bar{U} = \frac{\partial U_i}{\partial x_i} = A_{ii} = 0. \tag{4.34}$$

This corresponds to $P = 0$. In this case the discriminant is

$$D = Q^3 + \frac{27}{4}R^2 \quad (4.35)$$

and the invariants simplify to

$$\begin{aligned} Q &= -\frac{1}{2}A_{ik}A_{ki} \\ R &= -\frac{1}{3}A_{ik}A_{km}A_{mi}. \end{aligned} \quad (4.36)$$

The various possible elementary flow patterns for this case can be categorized on a plot of Q versus R shown in Figure 4.3

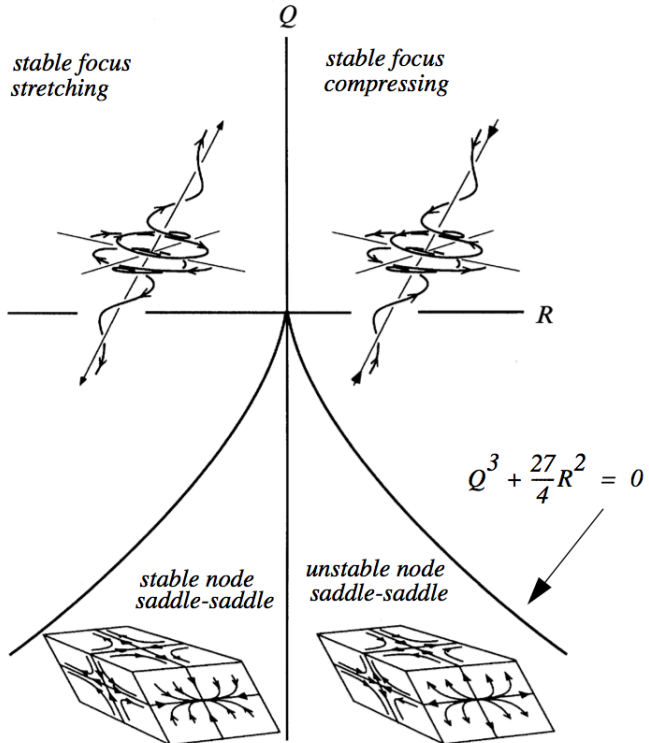


Figure 4.3: Three-dimensional flow patterns in the plane $P = 0$.

Figure 4.1 and Figure 4.3 are cuts through the surface (4.31) at $R = 0$ and $P = 0$ respectively.

4.1.5 Frames of reference

We introduced the transformation of coordinates between a fixed and moving frame in Chapter 1. Here we briefly revisit the subject again in the context of critical points. For a general smooth flow, the particle path equations (4.1) can be expanded as a Taylor series about any point \bar{x}_0 as follows

$$\frac{dx_i}{dt} = U_i|_{\bar{x}=\bar{x}_0} + A_{ik}|_{\bar{x}=\bar{x}_0} (x_k - x_{0k}) + O\left((x_k - x_{0k})^2\right) + \dots \quad (4.37)$$

If a coordinate system is attached to and moves with the particle at \bar{x}_0 with the velocity $U_i|_{\bar{x}=\bar{x}_0}$ so that

$$\begin{aligned} \bar{x}' &= \bar{x} - \bar{x}_0 \\ \bar{U}' &= \bar{U} - \bar{U}|_{\bar{x}=\bar{x}_0} \end{aligned} \quad (4.38)$$

then in that frame of reference the origin of coordinates in effect becomes a critical point (since the velocity is zero there) and the flow pattern that an observer in this coordinate system would see is determined by the second and higher order terms in (4.37).

$$\frac{dx'_i}{dt} = A_{ik}x'_k + O\left(x'_k{}^2\right) + \dots \quad (4.39)$$

The elementary flow patterns described above are what would be seen locally at an instant by an observer moving with a fluid element. Notice that the velocity gradient tensor referred to either frame is the same. In this way the velocity gradient tensor can be used to infer the geometry of the local flow pattern at any point in an unambiguous, frame-invariant manner.

Categorizing flow patterns using the invariants of the velocity gradient tensor has a long history of applications in fluid mechanics particularly in the kinematic description of flow separation and reattachment near a solid surface. More recently these methods have been used to describe light propagation near complex apertures and to describe changes in the electron charge density field in molecules during the making and breaking of chemical bonds.

4.2 Rate-of-strain and rate-of-rotation tensors

The velocity gradient tensor

$$A_{ij} = \partial U_i / \partial x_j \quad (4.40)$$

can be split into a symmetric and antisymmetric part

$$A_{ij} = \frac{\partial U_i}{\partial x_j} = \frac{1}{2} \left(\frac{\partial U_i}{\partial x_j} + \frac{\partial U_j}{\partial x_i} \right) + \frac{1}{2} \left(\frac{\partial U_i}{\partial x_j} - \frac{\partial U_j}{\partial x_i} \right). \quad (4.41)$$

The symmetric part is the rate-of-strain tensor

$$S_{ij} = \frac{1}{2} \left(\frac{\partial U_i}{\partial x_j} + \frac{\partial U_j}{\partial x_i} \right). \quad (4.42)$$

The anti-symmetric part is the rate-of-rotation tensor or spin tensor

$$W_{ij} = \frac{1}{2} \left(\frac{\partial U_i}{\partial x_j} - \frac{\partial U_j}{\partial x_i} \right). \quad (4.43)$$

The vorticity vector $\bar{\Omega} = \nabla \times \bar{U}$ is related to the velocity gradients by

$$\Omega_i = \varepsilon_{ijk} \left(\frac{\partial U_k}{\partial x_j} \right) \quad (4.44)$$

and the spin tensor is related to the vorticity by

$$W_{ik} = \frac{1}{2} \varepsilon_{ijk} \Omega_j. \quad (4.45)$$

All local flow patterns can be regarded as a linear sum of a purely rotational motion and a purely straining motion. The balance between these two components determines which of the local flow fields shown in Figure 4.1 or Figure 4.3 will exist at the point. As we move into our studies of compressible flow we shall see that a natural division exists between flows that are irrotational, where the effects of viscosity can often be neglected, and flows that are strain-rate dominated where viscosity plays an important and sometimes dominant role.

4.3 Problems

Problem 1 - The simplest 2-D flows imaginable are given by the linear system

$$\begin{aligned}\frac{dx}{dt} &= ax + by \\ \frac{dy}{dt} &= cx + dy.\end{aligned}\tag{4.46}$$

Sketch the corresponding flow pattern for the following cases.

- i) $(a, b, c, d) = (1, -1, -1, -1)$
- ii) $(a, b, c, d) = (1, -3, 1, -1)$
- iii) $(a, b, c, d) = (-1, 0, 0, -1)$

Work out the invariants of the velocity gradient tensor as well as the various components of the rate-of-rotation and rate-of-strain tensors and the vorticity vector. Which flows are incompressible?

Problem 2 - An unforced, damped, pendulum is governed by the second order ODE

$$\frac{d^2\theta}{dt^2} + \beta \frac{d\theta}{dt} + \frac{g}{L} \sin(\theta) = 0.\tag{4.47}$$

Let $x = \theta(t)$ and $y = d\theta(t)/dt$. Use these variables to convert the equation to the canonical form.

$$\begin{aligned}\frac{dx}{dt} &= U(x, y) \\ \frac{dy}{dt} &= V(x, y).\end{aligned}\tag{4.48}$$

Sketch the "streamlines" defined by (4.48). Locate and categorize any critical points using the methods developed in this chapter. Identify which points are dominated by rotation and which are dominated by the rate-of-strain. You can do this graphically by drawing line segments of the appropriate slope in (x, y) coordinates. The picture of the flow that results is called the *phase portrait* of the flow in reference to the fact that, for the pendulum, a point in the phase portrait represents the instantaneous relation between the position and velocity of the pendulum. For what value of β can the "flow" defined by the phase portrait be used as a model of an incompressible fluid flow?

Problem 3 - Use (4.25) to reduce (4.23) to (4.26).

Problem 4 - Sketch the flow pattern generated by the 3-D linear system

$$\begin{aligned}\frac{dx}{dt} &= -y \\ \frac{dy}{dt} &= x \\ \frac{dz}{dt} &= z.\end{aligned}\tag{4.49}$$

Work out the invariants of the velocity gradient tensor as well as the components of the rate-of-rotation and rate-of-strain tensors and vorticity vector. The vector field plotted in three dimensions is called the phase space of the system of ODEs. In fluid mechanics the phase portrait or phase space is the physical space of the flow.

Problem 5 - Show that

$$S_{ij}A_{ji} = S_{ij}S_{ji}\tag{4.50}$$

and is therefore greater than or equal to zero.

Problem 6 - Work out the formulas for the components of the vorticity vector and show that the spin tensor is related to the vorticity vector by

$$W_{ik} = \frac{1}{2}\varepsilon_{ijk}\Omega_j.\tag{4.51}$$

Problem 7 - The velocity field given below has been used in the fluid mechanics literature to model a two dimensional separation bubble.

$$\begin{aligned}U(x, y) &= -y + 3y^2 + x^2y - (2/3)y^3 \\ V(x, y) &= -3xy^2.\end{aligned}\tag{4.52}$$

Draw the phase portrait and identify critical points.

Chapter 5

The conservation equations

5.1 Leibniz' rule for differentiation of integrals

5.1.1 Differentiation under the integral sign

According to the fundamental theorem of calculus if f is a smooth function and the integral of f is

$$I(x) = \int_{\text{constant}}^x f(x') dx' \quad (5.1)$$

then the derivative of $I(x)$ is

$$\frac{dI}{dx} = f(x). \quad (5.2)$$

Similarly if

$$I(x) = \int_x^{\text{constant}} f(x') dx' \quad (5.3)$$

then

$$\frac{dI}{dx} = -f(x). \quad (5.4)$$

Suppose the function f depends on two variables and the integral is a definite integral

$$I(t) = \int_a^b f(x', t) dx' \quad (5.5)$$

where a and b are constant. The derivative with respect to t is

$$\frac{dI(t)}{dt} = \int_a^b \frac{\partial}{\partial t} (f(x', t)) dx'. \quad (5.6)$$

The order of the operations of integration and differentiation can be exchanged and so it is permissible to bring the derivative under the integral sign.

We are interested in applications to compressible flow and so from here on we will interpret the variable t as time. Now suppose that both the kernel of the integral and the limits of integration depend on time.

$$I(t, a(t), b(t)) = \int_{a(t)}^{b(t)} f(x', t) dx' \quad (5.7)$$

This situation is shown schematically below with movement of the boundaries indicated.

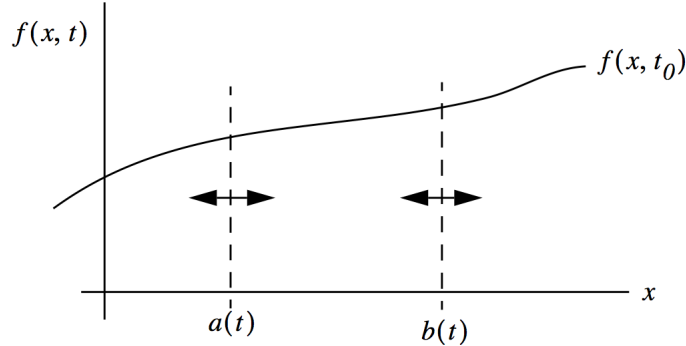


Figure 5.1: Integration with a moving boundary. The function $f(x, t)$ is shown at one instant of time.

Using the chain rule, the substantial derivative of (5.7) is

$$\frac{DI}{Dt} = \frac{\partial I}{\partial t} + \frac{\partial I}{\partial a} \frac{da}{dt} + \frac{\partial I}{\partial b} \frac{db}{dt} \quad (5.8)$$

Now make use of the results in (5.2), (5.4) and (5.6). Equation (5.8) becomes,

$$\frac{DI}{Dt} = \int_{a(t)}^{b(t)} \frac{\partial f(x', t)}{\partial t} dx' + f(b(t), t) \frac{db}{dt} - f(a(t), t) \frac{da}{dt}. \quad (5.9)$$

The various terms in (5.9) can be interpreted as follows. The first term is the time rate of change of I due to the integrated time rate of change of $f(x, t)$ within the domain $[a, b]$. The second and third terms are the contributions to the time rate of change of I due to the movement of the boundaries enclosing more or less f at a given instant in time. The relation (5.9) is called Leibniz' rule for the differentiation of integrals after Gottfried Wilhelm Leibniz (1646-1716) who, along with Isaac Newton, is credited with independently inventing differential and integral calculus.

5.1.2 Extension to three dimensions

Let $F(x_1, x_2, x_3, t)$ be some field variable defined as a function of space and time and $V(t)$ be a time-dependent control volume that encloses some finite region in space at each instant of time. The time dependent surface of the control volume is $A(t)$.

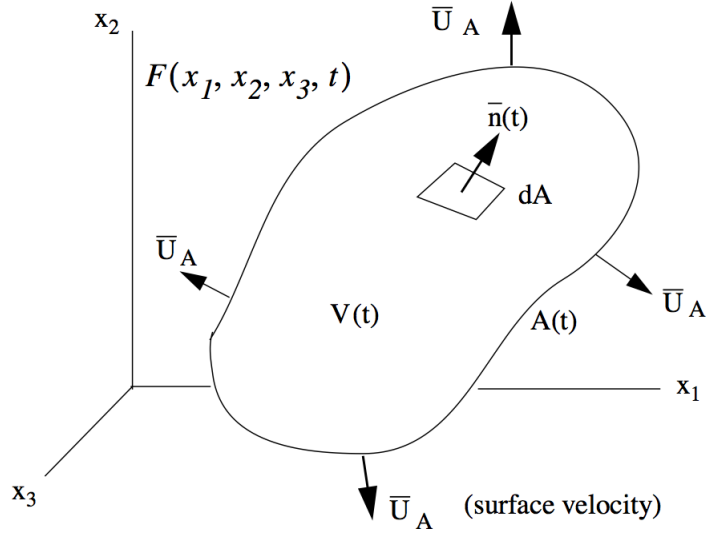


Figure 5.2: *Control volume definition.*

Leibniz' rule extended to three dimensions describes the time rate of change of the amount

of F contained inside V .

$$\frac{D}{Dt} \int_{V(t)} F dV = \int_{V(t)} \frac{\partial F}{\partial t} dV + \int_{A(t)} F \bar{U}_A \cdot \bar{n} dA \quad (5.10)$$

When (5.9) is generalized to three dimensions the boundary term in (5.9) becomes a surface integral. Equation (5.10) can be expressed in words as follows.

$$\left\{ \begin{array}{l} \text{Rate of} \\ \text{change of the} \\ \text{total amount of } F \\ \text{inside } V \end{array} \right\} = \left\{ \begin{array}{l} \text{Rate of change} \\ \text{due to changes} \\ \text{of } F \text{ within } V \end{array} \right\} + \left\{ \begin{array}{l} \text{Rate of change due to} \\ \text{movement of the} \\ \text{surface } A \text{ enclosing} \\ \text{more or less } F \text{ within } V \end{array} \right\} \quad (5.11)$$

The Leibniz relationship (5.10) is fundamental to the development of the transport theory of continuous media. The velocity vector \bar{U}_A is that of the control volume surface itself. If the medium is a moving fluid the surface velocity \bar{U}_A is specified independently of the fluid velocity \bar{U} . Consider a fluid with velocity vector \bar{U} which is a function of space and time.

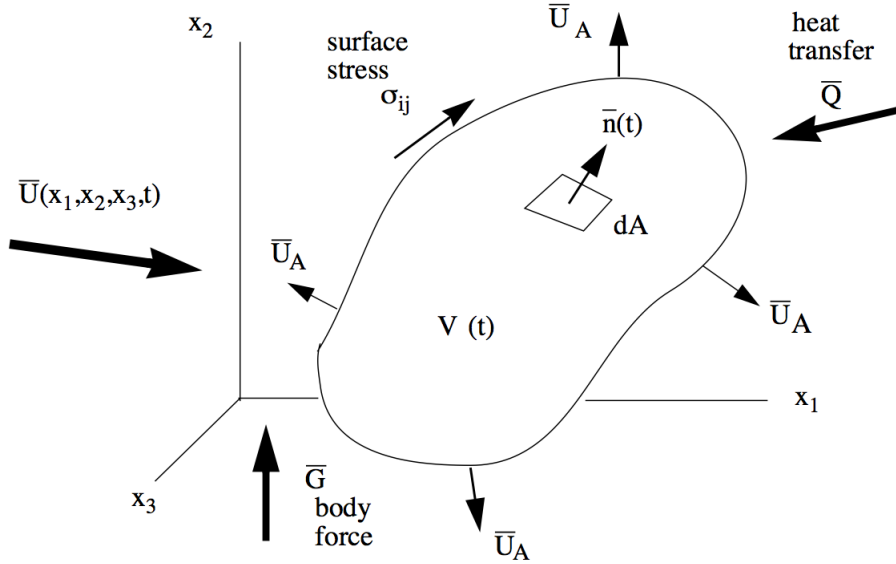


Figure 5.3: Control volume defined in a flow field subject to surface stresses, body forces and heat conduction.

Now let the velocity of each surface element of the control volume be the same as the velocity of the flow, $\bar{U} = \bar{U}_A$. In effect, we assume that the surface is attached to the fluid

and therefore the control volume always contains the same set of fluid elements. This is called a Lagrangian control volume. In this case Leibnitz' rule becomes

$$\frac{D}{Dt} \int_{V(t)} F dV = \int_{V(t)} \frac{\partial F}{\partial t} dV + \int_{A(t)} F \bar{U} \cdot \bar{n} dA \quad (5.12)$$

Use the Gauss theorem to convert the surface integral to a volume integral. The result is the Reynolds transport theorem.

$$\frac{D}{Dt} \int_{V(t)} F dV = \int_{V(t)} \left(\frac{\partial F}{\partial t} + \nabla \cdot (F \bar{U}) \right) dV \quad (5.13)$$

5.2 Conservation of mass

Let $F = \rho$ where ρ is the density of the fluid. The Reynolds transport theorem gives

$$\frac{D}{Dt} \int_{V(t)} \rho dV = \int_{V(t)} \left(\frac{\partial \rho}{\partial t} + \nabla \cdot (\rho \bar{U}) \right) dV. \quad (5.14)$$

The left-hand-side is the rate of change of the total mass inside the control volume. If there are no sources of mass within the control volume, the left-hand-side must be zero. Since the choice of control volume is arbitrary, the kernel of the right-hand-side must therefore be zero at every point in the flow.

Thus the continuity equation in the absence of mass sources is

$$\frac{\partial \rho}{\partial t} + \nabla \cdot (\rho \bar{U}) = 0 \quad (5.15)$$

This equation, expressed in coordinate independent vector notation, is the same one that we derived in Chapter 1 using an infinitesimal, cubic, Eulerian control volume. Expand (5.15)

$$\frac{\partial \rho}{\partial t} + U \cdot \nabla \rho + \rho \nabla \cdot \bar{U} = 0. \quad (5.16)$$

In terms of the substantial derivative the continuity equation is

$$\frac{D\rho}{Dt} + \rho \nabla \cdot \bar{U} = 0. \quad (5.17)$$

If the medium is incompressible then $\rho = \text{constant}$ and $\nabla \cdot \bar{U} = 0$.

5.3 Conservation of momentum

In this case the generic variable in Leibniz' rule is the vector momentum per unit volume, $F = \rho \bar{U}$. Momentum is convected about by the motion of the fluid itself and spatial variations of pressure and viscous stresses act as sources of momentum. Restricting ourselves to the motion of a continuous, viscous fluid (liquid or gas), the stress in a fluid is composed of two parts; a locally isotropic part proportional to the scalar pressure field and a non-isotropic part due to viscous friction. The stress tensor is

$$\sigma_{ij} = -P\delta_{ij} + \tau_{ij} \quad (5.18)$$

where P is the thermodynamic pressure, δ_{ij} is the Kronecker unit tensor defined in Chapter 3,

$$\bar{\bar{I}} = \begin{bmatrix} 1 & 0 & 0 \\ 0 & 1 & 0 \\ 0 & 0 & 1 \end{bmatrix} = \begin{cases} \delta_{ij} = 1; & i = j \\ \delta_{ij} = 0; & i \neq j \end{cases} \quad (5.19)$$

and τ_{ij} is the viscous stress tensor. The net force acting on the control volume is the integral of the stress tensor, σ_{ij} , over the surface plus the integral of any body force vectors per unit mass, G (gravitational acceleration, electromagnetic acceleration, etc.), over the volume.

The isotropy of the pressure implies that it acts normal to any surface element in the fluid regardless of how it is oriented. The viscous part of the stress can take on many different forms. In Aeronautics and Astronautics we deal almost exclusively with Newtonian fluids discussed in Chapter 1 such as air or water where the viscous stress is linearly proportional to the rate-of-strain tensor of the flow. The general form of the stress-rate-of-strain constitutive relation in Cartesian coordinates for a compressible Newtonian fluid is

$$\tau_{ij} = 2\mu S_{ij} - \left(\frac{2}{3}\mu - \mu_v\right) \delta_{ij} S_{kk} \quad (5.20)$$

where

$$S_{ij} = \frac{1}{2} \left(\frac{\partial U_i}{\partial x_j} + \frac{\partial U_j}{\partial x_i} \right). \quad (5.21)$$

Recall that $S_{kk} = \nabla \cdot \bar{U}$. The stress components in cylindrical and spherical polar coordinates are given in Appendix B.

Interestingly, there are actually two viscosity coefficients that are required to account for all possible stress fields that depend linearly on the rate-of-strain tensor. The so-called shear viscosity μ arises from momentum exchange due to molecular motion. A simple model of μ is described in Appendix A. The bulk viscosity μ_v is a little more mysterious. It contributes only to the viscous normal force and seems to arise from the exchange of momentum that can occur between colliding molecules and the internal degrees of freedom of the molecular system. Some typical values of the bulk viscosity are shown in Figure 5.4.

| Fluid | $\mu \times 10^5$, kg/(m)(s) | μ_v/μ | $\chi \times 10^2$, J/(m)(s)(K) | $\frac{\mu}{\rho} \times 10^5$, m ² /s | Pr |
|------------------------------------|----------------------------------|-------------|-------------------------------------|---|--------|
| He | 1.98 | 0 | 15.0 | 12.2 | 0.67 |
| Ar | 2.27 | 0 | 1.77 | 1.40 | 0.67 |
| H ₂ | 0.887 | 32 | 17.3 | 10.8 | 0.71 |
| N ₂ | 1.66 | 0.8 | 2.52 | 1.46 | 0.71 |
| O ₂ | 2.07 | 0.4 | 2.58 | 1.59 | 0.72 |
| CO ₂ | 1.50 | 1,000 | 1.66 | 0.837 | 0.75 |
| Air | 1.85 | 0.6 | 2.58 | 1.57 | 0.71 |
| H ₂ O (<i>liquid</i>) | 85.7 | 3.1 | 61 | 0.0857 | 6.0 |
| Ethyl alcohol | 110 | 4.5 | 18.3 | 0.14 | 15 |
| Glycerine | 134,000 | 0.4 | 29 | 109 | 11,000 |

Figure 5.4: Physical properties of some common fluids at one atmosphere and 298.15K.

For monatomic gases that lack such internal degrees of freedom, $\mu_v = 0$. For some polyatomic gases such as CO₂ the bulk viscosity is much larger than the shear viscosity. Recall the discussion of elementary flow patterns from Chapter 4. Any fluid flow can be decomposed into a rotational part and a straining part. According to the Newtonian model (5.20), only the straining part contributes to the viscous stress. Although μ is called the shear viscosity, it is clear from the diagonal terms in (5.20) that there are viscous normal

force components proportional to μ . However they make no net contribution to the mean normal stress defined as

$$\sigma_{mean} = (1/3) \sigma_{ii} = -P + \mu_v S_{kk}. \quad (5.22)$$

This is not to say that viscous normal stresses are unimportant. They play a key role in many compressible flow phenomena we will study later, especially shock waves.

A common assumption called Stokes' hypothesis is to assume that the bulk viscosity μ_v is equal to zero. Then only the so-called shear viscosity μ appears in the constitutive relation for the stress. While this assumption is strictly valid only for monatomic gases, it is applied very widely and works quite well, mainly because $\nabla \cdot \bar{U}$ tends to be relatively small in most situations outside of shock waves and high Mach number flow.

The rate of change of the total momentum inside the control volume is

$$\frac{D}{Dt} \int_{V(t)} \rho \bar{U} dV = \int_{A(t)} (-P \bar{I} + \bar{\tau}) \cdot \bar{n} dA + \int_{V(t)} \rho \bar{G} dV. \quad (5.23)$$

Use the Reynolds transport theorem to replace the left-hand-side of (5.23) and the Gauss theorem to convert the surface integral to a volume integral.

$$\int_{V(t)} \left(\frac{\partial \rho \bar{U}}{\partial t} + \nabla \cdot (\rho \bar{U} \bar{U} + P \bar{I} - \bar{\tau}) - \rho \bar{G} \right) dV = 0. \quad (5.24)$$

Since the equality must hold over an arbitrary control volume, the kernel must be zero at every point in the flow and we have the differential equation for conservation of momentum.

$$\frac{\partial \rho \bar{U}}{\partial t} + \nabla \cdot (\rho \bar{U} \bar{U} + P \bar{I} - \bar{\tau}) - \rho \bar{G} \quad (5.25)$$

This is the same momentum equation we derived in Chapter 1 except for the inclusion of the body force term.

5.4 Conservation of energy

The energy per unit mass of a moving fluid element is $e + k$ where e is the internal energy

per unit mass of the medium and

$$k = \frac{1}{2} U_i U_i = \frac{1}{2} (U_1^2 + U_2^2 + U_3^2) \quad (5.26)$$

is the kinetic energy per unit mass. In this case we use $F = \rho(e+k)$ in the Leibniz rule

The stress tensor acting over the surface does work on the control volume as do the body force vectors. In addition, there may be conductive heat flux Q through the surface. There could also be sources of heat within the flow due to chemical reactions, radiative heating, etc. For a general fluid the internal energy per unit mass is a function of temperature and pressure $e = f(T, P)$.

The rate of change of the energy inside the control volume in Figure 5.3 is

$$\frac{D}{Dt} \int_{V(t)} \rho (e + k) dV = \int_{A(t)} \left((-P \bar{I} + \bar{\tau}) \cdot \bar{U} - \bar{Q} \right) \cdot \bar{n} dA + \int_{V(t)} \rho \bar{G} \cdot \bar{U} dV. \quad (5.27)$$

The Reynolds transport theorem and Gauss's theorem lead to

$$\int_{V(t)} \left(\frac{\partial \rho (e + k)}{\partial t} + \nabla \cdot \left(\rho \bar{U} \left(e + \frac{P}{\rho} + k \right) - \bar{\tau} \cdot \bar{U} + \bar{Q} \right) - \rho \bar{G} \cdot \bar{U} \right) dV = 0. \quad (5.28)$$

Since the equality holds over an arbitrary volume, the kernel must be zero and we have the differential equation for conservation of energy.

$$\frac{\partial \rho (e + k)}{\partial t} + \nabla \cdot \left(\rho \bar{U} \left(e + \frac{P}{\rho} + k \right) - \bar{\tau} \cdot \bar{U} + \bar{Q} \right) - \rho \bar{G} \cdot \bar{U} = 0 \quad (5.29)$$

The sum of enthalpy and kinetic energy

$$h_t = e + \frac{P}{\rho} + k = h + \frac{1}{2} U_i U_i \quad (5.30)$$

is called the stagnation or total enthalpy and plays a key role in the transport of energy in compressible flow systems. Take care to keep in mind that the flow energy is purely the sum of internal and kinetic energy, $e + k$. Some typical gas transport properties at 300 K and one atmosphere are shown in Figure 5.4. According to Fick's law, the heat flux vector in a linear heat conducting medium is

$$Q_i = -\kappa (\partial T / \partial x_i) \quad (5.31)$$

where κ is the thermal conductivity.

The rightmost column in Figure 5.4 is the Prandtl number.

$$Pr = \frac{\mu C_p}{\kappa} \quad (5.32)$$

The Prandtl number can be thought of as comparing the rate at which momentum is transported by viscous diffusion to the rate at which temperature diffuses through thermal conductivity. For most gases the Prandtl number is around 0.7. This number is close to one due to the fact that heat and momentum transport are accomplished by the same basic mechanism of molecular collision with lots of space between molecules. Liquids are often characterized by large values of the Prandtl number and the underlying mechanisms of heat and momentum transport in a condensed fluid are more complex, since they depend much more on collisions that are heavily influenced by intermolecular forces.

5.5 Summary - differential form of the equations of motion

The coordinate-independent form of the equations of motion is

$$\begin{aligned} \frac{\partial \rho}{\partial t} + \nabla \cdot (\rho \bar{U}) &= 0 \\ \frac{\partial \rho \bar{U}}{\partial t} + \nabla \cdot \left(\rho \bar{U} \bar{U} + P \bar{I} - \bar{\tau} \right) - \rho \bar{G} &= 0 \\ \frac{\partial \rho (e + k)}{\partial t} + \nabla \cdot \left(\rho \bar{U} \left(e + \frac{P}{\rho} + k \right) - \bar{\tau} \cdot \bar{U} + \bar{Q} \right) - \rho \bar{G} \cdot \bar{U} &= 0. \end{aligned} \quad (5.33)$$

Using index notation the same equations in Cartesian coordinates are

$$\begin{aligned} \frac{\partial \rho}{\partial t} + \frac{\partial}{\partial x_j} (\rho U_j) &= 0 \\ \frac{\partial \rho U_i}{\partial t} + \frac{\partial}{\partial x_j} (\rho U_i U_j + P \delta_{ij} - \tau_{ij}) - \rho G_i &= 0 \\ \frac{\partial \rho (e + k)}{\partial t} + \frac{\partial}{\partial x_i} \left(\rho U_i \left(e + \frac{P}{\rho} + k \right) - \tau_{ij} U_j + Q_i \right) - \rho G_i U_i &= 0. \end{aligned} \quad (5.34)$$

The equations of motion in cylindrical and spherical polar coordinates are given in Appendix B.

5.6 Integral form of the equations of motion

In deriving the differential form of the conservation equations (5.33) we used a general Lagrangian control volume where the surface velocity is equal to the local fluid velocity and the surface always encloses the same set of fluid elements. In Chapter 1 we derived the same equations on a rectangular Eulerian control volume. It is important to recognize that these partial differential equations are valid at every point and at every instant in the flow of a compressible continuum and are completely independent of the particular control volume approach (Eulerian or Lagrangian) used to derive them.

With the equations of motion in hand we will now reverse the process and work out the integral form of these equations on control volumes that are adapted to solving useful problems. In this endeavor it is useful to consider other kinds of control volumes where the control surface may be stationary or where part of the control surface is stationary and part is moving but not necessarily attached to the fluid. Recall the general form of the Leibniz rule.

$$\frac{D}{Dt} \int_{V(t)} F dV = \int_{V(t)} \frac{\partial F}{\partial t} dV + \int_{A(t)} F \bar{U}_A \cdot \bar{n} dA \quad (5.35)$$

5.6.1 Integral equations on an Eulerian control volume

The simplest case to consider is the Eulerian control volume used in Chapter 1 where $\bar{U}_A = 0$. This is a stationary volume fixed in space through which the fluid moves. In this case the Leibniz rule reduces to

$$\frac{d}{dt} \int_V F dV = \int_V \frac{\partial F}{\partial t} dV. \quad (5.36)$$

Note that, since the Eulerian volume is fixed in space and not time dependent, the lower case form of the derivative d/dt is used in (5.36). See for comparison (5.6) and (5.9).

Let $F = \rho$ in Equation (5.36)

$$\frac{d}{dt} \int_V \rho dV = \int_V \frac{\partial \rho}{\partial t} dV \quad (5.37)$$

Use (5.15) to replace $\partial\rho/\partial t$ in (5.37).

$$\frac{d}{dt} \int_V \rho dV = - \int_V \nabla \cdot (\rho \bar{U}) dV \quad (5.38)$$

Now use the Gauss theorem to convert the volume integral on the right-hand-side of (5.38) to a surface integral. The integral form of the mass conservation equation valid on a finite Eulerian control volume of arbitrary shape is

$$\frac{d}{dt} \int_V \rho dV + \int_A \rho \bar{U} \cdot \bar{n} dA = 0. \quad (5.39)$$

The integral equations for conservation of momentum and energy are derived in a similar way using (5.25), (5.29), and (5.36). The result is

$$\begin{aligned} & \frac{d}{dt} \int_V \rho dV + \int_A \rho \bar{U} \cdot \bar{n} dA = 0 \\ & \frac{d}{dt} \int_V \rho \bar{U} dV + \int_A \left(\rho \bar{U} \bar{U} + P \bar{I} - \bar{\tau} \right) \cdot \bar{n} dA - \int_V \rho \bar{G} = 0 \\ & \frac{d}{dt} \int_V \rho (e + k) dV + \int_A \left(\rho \bar{U} \left(e + \frac{P}{\rho} + k \right) - \bar{\tau} \cdot \bar{U} + \bar{Q} \right) \cdot \bar{n} dA - \int_V \rho \bar{G} \cdot \bar{U} dV = 0. \end{aligned} \quad (5.40)$$

5.6.2 Mixed Eulerian-Lagrangian control volumes

More general control volumes where part of the surface may be at rest and other parts may be attached to the fluid are of great interest especially in the analysis of propulsion systems. Now use the general form of the Leibniz rule with $F = \rho$.

$$\frac{D}{Dt} \int_{V(t)} \rho dV = \int_{V(t)} \frac{\partial \rho}{\partial t} dV + \int_{A(t)} \rho \bar{U}_A \cdot \bar{n} dA = 0 \quad (5.41)$$

Use (5.15) to replace $\partial\rho/\partial t$ in (5.41) and use the Gauss theorem to convert the volume integral to a surface integral. The result is the integral form of mass conservation on an

arbitrary moving control volume.

$$\frac{D}{Dt} \int_{V(t)} \rho dV = - \int_{A(t)} \rho \bar{U} \cdot \bar{n} dA + \int_{A(t)} \rho \bar{U}_A \cdot \bar{n} dA \quad (5.42)$$

The integral equations for conservation of momentum and energy on a general, moving, finite control volume are derived in a similar way using (5.25), (5.29), and (5.35). Finally, the most general integrated form of the conservation equations is

$$\begin{aligned} & \frac{D}{Dt} \int_{V(t)} \rho dV + \int_{A(t)} \rho (\bar{U} - U_A) \cdot \bar{n} dA = 0 \\ & \frac{D}{Dt} \int_{V(t)} \rho \bar{U} dV + \int_{A(t)} \left(\rho \bar{U} (\bar{U} - U_A) + P \bar{\bar{I}} - \bar{\tau} \right) \cdot \bar{n} dA - \int_{V(t)} \rho \bar{G} = 0 \\ & \frac{D}{Dt} \int_{V(t)} \rho (e + k) dV + \int_{A(t)} \left(\rho (e + k) (\bar{U} - U_A) + P \bar{\bar{I}} \cdot \bar{U} - \bar{\tau} \cdot \bar{U} + \bar{Q} \right) \cdot \bar{n} dA - \\ & \int_{V(t)} (\rho \bar{G} \cdot \bar{U}) dV = 0. \end{aligned} \quad (5.43)$$

Remember, \bar{U}_A is the velocity of the control volume surface and can be selected at the convenience of the user.

5.7 Applications of control volume analysis

5.7.1 Example 1 - Solid body at rest in a steady flow

This is a simply connected Eulerian control volume where the segment A_2 surrounding (and attached to) the body is connected by a cut to the surrounding boundary A_1 . All fluxes on the cut A_3 cancel and therefore make no contribution to the integrated conservation laws. There is no mass injection through the surface of the body thus

$$\int_{A_1} (\rho \bar{U}) \cdot \bar{n} dA = 0. \quad (5.44)$$

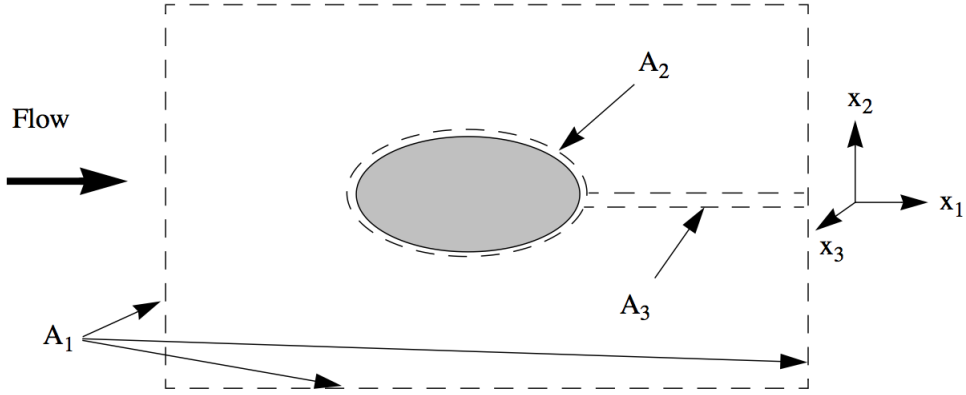


Figure 5.5: Eulerian control volume about a solid body at rest in a steady flow

Momentum fluxes integrated on A_1 are directly related to the lift and drag forces exerted on the body. The integrated momentum equation gives

$$\int_{A_1} \left(\rho \bar{U} \bar{U} + P \bar{I} - \bar{\tau} \right) \cdot \bar{n} dA + \int_{A_2} \left(P \bar{I} - \bar{\tau} \right) \cdot \bar{n} dA = 0. \quad (5.45)$$

The drag and lift forces by the flow on the body are

$$\begin{aligned} Drag &= \int_{A_2} \left(P \bar{I} - \bar{\tau} \right) \cdot \bar{n} dA \Big|_{x_1} \\ Lift &= \int_{A_2} \left(P \bar{I} - \bar{\tau} \right) \cdot \bar{n} dA \Big|_{x_2}. \end{aligned} \quad (5.46)$$

The integral momentum balance in the streamwise direction is

$$\int_{A_1} \left(\rho \bar{U} \bar{U} + P \bar{I} - \bar{\tau} \right) \cdot \bar{n} dA \Big|_{x_1} + Drag = 0 \quad (5.47)$$

and in the vertical direction is

$$\int_{A_1} \left(\rho \bar{U} \bar{U} + P \bar{I} - \bar{\tau} \right) \cdot \bar{n} dA \Big|_{x_2} + Lift = 0. \quad (5.48)$$

5.7.2 Example 2 - Channel flow with heat addition

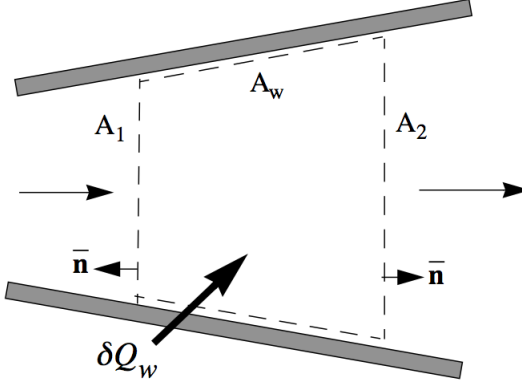


Figure 5.6: Steady flow in a channel with heat addition.

Heat addition to the compressible flow shown above occurs through heat transfer through the channel wall, δQ_w . There is no net mass addition to the control volume.

$$\int_{A_1} (\rho \bar{U}) \cdot \bar{n} dA + \int_{A_2} (\rho \bar{U}) \cdot \bar{n} dA = 0 \quad (5.49)$$

The flow is steady with no body forces. In this case, the energy balance is

$$\int_A (\rho \bar{U} (e + k) + P \bar{U} - \bar{\tau} \cdot \bar{U} + \bar{Q}) \cdot \bar{n} dA = 0. \quad (5.50)$$

The contribution of the viscous stresses to the energy balance is zero along the wall because of the no-slip condition, $\bar{U}|_{A_w} = 0$ and, as long as the streamwise velocity gradients are not large, the term $-\bar{\tau} \cdot \bar{U}$ is very small on the upstream and downstream faces, A_1 and A_2 . In this approximation, The energy balance becomes

$$\int_A \rho \left(e + \frac{P}{\rho} + k \right) \bar{U} \cdot \bar{n} dA = - \int_A \bar{Q} \cdot \bar{n} dA. \quad (5.51)$$

The effects of heat transfer through the wall and conduction through the upstream and downstream faces, A_1 and A_2 are accounted for by the change in the flux of stagnation enthalpy. Heat transfer through the upstream and downstream faces is usually small and

so most of the conductive heat transfer into the flow is through the wall.

$$-\int_A \bar{Q} \cdot \bar{n} dA \cong -\int_{A_w} \bar{Q} \cdot \bar{n} dA = \delta Q \quad (5.52)$$

The energy balance for this case reduces to

$$\int_{A_2} \rho h_t \bar{U} \cdot \bar{n} dA + \int_{A_1} \rho h_t \bar{U} \cdot \bar{n} dA = \delta Q. \quad (5.53)$$

When the vector multiplication is carried out (5.53) becomes

$$\int_{A_2} \rho_2 U_2 h_{t2} dA - \int_{A_1} \rho_1 U_1 h_{t1} dA = \delta Q. \quad (5.54)$$

The heat added to the flow is directly and simply related to the change of the integrated flow rate of stagnation enthalpy along the channel.

5.7.3 Example 3 - Stationary flow about a rotating fan

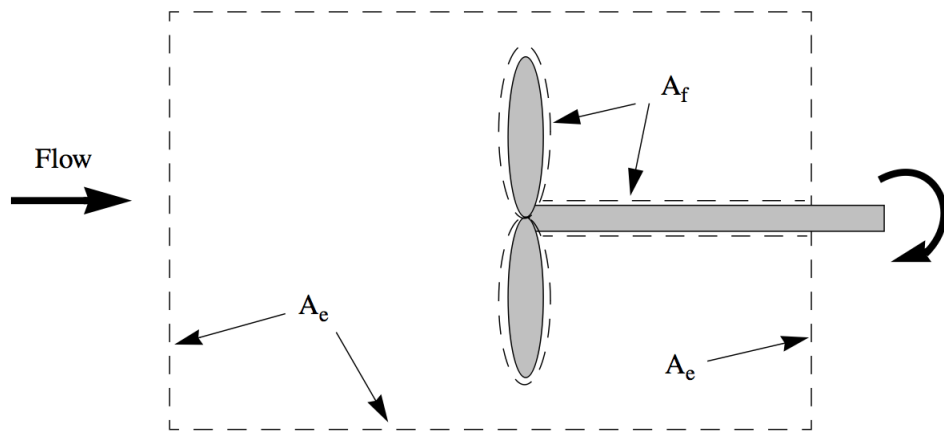


Figure 5.7: Mixed Eulerian-Lagrangian control volume about a rotating fan in a steady upstream flow.

This is the prototypical example for propellers, compressors and turbines. In contrast to a steady flow, a stationary flow is one where time periodic motions, such as the rotation of the fan illustrated above, do occur, but the properties of the flow averaged over one fan

rotation period or one blade passage period are constant. This will be the case if the fan rotation speed is held constant.

Here we make use of a mixed Eulerian-Lagrangian control volume. The Lagrangian part is attached to and moves with the fan blade surfaces and fan axle. Remember the fluid is viscous and subject to a no slip condition at the solid surface. The Eulerian surface elements are the upstream and downstream faces of the control volume as well as the cylindrical surrounding surface aligned with the axis of the fan. We will assume that the fan is adiabatic, $\bar{Q} = 0$ and there is no mass injection through the fan surface. The integrated mass fluxes are zero.

$$\int_{A_e} (\rho \bar{U}) \cdot \bar{n} dA = 0 \quad (5.55)$$

Momentum fluxes integrated on A_e are equal to the surface forces exerted by the flow on the fan

$$\int_{A_e} (\rho \bar{U} \bar{U} + P \bar{I} - \bar{\tau}) \cdot \bar{n} dA + \int_{A_f} (\rho \bar{U} (\bar{U} - \bar{U}_A) + P \bar{I} - \bar{\tau}) \cdot \bar{n} dA = 0 \quad (5.56)$$

or

$$\int_{A_e} (\rho \bar{U} \bar{U} + P \bar{I} - \bar{\tau}) \cdot \bar{n} dA + \bar{F} = 0 \quad (5.57)$$

where the vector force *by the flow on the fan* is

$$\bar{F} = \int_{A_f} (P \bar{I} - \bar{\tau}) \cdot \bar{n} dA. \quad (5.58)$$

Note that the flow and fan velocity on A_f are the same due to the no-slip condition

$$(\bar{U} - \bar{U}_A)|_{A_f} = 0. \quad (5.59)$$

For stationary flow, the integrated energy fluxes on A_e are equal to the *work/sec done by the flow on the fan*.

$$\int_{A_e} (\rho \bar{U} (e + k) + P \bar{U} - \bar{\tau} \cdot \bar{U} + \bar{Q}) \cdot \bar{n} dA + \int_{A_f} (P \bar{U} - \bar{\tau} \cdot \bar{U}) \cdot \bar{n} dA = 0 \quad (5.60)$$

$$Work = \int_{A_f} (P\bar{U} - \bar{\tau} \cdot \bar{U}) \cdot \bar{n} dA = \delta W \quad (5.61)$$

If the flow is adiabatic, and viscous normal stresses are neglected on A_e and A_f the energy equation becomes

$$\int_{A_e} \rho \left(e + \frac{P}{\rho} + k \right) \bar{U} \cdot \bar{n} dA + \delta W = 0. \quad (5.62)$$

5.7.4 Example 4 - Combined heat transfer and work

In a general situation where there is heat transfer and work done

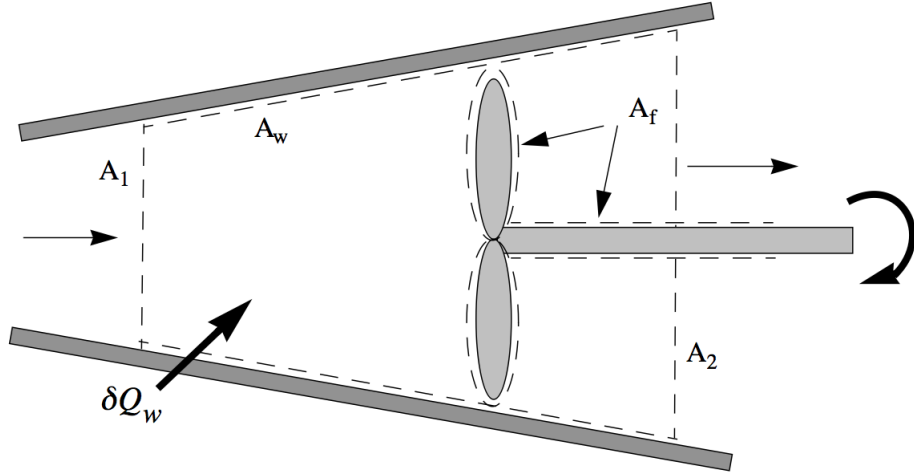


Figure 5.8: A general flow situation with heat transfer and work in a steady upstream flow.

the energy equation has the concise form

$$\int_{A_2} \rho_2 U_2 h_{t_2} dA - \int_{A_1} \rho_1 U_1 h_{t_1} dA = \delta Q - \delta W. \quad (5.63)$$

The effects of heat addition and work done are both accounted for by changes in the stagnation enthalpy of the flow. In general, changes due to thermal exchange are irreversible whereas changes due to the work done can be very nearly reversible except for entropy changes due to viscous friction.

5.8 Stagnation enthalpy, temperature and pressure

5.8.1 Stagnation enthalpy of a fluid element

It is instructive to develop an equation for the stagnation enthalpy change of a fluid element in a general unsteady flow. Using the energy equation

$$\frac{\partial \rho(e+k)}{\partial t} + \nabla \cdot \left(\rho \bar{U} \left(e + \frac{P}{\rho} + k \right) - \bar{\tau} \cdot \bar{U} + \bar{Q} \right) - \rho \bar{G} \cdot \bar{U} = 0 \quad (5.64)$$

along with the continuity equation

$$\frac{D\rho}{Dt} = -\rho \nabla \cdot \bar{U} \quad (5.65)$$

and the identity

$$\frac{D}{Dt} \left(\frac{P}{\rho} \right) = \frac{1}{\rho} \frac{DP}{Dt} - \frac{P}{\rho^2} \frac{D\rho}{Dt} \quad (5.66)$$

one can show that

$$\rho \frac{Dh_t}{Dt} = \nabla \cdot (\bar{\tau} \cdot \bar{U} - \bar{Q}) + \rho \bar{G} \cdot \bar{U} + \frac{\partial P}{\partial t}. \quad (5.67)$$

Equation (5.67) shows that changes in the stagnation enthalpy of a fluid element may be due to heat conduction as well as the work done by body forces and work by viscous forces. In addition, nonsteady changes in the pressure, generally associated with exchange of work by the system, can also change h_t .

In most aerodynamic problems body forces are negligible. Exceptions can occur at low speeds where density changes due to thermal gradients lead to gravity driven flows.

The work done by viscous forces is usually small (the work is zero at a wall where $\bar{U} = 0$) and energy transport by heat conduction, \bar{Q} , is often small. In this case the stagnation enthalpy of a fluid element is preserved if the flow is steady, $Dh_t/Dt = 0$.

The last term in (5.67) can be quite large in some nonsteady processes. For example, large temperature changes can occur in unsteady vortex formation in the wake of a bluff body in high speed flow due to this term.

If the flow is steady, inviscid and non-heat-conducting then (5.67) reduces to

$$\bar{U} \cdot \nabla (h_t + \Psi) = 0 \quad (5.68)$$

where the gravitational potential is related to the gravitational force by $\bar{G} = \nabla \Psi$.

5.8.2 Blowdown from a pressure vessel revisited

In Chapter 2 we looked at the blowdown of gas from an adiabatic pressure vessel through a small nozzle. The situation is shown below.

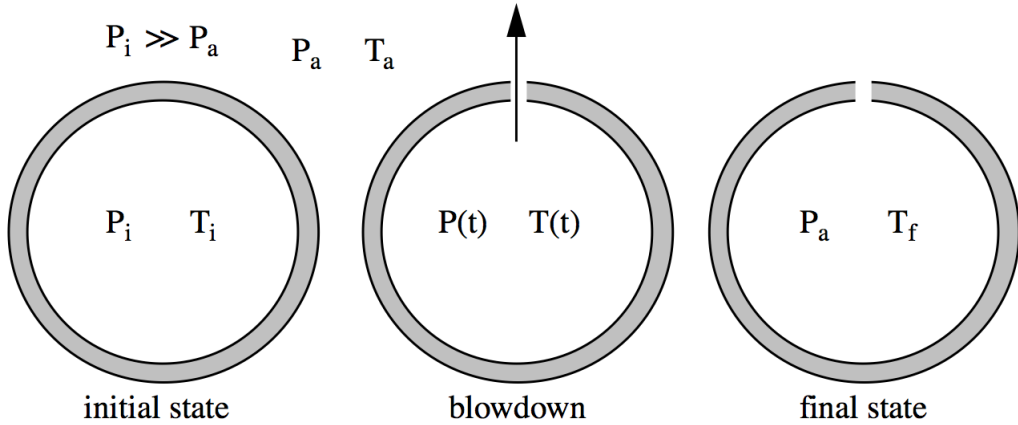


Figure 5.9: An adiabatic pressure vessel exhausting to the surroundings.

The stagnation enthalpy of the flow inside the pressure vessel is governed by (5.67). If we drop the body force term and assume the divergence term involving heat transfer and viscous work are small then (5.67) simplifies to

$$\rho \frac{Dh_t}{Dt} = \frac{\partial P}{\partial t}. \quad (5.69)$$

If we further assume that the vessel is very large and the hole is very small then the contribution of the flow velocity to the stagnation enthalpy can be neglected since most of the gas is almost at rest. Under these conditions the temperature and pressure can be regarded as approximately uniform over the interior of the vessel. With these assumptions (5.69) simplifies to

$$\rho \frac{dh}{dt} = \frac{dP}{dt}. \quad (5.70)$$

Equation (5.70) is the Gibbs equation for an isentropic process. If the gas is calorically perfect the final temperature is given by

$$\frac{T_f}{T_i} = \left(\frac{P_a}{P_i} \right)^{\frac{\gamma-1}{\gamma}}. \quad (5.71)$$

This is the result we were led to in Chapter 2 when we assumed the process in the vessel was isentropic. The difference is that by beginning with (5.67) the assumptions needed to reach (5.71) are clarified. This example nicely illustrates the role of the unsteady pressure term in (5.67).

5.8.3 Stagnation enthalpy and temperature in steady flow

The figure below shows the path of a fluid element in steady flow stagnating at the leading edge of an airfoil.

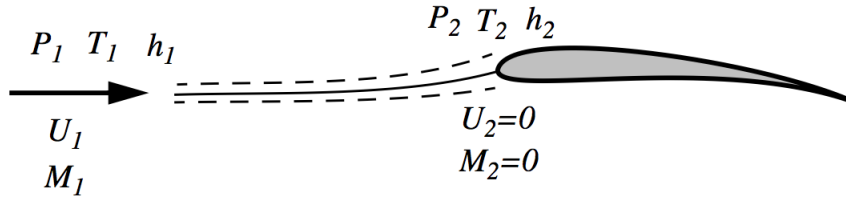


Figure 5.10: Schematic of a stagnation process in steady flow.

The dashed lines outline a small stream-tube surrounding the stagnation streamline. Lets interpret this problem in two ways, first as an extension of section 5.7 example 2 and then in the context of equation (5.67).

The result in example 2 applies to the flow in the streamtube.

$$\int_{A_2} \rho_2 U_2 h_{t_2} dA - \int_{A_1} \rho_1 U_1 h_{t_1} dA = \delta Q. \quad (5.72)$$

If we assume the airfoil is adiabatic and that there is no net heat loss or gain through the stream tube then

$$\int_{A_2} \rho_2 U_2 h_{t_2} dA = \int_{A_1} \rho_1 U_1 h_{t_1} dA. \quad (5.73)$$

Since the mass flow at any point in the stream tube is the same then one can conclude that the enthalpy per unit mass is also the same at any point along the stream tube (at least in an average sense across the tube which we can make arbitrarily narrow).

According to (5.67) the stagnation enthalpy of the fluid element can also change due to viscous work which we neglected in example 3. However as the element decelerates on its approach to the airfoil leading edge where viscous forces might be expected to play a role, the velocity becomes small and goes to zero at the stagnation point so one can argue that the viscous work terms are also small. An exception where this assumption needs to be re-examined is at very low Reynolds number where the viscous region can extend a considerable distance from the airfoil.

By either argument, we can conclude that to a good approximation in a steady flow

$$h_{t_1} = e_1 + \frac{P_1}{\rho_1} + k_1 = h_1 + \frac{1}{2}U_1^2 = h_2 + \frac{1}{2}U_2^2 = h_2. \quad (5.74)$$

With viscous work neglected, the stagnation enthalpy is conserved along an adiabatic path. When a fluid element is brought to rest adiabatically the enthalpy at the rest state is the stagnation enthalpy at the initial state.

The stagnation temperature is defined by the enthalpy relation

$$h_t - h = \int_T^{T_t} C_p dT = \frac{1}{2}U_i U_i. \quad (5.75)$$

The stagnation temperature is the temperature reached by an element of gas brought to rest adiabatically. For a calorically perfect ideal gas with constant specific heat in the range of temperatures between T and T_t (5.75) can be written

$$C_p T_t = C_p T + \frac{1}{2}U_i U_i. \quad (5.76)$$

In Figure 5.10 we would expect $T_2 = T_{t_1}$ to the extent that the heat capacity is constant. Divide through by $C_p T$ and introduce the speed of sound $a = \sqrt{\gamma R T}$. Equation (5.76) becomes

$$\frac{T_t}{T} = 1 + \left(\frac{\gamma - 1}{2} \right) M^2 \quad (5.77)$$

where M is the Mach number of the fluid element.

5.8.4 Frames of reference

In Chapter 1 we discussed how the momentum and kinetic energy of a fluid element change when the frame of reference is transformed from fixed to moving coordinates. Clearly since the stagnation temperature (5.76) depends on the kinetic energy then it too depends on the frame of reference. The stagnation temperatures in fixed and moving coordinates are

$$\begin{aligned} C_p T_t &= C_p T + \frac{1}{2} U_i U_i \\ C_p T'_t &= C_p T + \frac{1}{2} U'_i U'_i. \end{aligned} \quad (5.78)$$

The transformation of the kinetic energy is

$$\frac{1}{2} U'_i U'_i = \frac{1}{2} U_i U_i + \frac{1}{2} \dot{X} (\dot{X} - 2U) + \frac{1}{2} \dot{Y} (\dot{Y} - 2V) + \frac{1}{2} \dot{Z} (\dot{Z} - 2W) \quad (5.79)$$

where $(\dot{X}, \dot{Y}, \dot{Z})$ are the velocity components of the moving origin of coordinates. The thermodynamic variables density, temperature and pressure do not change and so the transformation of the stagnation temperature is

$$C_p T'_t = C_p T_t + \frac{1}{2} \dot{X} (\dot{X} - 2U) + \frac{1}{2} \dot{Y} (\dot{Y} - 2V) + \frac{1}{2} \dot{Z} (\dot{Z} - 2W). \quad (5.80)$$

5.8.5 Stagnation pressure

The stagnation pressure is defined using the Gibbs equation for an ideal gas.

$$ds = C_p \frac{dT}{T} - R \frac{dP}{P} \quad (5.81)$$

Note that while C_p and C_v depend on temperature, the gas constant $C_p - C_v$ is independent of temperature as long as there are no chemical reactions that might change the molecular weight of the gas. Integrate (5.81) along an isentropic path $ds = 0$. Between state 1 and state 2

$$R \int_{P_1}^{P_2} \frac{dP}{P} = \int_{T_1}^{T_2} C_p(T) \frac{dT}{T} \quad (5.82)$$

which becomes

$$\frac{P_2}{P_1} = \text{Exp} \left(\frac{1}{R} \int_{T_1}^{T_2} C_p(T) \frac{dT}{T} \right). \quad (5.83)$$

If an element of flowing gas at pressure P and temperature T is brought to rest adiabatically and isentropically to a temperature T_t , the stagnation pressure P_t is defined by

$$\frac{P_t}{P} = \text{Exp} \left(\frac{1}{R} \int_T^{T_t} C_p(T) \frac{dT}{T} \right). \quad (5.84)$$

If the heat capacities are constant (5.84) reduces to the isentropic relation

$$\frac{P_t}{P} = \left(\frac{T_t}{T} \right)^{\frac{\gamma}{\gamma-1}} = \left(1 + \left(\frac{\gamma-1}{2} \right) M^2 \right)^{\frac{\gamma}{\gamma-1}}. \quad (5.85)$$

If the stagnation path in Figure 5.10 is isentropic as well as adiabatic and the gas is calorically perfect then one would expect

$$P_2 = P_{t1} = P_1 \left(1 + \left(\frac{\gamma-1}{2} \right) M_1^2 \right)^{\frac{\gamma}{\gamma-1}}. \quad (5.86)$$

The stagnation state is just that, a thermodynamic state, and changes in the stagnation state of a material are described by the Gibbs equation

$$T_t \frac{Ds}{Dt} = \frac{Dh_t}{Dt} - \frac{1}{\rho_t} \frac{DP_t}{Dt} \quad (5.87)$$

where for an ideal gas $P_t = \rho_t RT_t$. Note that there is no distinction between the entropy and stagnation entropy. They are one and the same and the identity

$$\frac{1}{T_t} \frac{Dh_t}{Dt} - \frac{1}{\rho_t T_t} \frac{DP_t}{Dt} = \frac{1}{T} \frac{Dh}{Dt} - \frac{1}{\rho T} \frac{DP}{Dt} \quad (5.88)$$

is occasionally useful.

Let's return to Figure 5.10 for a moment and ask, what pressure and temperature would one measure at the stagnation point of the airfoil in a real experiment. In practice it is impossible to make the airfoil truly adiabatic and so some heat loss would be expected through conduction. In addition, as the gas approaches the airfoil, gradients in temperature arise

that tend to conduct heat away from the stagnation point. In addition, gradients in temperature and velocity near the stagnation point tend to produce an increase in entropy. As a result, the measured temperature and pressure both tend to be lower than predicted. The difference may vary by anywhere from a fraction of a percent to several percent depending on the Reynolds number and Mach number of the flow. At high Mach numbers a shock wave will be present ahead of the airfoil, substantially reducing the pressure measured at the stagnation point.

5.8.6 Transforming P_t between fixed and moving frames

The stagnation pressure and stagnation temperature in the fixed and moving frames are

$$\begin{aligned}\frac{P_t}{P} &= \left(\frac{T_t}{T}\right)^{\frac{\gamma}{\gamma-1}} \\ \frac{P'_t}{P} &= \left(\frac{T'_t}{T}\right)^{\frac{\gamma}{\gamma-1}}.\end{aligned}\tag{5.89}$$

Divide out the static pressure and temperature in (5.89).

$$\frac{P'_t}{P_t} = \left(\frac{T'_t}{T_t}\right)^{\frac{\gamma}{\gamma-1}}\tag{5.90}$$

Substitute (5.80) into (5.90). The transformation of stagnation pressure is

$$P'_t = P_t \left(1 + \frac{\dot{X}(\dot{X} - 2U) + \dot{Y}(\dot{Y} - 2V) + \dot{Z}(\dot{Z} - 2W)}{2C_p T_t}\right)^{\frac{\gamma}{\gamma-1}}.\tag{5.91}$$

5.9 Problems

Problem 1 - Work out the time derivative of the following integral.

$$I(t) = \int_{t^2}^{Sin(t)} e^{xt} dx\tag{5.92}$$

Obtain dI/dt in two ways: (1) by directly integrating, then differentiating the result and (2) by applying Leibniz' rule (5.9) then carrying out the integration.

Problem 2 - In Chapter 2, Problem 2 we worked out a hypothetical incompressible steady flow with the velocity components

$$(U, V) = (\cos(x)\cos(y), \sin(x)\sin(y)). \quad (5.93)$$

This 2-D flow clearly satisfies the continuity equation (conservation of mass), could it possibly satisfy conservation of momentum for an inviscid fluid? To find out work out the substantial derivatives of the velocity components and equate the results to the partial derivatives of the pressure that appear in the momentum equation. The differential of the pressure is

$$dP = \frac{\partial P}{\partial x}dx + \frac{\partial P}{\partial y}dy. \quad (5.94)$$

Show by the cross derivative test whether a pressure field exists that could enable (5.93) to satisfy momentum conservation. If such a pressure field exists work it out.

Problem 3 - Consider steady flow in one dimension where $\bar{U} = (U(x), 0, 0)$ and all velocity gradients are zero except

$$A_{11} = \frac{\partial U}{\partial x}. \quad (5.95)$$

Work out the components of the Newtonian viscous stress tensor τ_{ij} . Note the role of the bulk viscosity.

Problem 4 - A cold gas thruster on a spacecraft uses Helium (atomic weight 4) at a chamber temperature of 300 K and a chamber pressure of one atmosphere. The gas exhausts adiabatically through a large area ratio nozzle to the vacuum of space. Estimate the maximum speed of the exhaust gas.

Problem 5 - Work out equation (5.67).

Problem 6 - Steady flow through the empty test section of a wind tunnel with parallel walls and a rectangular cross-section is shown below. Use a control volume balance to relate the integrated velocity and pressure profiles at stations 1 and 2 to an integral of the wall shear stress.

State any assumptions used.

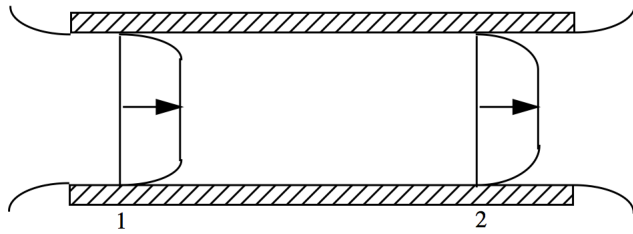


Figure 5.11: Steady flow in an empty wind tunnel

Problem 7 - Use a control volume balance to show that the drag of a circular cylinder at low Mach number can be related to an integral of the velocity and stress profile in the wake downstream of the cylinder. Be sure to use the continuity equation to help account for the x-momentum convected out of the control volume through the upper and lower surfaces. State any assumptions used.

Problem 8 - Use a control volume balance to evaluate the lift of a three dimensional wing in an infinite steady stream. Assume the Mach number is low enough so that there are no shock waves formed.

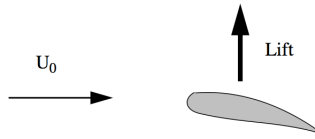


Figure 5.12: 3-D wing in an infinite stream

- 1) Select an appropriate control volume.
- 2) Write down the integral form of the mass conservation equation.
- 3) Write down the integral form of the momentum conservation equation.
- 4) Evaluate the various terms on the control volume boundary so as to express the lift of the wing in terms of an integral over the downstream wake.
- 5) Why did I stipulate that there are no shock waves? Briefly state any other assumptions that went in to your solution.

Problem 9 - Suppose a model 3-D wing is contained in a finite sized wind tunnel test section with horizontal and vertical walls as shown below.

What would a test engineer have to measure to determine lift and drag in the absence of sensors on the model or a mechanical balance for directly measuring forces? Consider a

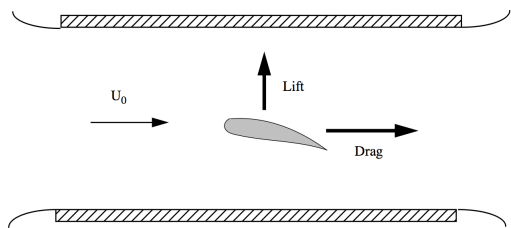


Figure 5.13: 3-D wing in a wind tunnel

control volume that coincides with the wind tunnel walls.

Chapter 6

Several forms of the equations of motion

6.1 The Navier-Stokes equations

Under the assumption of a Newtonian stress-rate-of-strain constitutive equation and a linear, thermally conductive medium, the equations of motion for compressible flow become the famous Navier-Stokes equations. In Cartesian coordinates,

$$\begin{aligned} \frac{\partial \rho}{\partial t} + \frac{\partial}{\partial x_i} (\rho U_i) &= 0 \\ \frac{\partial \rho U_i}{\partial t} + \frac{\partial}{\partial x_j} \left(\rho U_i U_j + P \delta_{ij} - 2\mu S_{ij} + \left(\frac{2}{3}\mu - \mu_v \right) \delta_{ij} S_{kk} \right) - \rho G_i &= 0 \\ \frac{\partial \rho (e + k)}{\partial t} + \frac{\partial}{\partial x_i} \left(\rho U_i h_t - \kappa (\partial T / \partial x_i) - 2\mu U_j S_{ij} + \left(\frac{2}{3}\mu - \mu_v \right) \delta_{ij} U_j S_{kk} \right) - \rho U_i G_i &= 0 \end{aligned} \quad (6.1)$$

The Navier-Stokes equations are the foundation of the science of fluid mechanics. With the inclusion of an equation of state, virtually all flow solving revolves around finding solutions of the Navier-Stokes equations. Most exceptions involve fluids where the relation between stress and rate-of-strain is nonlinear such as polymers, or where the equation of state is not very well understood (for example supersonic flow in water) or rarefied flows where the Boltzmann equation must be used to explicitly account for particle collisions. The equations can take on many forms depending on what approximations or assumptions may

be appropriate to a given flow. In addition, transforming the equations to different forms may enable one to gain insight into the nature of the solutions. It is essential to learn the many different forms of the equations and to become practiced in the manipulations used to transform them.

6.1.1 Incompressible Navier-Stokes equations

If there are no body forces and the flow is incompressible, $\nabla \cdot \bar{U} = 0$, the Navier-Stokes equations reduce to what is probably their most familiar form.

$$\begin{aligned}\frac{\partial U_i}{\partial x_i} &= 0 \\ \frac{\partial U_i}{\partial t} + \frac{\partial}{\partial x_j} \left(U_i U_j + \frac{P}{\rho} \delta_{ij} - 2 \left(\frac{\mu}{\rho} \right) S_{ij} \right) &= 0 \\ \frac{\partial T}{\partial t} + \frac{\partial}{\partial x_i} \left(U_i T - \left(\frac{\kappa}{\rho C} \right) \frac{\partial T}{\partial x_i} \right) - 2 \left(\frac{\mu}{\rho C} \right) S_{ij} S_{ij} &= 0\end{aligned}\tag{6.2}$$

where the internal energy is assumed to be $e = CT$ and C is the heat capacity of the material. The equation of state in this case is just $\rho = \text{constant}$. Notice that for incompressible flow the continuity and momentum equations are completely decoupled from the energy equation and can be solved separately. Once the velocity is known the energy equation can be solved for the temperature. The last term in the energy equation is always positive and represents a source of internal energy due to dissipation of kinetic energy by viscous friction. This will be discussed in much more detail in Chapter 7.

6.2 The momentum equation expressed in terms of vorticity

If the transport coefficients, μ and μ_v are assumed to be constant (a reasonable assumption if the Mach number is not too large), the compressible momentum equation can be written,

$$\frac{\partial \rho \bar{U}}{\partial t} + \nabla \cdot (\rho \bar{U} \bar{U}) + \nabla P - \mu \nabla^2 \bar{U} - \left(\frac{1}{3} \mu + \mu_v \right) \nabla (\nabla \cdot \bar{U}) - \rho \bar{G} = 0\tag{6.3}$$

where the body force is the gradient of a potential function $\bar{G} = -\nabla\Psi$. The vorticity is defined as the curl of the velocity.

$$\bar{\Omega} = \nabla \times \bar{U} \quad (6.4)$$

If we use the vector identities

$$\begin{aligned} \bar{U} \cdot \nabla \bar{U} &= (\nabla \times \bar{U}) \times \bar{U} + \nabla \left(\frac{\bar{U} \cdot \bar{U}}{2} \right) \\ \nabla \times (\nabla \times \bar{U}) &= \nabla (\nabla \cdot \bar{U}) - \nabla^2 \bar{U} \end{aligned} \quad (6.5)$$

together with the continuity equation, the momentum equation can be written in the form,

$$\rho \frac{\partial \bar{U}}{\partial t} + \rho (\bar{\Omega} \times \bar{U}) + \rho \nabla \left(\frac{\bar{U} \cdot \bar{U}}{2} \right) + \nabla P - \left(\frac{4}{3}\mu + \mu_v \right) \nabla (\nabla \cdot \bar{U}) + \mu \nabla \times \bar{\Omega} + \rho \nabla \Psi = 0 \quad (6.6)$$

If the flow is irrotational $\bar{\Omega} = 0$ equation (6.6) reduces to

$$\rho \frac{\partial \bar{U}}{\partial t} + \rho \nabla \left(\frac{\bar{U} \cdot \bar{U}}{2} \right) + \nabla P - \left(\frac{4}{3}\mu + \mu_v \right) \nabla (\nabla \cdot \bar{U}) + \rho \nabla \Psi = 0 \quad (6.7)$$

According to (6.7) viscous forces play very little role in momentum transport when the flow is irrotational. If the flow is compressible the effect of viscosity is only through a term that depends on $\nabla \cdot \bar{U}$ which is usually relatively small in flows at moderate Mach number. Remarkably, if the flow is incompressible the viscous term disappears altogether and viscosity plays no role whatsoever in momentum transport. Viscous stresses do act in the fluid but they generate no net momentum transfer in an irrotational flow. An example would be the flow over a wing outside the boundary layer near the surface of the wing and outside the viscous wake.

6.3 The momentum equation expressed in terms of the entropy and vorticity

In Chapter 2 we noted that when an equation of state is combined with Gibbs equation any thermodynamic variable can be expressed in terms of any two others. In an unsteady,

three-dimensional flow of a continuous medium

$$s = s(h(x, y, z, t), P(x, y, z, t)) \quad (6.8)$$

Taking the gradient of (6.8) leads to

$$T\nabla s = \nabla h - \frac{\nabla P}{\rho} \quad (6.9)$$

which we derived in Chapter 2.

Equation (6.9) can be used to replace the gradient of the pressure in (6.6). Thus the momentum equation in terms of the entropy is

$$\frac{\partial \bar{U}}{\partial t} + (\bar{\Omega} \times \bar{U}) + \nabla \left(h + \frac{\bar{U} \cdot \bar{U}}{2} + \Psi \right) - T\nabla s - \frac{1}{\rho} \left(\frac{4}{3}\mu + \mu_v \right) \nabla (\nabla \cdot \bar{U}) + \left(\frac{\mu}{\rho} \right) \nabla \times \bar{\Omega} = 0 \quad (6.10)$$

6.3.1 Crocco's theorem

The inviscid form of the above equation with $\mu = 0, \mu_v = 0$ is

$$\frac{\partial \bar{U}}{\partial t} + (\bar{\Omega} \times \bar{U}) + \nabla \left(h + \frac{\bar{U} \cdot \bar{U}}{2} + \Psi \right) - T\nabla s = 0 \quad (6.11)$$

Equation (6.11) is called Croccos theorem and demonstrates the close relationship between vorticity and the gradient of the entropy in a compressible flow.

The relation

$$\bar{\Omega} \times \bar{U} = 0 \quad (6.12)$$

is satisfied if $\bar{U} = 0$ (a trivial situation), if the vorticity and velocity are parallel (this is called a Beltrami flow) or if the flow is irrotational, $\nabla \times \bar{U} = 0$.

6.3.2 The energy equation for inviscid, non-heat conducting flow

With the viscosities and thermal conductivity, κ , set to zero, the energy equation in (6.1) becomes

$$\frac{\partial \rho(e+k)}{\partial t} + \frac{\partial}{\partial x_i}(\rho U_i h_t) - \rho G_i U_i = 0 \quad (6.13)$$

If we are going to assume that the fluid is inviscid then it is consistent to also assume that the heat conductivity is zero since the underlying molecular collision mechanisms for both fluid properties are fundamentally the same in a gas. In Chapter 7 we will come to recognize that assuming the gas is inviscid and non-heat-conducting is equivalent to assuming that the entropy of a fluid element cannot change.

In terms of the stagnation enthalpy $h_t = h + k$ (6.13) can be written as

$$\frac{\partial \rho h_t}{\partial t} + \frac{\partial}{\partial x_i}(\rho U_i h_t) - \rho G_i U_i = \frac{\partial P}{\partial t} \quad (6.14)$$

Use the continuity equation in (6.14) and $G_i = -\partial \Psi / \partial x_i$ to produce

$$\frac{\partial h_t}{\partial t} + U_i \frac{\partial}{\partial x_i}(h_t + \Psi) = \frac{1}{\rho} \frac{\partial P}{\partial t} \quad (6.15)$$

We developed the viscous, heat-conducting version of (6.15) previously in Chapter 5.

6.3.3 Steady flow

If the flow is steady, the inviscid energy equation (6.15) reduces to

$$U_i \frac{\partial}{\partial x_i} \left(h + \frac{U^2}{2} + \Psi \right) = \bar{U} \cdot \nabla \left(h + \frac{U^2}{2} + \Psi \right) = 0 \quad (6.16)$$

The quantity

$$h + \frac{U^2}{2} + \Psi \quad (6.17)$$

is called the steady Bernoulli integral or Bernoulli function. In a general, inviscid, non-heat-conducting, steady flow the energy equation reduces to the statement (6.16) that the

velocity field is normal to the gradient of the Bernoulli function. In the absence of body forces, $Dh_t/Dt = 0$ in such a flow. The flow is necessarily adiabatic and the stagnation enthalpy of a fluid element is preserved. If the flow is fed from a reservoir where the enthalpy is everywhere uniform then, since h_t is preserved for each fluid element, the enthalpy remains uniform and $\nabla h_t = 0$ everywhere. In this case the momentum equation (Crocinos theorem) reduces to

$$\bar{\Omega} \times \bar{U} = T \nabla s \quad (6.18)$$

If the flow is steady, inviscid and irrotational then both the stagnation enthalpy and the entropy are constant everywhere. A flow where $\nabla s = 0$ is called homentropic. In this instance both the momentum equation and energy equations reduce to the same result

$$h + \frac{U^2}{2} + \Psi = Const \quad (6.19)$$

6.4 Inviscid, irrotational, homentropic flow

It is instructive to examine this case further. Again, assume there are no body forces $\Psi = 0$, set $\mu = \mu_v = 0$, $\kappa = 0$ in the energy equation and $\nabla \times \bar{U} = 0$ in the momentum equation (6.6). The governing equations become

$$\begin{aligned} \frac{\partial \rho}{\partial t} + \frac{\partial}{\partial x_k} (\rho U_k) &= 0 \\ \rho \frac{\partial U_i}{\partial t} + \rho \frac{\partial}{\partial x_i} \left(\frac{U_k U_k}{2} \right) + \frac{\partial P}{\partial x_i} &= 0 \\ \frac{P}{P_0} &= \left(\frac{\rho}{\rho_0} \right)^\gamma \end{aligned} \quad (6.20)$$

In this approximation the energy equation reduces to the isentropic relation between pressure and density. These equations are the starting point for the development of inviscid flow theory as well as the theory for the propagation of sound.

6.4.1 Steady, inviscid, irrotational flow

If the flow is steady the equations (6.20) reduce to

$$\begin{aligned} \frac{\partial}{\partial x_k} (\rho U_k) &= 0 \\ \frac{\partial}{\partial x_i} \left(\frac{U_k U_k}{2} \right) + \frac{1}{\rho} \frac{\partial P}{\partial x_i} &= 0 \\ \frac{P}{P_0} &= \left(\frac{\rho}{\rho_0} \right)^\gamma \end{aligned} \quad (6.21)$$

Take the gradient of the isentropic relation. The result is

$$\nabla P = a^2 \nabla \rho \quad (6.22)$$

For an ideal gas

$$\nabla \left(\frac{P}{\rho} \right) = \frac{\nabla P}{\rho} - \frac{P}{\rho^2} \nabla \rho = \left(\frac{\gamma - 1}{\gamma} \right) \frac{\nabla P}{\rho} \quad (6.23)$$

where (6.22) is used. Using (6.23) the momentum equation now becomes

$$\nabla \left(\left(\frac{\gamma}{\gamma - 1} \right) \frac{P}{\rho} + \frac{\bar{U} \cdot \bar{U}}{2} \right) = 0 \quad (6.24)$$

The term in parentheses in (6.24) is the stagnation enthalpy. For this class of flows the momentum equation reduces to $\nabla h_t = 0$ and the entropy is the same everywhere as just noted in the previous section. Substitute (6.22) into the continuity equation.

$$\bar{U} \cdot \left(\frac{\nabla P}{\rho} \right) + a^2 \nabla \cdot \bar{U} = 0 \quad (6.25)$$

Using (6.23) the continuity equation becomes

$$\bar{U} \cdot \nabla (a^2) + (\gamma - 1) a^2 \nabla \cdot \bar{U} = 0 \quad (6.26)$$

Using (6.24) we can write

$$\left(\frac{a^2}{\gamma - 1} \right) = h_t - \frac{\bar{U} \cdot \bar{U}}{2} \quad (6.27)$$

The continuity equation now becomes

$$(\gamma - 1) \left(h_t - \frac{\bar{U} \cdot \bar{U}}{2} \right) \nabla \cdot \bar{U} - \bar{U} \cdot \nabla \left(\frac{\bar{U} \cdot \bar{U}}{2} \right) = 0 \quad (6.28)$$

The equations governing steady, inviscid, irrotational motion reduce to a single equation for the velocity vector \bar{U} .

6.5 The velocity potential

The condition $\nabla \times \bar{U} = 0$ implies that the velocity can be expressed in terms of a scalar potential.

$$\bar{U} = \nabla \Phi \quad (6.29)$$

Substitute (6.29) into (6.28). The result is the full potential equation for steady, irrotational flow.

$$(\gamma - 1) \left(h_t - \frac{\nabla \Phi \cdot \nabla \Phi}{2} \right) \nabla^2 \Phi - \nabla \Phi \cdot \nabla \left(\frac{\nabla \Phi \cdot \nabla \Phi}{2} \right) = 0 \quad (6.30)$$

The range of flows where (6.30) applies includes subsonic flow over bodies at Mach numbers below the critical Mach number at which shocks begin to form and supersonic flows that involve smooth expansion and compression such as the flow in a nozzle without shocks.

6.5.1 Unsteady potential flow, the unsteady Bernoulli integral

The irrotational, unsteady momentum equation is, from (6.10),

$$\frac{\partial \bar{U}}{\partial t} + \nabla \left(h + \frac{U^2}{2} + \Psi \right) - T \nabla s - \frac{1}{\rho} \left(\frac{4}{3} \mu + \mu_v \right) \nabla (\nabla \cdot \bar{U}) = 0 \quad (6.31)$$

Insert (6.29) into (6.31). The equation becomes

$$\nabla \left(\frac{\partial \Phi}{\partial t} + h + \frac{U^2}{2} + \Psi \right) - T \nabla s - \frac{1}{\rho} \left(\frac{4}{3} \mu + \mu_v \right) \nabla (\nabla^2 \Phi) = 0 \quad (6.32)$$

If the flow is inviscid,

$$\nabla \left(\frac{\partial \Phi}{\partial t} + h + \frac{U^2}{2} + \Psi \right) - T \nabla s = 0 \quad (6.33)$$

If the flow is inviscid and homentropic (homogeneously isentropic) with $\nabla s = 0$, the unsteady momentum equation reduces to

$$\nabla \left(\frac{\partial \Phi}{\partial t} + h + \frac{U^2}{2} + \Psi \right) = 0 \quad (6.34)$$

The quantity

$$\frac{\partial \Phi}{\partial t} + h + \frac{U^2}{2} + \Psi = F(t) \quad (6.35)$$

which can be at most a function of time is called the unsteady Bernoulli integral and is widely applied in the analysis of unsteady, inviscid, compressible flows.

If the flow is a calorically perfect gas with $h = C_p T$, then (6.35) can be written

$$\frac{\partial \Phi}{\partial t} + \left(\frac{\gamma}{\gamma - 1} \right) \frac{P}{\rho} + \frac{U^2}{2} + \Psi = F(t) \quad (6.36)$$

Generally $F(t)$ can be taken to be a constant independent of time. The sort of unusual situation where it could be time dependent might occur in a closed wind tunnel where the pressure throughout the system was forced to change due to some overall volume change of the tunnel. Such changes can occur but they are usually negligible unless there is some intention to change the volume for a particular purpose, perhaps to exert some form of flow control.

In summary, the equations of inviscid, homentropic flow in terms of the velocity potential are

$$\begin{aligned} \frac{1}{\rho} \frac{\partial \rho}{\partial t} + \frac{\nabla \Phi \cdot \nabla \rho}{\rho} + \nabla^2 \Phi &= 0 \\ \nabla \left(\frac{\partial \Phi}{\partial t} + \left(\frac{\gamma}{\gamma - 1} \right) \frac{P}{\rho} + \frac{\nabla \Phi \cdot \nabla \Phi}{2} + \Psi \right) &= 0 \\ \frac{P}{P_{ref}} &= \left(\frac{\rho}{\rho_{ref}} \right)^{\gamma} \end{aligned} \quad (6.37)$$

Note that the isentropic relation provides the needed equation to close the system in lieu of the energy equation. Equation (6.30) is the steady version of (6.37) all boiled down to one equation for the potential. We can reduce (6.37) to a single equation for the velocity potential as follows.

$$\frac{\partial \Phi}{\partial t} + \left(\frac{\gamma}{\gamma - 1} \right) \frac{P}{\rho} + \frac{\nabla \Phi \cdot \nabla \Phi}{2} + \Psi = F(t) \quad (6.38)$$

Replace the pressure in (6.38) with the density using the isentropic relation.

$$\begin{aligned} \rho &= \left(\frac{\rho_{ref}^{\gamma}}{P_{ref}} \left(\frac{\gamma - 1}{\gamma} \right) \left(F(t) - \frac{\partial \Phi}{\partial t} - \frac{\nabla \Phi \cdot \nabla \Phi}{2} - \Psi \right) \right)^{\left(\frac{1}{\gamma - 1} \right)} \\ \frac{1}{\rho} \frac{\partial \rho}{\partial t} &= \frac{1}{\gamma - 1} \left(\frac{dF(t)}{dt} - \Phi_{tt} - \nabla \Phi_t \cdot \nabla \Phi \right) \left(F(t) - \frac{\partial \Phi}{\partial t} - \frac{\nabla \Phi \cdot \nabla \Phi}{2} - \Psi \right)^{-1} \\ \frac{1}{\rho} \nabla \rho &= \frac{1}{\gamma - 1} \left(-\nabla \Phi_t - \nabla \left(\frac{\nabla \Phi \cdot \nabla \Phi}{2} \right) - \nabla \Psi \right) \left(F(t) - \frac{\partial \Phi}{\partial t} - \frac{\nabla \Phi \cdot \nabla \Phi}{2} - \Psi \right)^{-1} \end{aligned} \quad (6.39)$$

where the body force potential is assumed to be only a function of space. Substitute (6.39) into the continuity equation. The full unsteady potential equation becomes

$$\begin{aligned} \left(\frac{dF(t)}{dt} - \Phi_{tt} - \nabla \Phi_t \cdot \nabla \Phi \right) - \nabla \Phi \cdot \left(\nabla \Phi_t + \nabla \left(\frac{\nabla \Phi \cdot \nabla \Phi}{2} \right) + \nabla \Psi \right) + \\ (\gamma - 1) \left(F(t) - \frac{\partial \Phi}{\partial t} - \frac{\nabla \Phi \cdot \nabla \Phi}{2} - \Psi \right) \nabla^2 \Phi &= 0 \end{aligned} \quad (6.40)$$

6.5.2 Incompressible, irrotational flow

If the flow is incompressible, $\nabla \cdot \bar{U} = 0$, and irrotational, $\bar{\Omega} = 0$, the momentum equation in the absence of gravity, $\Psi = 0$, reduces to,

$$\frac{\partial \bar{U}}{\partial t} + \nabla \left(\frac{\bar{U} \cdot \bar{U}}{2} \right) + \nabla \left(\frac{P}{\rho} \right) = 0 \quad (6.41)$$

Note again that viscous forces, though present, have no effect on the momentum in an incompressible, irrotational flow. Since $\nabla \times \bar{U} = 0$ we can write $\bar{U} = \nabla \Phi$ and in terms of the velocity potential, the momentum equation for incompressible, irrotational flow becomes

$$\nabla \left(\frac{\partial \Phi}{\partial t} + \frac{U^2}{2} + \frac{P}{\rho} \right) = 0 \quad (6.42)$$

The quantity in parentheses is the incompressible form of the Bernoulli integral and, as in the compressible case, is at most a function of time.

$$\frac{\partial \Phi}{\partial t} + \frac{U^2}{2} + \frac{P}{\rho} = F(t) \quad (6.43)$$

An incompressible, irrotational flow (steady or unsteady) is governed by Laplace's equation

$$\nabla \cdot \bar{U} = \nabla^2 \Phi = 0 \quad (6.44)$$

which can be solved using a wide variety of well established techniques. Once the velocity potential Φ is known, the velocity field is generated by differentiation (6.29) and the pressure field is determined from the Bernoulli integral (6.43).

6.6 The vorticity equation

Earlier we cast the momentum equation in terms of the vorticity. Now let's derive a conservation equation for the vorticity itself. If we take the curl of the momentum equation

the result is

$$\nabla \times \left(\frac{\partial \bar{U}}{\partial t} + (\bar{\Omega} \times \bar{U}) + \nabla \left(h + \frac{\bar{U} \cdot \bar{U}}{2} + \Psi \right) - T \nabla s - \left(\frac{1}{\rho} \left(\frac{4}{3}\mu + \mu_v \right) \nabla (\nabla \cdot \bar{U}) + \left(\frac{\mu}{\rho} \right) \nabla \times \bar{\Omega} \right) \right) = 0 \quad (6.45)$$

or

$$\frac{\partial \bar{\Omega}}{\partial t} + \nabla \times (\bar{\Omega} \times \bar{U}) - \nabla \times (T \nabla s) - \left(\frac{4}{3}\mu + \mu_v \right) \nabla \times \left(\frac{\nabla (\nabla \cdot \bar{U})}{\rho} \right) + \mu \nabla \times \left(\frac{\nabla \times \bar{\Omega}}{\rho} \right) = 0 \quad (6.46)$$

Using vector identities, (6.46) can be rearranged to read

$$\frac{\partial \bar{\Omega}}{\partial t} + \bar{U} \cdot \nabla \bar{\Omega} - (\bar{\Omega} \cdot \nabla \bar{U}) + \bar{\Omega} \nabla \cdot \bar{U} - \nabla T \times \nabla s - \left(\frac{4}{3}\mu + \mu_v \right) \nabla \times \left(\frac{\nabla (\nabla \cdot \bar{U})}{\rho} \right) + \mu \nabla \times \left(\frac{\nabla \times \bar{\Omega}}{\rho} \right) = 0 \quad (6.47)$$

For inviscid, homentropic flow, $\nabla s = 0$, $\mu = 0$, $\mu_v = 0$, the vorticity equation reduces to

$$\frac{D \bar{\Omega}}{Dt} = \frac{\partial \bar{\Omega}}{\partial t} + \bar{U} \cdot \nabla \bar{\Omega} = (\bar{\Omega} \cdot \nabla \bar{U}) - \bar{\Omega} \nabla \cdot \bar{U} \quad (6.48)$$

Equation (6.48) is interpreted to mean that, in an inviscid fluid, if the flow is initially irrotational it will always remain irrotational. Conversely, if the flow has vorticity to begin with, then that vorticity can be convected or amplified through stretching or volume change but cannot disappear.

If the flow is incompressible and viscous, the vorticity equation is

$$\frac{D \bar{\Omega}}{Dt} = \frac{\partial \bar{\Omega}}{\partial t} + \bar{U} \cdot \nabla \bar{\Omega} = (\bar{\Omega} \cdot \nabla \bar{U}) + \left(\frac{\mu}{\rho} \right) \nabla^2 \bar{\Omega} \quad (6.49)$$

For planar, two-dimensional flow, $(\bar{\Omega} \cdot \nabla) \bar{U} = 0$ and there is only one non-zero component of the vorticity, Ω_z , which satisfies the diffusion equation

$$\frac{D\Omega_z}{Dt} = \left(\frac{\mu}{\rho} \right) \left(\frac{\partial^2 \Omega_z}{\partial x^2} + \frac{\partial^2 \Omega_z}{\partial y^2} \right) \quad (6.50)$$

This equation is of the same form as the incompressible equation for the transport of the temperature. See the energy equation in (6.2) with the viscous dissipation term neglected.

$$\frac{DT}{Dt} = \left(\frac{\kappa}{\rho} \right) \nabla^2 T \quad (6.51)$$

In two dimensions vorticity diffuses like a scalar such as temperature or concentration. But note that vorticity can be positive or negative and where mixing between opposite signs occurs, vorticity can disappear through diffusion. In three-dimensional flow, the vorticity can be amplified or reduced due to vortex stretching or compression arising from the nonlinear term $(\bar{\Omega} \cdot \nabla) \bar{U}$.

6.7 Fluid flow in three dimensions, the dual stream function

The equations for particle paths in a three-dimensional, steady fluid flow are

$$\begin{aligned} \frac{dx}{dt} &= U(x, y, z) \\ \frac{dy}{dt} &= V(x, y, z) \\ \frac{dz}{dt} &= W(x, y, z) \end{aligned} \quad (6.52)$$

The particle paths are determined by integrating (6.52)

$$\begin{aligned} x &= f(\tilde{x}, \tilde{y}, \tilde{z}, t) \\ y &= g(\tilde{x}, \tilde{y}, \tilde{z}, t) \\ z &= h(\tilde{x}, \tilde{y}, \tilde{z}, t) \end{aligned} \quad (6.53)$$

where $(\tilde{x}, \tilde{y}, \tilde{z})$ is the vector coordinate of a particle at $t = 0$. Elimination of t among these three relations leads to two infinite families of integral surfaces; the dual stream-function surfaces

$$\begin{aligned}\psi_1 &= \Psi_1(x, y, z) \\ \psi_2 &= \Psi_2(x, y, z)\end{aligned}\tag{6.54}$$

The total differential of the stream function is

$$d\psi = \frac{\partial \Psi}{\partial x} dx + \frac{\partial \Psi}{\partial y} dy + \frac{\partial \Psi}{\partial z} dz\tag{6.55}$$

Use (6.52) to replace the differentials in (6.55) and note that on a stream surface $d\psi = 0$, the stream-functions (6.54) are each integrals of the first order PDE

$$\bar{U} \cdot \nabla \Psi_j = U \frac{\partial \Psi_j}{\partial x} + V \frac{\partial \Psi_j}{\partial y} + W \frac{\partial \Psi_j}{\partial z} \quad j = 1, 2\tag{6.56}$$

A given initial point, $(\tilde{x}, \tilde{y}, \tilde{z})$, defines two stream-surfaces. The velocity vector through the point lies along the intersection of the surfaces as implied by (6.56) and shown in figure 6.1.

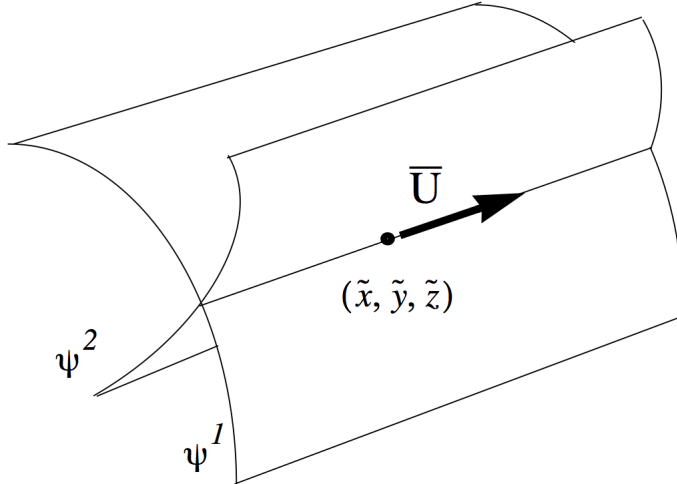


Figure 6.1: *Dual stream-function surfaces.*

Given the dual stream-functions, the velocity field can be reconstructed from

$$\bar{U} = \nabla\Psi_1 \times \nabla\Psi_2 \quad (6.57)$$

6.8 The vector potential

The velocity field of an incompressible flow can be represented as the curl of a vector potential, \bar{A} also called the vector stream function.

$$\bar{U} = \nabla \times \bar{A} \quad (6.58)$$

Use of the vector potential in (6.58) guarantees that the incompressibility condition $\nabla \cdot \bar{U} = 0$ is satisfied. In two-dimensional flow only the out-of-plane component of \bar{A} is nonzero and this corresponds to the stream function discussed in Chapter 1. Take the curl of (6.58).

$$\nabla \times \bar{U} = \nabla \times (\nabla \times \bar{A}) \quad (6.59)$$

Now use the vector identity

$$\nabla(\nabla \cdot \bar{A}) - \nabla^2 \bar{A} = \nabla \times (\nabla \times \bar{A}) \quad (6.60)$$

Equation (6.59) becomes

$$\bar{\Omega} = \nabla(\nabla \cdot \bar{A}) - \nabla^2 \bar{A} \quad (6.61)$$

6.8.1 Selection of a Coulomb gauge

There is a certain arbitrariness to the vector potential and we can take advantage of this to simplify (6.61). Suppose we add the gradient of a scalar function to the vector potential. Let

$$\bar{A}' = \bar{A} + \nabla f \quad (6.62)$$

Since $\bar{\nabla} \times \bar{\nabla} f \equiv 0$ the velocity field generated by A' or A is identically the same.

$$\nabla \times \bar{A}' = \nabla \times \bar{A} \quad (6.63)$$

Imagine that we are given A' . We can always find a function f such that

$$\nabla \cdot \bar{A}' = \nabla^2 f \quad (6.64)$$

which implies that

$$\nabla \cdot \bar{A} = 0 \quad (6.65)$$

This is called choosing a *Coloumb gauge* for \bar{A} . In effect we are free to impose the condition (6.65) on \bar{A} without affecting the velocity field generated from \bar{A} when we take the curl.

Using (6.65) in (6.61) generates the Poisson equation for the vector potential.

$$\nabla^2 \bar{A} = -\bar{\Omega} \quad (6.66)$$

In order for (6.66) to be useful one has to be given the vorticity field Ω . The vector potential is then determined using standard techniques for solving equations of Poisson type. The velocity field is then generated by taking the curl.

The vector potential is directly related to the dual stream-functions discussed in the previous section.

$$\bar{A} = \Psi_1 \nabla \Psi_2 = -\Psi_2 \nabla \Psi_1 \quad (6.67)$$

6.9 Incompressible flow with mass and vorticity sources

Consider an incompressible flow constructed from a distribution of mass sources, $Q(x, t)$ and distributed sources of vorticity, $\bar{\Omega}(x, t)$. The velocity field is constructed from a linear superposition of two fields.

$$\bar{U} = \bar{U}_{sources} + \bar{U}_{vortices} \quad (6.68)$$

The velocity field generated by the mass sources is irrotational and that generated by the vorticity sources is divergence free. The continuity equation for such a flow has a source term

$$\nabla \cdot \bar{U} = \nabla \cdot \bar{U}_{sources} = Q(\bar{x}, t) \quad (6.69)$$

and the curl of the velocity is

$$\nabla \times \bar{U} = \nabla \times \bar{U}_{vortices} = \bar{\Omega}(\bar{x}, t) \quad (6.70)$$

In terms of the potentials the velocity field is

$$\bar{U} = \nabla \Phi + \nabla \times \bar{A} \quad (6.71)$$

The potentials satisfy the system of Poisson equations

$$\begin{aligned} \nabla^2 \Phi &= Q(\bar{x}, t) \\ \nabla^2 \bar{A} &= -\bar{\Omega}(\bar{x}, t) \end{aligned} \quad (6.72)$$

This approach allows one to construct fairly complex flow fields that can be rotational while retaining the simplicity of working in terms of potentials governed by linear equations (6.72) and the associated law of superposition (6.68). Notice that the theory of potential flow is exactly analogous to the theory of potentials in electricity and magnetism. The mass sources coincide with the distribution of electric charges and the vorticity coincides with the electric currents.

6.10 Turbulent flow

Turbulent flows are characterized by unsteady eddying motions with a wide range of scales superimposed on a slowly changing or steady mean flow. The eddies mix fluid rapidly and are responsible for much higher rates of mass, momentum and heat transport than would occur if the flow was laminar. The primary difficulty with analyzing or numerically computing turbulent flows stems from the fact that, at high Reynolds number, the range of scales involved can be very large with velocity gradients at the finest scale, where most kinetic energy dissipation occurs, of order Re larger than the gradients at the largest scale that drive the flow. Computations designed to fully simulate the flow must be resolved on such a fine grid that often only a few simulations can be carried out even at moderate

Reynolds number. Very high Reynolds numbers are still beyond todays largest computers. Experiments designed to measure a turbulent flow are faced with a similar challenge requiring extremely small measurement volumes as well as the ability to measure over a large field comparable to the overall size of the flow.

Recall the equations of motion, repeated here for convenience

$$\begin{aligned} \frac{\partial \rho}{\partial t} + \frac{\partial}{\partial x_i} (\rho U_i) &= 0 \\ \frac{\partial \rho U_i}{\partial t} + \frac{\partial}{\partial x_j} \left(\rho U_i U_j + P \delta_{ij} - 2\mu S_{ij} + \left(\frac{2}{3}\mu - \mu_v \right) \delta_{ij} S_{kk} \right) - \rho G_i &= 0 \\ \frac{\partial \rho (e + k)}{\partial t} + \frac{\partial}{\partial x_i} \left(\rho U_i h_t - \kappa (\partial T / \partial x_i) - 2\mu U_j S_{ij} + \left(\frac{2}{3}\mu - \mu_v \right) \delta_{ij} U_j S_{kk} \right) - \rho U_i G_i &= 0 \end{aligned} \quad (6.73)$$

In this section we will discuss an alternative to fully resolving the unsteady flow introduced by Osborne Reynolds in 1895 in which each flow variable is decomposed into a mean and fluctuating part. When the equations of motion are suitably averaged, the result is a new set of equations that relate the mean flow to the correlated part of the fluctuating motion.

Imagine an ensemble of realizations of the time dependent flow that all satisfy the same set of initial and boundary conditions, perhaps in the form of a series of laboratory experiments repeated over and over. Decompose each flow variable into an ensemble mean and a fluctuation

$$F(x, y, z, t) = \hat{F}(x, y, z, t) + F'(x, y, z, t) \quad (6.74)$$

where F is a generic variable. The mean is defined by

$$\hat{F} = \frac{1}{N} \sum_{n=1}^N F_n \quad (6.75)$$

where the number of realizations of the flow is N and the index refers to the n th member of the ensemble. All members of the ensemble are aligned to have the same time origin and evolve with the same clock which is reset each time a new realization is initiated.

Apply the decomposition and averaging to a linear term in the equations of motion such as

$$\widehat{\frac{\partial}{\partial x_j} (P \delta_{ij})} = \frac{\partial}{\partial x_j} \left(\widehat{(\hat{P} + P')} \delta_{ij} \right) = \frac{\partial}{\partial x_j} (\hat{P} \delta_{ij}) + \widehat{\frac{\partial}{\partial x_j} (P' \delta_{ij})} = \frac{\partial}{\partial x_j} (\hat{P} \delta_{ij}) \quad (6.76)$$

Any term that is linear in the fluctuation is zero. Nonlinear terms are more complex. The decomposition of the density, pressure and velocity is

$$\begin{aligned} \rho &= \hat{\rho} + \rho' \\ P &= \hat{P} + P' \\ U &= \hat{U} + U' \\ V &= \hat{V} + V' \\ W &= \hat{W} + W' \end{aligned} \quad (6.77)$$

Consider averaging the momentum flux term ρUV .

$$\begin{aligned} \widehat{\rho UV} &= (\hat{\rho} + \rho') \left(\widehat{\hat{U} + U'} \right) \left(\widehat{\hat{V} + V'} \right) = \\ &= \widehat{\hat{\rho} \hat{U} \hat{V}} + \widehat{\rho' \hat{U} \hat{V}} + \widehat{\hat{\rho} U' \hat{V}} + \widehat{\rho' U' \hat{V}} + \widehat{\hat{\rho} \hat{U} V'} + \widehat{\rho' \hat{U} V'} + \widehat{\hat{\rho} U' V'} + \widehat{\rho' U' V'} = \\ &= \widehat{\hat{\rho} \hat{U} \hat{V}} + \widehat{\rho' U' \hat{V}} + \widehat{\rho' \hat{V}' \hat{U}} + \widehat{\hat{\rho} U' V'} + \widehat{\rho' U' V'} \end{aligned} \quad (6.78)$$

The transformation of the kinetic energy is

$$\widehat{\rho UV} = \hat{\rho} \hat{U} \hat{V} + \left(\widehat{\rho' U' \hat{V}} + \widehat{\rho' \hat{V}' \hat{U}} + \widehat{\hat{\rho} U' V'} + \widehat{\rho' U' V'} \right) = \hat{\rho} \hat{U} \hat{V} + \tau_{xy}|_{turbulent} \quad (6.79)$$

The terms in parentheses can be thought of as effective stresses due to the background fluctuations. Similar terms arise when generating the turbulent normal stresses in compressible flow

$$\begin{aligned} \widehat{\rho UU} &= \hat{\rho} \hat{U} \hat{U} + \left(2 \widehat{\rho' U' \hat{U}} + \widehat{\hat{\rho} U' U'} + \widehat{\rho' U' U'} \right) = \hat{\rho} \hat{U} \hat{U} + \tau_{xx}|_{turbulent} \\ \widehat{\rho VV} &= \hat{\rho} \hat{V} \hat{V} + \left(2 \widehat{\rho' V' \hat{V}} + \widehat{\hat{\rho} V' V'} + \widehat{\rho' V' V'} \right) = \hat{\rho} \hat{V} \hat{V} + \tau_{yy}|_{turbulent} \end{aligned} \quad (6.80)$$

Time dependent terms are ensemble averaged in the same way.

$$\begin{aligned}\widehat{\frac{\partial \rho}{\partial t}} &= \frac{1}{N} \sum_{n=1}^N \left. \frac{\partial \rho}{\partial t} \right|_n = \frac{\partial \hat{\rho}}{\partial t} + \widehat{\frac{\partial \rho'}{\partial t}} = \frac{\partial \hat{\rho}}{\partial t} \\ \widehat{\frac{\partial \rho U_i}{\partial t}} &= \frac{1}{N} \sum_{n=1}^N \left. \frac{\partial \rho U_i}{\partial t} \right|_n = \frac{\partial \hat{\rho} \hat{U}_i}{\partial t} + \widehat{\frac{\partial \rho' \hat{U}_i}{\partial t}} + \widehat{\frac{\partial \hat{\rho} U'_i}{\partial t}} + \widehat{\frac{\partial \rho' U'_i}{\partial t}} = \frac{\partial \hat{\rho} \hat{U}_i}{\partial t} + \widehat{\frac{\partial \rho' U'_i}{\partial t}}\end{aligned}\quad (6.81)$$

Since fluid properties such as μ , $m u_v$ and κ are temperature dependent they must also be included in the decomposition and averaging process.

6.10.1 Turbulent, incompressible, isothermal flow

If the flow is incompressible, the density is constant. If the temperature is also constant the equations of motion simplify to

$$\begin{aligned}\frac{\partial U_j}{\partial x_j} &= 0 \\ \frac{\partial U_i}{\partial t} + \frac{\partial U_i U_j}{\partial x_j} + \frac{1}{\rho} \frac{\partial P}{\partial x_i} - \left(\frac{\mu}{\rho} \right) \frac{\partial^2 U_i}{\partial x_j \partial x_j} &= 0\end{aligned}\quad (6.82)$$

Substitute the Reynolds decomposition (6.77) with density constant into (6.82) and ensemble average the equations.

$$\begin{aligned}\frac{\partial \hat{U}_j}{\partial x_j} &= 0 \\ \frac{\partial \hat{U}_i}{\partial t} + \frac{\partial \hat{U}_i \hat{U}_j}{\partial x_j} + \frac{\partial \widehat{U'_i U'_j}}{\partial x_j} + \frac{1}{\rho} \frac{\partial \hat{P}}{\partial x_i} - \left(\frac{\mu}{\rho} \right) \frac{\partial^2 \hat{U}_i}{\partial x_j \partial x_j} &= 0\end{aligned}\quad (6.83)$$

In incompressible flow the only nonlinear term is the convective term and the only term involving the fluctuations is the third term which can be viewed as an effective turbulent stress term, the Reynolds stress.

$$\tau_{ij}|_{turbulent} = -\rho \widehat{U'_i U'_j} \quad (6.84)$$

The advantage of this approach is that the entire unsteady motion does not need to be resolved, only the correlations (6.84) are needed. The fundamental difficulty is that the Reynolds stresses constitute an additional set of unknowns and the equations (6.83) are unclosed. The field of turbulence modeling is basically all about searching for model equations that can be used to relate the Reynolds stresses to the mean flow so the system (6.83) can be closed.

In free shear flows the laminar stress term in (6.83), $\mu \partial^2 U_i / \partial x_j \partial x_j$ is generally much smaller than the Reynolds stress term and some simplification can be achieved by neglecting the viscous term in the momentum equation altogether. In wall bounded flows this cannot be done. The Reynolds stresses tend to dominate the flow away from the wall but near the wall the velocity fluctuations are damped to zero and the viscous stress term is responsible for the friction on the wall. We will have more to say about the flow near a wall in Chapter 8.

6.11 Problems

Problem 1 - Derive equation (6.6) beginning with the Navier-Stokes equations. Do the same for equation (6.47).

Problem 2 - Show that for homentropic flow of an ideal gas $\nabla P = a^2 \nabla \rho$ where a is the local speed of sound.

Chapter 7

Entropy generation and transport

7.1 Convective form of the Gibbs equation

In this chapter we will address two questions.

- 1) How is Gibbs equation related to the energy conservation equation?
- 2) How is the entropy of a fluid affected by its motion?

We have touched on the latter questions several times in this text but without a rigorous analysis. In this chapter the precise form of the flow properties that represent the sources of entropy will be derived from first principles. In this endeavor we will use the Gibbs equation on a fluid element.

$$T \frac{Ds}{Dt} = \frac{De}{Dt} + P \frac{Dv}{Dt} \quad (7.1)$$

The Navier-Stokes equations are the foundation of the science of fluid mechanics. With the inclusion of an equation of state, virtually all flow solving revolves around finding solutions of the Navier-Stokes equations. Most exceptions involve fluids where the relation between stress and rate-of-strain is nonlinear such as polymers, or where the equation of state is not very well understood (for example supersonic flow in water) or rarefied flows where the Boltzmann equation must be used to explicitly account for particle collisions. The equations can take on many forms depending on what approximations or assumptions may be appropriate to a given flow. In addition, transforming the equations to different forms may enable one to gain insight into the nature of the solutions. It is essential to learn the

many different forms of the equations and to become practiced in the manipulations used to transform them.

7.2 The kinetic energy equation

To answer these questions we first need to form a conservation equation for the kinetic energy. This can be accomplished by manipulating the momentum and continuity equations. Multiply the momentum equation by U_i (sum over i).

$$U_i \frac{\partial \rho U_i}{\partial t} + U_i \frac{\partial}{\partial x_j} (\rho U_i U_j + P \delta_{ij} - \tau_{ij}) - \rho U_i G_i = 0 \quad (7.2)$$

First let's look at the temporal and convective terms in this equation.

$$\begin{aligned} & U_i \frac{\partial (\rho U_i)}{\partial t} + U_i \frac{\partial (\rho U_i U_j)}{\partial x_j} = \\ & U_i U_i \frac{\partial \rho}{\partial t} + U_i \rho \frac{\partial U_i}{\partial t} + U_i U_i U_j \frac{\partial \rho}{\partial x_j} + \rho U_i U_i \frac{\partial U_j}{\partial x_j} + \rho U_i U_j \frac{\partial U_i}{\partial x_j} \end{aligned} \quad (7.3)$$

The sum of the underlined terms is zero by continuity. Thus

$$U_i \frac{\partial (\rho U_i)}{\partial t} + U_i \frac{\partial (\rho U_i U_j)}{\partial x_j} = \rho \frac{\partial k}{\partial t} + \rho U_j \frac{\partial k}{\partial x_j} \quad (7.4)$$

where, $k = U_i U_i / 2$. Use continuity again in the form,

$$k \frac{\partial \rho}{\partial t} + k U_j \frac{\partial \rho}{\partial x_j} + k \rho \frac{\partial U_j}{\partial x_j} = 0 \quad (7.5)$$

Add the above two equations to get the temporal-convective part of the kinetic energy equation.

$$U_i \frac{\partial (\rho U_i)}{\partial t} + U_i \frac{\partial (\rho U_i U_j)}{\partial x_j} = \frac{\partial (\rho k)}{\partial t} + \frac{\partial (\rho k U_j)}{\partial x_j} \quad (7.6)$$

Now let's rearrange the pressure term.

$$U_i \frac{\partial (P \delta_{ij})}{\partial x_j} = \frac{\partial (P U_j)}{\partial x_j} - P \frac{\partial U_j}{\partial x_j} \quad (7.7)$$

and the viscous stress term

$$U_i \frac{\partial \tau_{ij}}{\partial x_j} = \frac{\partial (U_i \tau_{ij})}{\partial x_j} - \tau_{ij} \frac{\partial U_i}{\partial x_j} \quad (7.8)$$

which we derived in Chapter 2.

Finally, the kinetic energy equation is

$$\frac{\partial (\rho k)}{\partial t} + \frac{\partial}{\partial x_j} (\rho U_j k + P U_j - U_i \tau_{ij}) = \rho U_j G_j + P \frac{\partial U_j}{\partial x_j} - \tau_{ij} \frac{\partial U_i}{\partial x_j} \quad (7.9)$$

7.3 Internal energy

When the kinetic energy equation (7.9) is subtracted from the energy equation (7.2) the result is the conservation equation for internal energy.

$$\frac{\partial (\rho e)}{\partial t} + \frac{\partial}{\partial x_j} (\rho U_j e + Q_j) = -P \frac{\partial U_j}{\partial x_j} + \tau_{ij} \frac{\partial U_i}{\partial x_j} \quad (7.10)$$

Note that both of these equations are in the general conservation form

$$\frac{\partial (\)}{\partial t} + \nabla \cdot (\) = \text{sources} \quad (7.11)$$

The series of steps used to generate these equations are pretty standard and illustrate that the equations of motion can be (and often are) manipulated to create a conservation equation for practically any variable we wish.

The source term

$$P \frac{\partial U_j}{\partial x_j} = P \nabla \cdot \bar{U} \quad (7.12)$$

appears in both the kinetic and internal energy equations with opposite sign. It can be either positive or negative depending on the whether the fluid is expanding or being compressed. Recall the continuity equation in the form

$$\frac{1}{\rho} \frac{D\rho}{Dt} = -\nabla \cdot \bar{U} \quad (7.13)$$

Multiply by the pressure

$$P \nabla \cdot \bar{U} = -\frac{P}{\rho} \frac{D\rho}{Dt} = \rho \left(P \frac{Dv}{Dt} \right) \quad (7.14)$$

The term in parentheses we recognize as the work term in the Gibbs equation (the whole term is actually the work per second per unit volume). This term represents a reversible exchange between internal and kinetic energy due to the work of compression or expansion of a fluid element.

7.3.1 Viscous dissipation of kinetic energy

Now let's look at the term

$$\Phi = \tau_{ij} \frac{\partial U_i}{\partial x_j} \quad (7.15)$$

This needs to be worked a little further. Substitute the expression for the Newtonian stress tensor and decompose the velocity gradient into a symmetric and antisymmetric part.

$$\Phi = \left(2\mu S_{ij} - \left(\frac{2}{3}\mu - \mu_v \right) \delta_{ij} S_{kk} \right) (S_{ij} + W_{ij}) \quad (7.16)$$

The sum over the antisymmetric part is zero. Thus

$$\Phi = 2\mu (S_{ij} S_{ij}) - \frac{2}{3}\mu (S_{ii} S_{kk}) + \mu_v (S_{ii} S_{kk}) \quad (7.17)$$

We can write the first two terms as a square.

$$\Phi = 2\mu \left(S_{ij} - \frac{1}{3}\delta_{ij} S_{kk} \right) \left(S_{ij} - \frac{1}{3}\delta_{ij} S_{kk} \right) + \mu_v (S_{ii} S_{kk}) \quad (7.18)$$

The scalar quantity, Φ , is the viscous dissipation of kinetic energy and it is clear from the fact that (7.18) is a sum of squares that it is always positive. The dissipation term appears as a sink in the kinetic energy equation and as a source in the internal energy equation. It is the irreversible conversion of kinetic energy to internal energy due to viscous friction.

We can attach two physical interpretations to Stokes' hypothesis; the assumption that $\mu_v = 0$. Recall that the mean normal stress is

$$\sigma_{mean} = (1/3) \sigma_{ii} = -P + \mu_v S_{kk} \quad (7.19)$$

In terms of flow forces, Stokes' hypothesis implies that, in a viscous Newtonian fluid, the mean normal stress is everywhere equal to the pressure.

We can give a second interpretation to Stokes' hypothesis in terms of flow energy by noting that

$$\text{trace}(S_{ij} - (1/3) \delta_{ij} S_{kk}) = 0 \quad (7.20)$$

Under Stokes' hypothesis the second term in the dissipation expression (7.18) is zero and the only contributor to kinetic energy dissipation is the anisotropic (off diagonal) part of the rate of strain tensor.

7.4 Entropy

We are now in a position to say something about the entropy of the system. Recall the Gibbs equation.

$$\rho \frac{De}{Dt} - \left(\frac{P}{\rho} \right) \frac{D\rho}{Dt} = \rho T \frac{Ds}{Dt} \quad (7.21)$$

Write the internal energy equation,

$$\frac{\partial \rho e}{\partial t} + \frac{\partial}{\partial x_j} (\rho U_j e + Q_j) = -P \frac{\partial U_j}{\partial x_j} + \Phi \quad (7.22)$$

in terms of the substantial derivative.

$$\rho \frac{De}{Dt} + P \frac{\partial U_j}{\partial x_j} = -\frac{\partial Q_j}{\partial x_j} + \Phi \quad (7.23)$$

We have already written down the continuity equation in the form required to replace the second term on the left hand side.

$$\left(\frac{P}{\rho} \right) \frac{D\rho}{Dt} = -P \frac{\partial U_j}{\partial x_j} \quad (7.24)$$

The energy equation now becomes

$$\rho \frac{De}{Dt} - \left(\frac{P}{\rho} \right) \frac{D\rho}{Dt} = -\frac{\partial Q_j}{\partial x_j} + \Phi \quad (7.25)$$

Comparing this form of the energy equation with the Gibbs equation, we see that the left-hand-side corresponds to the entropy term

$$\rho T \frac{Ds}{Dt} = -\frac{\partial Q_j}{\partial x_j} + \Phi \quad (7.26)$$

Let's put this in the form of a conservation equation for the entropy. The approach is to use the continuity equation yet again!

$$\begin{aligned} \rho \frac{\partial s}{\partial t} + \rho U_j \frac{\partial s}{\partial x_j} &= -\frac{1}{T} \frac{\partial Q_j}{\partial x_j} + \frac{\Phi}{T} \\ s \frac{\partial \rho}{\partial t} + s U_j \frac{\partial \rho}{\partial x_j} + s \rho \frac{\partial U_j}{\partial x_j} &= 0 \end{aligned} \quad (7.27)$$

Add the two equations in (7.28) to get

$$\frac{\partial \rho s}{\partial t} + \frac{\partial}{\partial x_j} (\rho U_j s) = -\frac{1}{T} \frac{\partial Q_j}{\partial x_j} + \frac{\Phi}{T} \quad (7.28)$$

The heat flux term can be rearranged into a divergence term and a squared term.

$$\frac{\partial}{\partial x_j} \left(\frac{Q_j}{T} \right) = \frac{1}{T} \frac{\partial Q_j}{\partial x_j} - \frac{Q_j}{T^2} \frac{\partial T}{\partial x_j} \quad (7.29)$$

For a linear conducting material, the heat flux is

$$Q_j = -k \frac{\partial T}{\partial x_j} \quad (7.30)$$

Let

$$\Upsilon = \frac{k}{T} \left(\frac{\partial T}{\partial x_j} \frac{\partial T}{\partial x_j} \right) \quad (7.31)$$

Finally, the conservation equation for the entropy becomes

$$\frac{\partial \rho s}{\partial t} + \frac{\partial}{\partial x_j} \left(\rho U_j s - \frac{k}{T} \frac{\partial T}{\partial x_j} \right) = \frac{\Upsilon + \Phi}{T} \quad (7.32)$$

The integral form of the entropy transport equation on a general control volume is

$$\frac{D}{Dt} \int_{V(t)} \rho s dV + \int_{A(t)} \left(\rho (U_j - U_{A_j}) s - \frac{k}{T} \frac{\partial T}{\partial x_j} \right) n_j dA = \int_{V(t)} \left(\frac{\Upsilon + \Phi}{T} \right) dV \quad (7.33)$$

The right hand side of (7.32) is the entropy source term and is always positive. This remarkable result provides an explicit expression (in terms of squared temperature gradients and squared velocity gradients) for the irreversible changes in entropy that occur in a compressible flow. Notice that the body force term contributes nothing to the entropy.

Consider a closed adiabatic box containing a viscous, heat conducting fluid subject to the no slip condition on the walls. The fluid is stirred by a fan that is then turned off and the flow is allowed to settle.

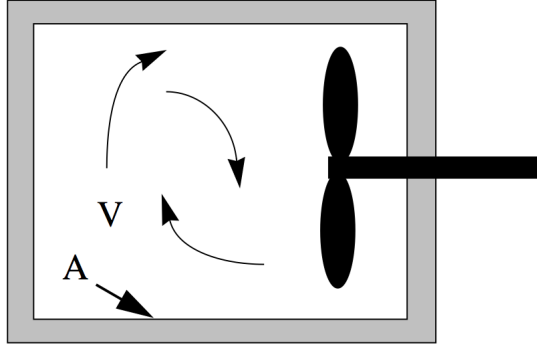


Figure 7.1: Fluid stirred in an adiabatic box.

The entropy of the fluid in the box behaves according to

$$\frac{D}{Dt} \int_V \rho s dV + \int_A \left(\rho U_j s - \frac{k}{T} \frac{\partial T}{\partial x_j} \right) n_j dA = \int_V \left(\frac{\Upsilon + \Phi}{T} \right) dV \quad (7.34)$$

The surface integral is zero by the no-slip condition and the assumption of adiabaticity. The

volume integral of the density times the intensive entropy is the extensive entropy.

$$S = \int_V \rho s dV \quad (7.35)$$

Thus as the closed, adiabatic, system comes to rest, the entropy continues to increase until all the gradients in velocity and temperature have vanished.

$$\frac{dS}{dt} = \int_V \left(\frac{\Upsilon + \Phi}{T} \right) dV > 0 \quad (7.36)$$

7.5 Problems

Problem 1 - Show that (7.17) can be expressed in the form (7.18).

Problem 2 - Imagine a spherically symmetric flow in the absence of shear.

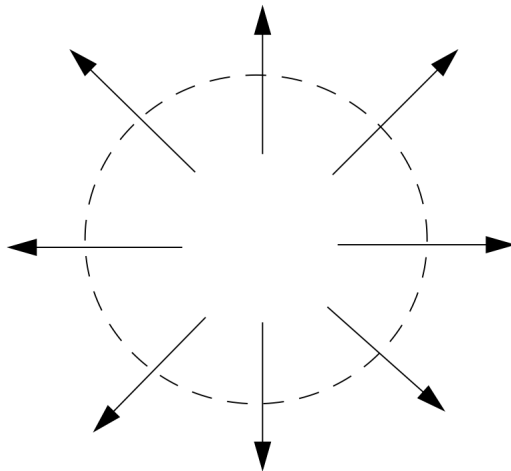


Figure 7.2: Radially directed viscous flow.

Let the fluid velocity in the radial direction be $f(r)$. Work out the expression for the kinetic energy dissipation in terms of f and the two viscosities μ and μ_v . Suppose the fluid is a monatomic gas for which $\mu_v = 0$. Does there exist a function f for which the dissipation is zero? Refer to Appendix B for the dissipation function in spherical polar coordinates.

Problem 3 - Suppose the fluid in the box shown in Section 7.5 is Air initially at 300 K and one atmosphere. Let the tip velocity of the propeller be 50 m/sec and the typical

boundary layer thickness over the surface of the propeller be 1 *millimeter*. The surface area of the propeller is 1 m^2 and the volume of the box is 1 m^3 . Roughly estimate the rate at which the temperature of the air in the box increases due to viscous dissipation.

Problem 4 - A simple pendulum of mass $m = 1.0 \text{ kilogram}$ is placed inside a rigid adiabatic container filled with 0.1 kilograms of Helium gas initially at rest (state 1). The gas pressure is one atmosphere and the temperature is 300 K . The acceleration due to gravity is $g = 9.8 \text{ meters/sec}^2$.

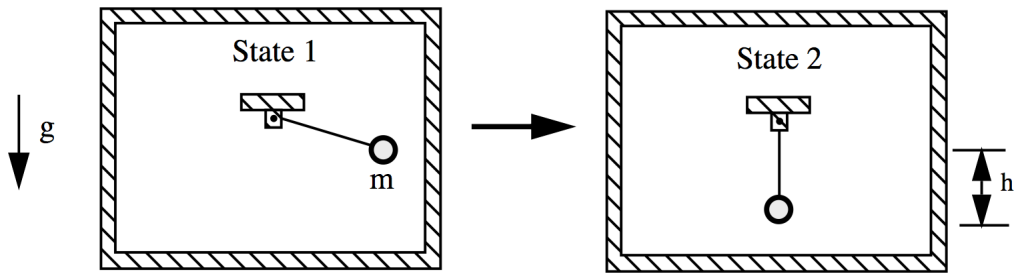


Figure 7.3: Pendulum released from rest in a viscous fluid in an adiabatic box.

At $t = 0$ the pendulum is released from an initial displacement height $h = 0.1 \text{ meters}$ and begins to oscillate and stir the gas. Eventually the pendulum and gas all come to rest (state 2).

- 1) Assume all the potential energy of the pendulum is converted to internal energy of the gas. What is the change in temperature of the Helium in going from state 1 to state 2?
- 2) What is the change in entropy per unit mass of the Helium in going from state 1 to state 2?

Chapter 8

Viscous flow along a wall

8.1 The no-slip condition

All liquids and gases are viscous and, as a consequence, a fluid near a solid boundary sticks to the boundary. The tendency for a liquid or gas to stick to a wall arises from momentum exchanged during molecular collisions with the wall. Viscous friction profoundly changes the fluid flow over a body compared to the ideal inviscid approximation that is widely applied in aerodynamic theory. Figure 8.1 below illustrates the effect of the no-slip condition on the flow over a curved boundary. Later we will see how the velocity U_e at the wall derived from irrotational flow theory is used as the outer boundary condition for the equations that govern the thin region of rotational flow near the wall imposed by the no-slip condition. This thin layer is called the boundary layer.

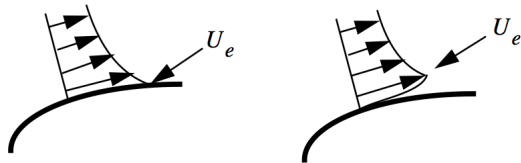


Figure 8.1: *Slip versus no-slip flow near a solid surface.*

The presence of low speed flow near the surface of a wing can lead to flow separation or stall. Separation can produce large changes in the pressure field surrounding the body leading to a decrease in lift and an increase in pressure related drag. The pressure drag due to stall may be much larger than the drag due to skin friction. In a supersonic flow the no-slip condition insures that there is always a subsonic flow near the wall enabling pressure disturbances to propagate upstream through the boundary layer. This may cause

flow separation and shock formation leading to increased wave drag. In Appendix A we worked out the mean free path between collisions in a gas

$$\lambda = \frac{1}{\sqrt{2\pi n\sigma^2}} \quad (8.1)$$

where n is the number of molecules per unit volume and σ is the collision diameter of the molecule. On an atomic scale all solid materials are rough and adsorb or retard gas molecules near the surface. When a gas molecule collides with a solid surface a certain fraction of its momentum parallel to the surface is lost due to Van der Walls forces and interpenetration of electron clouds with the molecules at the solid surface. Collisions of a rebounding gas molecule with other gas molecules within a few mean free paths of the surface will slow those molecules and cause the original molecule to collide multiple times with the surface. Within a few collision times further loss of tangential momentum will drop the average molecular velocity to zero. At equilibrium, the velocity of the gas within a small fraction of a mean free path of the surface and the velocity of the surface must match.

The exception to this occurs in the flow of a rarified gas where the distance a molecule travels after a collision with the surface is so large that a return to the surface may never occur and equilibrium is never established. In this case there is a slip velocity that can be modeled as

$$v_{slip} = C\lambda \frac{\partial U}{\partial y} \quad (8.2)$$

where C is a constant of order one. The slip velocity is negligible for typical values of the mean free path in gases of ordinary density. In situations where the velocity gradient is extremely large as in some gas lubrication flows there can be significant slip even at ordinary densities. For similar reasons there can be a discontinuity in temperature between the wall and gas in rarified flows or very high shear rate flows.

In this Chapter we will discuss two fundamental problems involving viscous flow along a wall at ordinary density and shear rate. The first is plane Couette flow between two parallel plates where the flow is perfectly parallel. This problem can be solved exactly. The second is the plane boundary layer along a wall where the flow is almost but not quite perfectly parallel. In this case an approximate solution to the equations of motion can be determined.

8.2 Equations of motion

Recall the equations of motion in Cartesian coordinates from Chapter 1; In the absence of body forces and internal sources of energy

Conservation of mass

$$\frac{\partial \rho}{\partial t} + \frac{\partial \rho U}{\partial x} + \frac{\partial \rho V}{\partial y} + \frac{\partial \rho W}{\partial z} = 0$$

Conservation of momentum

$$\begin{aligned} \frac{\partial \rho U}{\partial t} + \frac{\partial (\rho UU + P - \tau_{xx})}{\partial x} + \frac{\partial (\rho UV - \tau_{xy})}{\partial y} + \frac{\partial (\rho UW - \tau_{xz})}{\partial z} &= 0 \\ \frac{\partial \rho V}{\partial t} + \frac{\partial (\rho VU - \tau_{xy})}{\partial x} + \frac{\partial (\rho VV + P - \tau_{yy})}{\partial y} + \frac{\partial (\rho VW - \tau_{yz})}{\partial z} &= 0 \\ \frac{\partial \rho W}{\partial t} + \frac{\partial (\rho WU - \tau_{xz})}{\partial x} + \frac{\partial (\rho WV - \tau_{yz})}{\partial y} + \frac{\partial (\rho WW + P - \tau_{zz})}{\partial z} &= 0 \end{aligned} \quad (8.3)$$

Conservation of energy

$$\begin{aligned} \frac{\partial \rho (e + k)}{\partial t} + \frac{\partial (\rho (e + k) U + PU - \tau_{xx}U - \tau_{xy}V - \tau_{xz}W + Q_x)}{\partial x} \\ \frac{\partial (\rho (e + k) V + PV - \tau_{yx}U - \tau_{yy}V - \tau_{yz}W + Q_y)}{\partial y} \\ \frac{\partial (\rho (e + k) W + PW - \tau_{zx}U - \tau_{zy}V - \tau_{zz}W + Q_z)}{\partial z} = \end{aligned}$$

{Power generation due to energy sources inside the control volume}.

Throughout this chapter we will be looking at the steady flow over a flat wall and so the first simplification is to reduce the problem to the equations governing steady flow in two

space dimensions.

$$\begin{aligned}
 \frac{\partial \rho U}{\partial x} + \frac{\partial \rho V}{\partial y} &= 0 \\
 \frac{\partial (\rho U U + P - \tau_{xx})}{\partial x} + \frac{\partial (\rho U V - \tau_{xy})}{\partial y} &= 0 \\
 \frac{\partial (\rho V U - \tau_{xy})}{\partial x} + \frac{\partial (\rho V V + P - \tau_{yy})}{\partial y} &= 0 \\
 \frac{\partial (\rho h U + Q_x)}{\partial x} + \frac{\partial (\rho h V + Q_y)}{\partial y} - \left(U \frac{\partial P}{\partial x} + V \frac{\partial P}{\partial y} \right) \\
 - \left(\tau_{xx} \frac{\partial U}{\partial x} + \tau_{xy} \frac{\partial U}{\partial y} \right) - \left(\tau_{xy} \frac{\partial V}{\partial x} + \tau_{yy} \frac{\partial V}{\partial y} \right) &= 0
 \end{aligned} \tag{8.4}$$

8.3 Plane, compressible Couette flow

First let's study the two-dimensional, compressible flow produced between two parallel plates in relative motion as shown in Figure 8.2. This is the simplest possible compressible flow where viscous forces and heat conduction dominate the motion. We studied the incompressible version of this flow in Chapter 1. There the gas temperature is constant and the velocity profile is a straight line. In the compressible problem the temperature varies between the plates, as does the gas viscosity, leading to a more complex and more interesting problem.

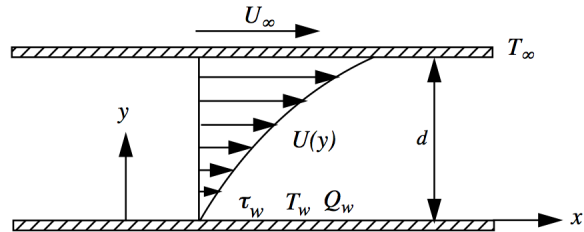


Figure 8.2: Flow produced between two parallel plates in relative motion.

The upper wall moves at a velocity U_∞ doing work on the fluid while the lower wall is at rest. The temperature of the upper wall is T_∞ . The flow is assumed to be steady with no variation in the z direction. The plates extend to plus and minus infinity in the x direction.

All gradients in the x direction are zero and the velocity in the y direction is zero.

$$\begin{aligned} V &= W = 0 \\ \frac{\partial}{\partial x} () &= \frac{\partial}{\partial z} () = 0 \end{aligned} \tag{8.5}$$

With these simplifications the equations of motion reduce to

$$\begin{aligned} \frac{\partial \tau_{xy}}{\partial y} &= 0 \\ \frac{\partial P}{\partial y} &= 0 \\ \frac{\partial (Q_y - \tau_{xy}U)}{\partial y} &= 0. \end{aligned} \tag{8.6}$$

The U velocity component and temperature only depend on y . The y momentum equation implies that the pressure is uniform throughout the flow (the pressure does not depend on x or y). The implication of the x momentum balance is that the shear stress τ_{xy} also must be uniform throughout the flow just like the pressure. Assume the fluid is Newtonian. With $V = 0$, the shear stress is

$$\tau_{xy} = \mu \frac{dU}{dy} = \tau_w = \text{constant} \tag{8.7}$$

where τ_w is the shear stress at the lower wall. For gases the viscosity depends only on temperature.

$$\mu = \mu(T) \tag{8.8}$$

Since the pressure is constant the density also depends only on the temperature. According to the perfect gas law

$$\rho(y) = \frac{P}{RT(y)}. \tag{8.9}$$

Using these equations, the solution for the velocity profile can be written as an integral.

$$U(y) = \tau_w \int_0^y \frac{dy}{\mu(T)} \quad (8.10)$$

To determine the velocity profile we need to know how the viscosity depends on temperature and the temperature distribution. The temperature distribution across the channel can be determined from the energy equation. Fourier's law for the heat flux is

$$Q_y = -\kappa \frac{dT}{dy}. \quad (8.11)$$

The coefficient of heat conductivity, like the viscosity is also only a function of temperature.

$$\kappa = \kappa(T) \quad (8.12)$$

The relative rates of diffusion of momentum and heat are characterized by the Prandtl number.

$$Pr = \frac{C_p \mu}{\kappa} \quad (8.13)$$

In gases, heat and momentum are transported by the same mechanism of molecular collisions. For this reason the temperature dependencies of the viscosity and heat conductivity approximately cancel in (8.13). The heat capacity is only weakly dependent on temperature and so to a reasonable approximation, the Prandtl number for gases tends to be a constant close to one. For Air $Pr = 0.71$.

8.3.1 The energy integral in plane Couette flow

The energy equation expresses the balance between heat flux and work done on the gas.

$$\frac{d}{dy} (-Q_y + \tau_w U) = 0 \quad (8.14)$$

Integrate (8.14).

$$-Q_y + \tau_w U = -Q_w \quad (8.15)$$

The constant of integration, $Q_w = \kappa(\partial T / \partial y)_{y=0}$, is the heat flux on the lower wall. Now insert the expressions for the shear stress and heat flux into (8.15).

$$\kappa \frac{dT}{dy} + \mu U \frac{dU}{dy} = \mu \frac{d}{dy} \left(\frac{1}{P_r} C_p T + \frac{1}{2} U^2 \right) = -Q_w \quad (8.16)$$

Integrate (8.16) from the lower wall.

$$C_p (T - T_w) + \frac{1}{2} P_r U^2 = -Q_w P_r \int_0^y \frac{dy}{\mu(T)} \quad (8.17)$$

The quantity T_w is the temperature of the lower wall. The integral on the right of (8.17) can be replaced by the velocity using (8.10). The result is the so-called *energy integral*.

$$C_p (T - T_w) + \frac{1}{2} P_r U^2 = -\frac{Q_w}{\tau_w} P_r U \quad (8.18)$$

At the upper wall, the temperature is T_∞ and this can now be used to evaluate the lower wall temperature.

$$C_p T_w = C_p T_\infty + P_r \left(\frac{U_\infty^2}{2} + \frac{Q_w}{\tau_w} U_\infty \right) \quad (8.19)$$

8.3.2 The adiabatic wall recovery temperature

Suppose the lower wall is insulated so that $Q_w = 0$. What temperature does the lower wall reach? This is called the adiabatic wall recovery temperature T_{wa} .

$$T_{wa} = T_\infty + \frac{P_r}{2C_p} U_\infty^2 \quad (8.20)$$

Introduce the Mach number $M_\infty = U_\infty / a_\infty$. Now

$$\frac{T_{wa}}{T_\infty} = 1 + P_r \left(\frac{\gamma - 1}{2} \right) M_\infty^2. \quad (8.21)$$

Equation (8.21) indicates that the recovery temperature equals the stagnation temperature at the upper wall only for a Prandtl number of one. The stagnation temperature at the upper wall is

$$\frac{T_{t\infty}}{T_\infty} = 1 + \left(\frac{\gamma - 1}{2} \right) M_\infty^2. \quad (8.22)$$

The recovery factor is defined as

$$\frac{T_{wa} - T_\infty}{T_{t\infty} - T_\infty} = r. \quad (8.23)$$

In Couette flow for a perfect gas with constant C_p equation (8.21) tells us that the recovery factor is the Prandtl number.

$$\frac{T_{wa} - T_\infty}{T_{t\infty} - T_\infty} = P_r \quad (8.24)$$

Equations (8.19) and (8.20) can be used to show that the heat transfer and shear stress are related by

$$\frac{Q_w}{\tau_w U_\infty} = \frac{C_p (T_w - T_{wa})}{P_r U_\infty^2}. \quad (8.25)$$

Equation (8.25) can be rearranged to read

$$\frac{\tau_w}{\frac{1}{2} \rho_\infty U_\infty^2} = 2P_r \left(\frac{Q_w}{\rho_\infty U_\infty C_p (T_w - T_{wa})} \right). \quad (8.26)$$

The left side of (8.26) is the friction coefficient.

$$C_f = \frac{\tau_w}{\frac{1}{2} \rho_\infty U_\infty^2} \quad (8.27)$$

On the right side of (8.26) there appears a dimensionless heat transfer coefficient called the Stanton number.

$$S_t = \frac{Q_w}{\rho_\infty U_\infty C_p (T_w - T_{wa})} \quad (8.28)$$

In order to transfer heat into the fluid, the lower wall temperature must exceed the recovery temperature. Equation (8.26) now becomes

$$C_f = 2P_r S_t. \quad (8.29)$$

The coupling between heat transfer and viscous friction indicated in (8.29) is a general property of all compressible flows near a wall. The numerical factor 2 may change and the dependence on Prandtl number may change depending on the flow geometry and on whether the flow is laminar or turbulent, but the general property that heat transfer and viscous friction are coupled is universal.

8.3.3 Velocity distribution in Couette flow

Now that the relation between temperature and velocity is known we can integrate the momentum relation for the stress. We use the energy integral written in terms of T_∞

$$C_p (T - T_\infty) = P_r \frac{Q_w}{\tau_w} (U_\infty - U) + \frac{1}{2} P_r (U_\infty^2 - U^2) \quad (8.30)$$

or

$$\frac{T}{T_\infty} = 1 + P_r \frac{Q_w}{U_\infty \tau_w} (\gamma - 1) M_\infty^2 \left(1 - \frac{U}{U_\infty} \right) + P_r \left(\frac{\gamma - 1}{2} \right) M_\infty^2 \left(1 - \frac{U^2}{U_\infty^2} \right). \quad (8.31)$$

Recall the momentum equation.

$$\mu(T) \frac{dU}{dy} = \tau_w \quad (8.32)$$

The temperature is a monotonic function of the velocity and so the viscosity can be regarded as a function of U . This enables the momentum equation to be integrated.

$$\int_0^U \mu(U) dU = \tau_w y \quad (8.33)$$

For gases, the dependence of viscosity on temperature is reasonably well approximated by Sutherland's law

$$\frac{\mu}{\mu_\infty} = \left(\frac{T}{T_\infty} \right)^{\frac{3}{2}} \left(\frac{T_\infty + T_S}{T + T_S} \right) \quad (8.34)$$

where T_S is the Sutherland reference temperature, which is $110.4K$ for Air. An approximation that is often used is the power law

$$\frac{\mu}{\mu_\infty} = \left(\frac{T}{T_\infty} \right)^\omega \quad 0.5 < \omega < 1.0. \quad (8.35)$$

Using (8.31) and (8.35), the momentum equation becomes

$$\int_0^U \left(1 + P_r \frac{Q_w}{U_\infty \tau_w} (\gamma - 1) M_\infty^2 \left(1 - \frac{U}{U_\infty} \right) + P_r \left(\frac{\gamma - 1}{2} \right) M_\infty^2 \left(1 - \frac{U^2}{U_\infty^2} \right) \right)^\omega dU = \frac{\tau_w}{\mu_\infty} y. \quad (8.36)$$

For Air the exponent ω is approximately 0.76. The simplest case, and a reasonable approximation, corresponds to $\omega = 1$. In this case the integral can be carried out explicitly. For an adiabatic wall $Q_w = 0$, the wall stress and velocity are related by

$$\frac{\tau_w}{\mu_\infty U_\infty} y = \frac{U}{U_\infty} + P_r \left(\frac{\gamma - 1}{2} \right) M_\infty^2 \left(\frac{U}{U_\infty} - \frac{1}{3} \left(\frac{U}{U_\infty} \right)^3 \right). \quad (8.37)$$

The shear stress is determined by evaluating (8.37) at the upper wall.

$$\frac{\tau_w}{\mu_\infty U_\infty} d = 1 + P_r \left(\frac{\gamma - 1}{3} \right) M_\infty^2 \quad (8.38)$$

The velocity profile is expressed implicitly as

$$\frac{y}{d} = \frac{\frac{U}{U_\infty} + P_r \left(\frac{\gamma - 1}{2} \right) M_\infty^2 \left(\frac{U}{U_\infty} - \frac{1}{3} \left(\frac{U}{U_\infty} \right)^3 \right)}{1 + P_r \left(\frac{\gamma - 1}{3} \right) M_\infty^2}. \quad (8.39)$$

At $M_\infty \rightarrow 0$ the profile reduces to the incompressible limit $U/U_\infty = y/d$. At high Mach number the profile is

$$\lim_{M_\infty \rightarrow \infty} \left(\frac{y}{d} \right) = \frac{3}{2} \left(\frac{U}{U_\infty} - \frac{1}{3} \left(\frac{U}{U_\infty} \right)^3 \right). \quad (8.40)$$

At high Mach number the profile is independent of the Prandtl number and Mach number. The two limiting cases are shown in Figure 8.3.

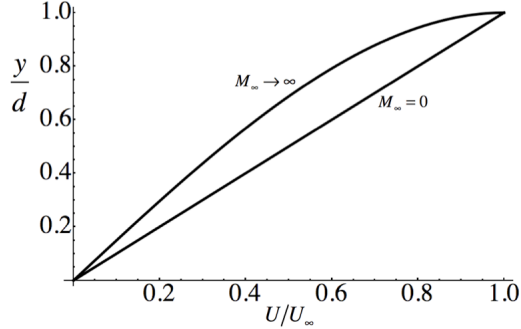


Figure 8.3: Velocity distribution in plane Couette flow for an adiabatic lower wall and $\omega = 1$.

Using (8.38) the wall friction coefficient for an adiabatic lower wall is expressed in terms of the Prandtl, Reynolds, and Mach numbers.

$$C_f = 2 \left(\frac{1 + P_r \left(\frac{\gamma-1}{3} \right) M_\infty^2}{R_e} \right) \quad (8.41)$$

The Reynolds number is

$$R_e = \frac{\rho_\infty U_\infty d}{\mu_\infty} \quad (8.42)$$

and can be expressed as

$$R_e = \frac{\rho_\infty U_\infty d}{\mu_\infty} = \frac{\frac{1}{2} \rho_\infty U_\infty^2}{\frac{1}{2} \mu_\infty \frac{U_\infty}{d}} = \frac{\text{dynamic pressure at the upper plate}}{\text{characteristic shear stress}}. \quad (8.43)$$

The last result nicely illustrates the interpretation of the Reynolds number as a ratio of convective to viscous forces.

Notice that if the upper and lower walls are both adiabatic the work done by the upper wall would lead to a continuous accumulation of energy between the two plates and a continuous rise in temperature. In this case a steady state solution to the problem would not exist. The upper wall has to be able to conduct heat into or out of the flow for a steady state solution to be possible.

8.4 The viscous boundary layer on a wall

The Couette problem provides a useful insight into the nature of compressible flow near a solid boundary. From a practical standpoint the more important problem is that of a compressible boundary layer where the flow originates at the leading edge of a solid body such as an airfoil. A key reference is the classic text *Boundary Layer Theory* by Hermann Schlichting. Recent editions are authored by Schlichting and Gersten.

To introduce the boundary layer concept we begin by considering viscous, compressible flow past a flat plate of length L as shown in Figure 8.4. The question of whether a boundary layer is present or not depends on the overall Reynolds number of the flow.

$$R_{eL} = \frac{\rho_\infty U_\infty L}{\mu_\infty} \quad (8.44)$$

Figure 8.4 depicts the case where the thickness of the viscous region, delineated, schematically by the parabolic boundary, is a significant fraction of the length of the plate and the Reynolds number based on the plate length is quite low. In this case there is no boundary layer and the full equations of motion must be solved to determine the flow.

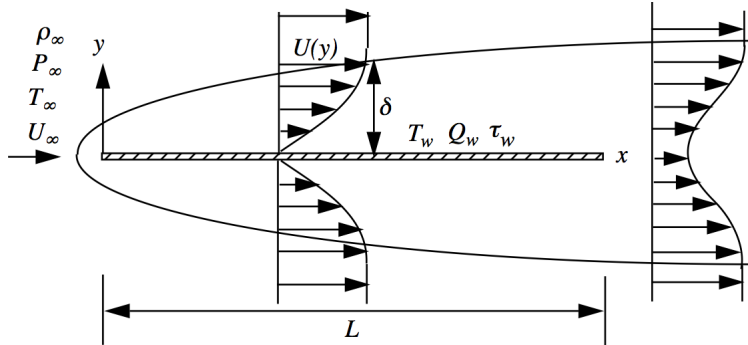


Figure 8.4: Low Reynolds number flow about a thin flat plate of length L . Re_L is less than a hundred or so. The parabolic envelope which extends upstream of the leading edge roughly delineates the region of rotational flow produced as a consequence of the no slip condition on the plate.

If the Reynolds number based on plate length is large then the flow looks more like that depicted in Figure 8.5.

At high Reynolds number the thickness of the viscous region is much less than the length

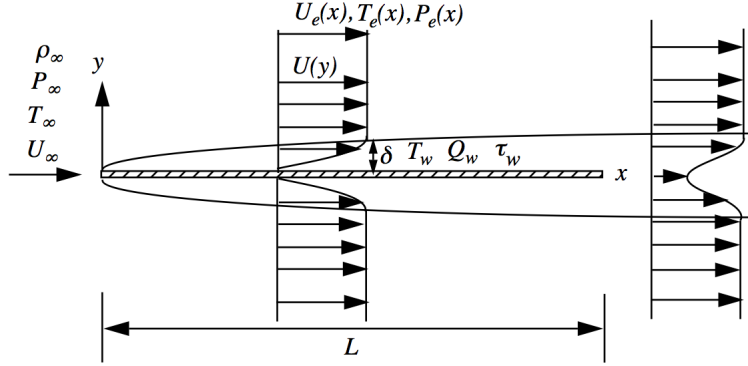


Figure 8.5: High Reynolds number flow developing from the leading edge of a flat plate of length L . Re_L is several hundred or more .

of the plate.

$$\frac{\delta}{L} \ll 1 \quad (8.45)$$

Moreover, there is a region of the flow away from the leading and trailing edges of the plate where the guiding effect of the plate produces a flow that is nearly parallel. In this region the transverse velocity component is much less than the streamwise component.

$$\frac{V}{U} \ll 1 \quad (8.46)$$

The variation of the flow in the streamwise direction is much smaller than the variation in the cross-stream direction. Thus

$$\begin{aligned} \frac{\partial(\cdot)}{\partial x} &\ll \frac{\partial(\cdot)}{\partial y} \\ U \frac{\partial(\cdot)}{\partial x} &\sim V \frac{\partial(\cdot)}{\partial y}. \end{aligned} \quad (8.47)$$

Moreover continuity tells us that

$$\frac{\partial U}{\partial x} \sim - \frac{\partial V}{\partial y}. \quad (8.48)$$

The convective and viscous terms in the stream wise momentum equation are of the same order, suggesting the following estimate for δ/L .

$$\frac{\rho_\infty U_\infty^2}{L} \approx \mu \frac{U_\infty}{\delta^2} \Rightarrow \frac{\delta}{L} \approx \frac{1}{(R_{eL})^{1/2}} \quad (8.49)$$

With this estimate in mind let's examine the y momentum equation.

$$\frac{\partial(\rho VU - \tau_{xy})}{\partial x} + \frac{\partial(\rho VV + P - \tau_{yy})}{\partial y} = 0 \quad (8.50)$$

Utilizing (8.46) and (8.47), equation (8.50) reduces to

$$\frac{\partial(P - \tau_{yy})}{\partial y} = 0. \quad (8.51)$$

Now integrate this equation at a fixed position x and evaluate the constant of integration in the free stream.

$$P(x, y) = \tau_{yy}(x, y) + P_e(x) \quad (8.52)$$

The pressure (8.52) is inserted into the x momentum equation in (8.4). The result is the boundary layer approximation to the x momentum equation.

$$\rho U \frac{\partial U}{\partial x} + \rho V \frac{\partial U}{\partial y} = -\frac{dP_e}{dx} + \frac{\partial}{\partial x}(\tau_{xx} - \tau_{yy}) + \frac{\partial \tau_{xy}}{\partial y} \quad (8.53)$$

Now consider the energy equation.

$$\frac{\partial(\rho hU + Q_x)}{\partial x} + \frac{\partial(\rho hV + Q_y)}{\partial y} - \left(U \frac{\partial P}{\partial x} + V \frac{\partial P}{\partial y} \right) - \left(\tau_{xx} \frac{\partial U}{\partial x} + \tau_{xy} \frac{\partial U}{\partial y} \right) - \left(\tau_{xy} \frac{\partial V}{\partial x} + \tau_{yy} \frac{\partial V}{\partial y} \right) = 0 \quad (8.54)$$

Using (8.46), (8.47) and (8.48) the energy equation simplifies to

$$\rho U \frac{\partial h}{\partial x} + \rho V \frac{\partial h}{\partial y} + \frac{\partial Q_y}{\partial y} - U \frac{\partial P_e}{\partial x} + U \frac{\partial}{\partial x}(\tau_{xx} - \tau_{yy}) - \frac{\partial(V\tau_{yy})}{\partial y} - \frac{\partial(U\tau_{xx})}{\partial x} - \tau_{xy} \frac{\partial U}{\partial y} = 0. \quad (8.55)$$

In laminar flow the normal stresses τ_{xx} and τ_{yy} are very small and the normal stress terms that appear in (8.53) and (8.55) can be neglected. In turbulent flow the normal stresses are not particularly small, with fluctuations of velocity near the wall that can be 10 to 20 percent of the velocity at the edge of the boundary layer. Nevertheless a couple of features of the turbulent boundary layer (compressible or incompressible) allow these normal stress terms in the boundary layer equations to be neglected.

- 1) τ_{xx} and τ_{yy} tend to be comparable in magnitude so that $\tau_{xx} - \tau_{yy}$ is small and the streamwise derivative $\partial(\tau_{xx} - \tau_{yy})/\partial x$ is generally quite small.
- 2) τ_{yy} has its maximum value in the lower part of the boundary layer where V is very small so the product $V\tau_{yy}$ is small.
- 3) τ_{xx} also has its maximum value relatively near the wall where U is small and the streamwise derivative of $U\tau_{xx}$ is small.

Using these assumptions to remove the normal stress terms, the compressible boundary layer equations become

$$\begin{aligned} \frac{\partial \rho U}{\partial x} + \frac{\partial \rho V}{\partial y} &= 0 \\ \rho U \frac{\partial U}{\partial x} + \rho V \frac{\partial U}{\partial y} + \frac{dP_e}{dx} - \frac{\partial \tau_{xy}}{\partial y} &= 0 \\ \rho U \frac{\partial h}{\partial x} + \rho V \frac{\partial h}{\partial y} + \frac{\partial Q_y}{\partial y} - U \frac{dP_e}{dx} - \tau_{xy} \frac{\partial U}{\partial y} &= 0. \end{aligned} \quad (8.56)$$

The only stress component that plays a role in this approximation is the shearing stress τ_{xy} . In a turbulent boundary layer both the laminar and turbulent shearing stresses are important.

$$\tau_{xy} = \tau_{xy}|_{laminar} + \tau_{xy}|_{turbulent} = \mu \frac{\partial U}{\partial y} + \tau_{xy}|_{turbulent} \quad (8.57)$$

In the outer part of the layer where the velocity gradient is relatively small the turbulent stresses dominate. But near the wall where the velocity fluctuations are damped and the velocity gradient is large, the viscous stress dominates.

The flow picture appropriate to the boundary layer approximation is shown in Figure 8.6.

The boundary layer is assumed to originate from a virtual origin near the plate leading edge and the wake is infinitely far off to the right. The velocity, temperature and pressure at

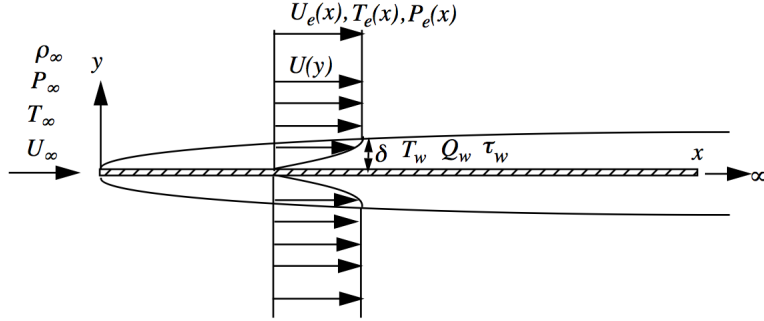


Figure 8.6: High Reynolds number flow developing from the leading edge of a semi-infinite flat plate.

the boundary layer edge are assumed to be known functions of the stream-wise coordinate. The appropriate measure of the Reynolds number in this flow is based on the distance from the leading edge.

$$R_{ex} = \frac{\rho_\infty U_\infty x}{\mu_\infty} \quad (8.58)$$

One would expect a thin flat plate to produce very little disturbance to the flow. So it is a bit hard at this point to see the origin of the variation in free stream velocity indicated in Figure 8.6. We will return to this question at the end of the chapter. For now we simply accept that the free stream pressure and velocity can vary with x even along a thin flat plate. By the way, an experimental method for generating a pressure gradient is to put the plate into a wind tunnel with variable walls that can be set at a geometry to accelerate or decelerate the flow.

For Newtonian laminar flow, the stress is

$$\begin{aligned} \tau_{ij} &= 2\mu S_{ij} - \left(\frac{2}{3}\mu - \mu_v \right) \delta_{ij} S_{kk} \\ \tau_{xy} &= \mu \left(\frac{\partial U}{\partial y} + \frac{\partial V}{\partial x} \right) \cong \mu \frac{\partial U}{\partial y}. \end{aligned} \quad (8.59)$$

The diffusion of heat is governed by Fourier's law introduced earlier.

$$Q_y = -k \frac{\partial T}{\partial y} \quad (8.60)$$

For laminar flow, the compressible boundary layer equations are

$$\begin{aligned} \frac{\partial \rho U}{\partial x} + \frac{\partial \rho V}{\partial y} &= 0 \\ \rho U \frac{\partial U}{\partial x} + \rho V \frac{\partial U}{\partial y} + \frac{dP_e}{dx} - \frac{\partial}{\partial y} \left(\mu \frac{\partial U}{\partial y} \right) &= 0 \\ \rho U C_p \frac{\partial T}{\partial x} + \rho V C_p \frac{\partial T}{\partial y} - U \frac{dP_e}{dx} - \frac{\partial}{\partial y} \left(\kappa \frac{\partial T}{\partial y} \right) - \mu \left(\frac{\partial U}{\partial y} \right)^2 &= 0. \end{aligned} \quad (8.61)$$

8.4.1 Measures of boundary layer thickness

The thickness of the boundary layer depicted in Figure 8.6 is denoted δ . There are several ways to define the thickness. The simplest is to identify the point where the velocity is some percentage of the free stream value, say $\delta_{0.95}$ or $\delta_{0.99}$. This is a somewhat arbitrary measure and it is generally better to use a thickness defined in terms of an integral over the boundary layer that converges at the boundary layer edge. The two most common measures are the displacement thickness and the momentum thickness.

Displacement thickness

$$\delta^* = \int_0^\delta \left(1 - \frac{\rho U}{\rho_e U_e} \right) dy \quad (8.62)$$

This is a measure of the distance by which streamlines are shifted away from the plate by the blocking effect of the boundary layer. This outward displacement of the flow comes from the reduced mass flux in the boundary layer compared to the mass flux that would occur if the flow were inviscid. Generally δ^* is a fraction of $\delta_{0.99}$. The integral (8.62) is terminated at the edge of the boundary layer where the velocity equals the free stream value U_e . This is important in a situation involving a pressure gradient where the velocity profile might look something like that depicted in Figure 8.1. The free stream velocity used as the outer boundary condition for the boundary layer calculation comes from the potential flow solution for the irrotational flow about the body evaluated at the wall. If the integral (8.62) is taken beyond this point it will begin to diverge.

Momentum thickness

$$\theta = \int_0^\delta \frac{\rho U}{\rho_e U_e} \left(1 - \frac{U}{U_e} \right) dy \quad (8.63)$$

This is a measure of the deficit in momentum flux within the boundary layer compared to the free stream value and is smaller than the displacement thickness. The evolution of the momentum thickness along the wall is directly related to the skin friction coefficient.

8.5 The Von Karman integral momentum equation

Often the detailed structure of the boundary layer velocity profile is not the primary object of interest. The most important properties of the boundary layer are the skin friction and the displacement effect. Boundary layer models usually focus primarily on these variables.

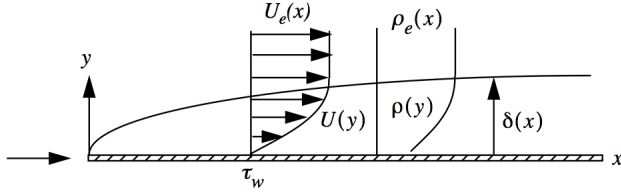


Figure 8.7: Boundary layer velocity and density profiles.

The steady compressible boundary layer equations, excluding the energy equation, are

$$\begin{aligned} \frac{\partial \rho U}{\partial x} + \frac{\partial \rho V}{\partial y} &= 0 \\ \frac{\partial \rho U^2}{\partial x} + \frac{\partial \rho UV}{\partial y} + \frac{dP_e}{dx} - \frac{\partial \tau_{xy}}{\partial y} &= 0. \end{aligned} \quad (8.64)$$

Integrate the continuity and momentum equations over the thickness of the boundary layer.

$$\begin{aligned} \int_0^{\delta(x)} \left(\frac{\partial \rho U}{\partial x} \right) dy + \int_0^{\delta(x)} \left(\frac{\partial \rho V}{\partial y} \right) dy &= 0 \\ \int_0^{\delta(x)} \left(\frac{\partial \rho U^2}{\partial x} \right) dy + \int_0^{\delta(x)} \left(\frac{\partial \rho UV}{\partial y} \right) dy + \int_0^{\delta(x)} \left(\frac{dP_e}{dx} \right) dy - \int_0^{\delta(x)} \left(\frac{\partial \tau_{xy}}{\partial y} \right) dy &= 0 \end{aligned} \quad (8.65)$$

Upon integration, the momentum equation becomes

$$\int_0^{\delta(x)} \left(\frac{\partial \rho U^2}{\partial x} \right) dy + \rho_e U_e V_e + \left(\frac{dP_e}{dx} \right) \delta(x) + \tau_{xy}|_{y=0} = 0. \quad (8.66)$$

The partial derivatives with respect to x in (8.65) can be taken outside the integral using Liebniz' rule.

$$\begin{aligned} \frac{d}{dx} \int_0^{\delta(x)} \rho U dy &= \int_0^{\delta(x)} \left(\frac{\partial \rho U}{\partial x} \right) dy + \rho_e U_e \frac{d\delta}{dx} \\ \frac{d}{dx} \int_0^{\delta(x)} \rho U^2 dy &= \int_0^{\delta(x)} \left(\frac{\partial \rho U^2}{\partial x} \right) dy + \rho_e U_e^2 \frac{d\delta}{dx} \end{aligned} \quad (8.67)$$

Use the second equation in (8.67) in (8.66)

$$\frac{d}{dx} \int_0^{\delta(x)} \rho U^2 dy - \rho_e U_e^2 \frac{d\delta}{dx} + \rho_e U_e V_e + \frac{dP_e}{dx} \delta(x) = -\tau_w \quad (8.68)$$

where $\tau_w(x) = \tau_{xy}(x, 0)$ and τ_w is positive. We will make use of the following relation.

$$\begin{aligned} \frac{d}{dx} \int_0^{\delta(x)} (\rho U U_e) dy &= \int_0^{\delta(x)} \left(\frac{\partial \rho U U_e}{\partial x} \right) dy + \rho_e U_e^2 \frac{d\delta}{dx} = \\ \int_0^{\delta(x)} \left(U_e \frac{\partial \rho U}{\partial x} + \rho U \frac{dU_e}{dx} \right) dy + \rho_e U_e^2 \frac{d\delta}{dx} &= \\ U_e \int_0^{\delta(x)} \left(\frac{\partial \rho U}{\partial x} \right) dy + \frac{dU_e}{dx} \int_0^{\delta(x)} \rho U dy + \rho_e U_e^2 \frac{d\delta}{dx} & \end{aligned} \quad (8.69)$$

Multiply the continuity equation in (8.65) by U_e and integrate with respect to y .

$$U_e \int_0^{\delta(x)} \left(\frac{\partial \rho U}{\partial x} \right) dy + \rho_e U_e V_e = 0 \quad (8.70)$$

Insert (8.70) into the last relation in (8.69).

$$\frac{d}{dx} \int_0^{\delta(x)} (\rho U U_e) dy + \rho_e U_e V_e - \frac{dU_e}{dx} \int_0^{\delta(x)} \rho U dy - \rho_e U_e^2 \frac{d\delta}{dx} = 0 \quad (8.71)$$

Subtract (8.71) from (8.68)

$$\frac{d}{dx} \int_0^{\delta(x)} (\rho U^2 - \rho U U_e) dy + \frac{dU_e}{dx} \int_0^{\delta(x)} \rho U dy + \frac{dP_e}{dx} \delta(x) = -\tau_w \quad (8.72)$$

and subtract the identity

$$\frac{dU_e}{dx} \int_0^{\delta(x)} \rho_e U_e dy - \rho_e U_e \frac{dU_e}{dx} \delta(x) = 0 \quad (8.73)$$

from (8.72). Now the integral momentum equation takes the form

$$\frac{d}{dx} \int_0^{\delta(x)} (\rho U^2 - \rho U U_e) dy + \frac{dU_e}{dx} \int_0^{\delta(x)} (\rho U - \rho_e U_e) dy + \left(\frac{dP_e}{dx} + \rho_e U_e \frac{dU_e}{dx} \right) \delta(x) = -\tau_w. \quad (8.74)$$

Recall the definitions of displacement thickness (8.62) and momentum thickness (8.63).

$$\begin{aligned} \delta^*(x) &= \int_0^{\delta(x)} \left(1 - \frac{\rho U}{\rho_e U_e} \right) dy \\ \theta(x) &= \int_0^{\delta(x)} \frac{\rho U}{\rho_e U_e} \left(1 - \frac{U}{U_e} \right) dy \end{aligned} \quad (8.75)$$

Substitute (8.75) into (8.74). The result is

$$-\frac{d}{dx} (\rho_e U_e^2 \theta) - \rho_e U_e \delta^* \frac{dU_e}{dx} + \left(\frac{dP_e}{dx} + \rho_e U_e \frac{dU_e}{dx} \right) \delta(x) = -\tau_w. \quad (8.76)$$

At the edge of the boundary layer both $\partial U / \partial y$ and τ_{xy} go to zero and the x -boundary layer momentum equation reduces to the Euler equation.

$$dP_e + \rho_e U_e dU_e = 0 \quad (8.77)$$

Using (8.77), the integral equation (8.76) reduces to

$$\frac{d}{dx} (\rho_e U_e^2 \theta) + \rho_e U_e \delta^* \frac{dU_e}{dx} = \tau_w. \quad (8.78)$$

The significance of this last step is that (8.78) does not depend explicitly on the perceived boundary layer thickness but only on the more precisely defined momentum and displacement thicknesses. It is customary to write (8.78) in a slightly different form. Introduce the wall friction coefficient and carry out the differentiation of the first term in (8.78).

$$C_f = \frac{\tau_w}{\frac{1}{2} \rho_e U_e^2} \quad (8.79)$$

$$\frac{d\theta}{dx} + (2\theta + \delta^*) \frac{1}{U_e} \frac{dU_e}{dx} + \frac{\theta}{\rho_e} \frac{d\rho_e}{dx} = \frac{C_f}{2} \quad (8.80)$$

If the free stream flow is adiabatic (not necessarily isentropic), then

$$\begin{aligned} \frac{dT_e}{T_e} + (\gamma - 1) M_e^2 \frac{dU_e}{U_e} &= 0 \\ \frac{dP_e}{P_e} + \gamma M_e^2 \frac{dU_e}{U_e} &= 0 \\ \frac{d\rho_e}{\rho_e} = \frac{dP_e}{P_e} - \frac{dT_e}{T_e} &= -M_e^2 \frac{dU_e}{U_e} \end{aligned} \quad (8.81)$$

Using the last relation in (8.81) in (8.78), the compressible Von Karman integral momentum equation is

$$\frac{d\theta}{dx} + ((2 - M_e^2)\theta + \delta^*) \frac{1}{U_e} \frac{dU_e}{dx} = \frac{C_f}{2}. \quad (8.82)$$

Another common form of (8.82) is generated by introducing the shape factor

$$H = \frac{\delta^*}{\theta}. \quad (8.83)$$

Equation (8.82) becomes

$$\frac{d\theta}{dx} + (2 - M_e^2 + H) \frac{\theta}{U_e} \frac{dU_e}{dx} = \frac{C_f}{2}. \quad (8.84)$$

8.6 The laminar boundary layer in the limit $M^2 \rightarrow 0$.

At very low Mach number the density is constant, temperature variations throughout the flow are very small, and the boundary layer equations (8.61) reduce to their incompressible form

$$\begin{aligned} \frac{\partial U}{\partial x} + \frac{\partial V}{\partial y} &= 0 \\ U \frac{\partial U}{\partial x} + V \frac{\partial U}{\partial y} &= -\frac{1}{\rho} \frac{dP_e}{dx} + \nu \left(\frac{\partial^2 U}{\partial y^2} \right) \end{aligned} \quad (8.85)$$

where the kinematic viscosity $\nu = \mu/\rho$ has been introduced. The boundary conditions are

$$\begin{aligned} U(0) &= V(0) = 0 \\ U(\delta) &= U_e. \end{aligned} \quad (8.86)$$

The pressure at the edge of the boundary layer at $y = \delta$ is determined using the Bernoulli relation.

$$P_t = P_e(x) + \frac{1}{2} \rho U_e(x)^2 \Rightarrow \frac{1}{\rho} \frac{dP_e}{dx} = -U_e \frac{dU_e}{dx} \quad (8.87)$$

The stagnation pressure is constant in the irrotational flow outside the boundary layer. The pressure at the boundary layer edge, $P_e(x)$, is assumed to be a given function determined from a potential flow solution for the flow outside the boundary layer.

The continuity equation is satisfied identically by introducing a stream function.

$$\begin{aligned} U &= \frac{\partial \psi}{\partial y} \\ V &= -\frac{\partial \psi}{\partial x}. \end{aligned} \quad (8.88)$$

In terms of the stream function, the governing momentum equation becomes a third-order partial differential equation.

$$\psi_y \psi_{xy} - \psi_x \psi_{yy} = U_e \frac{dU_e}{dx} + \nu \psi_{yyy} \quad (8.89)$$

8.6.1 The zero pressure gradient, incompressible boundary layer

For $dU_e/dx = 0$ the governing equation reduces to

$$\psi_y \psi_{xy} - \psi_x \psi_{yy} = \nu \psi_{yyy} \quad (8.90)$$

with boundary conditions

$$\begin{aligned} \psi(x, 0) &= \psi_y(x, 0) = 0 \\ \psi_y(x, \infty) &= U_e. \end{aligned} \quad (8.91)$$

We can solve this problem using a symmetry argument. Transform (8.90) using the following three parameter dilation Lie group.

$$\begin{aligned} \tilde{x} &= e^a x \\ \tilde{y} &= e^b y \\ \tilde{\psi} &= e^c \psi \end{aligned} \quad (8.92)$$

Equation (8.90) transforms as follows.

$$\tilde{\psi}_{\tilde{y}} \tilde{\psi}_{\tilde{x}\tilde{y}} - \tilde{\psi}_{\tilde{x}} \tilde{\psi}_{\tilde{y}\tilde{y}} - \nu \tilde{\psi}_{\tilde{y}\tilde{y}\tilde{y}} = e^{2c-a-2b} (\psi_y \psi_{xy} - \psi_x \psi_{yy}) - e^{c-3b} (\nu \psi_{yyy}) \quad (8.93)$$

Equation (8.90) is invariant under the group (8.92) if and only if $c = a - b$. The boundaries of the problem at the wall and at infinity are clearly invariant under (8.92).

$$\begin{aligned} \tilde{y} &= e^b y = 0 \Rightarrow y = 0 \\ \tilde{\psi}(\tilde{x}, 0) &= e^c \psi(e^a x, 0) = 0 \Rightarrow \psi(x, 0) = 0 \\ \tilde{\psi}_{\tilde{y}}(\tilde{x}, 0) &= e^{c-b} \psi_y(e^a x, 0) = 0 \Rightarrow \psi_y(x, 0) = 0 \end{aligned} \quad (8.94)$$

The free stream boundary condition requires some care.

$$\tilde{\psi}_{\tilde{y}}(\tilde{x}, \infty) = e^{c-b} \psi_y(e^a x, \infty) = U_e \quad (8.95)$$

Invariance of the free stream boundary condition only holds if $c = b$. So the problem as a whole, equation and boundary conditions, is invariant under the one-parameter group

$$\begin{aligned}\tilde{x} &= e^{2b}x \\ \tilde{y} &= e^b y \\ \tilde{\psi} &= e^b \psi.\end{aligned}\tag{8.96}$$

This process of showing that the problem is invariant under a Lie group is essentially a proof of the existence of a similarity solution to the problem. We can expect that the solution of the problem will also be invariant under the same group (8.96). That is we can expect a solution of the form

$$\frac{\psi}{\sqrt{x}} = F\left(\frac{y}{\sqrt{x}}\right).\tag{8.97}$$

The problem can be further simplified by using the parameters of the problem to non-dimensionalize the similarity variables. Introduce

$$\begin{aligned}\psi &= (2\nu U_\infty x)^{1/2} F(\alpha) \\ \alpha &= y \left(\frac{U_\infty}{2\nu x} \right)^{1/2}.\end{aligned}\tag{8.98}$$

In terms of these variables the velocities are

$$\begin{aligned}\frac{U}{U_\infty} &= F_\alpha \\ \frac{V}{U_\infty} &= \left(\frac{\nu}{2U_\infty x} \right)^{1/2} (\alpha F_\alpha - F).\end{aligned}\tag{8.99}$$

The Reynolds number in this flow is based on the distance from the leading edge. Recall Equation (8.58).

$$R_{ex} = \frac{U_\infty x}{\nu}\tag{8.100}$$

As the distance from the leading edge increases, the Reynolds number increases, V/U decreases, and the boundary layer approximation becomes more and more accurate. The vorticity in the boundary layer is

$$\omega = \frac{\partial V}{\partial x} - \frac{\partial U}{\partial y} \cong -U_\infty \left(\frac{U_\infty}{2\nu x} \right)^{1/2} F_{\alpha\alpha}. \quad (8.101)$$

The remaining derivatives that appear in (8.90) are

$$\begin{aligned} \psi_{xy} &= -\frac{U_\infty}{2x} \alpha F_{\alpha\alpha} \\ \psi_{yy} &= U_\infty \left(\frac{U_\infty}{2\nu x} \right)^{1/2} F_{\alpha\alpha} \\ \psi_{yyy} &= \frac{U_\infty^2}{2\nu x} F_{\alpha\alpha\alpha}. \end{aligned} \quad (8.102)$$

Substitute (8.99) and (8.102) into (8.90).

$$\begin{aligned} U_\infty F_\alpha \left(-\frac{U_\infty}{2x} \alpha F_{\alpha\alpha} \right) - U_\infty \left(\left(\frac{\nu}{2U_\infty x} \right)^{1/2} (\alpha F_\alpha - F) \right) U_\infty \left(\frac{U_\infty}{2\nu x} \right)^{1/2} F_{\alpha\alpha} &= \nu \left(\frac{U_\infty^2}{2\nu x} \right) F_{\alpha\alpha\alpha} \\ -F_\alpha (\alpha F_{\alpha\alpha}) + (\alpha F_\alpha - F) F_{\alpha\alpha} &= F_{\alpha\alpha\alpha} \\ -\alpha F_\alpha F_{\alpha\alpha} + \alpha F_\alpha F_{\alpha\alpha} - FF_{\alpha\alpha} - F_{\alpha\alpha\alpha} &= 0 \end{aligned} \quad (8.103)$$

Cancelling terms in (8.103) leads to the Blasius equation

$$F_{\alpha\alpha\alpha} + FF_{\alpha\alpha} = 0 \quad (8.104)$$

subject to the boundary conditions

$$\begin{aligned} F(0) &= 0 \\ F_\alpha(0) &= 0 \\ F_\alpha(\infty) &= 1. \end{aligned} \quad (8.105)$$

The numerical solution of the Blasius equation is shown below.

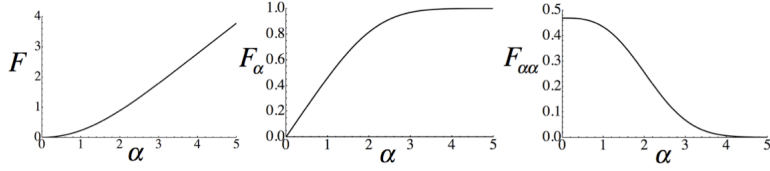


Figure 8.8: *Solution of the Blasius equation (8.104) for the stream function velocity and stress (or vorticity) profile in a zero pressure gradient laminar boundary layer.*

The friction coefficient derived from evaluating the velocity gradient at the wall is

$$C_f = \frac{\tau_w}{(1/2) \rho U_\infty^2} = \frac{0.664}{\sqrt{R_{ex}}}. \quad (8.106)$$

The transverse velocity component at the edge of the layer is

$$\frac{V_e}{U_\infty} = \frac{0.8604}{\sqrt{R_{ex}}}. \quad (8.107)$$

Notice that at a fixed value of x this velocity does not diminish with vertical distance from the plate which may seem a little surprising given our notion that the region of flow disturbed by a body should be finite and the disturbance should die away. But remember that in the boundary layer approximation, the body is semi-infinite. In the real flow over a finite length plate where the boundary layer solution only applies over a limited region, the disturbance produced by the plate would die off at infinity.

The various thickness measures of the Blasius boundary layer are

$$\begin{aligned} \frac{\delta_{0.99}}{x} &= \frac{4.906}{\sqrt{R_{ex}}} \\ \frac{\delta^*}{x} &= \frac{1.7208}{\sqrt{R_{ex}}} \\ \frac{\theta}{x} &= \frac{0.664}{\sqrt{R_{ex}}}. \end{aligned} \quad (8.108)$$

In terms of the similarity variable, the edge of the boundary layer at $\delta_{0.99}$ is at $\alpha_e = 4.906/\sqrt{2} = 3.469$.

We can use (8.104) to get some insight into the legitimacy of the boundary layer idea whereby the flow is separated into a viscous region where the vorticity is nonzero and an inviscid region where the vorticity is zero as depicted in Figure 8.8. The dimensionless vorticity (or shear stress) is given in (8.101). Let $\tau = F_{\alpha\alpha}$. The Blasius equation (8.104) can be expressed as follows

$$\frac{d\tau}{\tau} = -F d\alpha. \quad (8.109)$$

Integrate (8.109).

$$\frac{\tau}{\tau_w} = e^{-\int_0^\alpha F d\alpha} \quad (8.110)$$

The dimensionless stream function, the left panel in Figure 8.8, can be represented by

$$F(\alpha) = \alpha - G(\alpha). \quad (8.111)$$

The limiting behavior of G is $\lim_{\alpha \rightarrow \infty} G(\alpha) = C_1$ where C_1 is a positive constant related to the displacement thickness of the boundary layer. If we substitute (8.111) into (8.110) and integrate beyond the edge of the boundary layer the result is

$$\left. \frac{\tau}{\tau_w} \right|_{\alpha > \alpha_e} = e^{-\int_0^\alpha (\alpha - G(\alpha)) d\alpha} = C_2 e^{C_1 \alpha - \frac{\alpha^2}{2}}. \quad (8.112)$$

Equation (8.112) indicates that the shearing stress and vorticity decay exponentially at the edge of the layer. This rapid drop-off is the key point because it supports the fundamental boundary layer assumption noted above that the flow can be separated into two distinct zones.

8.7 The Falkner-Skan boundary layers

Finally, we address the question of free stream velocity distributions that lead to other similarity solutions beside the Blasius solution. We again analyze the stream function equation.

$$\psi_y \psi_{xy} - \psi_x \psi_{yy} - U_e \frac{dU_e}{dx} - \nu \psi_{yyy} = 0 \quad (8.113)$$

Let

$$U_e = Mx^\beta \quad (8.114)$$

where M has units

$$[M] = L^{1-\beta}/T. \quad (8.115)$$

Similarity solutions of (8.113) exist for the class of power law free-stream velocity distributions given by (8.114). This is the well-known Falkner-Skan family of boundary layers and the exponent β is the Falkner-Skan pressure gradient parameter.

The form of the similarity solution can be determined using a symmetry argument similar to that used to solve the zero pressure gradient case. Insert (8.115) into (8.113). The governing equation becomes

$$\psi_y\psi_{xy} - \psi_x\psi_{yy} - \beta M^2 x^{(2\beta-1)} - \nu\psi_{yyy} = 0. \quad (8.116)$$

Now transform (8.116) using a three parameter dilation Lie group.

$$\begin{aligned} \tilde{x} &= e^a x \\ \tilde{y} &= e^b y \\ \tilde{\psi} &= e^c \psi \end{aligned} \quad (8.117)$$

Equation (8.116) transforms as

$$\begin{aligned} \tilde{\psi}_{\tilde{y}}\tilde{\psi}_{\tilde{x}\tilde{y}} - \tilde{\psi}_{\tilde{x}}\tilde{\psi}_{\tilde{y}\tilde{y}} - \beta M^2 \tilde{x}^{(2\beta-1)} - \nu\tilde{\psi}_{\tilde{y}\tilde{y}\tilde{y}} = \\ e^{2c-a-2b} (\psi_y\psi_{xy} - \psi_x\psi_{yy}) - e^{(2\beta-1)a} (\beta M^2 x^{(2\beta-1)}) - e^{c-3b} (\nu\psi_{yyy}) = 0. \end{aligned} \quad (8.118)$$

Equation (8.116) is invariant under the group Equation (8.117) if and only if

$$2c - a - 2b = (2\beta - 1) a = c - 3b. \quad (8.119)$$

The boundaries of the problem at the wall and at infinity are invariant under (8.117).

$$\begin{aligned}\tilde{y} = e^b y = 0 &\Rightarrow y = 0 \\ \tilde{\psi}(\tilde{x}, 0) = e^c \psi(e^a x, 0) = 0 &\Rightarrow \psi(x, 0) = 0 \\ \tilde{\psi}_{\tilde{y}}(\tilde{x}, 0) = e^{c-b} \psi_y(e^a x, 0) = 0 &\Rightarrow \psi_y(x, 0) = 0\end{aligned}\tag{8.120}$$

As in the case of the Blasius problem, the free stream boundary condition requires some care.

$$\tilde{\psi}_{\tilde{y}}(\tilde{x}, \infty) = e^{c-b} \psi_y(e^a x, \infty) = e^{\beta a} M x^\beta\tag{8.121}$$

The boundary condition at the outer edge of the boundary layer is invariant if and only if

$$c - b = \beta a.\tag{8.122}$$

Solving (8.119) and (8.122) for a and c in terms of b leads to the group

$$\begin{aligned}\tilde{x} &= e^{\frac{2}{1-\beta} b} x \\ \tilde{y} &= e^b y \\ \tilde{\psi} &= e^{\frac{1+\beta}{1-\beta} b} \psi.\end{aligned}\tag{8.123}$$

We can expect that the solution of the problem will be invariant under the two-parameter group (8.123). That is we can expect a solution of the form

$$\frac{\psi}{x^{\left(\frac{1+\beta}{2}\right)}} = F\left(\frac{y}{x^{\left(\frac{1-\beta}{2}\right)}}\right).\tag{8.124}$$

As in the Blasius problem, we use M and ν to nondimensionalize the problem. The

similarity variables are

$$\alpha = \left(\frac{M}{2\nu} \right)^{1/2} \frac{y}{(x + x_0)^{\frac{1-\beta}{2}}} \quad (8.125)$$

$$F = \left(\frac{1}{2\nu M} \right)^{1/2} \frac{\psi}{(x + x_0)^{\frac{1+\beta}{2}}}.$$

Upon substitution of (8.125) and (8.114), the streamfunction equation (8.113) becomes

$$(x + x_0)^{2\beta-1} (F_\alpha((1 + \beta)F - (1 - \beta)\alpha F_\alpha)_\alpha - F_{\alpha\alpha}((1 + \beta)F - (1 - \beta)\alpha F_\alpha) - 2\beta - F_{\alpha\alpha\alpha}) = 0. \quad (8.126)$$

Cancelling terms produces the Falkner-Skan equation

$$F_{\alpha\alpha\alpha} + (1 + \beta)FF_{\alpha\alpha} - 2\beta(F_\alpha)^2 + 2\beta = 0 \quad (8.127)$$

with boundary conditions

$$\begin{aligned} F(0) &= 0 \\ F_\alpha(0) &= 0 \\ F_\alpha(\infty) &= 1. \end{aligned} \quad (8.128)$$

Note that $\beta = 0$ reduces (8.127) to the Blasius equation. It is fairly easy to reduce the order of (8.127) by one. The new variables are

$$\begin{aligned} \phi &= F \\ G &= F_\alpha. \end{aligned} \quad (8.129)$$

Differentiate G with respect to ϕ .

$$\frac{\frac{DG}{D\alpha}}{\frac{D\phi}{D\alpha}} = \frac{dG}{d\phi} = \frac{\frac{\partial G}{\partial \alpha} d\alpha + \frac{\partial G}{\partial F} dF + \frac{\partial G}{\partial F_\alpha} dF_\alpha}{\frac{\partial \beta}{\partial \alpha} d\alpha + \frac{\partial \beta}{\partial F} dF} = \frac{F_{\alpha\alpha}}{F_\alpha} \quad (8.130)$$

Rearrange (8.130) to read

$$\frac{d^2G}{d\phi^2} = \left(\frac{F_\alpha F_{\alpha\alpha\alpha} - F_{\alpha\alpha}^2}{F_\alpha^2} \right) \frac{1}{F_\alpha} = \frac{F_\alpha \left(-(1 + \beta) FF_{\alpha\alpha} + 2\beta(F_\alpha)^2 - 2\beta \right) - F_{\alpha\alpha}^2}{F_\alpha^3} \quad (8.131)$$

where the Falkner-Skan equation (8.127) has been used to replace the third derivative. Using (8.129) and (8.130), equation (8.131) can be expressed as the following second order ODE governing $G(\phi)$

$$GG_{\phi\phi} + (1 + \beta)\phi G_\phi + (G_\phi)^2 + 2\beta \left(\frac{1}{G} - G \right) = 0 \quad (8.132)$$

with boundary conditions

$$\begin{aligned} G(0) &= 0 \\ G(\infty) &= 1. \end{aligned} \quad (8.133)$$

Several velocity profiles are shown in Figure 8.9.

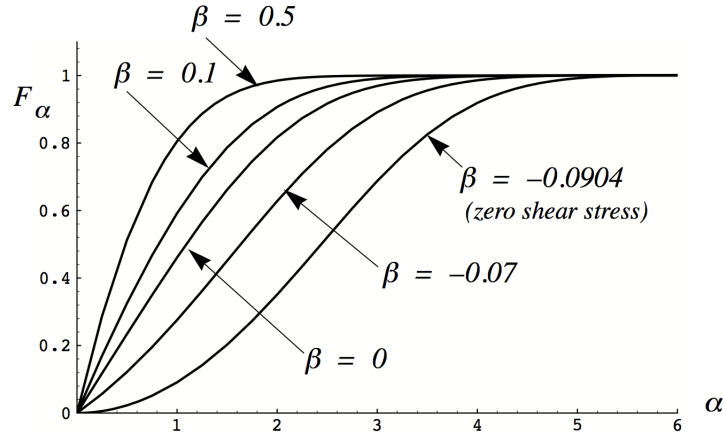
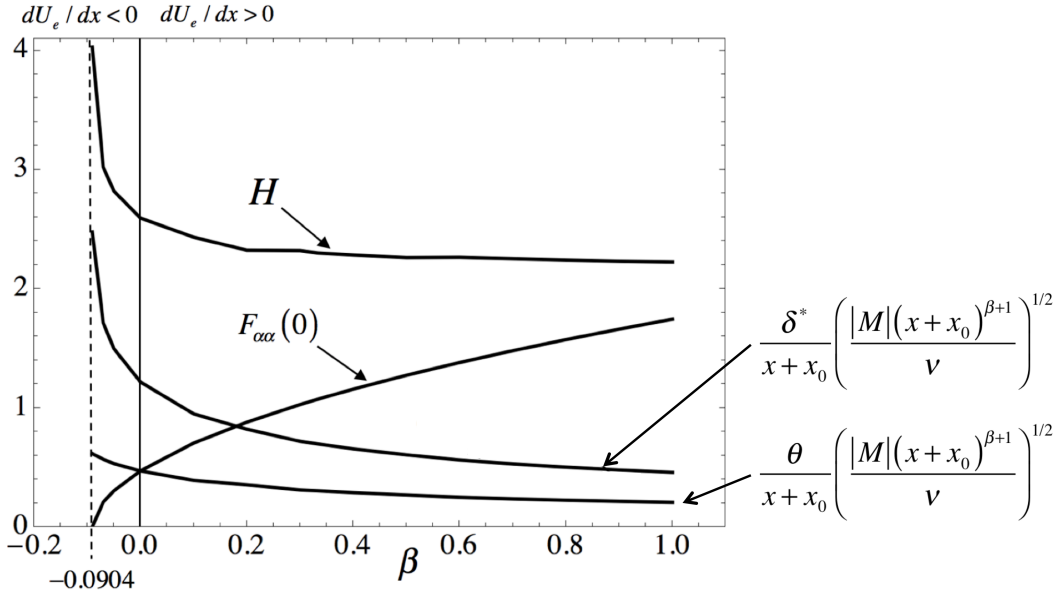


Figure 8.9: Falkner-Skan velocity profiles.

The various measures of boundary layer thickness including shape factor (8.83) and wall stress, are shown in Figure 8.10.

Figure 8.10: *Falkner-Skan boundary layer parameters versus β .*

8.7.1 The case $\beta = -1$.

A particularly interesting case occurs when $\beta = -1$. The pressure gradient term is

$$U_e = \frac{M}{x} \Rightarrow U_e \frac{dU_e}{dx} = -\frac{M^2}{x^3} \quad (8.134)$$

and the original variables become

$$\begin{aligned} \alpha &= \left(\frac{2\nu}{|M|} \right) \frac{y}{x+x_0} \\ F &= \pm \frac{\psi}{(2\nu|M|)^{1/2}}. \end{aligned} \quad (8.135)$$

The units of the governing parameter, $\hat{M} = L^2/T$, are the same as the kinematic viscosity. The ratio $|M|/\nu$ is the Reynolds number for the $\beta = -1$ flow. Note that the Reynolds number of this flow is a constant independent of space in contrast to flows governed by

other values of β . Equation (8.127) becomes

$$F_{\alpha\alpha\alpha} \pm \left(2(F_\alpha)^2 - 2\right) = 0. \quad (8.136)$$

The quantity M is an area flow rate and can change sign depending on whether the flow is created by a source or a sink. The plus sign corresponds to a source while the minus sign represents a sink. To avoid an imaginary root, the absolute value of M is used to non-dimensionalize the stream function in (8.135). The once reduced equation is

$$G^2 G_{\phi\phi} + G(G_\phi)^2 \pm 2(G^2 - 1) = 0 \quad (8.137)$$

where

$$\begin{aligned} \phi &= F \\ G &= F_\alpha. \end{aligned} \quad (8.138)$$

Choose new variables.

$$\begin{aligned} \gamma &= G \\ H &= G_\phi \end{aligned} \quad (8.139)$$

Differentiate the new variables in (8.139) with respect to ϕ and divide.

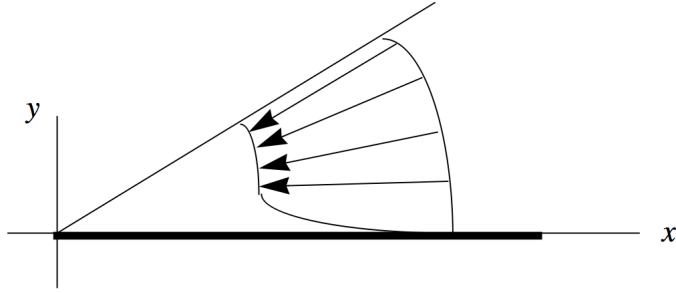
$$\frac{dH}{d\gamma} = \frac{H_\phi + H_G \frac{dG}{d\phi} + H_{G_\phi} \frac{dG_\phi}{d\phi}}{\gamma_\phi + \gamma G \frac{dG}{d\phi}} = \frac{G_{\phi\phi}}{G_\phi} = \frac{-\frac{G_\phi^2}{G} - \frac{2}{G^2} + 2}{G_\phi} \quad (8.140)$$

Equation (8.137) finally reduces to

$$\frac{dH}{d\gamma} = \frac{-\gamma H^2 \pm 2(1 - \gamma^2)}{\gamma^2 H}. \quad (8.141)$$

8.7.2 Falkner-Skan sink flow.

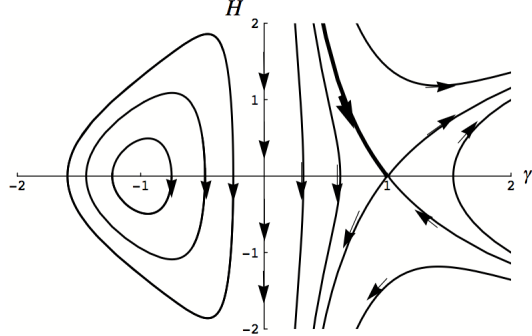
At this point we will restrict ourselves to the case of a sink flow (choose the minus sign in (8.137) and the plus sign in (8.141)). The flow we are considering is sketched in Figure 8.11.

Figure 8.11: *Falkner-Skan sink flow for $\beta = -1$.*

The negative sign in front of the F in (8.135) insures that the velocity derived from the stream function is directed in the negative x direction. The first order ODE, (8.141) (with the minus sign selected) can be broken into the autonomous pair

$$\begin{aligned} \frac{dH}{ds} &= -\gamma H^2 - 2(1 - \gamma^2) \\ \frac{d\gamma}{ds} &= \gamma^2 H \end{aligned} \tag{8.142}$$

with critical points at $(\gamma, H) = (0, \pm 1)$. The phase portrait of (8.142) is shown in Figure 8.12.

Figure 8.12: *Phase portrait of the Falkner-Skan case $\beta = -1$.*

Equation (8.141) is rearranged to read

$$(\gamma H^2 + 2 - 2\gamma^2) d\gamma + (\gamma^2 H) dH = 0 \tag{8.143}$$

which, by the cross derivative test can be shown to be a perfect differential with the integral

$$C = 2\gamma - \frac{2}{3}\gamma^3 + \frac{1}{2}\gamma^2 H^2. \quad (8.144)$$

Recall that

$$\begin{aligned} \gamma &= G = F_\alpha \\ H &= G_\phi = \frac{F_{\alpha\alpha}}{F_\alpha}. \end{aligned} \quad (8.145)$$

At the edge of the boundary layer

$$\left. \begin{aligned} \lim_{\alpha \rightarrow \infty} F_\alpha &= 1 \\ \lim_{\alpha \rightarrow \infty} F_{\alpha\alpha} &= 0 \end{aligned} \right\} \Rightarrow H(1) = 0. \quad (8.146)$$

This allows us to evaluate C in (8.144). The result is

$$C = \frac{4}{3}. \quad (8.147)$$

Solve (8.144) for H .

$$\begin{aligned} H &= \left(\frac{4\gamma}{3} - \frac{4}{\gamma} + \frac{8}{3\gamma^2} \right)^{1/2} \\ (0 < \gamma < 1) \end{aligned} \quad (8.148)$$

where the positive root is recognized to be the physical solution. The solution (8.148) is shown as the thicker weight trajectory in Figure 8.12. Equation (8.148) can be written as

$$\gamma H = \sqrt{\frac{4}{3}} \left((\gamma - 1)^2 (\gamma + 2) \right)^{1/2}. \quad (8.149)$$

In terms of the original variables

$$F_{\alpha\alpha} = \sqrt{\frac{4}{3}} \left((F_\alpha - 1)^2 (F_\alpha + 2) \right)^{1/2} \quad (8.150)$$

and

$$\alpha = \operatorname{Tanh}^{-1} \left(\sqrt{\frac{F_\alpha + 2}{3}} \right) - \operatorname{Tanh}^{-1} \left(\sqrt{\frac{2}{3}} \right). \quad (8.151)$$

The latter result can be solved for the negative of the velocity, F_α .

$$F_\alpha = 3 \operatorname{Tanh}^2 \left(\alpha + \operatorname{Tanh}^{-1} \sqrt{\frac{2}{3}} \right) - 2 \quad (8.152)$$

This is shown plotted in Figure 8.13.

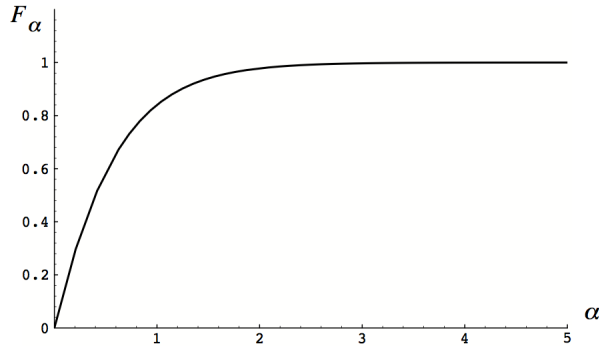


Figure 8.13: *Falkner-Skan sink flow velocity profile $\beta = -1$.*

The Falkner-Skan sink flow represents one of the few known exact solutions of the boundary layer equations. However the fact that an exact solution exists for the case $\beta = -1$ is no accident. Neither is the fact that this case corresponds to an independent variable of the form $\alpha \approx y/x$ where both coordinate directions are in some sense equivalent. Remember the essence of the boundary layer approximation is that the streamwise direction is in a sense "convective" while the transverse direction is regarded as "diffusive" producing a flow that is progressively more slender in the y direction as x increases. In the case of the Falkner-Skan sink flow the aspect ratio of the flow is constant.

8.8 Thwaites' method for approximate calculation of laminar boundary layer characteristics

At the wall, the momentum equation reduces to

$$\frac{\partial^2 U}{\partial y^2} \Big|_{y=0} = -\frac{U_e}{\nu} \frac{dU_e}{dx}. \quad (8.153)$$

Rewrite (8.84) as

$$\frac{\partial U}{\partial y} \Big|_{y=0} = (2 + H) \theta \frac{U_e}{\nu} \frac{dU_e}{dx} + \frac{U_e^2}{\nu} \frac{d\theta}{dx}. \quad (8.154)$$

Choose θ and U_e as length and velocity scales to non-dimensionalize the left sides of (8.153) and (8.154).

$$\begin{aligned} \left(\frac{\theta^2}{U_e} \right) \frac{\partial^2 U}{\partial y^2} \Big|_{y=0} &= -\frac{\theta^2}{\nu} \frac{dU_e}{dx} \\ \left(\frac{\theta}{U_e} \right) \frac{\partial U}{\partial y} \Big|_{y=0} &= (2 + H) \frac{\theta^2}{\nu} \frac{dU_e}{dx} + \frac{U_e}{2\nu} \frac{d\theta^2}{dx} \end{aligned} \quad (8.155)$$

In a landmark paper in 1948 Bryan Thwaites argued that the normalized derivatives on the left of (8.155) should depend only on the shape of the velocity profile and not explicitly on the free stream velocity or thickness. Moreover he argued that there should be a universal function relating the two. He defined

$$\begin{aligned} m &= \left(\frac{\theta^2}{U_e} \right) \frac{\partial^2 U}{\partial y^2} \Big|_{y=0} \\ l(m) &= \left(\frac{\theta}{U_e} \right) \frac{\partial U}{\partial y} \Big|_{y=0}. \end{aligned} \quad (8.156)$$

In terms of m the Von Karman equation is

$$\frac{U_e}{\nu} \frac{d\theta^2}{dx} = 2((2 + H)m + l(m)) = L(m) \quad (8.157)$$

where (8.153) has been used. Thwaites proceeded to examine a variety of known exact and approximate solutions of the boundary layer equations with a pressure gradient. The main results are shown in Figure 8.14.

The correlation of the data was remarkably good, especially the near straight line behavior of $L(m)$. Thwaites proposed the linear approximation

$$L(m) = 0.45 + 6m. \quad (8.158)$$

One of the classes of solutions included in Thwaites' data is the Falkner-Skan boundary layers discussed earlier. For these solutions the Thwaites functions can be calculated explicitly.

$$\begin{aligned} m &= F_{\alpha\alpha\alpha}(0) \left(\int_0^\alpha F_\alpha (1 - F_\alpha) d\alpha \right)^2 = -2\beta \left(\int_0^\alpha F_\alpha (1 - F_\alpha) d\alpha \right)^2 \\ l(m) &= F_{\alpha\alpha}(0) \int_0^\alpha F_\alpha (1 - F_\alpha) d\alpha \\ H(m) &= \frac{\int_0^\alpha (1 - F_\alpha) d\alpha}{\int_0^\alpha F_\alpha (1 - F_\alpha) d\alpha} \end{aligned} \quad (8.159)$$

The various measures of the Falkner-Skan solutions shown in Figure 8.10 can be related to m instead of β using the first equation in (8.159). The relation between m and β is shown in Figure 8.15.

The functions $l(m)$ and $H(m)$ for the Falkner-Skan boundary layer solutions are shown in Figure 8.16.

Thwaites' correlations were re-examined by N. Curle who came up with a very similar set of functions but with slightly improved prediction of boundary layer evolution in adverse pressure gradients. Figure 8.17 provides a comparison between the two methods.

Curle's tabulation of his functions for Thwaites' method is included in Figure 8.18.

A reasonable linear approximation to the data for $L(m)$ in Figure 8.18 is

$$L(m) = 0.441 + 6m. \quad (8.160)$$

Equation (8.160) is not the best linear approximation to Curle's data in Figure 8.18 but is consistent with the value of the friction coefficient for the zero-pressure gradient Blasius

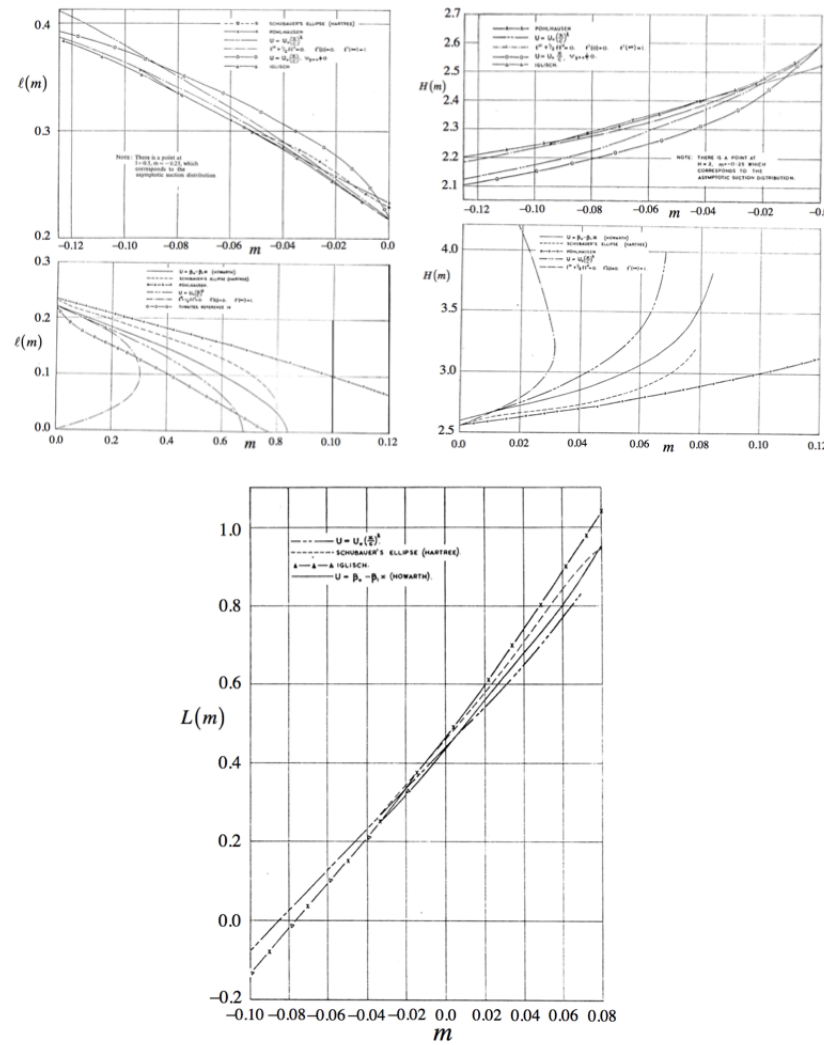


Figure 8.14: Data on skin friction collected by Thwaites: $l(m)$, shape factor $H(m)$ and $L(m)$ for a variety of boundary layer solutions.

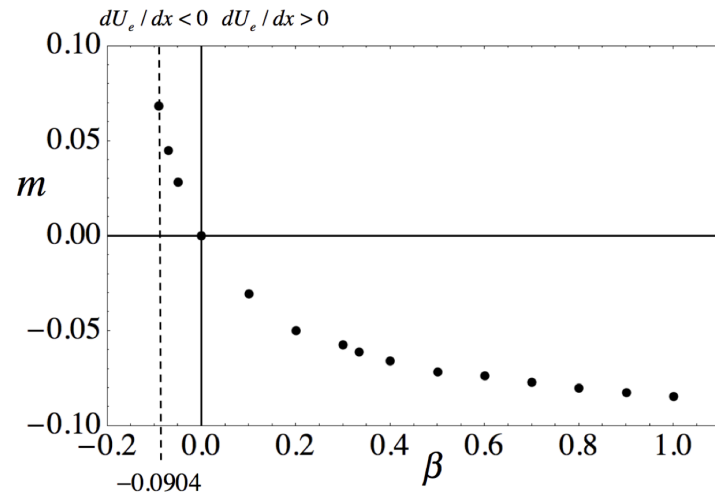


Figure 8.15: The variable m defined in (8.156) versus the free stream velocity exponent β for Falkner-Skan boundary layers.

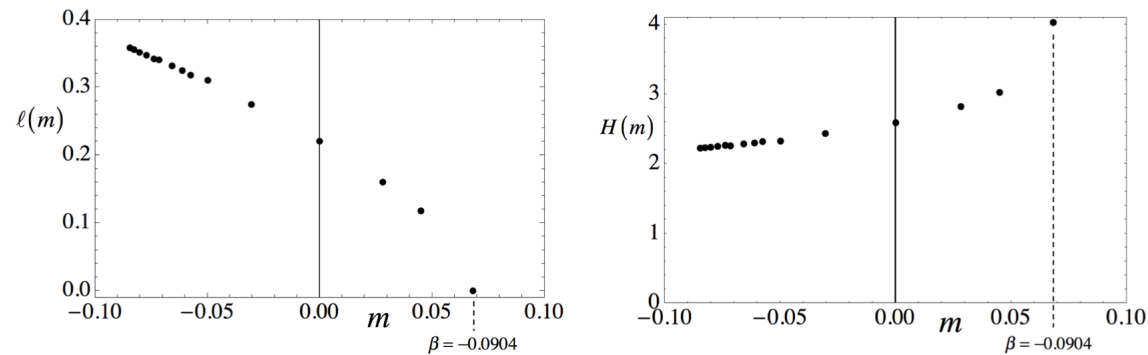


Figure 8.16: Thwaites functions for the Falkner-Skan solutions (8.159).

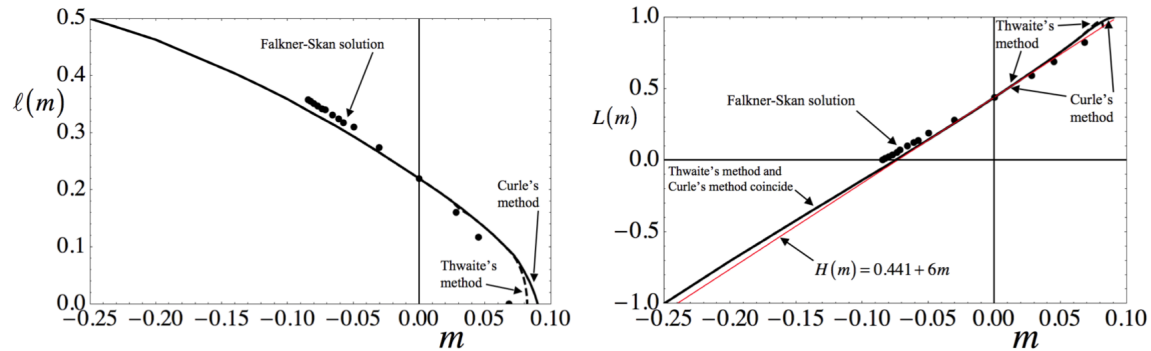


Figure 8.17: Comparison between Curle's functions and Thwaite's functions.

Universal functions for Thwaites's method

| m | $l(m)$ | $H(m)$ | m | $l(m)$ | $H(m)$ |
|--------|--------|--------|-------|--------|--------|
| -0.25 | 0.500 | 2.00 | 0.040 | 0.153 | 2.81 |
| -0.20 | 0.463 | 2.07 | 0.048 | 0.138 | 2.87 |
| -0.14 | 0.404 | 2.18 | 0.056 | 0.122 | 2.94 |
| -0.12 | 0.382 | 2.23 | 0.060 | 0.113 | 2.99 |
| -0.10 | 0.359 | 2.28 | 0.064 | 0.104 | 3.04 |
| -0.080 | 0.333 | 2.34 | 0.068 | 0.095 | 3.09 |
| -0.064 | 0.313 | 2.39 | 0.072 | 0.085 | 3.15 |
| -0.048 | 0.291 | 2.44 | 0.076 | 0.072 | 3.22 |
| -0.032 | 0.268 | 2.49 | 0.080 | 0.056 | 3.30 |
| -0.016 | 0.244 | 2.55 | 0.084 | 0.038 | 3.39 |
| 0 | 0.220 | 2.61 | 0.086 | 0.027 | 3.44 |
| +0.016 | 0.195 | 2.67 | 0.088 | 0.015 | 3.49 |
| 0.032 | 0.168 | 2.75 | 0.090 | 0 | 3.55 |

Figure 8.18: Curle's functions for Thwaites' method.

boundary layer ($\sqrt{0.441} = 0.664$). Insert (8.160) into (8.157) and use the definition of m in (8.155) and (8.156).

$$U_e \frac{d}{dx} \left(\frac{\theta^2}{\nu} \right) = 0.441 - 6 \left(\frac{\theta^2}{\nu} \right) \frac{dU_e}{dx} \quad (8.161)$$

Equation (8.161) can be integrated exactly.

$$\theta^2 = \frac{0.441\nu}{U_e(x)^6} \int_0^x U_e(x')^5 dx' \quad (8.162)$$

Equation (8.60) provides the momentum thickness of the boundary layer directly from the distribution of velocity outside the boundary layer $U_e(x)$. Although the von Karman integral equation (8.157) was used to generate the data for Thwaites method, it is no longer needed once (8.60) is known.

The procedure for applying Thwaites' method is as follows.

- 1) Given $U_e(x)$ use (8.162) to determine $\theta^2(x)$.

At a given x :

- 2) The parameter m is determined from (8.156) and (8.153).

$$m = -\frac{\theta^2}{\nu} \frac{dU_e}{dx} \quad (8.163)$$

- 3) The functions $l(m)$ and $H(m)$ are determined from the data in Figure 8.18.

- 4) The friction coefficient is determined from

$$C_f = \frac{2\nu}{U_e \theta} l(m). \quad (8.164)$$

- 5) The displacement thickness $\delta^*(m)$ is determined from $H(m)$.

The process is repeated while progressing along the wall to increasing values of x . Separation of the boundary layer is assumed to have occurred if a point is reached where $l(m) = 0$.

The key references used in this section are

- 1) Thwaites, B. 1948 Approximate calculations of the laminar boundary layer, VII International Congress of Applied Mechanics, London. Also *Aeronautical Quarterly* Vol. 1, page 245, 1949.

2) Curle, N. 1962 *The Laminar Boundary Layer Equations*, Clarendon Press.

8.8.1 Example - free stream velocity from the potential flow over a circular cylinder.

To illustrate the application of Thwaites' method let's see what it predicts for the flow over a circular cylinder where we take as the free stream velocity the potential flow solution.

$$\frac{U_e}{U_\infty} = 2 \sin\left(\frac{x}{R}\right) \quad (8.165)$$

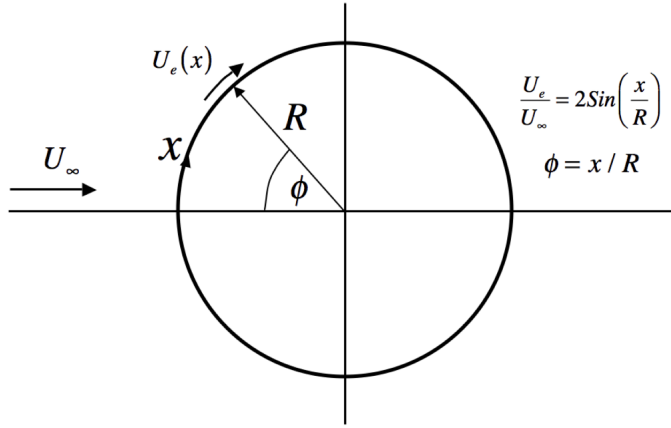


Figure 8.19: Example for Thwaites' method.

According to (8.162)

$$\left(\frac{\theta}{R}\right)^2 R_e = \frac{0.441}{\sin^6(\phi)} \int_0^\phi \sin^5(\phi') d\phi' \quad (8.166)$$

where

$$R_e = \frac{U_\infty (2R)}{\nu}. \quad (8.167)$$

Near the forward stagnation point

$$\lim_{\phi \rightarrow 0} \left(\frac{\theta}{R}\right)^2 R_e = \frac{0.441}{\phi^6} \int_0^\phi \phi'^5 d\phi' = \frac{0.441}{6}. \quad (8.168)$$

Interestingly the method gives a finite momentum thickness at the stagnation point. This is useful to know when we apply the method to an airfoil where the radius of the leading edge at the forward stagnation point will define the initial thickness for the boundary layer calculation. Next the relationship between m and ϕ is determined using (8.163).

$$m = -\frac{\theta^2}{\nu} \frac{dU_e}{dx} = -\frac{1}{2} \left(\frac{\theta}{R} \right)^2 R_e \frac{d}{d\phi} \left(\frac{U_e}{U_\infty} \right) = -\frac{0.441 \cos(\phi)}{\sin^6(\phi)} \int_0^\phi \sin^5(\phi') d\phi' \quad (8.169)$$

Once $m(\phi)$ is known, $l(m(\phi))$ is determined from the data in Figure 8.18. The friction coefficient determined using (8.164) is shown in Figure 8.21.

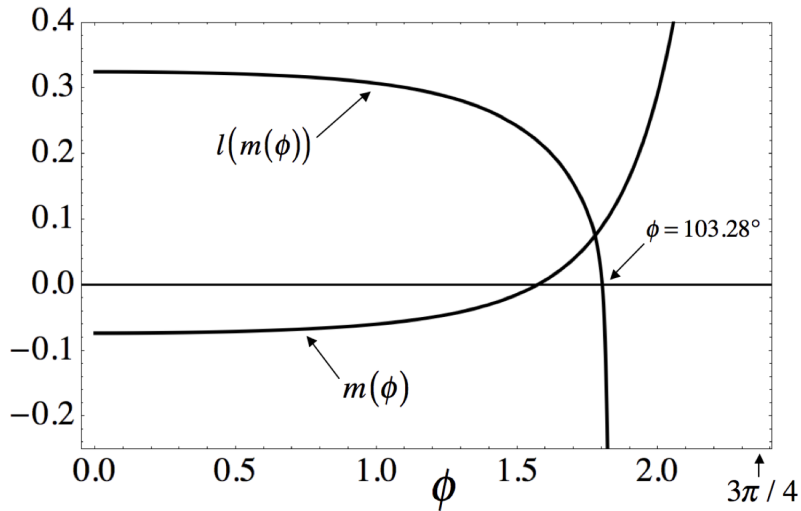


Figure 8.20: Thwaites' functions for the freestream distribution (8.165).

According to this method the boundary layer on the cylinder would separate. The boundary layer parameters, momentum thickness, displacement thickness, shape factor and friction coefficient are shown in figures 8.21 and 8.22. But the predicted separation point is well beyond the separation point measured in experiments. Part of the reason for this is that the pressure distribution is forced to be the potential solution. In practice the boundary layer and the free stream interact with each other leading to a forward surface pressure distribution that is quite different from the potential flow solution. If the experimentally measured pressure is used, the predicted separation point is much closer to the measured position of about $\phi_{separation} = 83^\circ$.

Notice the role of the Reynolds number. The momentum thickness and displacement thickness as well as the friction coefficient are all proportional to $1/\sqrt{R_e}$. We saw this same behavior in the Blasius solution, (8.106) and (8.108).

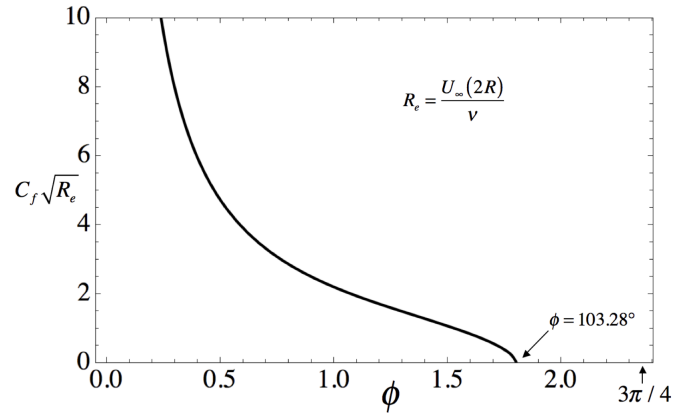


Figure 8.21: Friction coefficient for the freestream distribution (8.165).

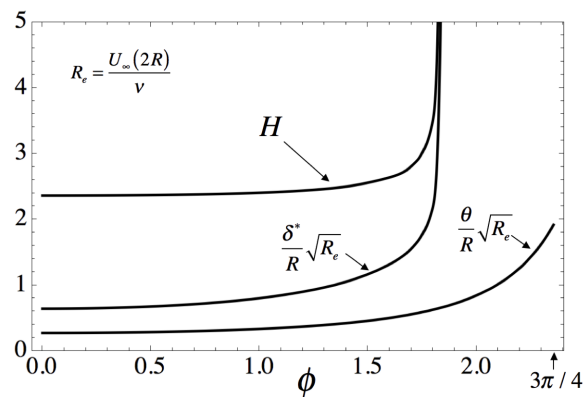


Figure 8.22: Boundary layer thicknesses and shape factor for the freestream distribution (8.165).

8.9 Compressible laminar boundary layers

The equations of motion for laminar flow are

$$\begin{aligned} \frac{\partial \rho U}{\partial x} + \frac{\partial \rho V}{\partial y} &= 0 \\ \rho U \frac{\partial U}{\partial x} + \rho V \frac{\partial U}{\partial y} + \frac{dP_e}{dx} - \frac{\partial}{\partial y} \left(\mu \frac{\partial U}{\partial y} \right) &= 0 \\ \rho U C_p \frac{\partial T}{\partial x} + \rho V C_p \frac{\partial T}{\partial y} - U \frac{dP_e}{dx} - \frac{\partial}{\partial y} \left(\kappa \frac{\partial T}{\partial y} \right) - \mu \left(\frac{\partial U}{\partial y} \right)^2 &= 0. \end{aligned} \quad (8.170)$$

Using the same approach as in the Couette flow problem, let the temperature in the boundary layer be expressed as a function of the local velocity, $T = T(U)$. Substitute this functional form into the energy equation.

$$\left(\rho U \frac{\partial U}{\partial x} + \rho V \frac{\partial U}{\partial y} \right) C_p \frac{dT}{dU} - U \frac{dP_e}{dx} - \frac{\partial}{\partial y} \left(\kappa \frac{dT}{dU} \frac{\partial U}{\partial y} \right) - \mu \left(\frac{\partial U}{\partial y} \right)^2 = 0 \quad (8.171)$$

Use the momentum equation to replace the factor in parentheses on the left hand side of (8.171)

$$\left(-\frac{dP_e}{dx} + \frac{\partial}{\partial y} \left(\mu \frac{\partial U}{\partial y} \right) \right) C_p \frac{dT}{dU} - U \frac{dP_e}{dx} - \frac{dT}{dU} \frac{\partial}{\partial y} \left(\kappa \frac{\partial U}{\partial y} \right) - \kappa \frac{d^2 T}{dU^2} \left(\frac{\partial U}{\partial y} \right)^2 - \mu \left(\frac{\partial U}{\partial y} \right)^2 = 0 \quad (8.172)$$

which we can write as

$$-\frac{dP_e}{dx} \left(C_p \frac{dT}{dU} + U \right) + C_p \frac{dT}{dU} \frac{\partial}{\partial y} \left(\left(\mu - \frac{\kappa}{C_p} \right) \frac{\partial U}{\partial y} \right) + \left(\kappa \frac{d^2 T}{dU^2} + \mu \right) \left(\frac{\partial U}{\partial y} \right)^2 = 0. \quad (8.173)$$

Introduce the Prandtl number (8.13) which can be assumed to be constant independent of position in the boundary layer. The energy equation becomes

$$-\frac{dP_e}{dx} \left(C_p \frac{dT}{dU} + U \right) + C_p \frac{dT}{dU} \left(\frac{Pr - 1}{Pr} \right) \frac{\partial}{\partial y} \left(\mu \frac{\partial U}{\partial y} \right) + \left(\kappa \frac{d^2 T}{dU^2} + \mu \right) \left(\frac{\partial U}{\partial y} \right)^2 = 0. \quad (8.174)$$

There are several important cases to consider.

8.9.1 The energy integral for a compressible boundary layer with an adiabatic wall and $P_r = 1$.

In this case (8.174) reduces to

$$-\frac{dP_e}{dx} \left(C_p \frac{dT}{dU} + U \right) + \left(\kappa \frac{d^2T}{dU^2} + \mu \right) \left(\frac{\partial U}{\partial y} \right)^2 = 0. \quad (8.175)$$

The flow at the wall satisfies

$$\begin{aligned} U|_{y=0} &= 0 \\ \frac{dT}{dy} \Big|_{y=0} &= \left(\frac{dT}{dU} \frac{\partial U}{\partial y} \right)_{y=0} = 0. \end{aligned} \quad (8.176)$$

The velocity gradient at the wall is finite as is the wall shear stress $(\partial U / \partial y)_{y=0} \neq 0$ so the second condition in (8.176) implies that $(\partial T / \partial y)_{y=0} = 0$. The pressure gradient along the wall is not necessarily zero so flow conditions at the edge of the boundary layer can vary with the streamwise coordinate. The temperature must satisfy

$$\frac{d^2T}{dU^2} = -\frac{\mu}{\kappa} \quad (8.177)$$

and

$$\frac{dT}{dU} = -\frac{U}{C_p}. \quad (8.178)$$

Both (8.177) and (8.178) are consistent with the definition of the Prandtl number and the assumption $P_r = 1$ and integrate to

$$T_{wa} - T = \frac{U^2}{2C_p} \quad (8.179)$$

where T_{wa} is the adiabatic wall temperature defined in (8.122). This temperature can be expressed in terms of the temperature and velocity at the edge of the boundary layer.

$$T_{wa} = T_e + \frac{U_e^2}{2C_p} \quad (8.180)$$

Introduce the Mach number at the edge of the boundary layer, $M_e = U_e/a_e$. Now

$$\frac{T_{wa}}{T_e} = 1 + \left(\frac{\gamma - 1}{2} \right) M_e^2 = \frac{T_{te}}{T_e}. \quad (8.181)$$

For a Prandtl number of one, the stagnation temperature is constant through the boundary layer at the value at the boundary layer edge.

8.9.2 Non-adiabatic wall with $dP/dx = 0$ and $P_r = 1$

Again, although for different reasons than in the previous section, the temperature is governed by

$$\frac{d^2 T}{dU^2} = -\frac{\mu}{\kappa}. \quad (8.182)$$

In this case, the temperature profile across the boundary layer is

$$C_p(T - T_w) + \frac{U^2}{2} = C_p U \left(\frac{dT}{dU} \right)_{y=0} \quad (8.183)$$

where T_w is the temperature at the no-slip wall. The heat transfer at the wall is

$$Q_w = -\kappa \left(\frac{\partial T}{\partial y} \right)_{y=0} = -\kappa \left(\frac{dT}{dU} \frac{\partial U}{\partial y} \right)_{y=0} = -\frac{\kappa}{\mu} \left(\mu \frac{\partial U}{\partial y} \right)_{y=0} \left(\frac{dT}{dU} \right)_{y=0}. \quad (8.184)$$

Thus

$$C_p \left(\frac{dT}{dU} \right)_{y=0} = - \left(\frac{C_p \mu}{\kappa} \right) \frac{Q_w}{\tau_w}. \quad (8.185)$$

The temperature profile with heat transfer is

$$C_p(T - T_w) + \frac{U^2}{2} = -\frac{Q_w}{\tau_w} U \quad (8.186)$$

which is identical to the temperature profile (8.18) derived for the Couette flow case for $P_r = 1$. Evaluate (8.186) at the edge of the boundary layer where the velocity and temperature U_e and T_e are the same as the free stream values U_∞ and T_∞ . The result is

$$T_w = T_\infty + \frac{U_\infty^2}{2C_p} + \frac{Q_w U_\infty}{\tau_w C_p}. \quad (8.187)$$

The Stanton number was defined in the previous section on Couette flow.

$$S_t = \frac{Q_w}{\rho_\infty U_\infty C_p (T_w - T_{wa})} \quad (8.188)$$

The adiabatic wall temperature is the free stream stagnation temperature. Using (8.187) in (8.188) gives the friction coefficient in terms of the Stanton number

$$C_f = 2S_t \quad (8.189)$$

which can be compared with the Couette flow result (8.29).

Using (8.186) and (8.187) the temperature profile can be expressed in terms of the free stream and wall temperatures as follows.

$$\frac{T - T_w}{T_\infty} = \left(1 - \frac{T_w}{T_\infty}\right) \frac{U}{U_\infty} + \left(\frac{U_\infty^2}{2C_p T_\infty}\right) \frac{U}{U_\infty} \left(1 - \frac{U}{U_\infty}\right) \quad (8.190)$$

8.10 Mapping a compressible to an incompressible boundary layer

In the late 1940's L. Howarth (*Proc. R. Soc. London A* 194, 16-42, 1948) and K. Stewartson (*Proc. R. Soc. London A* 200, 84-100, 1949) introduced a remarkable transformation that can be used to map the compressible boundary layer equations to the incompressible form including the effects of free stream velocity variation. The basic idea is to define a stream function for a virtual incompressible flow that carries the same mass flow, integrated to the wall, as the real compressible flow.

Figure 8.23 illustrates the idea. To satisfy the mass balance requirement, the constant density of the virtual flow is taken to be the stagnation density of the real flow at the edge

of the boundary layer.

$$\rho_t = \rho_e \left(1 + \left(\frac{\gamma - 1}{2} \right) M_e^2 \right)^{1/(\gamma-1)} \quad (8.191)$$

The flow at the edge of the boundary layer is assumed to be isentropic.

$$\frac{P_t}{P_e} = \left(\frac{T_t}{T_e} \right)^{\gamma/(\gamma-1)} = \left(\frac{a_t}{a_e} \right)^{2\gamma/(\gamma-1)} \quad (8.192)$$

The pressure through the boundary layer is constant, $P = P_e$ and $\tilde{P} = \tilde{P}_e$.

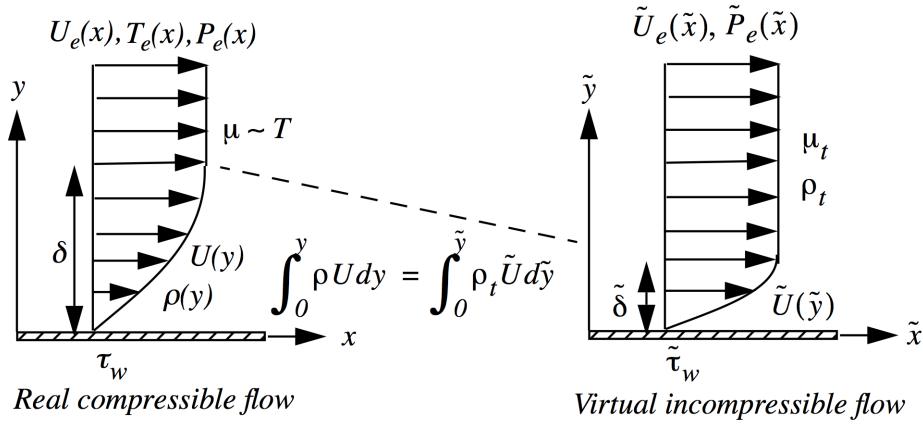


Figure 8.23: *Mapping of a compressible to an incompressible flow.*

Sutherland's law is referenced to the stagnation temperature T_t of the compressible flow at the edge of the boundary layer.

$$\frac{\mu}{\mu_t} = \left(\frac{T}{T_t} \right)^{3/2} \left(\frac{T_t + T_S}{T + T_S} \right) \quad (8.193)$$

The viscosity of the virtual flow, μ_t , is the viscosity of the gas evaluated at T_t . The key assumption needed to make the mapping work is that the viscosity of the gas is linearly proportional to temperature.

$$\frac{\mu}{\mu_t} = \sigma \frac{T}{T_t} \quad (8.194)$$

The constant σ is chosen to provide the best approximation to (8.193).

$$\sigma = \left(\frac{T_w}{T_t} \right)^{1/2} \left(\frac{T_t + T_S}{T_w + T_S} \right) \quad (8.195)$$

If $P_r = 1$ then $\sigma = 1$. The continuity and momentum equations governing the compressible flow are

$$\begin{aligned} \frac{\partial \rho U}{\partial x} + \frac{\partial \rho V}{\partial y} &= 0 \\ U \frac{\partial U}{\partial x} + V \frac{\partial U}{\partial y} + \frac{1}{\rho} \frac{dP_e}{dx} - \frac{1}{\rho} \frac{\partial}{\partial y} \left(\mu \frac{\partial U}{\partial y} \right) - \frac{1}{\rho} \frac{\partial \tau_{xy}}{\partial y} &= 0 \end{aligned} \quad (8.196)$$

where it is understood that τ_{xy} refers to the turbulent shearing stress. The coordinates of the virtual flow are defined as

$$\begin{aligned} \tilde{x} &= \sigma \int_0^x \left(\frac{P_e}{P_t} \left(\frac{a_e}{a_t} \right) \right) dx' = f(x) \\ \tilde{y} &= \left(\frac{a_e}{a_t} \right) \int_0^y \left(\frac{\rho(x, y')}{\rho_t} \right) dy' = g(x, y). \end{aligned} \quad (8.197)$$

Note that \tilde{y} is a function of x and y since the density depends on both spatial variables. The variables x' and y' are dummy variables of integration. From the fundamental theorem of calculus the derivatives of the coordinates are

$$\begin{aligned} \frac{\partial \tilde{x}}{\partial x} &= f_x = \sigma \left(\frac{P_e}{P_t} \left(\frac{a_e}{a_t} \right) \right) \\ \frac{\partial \tilde{x}}{\partial y} &= f_y = 0 \\ \frac{\partial \tilde{y}}{\partial x} &= g_x \\ \frac{\partial \tilde{y}}{\partial y} &= g_y = \left(\frac{a_e}{a_t} \right) \left(\frac{\rho}{\rho_t} \right). \end{aligned} \quad (8.198)$$

Each of the derivatives is known explicitly except $\partial \tilde{y} / \partial x$. However, as we will see in the analysis to follow, terms that involve this derivative will cancel. The continuity equation is

satisfied identically through the introduction of a compressible stream function. Let

$$\begin{aligned}\rho U &= \rho_t \frac{\partial \psi}{\partial y} \\ \rho V &= -\rho_t \frac{\partial \psi}{\partial x}.\end{aligned}\tag{8.199}$$

The stream function of the virtual incompressible flow is a function of $\tilde{x}(x)$ and $\tilde{y}(x, y)$ and has the same value as its counterpart in the real compressible flow since there is the same mass flow between the streamline and the wall in the two flows.

$$\psi(x, y) = \tilde{\psi}(\tilde{x}(x), \tilde{y}(x, y))\tag{8.200}$$

The mapping we are about to carry out is a bit complicated. In the discussion below I have tried to retain as much detail as possible to help the reader get through the derivation without requiring a lot of side work to see how one relation follows from another. Maybe there is more detail than needed but I decided to err on the side of more rather than less to try to give maximum help to the reader. The partial derivatives of the stream function are

$$\begin{aligned}\frac{\partial \psi}{\partial x} &= \frac{\partial \tilde{\psi}}{\partial \tilde{x}} \frac{\partial \tilde{x}}{\partial x} + \frac{\partial \tilde{\psi}}{\partial \tilde{y}} \frac{\partial \tilde{y}}{\partial x} = \frac{\partial \tilde{\psi}}{\partial \tilde{x}} \frac{d \tilde{x}}{dx} + \frac{\partial \tilde{\psi}}{\partial \tilde{y}} \frac{\partial \tilde{y}}{\partial x} \\ \frac{\partial \psi}{\partial y} &= \frac{\partial \tilde{\psi}}{\partial \tilde{x}} \frac{\partial \tilde{x}}{\partial y} + \frac{\partial \tilde{\psi}}{\partial \tilde{y}} \frac{\partial \tilde{y}}{\partial y} = \frac{\partial \tilde{\psi}}{\partial \tilde{y}} \frac{\partial \tilde{y}}{\partial y}.\end{aligned}\tag{8.201}$$

The velocities can be expressed in terms of the new coordinates as

$$\begin{aligned}U &= \frac{\rho_t}{\rho} \frac{\partial \psi}{\partial y} = \left(\frac{a_e}{a_t} \right) \frac{\partial \tilde{\psi}}{\partial \tilde{y}} = \left(\frac{a_e}{a_t} \right) \tilde{U} \\ V &= -\frac{\rho_t}{\rho} \frac{\partial \psi}{\partial x} = -\sigma \frac{\rho_t}{\rho} \left(\frac{P_e}{P_t} \frac{a_e}{a_t} \right) \frac{\partial \tilde{\psi}}{\partial \tilde{x}} - \frac{\rho_t}{\rho} \frac{\partial \tilde{\psi}}{\partial \tilde{y}} \frac{\partial \tilde{y}}{\partial x}.\end{aligned}\tag{8.202}$$

The streamwise velocity in the virtual flow is $\tilde{U} = \partial \tilde{\psi} / \partial \tilde{y}$. The mass flow between the streamline and the wall in the two flows is depicted in Figure 8.23.

$$\int_0^y \rho U dy = \int_0^{\tilde{y}} \rho_t \tilde{U} d\tilde{y}\tag{8.203}$$

Differentiate (8.203) at a fixed x and use (8.202). The result is

$$\frac{d\tilde{y}}{dy} = \frac{\rho U}{\rho_t \tilde{U}} = \left(\frac{a_e}{a_t} \right) \frac{\rho}{\rho_t} \quad (8.204)$$

which is consistent with the partial derivative $\partial\tilde{y}/\partial y$ in (8.198). Equation (8.204) confirms that the definition of \tilde{y} defined in (8.197) insures that the streamline values in the two flows are the same, that (8.200) holds. Use the chain rule to determine the first derivatives of U that appear in (8.196).

$$\begin{aligned} \frac{\partial U}{\partial x} &= \frac{\partial}{\partial \tilde{x}} \left(\left(\frac{a_e}{a_t} \right) \frac{\partial \tilde{\psi}}{\partial \tilde{y}} \right) \frac{d\tilde{x}}{dx} + \frac{\partial}{\partial \tilde{y}} \left(\left(\frac{a_e}{a_t} \right) \frac{\partial \tilde{\psi}}{\partial \tilde{y}} \right) \frac{\partial \tilde{y}}{\partial x} = \\ &\sigma \left(\frac{P_e}{P_t} \left(\frac{a_e}{a_t} \right)^2 \right) \left(\left(\frac{1}{a_e} \right) \frac{\partial a_e}{\partial \tilde{x}} \frac{\partial \tilde{\psi}}{\partial \tilde{y}} + \frac{\partial^2 \tilde{\psi}}{\partial \tilde{x} \partial \tilde{y}} \right) + \left(\frac{a_e}{a_t} \right) \frac{\partial^2 \tilde{\psi}}{\partial \tilde{y}^2} \frac{\partial \tilde{y}}{\partial x} \\ \frac{\partial U}{\partial y} &= \frac{\partial}{\partial \tilde{x}} \left(\left(\frac{a_e}{a_t} \right) \frac{\partial \tilde{\psi}}{\partial \tilde{y}} \right) \frac{d\tilde{x}}{dy} + \frac{\partial}{\partial \tilde{y}} \left(\left(\frac{a_e}{a_t} \right) \frac{\partial \tilde{\psi}}{\partial \tilde{y}} \right) \frac{\partial \tilde{y}}{\partial y} = \left(\frac{a_e}{a_t} \right)^2 \left(\frac{\rho}{\rho_t} \right) \left(\frac{\partial^2 \tilde{\psi}}{\partial \tilde{y}^2} \right) \end{aligned} \quad (8.205)$$

Now we can form the convective terms in (8.196).

$$\begin{aligned} U \frac{\partial U}{\partial x} + V \frac{\partial U}{\partial y} &= \\ &\sigma \left(\frac{P_e}{P_t} \left(\frac{a_e}{a_t} \right)^3 \right) \left(\left(\frac{1}{a_e} \right) \frac{\partial a_e}{\partial \tilde{x}} \left(\frac{\partial \tilde{\psi}}{\partial \tilde{y}} \right)^2 + \frac{\partial^2 \tilde{\psi}}{\partial \tilde{x} \partial \tilde{y}} \left(\frac{\partial \tilde{\psi}}{\partial \tilde{y}} \right) \right) + \left(\frac{a_e}{a_t} \right)^2 \left(\frac{\partial \tilde{\psi}}{\partial \tilde{y}} \frac{\partial^2 \tilde{\psi}}{\partial \tilde{y}^2} \frac{\partial \tilde{y}}{\partial x} \right) - \\ &\left(\sigma \left(\frac{P_e}{P_t} \frac{a_e}{a_t} \right) \left(\frac{a_e}{a_t} \right)^2 \left(\frac{\partial^2 \tilde{\psi}}{\partial \tilde{y}^2} \right) \frac{\partial \tilde{\psi}}{\partial \tilde{x}} + \left(\frac{a_e}{a_t} \right)^2 \left(\frac{\partial^2 \tilde{\psi}}{\partial \tilde{y}^2} \frac{\partial \tilde{\psi}}{\partial \tilde{y}} \frac{\partial \tilde{y}}{\partial x} \right) \right) \end{aligned} \quad (8.206)$$

Note the terms involving $\partial\tilde{y}/\partial x$ cancel in (8.206). Thus

$$\begin{aligned} U \frac{\partial U}{\partial x} + V \frac{\partial U}{\partial y} = \\ \sigma \left(\frac{P_e}{P_t} \left(\frac{a_e}{a_t} \right)^3 \right) \left(\left(\frac{1}{a_e} \right) \frac{\partial a_e}{\partial \tilde{x}} \left(\frac{\partial \tilde{\psi}}{\partial \tilde{y}} \right)^2 + \frac{\partial^2 \tilde{\psi}}{\partial \tilde{x} \partial \tilde{y}} \frac{\partial \tilde{\psi}}{\partial \tilde{y}} - \left(\frac{\partial^2 \tilde{\psi}}{\partial \tilde{y}^2} \right) \frac{\partial \tilde{\psi}}{\partial \tilde{x}} \right). \end{aligned} \quad (8.207)$$

Now consider the pressure gradient term. Assume the flow at the edge of the boundary layer is isentropic.

$$\left(\frac{P_e}{P_t} \right) = \left(\frac{a_e}{a_t} \right)^{\frac{2\gamma}{\gamma-1}} \quad (8.208)$$

The pressure gradient term can be expressed in terms of the speed of sound at the boundary layer edge.

$$\begin{aligned} \frac{dP_e}{dx} &= \frac{2\gamma P_t}{\gamma-1} \left(\frac{a_e}{a_t} \right)^{\frac{\gamma+1}{\gamma-1}} \frac{1}{a_t} \frac{da_e}{d\tilde{x}} \frac{d\tilde{x}}{dx} = \sigma \left(\frac{P_e}{P_t} \left(\frac{a_e}{a_t} \right) \right) \frac{2\gamma P_t}{\gamma-1} \left(\frac{a_e}{a_t} \right)^{\frac{\gamma+1}{\gamma-1}} \frac{1}{a_t} \frac{da_e}{d\tilde{x}} \\ \frac{dP_e}{dx} &= \sigma \left(\frac{P_e}{P_t} \left(\frac{a_e}{a_t} \right)^2 \right) \frac{2\gamma P_t}{\gamma-1} \left(\frac{a_e}{a_t} \right)^{\frac{\gamma+1}{\gamma-1}} \frac{1}{a_e} \frac{da_e}{d\tilde{x}} \end{aligned} \quad (8.209)$$

Now

$$\begin{aligned} U \frac{\partial U}{\partial x} + V \frac{\partial U}{\partial y} + \frac{1}{\rho} \frac{dP_e}{dx} &= \sigma \left(\frac{P_e}{P_t} \left(\frac{a_e}{a_t} \right)^3 \right) \left(\frac{\partial^2 \tilde{\psi}}{\partial \tilde{x} \partial \tilde{y}} \frac{\partial \tilde{\psi}}{\partial \tilde{y}} - \left(\frac{\partial^2 \tilde{\psi}}{\partial \tilde{y}^2} \right) \frac{\partial \tilde{\psi}}{\partial \tilde{x}} \right) + \\ \sigma \left(\frac{P_e}{P_t} \left(\frac{a_e}{a_t} \right)^3 \right) &\left(\left(\frac{\partial \tilde{\psi}}{\partial \tilde{y}} \right)^2 + \frac{1}{\rho} \frac{2\gamma P_t}{\gamma-1} \left(\frac{a_e}{a_t} \right)^{\frac{2}{\gamma-1}} \right) \frac{1}{a_e} \frac{da_e}{d\tilde{x}}. \end{aligned} \quad (8.210)$$

Note that, from (8.202).

$$\left(\frac{\partial \tilde{\psi}}{\partial \tilde{y}} \right)^2 = U^2 \left(\frac{a_t}{a_e} \right)^2. \quad (8.211)$$

So far

$$\begin{aligned} U \frac{\partial U}{\partial x} + V \frac{\partial U}{\partial y} + \frac{1}{\rho} \frac{dP_e}{dx} &= \sigma \left(\frac{P_e}{P_t} \left(\frac{a_e}{a_t} \right)^3 \right) \left(\frac{\partial^2 \tilde{\psi}}{\partial \tilde{x} \partial \tilde{y}} \frac{\partial \tilde{\psi}}{\partial \tilde{y}} - \left(\frac{\partial^2 \tilde{\psi}}{\partial \tilde{y}^2} \right) \frac{\partial \tilde{\psi}}{\partial \tilde{x}} \right) + \\ &\quad \sigma \left(\frac{P_e}{P_t} \left(\frac{a_e}{a_t} \right)^3 \right) \left(U^2 \left(\frac{a_t}{a_e} \right)^2 + \frac{1}{\rho} \frac{2\gamma P_t}{\gamma - 1} \left(\frac{a_e}{a_t} \right)^{\frac{2}{\gamma-1}} \right) \frac{1}{a_e} \frac{da_e}{d\tilde{x}}. \end{aligned} \quad (8.212)$$

The flow at the edge of the boundary layer is adiabatic

$$a_t^2 = a_e^2 + \left(\frac{\gamma - 1}{2} \right) U_e^2 \quad (8.213)$$

and

$$\frac{1}{a_e} \frac{da_e}{d\tilde{x}} = - \left(\frac{\gamma - 1}{2a_e^2} \right) U_e \frac{dU_e}{d\tilde{x}}. \quad (8.214)$$

Now

$$\begin{aligned} U \frac{\partial U}{\partial x} + V \frac{\partial U}{\partial y} + \frac{1}{\rho} \frac{dP_e}{dx} &= \sigma \left(\frac{P_e}{P_t} \left(\frac{a_e}{a_t} \right)^3 \right) \left(\frac{\partial^2 \tilde{\psi}}{\partial \tilde{x} \partial \tilde{y}} \frac{\partial \tilde{\psi}}{\partial \tilde{y}} - \left(\frac{\partial^2 \tilde{\psi}}{\partial \tilde{y}^2} \right) \frac{\partial \tilde{\psi}}{\partial \tilde{x}} \right) - \\ &\quad \sigma \left(\frac{P_e}{P_t} \left(\frac{a_e}{a_t} \right)^3 \right) \left(U^2 \left(\frac{\gamma - 1}{2a_e^2} \right) \left(\frac{a_t}{a_e} \right)^2 + \frac{1}{\rho} \frac{\gamma P_t}{a_e^2} \left(\frac{a_e}{a_t} \right)^{\frac{2}{\gamma-1}} \right) U_e \frac{dU_e}{d\tilde{x}}. \end{aligned} \quad (8.215)$$

Note that

$$\begin{aligned} U^2 \left(\frac{\gamma - 1}{2a_e^2} \right) \left(\frac{a_t}{a_e} \right)^2 + \frac{1}{\rho} \frac{\gamma P_t}{a_e^2} \left(\frac{a_e}{a_t} \right)^{\frac{2}{\gamma-1}} &= \\ U^2 \left(\frac{\gamma - 1}{2a_e^2} \right) \left(\frac{a_t}{a_e} \right)^2 + \frac{\rho_e}{\rho} \frac{\gamma P_e}{\rho_e a_e^2} \left(\frac{a_t}{a_e} \right)^{\frac{2\gamma}{\gamma-1}} \left(\frac{a_e}{a_t} \right)^{\frac{2}{\gamma-1}} &= \\ \left(\frac{a_t}{a_e} \right)^4 \left(\frac{a^2 + \left(\frac{\gamma-1}{2} \right) U^2}{a_t^2} \right) \end{aligned} \quad (8.216)$$

where we have used the isentropic relation $P_t/P_e = (a_t/a_e)^{2\gamma/(\gamma-1)}$ and $\gamma P_e/\rho = \gamma P/\rho = a^2$. Now work out the viscous term using $\rho T = P/R = P_e/R$.

$$\begin{aligned} \tau_{xy}|_{laminar} &= \mu \frac{\partial U}{\partial y} = \sigma \mu_t \left(\frac{T}{T_t} \right) \frac{\partial}{\partial y} \left(\left(\frac{a_e}{a_t} \right) \frac{\partial \tilde{\psi}}{\partial \tilde{y}} \right) = \sigma \mu_t \left(\frac{T}{T_t} \right) \left(\frac{a_e}{a_t} \right) \frac{\partial}{\partial y} \left(\frac{\partial \tilde{\psi}}{\partial \tilde{y}} \right) = \\ &\sigma \mu_t \left(\frac{a_e}{a_t} \right)^2 \left(\frac{T}{T_t} \right) \left(\frac{\rho}{\rho_t} \right) \frac{\partial}{\partial \tilde{y}} \left(\frac{\partial \tilde{\psi}}{\partial \tilde{y}} \right) = \sigma \left(\frac{a_e}{a_t} \right)^2 \left(\frac{\rho T}{\rho_t T_t} \right) \left(\mu_t \frac{\partial \tilde{U}}{\partial \tilde{y}} \right) = \sigma \left(\frac{a_e}{a_t} \right)^2 \left(\frac{P_e}{P_t} \right) \tilde{\tau}_{\tilde{x}\tilde{y}}|_{laminar} \end{aligned} \quad (8.217)$$

Recall $\tilde{U} = \partial \tilde{\psi} / \partial \tilde{y}$ and $\tilde{\tau}_{\tilde{x}\tilde{y}}|_{laminar} = \mu_t \partial \tilde{U} / \partial \tilde{y}$. The viscous stress term in the boundary layer equation is

$$\frac{1}{\rho} \frac{\partial}{\partial y} \left(\mu \frac{\partial U}{\partial y} \right) = \sigma \frac{\mu_t}{\rho_t} \frac{P_e}{P_t} \left(\frac{a_e}{a_t} \right)^3 \left(\frac{\partial^3 \tilde{\psi}}{\partial \tilde{y}^3} \right). \quad (8.218)$$

The turbulent stress term transforms as

$$\tau_{xy}|_{turbulent} = \sigma \left(\frac{a_e}{a_t} \right)^2 \frac{P_e}{P_t} \tilde{\tau}_{\tilde{x}\tilde{y}}|_{turbulent} \quad (8.219)$$

which can be expressed as

$$\frac{1}{\rho} \frac{\partial}{\partial y} (\tau_{xy}|_{turbulent}) = \sigma \left(\frac{a_e}{a_t} \right)^3 \frac{P_e}{\rho_t P_t} \frac{\partial}{\partial \tilde{y}} (\tilde{\tau}_{\tilde{x}\tilde{y}}|_{turbulent}). \quad (8.220)$$

Now the boundary layer momentum equation (8.196) becomes

$$\begin{aligned}
 U \frac{\partial U}{\partial x} + V \frac{\partial U}{\partial y} + \frac{1}{\rho} \frac{dP_e}{dx} - \frac{1}{\rho} \frac{\partial}{\partial y} \left(\mu \frac{\partial U}{\partial y} \right) - \frac{1}{\rho} \frac{\partial \tau_{xy}}{\partial y} = \\
 \sigma \left(\frac{P_e}{P_t} \left(\frac{a_e}{a_t} \right)^3 \right) \left(\frac{\partial^2 \tilde{\psi}}{\partial \tilde{x} \partial \tilde{y}} \frac{\partial \tilde{\psi}}{\partial \tilde{y}} - \left(\frac{\partial^2 \tilde{\psi}}{\partial \tilde{y}^2} \right) \frac{\partial \tilde{\psi}}{\partial \tilde{x}} \right) - \\
 \sigma \left(\frac{P_e}{P_t} \left(\frac{a_e}{a_t} \right)^3 \right) \left(\left(\frac{a_t}{a_e} \right)^4 \left(\frac{a^2 + \left(\frac{\gamma-1}{2} \right) U^2}{a_t^2} \right) \right) U_e \frac{dU_e}{d\tilde{x}} - \\
 \sigma \left(\frac{P_e}{P_t} \left(\frac{a_e}{a_t} \right)^3 \right) \frac{\mu_t}{\rho_t} \left(\frac{\partial^3 \tilde{\psi}}{\partial \tilde{y}^3} \right) - \sigma \left(\frac{P_e}{P_t} \left(\frac{a_e}{a_t} \right)^3 \right) \frac{1}{\rho_t} \frac{\partial}{\partial \tilde{y}} (\tilde{\tau}_{\tilde{x}\tilde{y}}|_{turbulent}) = 0.
 \end{aligned} \tag{8.221}$$

Drop the common factor multiplying each term on the right of (8.221). The transformed equation is nearly in incompressible form.

$$\begin{aligned}
 \left(\frac{\partial^2 \tilde{\psi}}{\partial \tilde{x} \partial \tilde{y}} \frac{\partial \tilde{\psi}}{\partial \tilde{y}} - \left(\frac{\partial^2 \tilde{\psi}}{\partial \tilde{y}^2} \right) \frac{\partial \tilde{\psi}}{\partial \tilde{x}} \right) - \left(\frac{a_t}{a_e} \right)^4 \left(\frac{a^2 + \left(\frac{\gamma-1}{2} \right) U^2}{a_t^2} \right) U_e \frac{dU_e}{d\tilde{x}} - \\
 \frac{\mu_t}{\rho_t} \left(\frac{\partial^3 \tilde{\psi}}{\partial \tilde{y}^3} \right) - \frac{1}{\rho_t} \frac{\partial}{\partial \tilde{y}} (\tilde{\tau}_{\tilde{x}\tilde{y}}|_{turbulent}) = 0
 \end{aligned} \tag{8.222}$$

The real and virtual free stream velocities are related by

$$\tilde{U}_e = \frac{a_t}{a_e} U_e \tag{8.223}$$

which comes from the expression for U in (8.202). Differentiate (8.223)

$$\tilde{U}_e \frac{d\tilde{U}_e}{d\tilde{x}} = \left(\frac{a_t}{a_e} \right)^2 \left(\frac{1}{a_e^2} \right) \left(a_e^2 + \left(\frac{\gamma-1}{2} \right) U_e^2 \right) U_e \frac{dU_e}{d\tilde{x}} = \left(\frac{a_t}{a_e} \right)^4 U_e \frac{dU_e}{d\tilde{x}} \tag{8.224}$$

and substitute (8.224) into (8.222).

$$\begin{aligned} & \left(\frac{\partial^2 \tilde{\psi}}{\partial \tilde{x} \partial \tilde{y}} \frac{\partial \tilde{\psi}}{\partial \tilde{y}} - \left(\frac{\partial^2 \tilde{\psi}}{\partial \tilde{y}^2} \right) \frac{\partial \tilde{\psi}}{\partial \tilde{x}} \right) - \left(\frac{a^2 + \left(\frac{\gamma-1}{2} \right) U^2}{a_t^2} \right) \tilde{U}_e \frac{d\tilde{U}_e}{d\tilde{x}} - \\ & \frac{\mu_t}{\rho_t} \left(\frac{\partial^3 \tilde{\psi}}{\partial \tilde{y}^3} \right) - \frac{1}{\rho_t} \frac{\partial}{\partial \tilde{y}} (\tilde{\tau}_{\tilde{x}\tilde{y}}|_{turbulent}) = 0 \end{aligned} \quad (8.225)$$

The velocities in the virtual flow are

$$\begin{aligned} \tilde{U} &= \frac{\partial \tilde{\psi}}{\partial \tilde{y}} \\ \tilde{V} &= -\frac{\partial \tilde{\psi}}{\partial \tilde{x}}. \end{aligned} \quad (8.226)$$

The transformed boundary layer momentum equation finally becomes

$$\left(\tilde{U} \frac{\partial \tilde{U}}{\partial \tilde{x}} + \tilde{V} \left(\frac{\partial \tilde{U}}{\partial \tilde{y}} \right) \right) - \left(\frac{a^2 + \left(\frac{\gamma-1}{2} \right) U^2}{a_e^2 + \left(\frac{\gamma-1}{2} \right) U_e^2} \right) \tilde{U}_e \frac{d\tilde{U}_e}{d\tilde{x}} - \nu_t \left(\frac{\partial^2 \tilde{U}}{\partial \tilde{y}^2} \right) - \frac{1}{\rho_t} \frac{\partial}{\partial \tilde{y}} (\tilde{\tau}_{\tilde{x}\tilde{y}}|_{turbulent}) = 0. \quad (8.227)$$

For an adiabatic wall and $P_r = 1$ the factor in brackets is equal to one. In this case the momentum equation maps exactly to the incompressible form

$$\left(\tilde{U} \frac{\partial \tilde{U}}{\partial \tilde{x}} + \tilde{V} \left(\frac{\partial \tilde{U}}{\partial \tilde{y}} \right) \right) - \tilde{U}_e \frac{d\tilde{U}_e}{d\tilde{x}} - \nu_t \left(\frac{\partial^2 \tilde{U}}{\partial \tilde{y}^2} \right) - \frac{1}{\rho_t} \frac{\partial}{\partial \tilde{y}} (\tilde{\tau}_{\tilde{x}\tilde{y}}|_{turbulent}) = 0 \quad (8.228)$$

with boundary conditions

$$\begin{aligned} \tilde{U}(0) &= 0 \\ \tilde{V}(0) &= 0 \\ \tilde{U}(\tilde{\delta}) &= \tilde{U}_e. \end{aligned} \quad (8.229)$$

The implication of (8.228) and (8.229) is that the effects of compressibility on the boundary layer can be almost completely accounted for by the scaling of coordinates presented in (8.197) which is driven in the y direction by the decrease in density near the wall due to heating and in the x direction by the isentropic changes in free stream temperature and boundary layer pressure due to flow acceleration or deceleration imposed by the surrounding potential flow.

Let's use this transformation to relate the skin friction in the compressible case to the incompressible skin friction. The definition of the friction coefficient is

$$\tilde{C}_f = \frac{\tilde{\tau}_w}{(1/2) \rho_t \tilde{U}_e^2} = \frac{\frac{1}{\sigma} \left(\left(\frac{a_t}{a_e} \right)^2 \frac{P_t}{P_e} \right) \tau_w}{\left(\frac{1}{2} \right) \left(\frac{\rho_t}{\rho_e} \right) \rho_e \left(\frac{a_t}{a_e} \right)^2 U_e^2} = \frac{1}{\sigma} \left(\frac{\rho_e}{\rho_t} \frac{P_t}{P_e} \right) \left(\frac{\tau_w}{(1/2) \rho_t U_e^2} \right) = \frac{1}{\sigma} \frac{T_t}{T_e} C_f. \quad (8.230)$$

Recall that for $P_r = 1$ the constant $\sigma = 1$. In terms of the Mach number, the ratio of friction coefficients in the real compressible flow and the virtual incompressible flow is

$$\frac{C_f}{\tilde{C}_f} = \frac{1}{1 + \left(\frac{\gamma-1}{2} \right) M_e^2}. \quad (8.231)$$

The physical velocity profiles in the compressible flow cannot be determined without solving for the temperature in the boundary layer. Here we will restrict our attention to the laminar, zero pressure gradient, Blasius case, $dU_e/dx = 0$, $\tau_{xy}|_{turbulent} = 0$. The temperature equation was integrated earlier to give

$$T = T_t - \frac{1}{2C_p} U^2. \quad (8.232)$$

Equation (8.232) can be expressed as

$$\frac{T}{T_e} = 1 + \left(\frac{\gamma-1}{2} \right) M_e^2 \left(1 - \left(\frac{U}{U_e} \right)^2 \right). \quad (8.233)$$

The compressible velocity profile is determined from the first relation in (8.202).

$$\frac{U}{U_e} = \frac{\tilde{U}}{\tilde{U}_e}. \quad (8.234)$$

Using the equality $\rho T = \rho_e T_e$ (8.233) becomes

$$\frac{T}{T_e} = 1 + \left(\frac{\gamma - 1}{2} \right) M_e^2 \left(1 - \left(\frac{\tilde{U}}{\tilde{U}_e} \right)^2 \right) = \frac{\rho_e}{\rho}. \quad (8.235)$$

Our goal is to relate the wall normal coordinate in compressible and incompressible flows. From (8.198)

$$dy = \left(\frac{a_t}{a_e} \right) \left(\frac{\rho_t}{\rho_e} \right) \left(\frac{\rho_e}{\rho} \right) d\tilde{y} = \left(\frac{a_t}{a_e} \right) \left(\frac{\rho_t}{\rho_e} \right) \left(1 + \left(\frac{\gamma - 1}{2} \right) M_e^2 \left(1 - \left(\frac{\tilde{U}}{\tilde{U}_e} \right)^2 \right) \right) d\tilde{y}. \quad (8.236)$$

The spatial similarity variable in the virtual flow is

$$\tilde{\alpha} = \tilde{y} \left(\frac{\tilde{U}_e}{2\nu_t \tilde{x}} \right)^{1/2}. \quad (8.237)$$

Now (8.236) becomes

$$dy = \left(\frac{a_t}{a_e} \right) \left(\frac{\rho_t}{\rho_e} \right) \left(\frac{2\nu_t \tilde{x}}{\tilde{U}_e} \right)^{1/2} \left(1 + \left(\frac{\gamma - 1}{2} \right) M_e^2 \left(1 - \left(\frac{\tilde{U}}{\tilde{U}_e} \right)^2 \right) \right) d \left(\tilde{y} \left(\frac{\tilde{U}_e}{2\nu_t \tilde{x}} \right)^{1/2} \right) \quad (8.238)$$

and we can write

$$\begin{aligned} d \left(y \left(\frac{U_e}{2\nu_e x} \right)^{1/2} \right) &= \\ \left(\frac{a_t}{a_e} \right) \left(\frac{\rho_t}{\rho_e} \right) \left(\frac{2\nu_t \tilde{x}}{\tilde{U}_e} \frac{U_e}{2\nu_e x} \right)^{1/2} &\left(1 + \left(\frac{\gamma - 1}{2} \right) M_e^2 \left(1 - \left(\frac{\tilde{U}}{\tilde{U}_e} \right)^2 \right) \right) d \left(\tilde{y} \left(\frac{\tilde{U}_e}{2\nu_t \tilde{x}} \right)^{1/2} \right). \end{aligned} \quad (8.239)$$

Rearrange the coefficient on the right hand side of (8.239) using (8.197) and (8.202).

$$\begin{aligned} \left(\frac{a_t}{a_e}\right) \left(\frac{\rho_t}{\rho_e}\right) \left(\frac{2\nu_t \tilde{x}}{\tilde{U}_e} \frac{U_e}{2\nu_e x}\right)^{1/2} &= \left(\frac{a_t}{a_e}\right) \left(\frac{\rho_t}{\rho_e}\right) \left(\frac{\mu_t \rho_e U_e}{\mu_e \rho_t \tilde{U}_e} \frac{\tilde{x}}{x}\right)^{1/2} = \\ \left(\frac{a_t}{a_e}\right) \left(\frac{\rho_t}{\rho_e}\right) \left(\frac{T_t \rho_e a_e P_e a_e}{T_e \rho_t a_t P_t a_t}\right)^{1/2} &= \left(\frac{\rho_t}{\rho_e}\right) \left(\frac{T_t \rho_e \rho_e T_e}{T_e \rho_t \rho_t T_t}\right)^{1/2} = 1 \end{aligned} \quad (8.240)$$

Finally

$$d\alpha = \left(1 + \left(\frac{\gamma - 1}{2}\right) M_e^2 \left(1 - \left(\frac{\tilde{U}}{\tilde{U}_e}\right)^2\right)\right) d\tilde{\alpha}. \quad (8.241)$$

Integrate (8.241). The similarity variables in the real and virtual flows are related by

$$\alpha(\tilde{\alpha}) = \tilde{\alpha} + \left(\frac{\gamma - 1}{2}\right) M_e^2 \int_0^{\tilde{\alpha}} \left(1 - \left(\frac{\tilde{U}}{\tilde{U}_e}\right)^2\right) d\tilde{\alpha}'. \quad (8.242)$$

The velocity ratio, \tilde{U}/\tilde{U}_e is a known function $\tilde{F}_{\tilde{\alpha}}(\tilde{\alpha})$ from the Blasius solution. The outer edge of the incompressible boundary layer is at $\tilde{\alpha}_e = 4.906/\sqrt{2} = 3.469$. The integral of the velocity term in (8.242) is

$$\int_0^{\tilde{\alpha}_e} \left(1 - \left(\frac{\tilde{U}}{\tilde{U}_e}\right)^2\right) d\tilde{\alpha}' = 1.67912. \quad (8.243)$$

This allows us to determine how the thickness of the compressible layer depends on Mach number. The outer edge of the compressible boundary layer is at

$$\alpha_e = \tilde{\alpha}_e + \left(\frac{\gamma - 1}{2}\right) M_e^2 \int_0^{\tilde{\alpha}_e} \left(1 - \left(\frac{\tilde{U}}{\tilde{U}_e}\right)^2\right) d\tilde{\alpha}' = 3.469 + 1.67912 \left(\frac{\gamma - 1}{2}\right) M_e^2. \quad (8.244)$$

The thickness of the compressible layer grows rapidly with Mach number. Knowing

$\alpha(\tilde{\alpha})$ enables the velocity and temperature profiles of the compressible layer to be determined,

$$\frac{U(\alpha(\tilde{\alpha}))}{U_e} = \frac{\tilde{U}(\tilde{\alpha})}{\tilde{U}_e} \quad (8.245)$$

and

$$\frac{T(\alpha(\tilde{\alpha}))}{T_e} = \frac{\rho_e}{\rho(\alpha(\tilde{\alpha}))} = 1 + \left(\frac{\gamma - 1}{2} \right) M_e^2 \left(1 - \left(\frac{\tilde{U}(\tilde{\alpha})}{\tilde{U}_e} \right)^2 \right). \quad (8.246)$$

Numerically determined solutions for the velocity profile at several Mach numbers are shown in Figure 8.24.

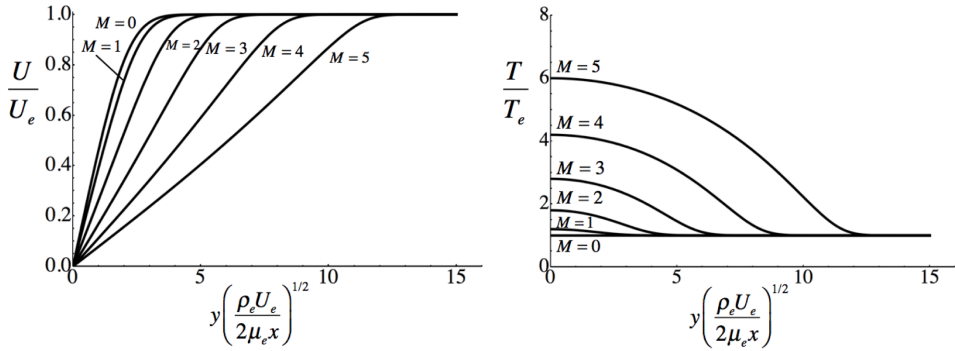


Figure 8.24: Compressible boundary layer profiles on an adiabatic plate for $P_r = 1$, viscosity exponent $\omega = 1$ and $\gamma = 1.4$.

The compressible layer is considerably thicker than the incompressible layer due to the high temperature and low density near the wall caused by the deceleration of the boundary layer flow imposed by the no-slip condition.

8.11 Turbulent boundary layers

As the Reynolds number increases along the plate a point is reached where the laminar boundary layer begins to be unstable to small disturbances. A complex series of events occurs by which the flow becomes turbulent characterized by very rapid mixing of momentum in the transverse direction. As a result the velocity profile becomes much fuller and the velocity gradient near the wall becomes much steeper compared to the velocity

gradient that would have occurred if the layer had remained laminar. The friction at the wall is also correspondingly much larger and the growth rate of the boundary layer is much faster as suggested schematically in Figure 8.25.

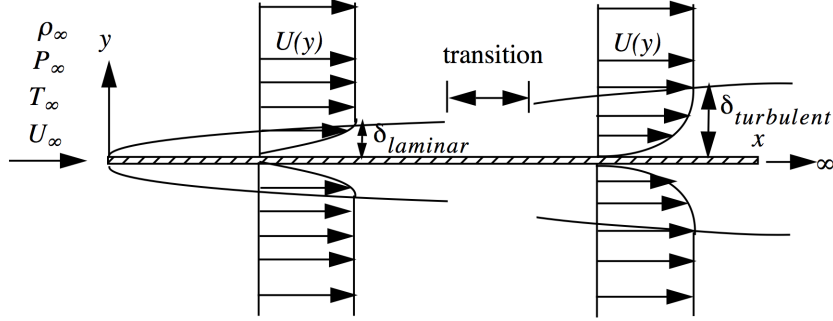


Figure 8.25: Sketch of boundary layer growth in the laminar and turbulent regions.

There is no ab-initio theory for the Reynolds shearing stress in a turbulent boundary layer and so there is no fundamental theory for the velocity profile, boundary layer thickness or skin friction. A reasonable and commonly used empirical formula for the thickness of an incompressible turbulent boundary layer is

$$\frac{\delta}{x} = \frac{0.37}{R_{ex}^{1/5}}. \quad (8.247)$$

There is no theoretical reason to assume that the thickness of a turbulent boundary layer grows according to a power law as there is in the laminar case. A relation that applies over a wider range of Reynolds number than (8.247) is Hansen's formula

$$\frac{\delta}{x} = \frac{0.14}{\ln(R_{ex})} G(\ln(R_{ex})). \quad (8.248)$$

Where G is a very slowly changing function of the Reynolds number with an asymptotic value of one at $\ln(R_{ex}) \rightarrow \infty$. In the Reynolds number range $10^5 < R_{ex} < 10^6$, $G = 1.5$.

The critical Reynolds number for transition is generally taken to be approximately 5×10^5 although in reality transition is affected by a wide variety of flow phenomena including such things as plate roughness, free stream turbulence, compressibility and the presence of acoustic noise in the free stream. Figure 8.26 is intended to illustrate this idea with the theoretical laminar and empirical turbulent skin friction lines connected by several curves reflecting the disturbance environment of a particular flow. In the transition zone the

physical wall shear stress can actually increase in the x direction due to the rapid filling out of the velocity profile as the turbulence develops.

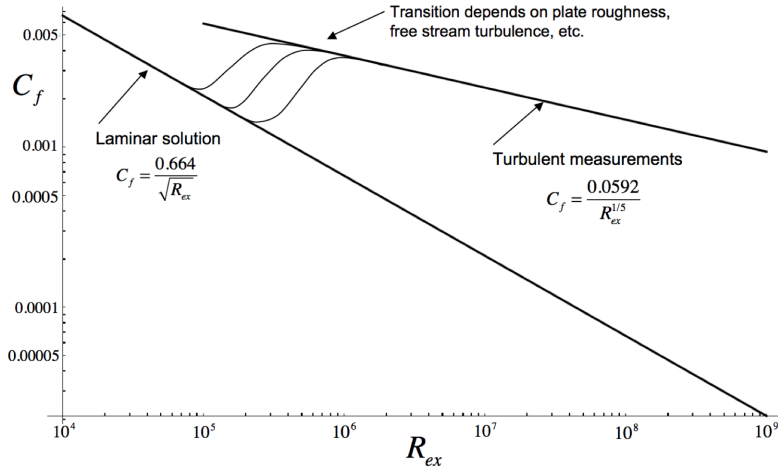


Figure 8.26: Laminar and turbulent wall friction coefficient in a zero pressure gradient flat plate boundary layer.

8.11.1 The incompressible turbulent boundary layer velocity profile

A commonly used empirical form of the velocity profile for a turbulent boundary layer is the so-called 1/7th power law.

$$\frac{U}{U_e} = \left(\frac{y}{\delta} \right)^{1/7} \quad (8.249)$$

This profile can be useful in a limited range of Reynolds numbers but it fails to capture one of the most important features of the turbulent boundary layer which is that the actual shape of the velocity profile depends on the Reynolds number. In contrast, the Blasius profile shape is completely independent of Reynolds number. Only the thickness changes with Reynolds number.

While there is no good theory for the velocity profile in a turbulent boundary, there is a very good correlation that accurately reflects certain fundamental flow properties and can be used to analyze and compare flows at different Reynolds numbers. The first thing to know is that the flow near the wall, when properly normalized, has a universal shape that is independent of the parameters that govern the outer flow. The idea is to normalize the

velocity near the wall by the so-called friction velocity.

$$\begin{aligned} u^* &= \sqrt{\frac{\tau_w}{\rho}} \\ \tau_w &= \mu \left. \frac{\partial U}{\partial y} \right|_{y=0} \end{aligned} \quad (8.250)$$

This leads to the definition of dimensionless wall variables.

$$\begin{aligned} y^+ &= \frac{yu^*}{\nu} \\ U^+ &= \frac{U}{u^*} \end{aligned} \quad (8.251)$$

The thickness of the boundary layer in wall units is

$$\delta^+ = \frac{\delta u^*}{\nu}. \quad (8.252)$$

If we use the empirical formulas for thickness and skin friction described above then

$$\frac{u^*}{U_e} = \left(\frac{\tau_w}{\rho U_e^2} \right)^{1/2} = \left(\frac{C_f}{2} \right)^{1/2} = \left(\frac{0.0592}{2R_{ex}^{1/5}} \right)^{1/2} = \frac{0.172}{R_{ex}^{1/10}} \quad (8.253)$$

and

$$\delta^+ = \frac{\delta}{x} \frac{u^*}{U_e} \frac{U_e x}{\nu} = \left(\frac{0.37}{R_{ex}^{1/5}} \right) \left(\frac{0.172}{R_{ex}^{1/10}} \right) R_{ex} = 0.0636 R_{ex}^{7/10}. \quad (8.254)$$

In other words, once R_{ex} is known most of the important properties of the boundary layer are known. A typical velocity profile is shown in Figure 8.27. I have chosen a relatively low Reynolds number so that the flow near the wall can be seen at a reasonable scale. The boundary layer is generally thought of as comprising several layers and these are indicated in Figure 8.27. Usually they are delineated in terms of wall variables.

Viscous sublayer - Wall to A, $0 \leq y^+ < 7$. In this region closest to the wall the velocity profile is linear.

$$U^+ = y^+ \quad (8.255)$$

Buffer layer - A to B, $7 \leq y^+ < 30$. Several alternative formulations are used to approximate the velocity in this region. An implicit relation that works reasonably well all the way to the wall is

$$y^+ = U^+ + e^{-\kappa C} \left(e^{\kappa U^+} - 1 - \kappa U^+ - \frac{1}{2}(\kappa U^+)^2 - \frac{1}{6}(\kappa U^+)^3 - \frac{1}{24}(\kappa U^+)^4 \right). \quad (8.256)$$

Logarithmic and outer layer - B to C to D, $30 \leq y^+ < \delta^+$. An empirical formula that works well and includes the effect of pressure gradient is

$$U^+ = \frac{1}{\kappa} \ln(y^+) + C + 2 \frac{\Pi(x)}{\kappa} \sin^2 \left(\frac{\pi}{2} \frac{y^+}{\delta^+} \right). \quad (8.257)$$

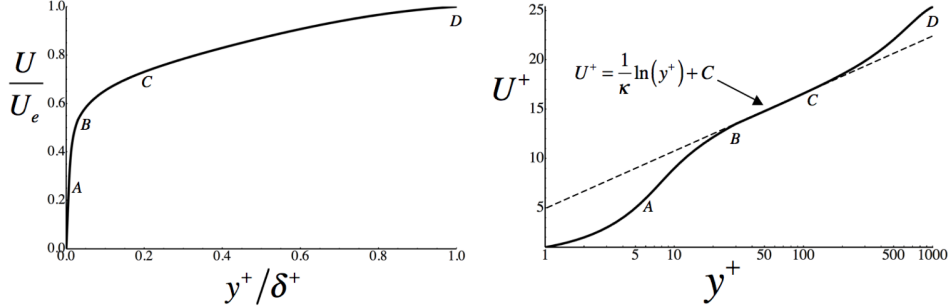


Figure 8.27: *Turbulent boundary layer velocity profile in linear and log-linear coordinates. The Reynolds number is $R_{ex} = 10^6$.*

The slope of the profile in the logarithmic region is inversely proportional to the Karman constant κ which is generally taken to be $\kappa = 0.4$ and is viewed as a universal constant of turbulent flows. However modelers of meteorological flows such as the atmospheric boundary layer have deduced values of κ as low as 0.35 while experiments in very high Reynolds number pipe flow at Princeton have suggested values as high as 0.436.

The constant C depends on the wall roughness. If k_s is a measure of the height of roughness elements at the wall (so-called sand grain roughness) one can define $R_{es} = u^* k_s / \nu$ as a roughness Reynolds number. The wall is considered hydraulically smooth if $R_{es} < 3$ and hydraulically rough if $R_{es} > 100$. For a hydraulically smooth wall $C = 5.1$ in (8.257) and increases with increasing R_{es} . The function $\Pi(x)$ is determined by the pressure gradient and layer Reynolds number. For $dP_e/dx = 0$, $\Pi(x) = 0.62$. The logarithmic term in (8.257) is remarkably robust in the presence of pressure gradients and roughness. The constant κ hardly changes at all with roughness.

The \sin^2 term in (8.257) is called the wake function because of the vaguely wake-like shape of the outer velocity profile. Something to notice is that the velocity profile (8.257) is not valid beyond $y^+ = \delta^+$ and the velocity profile has a small but finite slope at $y^+ = \delta^+$ because of the logarithmic term.

Figure 8.28 compares turbulent boundary layer profiles at various Reynolds numbers. The effect of Reynolds number on the flow expressed in wall variables is felt through the value of δ^+ in the wake function term in (8.257). In Figure 8.28 there is a slight mismatch between (8.256) and (8.257) at the outer edge of the buffer layer at a Reynolds number of 10^5 . This is because a turbulent boundary layer can hardly exist at such a low Reynolds number and the functions (8.256) and (8.257) which have been developed from boundary layer data were not designed to fit this case.

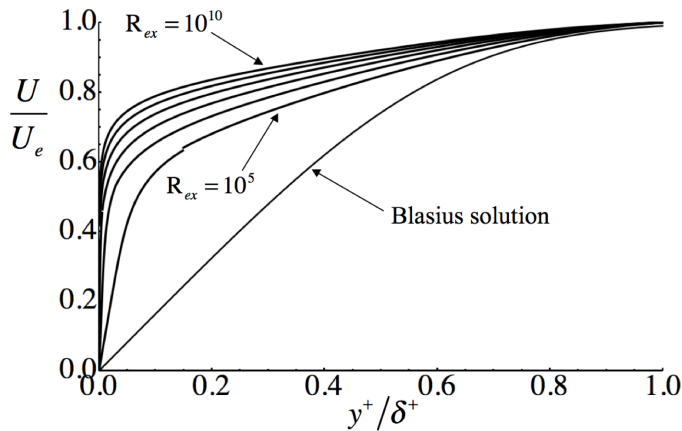


Figure 8.28: *Incompressible turbulent boundary layer profiles at several Reynolds numbers compared to the Blasius solution for a laminar boundary layer.*

The most remarkable feature of the turbulent boundary layer is the logarithmic region B to C governed by the so-called universal law of the wall. In this region the wake function is negligible and the velocity profile has the same shape regardless of the Reynolds number. The shape remains the same even in the presence of a pressure gradient which is remarkable in view of the sensitivity of the shape of the laminar velocity profile to pressure gradient. If the plate is rough the main effect is to increase the value of the constant C while preserving the logarithmic shape and the slope $1/\kappa$.

According to (8.254) δ^+ increases fairly rapidly with Reynolds number and this leads to an increasingly full velocity profile. At high Reynolds numbers the viscous sublayer becomes extremely thin and it is very difficult to make direct measurements of the linear part of the velocity profile to determine skin friction. Fortunately the skin friction can be determined using measurements in the much more accessible logarithmic region by utilizing the law of

the wall.

$$\frac{U}{U^*} = \frac{1}{\kappa} \ln \left(\frac{y U^*}{\nu} \right) + C \quad (8.258)$$

Measurements of U versus y in region B-C can be used to determine U^* and hence C_f . The friction coefficient in the compressible case can be estimated using (8.231).

The turbulent fluctuations about the mean velocity tend to peak near the wall in the general vicinity of the log layer. Figure 8.29 shows some classical data from Klebanoff (NACA report 1247, 1955). Generally the stream-wise velocity fluctuations are a factor of two larger than the wall normal or span-wise fluctuations. The peak turbulent shearing stress is generally quite close to the value at the wall indicating that there is a region of nearly constant shearing stress that extends from the wall out to the log layer. This can be used to develop a heuristic argument for the existence of a logarithmic segment of the mean velocity profile.

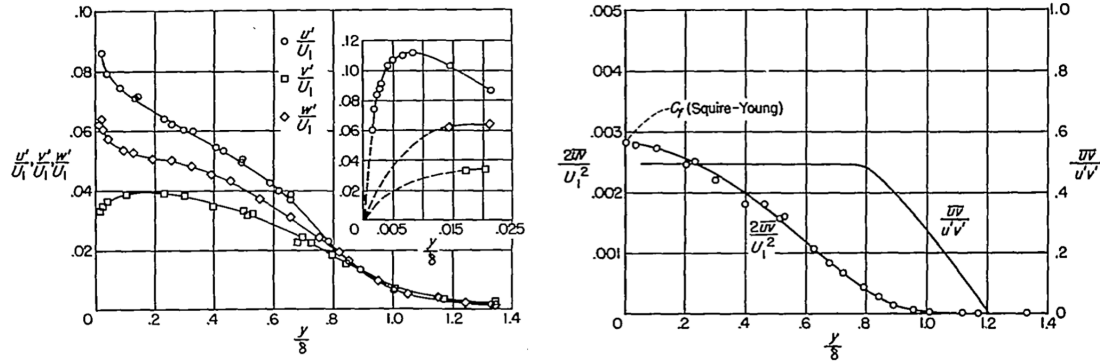


Figure 8.29: *Profiles of turbulent velocity fluctuations and turbulent shearing stress at $R_{ex} = 4.2 \times 10^6$ normalized by the free stream velocity.*

There is a great temptation to argue that the structure of a turbulent boundary layer near the wall is of universal character independent of the Reynolds number when the turbulent velocity fluctuations are normalized by the wall friction velocity. When turbulence data near the wall is normalized this way u'/U^* seems to have a value of about 2.5 independent of the Reynolds number. The great problem with this idea is that according to (8.253) the friction velocity decreases as a fraction of the free stream velocity as the Reynolds number increases. If the turbulent velocity fluctuations also decreased in the same way then in the limit of infinite Reynolds number the turbulent fluctuations would become a negligible fraction of the free stream speed. On the other hand if the turbulent velocity fluctuations scale with the free stream speed then the correlation between streamwise and

wall normal fluctuations would have to decrease to be consistent with the decrease of the friction coefficient with increasing Reynolds number. If an ab-initio theory of the turbulent boundary layer is ever developed this is the sort of issue that it should resolve.

8.12 Transformation between flat plate and curved wall boundary layers

One of the consequences of the boundary layer approximation is that the solution for the flow on a flat plate with a variable free stream velocity can be transformed directly to the solution on a curved wall with the same free stream velocity function. Once again the boundary layer equations are

$$\begin{aligned} \frac{\partial \rho U}{\partial x} + \frac{\partial \rho V}{\partial y} &= 0 \\ \rho U \frac{\partial U}{\partial x} + \rho V \frac{\partial U}{\partial y} + \frac{dP_e}{dx} - \frac{\partial \tau_{xy}}{\partial y} &= 0 \\ \rho U C_p \frac{\partial T}{\partial x} + \rho V C_p \frac{\partial T}{\partial y} - U \frac{dP_e}{dx} + \frac{\partial Q_y}{\partial y} - \tau_{xy} \frac{\partial U}{\partial y} &= 0. \end{aligned} \quad (8.259)$$

where τ_{xy} includes both laminar and turbulent components of shearing stress and Q_y includes laminar and turbulent components of heat flux. The transformation of variables

between the flat plate and curved wall is

$$\tilde{x} = x$$

$$\tilde{y} = y + g(x)$$

$$\tilde{U}(\tilde{x}, \tilde{y}) = U(x, y)$$

$$\tilde{V}(\tilde{x}, \tilde{y}) = V(x, y) + U(x, y) \frac{dg(x)}{dx} \quad (8.260)$$

$$\tilde{\rho}(\tilde{x}, \tilde{y}) = \rho(x, y)$$

$$\tilde{\tau}_{\tilde{x}\tilde{y}}(\tilde{x}, \tilde{y}) = \tau_{xy}(x, y)$$

$$\tilde{Q}_{\tilde{y}}(\tilde{x}, \tilde{y}) = Q_y(x, y)$$

$$\tilde{P}_e(\tilde{x}) = P_e(x).$$

The transformation (8.260) generates the transformation of derivatives using the chain

rule.

$$\begin{aligned}
 \frac{\partial \tilde{U}}{\partial \tilde{x}} &= \frac{\partial U}{\partial x} - \frac{dg}{dx} \frac{\partial U}{\partial y} \\
 \frac{\partial \tilde{U}}{\partial \tilde{y}} &= \frac{\partial U}{\partial y} \\
 \frac{\partial^2 \tilde{U}}{\partial \tilde{y}^2} &= \frac{\partial^2 U}{\partial y^2} \\
 \frac{\partial \tilde{V}}{\partial \tilde{y}} &= \frac{\partial V}{\partial y} + \frac{dg}{dx} \frac{\partial U}{\partial y} \\
 \frac{\partial \tilde{\rho}}{\partial \tilde{x}} &= \frac{\partial \rho}{\partial x} - \frac{dg}{dx} \frac{\partial \rho}{\partial y} \\
 \frac{\partial \tilde{\rho}}{\partial \tilde{y}} &= \frac{\partial \rho}{\partial y} \\
 \frac{\partial \tilde{T}}{\partial \tilde{x}} &= \frac{\partial T}{\partial x} - \frac{dg}{dx} \frac{\partial T}{\partial y} \\
 \frac{\partial \tilde{T}}{\partial \tilde{y}} &= \frac{\partial T}{\partial y} \\
 \frac{\partial \tilde{Q}_{\tilde{y}}}{\partial \tilde{y}} &= \frac{\partial Q_y}{\partial y} \\
 \frac{\partial \tilde{\tau}_{\tilde{x}\tilde{y}}(\tilde{x}, \tilde{y})}{\partial \tilde{y}} &= \frac{\partial \tau_{xy}(x, y)}{\partial y}.
 \end{aligned} \tag{8.261}$$

The transformation (8.260) and its extension to derivatives (8.261) maps (8.259) to it-

self.

$$\begin{aligned}
 \frac{\partial \tilde{\rho} \tilde{U}}{\partial \tilde{x}} + \frac{\partial \tilde{\rho} \tilde{V}}{\partial \tilde{y}} &= \frac{\partial \rho U}{\partial x} + \frac{\partial \rho V}{\partial y} = 0 \\
 \tilde{\rho} \tilde{U} \frac{\partial \tilde{U}}{\partial \tilde{x}} + \tilde{\rho} \tilde{V} \frac{\partial \tilde{U}}{\partial \tilde{y}} + \frac{d \tilde{P}_e}{d \tilde{x}} - \frac{\partial \tilde{\tau}_{\tilde{x}\tilde{y}}}{\partial \tilde{y}} &= \rho U \frac{\partial U}{\partial x} + \rho V \frac{\partial U}{\partial y} + \frac{d P_e}{d x} - \frac{\partial \tau_{xy}}{\partial y} = 0 \\
 \tilde{\rho} \tilde{U} C_p \frac{\partial \tilde{T}}{\partial \tilde{x}} + \tilde{\rho} \tilde{V} C_p \frac{\partial \tilde{T}}{\partial \tilde{y}} - \tilde{U} \frac{d \tilde{P}_e}{d \tilde{x}} + \frac{\partial \tilde{Q}_{\tilde{y}}}{\partial \tilde{y}} - \tilde{\tau}_{\tilde{x}\tilde{y}} \frac{\partial \tilde{U}}{\partial \tilde{y}} &= \\
 \rho U C_p \frac{\partial T}{\partial x} + \rho V C_p \frac{\partial T}{\partial y} - U \frac{d P_e}{d x} + \frac{\partial Q_y}{\partial y} - \tau_{xy} \frac{\partial U}{\partial y} &= 0
 \end{aligned} \tag{8.262}$$

In principle the function $g(x)$ added to the y coordinate is arbitrary, but in practice $g(x)$ is restricted to be smooth and slowly varying so as not to violate the boundary layer approximation.

It is the absence of the derivative $\partial V / \partial x$ from (8.259) that enables the transformation (8.260) and (8.261) to reproduce the same equations in the new coordinates. Figure 8.30 illustrates the idea.

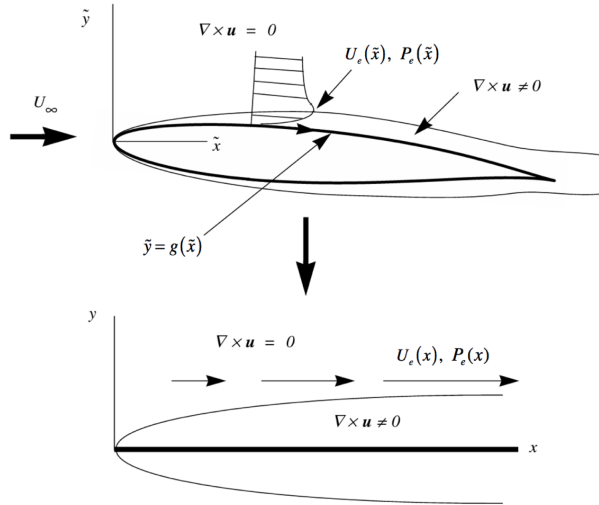


Figure 8.30: *Mapping of the boundary layer developing over an airfoil to the boundary layer on a flat plate with the same pressure gradient.*

The function $g(\tilde{x})$ defines the surface of the airfoil in the Cartesian coordinates (\tilde{x}, \tilde{y}) . The flow at a given \tilde{x} distance from the leading edge and a distance $\tilde{y} - g(\tilde{x})$ above the surface

of the airfoil is mapped to the same position in the boundary layer on a flat plate with the same free stream flow velocity $\tilde{U}_e(\tilde{x}) = U_e(x)$. The main restriction on $g(\tilde{x})$ is that it vary slowly enough so that the boundary layer does not approach separation and so that the approximation $\tilde{x} = x$ remains valid. The exponential decay of the vorticity at the edge of the boundary layer described earlier, together with this simple invariance of the boundary layer equations enables boundary layer theory to be applied to a wide variety of slender body shapes, creating one of the most powerful tools in fluid mechanics.

An iterative algorithm can be used to determine the viscous flow over a complex shape such as the airfoil shown in Figure 8.29. The procedure is the following.

- 1) Solve for the potential flow over the airfoil.
- 2) Use the potential flow velocity at the airfoil surface as the $U_e(x)$ for a boundary layer calculation beginning at the leading edge.
- 3) Determine the displacement thickness of the boundary layer and use the data to define a new airfoil shape. Repeat the potential flow calculation using the new airfoil shape to determine a new $U_e(x)$.
- 4) Using the new $U_e(x)$ repeat the boundary layer calculation.

A few iterations of this viscous-inviscid interaction procedure will converge to an accurate solution for the viscous, compressible flow over the airfoil.

8.13 Head's method for approximate calculation of turbulent boundary layer characteristics

In section 8.8 we discussed Thwaites' method for calculating the integral characteristics of laminar boundary layers in the presence of free stream velocity variation. Similar schemes have been developed for calculating the integral characteristics of turbulent boundary layers. One of the simplest to apply is the method described in the paper *Entrainment in the turbulent boundary layer*, Aero. Res. Council Research and Memoranda 3152, 1960 by M. R. Head.

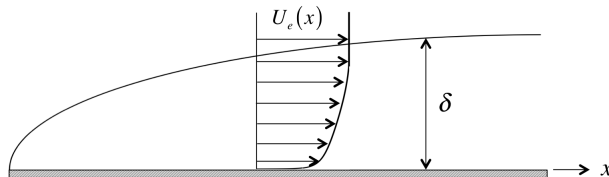


Figure 8.31: Incompressible turbulent boundary over a flat plate with pressure gradient.

In the boundary layer shown in figure 8.31 the area flow at any position x is

$$Q = \int_0^\delta U dy. \quad (8.263)$$

Equation (8.263) can be rearranged to express the area flow in terms of the boundary layer displacement thickness.

$$Q = \int_0^\delta U dy = \int_0^\delta U_e dy - \int_0^\delta U_e \left(1 - \frac{U}{U_e}\right) dy = U_e (\delta - \delta^*) \quad (8.264)$$

The entrainment velocity of the boundary layer is defined as the rate of change of Q with x .

$$V_e = \frac{dQ}{dx} = \frac{d}{dx} (U_e (\delta - \delta^*)) \quad (8.265)$$

Head defined a modified boundary layer shape factor as

$$H_1 = \frac{(\delta - \delta^*)}{\theta}. \quad (8.266)$$

He then analyzed a variety of boundary layer data and came up with the correlations shown in figure 8.32.

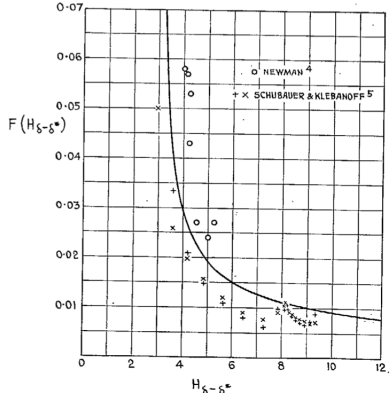


FIG. 1. $\frac{1}{U} \frac{d}{dx} [U(\delta - \delta^*)]$ as a function of $H_{\delta-\delta^*}$.

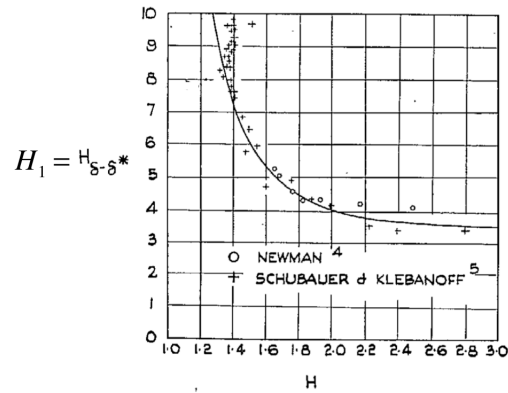


FIG. 2. Variation of $H_{\delta-\delta^*}$ with conventional form parameter H .

Figure 8.32: Correlated data from Head's paper.

The following quote from Head's paper is interesting in the insight that it provides into his thinking about his own model. He is brutally honest in describing the weaknesses of the assumptions of the model.

2.3. Determination of Functions F and G . For this purpose the experimental data of Newman² and of Schubauer and Klebanoff³ have been used†. In each case values of δ were obtained from tables of the measured profiles, δ being arbitrarily defined as the value of y for which $u/U = 0.995$.

From the values of δ and the corresponding values of H , θ , U and x , the quantities $\frac{1}{U} \frac{d}{dx} [U(\delta - \delta^*)]$ and $H_{\delta-\delta^*}$ were obtained and are shown plotted in Figs. 1 and 2. If the assumptions made in the previous Sections had been correct, and if both the analysis and the experimental data had been entirely free from error then, of course, the points obtained from the two sets of results should have coincided with common curves defining the two functions. In fact, however, as will be seen from the Figures there is considerable scatter of the points, and in Fig. 1 there is a fairly marked and consistent discrepancy between the two sets of results which makes the drawing of a hypothetical common curve, representing the function $F(H_{\delta-\delta^*})$, a somewhat arbitrary procedure. However, such a curve has been drawn, its justification being found *a posteriori*, in the accuracy with which it has enabled the form-parameter development to be predicted in the cases considered below. The curve relating $H_{\delta-\delta^*}$ to the normal form parameter H is rather more accurately defined, although here also there is some discrepancy between the two sets of results, and the values of H given by Schubauer and Klebanoff for the region where the pressure gradient was favourable appear somewhat high.

Figure 8.33: Head's frank comments about his method.

Based on the results in figure 8.32 Head assumed the existence of two universal functions for turbulent boundary layers, F and G where

$$\frac{V_e}{U_e} = \frac{1}{U_e} \frac{d}{dx} (U_e (\delta - \delta^*)) = \frac{1}{U_e} \frac{d}{dx} (U_e \theta H_1) = F(H_1) \quad (8.267)$$

and

$$H_1 = G(H) \quad (8.268)$$

where H is the conventional shape factor

$$H = \frac{\delta^*}{\theta}. \quad (8.269)$$

In addition he assumed that the skin friction coefficient followed the well-established empirical formula developed by Ludweig and Tillman. See *Investigations of the wall-shearing stress in turbulent boundary layers, NACA TM 1285, 1950*. The Ludweig-Tillman formula

is

$$C_f = \frac{0.246}{10^{0.678H} \left(\frac{U_e}{U_\infty} R_\theta \right)^{0.268}} \quad (8.270)$$

where the reference velocity for R_θ is the free stream velocity.

$$R_\theta = \frac{U_\infty \theta}{\nu} \quad (8.271)$$

In the paper *Calculation of separation points in incompressible turbulent flows, in J. Aircraft vol 9, No. 9, 1972 by T. Cebeci, G. J. Mosinskis and A. M. O. Smith of Douglas Aircraft*, the authors suggest

$$F(H_1) = \frac{0.0299}{(H_1 - 3.0)^{0.6169}} \quad (8.272)$$

and

$$G(H) = \begin{cases} 3.3 + \frac{0.8234}{(H - 1.1)^{1.287}} & H \leq 1.6 \\ 3.3 + \frac{1.5501}{(H - 0.6778)^{3.064}} & H > 1.6. \end{cases} \quad (8.273)$$

In the book *Boundary Layer Theory*, H. Schlichting suggests the same functions but uses the constant 0.0306 instead of 0.0299 in (8.272). The function (8.273) and its derivative are shown in figure 8.34.

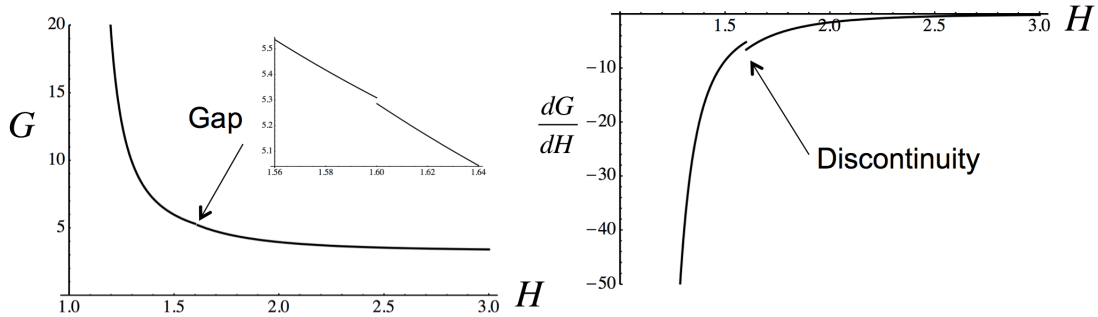


Figure 8.34: Empirical function G suggested in the references described above.

Unfortunately there is a discontinuity in the function and its derivative at $H = 1.6$. I prefer to use the smooth function

$$G(H) = 3.0445 + \frac{0.8702}{(H - 1.1)^{1.2721}} \quad (8.274)$$

shown in figure 8.35.

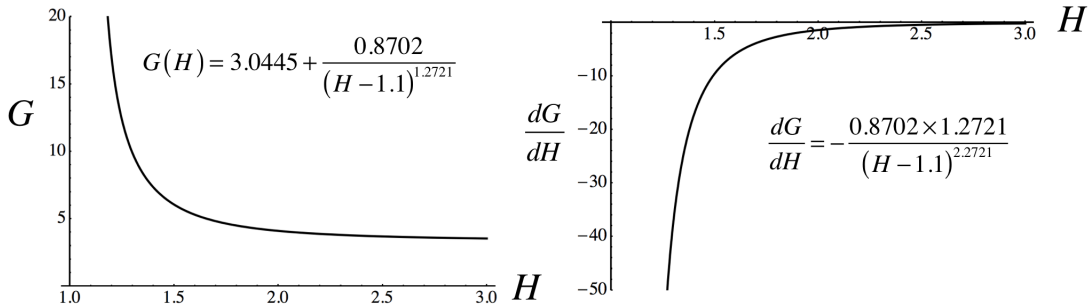


Figure 8.35: My preferred function G .

Figure 8.36 shows a comparison between (8.273) and (8.274).

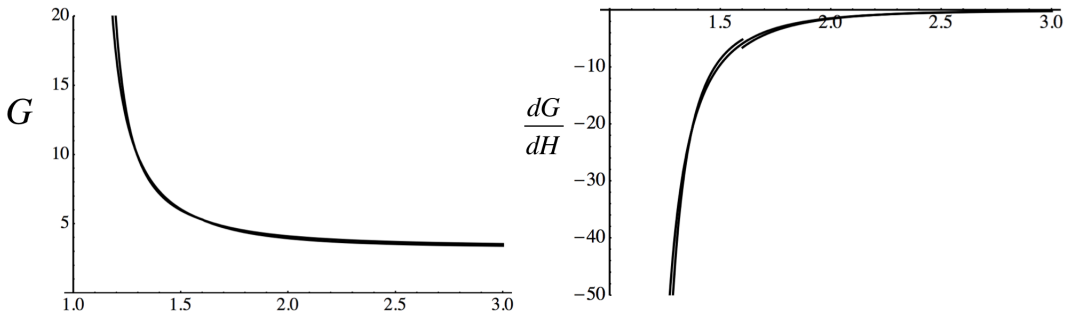


Figure 8.36: Comparison between G' s.

Expand the derivative in (8.267) to generate an equation for the shape factor.

$$\frac{dH}{dx} = \left(\frac{-\frac{G(H)}{\theta} \frac{d\theta}{dx} - G(H) \frac{1}{U_e} \frac{dU_e}{dx} + \frac{0.0299}{\theta(G(H)-3.0)^{0.6169}}}{\frac{dG}{dH}} \right) \quad (8.275)$$

Recall the von Karman integral momentum equation.

$$\frac{d\theta}{dx} + (2 + H) \frac{\theta}{U_e} \frac{dU_e}{dx} = \frac{C_f}{2} \quad (8.276)$$

Substitute (8.276) into (8.275).

$$\frac{dH}{dx} = \left(\frac{(1 + H) \frac{G(H)}{U_e} \frac{dU_e}{dx} - \frac{G(H)}{\theta} \frac{C_f}{2} + \frac{0.0299}{\theta(G(H)-3.0)^{0.6169}}}{\frac{dG}{dH}} \right) \quad (8.277)$$

Equations (8.276) and (8.277) constitute two equations for θ and H with known boundary layer edge velocity distribution $U_e(x)$. It is useful to put the equations into a normalized form that will make it easier to identify the inherent dependence of boundary layer parameters on Reynolds number. Refer the Reynolds number based on distance from the leading edge to the free stream velocity.

$$R_{ex} = \frac{U_\infty x}{\nu} \quad (8.278)$$

Using the Bernoulli equation

$$P_\infty + \frac{1}{2}\rho U_\infty^2 = P_e + \frac{1}{2}\rho U_e^2 \quad (8.279)$$

the pressure coefficient can be expressed in terms of the velocity at the edge of the boundary layer.

$$C_p = \frac{P_e - P_\infty}{\frac{1}{2}\rho U_\infty^2} = 1 - \left(\frac{U_e}{U_\infty} \right)^2 \quad (8.280)$$

Using (8.278), (8.280), and (8.270) express the von Karman equation as

$$\frac{dR_\theta}{dR_{ex}} = \frac{1}{2} \left(\frac{2 + H}{1 - C_p} \right) R_\theta \frac{dC_p}{dR_{ex}} + \frac{0.246}{10^{0.678H} (1 - C_p)^{0.268} R_\theta^{0.268}} \quad (8.281)$$

and the shape factor equation, (8.277) as

$$\frac{dH}{dR_{ex}} = \frac{\left(\frac{G(H)}{2} \left(\frac{1+H}{1-C_p} \right) \frac{dC_p}{dR_{ex}} + \frac{0.246 \times G(H)}{10^{0.678H} (1 - C_p)^{0.268} R_\theta^{1.268}} - \frac{0.0299}{(G(H)-3.0)^{0.6169} R_\theta} \right)}{\frac{0.8702 \times 1.2721}{(H-1.1)^{0.2721}}} \quad (8.282)$$

For given initial conditions on R_θ , H and known free stream pressure distribution $C_p(R_{ex})$, (8.281), (8.282) and (8.274) are solved for $R_\theta(R_{ex})$ and $H(R_{ex})$.

8.13.1 Head's method applied to the zero pressure gradient flat plate

In this case the governing equations (8.281) and (8.282) reduce to

$$\frac{dR_\theta}{dR_{ex}} = \frac{0.246}{10^{0.678H} R_\theta^{0.268}} \quad (8.283)$$

and

$$\frac{dH}{dR_{ex}} = \left(\frac{0.193381 \left(1 + 3.49862(H - 1.1)^{1.2721} \right)}{10^{0.678H} (H - 1.1) R_\theta^{1.268}} - \frac{0.0310393(H - 1.1)^{1.5442}}{\left(1 + 0.0511377(H - 1.1)^{1.2721} \right)^{0.6169} R_\theta} \right). \quad (8.284)$$

Figure 8.37 shows the results of a calculation of the momentum thickness and shape factor for this case. The calculation is initiated at a streamwise Reynolds number of 10,000 and the initial momentum thickness and shape factor are taken to be the Blasius values at that Reynolds number. Note the rapid decrease of the shape factor at low Reynolds number as the method adjusts to the turbulent value which is less than 1.5.

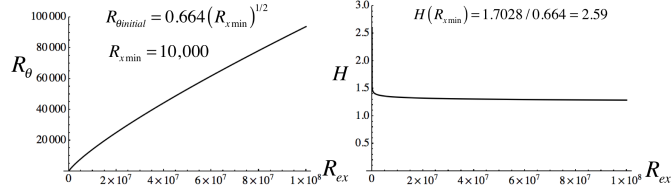


Figure 8.37: *Turbulent boundary layer parameters calculated using Head's method initiated with laminar values.*

Figure 8.38 shows the Ludweig-Tillman value of the friction coefficient calculated using Head's method and compared to the Blasius friction coefficient as well as the power law formula used in figure 8.26. The agreement is reasonable in a narrow range of Reynolds numbers around 10,000,000.

Figure 8.39 shows data from Head's paper for a variety of experiments for the shape factor of flat-plate zero-pressure-gradient turbulent boundary layers compared with the prediction of

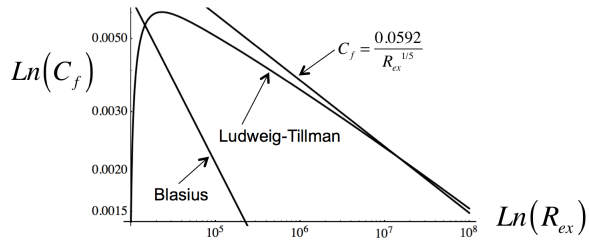


Figure 8.38: Data for the shape factor compared with Head's method.

Head's method over almost three orders of magnitude in R_{ex} . The method works reasonably well although the prediction seems a little high at high Reynolds numbers.

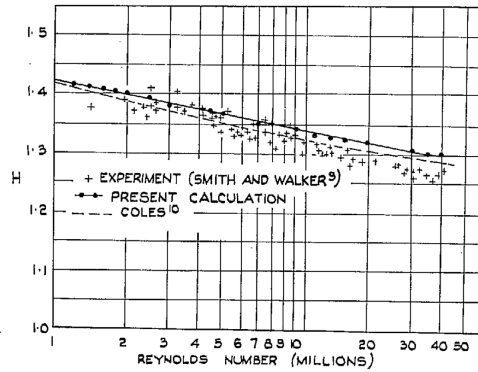


Figure 8.39: Data for the shape factor compared with Head's method.

8.13.2 Head's method used to study the effect of Reynolds number on flow separation on a circular cylinder

Since Head's method can be used to determine skin friction for an evolving boundary layer one might expect the method to be able to predict the point where the skin friction approaches zero and flow separation occurs, say on a wing at high angle of attack. With a healthy dose of skepticism and accepting a fair amount of uncertainty in the actual predicted separation point, the method can reasonably be used to predict trends in the separation point with, say, changing angle of attack.

Perhaps the most challenging problem for predicting separation is flow past a bluff body such as a circular cylinder shown in Figure 8.40. In section 8.8 we used Thwaites' method and the potential flow solution for U_e/U_∞ to predict the separation point of a laminar boundary layer developing from the forward stagnation point. See figure 8.20. The pre-

dicted separation point was somewhat aft of $\phi = 90^\circ$ mainly because the pressure distribution was forced to be the potential flow solution.

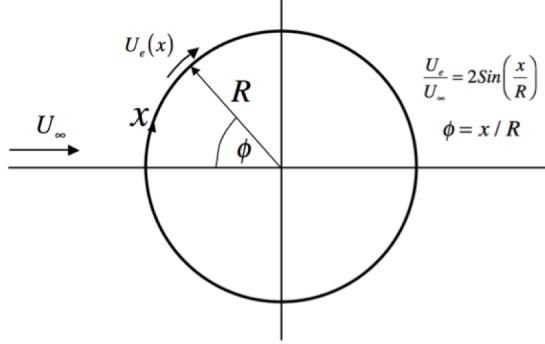


Figure 8.40: *Flow past a circular cylinder.*

Figures 8.41 and 8.42 show results for a relatively low cylinder Reynolds number that would not be expected to have a turbulent boundary layer on the forward surface unless it was artificially tripped. Note that separation is pretty clearly indicated by a rapidly increasing shape factor and decreasing skin friction with increasing R_{ex} . The calculation becomes singular when the friction goes to zero and there is no data beyond separation.

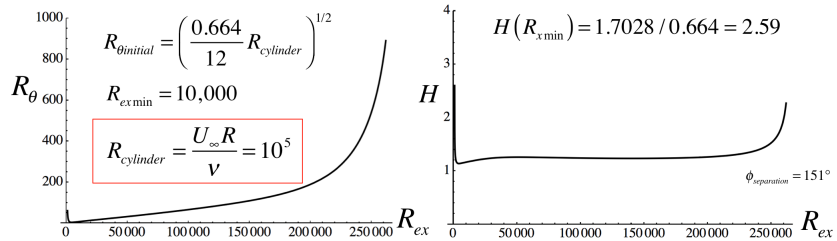


Figure 8.41: *Assumed turbulent boundary layer on a circular cylinder at low cylinder Reynolds number computed using Head's method. The flow is initiated with laminar values and the pressure distribution is taken to be the potential flow solution.*

Figures 8.43 and 8.44 show results for a high cylinder Reynolds number that would be expected to have a turbulent boundary layer on the forward surface. The separation point moves aft compared to the low Reynolds number case but is also probably too far aft because of the use of the potential flow solution for the pressure.

In both cases the effect of a turbulent boundary layer is to move the separation point aft with the high Reynolds number case furthest back. But in both cases the separation point is probably too far back compared the prediction that would come from using the

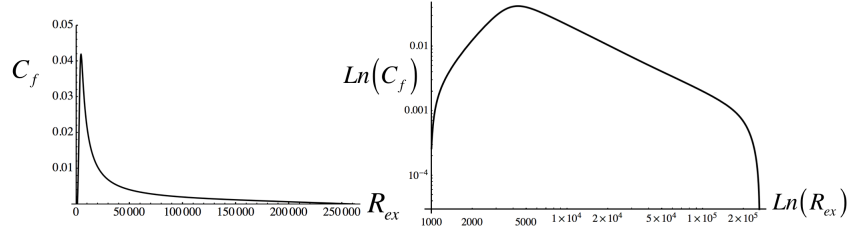


Figure 8.42: Skin friction for an assumed turbulent boundary layer on a low Reynolds number circular cylinder computed using Head's method. Separation is predicted to occur at the back of the cylinder.

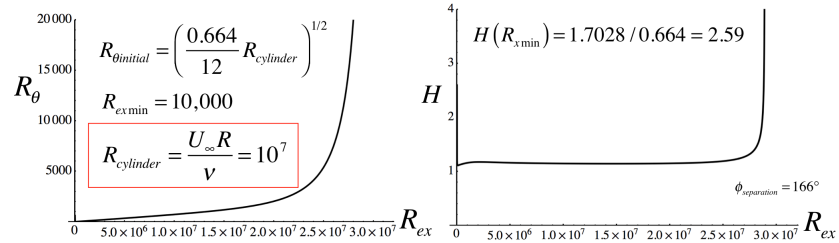


Figure 8.43: Assumed turbulent boundary layer on a circular cylinder at high cylinder Reynolds number computed using Head's method. The flow is initiated with laminar values and the pressure distribution is taken to be the potential flow solution.

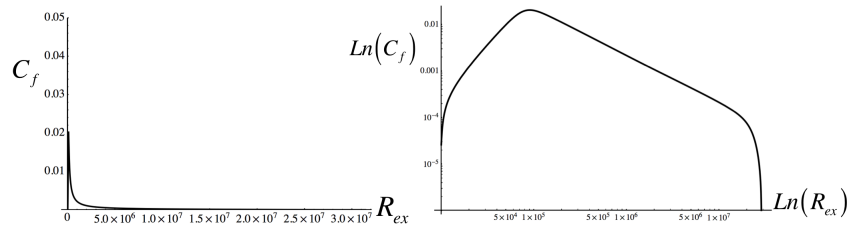


Figure 8.44: Skin friction for an assumed turbulent boundary layer on a high Reynolds number circular cylinder computed using Head's method. Separation is predicted to occur at the back of the cylinder somewhat further aft than in the low Reynolds number case.

experimental pressure distribution. See the paper by Cebici et al mentioned earlier, where the actual pressure distribution is used.

8.14 Problems

Problem 1 - Figure 8.45 depicts Couette flow of an ideal gas between two infinite parallel plates. The lower wall is adiabatic. Determine the entropy difference between the lower and upper walls.

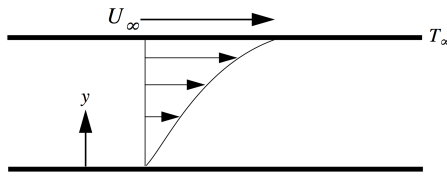


Figure 8.45: *Couette flow, adiabatic lower wall.*

Problem 2 - Figure 8.46 depicts Couette flow of helium gas between two infinite parallel walls spaced 1 cm apart. The lower wall is adiabatic and the speed of the upper wall is 400 meters/sec. The temperature of the upper wall is 300K.

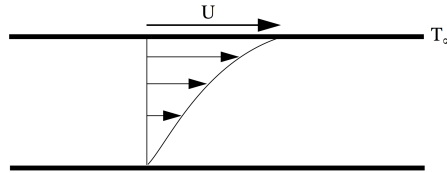


Figure 8.46: *Couette flow of helium, adiabatic lower wall.*

Assume the viscosity depends linearly on temperature.

$$\mu/\mu_\infty = T/T_\infty \quad (8.285)$$

Set up and solve the compressible flow equations for this simple flow. Note that the flow is assumed to be steady and all flow variables depend only on the coordinate normal to the wall.

- 1) Determine the speed of sound at the upper wall.
- 2) Determine the temperature of the lower wall.
- 3) Determine the shear stress.

- 4) Is there work done on the flow? How much?
- 5) Determine the heat flux through the upper wall.
- 6) Sketch the distribution of stagnation temperature across the channel.
- 7) Sketch the distribution of entropy across the channel.

Problem 3 - Figure 8.47 depicts Couette flow of a gas between two infinite parallel walls spaced a distance d apart. The lower wall is adiabatic. The reference Mach number is $M_\infty = U_\infty / \sqrt{\gamma R T_\infty}$. The viscosity is assumed to depend linearly on temperature $\mu/\mu_\infty = T/T_\infty$ and the reference Reynolds number is $R_e = \rho_\infty U_\infty d / \mu_\infty$.

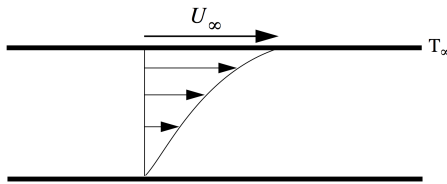


Figure 8.47: Couette flow of an ideal gas, adiabatic lower wall.

Sketch how the friction coefficient C_f depends on U_∞ . At what Mach number is the friction coefficient an extremum? Is it a maximum or a minimum? Express your answer in terms of γ and the Prandtl number. What are the values for helium and air?

Problem 4 - Figure 8.48 shows the unsteady flow produced by a flat plate set into motion impulsively at velocity U_∞ .

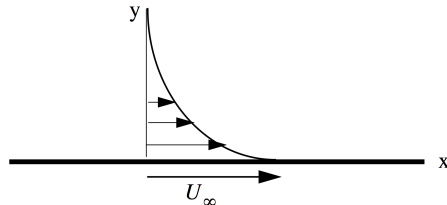


Figure 8.48: Impulsively started flat plate.

The plate extends to infinity in both directions. Simplify the compressible flow equations. Note that the fluid near the wall is heated when the plate is started. Solve for the velocity and vorticity in the incompressible case.

Problem 5 - In the discussion of boundary layers we considered several definitions of the thickness. How would you define a thickness based on the vorticity distribution? What might be the advantage of such a definition?

Problem 6 - Use the Howarth-Stewartson transformation to generate the velocity and temperature profiles in a laminar, compressible, zero pressure-gradient boundary layer at a free stream Mach number $M_\infty = 8$.

Problem 7 - The 2-D stream function for potential flow over an elliptically shaped body at zero angle of attack is produced by the superposition of a uniform flow plus a source and a sink of equal strength. The stream function and flow pattern are

$$\Psi = U_\infty y + \frac{Q}{2\pi} \operatorname{ArcTan} \left(\frac{y}{x+a} \right) - \frac{Q}{2\pi} \operatorname{ArcTan} \left(\frac{y}{x-a} \right) \quad (8.286)$$

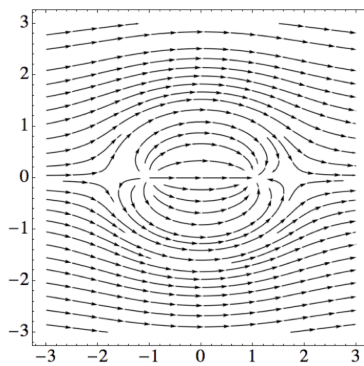


Figure 8.49: Potential flow over a 2-D elliptical body.

Choose two aspect ratios for the ellipse (length/width = 2, length/width = 20).

- 1) Use the potential flow solution to determine the pressure coefficient on the body.
- 2) Use Thwaites' method to calculate the properties of the laminar boundary layer up to separation. How does the separation point depend on the aspect ratio of the ellipse? Use the radius of curvature at the forward stagnation point to initiate the calculation.
- 3) Use Head's method to do the same for a turbulent boundary layer. For a given aspect ratio how does the separation point depend on the Reynolds number based on the length of the body?

Chapter 9

Quasi-one-dimensional flow

9.1 Control volume and integral conservation equations

In this chapter we will treat the very general stationary flow of a compressible fluid in a channel without body forces ($G_i = 0$) shown in figure 9.1 .

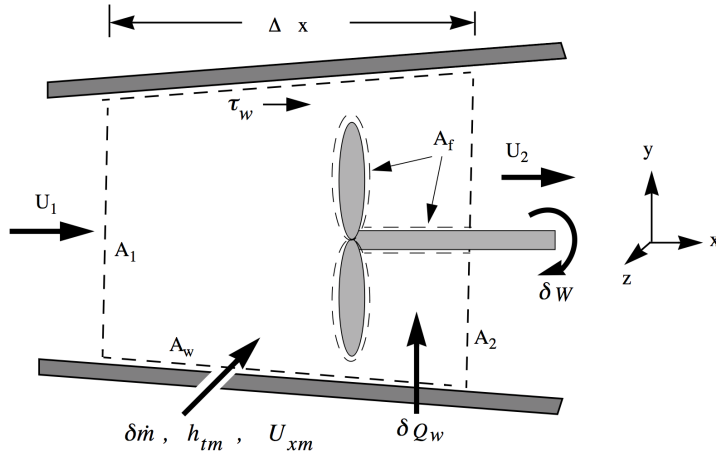


Figure 9.1: *Control volume enclosing a general stationary channel flow.*

Viscous friction imposes a no-slip condition at all solid surfaces. There may be mass addition as well as heat conduction through the wall. The added mass has total enthalpy, h_{tm} and stream wise velocity component, U_{xm} . In addition there may be work done on the flow by a fan or by the flow on a turbine. The work exchanged with the control volume is symbolized by a fan assumed to be rotating at a constant angular frequency.

The appropriate Eulerian-Lagrangian control volume is shown in figure 9.1 . The Eulerian inlet and outlet surfaces of the control volume, A_1 , and A_2 are fixed in space as is A_w which is attached to the non-moving wall of the channel. The Lagrangian surface A_f is attached to, and moves with, the surface of the rotating fan. The area where the control volume is constantly being stretched and twisted at the corner where A_2 and A_f meet is negligibly small and therefore involves no net contribution to the mass momentum and energy entering or leaving the control volume.

In chapter 5 we briefly discussed the distinction between steady flow and stationary flow. The flow in the neighborhood of the rotating fan with moving blades is surely unsteady but as long as the rotation speed of the fan is constant there will be no net gain or loss of mass, momentum or energy inside the control volume. This justifies dropping the time derivative terms in the conservation equations. Another way to look at this is to imagine that the fan blades are smeared out onto a continuous disk called an actuator disk. This would make the flow truly steady but begs the question as to how such a disk could be constructed. A third way to justify the use of the steady flow equations is to view any flow variable as a time average over precisely one blade passage period, or one full fan rotation period, or for an averaging time that is so long compared to the blade passage period that a small additional contribution from a portion of a period is negligible.

There are other aspects of the flow that might have to be treated as stationary. For example the flow in figure 9.1 could be turbulent in which case unsteady fluctuations in the flow properties, particularly near the wall, would be characterized by a wide range of time scales lacking any obvious periodicity. In this case the flow is stationary as long as the time average of any flow property such as velocity, pressure or density is constant. This brings in some subtle questions as to the length of the time average and specific times when the averaging begins and ends. For our purposes it is sufficient to require that the averaging is long compared to both the rotation period of the fan and any low frequency variations in the turbulent fluctuations.

As a practical matter we are not attempting to treat the case where the flow is being turned on or off or where the fan is changing speed. These cases would require a full unsteady analysis. This is quite do-able but beyond the scope of this course.

9.1.1 Conservation of mass

The integral form of the mass conservation equation in steady flow is evaluated on each

surface of the control volume.

$$\begin{aligned} \int_{A(t)} \rho (\bar{U} - \bar{U}_A) \cdot \bar{n} dA &= \\ \int_{A_1} \rho_2 U_2 dA - \int_{A_1} \rho_1 U_1 dA + \int_{A_w} \rho \bar{U} \cdot \bar{n} dA + \int_{A_f(t)} \rho (\bar{U} - \bar{U}_A) \cdot \bar{n} dA &= 0 \end{aligned} \quad (9.1)$$

The integral of the mass flux over the wall is simply the total mass added.

$$\int_{A_w} \rho \bar{U} \cdot \bar{n} dA = -\delta \dot{m} \quad (9.2)$$

There is no mass addition through the fan surface (the last term in equation (9.1)) and so the integrated form of the mass equation becomes

$$\int_{A_2} \rho_2 U_2 dA - \int_{A_1} \rho_1 U_1 dA = \delta \dot{m}. \quad (9.3)$$

9.1.2 Conservation of x -momentum

Now evaluate the integral form of the momentum equation over the control volume. Note that $U - U_A = 0$ on the fan surface by the no-slip condition.

$$\begin{aligned} \int_{A(t)} (\rho \bar{U} (\bar{U} - \bar{U}_A) + P \bar{\delta} - \bar{\tau}) \cdot \bar{n} dA &= \\ \int_{A_2} (\rho_2 U_2 U_2 + P_2 - \tau_{xx2}) dA - \int_{A_1} (\rho_1 U_1 U_1 + P_1 - \tau_{xx1}) dA &+ \\ \int_{A_w} (\rho \bar{U} \bar{U} + P \bar{\delta} - \bar{\tau}) \cdot \bar{n} dA &+ \int_{A_f(t)} (\rho \bar{U} (\bar{U} - \bar{U}_A) + P \bar{\delta} - \bar{\tau}) \cdot \bar{n} dA = 0 \end{aligned} \quad (9.4)$$

Over most of the wall the velocity is zero due to the no slip condition. However over the duct through which the added mass enters the control volume there is a contribution to the x -momentum in the amount

$$U_{xm} \delta \dot{m}. \quad (9.5)$$

Any small contributions from the pressure and stress forces acting over the control volume in the neighborhood of the mass injector as well as any non-uniformities in the injector velocity field have been included in the effective value that might be assigned to U_{xm} in (9.5). The integrated x -momentum equation now becomes

$$\begin{aligned} \int_{A(t)} (\rho \bar{U} (\bar{U} - \bar{U}_A) + P \bar{\delta} - \bar{\tau}) \cdot \bar{n} dA \Big|_x = \\ \int_{A_2} (\rho_2 U_2 U_2 + P_2 - \tau_{xx2}) dA - \int_{A_1} (\rho_1 U_1 U_1 + P_1 - \tau_{xx1}) dA + \\ \int_{A_w} (P \bar{\delta} - \bar{\tau}) \cdot \bar{n} dA \Big|_x - U_{xm} \delta \dot{m} + \delta F_x = 0. \end{aligned} \quad (9.6)$$

On the fan $U = U_A$ and so only the surface pressure and stress contribute an amount F_x to the momentum flux. The force *by the flow on the fan* is

$$\delta F_x = \int_{A_f(t)} (P \bar{\delta} - \bar{\tau}) \cdot \bar{n} dA \Big|_x. \quad (9.7)$$

If the Reynolds number of the flow is relatively high the major contribution to the total force in the x -direction, (9.7), comes from pressure forces integrated over the fan surface. The way to evaluate this force is to sum the stream-wise lift components of all the fan blades. If the sum is negative the fan is adding momentum to the flow. If the sum is positive, the fan is actually a windmill or turbine taking momentum out of the flow.

9.1.3 Conservation of energy

Next we evaluate the integral form of the energy equation over the control volume.

$$\begin{aligned}
 & \int_{A(t)} (\rho(e+k)(\bar{U} - \bar{U}_A) + P\bar{U} - \bar{\tau} \cdot \bar{U} + \bar{Q}) \cdot \bar{n} dA = \\
 & \int_{A_2} (\rho_2 h_{t2} U_2 - \tau_{xx2} U_2 + Q_2) dA - \int_{A_1} (\rho_1 h_{t1} U_1 - \tau_{xx1} U_1 + Q_1) dA + \\
 & \int_{A_w} (\rho h_t \bar{U} - \bar{\tau} \cdot \bar{U} + \bar{Q}) \cdot \bar{n} dA + \\
 & \int_{A_f(t)} (\rho(e+k)(\bar{U} - \bar{U}_A) + P\bar{U} - \bar{\tau} \cdot \bar{U} + \bar{Q}) \cdot \bar{n} dA = 0
 \end{aligned} \tag{9.8}$$

The integral over the wall includes the total enthalpy of the mass injected through the wall.

$$\int_{A_w} (\rho h_t \bar{U} - \bar{\tau} \cdot \bar{U} + \bar{Q}) \cdot \bar{n} dA = -\delta Q_w - h_{tm} \delta \dot{m} \tag{9.9}$$

The last integral in (9.8) is the work done *by the flow on the fan*.

$$\delta W = \int_{A_f(t)} (P\bar{U} - \bar{\tau} \cdot \bar{U}) \cdot \bar{n} dA \tag{9.10}$$

Using (9.9) and (9.10) the integrated energy conservation equation is

$$\int_{A_2} (\rho_2 h_{t2} U_2 - \tau_{xx2} U_2 + Q_2) dA - \int_{A_1} (\rho_1 h_{t1} U_1 - \tau_{xx1} U_1 + Q_1) dA = \delta Q_w + h_{tm} \delta \dot{m} - \delta W. \tag{9.11}$$

9.2 Area averaged flow

Every flow variable is a three-dimensional function of space. By averaging the flow across the channel we can produce approximate flow variables that depend only on the stream-wise

coordinate. For example

$$\hat{\rho}(x) = \frac{1}{A(x)} \int \rho(x, y, z) dy dz. \quad (9.12)$$

Similarly we can define the following area averages.

$$\begin{aligned} \hat{T}(x) &= \frac{1}{A(x)} \int T(x, y, z) dy dz \\ \hat{P}(x) &= \frac{1}{A(x)} \int P(x, y, z) dy dz \\ \hat{s}(x) &= \frac{1}{A(x)} \int s(x, y, z) dy dz \\ \hat{U}(x) &= \frac{1}{A(x)} \int U(x, y, z) dy dz \\ \hat{\tau}_{xx}(x) &= \frac{1}{A(x)} \int \tau_{xx}(x, y, z) dy dz \\ \hat{Q}_x(x) &= \frac{1}{A(x)} \int Q_x(x, y, z) dy dz \end{aligned} \quad (9.13)$$

Thus every variable in the flow can be written as a mean plus a deviation.

$$\begin{aligned} \rho(x, y, z) &= \hat{\rho}(x) + \rho'(x, y, z) \\ T(x, y, z) &= \hat{T}(x) + T'(x, y, z) \\ P(x, y, z) &= \hat{P}(x) + P'(x, y, z) \\ s(x, y, z) &= \hat{s}(x) + s'(x, y, z) \\ U(x, y, z) &= \hat{U}(x) + U'(x, y, z) \\ \tau_{xx}(x, y, z) &= \hat{\tau}_{xx}(x) + \tau'_{xx}(x, y, z) \\ Q_x(x, y, z) &= \hat{Q}_x(x) + Q'_x(x, y, z) \end{aligned} \quad (9.14)$$

Consider the mass flux integral.

$$\int_A \rho U dA = \int_A (\hat{\rho} + \rho') (\hat{U} + U') dA = \int_A \hat{\rho} \hat{U} dA + \int_A \rho' U' dA = \\ \hat{\rho}(x) \hat{U}(x) A(x) + \widehat{\rho' U'}(x) A(x) \quad (9.15)$$

The terms that are linear in the deviations are zero by the definition of the average. As long as spatial correlations of flow variables such as $\widehat{\rho' U'}$ are small and can be neglected, the area average is a useful approximation to the flow. In terms of area averaged variables, the integral equations of motion become

$$\begin{aligned} \hat{\rho}_2 \hat{U}_2 A_2 - \hat{\rho}_1 \hat{U}_1 A_1 &= \delta \dot{m} \\ \left(\hat{\rho}_2 \hat{U}_2 \hat{U}_2 + \hat{P}_2 - \hat{\tau}_{xx2} \right) A_2 - \left(\hat{\rho}_1 \hat{U}_1 \hat{U}_1 + \hat{P}_1 - \hat{\tau}_{xx1} \right) A_1 + \\ \int_{A_w} (P\bar{\delta} - \bar{\tau}) \cdot \bar{n} dA \Big|_x - U_{xm} \delta \dot{m} + \delta F_x &= 0 \\ \left(\hat{\rho}_2 \hat{h}_{t2} \hat{U}_2 - \hat{\tau}_{xx2} \hat{U}_2 + \hat{Q}_{x2} \right) A_2 - \left(\hat{\rho}_1 \hat{h}_{t1} \hat{U}_1 - \hat{\tau}_{xx1} \hat{U}_1 + \hat{Q}_{x1} \right) A_1 = \\ \delta Q_w + h_{tm} \delta \dot{m} - \delta W. \end{aligned} \quad (9.16)$$

9.2.1 The traction vector

The pressure-stress integral on the wall in (9.16) (see also (9.7)) needs to be examined a little further.

The unit outward normal to the wall is $\bar{n} = (n_x, n_y, n_z)$ and the components of the so-called traction vector are

$$\bar{T} = (P\bar{\delta} - \bar{\tau}) \cdot \bar{n} = \begin{bmatrix} Pn_x - \tau_{xx}n_x - \tau_{xy}n_y - \tau_{xz}n_z \\ -\tau_{xy}n_x + Pn_y - \tau_{yy}n_y - \tau_{yz}n_z \\ -\tau_{zx}n_x - \tau_{zy}n_y + Pn_z - \tau_{zz}n_z \end{bmatrix}. \quad (9.17)$$

The x -component of the traction vector is indicated in figure 9.2.

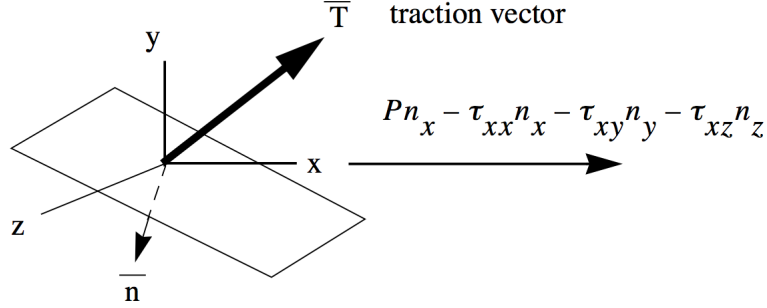


Figure 9.2: *Traction force on the wall due to pressure and viscous forces.*

If we imagine that the length of the control volume is made very small (\$\Delta x \rightarrow 0\$) then the pressure and viscous stress variation along the wall of the control volume is small and so the pressure-viscous stress integral over the surface in (9.16) can be approximated using average values as follows.

$$\begin{aligned} \int_{A_w} (P\bar{\delta} - \bar{\tau}) \cdot \bar{n} dA \Big|_x &= \int_{A_w} (Pn_x - \tau_{xx}n_x - \tau_{xy}n_y - \tau_{xz}n_z) dA \cong \\ &\left(\frac{P_1 + P_2}{2} \right) (A_1 - A_2) - \left(\frac{\tau_{xx1} + \tau_{xx2}}{2} \right) (A_1 - A_2) + \tau_w \pi \left(\frac{D_1 + D_2}{2} \right) \Delta x \end{aligned} \quad (9.18)$$

where we have used

$$\int_{A_w} n_x dA = (A_1 - A_2) \quad (9.19)$$

and

$$\int_{A_w} (\tau_{xy}n_y + \tau_{xz}n_z) dA \equiv -\tau_w \pi \left(\frac{D_1 + D_2}{2} \right) \Delta x. \quad (9.20)$$

This last relation is essentially a definition for the effective wall shear stress \$\tau_w\$ which is always taken to be positive. The wetted surface of the channel is defined using the hydraulic diameter of the channel defined as

$$D = \left(\frac{4A}{\pi} \right)^{1/2}. \quad (9.21)$$

The integrated equations of motion (for small Δx) now take the form

$$\rho_2 U_2 A_2 - \rho_1 U_1 A_1 = \delta \dot{m}$$

$$\begin{aligned}
& (\rho_2 U_2 U_2 + P_2 - \tau_{xx2}) A_2 - (\rho_1 U_1 U_1 + P_1 - \tau_{xx1}) A_1 - \\
& \left(\frac{P_1 + P_2}{2} \right) (A_1 - A_2) + \left(\frac{\tau_{xx1} + \tau_{xx2}}{2} \right) (A_1 - A_2) - \tau_w \pi \left(\frac{D_1 + D_2}{2} \right) \Delta x = U_{xm} \delta \dot{m} - \delta F_x \\
& (\rho_2 H_2 U_2 - \tau_{xx2} U_2 + Q_2) A_2 - (\rho_1 H_1 U_1 - \tau_{xx1} U_1 + Q_1) A_1 = \delta Q_w + h_{tm} \delta \dot{m} - \delta W
\end{aligned} \tag{9.22}$$

where the averaging symbol has been dropped for convenience. Now take the limit $\Delta x \rightarrow 0$ of each of the equations in (9.22). Each of the terms in the integrated equations becomes a differential.

$$\begin{aligned}
& \rho_2 U_2 A_2 - \rho_1 U_1 A_1 \Rightarrow d(\rho U A) \\
& \rho_2 U_2 U_2 A_2 - \rho_1 U_1 U_1 A_1 \Rightarrow d(\rho U^2 A) \\
& P_2 A_2 - P_1 A_1 \Rightarrow d(PA) \\
& \tau_{xx2} A_2 - \tau_{xx1} A_1 \Rightarrow d(\tau_{xx} A) \\
& \left(\frac{P_1 + P_2}{2} \right) (A_1 - A_2) \Rightarrow P dA \\
& \left(\frac{\tau_{xx1} + \tau_{xx2}}{2} \right) (A_1 - A_2) \Rightarrow \tau_{xx} dA \\
& \tau_w \pi \left(\frac{D_1 + D_2}{2} \right) \Delta x \Rightarrow \tau_w \pi D dx \\
& \rho_2 h_{t2} U_2 A_2 - \rho_1 h_{t1} U_1 A_1 \Rightarrow d(\rho U h_t A) \\
& \tau_{xx2} U_2 A_2 - \tau_{xx1} U_1 A_1 \Rightarrow d(\tau_{xx} U A) \\
& Q_{x2} A_2 - Q_{x1} A_1 \Rightarrow d(Q_x A)
\end{aligned} \tag{9.23}$$

Now the equations of motion (9.22) become

$$d(\rho U A) = \delta \dot{m}$$

$$d(\rho U^2 A) + d(PA) - d(\tau_{xx} A) - PdA + \tau_{xx} dA = -\tau_w \pi D dx + U_{xm} \delta \dot{m} - \delta F_x \quad (9.24)$$

$$d(\rho U h_t A) - d(\tau_{xx} U A) + d(Q_x A) = \delta Q_w + h_{tm} \delta \dot{m} - \delta W.$$

Both the momentum and energy equations can be simplified using continuity.

$$U \delta \dot{m} + \rho U A dU + A dP - A d\tau_{xx} = -\tau_w \pi D dx + U_{xm} \delta \dot{m} - \delta F_x$$

$$h_t \delta \dot{m} + \rho U A d h_t - \frac{\tau_{xx}}{\rho} \delta \dot{m} - \rho U A d \left(\frac{\tau_{xx}}{\rho} \right) + \frac{Q_x}{\rho U} \delta \dot{m} + \rho U A d \left(\frac{Q_x}{\rho U} \right) = \quad (9.25)$$

$$\delta Q_w + h_{tm} \delta \dot{m} - \delta W$$

Finally our quasi-one-dimensional equations of motion are

$$d(\rho U A) = \delta \dot{m}$$

$$d(P - \tau_{xx}) + \rho U dU = -\tau_w \left(\frac{\pi D dx}{A} \right) + \frac{(U_{xm} - U) \delta \dot{m}}{A} - \frac{\delta F_x}{A} \quad (9.26)$$

$$d \left(h_t - \frac{\tau_{xx}}{\rho} + \frac{Q_x}{\rho U} \right) = \frac{\delta Q_w}{\rho U A} - \frac{\delta W}{\rho U A} + \left(h_{tm} - \left(h_t - \frac{\tau_{xx}}{\rho} + \frac{Q_x}{\rho U} \right) \right) \frac{\delta \dot{m}}{\rho U A}.$$

It is convenient to introduce the friction coefficient defined as

$$C_f = \frac{\tau_w}{\frac{1}{2} \rho U^2}. \quad (9.27)$$

The heat added through the wall and work done per unit mass flow are

$$\begin{aligned} \delta q_w &= \frac{\delta Q_w}{\rho U A} \\ \delta w &= \frac{\delta W}{\rho U A}. \end{aligned} \quad (9.28)$$

With these definitions, the area-averaged equations of motion take on the fairly concise form

$$\begin{aligned} d(\rho U) &= \frac{\delta \dot{m}}{A} - \rho U \frac{dA}{A} \\ d(P - \tau_{xx}) + \rho U dU &= -\frac{1}{2} \rho U^2 \left(\frac{4C_f dx}{D} \right) + \frac{(U_{xm} - U) \delta \dot{m}}{A} - \frac{\delta F_x}{A} \\ d \left(h_t - \frac{\tau_{xx}}{\rho} + \frac{Q_x}{\rho U} \right) &= \delta q_w - \delta w + \left(h_{tm} - \left(h_t - \frac{\tau_{xx}}{\rho} + \frac{Q_x}{\rho U} \right) \right) \frac{\delta \dot{m}}{\rho U A}. \end{aligned} \quad (9.29)$$

The heat added to the flow through the wall per unit mass is δq_w and the work done by the flow per unit mass is δw . The spirit of these equations is that the differential terms on the right hand sides of (9.29) such as dA/A , $\delta \dot{m}$, $4C_f dx/D$, δq_w and δw are assumed to be known or given quantities. They can be thought of as inputs to the flow whereas the resulting variations in ρ , U , P and temperature T (recall $Q_x = -k \partial T / \partial x$ for a linear conducting medium) are the output changes in the flow.

Notice that up to this point we have not invoked an equation of state. Equations (9.29) apply to the steady flow of any continuous medium in the absence of body forces. By the same token (9.29) is not a closed system; We have four unknowns but only three equations.

9.2.2 Example - steady, gravity-free, adiabatic flow of a compressible fluid in a channel

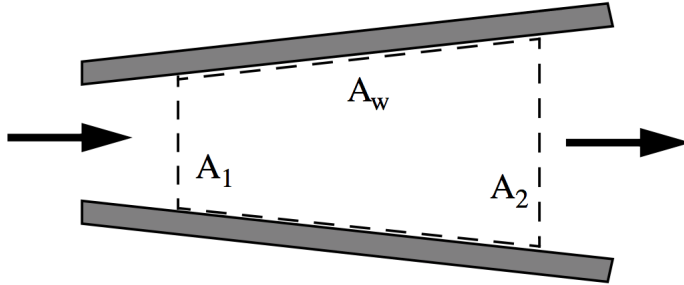


Figure 9.3: Adiabatic channel flow

The integral form of the energy equation in this case is simply

$$d \left(h_t - \frac{\tau_{xx}}{\rho} + \frac{Q_x}{\rho U} \right) = 0. \quad (9.30)$$

For typical cases such as the flow of gases at more than a few meters per second, the stress and heat conduction terms on A_1 and A_2 are very small and can be neglected. Thus

$$h_{t2} = h_{t1}. \quad (9.31)$$

This is, of course, a result we have seen before. It is extraordinarily useful because there are so many flow situations where an adiabatic approximation can be assumed and where the stagnation enthalpy of a fluid particle is approximately conserved. This applies generally, except for flow near a non-adiabatic wall where significant heat conduction may take place and within a shock wave where large stream-wise velocity and temperature gradients occur.

9.3 Normal shock waves

Lets consider uni-directional flow in the absence of mass addition, wall friction, and heat addition. The continuity equation in this case is

$$d(\rho U) = 0. \quad (9.32)$$

If the fluid is incompressible (9.32) gives the trivial result $dU = 0$. But if the fluid is compressible then a non-trivial flow can exist where U and ρ vary inversely. The prime example of such a flow is the shock wave where the properties of the flow change almost discontinuously.

The shaded region in figure 9.4 (the shock) contains gradients in temperature, pressure, density and velocity while the upstream and downstream conditions are perfectly uniform. The thickness of the shock is δ . The equations of motion in this case are

$$\begin{aligned} d(\rho U) &= 0 \\ d(P - \tau_{xx} + \rho U^2) &= 0 \\ d \left(h_t - \frac{\tau_{xx}}{\rho} + \frac{Q_x}{\rho U} \right) &= 0. \end{aligned} \quad (9.33)$$

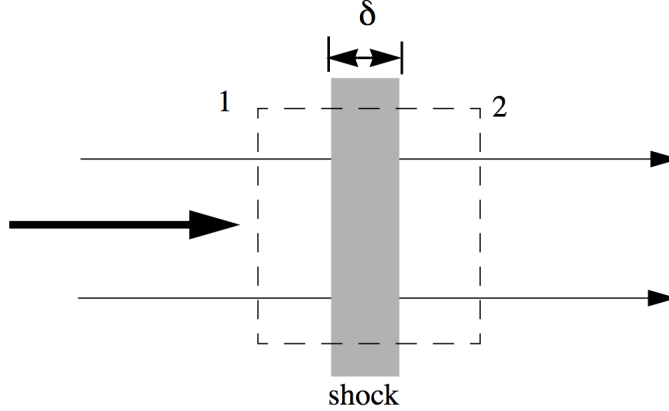


Figure 9.4: Shock wave schematic

Notice that the continuity equation has been used to make the momentum equation a perfect differential. There are three conserved quantities in this flow.

$$\rho U = \text{constant}1$$

$$P - \tau_{xx} + \rho U^2 = \text{constant}2 \quad (9.34)$$

$$h_t - \frac{\tau_{xx}}{\rho} + \frac{Q_x}{\rho U} = \text{constant}3$$

These combinations of flow variables have the same value at every point in the flow including within the shock. Integrate (9.34) between states 1 and 2.

$$\rho_1 U_1 = \rho_2 U_2$$

$$P_1 - \tau_{xx1} + \rho_1 U_1^2 = P_2 - \tau_{xx2} + \rho_2 U_2^2 \quad (9.35)$$

$$h_{t1} - \frac{\tau_{xx1}}{\rho_1} + \frac{Q_{x1}}{\rho_1 U_1} = h_{t2} - \frac{\tau_{xx2}}{\rho_2} + \frac{Q_{x2}}{\rho_2 U_2}$$

Recall that for a Newtonian fluid

$$\tau_{xx} = \left(\frac{4}{3} \mu + \mu_\nu \right) \frac{\partial U}{\partial x} \quad (9.36)$$

where μ_v is the bulk viscosity, and

$$Q_x = -k \frac{\partial T}{\partial x}. \quad (9.37)$$

The flow at 1 and 2 is uniform, i.e., the velocity and temperature gradients are zero and so the equations of motion reduce to the classical shock jump conditions.

$$\begin{aligned} \rho_1 U_1 &= \rho_2 U_2 \\ P_1 + \rho_1 U_1^2 &= P_2 + \rho_2 U_2^2 \\ h_{t1} &= h_{t2} \end{aligned} \quad (9.38)$$

It is important to recognize that in deriving (9.38) viscosity and heat conduction were not neglected. They vanish from the jump conditions because of the uniformity of the upstream and downstream flows. Nevertheless their effects are felt through the mechanism of molecular collision by which changes in the state of the fluid are accomplished within the shock. Notice also that we still have not invoked an equation of state. The equations (9.38) govern the propagation of shock waves in any continuous medium, air, water, rock, etc.

9.3.1 The Rankine-Hugoniot relations

A general set of jump relations in which the velocity does not appear can be derived from (9.38). Combine the mass and momentum jump relations to generate the following equation for the product $U_1 U_2$.

$$U_1 U_2 = \frac{P_2 - P_1}{\rho_2 - \rho_1}. \quad (9.39)$$

The energy equation for a calorically perfect gas is

$$\left(\frac{\gamma}{\gamma - 1} \right) \frac{P_1}{\rho_1} + \frac{1}{2} U_1^2 = \left(\frac{\gamma}{\gamma - 1} \right) \frac{P_2}{\rho_2} + \frac{1}{2} U_2^2. \quad (9.40)$$

Multiply (9.40) by $\rho_1 \rho_2$ and use continuity.

$$\left(\frac{\gamma}{\gamma - 1} \right) P_1 \rho_2 + \frac{1}{2} \rho_2^2 U_1 U_2 = \left(\frac{\gamma}{\gamma - 1} \right) P_2 \rho_1 + \frac{1}{2} \rho_1^2 U_1 U_2. \quad (9.41)$$

Energy conservation generates a second equation for $U_1 U_2$.

$$U_1 U_2 = \left(\frac{2\gamma}{\gamma - 1} \right) \frac{P_2 \rho_1 - P_1 \rho_2}{(\rho_2 - \rho_1)(\rho_2 + \rho_1)} \quad (9.42)$$

Equate (9.42) and (9.39). After some rearrangement the result is

$$\frac{P_2}{P_1} = \frac{\frac{\gamma+1}{\gamma-1} \left(\frac{\rho_2}{\rho_1} \right) - 1}{\frac{\gamma+1}{\gamma-1} - \left(\frac{\rho_2}{\rho_1} \right)}. \quad (9.43)$$

Equation (9.43) is the famous Rankine-Hugoniot relation. Another form of (9.43) is

$$\frac{\frac{P_2}{P_1} - 1}{\frac{P_2}{P_1} + 1} = \gamma \left(\frac{\frac{\rho_2}{\rho_1} - 1}{\frac{\rho_2}{\rho_1} + 1} \right). \quad (9.44)$$

which can be rearranged to read

$$\frac{P_2 - P_1}{\rho_2 - \rho_1} = \gamma \left(\frac{P_2 + P_1}{\rho_2 + \rho_1} \right). \quad (9.45)$$

9.3.2 Shock property ratios in a calorically perfect ideal gas

The jump conditions (9.38) can be used to generate all of the important property ratios for a normal shock. Consider a reference state where the flow speed equals the local speed of sound. The flow variables at this state will be denoted with a superscript *; Thus $U^* = a^*$, and $\rho = \rho^*$, $P = P^*$, $T = T^*$. The third jump condition is $h_{t1} = h_{t2}$. Assume a calorically perfect gas and equate the stagnation enthalpy at stations 1 and 2 to the reference state.

$$\begin{aligned} C_p T_1 + \frac{1}{2} U_1^2 &= \frac{\gamma + 1}{2(\gamma - 1)} a^{*2} \\ C_p T_2 + \frac{1}{2} U_2^2 &= \frac{\gamma + 1}{2(\gamma - 1)} a^{*2} \end{aligned} \quad (9.46)$$

Use the ideal gas law to write (9.46) in the form

$$\begin{aligned}\frac{\gamma}{\gamma-1}P_1 + \frac{1}{2}\rho_2U_2U_1 &= \frac{\gamma+1}{2(\gamma-1)}\rho_1a^{*2} \\ \frac{\gamma}{\gamma-1}P_2 + \frac{1}{2}\rho_1U_2U_1 &= \frac{\gamma+1}{2(\gamma-1)}\rho_2a^{*2}.\end{aligned}\tag{9.47}$$

Subtract the relations in (9.47)

$$\frac{\gamma}{\gamma-1}(P_2 - P_1) - \frac{1}{2}(\rho_2 - \rho_1)U_1U_2 = \frac{\gamma+1}{2(\gamma-1)}a^{*2}(\rho_2 - \rho_1).\tag{9.48}$$

Now use (9.39) to replace $P_2 - P_1$ in (9.48) and gather terms. The result is the famous Prandtl relation

$$U_1U_2 = a^{*2}.\tag{9.49}$$

Note that a^* is essentially defined by (9.46) and can be determined entirely by values in either region 1 ahead of the shock or region 2 behind the shock. Prandtl's relation is the Rosetta stone for generating all of the shock jump relations in terms of the upstream shock Mach number, M_1 . For example, substitute (9.49) into the first relation in (9.46).

$$C_pT_1 + \frac{1}{2}U_1^2 = \frac{\gamma+1}{2(\gamma-1)}U_1U_2\tag{9.50}$$

Divide (9.50) by U_1^2 . The result is

$$\frac{U_2}{U_1} = \frac{2}{\gamma+1} \left(\frac{\gamma RT_1}{U_1^2} \right) + \left(\frac{\gamma-1}{\gamma+1} \right).\tag{9.51}$$

The Mach number ahead of the shock is

$$M_1 = \frac{U_1}{\sqrt{\gamma RT_1}}.\tag{9.52}$$

Equation (9.51) becomes the basic relation for the velocity ratio (and density ratio) across the shock in terms of the upstream Mach number.

$$\frac{U_2}{U_1} = \frac{1 + \left(\frac{\gamma-1}{2}\right) M_1^2}{\left(\frac{\gamma+1}{2}\right) M_1^2} = \frac{\rho_1}{\rho_2} \quad (9.53)$$

All of the other important property ratios of a normal shock wave can now be expressed in terms of the upstream Mach number. Using (9.53) and the Rankine-Hugoniot relation (9.43) we can work out the pressure ratio across the shock.

$$\frac{P_2}{P_1} = \frac{\left(\frac{\gamma+1}{\gamma-1}\right) \left(\frac{\rho_2}{\rho_1}\right) - 1}{\frac{\gamma+1}{\gamma-1} - \left(\frac{\rho_2}{\rho_1}\right)} = \frac{\left(\frac{\gamma+1}{\gamma-1}\right) \left(\frac{\left(\frac{\gamma+1}{2}\right) M_1^2}{1 + \left(\frac{\gamma-1}{2}\right) M_1^2}\right) - 1}{\frac{\gamma+1}{\gamma-1} - \left(\frac{\left(\frac{\gamma+1}{2}\right) M_1^2}{1 + \left(\frac{\gamma-1}{2}\right) M_1^2}\right)} \quad (9.54)$$

Simplify (9.54).

$$\frac{P_2}{P_1} = \frac{\frac{2\gamma}{\gamma-1} M_1^2 - 1}{\frac{\gamma+1}{\gamma-1}} \quad (9.55)$$

The pressure ratio (9.55) is called the *shock strength*. Note the rapid increase with Mach number. The temperature ratio is generated using the ideal gas law.

$$\frac{T_2}{T_1} = \left(\frac{P_2}{P_1}\right) \left(\frac{\rho_1}{\rho_2}\right) = \left(\frac{\gamma M_1^2 - \left(\frac{\gamma-1}{2}\right)}{\frac{\gamma+1}{2}}\right) \left(\frac{1 + \left(\frac{\gamma-1}{2}\right) M_1^2}{\left(\frac{\gamma+1}{2}\right) M_1^2}\right) \quad (9.56)$$

The downstream Mach number is

$$\left(\frac{M_2}{M_1}\right)^2 = \left(\frac{U_2}{U_1}\right)^2 \frac{T_1}{T_2}. \quad (9.57)$$

Substitute (9.53) and (9.56) into (9.57). Several factors cancel and the final result for the downstream Mach number is

$$M_2^2 = \left(\frac{1 + \left(\frac{\gamma-1}{2}\right) M_1^2}{\gamma M_1^2 - \left(\frac{\gamma-1}{2}\right)}\right). \quad (9.58)$$

The relation (9.58) is plotted below for $\gamma = 1.4$.

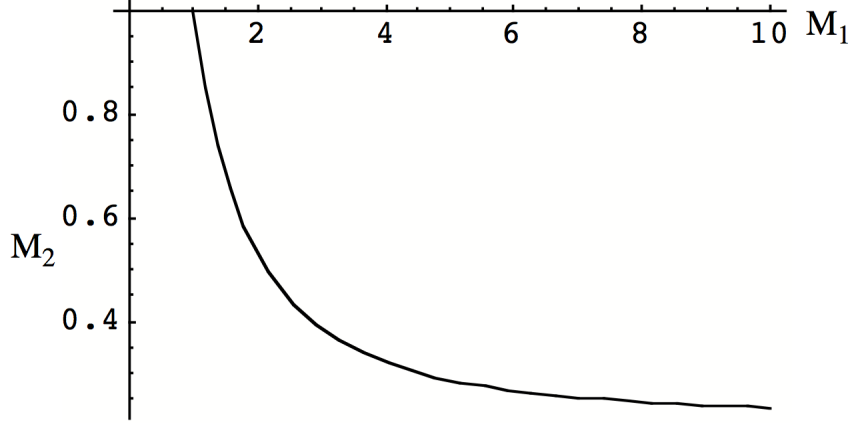


Figure 9.5: Downstream Mach number versus upstream Mach number for a normal shock.

Note that the downstream Mach number is subsonic and has a finite lower limit.

$$\lim_{M_1 \rightarrow \infty} M_2 = \sqrt{\frac{\gamma - 1}{2\gamma}} \quad (9.59)$$

9.3.3 Stagnation pressure ratio across a normal shock wave

The stagnation pressure is determined from the isentropic relations in regions 1 and 2.

$$\begin{aligned} \frac{P_{t1}}{P_1} &= \left(1 + \left(\frac{\gamma - 1}{2} \right) M_1^2 \right)^{\frac{\gamma}{\gamma-1}} \\ \frac{P_{t2}}{P_2} &= \left(1 + \left(\frac{\gamma - 1}{2} \right) M_2^2 \right)^{\frac{\gamma}{\gamma-1}} \end{aligned} \quad (9.60)$$

Divide these two relations.

$$\frac{P_{t2}}{P_{t1}} = \frac{P_2}{P_1} \left(\frac{1 + \left(\frac{\gamma-1}{2} \right) M_2^2}{1 + \left(\frac{\gamma-1}{2} \right) M_1^2} \right)^{\frac{\gamma}{\gamma-1}} \quad (9.61)$$

In (9.61) replace P_2/P_1 with (9.55) and M_2^2 with (9.58).

$$\frac{P_{t2}}{P_{t1}} = \left(\frac{\frac{2\gamma}{\gamma-1} M_1^2 - 1}{\frac{\gamma+1}{\gamma-1}} \right) \left(\frac{1 + \left(\frac{\gamma-1}{2}\right) \left(\frac{1+(\gamma-1)M_1^2}{\gamma M_1^2 - (\gamma-1)}\right)}{1 + \left(\frac{\gamma-1}{2}\right) M_1^2} \right)^{\frac{\gamma}{\gamma-1}} \quad (9.62)$$

Rearrange (9.62).

$$\frac{P_{t2}}{P_{t1}} = \left(\frac{\frac{2\gamma}{\gamma-1} M_1^2 - 1}{\frac{\gamma+1}{\gamma-1}} \right) \left(\frac{\left(\frac{\gamma+1}{2}\right)^2 M_1^2}{\left(\frac{\gamma-1}{2}\right) \left(\frac{2\gamma}{\gamma-1} M_1^2 - 1\right) \left(1 + \left(\frac{\gamma-1}{2}\right) M_1^2\right)} \right)^{\frac{\gamma}{\gamma-1}} \quad (9.63)$$

Combine factors in (9.63). The stagnation pressure ratio across the shock wave is

$$\frac{P_{t2}}{P_{t1}} = \left(\frac{\frac{\gamma+1}{\gamma-1}}{\frac{2\gamma}{\gamma-1} M_1^2 - 1} \right)^{\frac{1}{\gamma-1}} \left(\frac{\left(\frac{\gamma+1}{2}\right) M_1^2}{1 + \left(\frac{\gamma-1}{2}\right) M_1^2} \right)^{\frac{\gamma}{\gamma-1}}. \quad (9.64)$$

The stagnation pressure ratio across a normal shock wave is plotted in figure 9.6 for two values of γ .

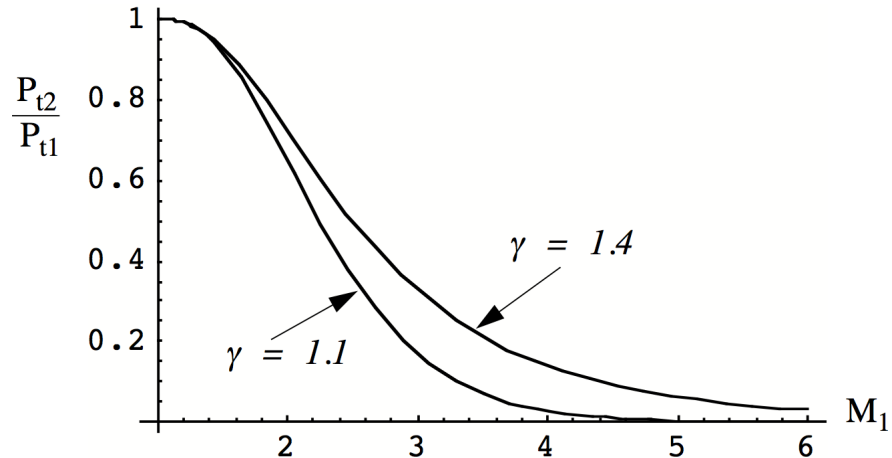


Figure 9.6: Stagnation pressure ratio across a normal shock as a function of shock Mach number.

Two important features of figure 9.6 need to be noted.

- 1) At Mach numbers close to one the change in stagnation pressure across a normal shock wave is very small.
- 2) At high Mach numbers the stagnation pressure loss is very large with

$$\lim_{M_1 \rightarrow \infty} \frac{P_{t2}}{P_{t1}} = \left(\frac{\gamma + 1}{\gamma - 1} \right)^{\frac{\gamma}{\gamma-1}} \left(\frac{\gamma + 1}{2\gamma M_1^2} \right)^{\frac{1}{\gamma-1}}. \quad (9.65)$$

Recall that we can write the Gibbs equation in terms of the stagnation state of the gas.

$$ds = \frac{dh_t}{T_t} - R \frac{dP_t}{P_t} \quad (9.66)$$

Integrate (9.66) from state 1 to state 2. Since $dh_t = 0$ the entropy change across the wave is determined directly from the change in stagnation pressure.

$$\frac{P_{t2}}{P_{t1}} = e^{-\left(\frac{s_2-s_1}{R}\right)} \quad (9.67)$$

The connection (9.67) between the stagnation pressure and entropy in an adiabatic flow is an extremely important one that we see often when we solve problems in compressible channel flow.

The equations for the flow property ratios across the shock are the fundamental relations used to generate shock tables.

9.3.4 Example - stagnation at a leading edge in supersonic flow

The figure below shows a supersonic flow of Helium (atomic weight equals 4) over the leading edge of a thick flat plate at a free stream Mach number $M_1 = 2.0$.

The temperature of the free stream is 300 K and the pressure is one atmosphere.

- 1) Determine the *energy* per unit mass of a fluid element located at points 1 (free stream), 2 (just behind the shock) and 3 (at the stagnation point on the body). State the assumptions used to solve the problem. Express your answer in Joules/kg.

Solution

The energy per unit mass of a flowing gas is the sum of internal energy and kinetic energy per unit mass, $e + k$.

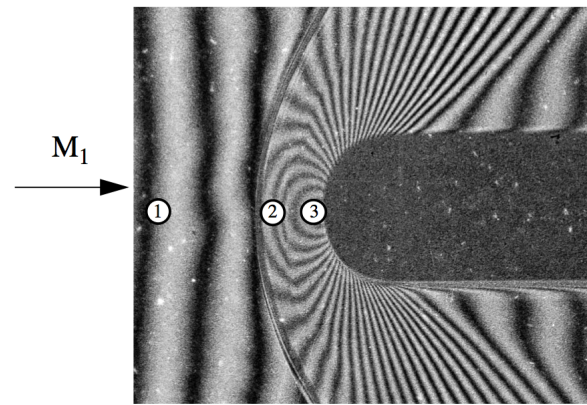


Figure 9.7: Supersonic flow of helium over a leading edge.

- a) Assume the gas is calorically perfect - constant heat capacities.
- b) Assume the flow is adiabatic from station 1 to station 3.
- c) Assume the body is adiabatic.

For Helium the number of degrees of freedom equals 3 and at the conditions of the free

stream we have the following values.

$$R = \frac{8314.472}{4} = 2078.62 \text{ m}^2/\text{sec}^2 - K$$

$$C_v = \frac{3}{2}R = 3117.93 \text{ m}^2/\text{sec}^2 - K$$

$$C_p = \frac{3+2}{2}R = 5196.55 \text{ m}^2/\text{sec}^2 - K$$

$$\gamma = 5/3$$

$$a = \sqrt{\gamma RT} = \sqrt{\frac{5}{3}2078.62(300)} = 1019.46 \text{ m}^2/\text{sec}^2 \quad (9.68)$$

$$U_1 = 2(1019.46) = 2038.92 \text{ m/sec}$$

$$e_1 + k_1 = C_v T_1 + \frac{1}{2} U_1^2 = 3117.93(300) + 0.5(2038.92)^2 = 935379 + 2078597$$

$$e_1 + k_1 = 3013976 \text{ J/kg}$$

The stagnation temperature of the free stream is determined from

$$\frac{T_t}{T} = 1 + \left(\frac{\gamma - 1}{2} \right) M^2. \quad (9.69)$$

Thus

$$T_{t1} = 300 \left(1 + \frac{4}{3} \right) = 700 \text{ K} \quad (9.70)$$

Across a normal shock at Mach 2 the temperature ratio is

$$\frac{T_2}{T_1} = \frac{\left(1 + \left(\frac{\gamma-1}{2} \right) M_1^2 \right) \left(\gamma M_1^2 - \left(\frac{\gamma-1}{2} \right) \right)}{\left(\frac{\gamma+1}{2} \right)^2 M_1^2} \quad (9.71)$$

which gives

$$\frac{T_2}{T_1} = \frac{\left(1 + \frac{4}{3}\right) \left(\frac{5}{3}(4) - \left(\frac{1}{3}\right)\right)}{\left(\frac{4}{3}\right)^2 (4)} = \frac{\left(\frac{7}{3}\right) \left(\frac{19}{3}\right)}{\left(\frac{4}{3}\right) \left(\frac{16}{3}\right)} = \frac{7}{4} \left(\frac{19}{16}\right) = 2.078. \quad (9.72)$$

Assume the flow is adiabatic from the free stream to the stagnation point.

$$h_1 + \frac{1}{2}U_1^2 = h_2 + \frac{1}{2}U_2^2 = h_3 + \frac{1}{2}U_3^2 \quad (9.73)$$

We can rewrite this equation as follows.

$$RT_1 + (e_1 + k_1) = RT_2 + (e_2 + k_2) = RT_3 + (e_3 + k_3) \quad (9.74)$$

The temperatures at stations 1, 2 and 3 are respectively

$$T_1 = 300 K$$

$$T_2 = 2.078 (300) = 623.44 K \quad (9.75)$$

$$T_3 = T_{t1} = 700 K.$$

Now

$$e_1 + k_1 = 3.014 \times 10^6 J/kg$$

$$\begin{aligned} (e_2 + k_2) &= (e_1 + k_1) - R(T_2 - T_1) = 3.014 \times 10^6 - 2078.62 (623.44 - 300) \\ &= 3.014 \times 10^6 - 0.6723 \times 10^6 = 2.3417 \times 10^6 J/kg \end{aligned} \quad (9.76)$$

$$\begin{aligned} (e_3 + k_3) &= (e_1 + k_1) - R(T_3 - T_1) = 3.014 \times 10^6 - 2078.62 (700 - 300) \\ &= 3.014 \times 10^6 - 0.8314 \times 10^6 = 2.1826 \times 10^6 J/kg. \end{aligned}$$

The energy of a fluid element decreases considerably across the shock and then decreases further to the stagnation point.

2) Describe the mechanism by which the energy of the fluid element changes as it moves from station 1 to station 3.

The work done by the pressure and viscous normal force field on the fluid element is the mechanism by which the energy decreases in moving from station 1 to station 3. The flow

energy decreases across the shock wave through a combination of pressure and viscous normal stress forces of roughly equal magnitude that act to compress the fluid element increasing its internal energy while decelerating it and reducing its kinetic energy. The loss of kinetic energy dominates the increase in internal energy.

Between stations 2 and 3 the flow further decelerates as the pressure increases toward the stagnation point. Viscous normal forces also act in region 2 to 3 but because the streamwise velocity gradients are small (compared to the shock) viscous forces are generally much smaller than the pressure forces.

9.4 Shock wave thickness

Let's use the jump conditions and our knowledge of entropy generation to *estimate* the thickness of a shock wave.

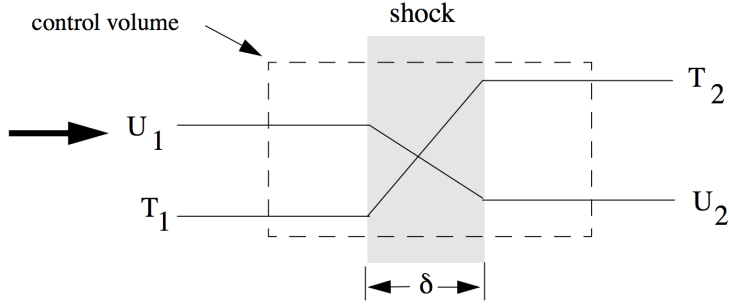


Figure 9.8: *Linear model for temperature and pressure variation within a shock.*

The integral form of the entropy transport equation, derived in Chapter 7, over an Eulerian control volume is

$$\frac{d}{dt} \int_V \rho s dV + \int_A \left(\rho \bar{U} s - \frac{k}{T} \nabla T \right) \cdot \bar{n} dA = \int_V \left(\frac{\Upsilon + \Phi}{T} \right) dV \quad (9.77)$$

where for a Newtonian, linear, heat conducting medium

$$\Phi = 2\mu \left(S_{ij} - \frac{1}{3} \delta_{ij} S_{kk} \right) \left(S_{ij} - \frac{1}{3} \delta_{ij} S_{kk} \right) + \mu_v (S_{ii} S_{kk}) \quad (9.78)$$

and

$$\Upsilon = \frac{k}{T} \left(\frac{\partial T}{\partial x_j} \frac{\partial T}{\partial x_j} \right). \quad (9.79)$$

The stress tensor is

$$\tau_{ij} = 2\mu S_{ij} - ((2/3)\mu - \mu_v) \delta_{ij} S_{kk}. \quad (9.80)$$

For the unidirectional flow within the shock wave the stress tensor reduces to

$$\tau_{ij} = \begin{bmatrix} \left(\frac{4}{3}\mu + \mu_v\right) \frac{dU}{dx} & 0 & 0 \\ 0 & \left(-\frac{2}{3}\mu + \mu_v\right) \frac{dU}{dx} & 0 \\ 0 & 0 & \left(-\frac{2}{3}\mu + \mu_v\right) \frac{dU}{dx} \end{bmatrix}. \quad (9.81)$$

Note that the viscous normal stresses in the y and z directions are not zero since $S_{kk} = \nabla \cdot \bar{U} = dU/dx$. The modified rate-of-strain tensor that appears in the dissipation is

$$S_{ij} - \frac{1}{3}\delta_{ij}S_{kk} = \begin{bmatrix} \frac{2}{3}\frac{dU}{dx} & 0 & 0 \\ 0 & -\frac{1}{3}\frac{dU}{dx} & 0 \\ 0 & 0 & -\frac{1}{3}\frac{dU}{dx} \end{bmatrix} \quad (9.82)$$

and therefore the kinetic energy dissipation within the shock is

$$\Phi = \left(\frac{4}{3}\mu + \mu_v\right) \left(\frac{dU}{dx}\right)^2. \quad (9.83)$$

The temperature dissipation is

$$\Upsilon = \frac{k}{T} \left(\frac{dT}{dx}\right)^2. \quad (9.84)$$

Now we integrate the entropy transport equation over the control volume indicated in the figure 9.8. Since the flow is steady

$$\frac{d}{dt} \int_V \rho s dV = 0. \quad (9.85)$$

The integrated entropy equation becomes

$$\left(\rho U s A - \frac{k}{T} \frac{dT}{dx} A \right)_2 - \left(\rho U s A - \frac{k}{T} \frac{dT}{dx} A \right)_1 = \left(\int_0^\delta \left(\frac{\Upsilon + \Phi}{T} \right) dx \right) A. \quad (9.86)$$

The areas cancel on both sides of the equation and the temperature gradients at stations 1 and 2 are zero. The product ρU is constant through the wave.

$$\rho U (s_2 - s_1) = \int_0^\delta \left(\left(\frac{\frac{4}{3}\mu + \mu_v}{T} \right) \left(\frac{dU}{dx} \right)^2 + \frac{k}{T^2} \left(\frac{dT}{dx} \right)^2 \right) dx \quad (9.87)$$

In order to model the integral on the right-hand-side of (9.87) we make the following linear approximations for the gradients inside the wave and for the mean temperature.

$$\begin{aligned} \frac{dU}{dx} &\cong \frac{U_2 - U_1}{\delta} \\ \frac{dT}{dx} &\cong \frac{T_2 - T_1}{\delta} \\ T &\cong \frac{T_2 + T_1}{2} \end{aligned} \quad (9.88)$$

We assume that the viscosity and thermal conductivity are evaluated at the mean temperature. The control volume balance of entropy now becomes

$$\rho U (s_2 - s_1) \left(\frac{T_2 + T_1}{2} \right) \delta = \left(\left(\frac{4}{3}\mu + \mu_v \right) (U_2 - U_1)^2 + 2k \frac{(T_2 - T_1)^2}{(T_2 + T_1)} \right) \quad (9.89)$$

which can be expressed as

$$\rho U (s_2 - s_1) \delta = \left(\frac{2 \left(\frac{4}{3} \mu + \mu_v \right) \frac{U_1^2}{T_1} \left(\frac{U_2}{U_1} - 1 \right)^2 + 4k \frac{\left(\frac{T_2}{T_1} - 1 \right)^2}{\left(\frac{T_2}{T_1} + 1 \right)}}{\left(\frac{T_2}{T_1} + 1 \right)} \right). \quad (9.90)$$

Use $U_2/U_1 = \rho_1/\rho_2$ and move the entropy term to the right-hand-side.

$$\frac{\rho U \delta}{\mu} = \left(\frac{2(\gamma - 1) \left(\frac{4}{3} + \frac{\mu_v}{\mu} \right) M_1^2 \left(\frac{\rho_1}{\rho_2} - 1 \right)^2 + 4 \frac{k}{\mu C_p} \frac{\left(\frac{T_2}{T_1} - 1 \right)^2}{\left(\frac{T_2}{T_1} + 1 \right)}}{\frac{1}{\gamma} \left(\frac{T_2}{T_1} + 1 \right) \left(\frac{s_2 - s_1}{C_v} \right)} \right) \quad (9.91)$$

Recall that the Prandtl number is defined as

$$P_r = \frac{\mu C_p}{k}. \quad (9.92)$$

The entropy jump across the shock can be expressed in terms of the density and temperature ratio using Gibbs' equation.

$$\frac{s_2 - s_1}{C_v} = \ln \left(\frac{T_2}{T_1} \left(\frac{\rho_1}{\rho_2} \right)^{(\gamma-1)} \right) \quad (9.93)$$

Finally

$$\frac{\rho U \delta}{\mu} = \left(\frac{2\gamma(\gamma - 1) \left(\frac{4}{3} + \frac{\mu_v}{\mu} \right) M_1^2 \left(\frac{\rho_1}{\rho_2} - 1 \right)^2 + 4 \frac{\gamma}{P_r} \frac{\left(\frac{T_2}{T_1} - 1 \right)^2}{\left(\frac{T_2}{T_1} + 1 \right)}}{\left(\frac{T_2}{T_1} + 1 \right) \ln \left(\frac{T_2}{T_1} \left(\frac{\rho_1}{\rho_2} \right)^{(\gamma-1)} \right)} \right). \quad (9.94)$$

The right hand side of (9.94) is expressed in terms of ratios across the shock and can

be written entirely in terms of the upstream Mach number using the shock jump relations.

$$\frac{\rho_1}{\rho_2} = \frac{(\gamma - 1) M_1^2 + 2}{(\gamma + 1) M_1^2}$$

$$\frac{T_2}{T_1} = \frac{(2\gamma M_1^2 - (\gamma - 1)) ((\gamma - 1) M_1^2 + 2)}{(\gamma + 1)^2 M_1^2} \quad (9.95)$$

The left hand side of (9.94) can be interpreted as the shock Reynolds number where the characteristic length is taken to be the shock thickness. In summary

$$\frac{\rho U \delta}{\mu} = F \left(M_1^2, \gamma, P_r, \frac{\mu_v}{\mu} \right). \quad (9.96)$$

The function $F(M_1^2, \gamma, P_r, \mu_v/\mu)$ in (9.94) is plotted in figure 9.9 for two values of the ratio of bulk to shear viscosity μ_v/μ .

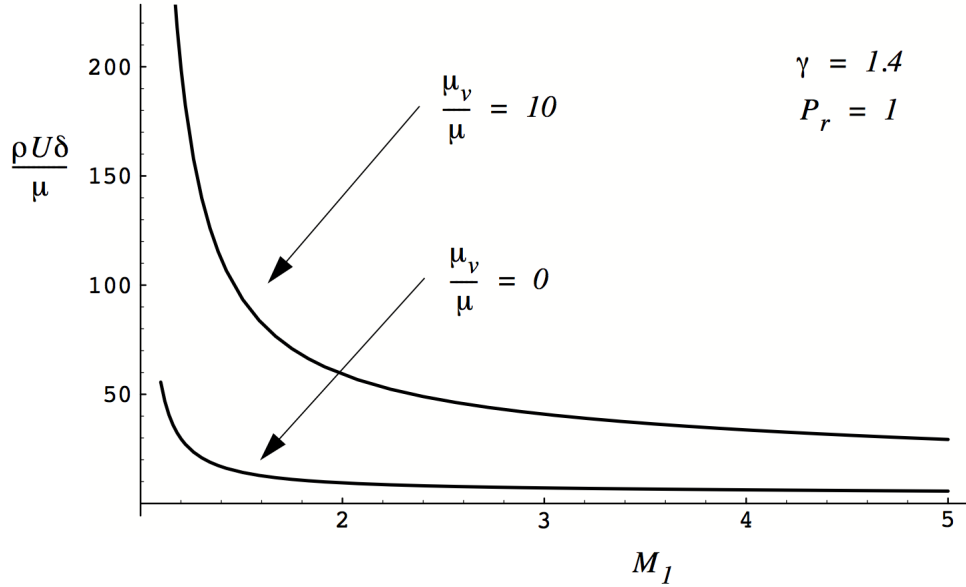


Figure 9.9: Shock Reynolds number as a function of Mach number.

The results of our model indicate that the Reynolds number of a shock wave is small and decreases with increasing Mach number, affirming the strongly viscous nature of the flow

through the wave. Note also that, at a given Mach number, a gas with a large bulk viscosity will generate a much thicker shock wave.

Results from kinetic theory relating the viscosity to the mean free path are provided in Appendix A. To a good approximation $\mu = \rho a \lambda$ where λ is the mean free path and a is the speed of sound. Equation (9.96) can be written

$$\frac{\rho U \delta}{\rho a \lambda} \cong F \left(M_1^2, \gamma, P_r, \frac{\mu_v}{\mu} \right). \quad (9.97)$$

In the spirit of the approximations used earlier let the Mach number appearing on the left hand side of (9.97) be approximated as

$$\frac{U}{a} = \left(\frac{U_1 + U_2}{2} \right) \left(\frac{2}{a_1 + a_2} \right) = M_1 \left(\frac{\frac{\rho_1}{\rho_2} + 1}{\sqrt{\frac{T_2}{T_1}} + 1} \right). \quad (9.98)$$

Now the ratio of shock thickness to the mean free path in the gas (the inverse of the shock Knudsen number) can be estimated.

$$\frac{\delta}{\lambda} \cong \frac{F \left(M_1^2, \gamma, P_r, \frac{\mu_v}{\mu} \right)}{M_1} \left(\frac{\sqrt{\frac{T_2}{T_1}} + 1}{\frac{\rho_1}{\rho_2} + 1} \right) \quad (9.99)$$

This function is plotted in figure 9.10.

We can see from this final result that in fact a shock is extremely thin, on the order of a few mean free paths thick. It is important that the model gives a shock thickness greater than the mean free path so as to be consistent with the fact that the shock is viscous and that a molecule experiences at least several collisions as it passes through the shock. It is the increased randomization of the molecular motion due to these collisions that leads to the entropy rise across the shock imposed by the shock jump conditions.

This result also serves as a warning that the model, based on the Navier-Stokes equations, has its limitations! Notice that for Mach numbers above about 2, the shock is a very small number of mean free paths thick. This is inconsistent with the assumption that the gas is in local thermodynamic equilibrium. The equilibrium state of the gas, with well defined values of temperature (to which the viscosity and thermal conductivity are related) and pressure, can only be established through collisions and four or five collisions is barely enough.

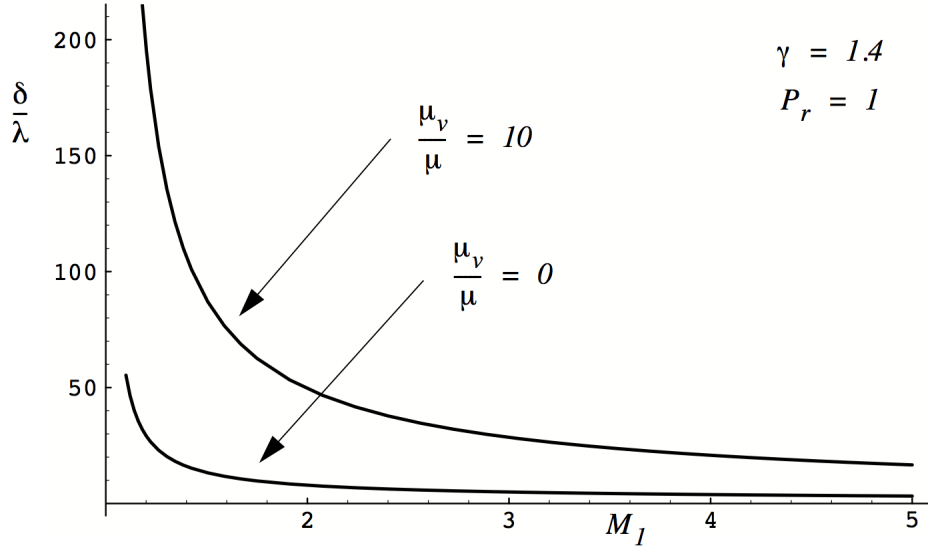


Figure 9.10: Shock thickness number as a function of Mach number.

The state of the gas inside a very strong shock wave is far from thermodynamic equilibrium and a proper theory for the flow requires a much more sophisticated treatment. One is forced to a much more complex analysis based on the Boltzmann equation which describes the space-time evolution of the velocity probability density function and explicitly accounts for molecular collisions.

9.5 Problems

Problem 1 - Heat in the amount of 10^6 J/kg is added to a compressible flow of helium in a diverging channel. The heat is distributed so that the area averaged velocities at stations 1 and 2 are the same.

The temperature at station 1 is 1000 K and the area ratio is $A_2/A_1 = 2$. Determine T_2/T_1 , ρ_2/ρ_1 , P_2/P_1 , and $(s_2 - s_1)/C_p$.

Problem 2 - Recall Problem 5.3. Consider steady flow in one dimension where $\bar{U} = (U(x), 0, 0)$ and all velocity gradients are zero except

$$A_{11} = \frac{\partial U}{\partial x}. \quad (9.100)$$

Work out the components of the Newtonian viscous stress tensor τ_{ij} . Note the role of

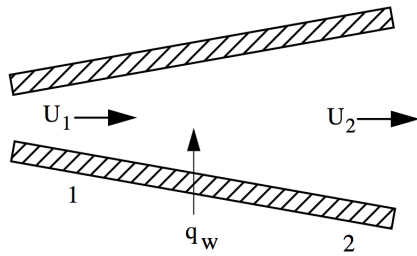


Figure 9.11: Heat added to a diverging channel flow.

the bulk viscosity. Inside a normal shock wave the velocity gradient can be as high as 10^{10} sec^{-1} . Using values for Air at 300 K and one atmosphere, estimate the magnitude of the viscous normal stress inside a shock wave. Express your answer in atmospheres.

Problem 3 - Consider a normal shock wave in helium with Mach number $M_1 = 3$. The temperature of the upstream gas is 300 K and the pressure is 10^5 N/m^2 .

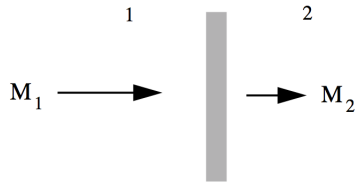


Figure 9.12: Normal shock wave in helium

- 1) Determine the stagnation temperature in region 2 as measured by an observer at rest with respect to the upstream gas. This is an observer that sees the shock wave propagating to the left at Mach 3.
- 2) Determine the stagnation pressure in region 2 as measured by an observer at rest with respect to the upstream gas.

Problem 4 - The figure below shows supersonic flow of carbon dioxide, $\gamma = 4/3$, past a cylindrical bullet at a free stream Mach number, $M_1 = 2.77$.

The temperature of the free stream is 300 K and the pressure is one atmosphere.

- a) Determine the temperature, pressure and Mach number of the gas on the centerline just downstream of the shock wave.
- b) Estimate the temperature and pressure at the stagnation point on the upstream face of the cylinder.

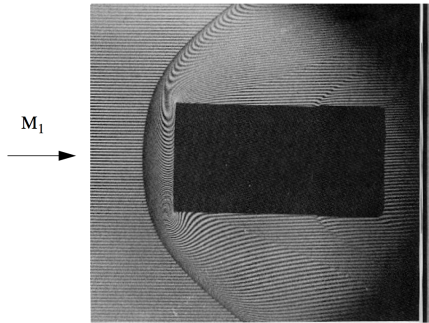


Figure 9.13: Supersonic flow of carbon dioxide past a bullet. See Van Dyke page 163.

- c) Determine the entropy increase across the shock wave.
- d) Estimate the thickness of the shock wave.
- e) Estimate the acceleration of the fluid element as it traverses the shock wave. Express your answer in m/sec^2 .

Problem 5 - Estimate the thickness of the shock wave in Helium discussed in section 9.3.4.

Problem 6 - The sketch below shows supersonic flow of air, $\gamma = 1.4$, past a sphere at a free stream Mach number, $M_1 = 1.53$. See Van Dyke page 164.

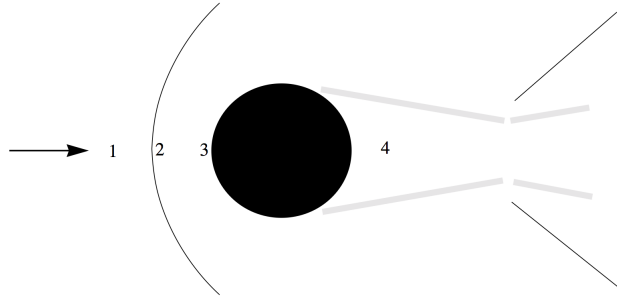


Figure 9.14: Supersonic flow past a sphere.

- a) Compare each of the following properties of the gas; stagnation enthalpy, h_t , stagnation pressure, P_t and entropy per unit mass, s at locations 1, 2 and 3 identified in the figure. State the assumptions needed to make your comparisons.
- b) What can you say about the same properties of the gas at station 4? How certain is your answer? Why?

- c) Determine the Mach number at station 2.
- d) Is the energy per unit mass (internal plus kinetic) of a gas particle at 1 and 2 the same? Prove your answer.

Problem 7 - We often encounter practical situations involving weak shock waves where the Mach number upstream of the wave is very close to one.

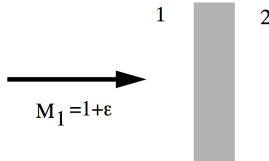


Figure 9.15: Weak normal shock

Let the Mach number ahead of the wave be $M_1 = 1 + \varepsilon$ where $\varepsilon < 1$. Derive the weak shock jump relations $M_2 \cong 1 - \varepsilon$ and

$$\begin{aligned} \frac{U_2 - U_1}{a_1} &\cong -\frac{4}{\gamma + 1}\varepsilon \\ \frac{T_2 - T_1}{T_1} &\cong ? \\ \frac{P_2 - P_1}{P_1} &\cong ? \\ \frac{P_{t2} - P_{t1}}{P_{t1}} &\cong -\frac{16}{3} \frac{\gamma}{(\gamma + 1)^2} \varepsilon^3. \end{aligned} \tag{9.101}$$

The last result in (9.101) is extremely important in that it shows that the stagnation loss across a weak shock is extremely small indeed. This fact is exploited in the design of supersonic inlets. Note that first and second order terms in ε have cancelled. I suggest you use symbol manipulation software such as Mathematica to derive this result.

Problem 8 - The photo below shows a rifle bullet moving in air at a Mach number of 1.1. The air temperature is 300 K. On the centerline the flow from the left passes through a normal shock wave and then stagnates on the nose of the bullet.

- a) Determine the temperature, pressure and density change across the wave.
- b) Compare the temperature, pressure and density of the gas at the nose of the bullet to values in the freestream.

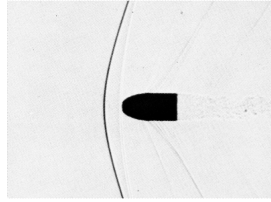


Figure 9.16: *Supersonic rifle bullet.*

- c) Evaluate the entropy change.
- d) State any assumptions used.

Problem 9 - Use the weak shock theory developed in problem 7 to estimate the thickness of the shock wave depicted in Problem 8. Develop an expression for estimating the thickness of a weak shock wave δ in terms of ε and γ .

Problem 10 - The figure below shows supersonic flow of air over a model of a re-entry body at a free stream Mach number, $M_1 = 2$.

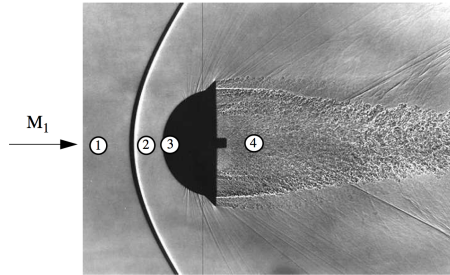


Figure 9.17: *Supersonic flow over a re-entry body.*

The temperature of the free stream is 300 K and the pressure is one atmosphere.

- 1) Determine the stagnation temperature and pressure of a fluid element located at stations 1 (free stream), 2 (just behind the shock) and 3 (at the stagnation point on the body). State the assumptions used to solve the problem. Express your answers in degrees Kelvin and atmospheres.
- 2) What can you say about the state of the gas at point 4?
- 3) Refer the stagnation temperatures at 1, 2 and 3 to an observer at rest with respect to the upstream gas. To such an observer the body is moving to the left at a Mach number of 2.0.

Problem 11 - The photo below shows the flow of Helium gas past a sphere at a Mach number of 1.05. The pressure is one atmosphere ($1.01325 \times 10^5 \text{ N/m}^2$) and the temperature is 300 K . The viscosity of Helium at that temperature is $\mu_1 = 1.98 \times 10^{-5} \text{ kg/m} - \text{sec}$. Consider a fluid element that passes through the shock on the flow centerline.

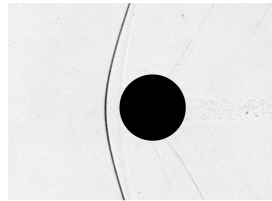


Figure 9.18: *Slightly supersonic flow past a sphere.*

Estimate the acceleration of the fluid element as it traverses the shock wave. Express your answer in m/sec^2 .

Chapter 10

Gasdynamics of nozzle flow

A nozzle is an extremely efficient device for converting thermal energy to kinetic energy. Nozzles come up in a vast range of applications. Obvious ones are the thrust nozzles of rocket and jet engines. Converging-diverging ducts also come up in aircraft engine inlets, wind tunnels and in all sorts of piping systems designed to control gas flow. The flows associated with volcanic and geyser eruptions are influenced by converging-diverging nozzle geometries that arise naturally in geological formations.

10.1 Area-Mach number function

In Chapter 8 we developed the area-averaged equations of motion.

$$\begin{aligned} d(\rho U) &= \frac{\delta \dot{m}}{A} - \rho U \frac{dA}{A} \\ d(P - \tau_{xx}) + \rho U dU &= -\frac{1}{2} \rho U^2 \left(\frac{4C_f dx}{D} \right) + \frac{(U_{xm} - U) \delta \dot{m}}{A} - \frac{\delta F_x}{A} \\ d \left(h_t - \frac{\tau_{xx}}{\rho} + \frac{Q_x}{\rho U} \right) &= \delta q_w - \delta w + \left(h_{tm} - \left(h_t - \frac{\tau_{xx}}{\rho} + \frac{Q_x}{\rho U} \right) \right) \frac{\delta \dot{m}}{\rho U A} \end{aligned} \quad (10.1)$$

Assume the only effect on the flow is streamwise area change so that

$$\delta \dot{m} = C_f = \delta F_x = \delta q = \delta w = 0. \quad (10.2)$$

Also assume that streamwise normal stresses and heat fluxes τ_{xx} , Q_x are small enough to be neglected. With these assumptions the governing equations (10.1) together with the perfect gas law reduce to

$$\begin{aligned} d(\rho U A) &= 0 \\ dP + \rho U dU &= 0 \\ C_p dT + U dU &= 0 \\ P &= \rho R T. \end{aligned} \tag{10.3}$$

Introduce the Mach number

$$U^2 = \gamma R T M^2. \tag{10.4}$$

Each of the equations in (10.3) can be expressed in fractional differential form.

$$\begin{aligned} \frac{d\rho}{\rho} + \frac{dU^2}{2U^2} + \frac{dA}{A} &= 0 \\ \frac{dP}{P} + \frac{\gamma M^2}{2} \frac{dU^2}{U^2} &= 0 \\ \frac{dT}{T} + \frac{(\gamma - 1) M^2}{2} \frac{dU^2}{U^2} &= 0 \\ \frac{dP}{P} &= \frac{d\rho}{\rho} + \frac{dT}{T} \end{aligned} \tag{10.5}$$

Equation (10.4) can also be written in fractional differential form.

$$\frac{dU^2}{U^2} = \frac{dT}{T} + \frac{dM^2}{M^2} \tag{10.6}$$

Use the equations for mass, momentum and energy to replace the terms in the equation of state.

$$-\frac{\gamma M^2}{2} \frac{dU^2}{U^2} = -\frac{dU^2}{2U^2} - \frac{dA}{A} - \frac{(\gamma - 1) M^2}{2} \frac{dU^2}{U^2} \tag{10.7}$$

Solve for dU^2/U^2 .

$$\frac{dU^2}{U^2} = \left(\frac{2}{M^2 - 1} \right) \frac{dA}{A} \quad (10.8)$$

Equation (10.8) shows the effect of streamwise area change on the speed of the flow. If the Mach number is less than one then increasing area leads to a decrease in the velocity. But if the Mach number is greater than one then increasing area leads to an increase in flow speed. Use (10.8) to replace dU^2/U^2 in each of the relations in (10.5).

$$\begin{aligned} \frac{d\rho}{\rho} &= - \left(\frac{M^2}{M^2 - 1} \right) \frac{dA}{A} \\ \frac{dP}{P} &= - \left(\frac{\gamma M^2}{M^2 - 1} \right) \frac{dA}{A} \\ \frac{dT}{T} &= - \left(\frac{(\gamma - 1) M^2}{M^2 - 1} \right) \frac{dA}{A} \end{aligned} \quad (10.9)$$

Equations (10.9) describe the effects of area change on the thermodynamic state of the flow. Now use (10.8) and the temperature equation in (10.6).

$$\left(\frac{2}{M^2 - 1} \right) \frac{dA}{A} = - \frac{(\gamma - 1) M^2}{M^2 - 1} \frac{dA}{A} + \frac{dM^2}{M^2} \quad (10.10)$$

Rearrange (10.10). The effect of area change on the Mach number is

$$\frac{dA}{A} = \frac{M^2 - 1}{2 \left(1 + \left(\frac{\gamma-1}{2} \right) M^2 \right)} \frac{dM^2}{M^2}. \quad (10.11)$$

Equation (10.11) is different from (10.8) and (10.9) in that it can be integrated from an initial to a final state. Integrate (10.11) from an initial Mach number M to one.

$$\int_{M^2}^1 \frac{M^2 - 1}{2 \left(1 + \left(\frac{\gamma-1}{2} \right) M^2 \right)} \frac{dM^2}{M^2} = \int_A^{A^*} \frac{dA}{A} \quad (10.12)$$

The result is

$$\ln\left(\frac{A^*}{A}\right) = \left\{ -\ln(M) + \ln\left(2\left(1 + \left(\frac{\gamma-1}{2}\right)M^2\right)^{\frac{\gamma+1}{2(\gamma-1)}}\right) \right\} \Big|_{M^2}^1. \quad (10.13)$$

Evaluate (10.13) at the limits

$$\ln\left(\frac{A^*}{A}\right) = \ln\left(\left(\frac{\gamma+1}{2}\right)^{\frac{\gamma+1}{2(\gamma-1)}}\right) - \left\{ -\ln(M) + \ln\left(\left(1 + \left(\frac{\gamma-1}{2}\right)M^2\right)^{\frac{\gamma+1}{2(\gamma-1)}}\right) \right\}_{(10.14)}$$

which becomes

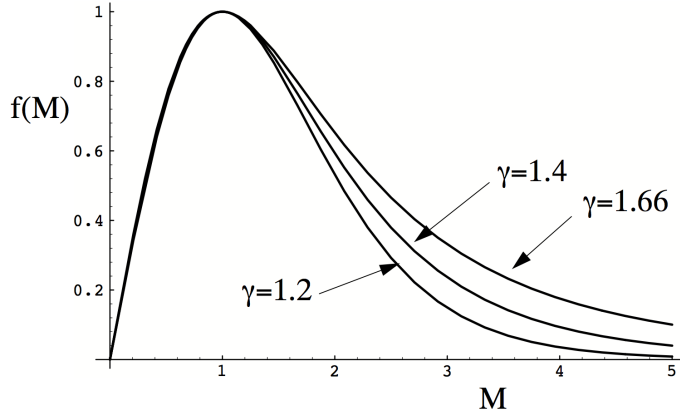
$$\ln\left(\frac{A^*}{A}\right) = \ln\left(\left(\frac{\gamma+1}{2}\right)^{\frac{\gamma+1}{2(\gamma-1)}} \frac{M}{\left(1 + \left(\frac{\gamma-1}{2}\right)M^2\right)^{\frac{\gamma+1}{2(\gamma-1)}}}\right). \quad (10.15)$$

Exponentiate both sides of (10.15). The result is the all-important area-Mach number equation.

$$f(M) = \frac{A^*}{A} = \left(\frac{\gamma+1}{2}\right)^{\frac{\gamma+1}{2(\gamma-1)}} \frac{M}{\left(1 + \left(\frac{\gamma-1}{2}\right)M^2\right)^{\frac{\gamma+1}{2(\gamma-1)}}} \quad (10.16)$$

In (10.16) we referenced the integration process to $M = 1$. The area A^* is a reference area at some point in the channel where $M = 1$ although such a point need not actually be present in a given problem. The area-Mach-number function is plotted below for three values of γ .

Note that for smaller values of γ it takes an extremely large area ratio to generate high Mach number flow. A value of $\gamma = 1.2$ would be typical of the very high temperature mixture of gases in a rocket exhaust. Conversely, if we want to produce a high Mach number flow in a reasonable size nozzle, say for a wind tunnel study, an effective method is to select a monatomic gas such as Helium which has $\gamma = 1.66$. A particularly interesting feature of (10.16) is the insensitivity of $f(M)$ to γ for subsonic flow.

Figure 10.1: *Area-Mach number function.*

10.1.1 Mass conservation

The result (10.16) can also be derived simply by equating mass flows at any two points in the channel and using the mass flow relation.

$$\dot{m} = \rho U A \quad (10.17)$$

This can be expressed as

$$\dot{m} = \rho U A = \frac{P}{RT} (\gamma RT)^{1/2} M A. \quad (10.18)$$

Insert

$$\begin{aligned} \frac{T_t}{T} &= 1 + \frac{\gamma - 1}{2} M^2 \\ \frac{P_t}{P} &= \left(1 + \frac{\gamma - 1}{2} M^2 \right)^{\frac{\gamma}{\gamma-1}} \end{aligned} \quad (10.19)$$

into (10.18) to produce

$$\dot{m} = \rho U A = \frac{\gamma}{\left(\frac{\gamma+1}{2}\right)^{\frac{\gamma+1}{2(\gamma-1)}}} \left(\frac{P_t A}{\sqrt{\gamma R T_t}} \right) f(M). \quad (10.20)$$

If we equate the mass flows at any two points in a channel (10.20) gives

$$\begin{aligned} \dot{m}_1 &= \dot{m}_2 \\ \frac{P_{t1}A_1}{\sqrt{T_{t1}}} f(M_1) &= \frac{P_{t2}A_2}{\sqrt{T_{t2}}} f(M_2). \end{aligned} \quad (10.21)$$

In the case of an adiabatic ($T_t = \text{constant}$), isentropic ($P_t = \text{constant}$) flow in a channel (10.16) provides a direct relation between the local area and Mach number.

$$A_1 f(M_1) = A_2 f(M_2) \quad (10.22)$$

10.2 A simple convergent nozzle

Figure 10.2 shows a large adiabatic reservoir containing an ideal gas at pressure P_t . The gas exhausts through a simple convergent nozzle with throat area A_e to the ambient atmosphere at pressure P_{ambient} . Gas is continuously supplied to the reservoir so that the reservoir pressure is effectively constant. Assume the gas is calorically perfect, ($P = \rho RT$, C_p and C_v are constant) and assume that wall friction is negligible.

Let's make this last statement a little more precise. Note that we do not assume that the gas is inviscid since we want to accommodate the possibility of shock formation somewhere in the flow. Rather, we make use of the fact that, if the nozzle is large enough, the boundary layer thickness will be small compared to the diameter of the nozzle enabling most of the flow to be treated as irrotational and isentropic.

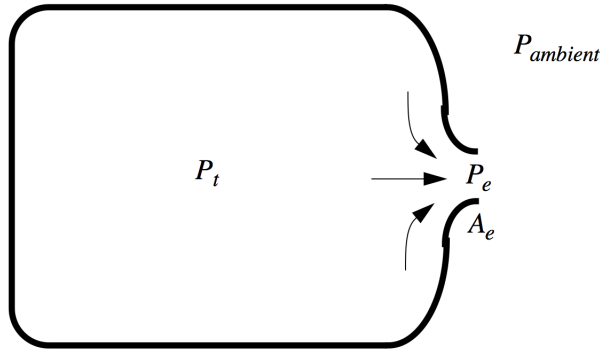


Figure 10.2: Reservoir with a convergent nozzle.

The isentropic assumption works quite well for nozzles that are encountered in most applications. But if the plenum falls below a few centimeters in size with a nozzle diameter less than a few millimeters then a fully viscous, non-isentropic treatment of the flow is required. Accurate nozzle design, regardless of size, virtually always requires that the boundary layer on the wall of the plenum and nozzle is taken into account.

If the ambient pressure equals the reservoir pressure there is, of course, no flow. If $P_{ambient}$ is slightly below P_t then there is a low-speed, subsonic, approximately isentropic flow from the plenum to the nozzle. If $P_t/P_{ambient}$ is less than a certain critical value then the condition that determines the speed of the flow at the exit is that the exit static pressure is very nearly equal to the ambient pressure.

$$P_e = P_{ambient} \quad (10.23)$$

The reason this condition applies is that large pressure differences cannot occur over small distances in a subsonic flow. Any such difference that might arise, say between the nozzle exit and a point slightly outside of and above the exit, will be immediately smoothed out by a readjustment of the whole flow. Some sort of shock or expansion is required to maintain a pressure discontinuity and this can only occur in supersonic flow. Slight differences in pressure are present due to the mixing zone that exists outside the nozzle but in subsonic flow these differences are very small compared to the ambient pressure. Since the flow up to the exit is approximately isentropic the stagnation pressure P_t is approximately constant from the reservoir to the nozzle exit and we can write

$$\frac{P_t}{P_e} = \left(1 + \left(\frac{\gamma - 1}{2} \right) M_e^2 \right)^{\frac{\gamma}{\gamma-1}}. \quad (10.24)$$

Using (10.23) and (10.24) we can solve for the Mach number at the nozzle exit in terms of the applied pressure ratio.

$$M_e = \left(\frac{2}{\gamma - 1} \right)^{1/2} \left(\left(\frac{P_t}{P_{ambient}} \right)^{\frac{\gamma-1}{\gamma}} - 1 \right)^{1/2} \quad (10.25)$$

Note that the nozzle area does not appear in this relationship.

10.2.1 The phenomenon of choking

The exit Mach number reaches one when

$$\frac{P_t}{P_{ambient}} = \left(\frac{\gamma + 1}{2} \right)^{\frac{\gamma}{\gamma - 1}}. \quad (10.26)$$

For Air with $\gamma = 1.4$ this critical pressure ratio is $P_t/P_{ambient} = 1.893$ and the condition (10.23) holds for $1 \leq P_t/P_{ambient} \leq 1.893$. At $P_t/P_{ambient} = 1.893$ the area-Mach number function $f(M)$ is at its maximum value of one. At this condition the mass flow through the nozzle is as large as it can be for the given reservoir stagnation pressure and temperature and the nozzle is said to be choked.

If $P_t/P_{ambient}$ is increased above the critical value the flow from the reservoir to the nozzle throat will be unaffected; the Mach number will remain $M_e = 1$ and $P_t/P_{ambient} = 1.893$. However condition (10.23) will no longer hold because now $P_e > P_{ambient}$. The flow exiting the nozzle will tend to expand supersonically eventually adjusting to the ambient pressure through a system of expansions and shocks.

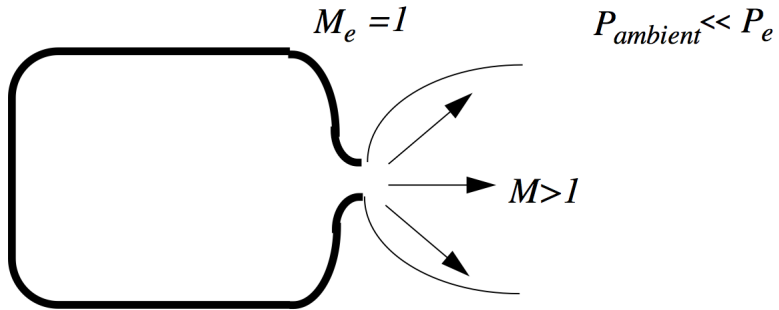
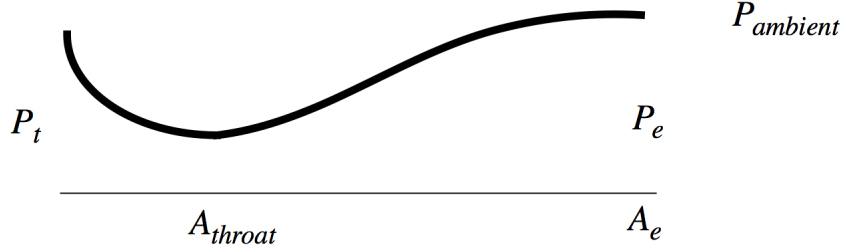


Figure 10.3: Plenum exhausting to very low pressure.

10.3 The converging-diverging nozzle

Now let's generalize these ideas to the situation where the nozzle consists of a converging section upstream of the throat and a diverging section downstream. Consider the nozzle geometry shown below.

The goal is to completely determine the flow in the nozzle given the pressure ratio $P_t/P_{ambient}$ and the area ratio A_e/A_{throat} . Before analyzing the flow we should first work out the critical

Figure 10.4: *Converging-diverging geometry*

exit Mach numbers and pressures for the selected area ratio. Solving

$$\frac{A_{throat}}{A_e} = \left(\frac{\gamma + 1}{2} \right)^{\frac{\gamma+1}{2(\gamma-1)}} \frac{M_e}{\left(1 + \left(\frac{\gamma-1}{2} \right) M_e^2 \right)^{\frac{\gamma+1}{2(\gamma-1)}}} \quad (10.27)$$

gives two critical Mach numbers $M_{ea} < 1$ and $M_{eb} > 1$ for isentropic flow in the nozzle with $M = 1$ at the throat. The corresponding critical exit pressures are determined from

$$\begin{aligned} \frac{P_t}{P_{ea}} &= \left(1 + \left(\frac{\gamma - 1}{2} \right) M_{ea}^2 \right)^{\frac{\gamma}{\gamma-1}} \\ \frac{P_t}{P_{eb}} &= \left(1 + \left(\frac{\gamma - 1}{2} \right) M_{eb}^2 \right)^{\frac{\gamma}{\gamma-1}}. \end{aligned} \quad (10.28)$$

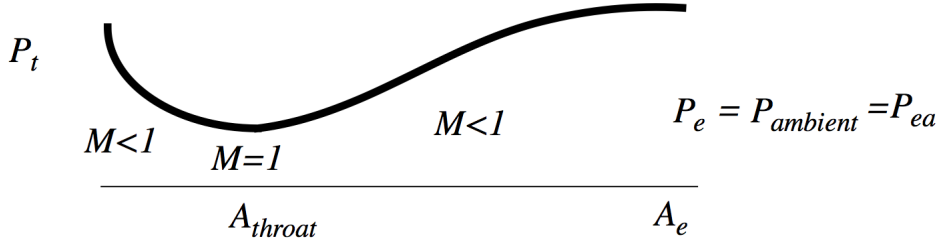
There are several possible cases to consider.

10.3.1 Case 1 - Isentropic subsonic flow in the nozzle

If $P_t/P_{ambient}$ is not too large then the flow throughout the nozzle will be sub- sonic and isentropic and the pressure at the exit will match the ambient pressure. In this instance the exit Mach number is determined using (10.25).

If $P_t/P_{ambient}$ is increased there is a critical value that leads to choking at the throat. This flow condition is sketched below.

The exit Mach number is M_{ea} and the pressure ratio is $P_t/P_{ambient} = P_t/P_{ea}$. Note that when a diverging section is present the pressure ratio that leads to choking is less than

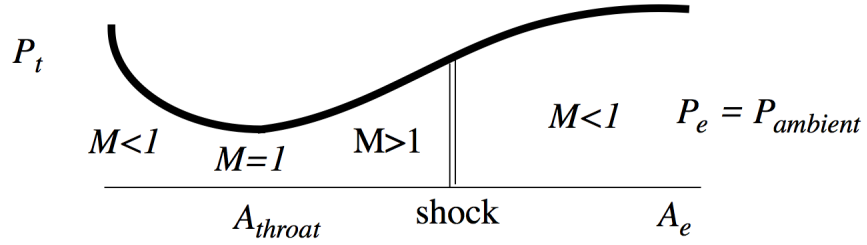
Figure 10.5: *Onset of choking.*

that given by (10.26). The flow in the nozzle is all subsonic when the pressure ratio is in the range

$$1 < \frac{P_t}{P_{ambient}} < \frac{P_t}{P_{ea}}. \quad (10.29)$$

10.3.2 Case 2 - Non-isentropic flow - shock in the nozzle

If the pressure ratio is increased above P_t/P_{ea} a normal shock will form downstream of the throat, the exit Mach number remains subsonic and the exit pressure will continue to match the ambient pressure. This flow condition is shown below.

Figure 10.6: *Shock in nozzle.*

The entropy is constant up to the shock wave, increases across the wave and remains constant to the exit. To work out the flow properties, first equate mass flows at the throat and nozzle exit

$$\dot{m}_{throat} = \dot{m}_{exit} \quad (10.30)$$

or

$$P_t A_{throat} = P_{te} A_e f(M_e). \quad (10.31)$$

The key piece of information that enables us to solve for the flow is that the exit pressure still matches the ambient pressure and so we can write

$$P_{te} = P_e \left(1 + \left(\frac{\gamma - 1}{2} \right) M_e^2 \right)^{\frac{\gamma}{\gamma-1}} = P_{ambient} \left(1 + \left(\frac{\gamma - 1}{2} \right) M_e^2 \right)^{\frac{\gamma}{\gamma-1}}. \quad (10.32)$$

When (10.32) is incorporated into (10.31) the result is

$$\left(\frac{P_t}{P_{ambient}} \right) \left(\frac{A_{throat}}{A_e} \right) = \left(\frac{\gamma + 1}{2} \right)^{\frac{\gamma+1}{2(\gamma-1)}} M_e \left(1 + \left(\frac{\gamma - 1}{2} \right) M_e^2 \right)^{\frac{1}{2}}. \quad (10.33)$$

The items on the left side of (10.33) are known quantities and so one solves (10.33) implicitly for $M_e < 1$. With the exit Mach number known, (10.31) is used to determine the stagnation pressure ratio across the nozzle.

$$\left(\frac{P_{te}}{P_t} \right) = \left(\frac{A_{throat}}{A_e} \right) \frac{1}{f(M_e)} < 1 \quad (10.34)$$

Since the only mechanism for stagnation pressure loss is the normal shock, the value of P_{te}/P_t determined from (10.34) can be used to infer the shock Mach number from

$$\left(\frac{P_{te}}{P_t} \right) = \left(\frac{\left(\frac{\gamma+1}{2} \right) M_{shock}^2}{1 + \left(\frac{\gamma-1}{2} \right) M_{shock}^2} \right)^{\frac{\gamma}{\gamma-1}} \left(\frac{\frac{\gamma+1}{2}}{\gamma M_{shock}^2 - \left(\frac{\gamma-1}{2} \right)} \right)^{\frac{1}{\gamma-1}}. \quad (10.35)$$

Thus all of the important properties of the flow in the nozzle are known given the plenum to ambient pressure ratio and the nozzle area ratio.

As the nozzle pressure ratio is increased, the shock moves more and more downstream until it is situated at the nozzle exit. This flow condition is shown below.

In this case the Mach number just ahead of the shock is the supersonic critical value M_{eb} and the Mach number just behind is the corresponding subsonic value derived from normal

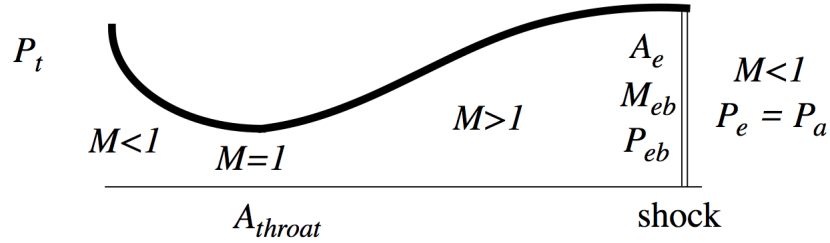


Figure 10.7: Normal shock at the nozzle exit.

shock relations.

$$M_{e(\text{behindshock})}^2 = \frac{1 + \left(\frac{\gamma-1}{2}\right) M_{eb}^2}{\gamma M_{eb}^2 - \left(\frac{\gamma-1}{2}\right)} \quad (10.36)$$

The value of $P_t/P_{ambient}$ that produces this flow is

$$\left. \frac{P_t}{P_{ambient}} \right|_{\text{exit} \perp \text{shock}} = \left(\frac{A_e}{A_{throat}} \right) \left(\frac{\gamma+1}{2} \right)^{\frac{\gamma+1}{2(\gamma-1)}} M_{e(\text{behindshock})} \left(1 + \left(\frac{\gamma-1}{2} \right) M_{e(\text{behindshock})}^2 \right)^{\frac{1}{2}}. \quad (10.37)$$

The shock-in-the-nozzle case occurs over the range

$$\frac{P_t}{P_{ea}} < \frac{P_t}{P_{ambient}} < \left. \frac{P_t}{P_{ambient}} \right|_{\text{exit} \perp \text{shock}}. \quad (10.38)$$

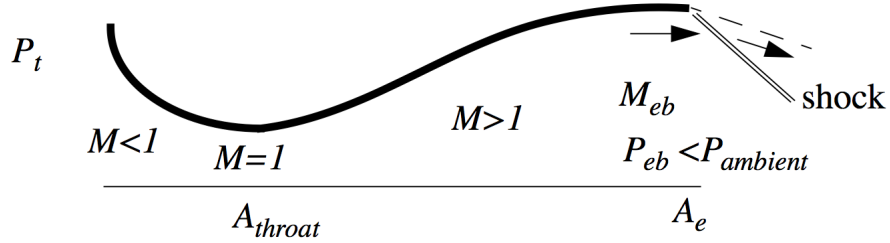
10.3.3 Case 3 - Isentropic supersonic flow in the nozzle

If the nozzle pressure ratio exceeds the value given in (10.37) then no further changes occur in the flow within the nozzle. Three different cases are distinguished.

i) Over expanded flow - This corresponds to the range

$$\left. \frac{P_t}{P_{ambient}} \right|_{\text{exit} \perp \text{shock}} < \frac{P_t}{P_{ambient}} < \frac{P_t}{P_{eb}}. \quad (10.39)$$

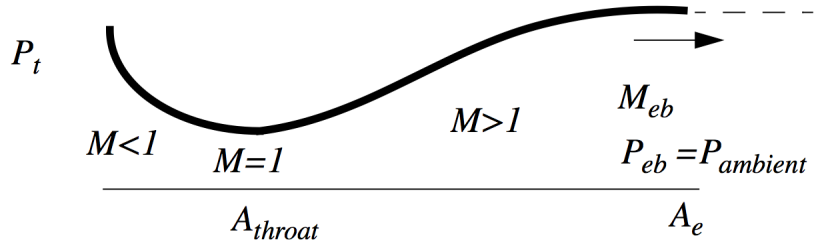
In this case the flow passes through an oblique shock as it exhausts.

Figure 10.8: *Oblique shock at the nozzle exit.*

ii) Fully expanded flow - This is the case where

$$\frac{P_t}{P_{ambient}} = \frac{P_t}{P_{eb}}. \quad (10.40)$$

The exit pressure now matches the ambient pressure and the flow exhausts smoothly.

Figure 10.9: *Fully expanded flow.*

iii) Under expanded flow - This corresponds to the range

$$\frac{P_t}{P_{ambient}} > \frac{P_t}{P_{eb}}. \quad (10.41)$$

In this case the exit pressure exceeds the ambient pressure and the flow expands outward as it leaves the nozzle.

A good example of the occurrence of all three conditions is the Space Shuttle Main Engine which leaves the pad in an over expanded state, becomes fully expanded at high altitude and then extremely under expanded as the Shuttle approaches the vacuum of space.

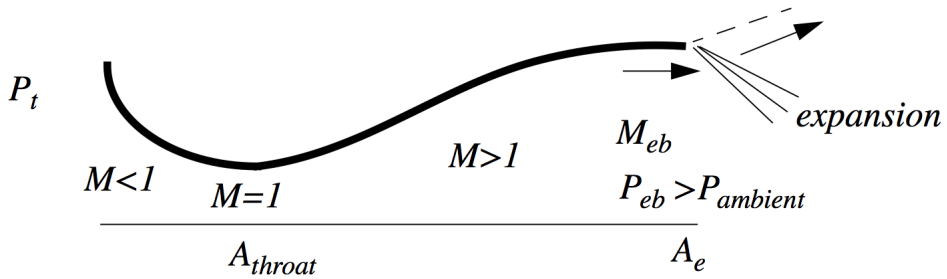


Figure 10.10: Expansion fan at the nozzle exit.

10.4 Examples

10.4.1 Shock in a nozzle

A normal shock is stabilized in the diverging section of a nozzle. The area ratios are, $A_s/A_{throat} = 2$, $A_e/A_{throat} = 4$ and $A_1 = A_e$.

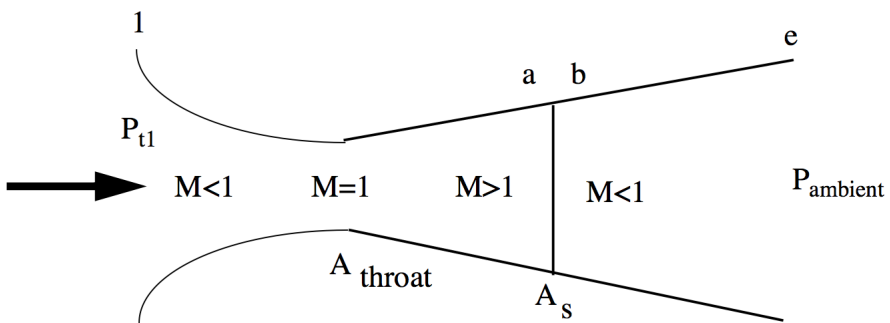


Figure 10.11: Converging-diverging nozzle with shock.

- Determine M_1 , M_e , the Mach number just ahead of the shock M_a , and the Mach number just behind the shock, M_b . Assume the gas is Air with $\gamma = 1.4$.

Solution

The area ratio from the throat to the shock is 2. One needs to solve

$$f(M_a) = 1/2 \quad (10.42)$$

for the supersonic root. The solution from tables or a calculator is $M_a = 2.197$. The

normal shock relation for the downstream Mach number is

$$M_b^2 = \frac{1 + \left(\frac{\gamma-1}{2}\right) M_a^2}{\gamma M_a^2 - \left(\frac{\gamma-1}{2}\right)} \quad (10.43)$$

which gives $M_b = 0.547$. At station 1 the area ratio to the throat is 4 and the Mach number is subsonic. Solve for the subsonic root of

$$f(M_1) = 1/4. \quad (10.44)$$

The solution is $M_1 = 0.147$. The area ratio from behind the shock to station e is two. If we equate mass flows at both points and assume isentropic flow from station b to e we can write

$$A_b f(M_b) = A_e f(M_e). \quad (10.45)$$

Solve (10.45) for $f(M_e)$.

$$f(M_e) = \frac{A_b}{A_e} f(M_b) = (1/2)(0.794) = 0.397 \quad (10.46)$$

The exit Mach number is $M_e = 0.238$. So far the structure of the flow is as shown below.

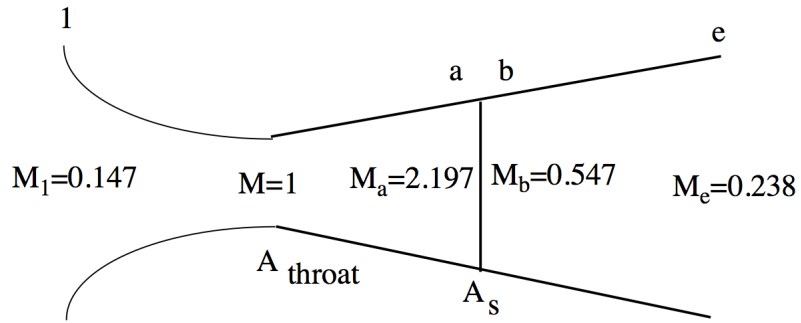


Figure 10.12: *Converging-diverging nozzle with Mach numbers labeled.*

- 2) Determine the pressure ratio across the nozzle, P_e/P_{t1} .

Solution

Since the exit flow is subsonic the exit pressure matches the ambient pressure. Use (10.33).

$$\begin{aligned}\frac{P_e}{P_{t1}} &= \frac{(A_{throat}/A_e)}{\left(\frac{\gamma+1}{2}\right)^{\frac{\gamma+1}{2(\gamma-1)}} M_e \left(1 + \left(\frac{\gamma-1}{2}\right) M_e^2\right)^{1/2}} \\ &= \frac{(1/4)}{\left(\frac{1}{2}\right)^3 (0.238) \left(1 + (1/5)(0.238)^2\right)^{1/2}} = 0.604\end{aligned}\quad (10.47)$$

3) What pressure ratio would be required to position the shock at station *e*?

Solution

The structure of the flow in this case would be as shown in 10.13. To determine the pressure ratio that produces this flow use (10.37).

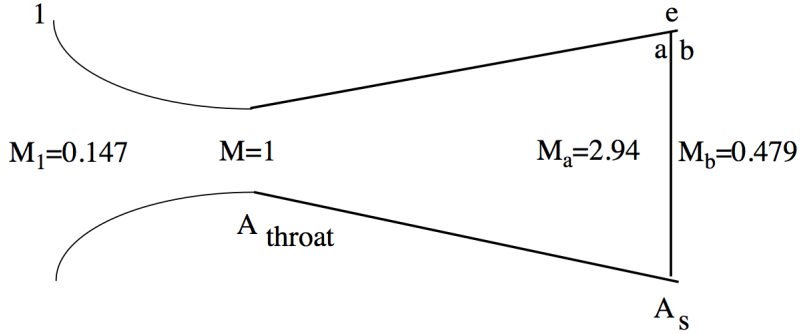


Figure 10.13: *Converging-diverging nozzle with shock at the exit.*

$$\begin{aligned}\frac{P_t}{P_{ambient}} \Big|_{exit \perp shock} &= \frac{P_{t1}}{P_e} \Big|_{exit \perp shock} = \\ \left(\frac{A_e}{A_{throat}}\right) \left(\frac{\gamma+1}{2}\right)^{\frac{\gamma+1}{2(\gamma-1)}} M_e &\left(1 + \left(\frac{\gamma-1}{2}\right) M_e^2\right)^{\frac{1}{2}} = \\ \frac{P_e}{P_{t1}} \Big|_{exit \perp shock} &= \frac{1}{4(1.2)^3 (0.479) \left(1 + (1/5)(0.479)^2\right)^{\frac{1}{2}}} = 0.295\end{aligned}\quad (10.48)$$

This is considerably lower than the pressure ratio determined in part 2.

10.4.2 Cold gas thruster

A cold gas thruster on a spacecraft uses Helium (atomic weight 4) as the working gas. The gas exhausts through a large area ratio nozzle to the vacuum of space. Compare the energy of a parcel of gas in the fully-expanded exhaust to the energy it had when it was in the chamber.

Answer

In the chamber the energy per unit mass, neglecting kinetic energy is

$$E_{chamber} = C_v T_{chamber}. \quad (10.49)$$

Assume the expansion takes place adiabatically. Under that assumption, the stagnation enthalpy is conserved.

$$C_p T_{chamber} = C_p T + \frac{1}{2} U^2 = \text{constant} \quad (10.50)$$

Since the area ratio is large the thermal energy of the exhaust gas is small compared to the kinetic energy.

$$E_{exhaust} = C_v T_{exhaust} + \frac{1}{2} U_{exhaust}^2 \cong \frac{1}{2} U_{exhaust}^2 \cong C_p T_{chamber} \quad (10.51)$$

Divide (10.51) by U_1^2 . The result is

$$\frac{E_{exhaust}}{E_{chamber}} = \frac{C_p T_{chamber}}{C_v T_{exhaust}} = \gamma = \frac{5}{3}. \quad (10.52)$$

The energy gained by the fluid element during the expansion process is due to the pressure forces that accelerate the element. In fact what is recovered is exactly the work required to create the original pressurized state.

10.4.3 Gasdynamics of a double throat, starting and unstarting supersonic flow

One of the most important applications of the gas-dynamic tools we have been developing is to a channel with multiple throats. Virtually all air-breathing propulsion systems utilize at least two throats; one to decelerate the incoming flow and a second to accelerate the exit flow. When a compressor and turbine are present several more throats may be involved.

The simplest application of two throats is to the design of a supersonic wind tunnel. Shown below is a supersonic wind tunnel that uses air as the working gas.

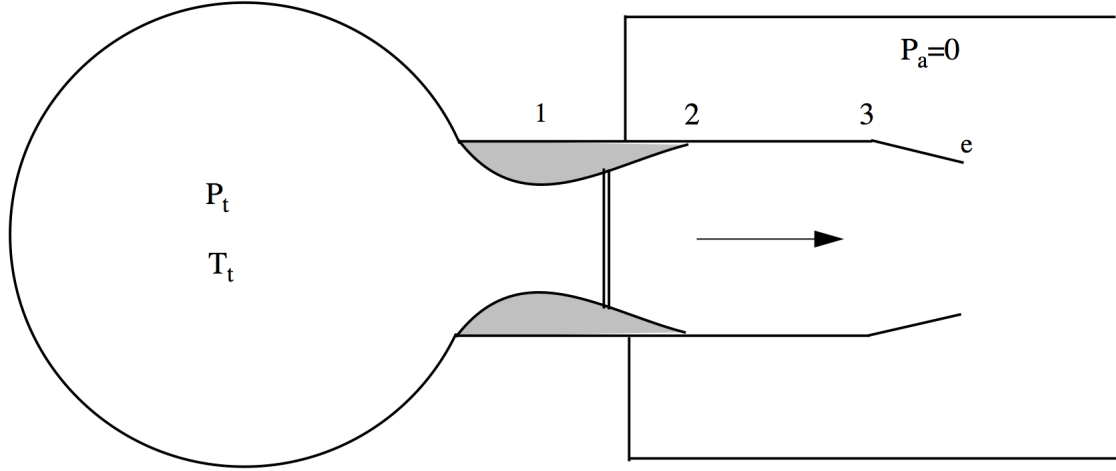


Figure 10.14: Supersonic wind tunnel with two throats.

A very large plenum contains the gas at constant stagnation pressure and temperature, P_t , T_t . The flow exhausts to a large tank that is maintained at vacuum $P_a = 0$. The upstream nozzle area ratio is $A_2/A_1 = 6$ and the ratio of exit area to throat area is $A_e/A_1 = 2$. The test section has a constant area $A_3 = A_2$. A shock wave is stabilized in the diverging portion of the nozzle. The wall friction coefficient is very small.

- 1) Determine P_{te}/P_e .

Solution

The mass balance between stations 1 and e is

$$\dot{m}_1 = \dot{m}_e$$

$$\frac{P_{t1}A_1}{\sqrt{\gamma RT_{t1}}} f(M_1) = \frac{P_{te}A_e}{\sqrt{\gamma RT_{te}}} f(M_e). \quad (10.53)$$

The flow exits to vacuum and so the large pressure ratio across the system essentially guarantees that both throats must be choked, $M_1 = 1$ and $M_e = 1$. Assume the flow is adiabatic and neglect wall friction. With these assumptions the mass balance (10.53).

reduces to

$$\frac{P_{te}}{P_t} = \frac{A_1}{A_e} = 0.5. \quad (10.54)$$

- 2) Determine the shock Mach number

Solution

From the relations for shock wave flow, the shock Mach number that reduces the stagnation pressure by half for a gas with $\gamma = 1.4$ is $M_s = 2.5$.

- 3) Determine the Mach numbers at stations 2 and 3.

Solution

The Mach number at station 3 is determined by the area ratio from 3 to e and the fact that the exit is choked.

$$\frac{A_e}{A_3} = \frac{1}{3} \Rightarrow M_3 = 0.195 \quad (10.55)$$

Since the area of the test section is constant and friction is neglected the Mach number at station 2 is the same $M_2 = 0.195$.

- 4) Suppose A_e is reduced to the point where $A_e = A_1$. What happens to the shock?

Solution

Again use the mass flow equation (10.20) and equate mass flows at the two throats. In this case (10.53) is

$$\frac{P_{te}}{P_t} = \frac{A_1}{A_e} = 1.0. \quad (10.56)$$

There is no shock and therefore there is no stagnation pressure loss between the two throats. As A_e is reduced the shock moves upstream to lower Mach numbers till a point is reached when the two areas are equal. At that point the shock has essentially weakened to the point of disappearing altogether.

- 5) Suppose A_e is made smaller than A_1 , what happens?

Solution

Since both the stagnation pressure and temperature are now constant along the channel and the exit throat is choked the mass balance (10.53) becomes

$$f(M_1) = \frac{A_e}{A_1}. \quad (10.57)$$

The Mach number at the upstream throat becomes subsonic and satisfies (10.57) as the area is further reduced.

- 6) Suppose A_e is increased above $A_e/A_1 = 2$. What happens to the shock?

Solution

In this case the shock moves downstream to higher Mach numbers. The highest Mach number that the shock can reach is at the end of the expansion section of the upstream nozzle where the area ratio is $A_2/A_1 = 6$. Equation (10.16) gives the Mach number of the shock at that point as $M_2 = 3.368$. The corresponding stagnation pressure ratio across the shock is $P_{te}/P_t = 0.2388$. Using the mass balance again, the throat area ratio that produces this condition is

$$\frac{A_e}{A_1} = \frac{P_t}{P_{te}} = 4.188. \quad (10.58)$$

Throughout this process the exit is at $M_e = 1$ and the flow in the test section is subsonic due to the presence of the shock. In fact the Mach number in the test section from station 2 to 3 would be the Mach number behind a Mach 3.368 shock which is 0.4566. Note that this is consistent with the area ratio $A_3/A_e = 6/4.188 = 1.433$ for which the subsonic solution of (10.16) is 0.4566.

- 7) Now suppose A_e/A_1 is increased just slightly above 4.188, what happens?

Solution

Again go back to the mass flow relation (10.53). Write (10.53) as

$$P_{t1}A_1 = P_{te}A_e f(M_e). \quad (10.59)$$

The upstream throat is choked and so the mass flow is fixed and the left-hand-side of (10.59) is fixed. The shock is at the highest Mach number it can reach given the area ratio of the upstream nozzle. So as A_e/A_1 is increased above 4.188 there is no way for P_{te}/P_t to decrease so as to maintain the equality (10.59) enforced by mass conservation. Instead an event occurs and that event is that the shock is swallowed by the downstream throat and supersonic flow is established in the test section. The supersonic wind tunnel is said to be

started. Since there is no shock present the flow throughout the system is isentropic and the mass balance (10.59) becomes

$$f(M_e) = \frac{A_1}{A_e} = \frac{1}{4.188}. \quad (10.60)$$

The Mach number at the exit throat is now the supersonic root of (10.60), $M_e = 2.99$. If A_e/A_1 is increased further the exit Mach number increases according to Equation (10.60). If A_e/A_1 is reduced below 4.188 the exit Mach number reduces below 2.99 until it approaches one from above as $A_e/A_1 \rightarrow 1 + \varepsilon$. If A_e/A_1 is reduced below one the wind tunnel unstarts and the flow between 1 and the exit is all subsonic (no shock) with $M_1 = M_e = 1$.

10.5 Problems

Problem 1 - Consider the expression ρU^n . The value $n = 1$ corresponds to the mass flux, $n = 2$ corresponds to the momentum flux and $n = 3$ corresponds to the energy flux of a compressible gas. Use the momentum equation

$$dP + \rho U dU = 0 \quad (10.61)$$

to determine the Mach number (as a function of n) at which ρU^n ; $n = 1$ is a maximum in steady flow.

Problem 2 - In the double-throat example above the flow exhausts into a vacuum chamber. Suppose the pressure P_a is not zero. What is the maximum pressure ratio P_a/P_t that would be required for the supersonic tunnel to start as described in the example? The exit area can be varied as required.

Problem 3 - In the double-throat example above suppose the effect of wall friction is included. How would the answers to the problem change? Would the various values calculated in the problem increase, decrease or remain the same and why?

Problem 4 - Figure 10.15 shows a supersonic wind tunnel which uses helium as a working gas. A very large plenum contains the gas at constant stagnation pressure and temperature P_t , T_t . Supersonic flow is established in the test section and the flow exhausts to a large tank at pressure P_a .

The exit area A_e can be varied in order to change the flow conditions in the tunnel. Initially $A_2/A_e = 4$, and $A_2/A_1 = 8$. The gas temperature in the plenum is $T_t = 300\text{K}$. Neglect wall friction. Let $P_t/P_a = 40$.

- 1) Determine the Mach numbers at A_e , A_1 and A_2 .

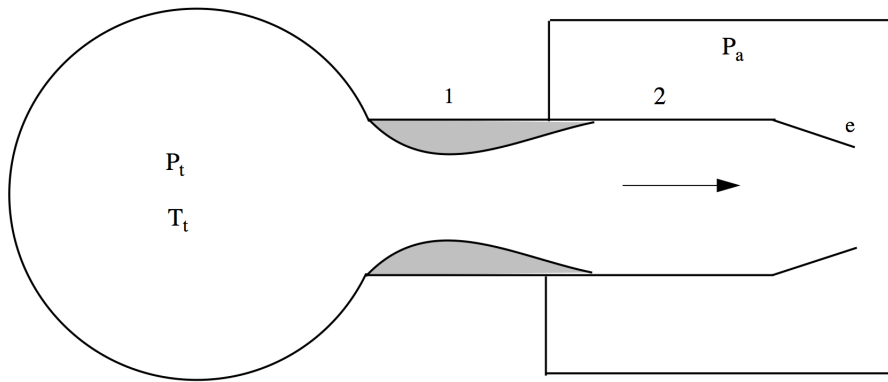


Figure 10.15: Supersonic wind tunnel with variable area exit.

- 2) Determine the velocity U_e and pressure ratio P_e/P_a .
- 3) Suppose A_e is reduced. Determine the value of A_e/A_2 which would cause the Mach number at A_e to approach one (from above). Suppose A_e is reduced slightly below this value - what happens to the supersonic flow in the tunnel? Determine P_{te}/P_t and the Mach numbers at A_1 , A_2 and A_e for this case.

Problem 5 - Figure 10.16 shows a supersonic wind tunnel which uses air as the working gas. A very large plenum contains the gas at constant stagnation pressure and temperature, P_t , T_t . The flow exhausts to a large tank that is maintained at vacuum $P_a = 0$. The upstream nozzle area ratio is $A_2/A_1 = 3$. The downstream throat area A_e can be varied in order to change the flow conditions in the tunnel. Initially, $A_e = 0$. Neglect wall friction. Assign numerical values where appropriate.

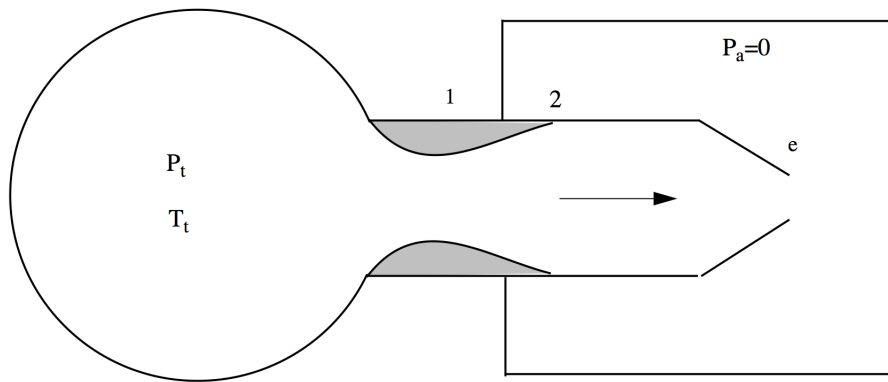


Figure 10.16: Supersonic wind tunnel exiting to vacuum.

1) Suppose A_e/A_1 is slowly increased from zero. Plot P_{te}/P_t as a function of A_e/A_1 for the range $0 \leq A_e/A_1 \leq 3$.

2) Now with $A_e/A_1 = 3$ initially, let A_e be decreased back to zero. Plot P_{te}/P_t as a function of A_e/A_1 for this process.

Problem 6 - In Chapter 2 we looked at the blowdown through a small nozzle of a calorically perfect gas from a large adiabatic pressure vessel at initial pressure P_i and temperature T_i to the surroundings at pressure P_a and temperature T_a . I would like you to reconsider that problem from the point of view of the conservation equations for mass and energy. Use a control volume analysis to determine the relationship between the pressure, density and temperature in the vessel as the mass is expelled. Show that the final temperature derived from a control volume analysis is the same as that predicted by integrating the Gibbs equation.

Problem 7 - Consider the inverse of Problem 6. A highly evacuated, thermally insulated flask is placed in a room with air temperature T_a . The air is allowed to enter the flask through a slightly opened stopcock until the pressure inside equals the pressure in the room. Assume the air to be calorically perfect. State any other assumptions needed to solve the problem.

(i) Use a control volume analysis to determine the relationship between the pressure, density and temperature in the vessel as mass enters the vessel.

(ii) Determine the entropy change per unit mass during the process for the gas that enters the vessel.

(iii) Determine the final temperature of the gas in the vessel.

May I suggest that you break the process into two parts. When the stopcock is first opened, the opening is choked and the flow outside the flask is steady. But after a while the opening un-choke and the pressure at the opening increases with time. In the latter case the flow outside the flask is unsteady and one needs to think of a reasonable model of the flow in order to solve the problem.

Chapter 11

Area change, wall friction and heat transfer

11.1 Control volume

Assume a calorically perfect gas, ($P = \rho RT$, C_p and C_v constant) is flowing in a channel in the absence of body forces. Viscous friction acts along the wall and there may be heat conduction through the wall but there is no mass addition. Consider a differential length of the channel.

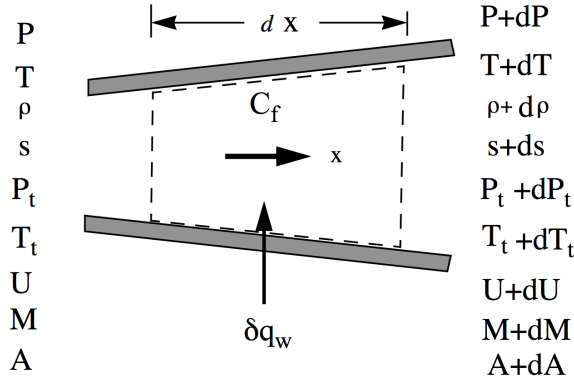


Figure 11.1: Differential changes along a channel.

The area-averaged equations of motion are

$$\begin{aligned} d(\rho U A) &= 0 \\ dP + \rho U dU &= -\frac{1}{2} \rho U^2 \left(\frac{4C_f dx}{D} \right) \\ C_p dT + U dU &= \delta q_w = C_p dT_t. \end{aligned} \quad (11.1)$$

For convenience let's put these equations into fractional differential form.

$$\begin{aligned} \frac{d\rho}{\rho} + \frac{1}{2} \frac{dU^2}{U^2} &= -A \frac{dA}{U^2} \\ \frac{dP}{P} + \frac{\gamma M^2}{2} \frac{dU^2}{U^2} &= -\frac{\gamma M^2}{2} \left(\frac{4C_f dx}{D} \right) \\ \frac{dT}{T} + \frac{(\gamma - 1) M^2}{2} \frac{dU^2}{U^2} &= \frac{dT_t}{T} \\ \frac{dP}{P} - \frac{d\rho}{\rho} - \frac{dT}{T} &= 0 \end{aligned} \quad (11.2)$$

As noted when we developed the quasi-one-dimensional equations, the spirit of this analysis is that $A(x)$, $C_f(x)$ and $T_t(x)$ are specified input functions along the channel. The problem is to use the equations of motion to determine how the various (output) properties of the flow change along the channel particularly the Mach number.

11.2 Entropy and stagnation pressure

At any point in the flow the static and stagnation states of the gas are related by

$$\frac{P_t}{P} = \left(\frac{T_t}{T} \right)^{\frac{\gamma}{\gamma-1}}. \quad (11.3)$$

This relationship essentially defines P_t . If we take the log of this equation and differentiate, the result is Gibbs equation in terms of stagnation quantities.

$$\left(\frac{\gamma}{\gamma-1} \right) \frac{dT_t}{T_t} - \frac{dP_t}{P_t} = \left(\frac{\gamma}{\gamma-1} \right) \frac{dT}{T} - \frac{dP}{P} = \frac{ds}{R} \quad (11.4)$$

Now use the fractional differential form of the area averaged equations to replace dT/T and dP/P in Gibbs equation. The result is a differential form describing the effect of heat transfer and friction on the stagnation pressure.

$$\frac{dP_t}{P_t} = -\frac{\gamma M^2}{2} \left(\frac{dT_t}{T_t} \right) - \frac{\gamma M^2}{2} \left(\frac{4C_f dx}{D} \right) \quad (11.5)$$

Stagnation pressure losses are proportional to M^2 indicating that the losses due to both heat transfer and friction are very small in a low Mach number flow and, conversely, very large in a high Mach number flow.

The entropy relation is

$$\frac{ds}{R} = \left(\frac{\gamma}{\gamma - 1} \right) \left(1 + \left(\frac{\gamma - 1}{2} \right) M^2 \right) \left(\frac{dT_t}{T_t} \right) + \frac{\gamma M^2}{2} \left(\frac{4C_f dx}{D} \right) \quad (11.6)$$

which describes the 1-D variation of entropy due to viscous friction and heat conduction effects.

It would appear from this result that one can increase the stagnation pressure of a flow by cooling through the wall. Lets investigate this possibility. Consider the combined effects of friction and heat transfer through the wall on the stagnation pressure. The heat transfer process is characterized by the Stanton number defined as

$$S_t = \frac{Q_w}{\rho U C_p (T_{wall} - T_t)}. \quad (11.7)$$

In (11.7)

T_t = the adiabatic wall recovery temperature, equal to the stagnation temperature of the free stream for a recovery factor of one ($P_r = 1$),

T_{wall} = the actual wall temperature,

Q_w = the heat transfer rate to the fluid (energy/area-sec).

The total heat per unit mass transferred to the fluid is

$$dh_t = \frac{Q_w \pi D dx}{\rho U A} = S_t C_p (T_{wall} - T_t) \left(\frac{\pi D dx}{\frac{\pi D^2}{4}} \right) = C_p (T_{wall} - T_t) \left(\frac{4S_t dx}{D} \right). \quad (11.8)$$

Now the stagnation pressure change is

$$\frac{dP_t}{P_t} = -\frac{\gamma M^2}{2} \left(\frac{4C_f dx}{D} + \left(\frac{T_{wall} - T_t}{T_t} \right) \frac{4S_t dx}{D} \right). \quad (11.9)$$

A careful study of boundary layer flows with heat transfer leads to the recognition that heat transfer and viscous friction are coupled. This is expressed in terms of the well known Reynolds analogy discussed in Chapter 5 which states that

$$2S_t = C_f. \quad (11.10)$$

Using (11.10), the fractional differential equation for the stagnation pressure becomes

$$\frac{dP_t}{P_t} = -\frac{\gamma M^2}{2} \left(\frac{T_{wall} + T_t}{2T_t} \right) \frac{4C_f dx}{D} \quad (11.11)$$

which is always positive, implying a loss of stagnation pressure regardless of whether Q_w is positive or negative. Cooling the wall does decrease the rate at which the stagnation pressure drops in the direction of the flow.

11.3 Velocity, density, temperature and pressure

Now let's examine the effects of dA , $C_f dx$ and dT_t on the other properties of the gas. In equation (11.2) replace each term in the ideal gas law using the mass, momentum and energy equations. The result is an equation for the differential change in velocity.

$$\left(\frac{1 - M^2}{2} \right) \frac{dU^2}{U^2} = -\frac{dA}{A} + \frac{\gamma M^2}{2} \left(\frac{4C_f dx}{D} \right) + \frac{dT_t}{T} \quad (11.12)$$

Now the velocity equation is used in each of the mass, momentum and energy equations in turn to generate equations for the differential changes in density, temperature and pressure.

$$\left(\frac{1 - M^2}{2} \right) \frac{d\rho}{\rho} = \left(\frac{M^2}{2} \right) \frac{dA}{A} - \frac{\gamma M^2}{4} \left(\frac{4C_f dx}{D} \right) - \frac{1}{2} \frac{dT_t}{T} \quad (11.13)$$

$$\left(\frac{1 - M^2}{2} \right) \frac{dT}{T} = \left(\frac{\gamma - 1}{2} \right) M^2 \frac{dA}{A} - \frac{\gamma}{2} \left(\frac{\gamma - 1}{2} \right) M^4 \left(\frac{4C_f dx}{D} \right) + \left(\frac{1 - \gamma M^2}{2} \right) \frac{dT_t}{T} \quad (11.14)$$

$$\left(\frac{1-M^2}{2}\right)\frac{dP}{P} = \frac{\gamma M^2}{2}\frac{dA}{A} - \frac{\gamma M^2}{4}(1+(\gamma-1)M^2)\left(\frac{4C_f dx}{D}\right) - \frac{\gamma M^2}{2}\frac{dT_t}{T} \quad (11.15)$$

These equations provide some insight into how various inputs affect the flow but they are not particularly useful for solving problems because, as they stand they cannot be integrated.

11.4 The Mach number

Lets determine the differential equation for the Mach number. Recall

$$U^2 = M^2\gamma RT. \quad (11.16)$$

Take the derivative of (11.16).

$$\frac{dM^2}{M^2} = \frac{dU^2}{U^2} - \frac{dT}{T} \quad (11.17)$$

Replace the differentials on the right-hand-side of (11.17) using (11.12) and (11.14).

$$\left(\frac{1-M^2}{1+\left(\frac{\gamma-1}{2}\right)M^2}\right)\frac{dM^2}{2M^2} = -\frac{dA}{A} + \frac{\gamma M^2}{2}\left(\frac{4C_f dx}{D}\right) + \left(\frac{1+\gamma M^2}{2}\right)\frac{dT_t}{T_t} \quad (11.18)$$

When only one effect occurs at a time, the above equation can be integrated exactly and this is the basis for the gas tables relating Mach number to friction (Fanno line - C_f assumed constant), heat addition (Rayleigh line) and area change. When two or more effects are present, it is generally necessary to specify $A(x)$, $T_t(x)$ and $C_f(x)$ in detail and to integrate the equations numerically. Notice that when heat transfer and or friction are present the sonic point does not have to occur at the minimum area point. In (11.18) let $M = 1$. The relation becomes

$$\frac{dA}{A} = \frac{\gamma}{2}\left(\frac{4C_f dx}{D}\right) + \left(\frac{1+\gamma}{2}\right)\frac{dT_t}{T_t}. \quad (11.19)$$

If we introduce the Stanton number

$$\frac{dA}{A} = \frac{\gamma}{2} \left(\frac{4C_f dx}{D} \right) + \left(\frac{1+\gamma}{2} \right) \left(\frac{T_{wall} - T_t}{T_t} \right) \left(\frac{4S_t dx}{D} \right) \quad (11.20)$$

and the Reynolds analogy $2S_t = C_f$, then the sonic point occurs where

$$\frac{dA}{A} = \left(\frac{(\gamma - 1) T_t + (\gamma + 1) T_{wall}}{4T_t} \right) \left(\frac{4C_f dx}{D} \right). \quad (11.21)$$

According to (11.21) in a real flow, the sonic point will always occur slightly downstream of the throat in the diverging part of the nozzle where dA is slightly positive.

11.5 Mass flow, area-Mach-number function

Note that the heat addition and friction terms on the right hand side of (11.18) can be rearranged with the use of (11.5) to yield

$$\left(\frac{1 - M^2}{1 + \left(\frac{\gamma-1}{2} \right) M^2} \right) \frac{dM^2}{2M^2} = -\frac{dA}{A} - \frac{dP_t}{P_t} + \frac{1}{2} \frac{dT_t}{T_t}. \quad (11.22)$$

Equation (11.22) can be integrated to

$$\frac{P_{t2} A_2}{P_{t1} A_1} \sqrt{\frac{T_{t1}}{T_{t2}}} = \frac{f(M_1)}{f(M_2)}. \quad (11.23)$$

where

$$f(M) = \frac{A^*}{A} = \left(\frac{\gamma + 1}{2} \right)^{\frac{\gamma+1}{2(\gamma-1)}} \frac{M}{\left(1 + \frac{\gamma-1}{2} M^2 \right)^{\frac{\gamma+1}{2(\gamma-1)}}} \quad (11.24)$$

is the area-Mach number function introduced in Chapter 9 and A^* is a reference area where $M = 1$. Between any two points in a channel in the presence of friction and heat transfer,

we can equate mass flows.

$$\dot{m}_1 = \dot{m}_2$$

$$\frac{P_{t1}A_1}{\sqrt{T_{t1}}} f(M_1) = \frac{P_{t2}A_2}{\sqrt{T_{t2}}} f(M_2) \quad (11.25)$$

This simple equality, used so heavily in Chapter 9 to analyze a channel with two throats, is one of the most important in all of gas dynamics. It is amazingly useful in solving seemingly very complex problems as we shall see in several examples.

11.6 Integrated relations

11.6.1 1-D, adiabatic, constant area flow with friction (Fanno line flow)

The relationship between Mach number and friction from (11.18) is

$$\frac{4C_f dx}{D} = \left(\frac{1 - M^2}{1 + \frac{\gamma-1}{2}M^2} \right) \frac{dM^2}{\gamma M^4}. \quad (11.26)$$

Assume the friction coefficient is constant (or equal to some mean value averaged over the length of the duct in question). Let the final state correspond to the reference value $M = 1$.

$$\int_0^{L_{\max}} \left(\frac{4C_f dx}{D} \right) = \int_{M^2}^1 \left(\frac{1 - M^2}{1 + \frac{\gamma-1}{2}M^2} \right) \frac{dM^2}{\gamma M^4} \quad (11.27)$$

Carry out the integration.

$$\frac{4C_f L_{\max}}{D} = \frac{1 - M^2}{\gamma M^2} + \left(\frac{\gamma + 1}{2\gamma} \right) \ln \left(\frac{(\gamma + 1) M^2}{2 \left(1 + \frac{\gamma-1}{2} M^2 \right)} \right) \quad (11.28)$$

The length of duct L required for the flow to pass from a given initial Mach number M_1 to a final Mach number M_2 is found from

$$\frac{4C_f L}{D} = \left(\frac{4C_f L_{\max}}{D} \right)_{M_1} - \left(\frac{4C_f L_{\max}}{D} \right)_{M_2}. \quad (11.29)$$

In each of the following

$$\begin{aligned}
 \left(\frac{1-M^2}{2}\right) \frac{dU^2}{U^2} &= \frac{\gamma M^2}{2} \left(\frac{4C_f dx}{D}\right) \\
 \left(\frac{1-M^2}{2}\right) \frac{d\rho}{\rho} &= -\frac{\gamma M^2}{4} \left(\frac{4C_f dx}{D}\right) \\
 \left(\frac{1-M^2}{2}\right) \frac{dT}{T} &= -\frac{\gamma}{2} \left(\frac{\gamma-1}{2}\right) M^4 \left(\frac{4C_f dx}{D}\right) \\
 \left(\frac{1-M^2}{2}\right) \frac{dP}{P} &= -\frac{\gamma M^2}{2} (1 + (\gamma-1) M^2) \left(\frac{4C_f dx}{D}\right)
 \end{aligned} \tag{11.30}$$

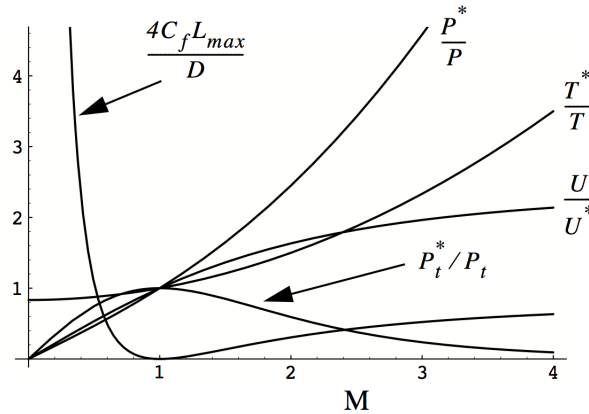
replace $4C_f dx/D$ with $((1-M^2)/(1+((\gamma-1)/2)M^2)) dM^2 / (\gamma M^4)$ and carry out the integration. The result is the set of Fanno line relations.

$$\begin{aligned}
 \frac{U}{U^*} &= \left(\frac{\frac{\gamma+1}{2}M^2}{1+\frac{\gamma-1}{2}M^2}\right)^{1/2} = \frac{\rho^*}{\rho} \\
 \frac{T^*}{T} &= \left(\frac{1+\frac{\gamma-1}{2}M^2}{\frac{\gamma+1}{2}}\right) \\
 \frac{P^*}{P} &= M \left(\frac{1+\frac{\gamma-1}{2}M^2}{\frac{\gamma+1}{2}}\right)^{1/2} \\
 \frac{P_t^*}{P_t} &= \left(\frac{\gamma+1}{2}\right)^{\frac{\gamma+1}{2(\gamma-1)}} \frac{M}{\left(1+\frac{\gamma-1}{2}M^2\right)^{\frac{\gamma+1}{2(\gamma-1)}}
 \end{aligned} \tag{11.31}$$

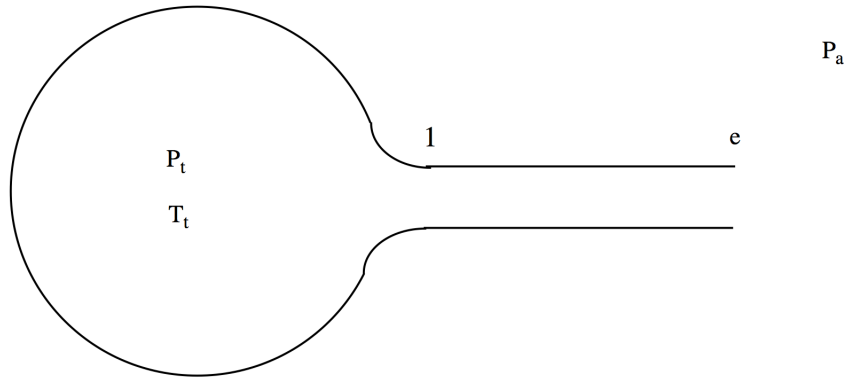
Recall that friction exerted by a no-slip wall at rest does not affect the stagnation enthalpy. The various Fanno line relations (11.28) and (11.31) are plotted in Figure 11.2 for $\gamma = 1.4$.

11.6.2 Example - frictional flow in a long pipe

Figure 11.3 shows air at constant stagnation pressure and temperature, P_t , T_t exhausting from a very large plenum to the surrounding atmosphere through a long straight pipe. The

Figure 11.2: *Fanno line relations.*

gas temperature in the plenum is $T_t = 300\text{K}$ and $P_t/P_a = 10$.

Figure 11.3: *Frictional flow in a long constant-area pipe.*

The friction coefficient in the pipe is $C_f = 0.01$ and the pipe is 10 diameters long.

- 1) Determine the Mach number at the entrance to the pipe M_1 .

Solution

Begin with the assumption that the flow is choked at the exit. Solve for M_1 using (11.28). The result is

$$\frac{4C_f L_{\max}}{D} = 0.4 \Rightarrow M_1 = 0.625. \quad (11.32)$$

2) Determine P_{te}/P_t and P_e/P_a .

Solution

The Fanno line relations (11.31) give the stagnation pressure drop along the pipe.

$$\frac{P_{te}}{P_t} = 0.862 \quad (11.33)$$

Alternatively, we could get the same result using (11.25) evaluated at the entrance and exit of the pipe where the Mach numbers are known. Thus at the pipe exit

$$\frac{P_{te}}{P_a} = 10 \times 0.862 = 8.62. \quad (11.34)$$

Since the exit Mach number is one

$$\frac{P_{te}}{P_e} = \left(\frac{\gamma + 1}{2} \right)^{\frac{\gamma}{\gamma - 1}} = 1.2^{3.5} = 1.893 \quad (11.35)$$

and the static pressure ratio at the exit is

$$\frac{P_e}{P_a} = \frac{8.62}{1.893} = 4.554. \quad (11.36)$$

The fact that the exit static pressure comes out so much larger than the ambient, solidly confirms our assumption that the exit is choked.

3) Suppose the pipe is lengthened. What value of L/D will produce $P_e/P_a = 1$?

Solution

At this condition the exit is choked, $M_e = 1$ and the exit pressure is no longer above the ambient pressure, that is $P_e = P_a$. Note the identity

$$\frac{P_e}{P_a} = \left(\frac{P_t}{P_a} \right) \left(\frac{P_{te}}{P_t} \right) \left(\frac{P_e}{P_{te}} \right). \quad (11.37)$$

The condition $P_e/P_a = 1$ implies that the stagnation pressure drop along the pipe must be

$$1 = 10 \left(\frac{P_{te}}{P_t} \right) \frac{1}{1.893} \Rightarrow \frac{P_{te}}{P_t} = \frac{1.893}{10} = \frac{1}{5.28}. \quad (11.38)$$

From the Fanno line stagnation pressure relation in (11.31) we find that this stagnation pressure ratio corresponds to $M_1 = 0.11$. Using this entrance Mach number (11.28) gives the length of the pipe.

$$\frac{4C_f L_{\max}}{D} = 54.32 \quad (11.39)$$

The value of L/D that unchoke the exit is

$$\frac{L}{D} = \frac{54.32}{4 \times 0.01} = 1358. \quad (11.40)$$

11.6.3 Integrated relations - 1-D frictionless, constant area flow with heat transfer (Rayleigh line flow)

In the presence of heat transfer, the relationship between Mach number and stagnation temperature from (11.18) is

$$\frac{dT_t}{T_t} = \left(\frac{1 - M^2}{1 + \gamma M^2} \right) \left(\frac{1}{1 + \frac{\gamma-1}{2} M^2} \right) \frac{dM^2}{M^2}. \quad (11.41)$$

Let the final state correspond to $M = 1$.

$$\int_{T_t}^{T_t^*} \frac{dT_t}{T_t} = \int_{M^2}^1 \left(\frac{1 - M^2}{1 + \gamma M^2} \right) \left(\frac{1}{1 + \frac{\gamma-1}{2} M^2} \right) \frac{dM^2}{M^2} \quad (11.42)$$

Carry out the integration indicated in (11.42).

$$\frac{T_t^*}{T_t} = \frac{(1 + \gamma M^2)^2}{2(1 + \gamma) M^2 \left(1 + \frac{\gamma-1}{2} M^2 \right)} \quad (11.43)$$

The stagnation temperature change required for the flow to pass from a given initial Mach number M_1 to a final Mach number, M_2 is found from

$$\frac{T_{t2}}{T_{t1}} = \left(\frac{T_t}{T_t^*} \right)_{M_2} \left(\frac{T_t^*}{T_t} \right)_{M_1}. \quad (11.44)$$

In each of the following relations

$$\begin{aligned} \left(\frac{1-M^2}{2}\right) \frac{dU^2}{U^2} &= \frac{dT_t}{T} \\ \left(\frac{1-M^2}{2}\right) \frac{d\rho}{\rho} &= -\frac{1}{2} \frac{dT_t}{T} \end{aligned} \quad (11.45)$$

and

$$\begin{aligned} \left(\frac{1-M^2}{2}\right) \frac{dT}{T} &= \left(\frac{1-\gamma M^2}{2}\right) \frac{dT_t}{T} \\ \left(\frac{1-M^2}{2}\right) \frac{dP}{P} &= -\left(\frac{\gamma M^2}{2}\right) \frac{dT_t}{T} \end{aligned} \quad (11.46)$$

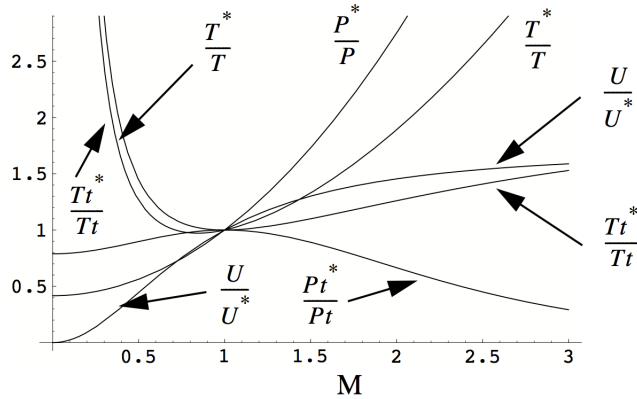
replace dT_t/T_t with $((1-M^2)/(1+((\gamma-1)/2)M^2))dM^2/(\gamma M^4)$ and carry out the integration. The result is the set of Rayleigh line relations.

$$\begin{aligned} \frac{U}{U^*} &= \frac{(\gamma+1)M^2}{1+\gamma M^2} = \frac{\rho^*}{\rho} \\ \frac{T^*}{T} &= \left(\frac{1+\gamma M^2}{(\gamma+1)M}\right)^2 \\ \frac{P^*}{P} &= \frac{1+\gamma M^2}{\gamma+1} \\ \frac{P_t^*}{P_t} &= \left(\frac{1+\gamma M^2}{\gamma+1}\right) \left(\frac{\frac{\gamma+1}{2}}{1+\frac{\gamma-1}{2}M^2}\right)^{\frac{\gamma}{\gamma-1}} \end{aligned} \quad (11.47)$$

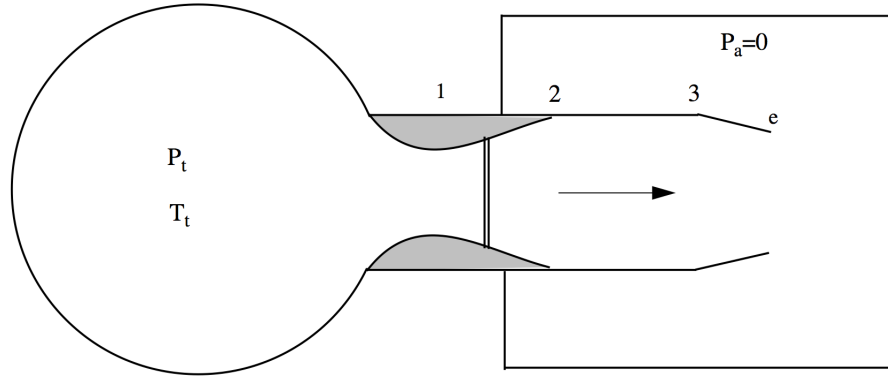
The various Rayleigh line relations (11.42) and (11.47) are plotted below for $\gamma = 1.4$.

11.6.4 Example - double throat with heat addition

In Chapter 9 we studied the flow in a channel with two throats. Here we will revisit the problem and add heat to the flow. Lets recall the flow situation. The figure below shows a supersonic wind tunnel that uses Air as a working gas. A very large plenum contains the gas at constant stagnation pressure and temperature, P_t , T_t . The flow exhausts to a large

Figure 11.4: *Rayleigh line relations.*

tank that is maintained at vacuum $P_a = 0$. The upstream nozzle area ratio is $A_2/A_1 = 6$ and the ratio of exit area to throat area is $A_e/A_1 = 2$. The test section has a constant area $A_3 = A_2$. A shock wave is stabilized in the diverging portion of the nozzle. Neglect wall friction.

Figure 11.5: *Supersonic wind tunnel with normal shock and heat addition.*

Suppose heat is added to the flow between stations 2 and 3.

- 1) Does the shock Mach number increase, decrease or remain the same? Explain.

Solution

The mass balance between stations 1 and e gives

$$\frac{P_t A_1}{\sqrt{T_t}} = \frac{P_{te} A_e}{\sqrt{T_{te}}} = \text{constant} \quad (11.48)$$

which is considerably lower than the pressure ratio determined in part 2.

As heat is added, the shock must move upstream to a lower Mach number so that the ratio $P_{te}/\sqrt{T_{te}}$ remains constant. This is essentially a constraint imposed by the fixed mass flow through the upstream throat. Through the shock movement upstream, the stagnation pressure at the exit goes up as the temperature goes up. The mechanism for stagnation pressure loss between stations 1 and e is a combination of shock loss and heat addition.

- 2) What happens to the Mach numbers at stations 2 and 3 as the heat is added?

Solution

The Mach number at station 3 is fixed by choking at the exit and, because of the geometry constraint, must remain constant during the heat addition process. With the Mach number at 3 fixed, the heat addition between 2 and 3 must lead to a decrease in Mach number at station 2. This is consistent with the upstream movement of the shock.

- 3) Suppose sufficient heat is added between 2 and 3 so that the throat at Station 1 just barely becomes un-choked. Determine the Mach numbers at stations 2 and 3 for this condition. How sensitive are these Mach number values to the choice of working gas? If the gas were changed to Argon (atomic weight = 40) would the Mach numbers at 2 and 3 be much different? If not, why not?

Solution

As noted above, the Mach number at station 3 is fixed by choking at the exit. For $A_e/A_3 = 1/3$ the Mach number at station 3 is $M_3 = 0.197$. The Mach number at station one is very close to one and the section from 1 to 2 is shock free thus the Mach number at station 2 for an area ratio $A_1/A_2 = 6$ is $M_2 = 0.097$.

Note that the subsonic branch of $f(M)$ is practically the same for various values of γ . Thus the Mach numbers at 2 and 3 would not be expected to change much when the test gas is changed from air $\gamma = 7/5$ to argon $\gamma = 5/3$. The factor $((\gamma + 1)/2)^{((\gamma+1)/(2(\gamma-1)))}$ out in front of $f(M)$ evaluates to 1.893 for $\gamma = 1.4$ versus 1.77 for $\gamma = 1.66$.

- 4) Recall the relationship between stagnation pressure loss and heat addition. Argue whether the stagnation pressure loss between stations 2 and 3 is large or small?

Solution

At the point where the upstream throat barely chokes, the Mach number at station 2 is $M_2 = 0.097$. The stagnation pressure loss between stations 2 and 3 is proportional to the Mach number squared and would be expected to be very small. To a pretty decent approximation at this Mach number, $P_{te} \cong P_t$.

- 5) At approximately what ratio of T_{te}/T_t does the un-choking of the throat at station 1 occur?

Solution

Since there is no shock and the heat addition takes place at low Mach number and we are asked for an approximate result, the stagnation temperature ratio at which the flow un-chokes can be determined from the mass flow balance.

$$\frac{A_1}{\sqrt{T_t}} = \frac{A_e}{\sqrt{T_{te}}} \Rightarrow \frac{T_{te}}{T_t} = 4 \quad (11.49)$$

11.7 Detonations and deflagrations

To complete this chapter, we will consider an important class of 1-D flows with heat addition where the source of heat is a combustible gas mixture of fuel and oxidizer. The 1-D governing equations are

$$\begin{aligned} d(\rho U) &= 0 \\ d(P + \rho U^2) &= 0 \\ d\left(C_p T + \frac{1}{2} U^2\right) &= \delta q \end{aligned} \quad (11.50)$$

The flows governed by these equations are characterized by waves that combine the features of shock waves and heat addition. Consider a channel filled with a combustible mixture as shown in 11.6.

Upon ignition with a spark, the subsequent process of heat release and expansion of hot gases is energetic enough to produce pressure disturbances that propagate along the tube away from the source forming a self-sustaining combustion wave. One of two things may happen.

- 1) A weak deflagration wave may occur in which heat is transferred to the upstream gas by conduction. In this case the wave speed is generally very low, a few tens of centimeters per second for hydrocarbon-air mixtures up to some tens of meters per second for a mixture

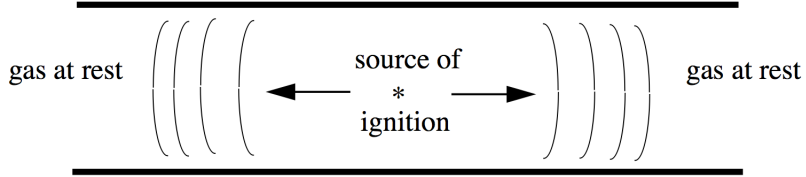


Figure 11.6: *Compression waves created by a source of ignition in a combustible mixture.*

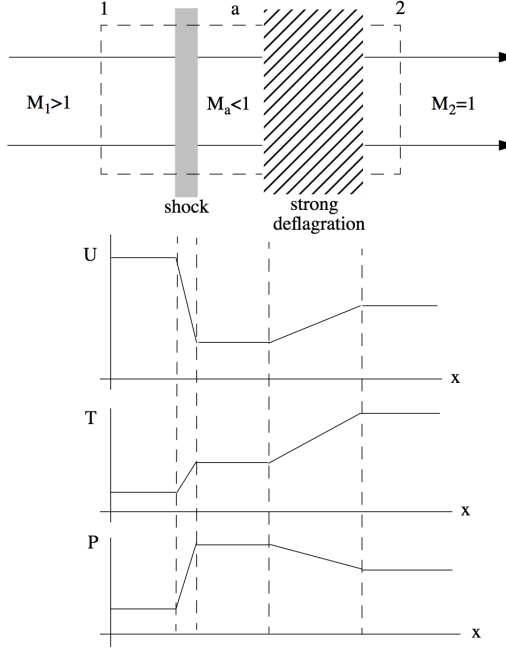
of hydrogen and oxygen. The speed of the wave cannot be determined from the heat of reaction and jump conditions alone. It can only be determined by a model that treats the details of the wave and includes the effects of heat conduction and viscosity. This is the sort of combustion wave one observes when a gas flame on a stove is ignited.

2) If the reaction is sufficiently energetic and heat loss mechanisms such as radiation and conduction to the channel walls are sufficiently small then the pressure waves preceding the flame front can catch up to one another in a process of non-linear steepening due to the dependence of acoustic speed on gas temperature. The steepening of the pressure front quickly forms a shock wave. The shock preheats the unburned gas passing through it causing the reaction to proceed at an even faster rate. Eventually the flow behind the combustion wave becomes thermally choked and the shock-combustion wave combination, called a detonation, moves along the pipe at an extreme speed on the order of thousands of meters per second. In this case the wave speed can be determined from the heat of reaction and the jump conditions across a region of heat addition.

Figure 11.7 somewhat artificially decomposes the detonation into a conventional shock followed by a thermally choked region of heat addition called a strong deflagration. Depending on the speed of the reaction and the mean free path of the gas, the whole region of change is extremely thin (a fraction of a millimeter) and the intermediate zone a is an idealization of a state that only exists at one point in the wave if at all. The equations of motion can be integrated to form the jump conditions

$$\begin{aligned} \rho_1 U_1 &= \rho_2 U_2 \\ P_1 + \rho_1 U_1^2 &= P_2 + \rho_2 U_2^2 \\ C_p T_1 + \frac{1}{2} U_1^2 + \Delta h_t &= C_p T_2 + \frac{1}{2} U_2^2 \\ P &= \rho R T \end{aligned} \tag{11.51}$$

where Δh_t is the stagnation enthalpy change per unit mass across the wave. Now we need

Figure 11.7: *Chapman-Jouget detonation wave structure.*

to determine the possible states of motion that can occur and the Mach number of the wave for a given enthalpy change. First combine the mass and momentum equation to form the equation

$$\left(\frac{P_2}{P_1} - 1 \right) = \gamma M_1^2 \left(1 - \frac{\rho_1}{\rho_2} \right). \quad (11.52)$$

The energy equation can be rearranged to read

$$\frac{1}{2} \frac{U_1^2}{C_p T_1} + 1 + \frac{\Delta h_t}{C_p T_1} = \frac{T_2}{T_1} + \frac{1}{2} \left(\frac{\rho_1}{\rho_2} \right)^2 \frac{U_1^2}{C_p T_1} \quad (11.53)$$

or

$$\left(1 + \frac{\Delta h_t}{C_p T_1} \right) + \left(\frac{\gamma - 1}{2} \right) M_1^2 \left(1 - \left(\frac{\rho_1}{\rho_2} \right)^2 \right) = \left(\frac{P_2}{P_1} \right) \left(\frac{\rho_1}{\rho_2} \right). \quad (11.54)$$

Use (11.52) to eliminate M_1 in (11.54). The result is

$$\left(\frac{P_2}{P_1} - 1\right) = \frac{2\gamma}{\gamma-1} \left(\frac{\frac{\Delta h_t}{C_p T_1} + \left(1 - \frac{\rho_1}{\rho_2}\right)}{\left(\frac{\gamma+1}{\gamma-1}\right) \frac{\rho_1}{\rho_2} - 1} \right). \quad (11.55)$$

Equations (11.52) and (11.55) are two functions relating pressure and density that are both satisfied simultaneously and fully define the state of the gas.

$$\begin{aligned} \frac{P_2}{P_1} - 1 &= F \left(\gamma, \frac{\rho_1}{\rho_2}, M_1 \right) \\ \frac{P_2}{P_1} - 1 &= G \left(\gamma, \frac{\rho_1}{\rho_2}, \frac{\Delta h_t}{C_p T_1} \right) \end{aligned} \quad (11.56)$$

If $\Delta h_t/C_p T_1 = 0$ (11.55) reduces to the Hugoniot relation for a normal shock. Equating (11.52) and (11.55) leads to a quadratic equation for ρ_1/ρ_2 the roots of which are

$$\frac{\rho_1}{\rho_2} = \frac{1 + \gamma M_1^2 \pm \left((M_1^2 - 1)^2 - 2(\gamma + 1) M_1^2 \frac{\Delta h_t}{C_p T_1} \right)^{1/2}}{(\gamma + 1) M_1^2}. \quad (11.57)$$

For $\Delta h_t/C_p T_1 = 0$ the roots are $\rho_1/\rho_2 = (1, (2 + (\gamma - 1) M_1^2) / ((\gamma + 1) M_1^2))$ which are the normal shock wave values. Note that the upstream Mach number M_1 may be either subsonic or supersonic. A cross-plot of (11.52) and (11.55) will define the state of the gas for a given $\Delta h_t/C_p T_1$. Several different types of combustion waves can occur.

- 1) A weak deflagration where $M_1 < 1$ and $M_2 < 1$.
- 2) A strong deflagration or thermally choked wave where $M_1 < 1$ and $M_2 = 1$.
- 3) A weak detonation where $M_1 > 1$ and $M_2 < 1$.
- 4) A thermally choked detonation where $M_1 > 1$ and $M_2 = 1$. This is also called a Chapman-Jouget detonation. Virtually all stable detonations are of Chapman-Jouget type. In this case the wave can be decomposed into a shock wave and a strong deflagration as shown in figure 11.7.

The Mach number of a Chapman-Jouget wave for a given value of $\Delta h_t/C_p T_1$ can be determined using the Rayleigh line equation for stagnation temperature change. Note that

$$\frac{\Delta h_t}{C_p T_1} = \left(\frac{T_{t2}}{T_{t1}} - 1 \right) \frac{T_{t1}}{T_1}. \quad (11.58)$$

Now substitute (11.43) into (11.58) to get

$$\frac{\Delta h_t}{C_p T_1} = \left(\frac{(1 + \gamma M_1^2)^2}{2(\gamma + 1) M_1^2 \left(1 + \frac{\gamma - 1}{2} M_1^2 \right)} - 1 \right) \left(1 + \frac{\gamma - 1}{2} M_1^2 \right) \quad (11.59)$$

or

$$\frac{\Delta h_t}{C_p T_1} = \frac{(1 - M_1^2)^2}{2(\gamma + 1) M_1^2}. \quad (11.60)$$

Solve Equation (11.60) for the Mach number.

$$M_1^2 = \left(1 + (\gamma + 1) \frac{\Delta h_t}{C_p T_1} \right) \pm \left(\left(1 + (\gamma + 1) \frac{\Delta h_t}{C_p T_1} \right)^2 - 1 \right)^{1/2} \quad (11.61)$$

The subsonic and supersonic roots of (11.61) are plotted below.

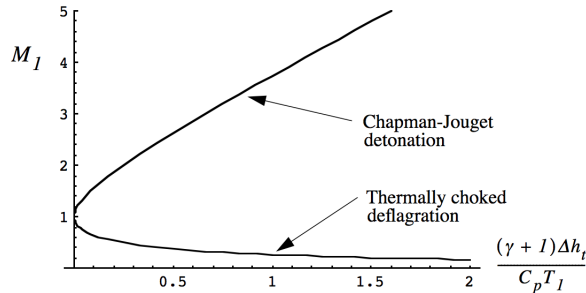


Figure 11.8: *Mach number of a detonation wave determined by heat release.*

11.7.1 Example - detonation in a mixture of fluorine and hydrogen diluted by nitrogen.

As an example, consider a stoichiometric mixture of 5% H_2 and 5% F_2 in 90% N_2 where the percentages are mole fractions. Let the initial temperature of the nitrogen be 300K. For fluorine reacting with hydrogen the heat of reaction is 1.35×10^5 calories per mole

or $1.36 \times 10^7 \text{ m}^2/\text{sec}^2$ per unit mass. The stagnation enthalpy change across the wave compared to the enthalpy of the free stream gas is approximately

$$\frac{\Delta h_t}{C_p T_1} = \frac{1.36 \times 10^7}{929 \times 300 \times 10} = 4.88. \quad (11.62)$$

The extra factor of ten in the denominator comes from the 90% dilution of the reactants with nitrogen. Using (11.61) and (11.62) with $\gamma = 1.4$ gives $M_1 = 5.0$, $M_a = 0.41$. This latter result is consistent with the normal shock value. Using normal shock and Rayleigh relations the conditions through the detonation wave in the rest frame of the wave are shown below.

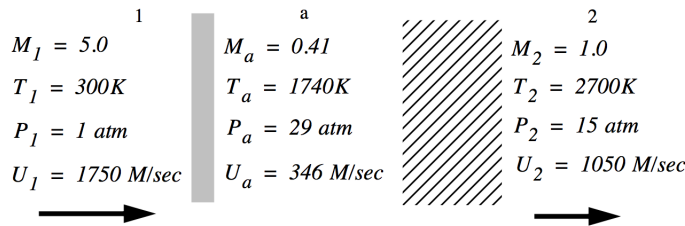


Figure 11.9: *Detonation wave example.*

Note that the drift speed of the gas behind the detonation in a frame of reference at rest with respect to the upstream gas is $U_2 - U_1 = -700 \text{ m/sec}$. The high pressure and strong wind generated by the detonation is responsible for the extreme destructive force of this type of explosion.

11.8 Problems

Problem 1 - Frictional flow of a compressible gas in an adiabatic pipe is sketched in figure 11.10. The gas comes from a large plenum at rest at constant P_t and T_t .

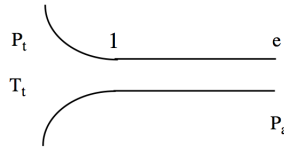


Figure 11.10: *Frictional flow in an adiabatic pipe.*

Show that the maximum Mach number must occur at the pipe exit, that the maximum possible Mach number is one and that supersonic flow cannot occur in the pipe.

Problem 2 - Natural gas, which is composed almost entirely of methane (molecular weight 16, $\gamma = 1.3$) is to be pumped through an insulated pipe one meter in diameter connecting two compressor stations 60 kilometers apart. At the upstream station, the stagnation pressure is 7 atmospheres and the stagnation temperature is 300 K. The mean friction coefficient is $C_f = 0.001$. Calculate the maximum mass flow rate that can be pumped through the pipe by the downstream station.

Problem 3 - In figure 11.11 Air flows from a large plenum through an adiabatic pipe with $L/D = 100$. The pressure ratio is $P_t/P_a = 1.5$ and the friction coefficient is $C_f = 0.01$.

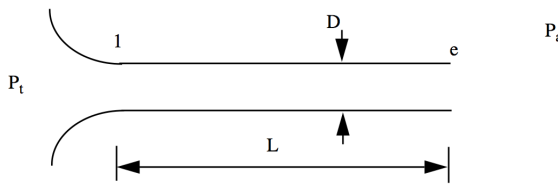


Figure 11.11: Frictional flow in an adiabatic pipe with given parameters.

Determine M_1 , M_e and P_{te}/P_t .

Problem 4 - In figure 11.12 a heater is used to increase the stagnation temperature of a compressible flow of air exhausting from a large plenum at constant P_t and T_t to vacuum.

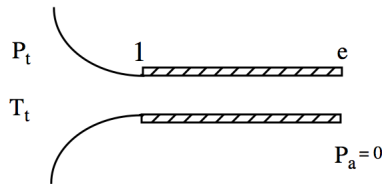


Figure 11.12: Flow in a constant area pipe with heat addition.

- 1) When T_{te}/T_t is increased does M_1 increase, decrease or remain the same ?
- 2) Consider the case where the increase in stagnation temperature is very large, $T_{te}/T_t \gg 1$. What is the value of P_{te}/P_t in this case?

Problem 5 - Figure 11.13 shows air at constant stagnation pressure and temperature, P_t , T_t exhausting from a very large plenum to the surrounding atmosphere through a long

straight pipe surrounded by a heater.

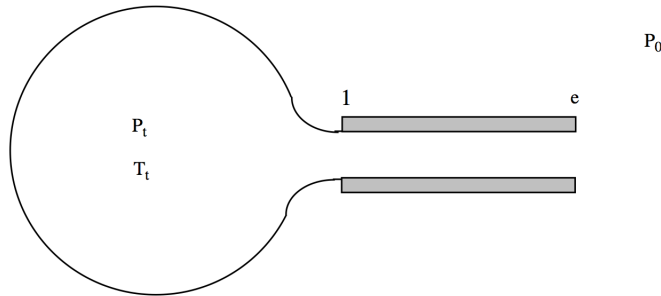


Figure 11.13: *Flow in a constant area pipe with heat addition and friction neglected.*

The gas temperature in the plenum is $T_t = 300\text{ K}$ and $P_t/P_0 = 10$. The heater increases the stagnation temperature to $T_{te} = 400\text{ K}$. Neglect the effects of friction.

- 1) Determine the Mach number at the entrance to the pipe.
- 2) Determine P_{te}/P_t and P_e/P_0 . Recall (11.25).
- 3) Suppose the amount of heat added is increased. What value of T_{te} , if any, will produce $P_e/P_0 = 1$?

Problem 6 - The figure below shows a supersonic wind tunnel supplied with Carbon Dioxide ($\gamma = 4/3$, Molecular weight = 44) from a very large plenum. The CO_2 passes through the test section and exhausts to a large vacuum chamber, $P_a = 0$. A high power, infrared laser tuned to one of the absorption lines of CO_2 is used to heat the gas between stations 2 and 3.

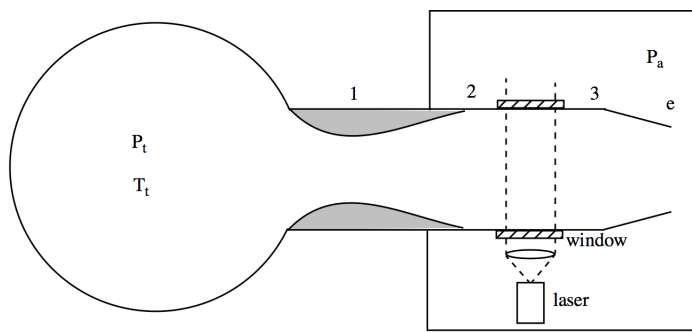


Figure 11.14: *Supersonic wind tunnel with two throats and heat addition by laser absorption.*

Relevant areas are $A_e/A_1 = 3$, $A_2 = A_3$, $A_2/A_1 = 5$. Neglect wall friction.

- 1) The laser is initially turned off and supersonic flow is established in the test section. Determine M_2 and M_e .
- 2) The laser is turned on and the stagnation temperature is increased slightly between 2 and 3 so that $T_{t3}/T_{t2} = 1.01$. Determine M_2 . Estimate P_{t3}/P_{t2} and M_e .
- 3) How much stagnation temperature increase can occur between stations 2 and 3 before the wind tunnel un-starts?
- 4) Suppose the stagnation temperature increase between stations 2 and 3 is such that $T_{t3}/T_{t2} = 4$. Determine P_{te}/P_t .

Problem 7 - Include the effects of friction and heat addition in a problem similar to Problem 2. The gas temperature in the plenum is $T_t = 300\text{ K}$ and $P_t/P_0 = 10$. The exit stagnation temperature T_{te} is not specified, rather a model for the wall temperature will be specified and T_{te} will be determined for a given length of pipe. Let $C_f = 0.01$ and $L/D = 10$. The differential change in stagnation temperature in terms of the Stanton number is

$$\frac{dT_t}{T_t} = \left(\frac{T_{wall}}{T_t} - 1 \right) \left(\frac{4S_t dx}{D} \right). \quad (11.63)$$

To solve the problem you will need the constant area Mach number relation

$$\left(\frac{1 - M^2}{1 + \left(\frac{\gamma-1}{2} \right) M^2} \right) \frac{dM^2}{2M^2} = \frac{\gamma M^2}{2} \left(\frac{4C_f dx}{D} \right) + \left(\frac{1 + \gamma M^2}{2} \right) \left(\frac{T_{wall}}{T_t} - 1 \right) \left(\frac{4S_t dx}{D} \right). \quad (11.64)$$

Let the wall temperature be distributed such that

$$\frac{T_{wall}}{T_t} = 3 \quad (11.65)$$

all along the wall.

- 1) Use (11.63) to determine T_{te} .
- 2) Use the Reynolds analogy (11.10) and integrate (11.64) to determine the Mach number at the entrance to the pipe.
- 3) Use mass conservation in the form of (11.25) to determine the stagnation pressure ratio across the pipe and confirm that the exit flow is choked.

4) What value of L/D (if any) would cause the exit flow to un-choke?

Problem 8 - Consider the frictionless flow of a calorically perfect gas in a channel with heat addition. The wall is shaped so as to keep the static pressure constant. The flow enters at condition 1 and departs at condition 2. Let the ratio of stagnation temperature between the entrance and exit be $\tau = T_{t2}/T_{t1}$.

(a) Find an expression for M_2 in terms of γ , M_1 and τ .

(b) Show that

$$\frac{A_2}{A_1} = \tau + \frac{\gamma - 1}{2} M_1^2 (\tau - 1). \quad (11.66)$$

(c) Show that

$$\frac{P_{t2}}{P_{t1}} = \left(\frac{\tau}{\tau + \frac{\gamma-1}{2} M_1^2 (\tau - 1)} \right)^{\gamma/(\gamma-1)}. \quad (11.67)$$

Problem 9 - Plot the temperature versus entropy of a calorically perfect gas in a constant area flow with friction. This is done by creating a chart of temperature versus Mach number and a chart of entropy versus Mach number. When the two variables are plotted versus one another with the Mach number as a parameter along the trajectory (ranging, say, from zero to 4), the resulting curve is called the Fanno line. Repeat the process for the case of constant area flow with heat transfer to produce the Rayleigh line.

Problem 10 - Figure 11.15 shows a supersonic wind tunnel supplied with Air from a very large plenum. The air passes through the test section and exhausts to a large vacuum chamber, $P_a = 0$. A sphere is placed in the test section between stations 2 and 3. The tunnel and sphere are adiabatic. The effect of wall friction on the flow can be neglected compared to the effect of the drag of the sphere.

Relevant areas are $A_2/A_1 = 5$, $A_2 = A_3$ and $A_e/A_1 = 3$. A reasonable model for the stagnation pressure drop due to the sphere is

$$\frac{P_{t3}}{P_{t2}} = 1 - \frac{\gamma M_2^2}{2} \left(\frac{A_{sphere}}{A_{tunnel}} \right) C_d. \quad (11.68)$$

Let $C_d = 1$ and $A_{sphere}/A_{tunnel} = 0.04$.

1) Supersonic flow is established in the test section. Determine, M_2 and M_3 .

2) Suppose A_e is decreased. At what value of A_e/A_1 does the wind tunnel un-start?

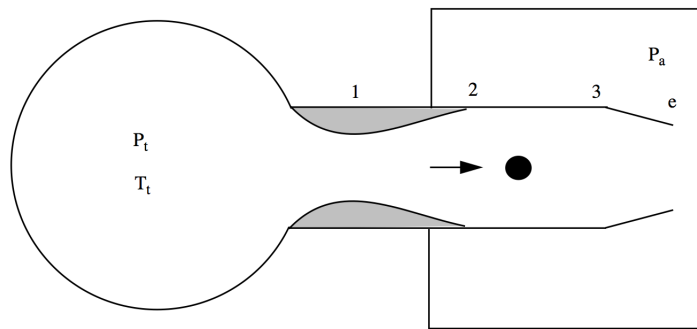


Figure 11.15: Supersonic wind tunnel with two throats and a drag producing sphere in the test section.

- 3) Is there a normal shock between 1 and 2 after the tunnel un-starts? If so, estimate the Mach number of the normal shock.
- 4) With the tunnel unstated suppose A_e is increased. Estimate the value of A_e/A_1 at which the wind tunnel starts.

Chapter 12

Steady waves in compressible flow

12.1 Oblique shock waves

Figure 12.1 shows an oblique shock wave produced when a supersonic flow is deflected by an angle θ .

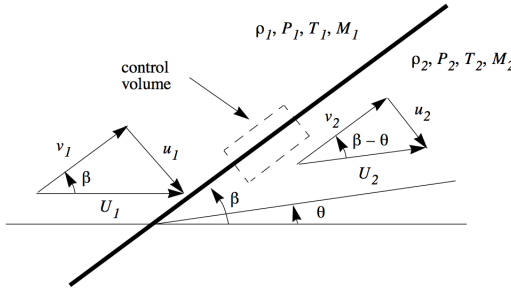


Figure 12.1: Flow geometry near a plane oblique shock wave.

We can think of the deflection as caused by a planar ramp at this angle although it could be generated by the blockage produced by a solid body placed some distance away in the flow. In general, a 3-D shock wave will be curved, and will separate two regions of non-uniform flow. However, at each point along the shock, the change in flow properties takes place in a very thin region much thinner than the radius of curvature of the shock. If we consider a small neighborhood of the point in question then within the small neighborhood, the shock may be regarded as locally planar to any required level of accuracy and the flows on either

side can be regarded as uniform. With the proper orientation of axes the flow is locally two-dimensional. Therefore it is quite general to consider a straight oblique shock wave in a uniform parallel stream in two-dimensions as shown below.

Balancing mass, two components of momentum and energy across the indicated control volume leads to the following oblique shock jump conditions.

$$\begin{aligned} \rho_1 u_1 &= \rho_2 u_2 \\ P_1 + \rho_1 u_1^2 &= P_2 + \rho_2 u_2^2 \\ \rho_1 u_1 v_1 &= \rho_2 u_2 v_2 \\ h_1 + \frac{1}{2} (u_1^2 + v_1^2) &= h_2 + \frac{1}{2} (u_2^2 + v_1^2) \end{aligned} \tag{12.1}$$

Since ρu is constant, $v_1 = v_2$ and the jump conditions become

$$\begin{aligned} \rho_1 u_1 &= \rho_2 u_2 \\ P_1 + \rho_1 u_1^2 &= P_2 + \rho_2 u_2^2 \\ v_1 &= v_2 \\ h_1 + \frac{1}{2} u_1^2 &= h_2 + \frac{1}{2} u_2^2. \end{aligned} \tag{12.2}$$

When the ideal gas law $P = \rho RT$ is included, the system of equations (12.2) closes allowing all the properties of the shock to be determined. Note that, with the exception of the additional equation, $v_1 = v_2$, the system is identical to the normal shock jump conditions. The oblique shock acts like a normal shock to the flow perpendicular to it. Therefore almost all of the normal shock relations can be converted to oblique shock relations with the substitution

$$\begin{aligned} M_1 &\rightarrow M_1 \sin(\beta) \\ M_2 &\rightarrow M_2 \sin(\beta - \theta). \end{aligned} \tag{12.3}$$

Recall the Rankine-Hugoniot relation

$$\frac{\rho_2}{\rho_1} = \frac{\gamma \left(\frac{P_2}{P_1} + 1 \right) + \left(\frac{P_2}{P_1} - 1 \right)}{\gamma \left(\frac{P_2}{P_1} + 1 \right) - \left(\frac{P_2}{P_1} - 1 \right)} \quad (12.4)$$

plotted in figure 12.2.

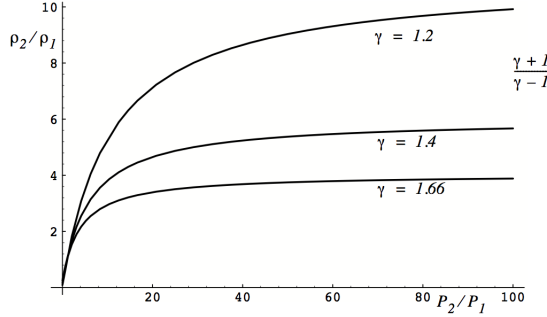


Figure 12.2: Plot of the Hugoniot relation (12.4)

This shows the close relationship between the pressure rise across the wave (oblique or normal) and the associated density rise. The jump conditions for oblique shocks lead to a modified form of the very useful Prandtl relation

$$u_1 u_2 = (a^*)^2 - \left(\frac{\gamma - 1}{\gamma + 1} \right) v_1^2 \quad (12.5)$$

where $(a^*)^2 = \gamma R T^*$. From the conservation of total enthalpy, for a calorically perfect gas in steady adiabatic flow

$$C_p T_t = C_p T + \frac{1}{2} U^2 = \frac{a^2}{\gamma - 1} + \frac{1}{2} U^2 = \frac{\gamma + 1}{2(\gamma - 1)} (a^*)^2. \quad (12.6)$$

The Prandtl relation is extremely useful for easily deriving all the various normal and

oblique shock relations. The oblique shock relations generated using (12.3) are

$$\begin{aligned}\frac{P_2}{P_1} &= \frac{2\gamma M_1^2 \sin^2(\beta) - (\gamma - 1)}{\gamma + 1} \\ \frac{\rho_2}{\rho_1} = \frac{u_1}{u_2} &= \frac{(\gamma + 1) M_1^2 \sin^2(\beta)}{(\gamma - 1) M_1^2 \sin^2(\beta) + 2} \\ \frac{T_2}{T_1} &= \frac{(2\gamma M_1^2 \sin^2(\beta) - (\gamma - 1)) ((\gamma - 1) M_1^2 \sin^2(\beta) + 2)}{(\gamma + 1)^2 M_1^2 \sin^2(\beta)} \\ M_2^2 \sin^2(\beta - \theta) &= \frac{(\gamma - 1) M_1^2 \sin^2(\beta) + 2}{2\gamma M_1^2 \sin^2(\beta) - (\gamma - 1)}.\end{aligned}\tag{12.7}$$

The stagnation pressure ratio across the shock is

$$\frac{P_{t2}}{P_{t1}} = \left(\frac{(\gamma + 1) M_1^2 \sin^2(\beta)}{(\gamma - 1) M_1^2 \sin^2(\beta) + 2} \right)^{\frac{\gamma}{\gamma-1}} \left(\frac{\gamma + 1}{2\gamma M_1^2 \sin^2(\beta) - (\gamma - 1)} \right)^{\frac{1}{\gamma-1}}.\tag{12.8}$$

Note that (12.8) can also be generated by the substitution (12.3).

12.1.1 Exceptional relations

One all new relation that has no normal shock counterpart is the equation for the absolute velocity change across the shock.

$$\left(\frac{U_2}{U_1} \right)^2 = 1 - 4 \frac{(M_1^2 \sin^2(\beta) - 1)(\gamma M_1^2 \sin^2(\beta) + 1)}{(\gamma + 1)^2 M_1^4 \sin^2(\beta)}\tag{12.9}$$

Exceptions to the substitution rule (12.3) are the relations involving the static and stagnation pressure, P_{t2}/P_1 and P_{t1}/P_2 across the wave. The reason for this is as follows. Consider

$$\frac{P_{t2}}{P_1} = \frac{P_{t2}}{P_{t1}} \frac{P_{t1}}{P_1} = \frac{P_{t2}}{P_{t1}} \left(1 + \frac{\gamma - 1}{2} M_1^2 \right)^{\frac{\gamma}{\gamma-1}}.\tag{12.10}$$

Similarly

$$\frac{P_{t1}}{P_2} = \frac{P_{t1}}{P_{t2}} \frac{P_{t2}}{P_2} = \frac{P_{t1}}{P_{t2}} \left(1 + \frac{\gamma - 1}{2} M_2^2\right)^{\frac{\gamma}{\gamma-1}}. \quad (12.11)$$

The stagnation to static pressure ratio in each region depends on the full Mach number, not just the Mach number perpendicular to the shock wave.

12.1.2 Flow deflection versus shock angle

The most basic question connected with oblique shocks is: given the free stream Mach number, M_1 , and flow deflection, θ , what is the shock angle, β ? The normal velocity ratio is

$$\frac{u_2}{u_1} = \frac{(\gamma - 1) M_1^2 \sin^2 \beta + 2}{(\gamma + 1) M_1^2 \sin^2 \beta} = \frac{u_2}{u_1} \frac{v_1}{v_2}. \quad (12.12)$$

From the velocity triangles in figure 12.1

$$\begin{aligned} \tan(\beta) &= \frac{u_1}{v_1} \\ \tan(\beta - \theta) &= \frac{u_2}{v_2}. \end{aligned} \quad (12.13)$$

Now

$$\tan(\beta - \theta) = \tan(\beta) \left(\frac{(\gamma - 1) M_1^2 \sin^2(\beta) + 2}{(\gamma + 1) M_1^2 \sin^2(\beta)} \right). \quad (12.14)$$

An alternative form of this relation is

$$\tan(\theta) = \cot(\beta) \left(\frac{M_1^2 \sin^2(\beta) - 1}{1 + \left(\frac{\gamma+1}{2}\right) M_1^2 - M_1^2 \sin^2(\beta)} \right). \quad (12.15)$$

The shock-angle-deflection-angle relation (12.15) is plotted in figure 12.3 for several values of the Mach number.

Corresponding points in the supersonic flow past a circular cylinder sketched below are indicated on the $M_1 = 1.5$ contour. At point a the flow is perpendicular to the shock wave

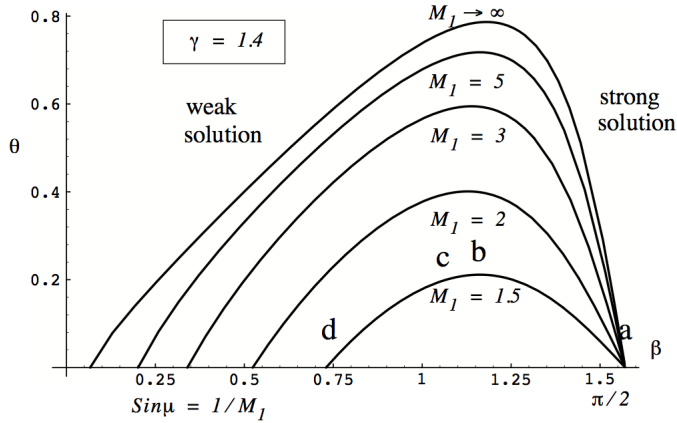


Figure 12.3: Flow deflection versus shock angle for oblique shocks.

and the properties of the flow are governed by the normal shock relations. In moving from point a to b the shock weakens and the deflection of the flow behind the shock increases until a point of maximum flow deflection is reached at b . The flow solution between a and b is referred to as the strong solution in figure 12.3. Notice that the Mach number behind the shock is subsonic up to point c where the Mach number just downstream of the shock is one. Between c and d the flow corresponds to the weak solutions indicated in figure 12.3. If one continued along the shock to very large distances from the sphere the shock will have a more and more oblique angle eventually reaching the Mach angle $\beta \rightarrow \mu = Sin^{-1}(1/M_1)$ corresponding to an infinitesimally small disturbance.

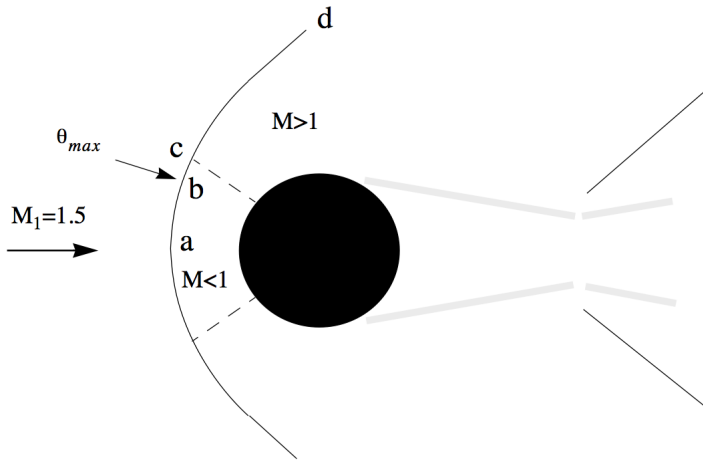


Figure 12.4: Supersonic flow past a cylinder with shock structure shown.

Note that as the free-stream Mach number becomes large, the shock angle becomes independent of the Mach number.

$$\lim_{M_1 \rightarrow \infty} \tan(\theta) = \frac{\cos(\beta) \sin(\beta)}{\left(\frac{\gamma+1}{2}\right) - \sin^2 \beta} \quad (12.16)$$

12.2 Weak oblique waves

In this section we will develop the differential equations that govern weak waves generated by a small disturbance. The theory will be based on infinitesimal changes in the flow and for this reason it is convenient to drop the subscript '1' on the flow variables upstream of the wave. The sketch below depicts the case where the flow deflection is very small $d\theta \ll 1$. Note that M is *not* close to one.

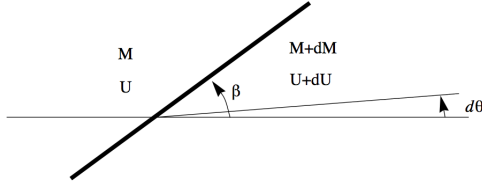


Figure 12.5: Small deflection in supersonic flow.

In terms of figure 12.3 we are looking at the behavior of weak solutions close to the horizontal axis of the figure. For a weak disturbance, the shock angle is very close to the Mach angle $\sin(\mu) = 1/M$. Let

$$\sin(\beta) = \frac{1}{M} + \varepsilon \quad (12.17)$$

and make the approximation

$$M^2 \sin^2(\beta) \cong 1 + 2M\varepsilon. \quad (12.18)$$

Using (12.18) we can also develop the approximation

$$\cot(\beta) \cong (M^2 - 1)^{1/2} \left(1 - \frac{M^3}{M^2 - 1} \varepsilon \right). \quad (12.19)$$

Using (12.18) and (12.19) the (β, θ) relation (12.15) can be expanded to yield

$$\tan(d\theta) \cong d\theta \cong \frac{4}{\gamma+1} \frac{(M^2 - 1)^{1/2}}{M} \varepsilon. \quad (12.20)$$

The velocity change across the shock (12.9) is expanded as

$$\left(\frac{U_2 - U_1}{U_1} + 1 \right)^2 = 1 - 4 \frac{\left(M^2 \left(\frac{1}{M} + \varepsilon \right)^2 - 1 \right) \left(\gamma M^2 \left(\frac{1}{M} + \varepsilon \right)^2 + 1 \right)}{(\gamma+1)^2 M^4 \left(\frac{1}{M} + \varepsilon \right)^2}. \quad (12.21)$$

Retaining only terms of order ε the fractional velocity change due to the small deflection is

$$\left(\frac{dU}{U} + 1 \right)^2 = 1 - \frac{8}{(\gamma+1) M} \varepsilon. \quad (12.22)$$

Equation (12.22) is approximated as

$$\frac{dU}{U} = - \frac{4}{(\gamma+1) M} \varepsilon. \quad (12.23)$$

Write (12.23) in terms of the deflection angle

$$\frac{dU}{U} = - \frac{4}{(\gamma+1) M} \varepsilon = - \frac{4}{(\gamma+1) M} \left(\frac{\gamma+1}{4} \right) \frac{M}{(M^2 - 1)^{1/2}} d\theta \quad (12.24)$$

or

$$\frac{dU}{U} = - \frac{1}{(M^2 - 1)^{1/2}} d\theta \quad (12.25)$$

where $d\theta$ is measured in radians. Other small deflection relations are

$$\begin{aligned}\frac{dP}{P} &= \frac{\gamma M^2}{(M^2 - 1)^{1/2}} d\theta \\ \frac{d\rho}{\rho} &= \frac{M^2}{(M^2 - 1)^{1/2}} d\theta \\ \frac{dT}{T} &= \frac{(\gamma - 1) M^2}{(M^2 - 1)^{1/2}} d\theta\end{aligned}\tag{12.26}$$

and

$$\frac{dP_t}{P_t} = -\frac{2\gamma}{3(\gamma + 1)^2} (M^2 \sin^2 \beta - 1)^3 = -\frac{16\gamma M^3}{3(\gamma + 1)^2} \varepsilon^3 = -\frac{ds}{R}\tag{12.27}$$

or using (12.20)

$$\frac{dP_t}{P_t} = -\frac{\gamma(\gamma + 1) M^6}{12(M^2 - 1)^{3/2}} (d\theta)^3 = -\frac{ds}{R}.\tag{12.28}$$

Note that the entropy change across a weak oblique shock wave is extremely small; the wave is nearly isentropic. The Mach number is determined from

$$\frac{dM^2}{M^2} = \frac{dU^2}{U^2} - \frac{dT}{T} = -\frac{2}{(M^2 - 1)^{1/2}} d\theta - \frac{(\gamma - 1) M^2}{(M^2 - 1)^{1/2}} d\theta.\tag{12.29}$$

Adding terms

$$\frac{dM^2}{M^2} = -2 \frac{\left(1 + \frac{\gamma-1}{2} M^2\right)}{(M^2 - 1)^{1/2}} d\theta.\tag{12.30}$$

Eliminate $d\theta$ between (12.25) and (12.30) to get an integrable equation relating velocity and Mach number changes.

$$\frac{dU^2}{U^2} = \frac{1}{\left(1 + \frac{\gamma-1}{2} M^2\right)} \frac{dM^2}{M^2}\tag{12.31}$$

The weak oblique shock relations (12.26) are, in terms of the velocity.

$$\begin{aligned}\frac{dP}{P} &= -\frac{\gamma}{2} M^2 \frac{dU^2}{U^2} \\ \frac{dT}{T} &= -\left(\frac{\gamma-1}{2}\right) M^2 \frac{dU^2}{U^2} \\ \frac{dp}{\rho} &= -M^2 \frac{dU^2}{U^2}\end{aligned}\tag{12.32}$$

These last relations are precisely the same ones we developed for one dimensional flow with area change in the absence of wall friction and heat transfer in chapter 9. From that development we had

$$\begin{aligned}\frac{1-M^2}{2} \frac{dU^2}{U^2} &= -\frac{dA}{A} \\ \frac{1-M^2}{2\left(1+\frac{\gamma-1}{2}M^2\right)} \frac{dM^2}{M^2} &= -\frac{dA}{A}.\end{aligned}\tag{12.33}$$

If we eliminate dA/A between these two relations, the result is

$$\frac{dU^2}{U^2} = \frac{1}{\left(1+\frac{\gamma-1}{2}M^2\right)} \frac{dM^2}{M^2}\tag{12.34}$$

which we just derived in the context of weak oblique shocks.

12.3 The Prandtl-Meyer expansion

The upshot of all this is that

$$\frac{dU^2}{U^2} = -\frac{2}{(M^2-1)^{1/2}} d\theta\tag{12.35}$$

is actually a general relationship valid for steady, isentropic flow. In particular it can be applied to negative values of $d\theta$. Consider flow over a corner.

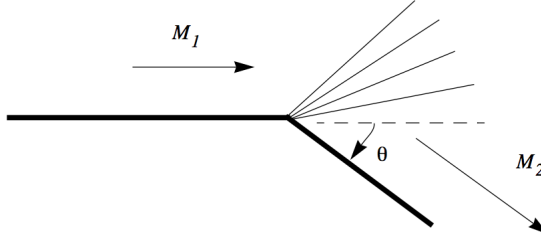


Figure 12.6: Supersonic flow over a corner.

Express the angle in terms of the Mach number.

$$d\theta = -\frac{(M^2 - 1)^{1/2}}{2 \left(1 + \frac{\gamma-1}{2}M^2\right)} \frac{dM^2}{M^2} \quad (12.36)$$

Now integrate the angle between the initial and final Mach numbers.

$$\int_0^\theta d\theta' = - \int_{M_1}^{M_2} \frac{(M^2 - 1)^{1/2}}{2 \left(1 + \frac{\gamma-1}{2}M^2\right)} \frac{dM^2}{M^2} \quad (12.37)$$

Let ω be the angle change beginning at the reference mach number $M_1 = 1$. The integral (12.37) is

$$\omega(M) = \left(\frac{\gamma+1}{\gamma-1}\right)^{1/2} \operatorname{Tan}^{-1} \left(\left(\frac{\gamma-1}{\gamma+1}\right)^{1/2} (M^2 - 1)^{1/2} \right) - \operatorname{Tan}^{-1} (M^2 - 1)^{1/2}. \quad (12.38)$$

This expression provides a unique relationship between the local Mach number and the angle required to accelerate the flow to that Mach number beginning at Mach one. The straight lines in figure 12.5 are called *characteristics* and represent particular values of the flow deflection. According to (12.38) the Mach number is the same at every point on a given characteristic. This flow is called a Prandtl-Meyer expansion and (12.38) is called the Prandtl-Meyer function, plotted below for several values of γ .

Note that for a given γ there is a limiting angle at $M^2 \rightarrow \infty$.

$$\omega_{\max} = \frac{\pi}{2} \left(\left(\frac{\gamma+1}{\gamma-1}\right)^{1/2} - 1 \right) \quad (12.39)$$

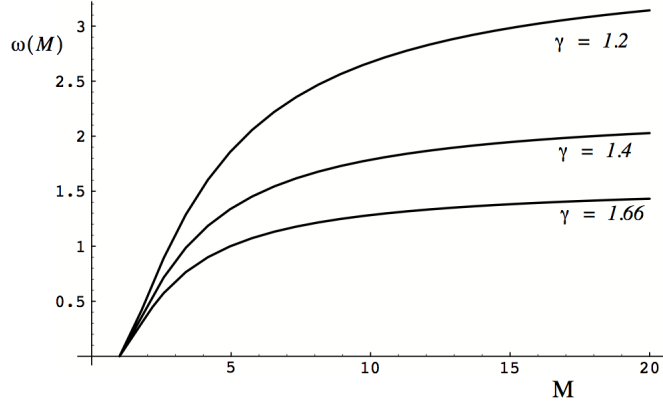


Figure 12.7: Prandtl-Meyer function for several values of γ .

For $\gamma = 1.4$, $\omega_{\max} = 1.45 \left(\frac{\pi}{2}\right)$. The expansion angle can be greater than 90° . If the deflection is larger than this angle there will be a vacuum between ω_{\max} and the wall.

12.3.1 Example - supersonic flow over a bump

Air flows past a symmetric 2-D bump at a Mach number of 3. The aspect ratio of the bump is $a/b = \sqrt{3}$.

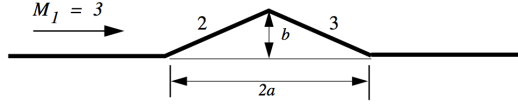


Figure 12.8: Supersonic flow over a bump.

Determine the drag coefficient of the bump assuming zero wall friction.

$$C_d = \frac{\text{Drag force per unit span}}{\frac{1}{2} \rho_1 U_1^2 b} \quad (12.40)$$

Solution

The ramp angle is 30° producing a 52° oblique shock with pressure ratio

$$\frac{P_2}{P_1} = 6.356. \quad (12.41)$$

The expansion angle is 60° producing a Mach number

$$\begin{aligned} M_2 &= 1.406 \\ \omega &= 9.16^\circ. \end{aligned} \tag{12.42}$$

The stagnation pressure is constant through the expansion wave and so the pressure ratio over the downstream face is

$$\begin{aligned} M_3 &= 4.268 \\ \omega &= 69.16^\circ \end{aligned} \tag{12.43}$$

and

$$\frac{P_3}{P_2} = \left(\frac{1 + \left(\frac{\gamma-1}{2}\right) M_2^2}{1 + \left(\frac{\gamma-1}{2}\right) M_3^2} \right)^{\frac{\gamma}{\gamma-1}} = \left(\frac{1 + 0.2(1.406)^2}{1 + 0.2(4.268)^2} \right)^{3.5} = \left(\frac{1.395}{4.643} \right)^{3.5} = 0.0149 \tag{12.44}$$

and

$$\frac{P_3}{P_1} = \frac{P_3}{P_2} \frac{P_2}{P_1} = 0.0149 \times 6.356 = 0.0945. \tag{12.45}$$

The drag coefficient becomes

$$C_d = \frac{P_2 2b \sin(30) - P_3 2b \sin(30)}{\frac{\gamma}{2} M_1^2 P_1 b} = \frac{6.356 - 0.0945}{\frac{1.4}{2} (9)} = 0.994. \tag{12.46}$$

12.4 Problems

Problem 1 - Use the oblique shock jump conditions (12.2) to derive the oblique shock Prandtl relation (12.5).

Problem 2 - Consider the supersonic flow past a bump discussed in the example above. Carefully sketch the flow putting in the shock waves as well as the leading and trailing characteristics of the expansion.

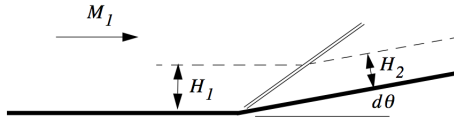


Figure 12.9: Supersonic flow past a 2-D ramp.

Problem 3 - Consider a streamline in compressible flow past a 2-D ramp with a very small ramp angle.

Determine the ratio of the heights of the streamline above the wall before and after the oblique shock in terms of M_1 and $d\theta$ find the unknown coefficient in (12.47).

$$\frac{H_2}{H_1} = 1 + (\text{????}) d\theta \quad (12.47)$$

Pay careful attention to signs.

Problem 4 - Consider a body in subsonic flow. As the free-stream Mach number is increased there is a critical value, M_c , such that there is a point somewhere along the body where the flow speed outside the boundary layer reaches the speed of sound. Figure 12.10 illustrates this phenomena for flow over a projectile.

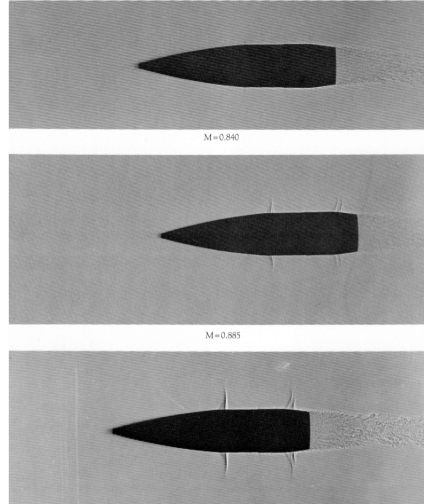


Figure 12.10: Projectile in high subsonic flow.

In this figure 12.10 the critical Mach number is somewhere between 0.840 and 0.885 as evidenced by the weak shocks that appear toward the back of the projectile in the middle

picture. The local pressure in the neighborhood of the body is expressed in terms of the pressure coefficient.

$$C_P = \frac{P - P_\infty}{\frac{1}{2} \rho_\infty U_\infty^2} \quad (12.48)$$

Show that the value of the pressure coefficient at the point where sonic speed occurs is

$$C_{P_c} = \frac{\left(\frac{1 + \frac{\gamma-1}{2} M_{\infty c}^2}{\frac{\gamma+1}{2}} \right)^{\frac{\gamma}{\gamma-1}} - 1}{\frac{\gamma}{2} M_{\infty c}^2}. \quad (12.49)$$

State any assumptions needed to solve the problem.

Problem 5 - Consider frictionless (no wall friction) supersonic flow over a flat plate of chord C at a small angle of attack as shown in figure 12.11.

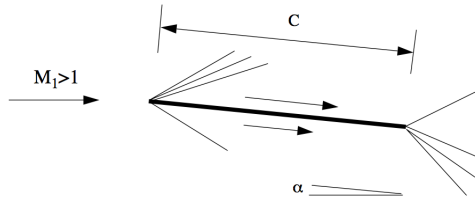


Figure 12.11: Supersonic flow past a flat plate at a small angle of attack.

The circulation about the plate is defined as

$$\Gamma = \oint U ds. \quad (12.50)$$

where the integration is along any contour surrounding the plate.

1) Show that, to a good approximation, the circulation is given by

$$\Gamma = \frac{2U_1 C}{(M_1^2 - 1)^{1/2}} \alpha \quad (12.51)$$

where the integration is clockwise around the plate.

2) Show that, to the same approximation, $Lift per unit span = \rho_1 U_1 \Gamma$.

Problem 6 - Consider frictionless (no wall friction) flow of air at $M = 2$ over a flat plate of chord C at 5° angle of attack as shown in figure 12.12.

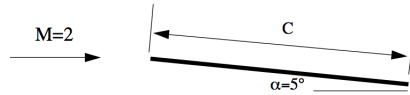


Figure 12.12: Supersonic flow over a flat plate at 5° angle of attack.

Evaluate the drag coefficient of the plate. Compare with the value obtained using a weak wave approximation.

Problem 7 - Consider frictionless (no wall friction) supersonic flow of Air over a flat plate of chord C at an angle of attack of 15 degrees as shown in figure 12.13.

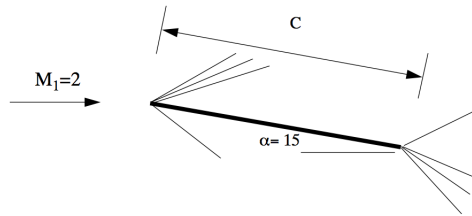


Figure 12.13: Supersonic flow over a flat plate at 15° angle of attack.

Determine the lift coefficient

$$C_L = \frac{L}{\frac{1}{2} \rho_\infty U_\infty^2 C} \quad (12.52)$$

where L is the lift force per unit span.

Problem 8 - Figure 12.14 shows a symmetrical, diamond shaped airfoil at a 5° angle of attack in a supersonic flow of air.

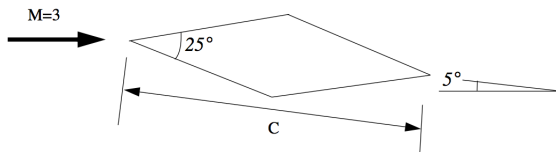


Figure 12.14: Supersonic flow past a diamond shaped airfoil.

Determine the lift and drag coefficients of the airfoil.

$$C_L = \frac{\text{Lift per unit span}}{\frac{1}{2}\rho_\infty U_\infty^2 C} \quad (12.53)$$

$$C_D = \frac{\text{Drag per unit span}}{\frac{1}{2}\rho_\infty U_\infty^2 C}$$

What happens to the flow over the airfoil if the free-stream Mach number is decreased to 1.5? Compare your result with the lift and drag of a thin flat plate at 5° angle of attack and free-stream Mach number of 3.

Problem 9 - The figure below shows supersonic flow of Air over a 30° wedge followed by a 10° wedge. The free stream Mach number is 3.

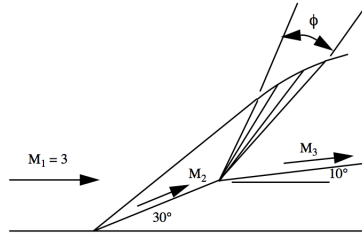


Figure 12.15: Supersonic over a wedge with a shoulder.

- 1) Determine M_2 , M_3 and the included angle of the expansion fan, ϕ .
- 2) Suppose the flow was turned through a single 10° wedge instead of the combination shown above. Would the stagnation pressure after the turn be higher or lower than in the case shown? Why?

Problem 10 - Figure 12.16 shows a smooth compression of a supersonic flow of air by a concave surface. The free-stream Mach number is 1.96. The weak oblique shock at the nose produces a Mach number of 1.932 at station 1. From station 1 to station 2 the flow is turned 20 degrees.

- 1) Determine the Mach number at station 2.
- 2) Determine the pressure ratio P_2/P_1 .
- 3) State any assumptions used.

Problem 11 - Figure 12.17 shows supersonic flow of air in a channel or duct at a Mach number of three. The flow produces an oblique shock off a ramp at an angle of 16 degrees.

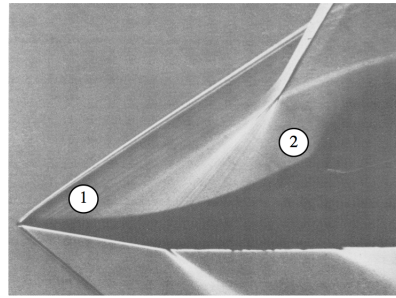


Figure 12.16: *Supersonic flow compressed by a concave surface.*

The shock reflects off the upper surface of the wind tunnel as shown below. Beyond the ramp the channel height is the same at the height ahead of the ramp.

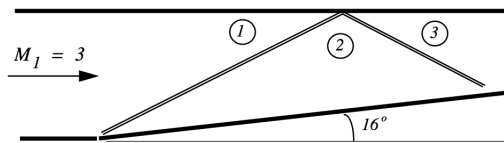


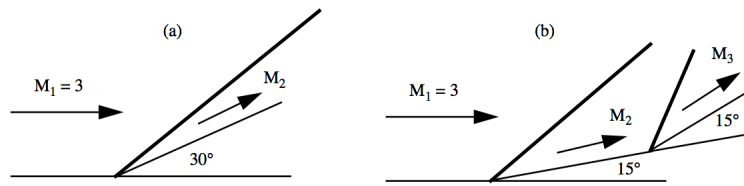
Figure 12.17: *Mach 3 flow in a duct with a ramp.*

- 1) Determine the Mach number in region 2.
- 2) Determine the Mach number in region 3.
- 3) Describe qualitatively how P_t and T_t vary between regions 1, 2 and 3.
- 4) Suppose the channel height is 10 cm . Precisely locate the shock reflections on the upper and lower walls.
- 5) Suppose the walls were lengthened. At roughly what point would the Mach number tend to one?

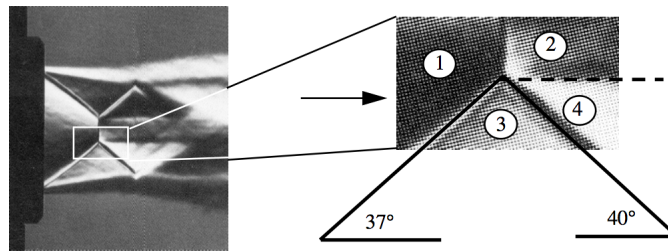
Problem 12 - Figure 12.18 shows supersonic flow of air turned through an angle of 30° . The free stream Mach number is 3.

In case (a) the turning is accomplished by a single 30° wedge whereas in case (b) the turning is accomplished by two 15° degree wedges in tandem. Determine the stagnation pressure change in each case, $(P_{t2}/P_{t1})|_{(a)}$ and $(P_{t3}/P_{t1})|_{(b)}$ and comment on the relative merit of one design over the other.

Problem 13 - Figure 12.19 shows the flow of helium from a supersonic over-expanded round jet. If we restrict our attention to a small region near the intersection of the first

Figure 12.18: *Supersonic flow turned 30°.*

two oblique shocks and the so-called Mach disc as shown in the blow-up, then we can use oblique shock theory to determine the flow properties near the shock intersection (despite the generally non-uniform 3-D nature of the rest of the flow). The shock angles with respect to the horizontal measured from the image are as shown.

Figure 12.19: *Supersonic flow from an over expanded round jet.*

- 1) Determine the jet exit Mach number. Hint, you will need to select a Mach number that balances the pressures in regions 2 and 4 with a dividing streamline that is very nearly horizontal as shown in the picture.
- 2) Determine the Mach number in region 2.
- 3) Determine the flow angles and Mach numbers in regions 3 and 4.
- 4) Determine P_2/P_1 and P_4/P_1 . How well do the static pressures match across the dividing streamline (dashed line) between regions 2 and 4?

Problem 14 - Figure 12.20 shows the reflection of an expansion wave from the upper wall of a 2-D, adiabatic, inviscid channel flow. The gas is helium at an incoming Mach number, $M_1 = 1.5$ and the deflection angle is 20° . The flow is turned to horizontal by the lower wall which is designed to follow a streamline producing no reflected wave. Determine M_2 , M_3 and H/h .

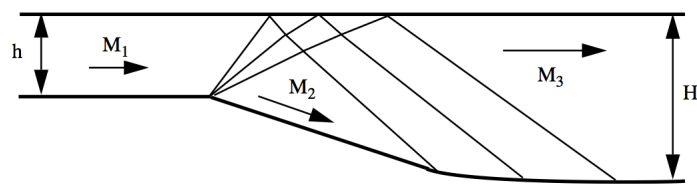


Figure 12.20: Supersonic flow in an expansion.

Chapter 13

Unsteady waves in compressible flow

13.1 Governing equations

One of the most important applications of compressible flow theory is to the analysis of the generation and propagation of sound. In Chapter 6 we worked out the equations for homentropic, unsteady flow that are the starting point for the derivation of the acoustic equations. For $\nabla \times \bar{U} = 0$, and $\nabla s = 0$, the equations of motion are

$$\begin{aligned}\frac{\partial \rho}{\partial t} + \frac{\partial}{\partial x_k} (\rho U_k) &= 0 \\ \rho \frac{\partial U_i}{\partial t} + \rho \frac{\partial}{\partial x_i} \left(\frac{U_k U_k}{2} \right) + \frac{\partial P}{\partial x_i} &= 0 \\ \frac{P}{P_0} &= \left(\frac{\rho}{\rho_0} \right)^\gamma.\end{aligned}\tag{13.1}$$

The role of the energy equation is played by the isentropic relation between pressure and density.

13.2 The acoustic equations

Now consider an unsteady flow where disturbances in density and pressure are extremely

small compared to constant background values.

$$\begin{aligned}\rho &= \rho_0 + \rho' \quad ; \quad \frac{\rho'}{\rho_0} \ll 1 \\ P &= P_0 + P' \quad ; \quad \frac{P'}{P_0} \ll 1\end{aligned}\tag{13.2}$$

In addition, assume that the velocity field involves very small fluctuations about zero. Linearize (13.1) by dropping higher order nonlinear terms.

$$\begin{aligned}\frac{\partial \rho}{\partial t} + \rho_0 \frac{\partial U_k}{\partial x_k} &= 0 \\ \rho_0 \frac{\partial U_i}{\partial t} + \frac{\partial P}{\partial x_i} &= 0\end{aligned}\tag{13.3}$$

Now define the dimensionless density disturbance

$$r = \frac{\rho - \rho_0}{\rho_0}.\tag{13.4}$$

In terms of this variable the equations of motion become

$$\begin{aligned}\frac{\partial r}{\partial t} + \frac{\partial U_k}{\partial x_k} &= 0 \\ \rho_0 \frac{\partial U_i}{\partial t} + \frac{\partial P}{\partial x_i} &= 0 \\ \frac{P}{P_0} &= (1 + r)^\gamma \cong 1 + \gamma r.\end{aligned}\tag{13.5}$$

Slight rearrangement produces the acoustic equations

$$\begin{aligned}\frac{\partial r}{\partial t} + \frac{\partial U_k}{\partial x_k} &= 0 \\ \frac{\partial U_i}{\partial t} + a_0^2 \frac{\partial r}{\partial x_i} &= 0\end{aligned}\tag{13.6}$$

where

$$a_0^2 = \gamma \frac{P_0}{\rho_0}. \quad (13.7)$$

Now differentiate the linearized continuity equation with respect to time and the linearized momentum equation with respect to space.

$$\begin{aligned} \frac{\partial^2 r}{\partial t^2} + \frac{\partial^2 U_k}{\partial x_k \partial t} &= 0 \\ \frac{\partial^2 U_k}{\partial x_k \partial t} + a_0^2 \frac{\partial^2 r}{\partial x_k \partial x_k} &= 0 \end{aligned} \quad (13.8)$$

Subtract one from the other in (13.8). The dimensionless density disturbance satisfies the linear wave equation.

$$\frac{\partial^2 r}{\partial t^2} - a_0^2 \frac{\partial^2 r}{\partial x_k \partial x_k} = 0 \quad (13.9)$$

Now repeat the process with the differentiation reversed. The result is

$$\begin{aligned} \frac{\partial^2 r}{\partial t \partial x_i} + \frac{\partial^2 U_k}{\partial x_k \partial x_i} &= 0 \\ \frac{\partial^2 U_i}{\partial t^2} + a_0^2 \frac{\partial^2 r}{\partial x_i \partial t} &= 0. \end{aligned} \quad (13.10)$$

Again, subtract one equation from the other in (13.10). The velocity fluctuation satisfies the equation

$$\frac{\partial^2 U_i}{\partial t^2} - a_0^2 \frac{\partial^2 U_k}{\partial x_k \partial x_i} = 0. \quad (13.11)$$

Recall the vector identity $\nabla \times (\nabla \times \bar{U}) = \nabla(\nabla \cdot \bar{U}) - \nabla^2 \bar{U}$. Using this identity and the fact that the flow is irrotational, (13.11) can be expressed as the linear wave equation

$$\frac{\partial^2 U_i}{\partial t^2} - a_0^2 \frac{\partial^2 U_i}{\partial x_k \partial x_k} = 0. \quad (13.12)$$

Similarly, the pressure satisfies the wave equation. Substitute

$$r = \frac{1}{\gamma} \left(\frac{P - P_0}{P_0} \right) \quad (13.13)$$

into (13.9)

$$\frac{\partial^2 P}{\partial t^2} - a_0^2 \frac{\partial^2 P}{\partial x_k \partial x_k} = 0. \quad (13.14)$$

Finally, the temperature also satisfies the wave equation.

$$\frac{\partial^2 T}{\partial t^2} - a_0^2 \frac{\partial^2 T}{\partial x_k \partial x_k} = 0 \quad (13.15)$$

13.3 Propagation of acoustic waves in one space dimension

In one dimensional flow the acoustic equations become

$$\begin{aligned} \frac{\partial r}{\partial t} + \frac{\partial U}{\partial x} &= 0 \\ \frac{\partial U_i}{\partial t} + a_0^2 \frac{\partial r}{\partial x} &= 0. \end{aligned} \quad (13.16)$$

The wave equation

$$\frac{\partial^2 r}{\partial t^2} - a_0^2 \frac{\partial^2 r}{\partial x^2} = 0 \quad (13.17)$$

can be solved in a very general form

$$r(x, t) = F(x - a_0 t) + G(x + a_0 t) \quad (13.18)$$

where F and G are arbitrary functions. The character of the solution can be understood by considering first the case $G = 0$. Figure 13.1 illustrates the evolution of an initial distribution of F propagating to the right in the $x - t$ plane.

The disturbance moves to the right unchanged in shape. Acoustic waves are nondispersive meaning that the wave speed does not depend on the wavelength. The figure below

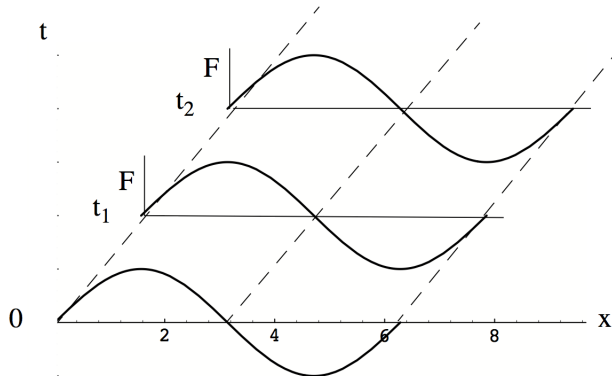


Figure 13.1: Right propagating wave.

illustrates the evolution of an initial distribution of G propagating to the left in the $x - t$ plane.

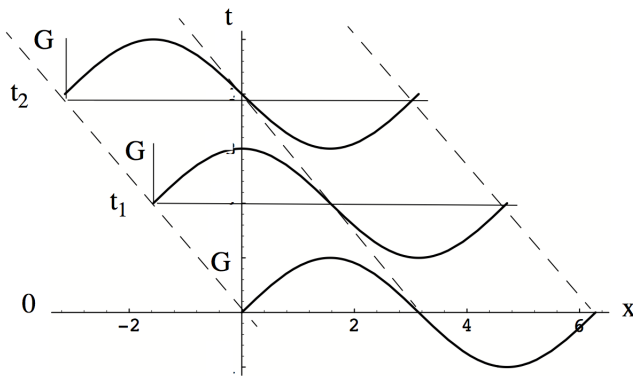


Figure 13.2: Left propagating wave

In the absence of dispersion and dissipation, the waves simply translate while retaining their form. The pressure disturbance produced by the wave is related to the density by

$$\frac{P - P_0}{P_0} = \gamma r = \gamma \left(\frac{\rho - \rho_0}{\rho_0} \right). \quad (13.19)$$

In differential form

$$\frac{dP}{P} = \gamma \frac{d\rho}{\rho}. \quad (13.20)$$

The velocity induced by the acoustic disturbance can also be written in a very general form.

$$U(x, t) = f(x - a_0 t) + g(x + a_0 t) \quad (13.21)$$

Substitute the expressions for r and U into the acoustic equations.

$$\begin{aligned} \frac{\partial}{\partial t} (F(x - a_0 t) + G(x + a_0 t)) + \frac{\partial}{\partial x} (f(x - a_0 t) + g(x + a_0 t)) &= 0 \\ \frac{\partial}{\partial t} (f(x - a_0 t) + g(x + a_0 t)) + a_0^2 \frac{\partial}{\partial x} (F(x - a_0 t) + G(x + a_0 t)) &= 0 \end{aligned} \quad (13.22)$$

Let

$$\begin{aligned} \xi &= x - a_0 t \\ \eta &= x + a_0 t. \end{aligned} \quad (13.23)$$

Equation (13.22) becomes

$$\begin{aligned} -a_0 F_\xi + a_0 G_\eta + f_\xi + g_\eta &= 0 \\ a_0 F_\xi + a_0 G_\eta - f_\xi + g_\eta &= 0. \end{aligned} \quad (13.24)$$

Add and subtract the relations in (13.24)

$$\begin{aligned} -a_0 F_\xi + f_\xi &= 0 \\ a_0 G_\eta + g_\eta &= 0. \end{aligned} \quad (13.25)$$

From (13.25) we can conclude that $g = -a_0 G$; $f = a_0 F$. The result (13.25) gives us the relationship between density and velocity in left and right running waves.

$$U(x, t) = a_0 F(x - a_0 t) - a_0 G(x + a_0 t) \quad (13.26)$$

Now

$$\frac{U}{a_0 r} = \frac{F - G}{F + G}. \quad (13.27)$$

In a right running wave

$$\frac{U}{a_0 r} = 1. \quad (13.28)$$

In a left running wave

$$\frac{U}{a_0 r} = -1. \quad (13.29)$$

In differential form (13.27) is equivalent to

$$\begin{aligned} dU &= \pm a_0 \frac{d\rho}{\rho} \\ \frac{dP}{P} &= \gamma \frac{d\rho}{\rho}. \end{aligned} \quad (13.30)$$

13.4 Isentropic, finite amplitude waves

The speed of sound may vary from one point to another and in a general, 1-D, isentropic flow.

$$a = a_0 \left(\frac{\rho}{\rho_0} \right)^{\frac{\gamma-1}{2}} \quad (13.31)$$

Locally, the particle disturbance velocity is given by (13.30) with the speed of sound regarded as a function of space and time.

$$dU = \pm a \frac{d\rho}{\rho} \quad (13.32)$$

Equation (13.32) is one of the most important equations in unsteady gas dynamics and is often introduced as an intuitively obvious extension of equation (13.30). We can put (13.32)

on a firmer foundation by returning to the full nonlinear equations for one-dimensional, isentropic flow. In one dimension (13.1) becomes

$$\begin{aligned}\frac{\partial \rho}{\partial t} + \rho \frac{\partial U}{\partial x} + U \frac{\partial \rho}{\partial x} &= 0 \\ \frac{\partial U}{\partial t} + U \frac{\partial U}{\partial x} + \frac{\gamma P_0}{\rho_0^2} \left(\frac{\rho}{\rho_0} \right)^{\gamma-2} \frac{\partial \rho}{\partial x} &= 0.\end{aligned}\tag{13.33}$$

Now assume that the density can be written as a function of the velocity.

$$\rho = \rho(U)\tag{13.34}$$

The derivatives of the density are

$$\begin{aligned}\frac{\partial \rho}{\partial t} &= \frac{d\rho}{dU} \frac{\partial U}{\partial t} \\ \frac{\partial \rho}{\partial x} &= \frac{d\rho}{dU} \frac{\partial U}{\partial x}.\end{aligned}\tag{13.35}$$

Substitute (13.35) into (13.33).

$$\begin{aligned}\frac{d\rho}{dU} \frac{\partial U}{\partial t} + \rho \frac{\partial U}{\partial x} + U \frac{d\rho}{dU} \frac{\partial U}{\partial x} &= 0 \\ \frac{\partial U}{\partial t} + U \frac{\partial U}{\partial x} + \frac{\gamma P_0}{\rho_0^2} \left(\frac{\rho}{\rho_0} \right)^{\gamma-2} \frac{d\rho}{dU} \frac{\partial U}{\partial x} &= 0\end{aligned}\tag{13.36}$$

Rearrange (13.36).

$$\begin{aligned}\frac{\partial U}{\partial t} + U \frac{\partial U}{\partial x} + \frac{\rho}{d\rho/dU} \frac{\partial U}{\partial x} &= 0 \\ \frac{\partial U}{\partial t} + U \frac{\partial U}{\partial x} + \frac{\gamma P_0}{\rho_0^2} \left(\frac{\rho}{\rho_0} \right)^{\gamma-2} \frac{d\rho}{dU} \frac{\partial U}{\partial x} &= 0\end{aligned}\tag{13.37}$$

Comparing the continuity and momentum equation in (13.37) we see that in order for (13.34) to be a solution of (13.33) we must have

$$\frac{\rho}{d\rho/dU} = \frac{\gamma P_0}{\rho_0^2} \left(\frac{\rho}{\rho_0} \right)^{\gamma-2} \frac{d\rho}{dU}. \quad (13.38)$$

Equation (13.38) can be rearranged to read

$$\left(\frac{d\rho}{dU} \right)^2 = \frac{\rho_0^2}{a_0^2} \left(\frac{\rho}{\rho_0} \right)^{3-\gamma}. \quad (13.39)$$

Take the square root of (13.39).

$$\frac{d\rho}{dU} = \pm \frac{\rho_0}{a_0} \left(\frac{\rho}{\rho_0} \right)^{\frac{3-\gamma}{2}} \quad (13.40)$$

Now substitute the isentropic relation between the speed of sound and density

$$\frac{a}{a_0} = \left(\frac{\rho}{\rho_0} \right)^{\frac{\gamma-1}{2}} \quad (13.41)$$

into (13.40). Equation (13.40) becomes

$$dU = \pm a \frac{d\rho}{\rho} \quad (13.42)$$

which confirms the general validity of (13.32). Using the isentropic assumption, (13.32) can be integrated from some initial state to a final state.

$$U = \pm \int_{\rho_1}^{\rho} a \frac{d\rho}{\rho} = \pm a_1 \int_{\rho_1}^{\rho} \left(\frac{\rho}{\rho_1} \right)^{\frac{\gamma-1}{2}} \frac{d\rho}{\rho} \quad (13.43)$$

Integrating,

$$U = \pm \frac{2a_1}{\gamma - 1} \left(\left(\frac{\rho}{\rho_1} \right)^{\frac{\gamma-1}{2}} - 1 \right) = \pm \frac{2}{\gamma - 1} (a - a_1). \quad (13.44)$$

The local acoustic speed is

$$a = a_1 \pm \left(\frac{\gamma - 1}{2} \right) U \quad (13.45)$$

and the wave speed at any point is

$$c = a \pm U = a_1 \pm \left(\frac{\gamma - 1}{2} \right) U \pm U = a_1 \pm \left(\frac{\gamma + 1}{2} \right) U. \quad (13.46)$$

13.5 Centered expansion wave

Now consider the situation shown below where a piston is withdrawn from a fluid at rest.

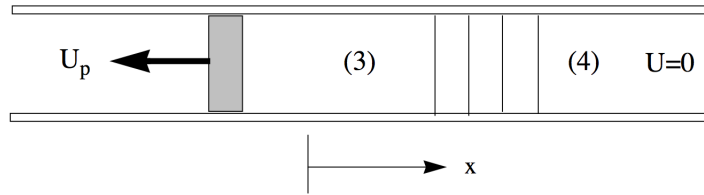


Figure 13.3: Withdrawal of a piston from a compressible gas.

The speed of the fluid in region (3) is equal to the piston speed.

$$U_p = \frac{2}{\gamma - 1} (a_3 - a_4) \quad (13.47)$$

Note that U_p is negative. In effect (13.47) gives us the sound speed in region (3) in terms of the known piston speed and the known speed of sound in region (4).

$$a_3 = a_4 + \left(\frac{\gamma - 1}{2} \right) U_p \quad (13.48)$$

From this we can see that the gas in region (3) is cooler than that in region (4), consistent with what we would expect for an expansion. The front or leading characteristic of the

wave propagates to the right with wave speed equal to the speed of sound $c_4 = a_4$. The tail of the wave (terminating characteristic) moves to the right with wave speed

$$c_3 = a_3 + U_p = a_4 + \left(\frac{\gamma + 1}{2} \right) U_p \quad (13.49)$$

and the expansion zone widens at the rate $(\gamma + 1) |U_p| / 2$. It is useful to visualize this flow in the $x - t$ plane.

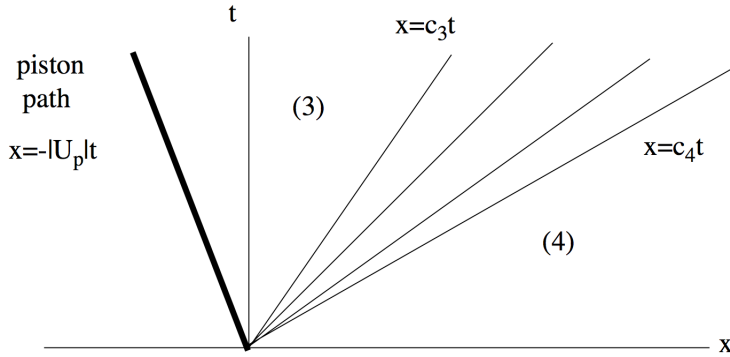


Figure 13.4: Trajectory of a piston and an expansion wave in the x - t plane.

The density ratio across the wave is given by the isentropic relation

$$\frac{\rho_3}{\rho_4} = \left(\frac{a_3}{a_4} \right)^{\frac{2}{\gamma-1}} \quad (13.50)$$

or, using (13.48)

$$\frac{\rho_3}{\rho_4} = \left(1 + \frac{\gamma - 1}{2} \frac{U_p}{a_4} \right)^{\frac{2}{\gamma-1}}. \quad (13.51)$$

The pressure ratio is

$$\frac{P_3}{P_4} = \left(1 + \frac{\gamma - 1}{2} \frac{U_p}{a_4} \right)^{\frac{2\gamma}{\gamma-1}} \quad (13.52)$$

and the temperature ratio is

$$\frac{T_3}{T_4} = \left(\frac{P_3}{P_4} \right)^{\frac{\gamma-1}{\gamma}} = \left(1 + \frac{\gamma-1}{2} \frac{U_p}{a_4} \right)^2. \quad (13.53)$$

In summary, our solution of the small disturbance wave equation from the previous section has allowed us to determine all the properties of a finite expansion wave. Things worked out this way because the expansion wave is isentropic to a high degree of accuracy. Note the similarity between the 1-D unsteady expansion wave and the steady Prandtl-Meyer expansion, and the presence of space-time characteristics in the $x - t$ plane along which the properties of the flow are constant.

13.6 Compression wave

Suppose the piston motion is to the right into the gas. None of the above relations change but the physics does change and this can be seen from the $x - t$ diagram.

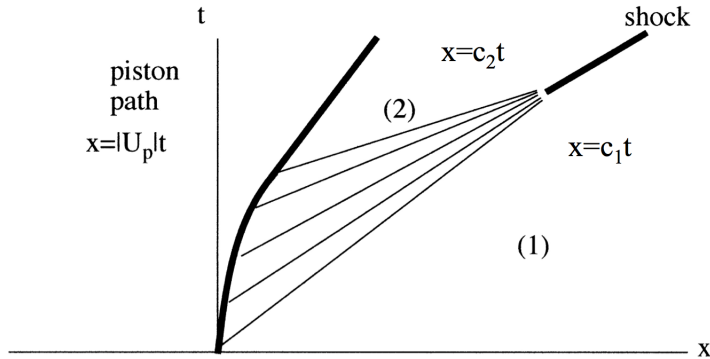


Figure 13.5: *Compression wave converging to a shock in the x - t plane.*

The wave speed at the surface of the piston is

$$c_2 = a_2 + U_p = a_1 + \frac{\gamma+1}{2} U_p. \quad (13.54)$$

In this case the characteristics tend to cross, at which point the isentropic assumption is no longer valid. The system of compression waves catches up to itself (nonlinear steepening) in a very short time collapsing to form a shock wave.

13.7 The shock tube

A very important device used to study shock waves in the laboratory is the shock tube shown schematically in figure 13.6.

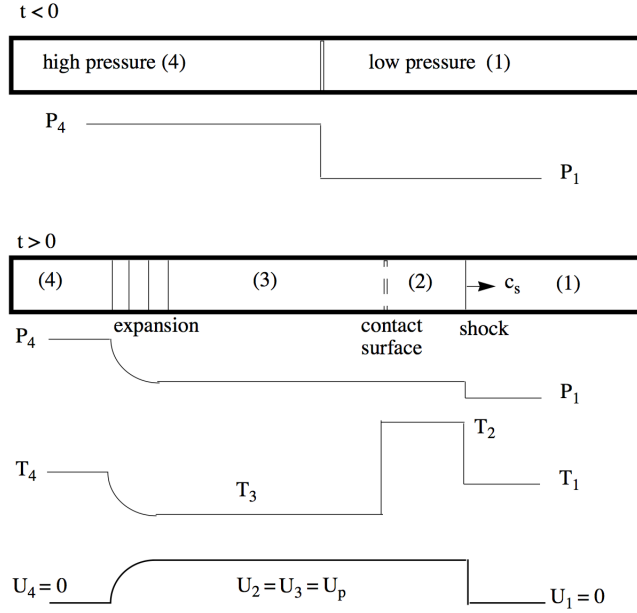


Figure 13.6: Shock tube flow.

Regions (1) and (2) of the shock tube are initially separated into high and low pressure sections by a diaphragm. At $t = 0$ the diaphragm bursts and the high pressure driver gas rushes into the low pressure test gas. The contact surface between the two surfaces acts like a piston and the piston motion produces a shock wave moving at the speed c_s . The shock wave arises through a process of nonlinear steepening based on the fact that the speed of a pressure wave increases with an increase in the temperature of the gas. Pressure waves to the rear of the compression front move more rapidly than those near the front, quickly catching up to form a very thin pressure jump as illustrated in figure 13.5. The important gas-dynamic problem is to determine the pressure ratio across the shock P_2/P_1 for a given choice of gases ($\gamma_1, a_1, \gamma_4, a_4$) and diaphragm pressure ratio P_4/P_1 . In the following we will combine the results for expansion waves with normal shock relations to derive the so-called

shock tube equation. The conditions at the contact surface are

$$\begin{aligned} P_2 &= P_3 \\ U_2 &= U_3 = U_p. \end{aligned} \tag{13.55}$$

where U_2 is the speed of the slug of gas set into motion by the opening of the diaphragm. This is the effective piston speed of the fluid released by the diaphragm.

In a frame of reference moving with the shock wave the gas velocities are

$$\begin{aligned} U'_1 &= -c_s \\ U'_2 &= -c_s + U_p \end{aligned} \tag{13.56}$$

and the shock jump conditions are

$$\begin{aligned} \frac{U'_2}{U'_1} &= \frac{1 + \frac{\gamma_1 - 1}{2} M_1^2}{\frac{\gamma_1 + 1}{2} M_1^2} \\ \frac{P_2}{P_1} &= \frac{\gamma_1 M_1^2 - \frac{\gamma_1 - 1}{2}}{\frac{\gamma_1 + 1}{2}} \end{aligned} \tag{13.57}$$

where $M_1 = c_s/a_1 = -U'_1/a_1$. Using the first relation in (13.57) we can write

$$\frac{U'_2 - U'_1}{U'_1} = \frac{1 + \frac{\gamma_1 - 1}{2} M_1^2}{\frac{\gamma_1 + 1}{2} M_1^2} - 1 = \frac{1 - M_1^2}{\frac{\gamma_1 + 1}{2} M_1^2}. \tag{13.58}$$

The piston velocity is

$$U_p = U'_2 - U'_1 = U'_1 \left(\frac{1 - M_1^2}{\frac{\gamma_1 + 1}{2} M_1 \left(-\frac{U'_1}{a_1} \right)} \right) = a_1 \left(\frac{M_1^2 - 1}{\frac{\gamma_1 + 1}{2} M_1} \right). \tag{13.59}$$

Note that U_p is positive. Using the second relation in (13.57), equation (13.59) can be expressed in terms of the shock pressure ratio as

$$U_p = a_1 \left(\frac{P_2}{P_1} - 1 \right) \left(\frac{2}{\gamma_1 (\gamma_1 + 1) \left(\frac{P_2}{P_1} \right) + \gamma_1 (\gamma_1 - 1)} \right)^{1/2}. \tag{13.60}$$

Equation (13.60) is the expression for the piston velocity derived using normal shock theory. Now let's work out an expression for the piston velocity using isentropic expansion theory. The velocity behind the expansion is

$$U_3 = U_p = \frac{2a_4}{\gamma_4 - 1} \left(1 - \left(\frac{P_3}{P_4} \right)^{\frac{\gamma_4 - 1}{2\gamma_4}} \right). \quad (13.61)$$

Equate (13.60) and (13.61).

$$a_1 \left(\frac{P_2}{P_1} - 1 \right) \left(\frac{2}{\gamma_1 (\gamma_1 + 1) \left(\frac{P_2}{P_1} \right) + \gamma_1 (\gamma_1 - 1)} \right)^{1/2} = \frac{2a_4}{\gamma_4 - 1} \left(1 - \left(\frac{P_3 P_2 P_1}{P_2 P_1 P_4} \right)^{\frac{\gamma_4 - 1}{2\gamma_4}} \right) \quad (13.62)$$

Using the following identity

$$\frac{P_3}{P_4} = \frac{P_3 P_2 P_1}{P_2 P_1 P_4} \quad (13.63)$$

and noting that $P_3/P_2 = 1$ solve (13.61) for $P_4/P_1 = 1$. The result is the basic shock tube equation

$$\frac{P_4}{P_1} = \frac{P_2}{P_1} \left(1 - \frac{(\gamma_4 - 1) \left(\frac{a_1}{a_4} \right) \left(\frac{P_2}{P_1} - 1 \right)}{\left(4\gamma_1^2 + 2\gamma_1 (\gamma_1 + 1) \left(\frac{P_2}{P_1} - 1 \right) \right)^{1/2}} \right)^{-\left(\frac{2\gamma_4}{\gamma_4 - 1} \right)} \quad (13.64)$$

plotted in figure 13.7. Given $(P_4/P_1, \gamma_1, \gamma_4, a_1, a_4)$ we can determine the shock strength P_2/P_1 from (13.64).

Once the shock strength is determined, the shock Mach number can be determined from

$$\frac{P_2}{P_1} = \frac{2\gamma_1}{\gamma_1 + 1} M_s^2 - \left(\frac{\gamma_1 - 1}{\gamma_1 + 1} \right) \quad (13.65)$$

or

$$M_s^2 = \frac{\gamma_1 + 1}{2\gamma_1} \left(\frac{P_2}{P_1} + \frac{\gamma_1 - 1}{\gamma_1 + 1} \right). \quad (13.66)$$

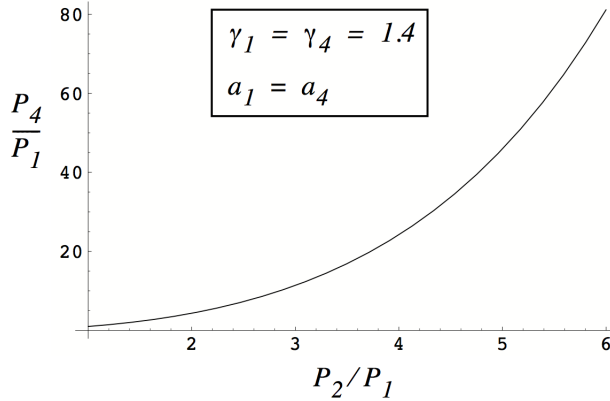


Figure 13.7: Shock tube pressure ratio versus shock strength.

Notice that very large values of P_4/P_1 are required to generate strong shocks. One way to improve the performance of the shock tube is to select a driver gas with a large speed of sound. Helium driving into nitrogen will produce a much stronger shock wave than say Argon driving into nitrogen at a given P_4/P_1 . In essence Helium provides a much lighter piston that can translate much more rapidly into the test gas. The figure below provides this comparison.

Hydrogen as the driver gas produces the strongest shock waves however the fire and explosion hazard involved has limited its use.

13.7.1 Example - flow induced by the shock in a shock tube

The flow in a shock tube is shown below.

The shock wave induces a gas velocity in the laboratory frame, $U_p = U_2 = U_3$ where

$$U_2 = a_1 \left(\frac{P_2}{P_1} - 1 \right) \left(\frac{2}{\gamma_1(\gamma_1 + 1) \left(\frac{P_2}{P_1} \right) + \gamma_1(\gamma_1 - 1)} \right)^{1/2}. \quad (13.67)$$

Suppose the gas in the driver section and test section is Air initially at 300 K. A shock wave with a Mach number of 2 is produced in the tube.

- 1) Determine the stagnation temperature of the gas in region (2) in the laboratory frame.
- 2) Determine the stagnation temperature of the gas in region (3) in the laboratory frame.

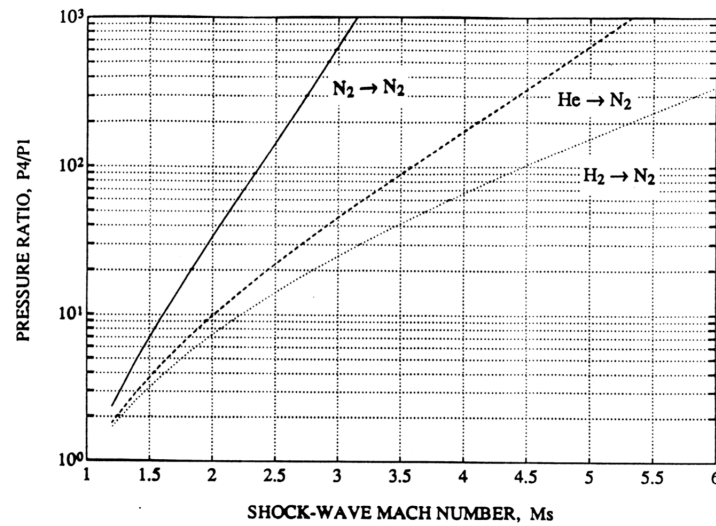


Figure 13.8: Shock Mach number for several driver gases.

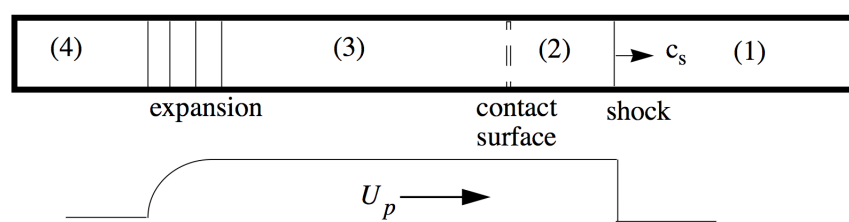


Figure 13.9: Flow induced in a shock tube.

Answer

The pressure ratio across a Mach number 2 shock in air is

$$\frac{P_2}{P_1} = 4.5 \quad (13.68)$$

and the temperature ratio is

$$\frac{T_2}{T_1} = 1.687. \quad (13.69)$$

The speed of sound in air is $a_1 = \sqrt{\gamma RT} = 347\text{m/sec}$ and the heat capacity at constant pressure is, $C_p = 1005\text{m}^2/\text{sec}^2 - K$. The piston velocity is

$$U_2 = a_1 \left(\frac{P_2}{P_1} - 1 \right) \left(\frac{2}{\gamma_1(\gamma_1 + 1) \left(\frac{P_2}{P_1} \right) + \gamma_1(\gamma_1 - 1)} \right)^{1/2} = .$$

$$347 \times 3.5 \times \left(\frac{2}{15.68} \right)^{1/2} = 433.75 \text{ m/sec}$$
(13.70)

The temperature in region (3) is obtained from (13.53).

$$\frac{T_3}{T_4} = \left(1 + \frac{\gamma - 1}{2} \frac{U_p}{a_4} \right)^2 = \left(1 - 0.2 \left(\frac{433.75}{347} \right) \right)^2 = 0.5625 \quad (13.71)$$

Now, in region (2)

$$T_{t2} = T_2 + \frac{1}{2} \frac{U_p^2}{C_p} = 1.687 \times 300 + \frac{433.75^2}{2 \times 1005} = 506.1 + 93.6 = 599.7 K \quad (13.72)$$

and in region (3)

$$T_{t3} = T_3 + \frac{1}{2} \frac{U_p^2}{C_p} = 0.5625 \times 300 + \frac{433.75^2}{2 \times 1005} = 168.75 + 93.6 = 262.35 K. \quad (13.73)$$

13.8 Problems

Problem 1 - Consider the expression ρU^n , $n = 1$ corresponds to the mass flux, $n = 2$ corresponds to the momentum flux and $n = 3$ corresponds to the energy flux of a compressible gas. Use the acoustic relation

$$dU = \pm a \frac{d\rho}{\rho} \quad (13.74)$$

to determine the Mach number (as a function of n) at which ρU^n is a maximum in a one-dimensional, unsteady expansion wave. The steady case is considered in one of the problems at the end of Chapter 9.

Problem 2 - In the shock tube example discussed above, determine the stagnation pressure of the gas in regions (2) and (3). Determine the stagnation pressure in both the laboratory frame and in the frame of reference moving with the shock wave.

Problem 3 - Figure 13.10 below shows a sphere moving over a flat plate in a ballistic range. The sphere has been fired from a gun and is translating to the left at a Mach number of 3. The static temperature of the air upstream of the sphere is 300 K and the pressure is one atmosphere. On the plane of symmetry of the flow (the plane of the photo) the shock intersects the plate at an angle of 25 degrees as indicated.

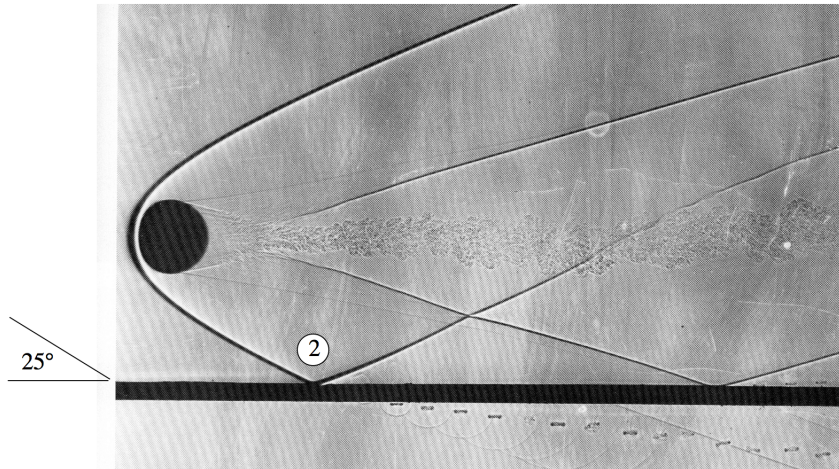


Figure 13.10: *Sphere moving supersonically over a flat plate.*

- i) Determine the flow Mach number, speed and angle behind the shock in region 2 close to the intersection with the plate. Work out your results in a frame of reference moving with

the sphere. In this frame the upstream air is moving to the right at 3 times the speed of sound.

- ii) What are the stream-wise and plate normal velocity components of the flow in region 2 referred to a frame of reference at rest with respect to the upstream gas.
- iii) Determine the stagnation temperature and pressure of the flow in region 2 referred to a frame of reference at rest with respect to the upstream gas.

Problem 4 - We normally think of the shock tube as a device that can be used to study relatively strong shock waves. But shock tubes have also been used to study weak shocks relevant to the sonic boom problem. Suppose the shock tube is used to generate weak shock waves with $P_2/P_1 = 1 + \varepsilon$. Show that for small ε the relationship between P_2/P_1 and P_4/P_1 is approximated by

$$\frac{P_4}{P_1} = 1 + A\varepsilon. \quad (13.75)$$

How does A depend on the properties of the gases in regions 1 and 4? Use the exact theory to determine the strength of a shock wave generated in an air-air shock tube operated at $P_4/P_1 = 1.2$. Compare with the approximate result.

Problem 5 - The sketch below shows a one meter diameter tube filled with air and divided into two volumes by a heavy piston of weight W . The piston is held in place by a mechanical stop and the pressure and temperature are uniform throughout the tube at one atmosphere and 300K. Body force effects in the gas may be neglected.

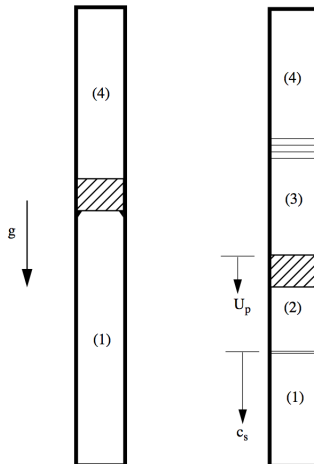


Figure 13.11: *Gravity driven frictionless piston in a shock tube.*

The piston is released and accelerates downward due to gravity. After a short transient the piston reaches a constant velocity U_p . The piston drives a shock wave ahead of it at a wave speed c_s equal to twice the sound speed in region 1. What is the weight of the piston?

Problem 6 - Each time Stanford makes a touchdown an eight inch diameter, open ended shock tube is used to celebrate the score. Suppose the shock wave developed in the tube is required to have a pressure ratio of 2. What pressure is needed in the driver section? Assume the driver gas is air. What is the shock Mach number? Suppose the shock tube is mounted vertically on a cart as shown in figure 13.12 below. Estimate the force that the cart must withstand when the tube fires.

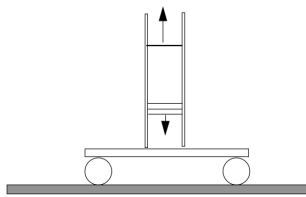


Figure 13.12: Shock tube mounted on a cart.

Problem 7 - In figure 13.13 a moveable piston sits in the middle of a long tube filled with air at one atmosphere and 300 K. At time zero the piston is moved impulsively to the right at $U_p = 200 \text{ m/sec}$.

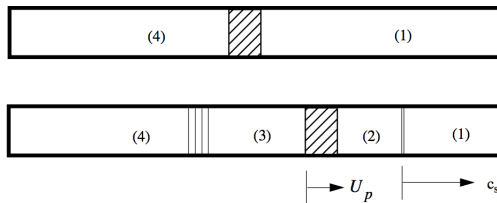


Figure 13.13: Frictionless piston in a shock tube.

- 1) What is the pressure on the right face of the piston (region 2) in atmospheres?
- 2) What is the pressure on the left face of the piston (region 3) in atmospheres?

Problem 8 - One of the most versatile instruments used in the study of fluid flow is the shock tube. It can even be used as a wind tunnel as long as one is satisfied with short test times. Figure 13.14 below illustrates the idea. An airfoil is placed in the shock tube and after the passage of the shock it is subject to flow of the test gas at constant velocity U_p and temperature T_2 . In a real experiment the contact surface is quite turbulent and so the

practical usefulness of the flow is restricted to the time after the arrival of the shock and before the arrival of the contact surface, typically a millisecond or so.

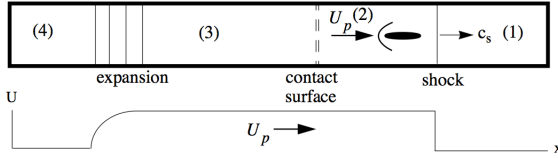


Figure 13.14: Shock tube used as a wind tunnel.

Proponents of this idea point out that if the shock Mach number is very large the flow over the body can be supersonic as suggested in the sketch above.

- 1) Show that this is the case.
- 2) For very large shock Mach number, which test gas would produce a higher Mach number over the body, helium or air. Estimate the Mach number over the body for each gas.

Problem 9 - Figure 13.15 below shows a shock wave reflecting from the endwall of a shock tube. The reflected shock moves to the left at a constant speed c_{rs} into the gas that was compressed by the incident shock. The gas behind the reflected shock, labeled region (5), is at rest and at a substantially higher temperature and pressure than it was in state (1) before the arrival of the incident shock.

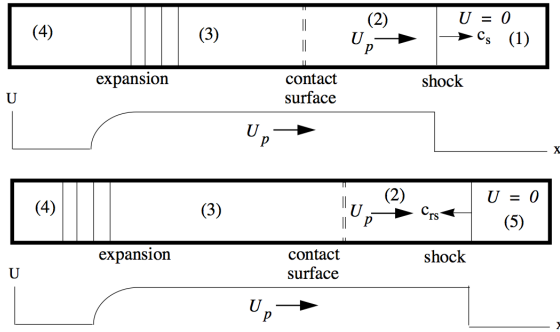


Figure 13.15: Shock wave reflecting from an end wall.

- 1) Suppose the gas in the driver and test sections is helium at an initial temperature of 300K prior to opening the diaphragm. The Mach number of the incident shock wave is 3. Determine the Mach number of the reflected shock.
- 2) Determine T_5/T_1 .

Problem 10 - One of the key variables in the design of a shock tube is the length needed for a shock to develop from the initial compression process. Suppose a piston is used to compress a gas initially at rest in a tube. During the startup transient $0 < t < t_1$ the piston speed increases linearly with time as shown on the $x - t$ diagram in figure 13.16.

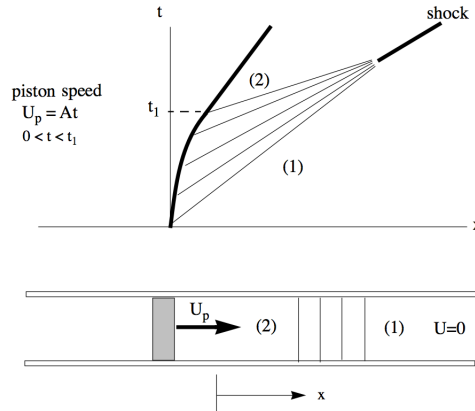


Figure 13.16: *Piston compressing air.*

In a shock tube the startup time t_1 is generally taken to be the time required for the diaphragm to open. Let the gas be air at $T_1 = 300 K$. Use $t_1 = 5 \times 10^{-3} \text{ sec}$ and $A = 4 \times 10^4 \text{ m/sec}^2$ to estimate the distance needed for the shock wave to form.

Chapter 14

Thin airfoil theory

14.1 Compressible potential flow

14.1.1 The full potential equation

In compressible flow, both the lift and drag of a thin airfoil can be determined to a reasonable level of accuracy from an inviscid, irrotational model of the flow. Recall the equations developed in Chapter 6 governing steady, irrotational, homentropic ($\nabla s = 0$) flow in the absence of body forces.

$$\begin{aligned}\nabla(\rho\bar{U}) &= 0 \\ \nabla\left(\frac{\bar{U} \cdot \bar{U}}{2}\right) + \frac{\nabla P}{\rho} &= 0 \\ \frac{P}{P_0} &= \left(\frac{\rho}{\rho_0}\right)^\gamma\end{aligned}\tag{14.1}$$

The gradient of the isentropic relation is

$$\nabla P = a^2 \nabla \rho.\tag{14.2}$$

Recall from the development in Chapter 6 that

$$\nabla\left(\frac{P}{\rho}\right) = \left(\frac{\gamma - 1}{\gamma}\right) \frac{\nabla P}{\rho}.\tag{14.3}$$

Using (14.3) the momentum equation becomes

$$\nabla \left(\left(\frac{\gamma}{\gamma - 1} \right) \frac{P}{\rho} + \frac{\bar{U} \cdot \bar{U}}{2} \right) = 0. \quad (14.4)$$

Substitute (14.2) into the continuity equation and use (14.3). The continuity equation becomes

$$\bar{U} \cdot \nabla a^2 + (\gamma - 1) a^2 \nabla \cdot \bar{U} = 0. \quad (14.5)$$

Equate the Bernoulli integral to free stream conditions.

$$\frac{a^2}{\gamma - 1} + \frac{\bar{U} \cdot \bar{U}}{2} = \frac{a_\infty^2}{\gamma - 1} + \frac{U_\infty^2}{2} = \frac{a_\infty^2}{\gamma - 1} \left(1 + \frac{\gamma - 1}{2} M_\infty^2 \right) = C_p T_t \quad (14.6)$$

Note that the momentum equation is essentially equivalent to the statement that the stagnation temperature T_t is constant throughout the flow. Using (14.6) we can write

$$\frac{a^2}{\gamma - 1} = h_t - \frac{\bar{U} \cdot \bar{U}}{2}. \quad (14.7)$$

The continuity equation finally becomes

$$(\gamma - 1) \left(h_t - \frac{\bar{U} \cdot \bar{U}}{2} \right) \nabla \cdot \bar{U} - \bar{U} \cdot \nabla \left(\frac{\bar{U} \cdot \bar{U}}{2} \right) = 0. \quad (14.8)$$

The equations governing compressible, steady, inviscid, irrotational motion reduce to a single equation for the velocity vector \mathbf{U} . The irrotationality condition $\nabla \times \bar{U} = 0$ permits the introduction of a velocity potential.

$$\bar{U} = \nabla \Phi \quad (14.9)$$

and (14.8) becomes

$$(\gamma - 1) \left(h_t - \frac{\nabla \Phi \cdot \nabla \Phi}{2} \right) \nabla^2 \Phi - \nabla \Phi \cdot \nabla \left(\frac{\nabla \Phi \cdot \nabla \Phi}{2} \right) = 0. \quad (14.10)$$

For complex body shapes numerical methods are normally used to solve for Φ . However the equation is of relatively limited applicability. If the flow is over a thick airfoil or a bluff

body for instance then the equation only applies to the subsonic Mach number regime at Mach numbers below the range where shocks begin to appear on the body. At high subsonic and supersonic Mach numbers where there are shocks then the homentropic assumption (14.2) breaks down. Equation (14.8) also applies to internal flows without shocks such as fully expanded nozzle flow.

14.1.2 The nonlinear small disturbance approximation

In the case of a thin airfoil that only slightly disturbs the flow, equation (14.8) can be simplified using small disturbance theory. Consider the flow past a thin 3-D airfoil shown in Figure 14.1.

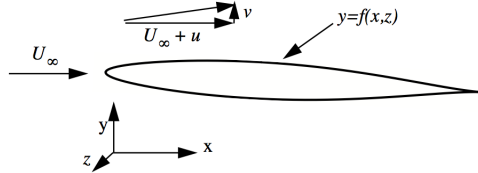


Figure 14.1: Flow past a thin 3-D airfoil

The velocity field consists of a free-stream flow plus a small disturbance

$$\begin{aligned}\bar{U} &= U_{\infty} + u \\ V &= v \\ W &= w\end{aligned}\tag{14.11}$$

where

$$\begin{aligned}\frac{u}{U_{\infty}} &<< 1 \\ \frac{v}{U_{\infty}} &<< 1 \\ \frac{w}{U_{\infty}} &<< 1.\end{aligned}\tag{14.12}$$

Similarly the state variables deviate only slightly from free-stream values

$$\begin{aligned} P &= P_\infty + P' \\ T &= T_\infty + T' \\ \rho &= \rho_\infty + \rho' \end{aligned} \tag{14.13}$$

and

$$a = a_\infty + a'. \tag{14.14}$$

This decomposition of variables is substituted into equation (14.8). Various terms are

$$\begin{aligned} \frac{\bar{U} \cdot \bar{U}}{2} &= \frac{U_\infty^2}{2} + uU_\infty + \frac{u^2}{2} + \frac{v^2}{2} + \frac{w^2}{2} \\ \nabla \cdot \bar{U} &= u_x + v_y + w_z \end{aligned} \tag{14.15}$$

and

$$\nabla \left(\frac{\bar{U} \cdot \bar{U}}{2} \right) = (u_x U_\infty + uu_x + vv_x + ww_x, u_y U_\infty + uu_y + vv_y + ww_y, u_z U_\infty + uu_z + vv_z + ww_z) \tag{14.16}$$

as well as

$$\begin{aligned} (\gamma - 1) \left(h_t - \frac{\bar{U} \cdot \bar{U}}{2} \right) \nabla \cdot \bar{U} &= \\ (\gamma - 1) \left(h_t - \left(\frac{U_\infty^2}{2} + uU_\infty + \frac{u^2}{2} + \frac{v^2}{2} + \frac{w^2}{2} \right) \right) u_x &+ \\ (\gamma - 1) \left(h_t - \left(\frac{U_\infty^2}{2} + uU_\infty + \frac{u^2}{2} + \frac{v^2}{2} + \frac{w^2}{2} \right) \right) u_y &+ \\ (\gamma - 1) \left(h_t - \left(\frac{U_\infty^2}{2} + uU_\infty + \frac{u^2}{2} + \frac{v^2}{2} + \frac{w^2}{2} \right) \right) u_z & \end{aligned} \tag{14.17}$$

and, finally

$$\begin{aligned}
 & (\gamma - 1) \left(h_t - \frac{\bar{U} \cdot \bar{U}}{2} \right) \nabla \cdot \bar{U} - \bar{U} \cdot \nabla \left(\frac{\bar{U} \cdot \bar{U}}{2} \right) \cong \\
 & (\gamma - 1) \left(h_t - \left(\frac{U_\infty^2}{2} + uU_\infty \right) \right) u_x + \\
 & (\gamma - 1) \left(h_t - \left(\frac{U_\infty^2}{2} + uU_\infty \right) \right) v_y + \\
 & (\gamma - 1) \left(h_t - \left(\frac{U_\infty^2}{2} + uU_\infty \right) \right) w_z - \\
 & (u_x U_\infty^2 + uu_x U_\infty + vv_x U_\infty + ww_x U_\infty) - \\
 & uu_x U_\infty - vu_y U_\infty - wu_z U_\infty.
 \end{aligned} \tag{14.18}$$

Neglect terms in (14.17) and (14.18) that are of third order in the disturbance velocities. Now

$$\begin{aligned}
 & (\gamma - 1) \left(h_t - \frac{\bar{U} \cdot \bar{U}}{2} \right) \nabla \cdot \bar{U} - \bar{U} \cdot \nabla \left(\frac{\bar{U} \cdot \bar{U}}{2} \right) \cong \\
 & (\gamma - 1) \left(h_t - \left(\frac{U_\infty^2}{2} + uU_\infty \right) \right) u_x + \\
 & (\gamma - 1) \left(h_t - \left(\frac{U_\infty^2}{2} + uU_\infty \right) \right) v_y + \\
 & (\gamma - 1) \left(h_t - \left(\frac{U_\infty^2}{2} + uU_\infty \right) \right) w_z - \\
 & (u_x U_\infty^2 + uu_x U_\infty + vv_x U_\infty + ww_x U_\infty) - \\
 & uu_x U_\infty - vu_y U_\infty - wu_z U_\infty
 \end{aligned} \tag{14.19}$$

or

$$\begin{aligned}
 & (\gamma - 1) \left(h_t - \frac{\bar{U} \cdot \bar{U}}{2} \right) \nabla \cdot \bar{U} - \bar{U} \cdot \nabla \left(\frac{\bar{U} \cdot \bar{U}}{2} \right) \cong \\
 & (\gamma - 1) (h_\infty - u U_\infty) (u_x + v_y + w_z) - \\
 & (u_x U_\infty^2 + uu_x U_\infty + vv_x U_\infty + ww_x U_\infty) - \\
 & uu_x U_\infty - vu_y U_\infty - wu_z U_\infty.
 \end{aligned} \tag{14.20}$$

Recall that $(\gamma - 1) h_\infty = a_\infty^2$. Equation (14.20) can be rearranged to read

$$\begin{aligned}
 & (\gamma - 1) \left(h_t - \frac{\bar{U} \cdot \bar{U}}{2} \right) \nabla \cdot \bar{U} - \bar{U} \cdot \nabla \left(\frac{\bar{U} \cdot \bar{U}}{2} \right) \cong \\
 & a_\infty^2 (u_x + v_y + w_z) - u_x U_\infty^2 - (\gamma + 1) uu_x U_\infty - (vv_x U_\infty + ww_x U_\infty) - \\
 & (\gamma - 1) (uv_y U_\infty + uw_z U_\infty) - vu_y U_\infty - wu_z U_\infty.
 \end{aligned} \tag{14.21}$$

Divide through by a_∞^2 .

$$\begin{aligned}
 & \left(\frac{\gamma - 1}{a_\infty^2} \right) \left(h_t - \frac{\bar{U} \cdot \bar{U}}{2} \right) \nabla \cdot \bar{U} - \left(\frac{1}{a_\infty^2} \right) \bar{U} \cdot \nabla \left(\frac{\bar{U} \cdot \bar{U}}{2} \right) \cong \\
 & (1 - M_\infty^2) u_x + v_y + w_z - \frac{(\gamma + 1) M_\infty}{a_\infty} uu_x - \\
 & \frac{M_\infty}{a_\infty} ((\gamma - 1) (uv_y + uw_z) + vu_y + wu_z + vv_x + ww_x)
 \end{aligned} \tag{14.22}$$

Equation (14.22) contains both linear and quadratic terms in the velocity disturbances and one might expect to be able to neglect the quadratic terms. But note that the first term becomes very small near $M_\infty = 1$. Thus in order to maintain the small disturbance approximation at transonic Mach numbers the uu_x term must be retained. The remaining quadratic terms are small at all Mach numbers and can be dropped. Finally the small disturbance equation is

$$(1 - M_\infty^2) u_x + v_y + w_z - \frac{(\gamma + 1) M_\infty}{a_\infty} uu_x = 0. \tag{14.23}$$

The velocity potential is written in terms of a free-stream potential and a disturbance potential.

$$\Phi = U_\infty x + \phi(x, y, z) \quad (14.24)$$

The small disturbance equation in terms of the disturbance potential is

$$(1 - M_\infty^2) \phi_{xx} + \phi_{yy} + \phi_{zz} = \frac{(\gamma + 1) M_\infty}{a_\infty} \phi_x \phi_{xx}. \quad (14.25)$$

Equation (14.25) is valid over the whole range of subsonic, transonic and supersonic Mach numbers.

14.1.3 Linearized potential flow

If we restrict our attention to subsonic and supersonic flow, staying away from Mach numbers close to one, the nonlinear term on the right side of (14.25) can be dropped and the small disturbance potential equation reduces to the linear wave equation

$$\beta^2 \phi_{xx} - (\phi_{yy} + \phi_{zz}) = 0 \quad (14.26)$$

where $\beta = \sqrt{M_\infty^2 - 1}$. In two dimensions

$$\beta^2 \phi_{xx} - \phi_{yy} = 0. \quad (14.27)$$

The general solution of (14.27) can be expressed as a sum of two arbitrary functions

$$\phi(x, y) = F(x - \beta y) + G(x + \beta y). \quad (14.28)$$

Note that if $M_\infty^2 < 1$ the 2-D linearized potential equation (14.27) is an elliptic equation that can be rescaled to form Laplace's equation and (14.28) expresses the solution in terms of conjugate complex variables. In this case the subsonic flow can be analyzed using the methods of complex analysis. Presently we will restrict our attention to the supersonic case. The subsonic case is treated later in the chapter.

If $M_\infty^2 > 1$ then (14.27) is the 2-D wave equation and has solutions of hyperbolic type. Supersonic flow is analyzed using the fact that the properties of the flow are constant along the characteristic lines $x \pm \beta y = \text{constant}$. Figure 14.2 illustrates supersonic flow past a

thin airfoil with several characteristics shown. Notice that in the linear approximation the characteristics are all parallel to one another and lie at the Mach angle μ_∞ of the free stream. Information about the flow is carried in the value of the potential assigned to a given characteristic and in the spacing between characteristics for a given flow change. Right-leaning characteristics carry the information about the flow on the upper surface of the wing and left-leaning characteristics carry information about the flow on the lower surface.

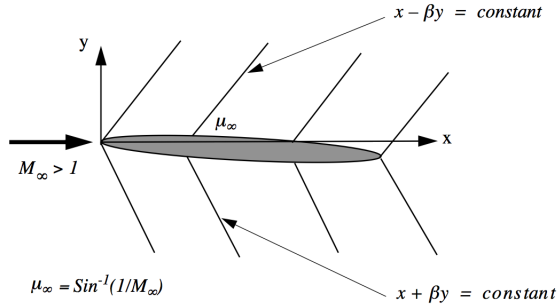


Figure 14.2: Right and left leaning characteristics on a thin 2-D airfoil.

All properties of the flow, velocity, pressure, temperature, etc. are constant along the characteristics. Since disturbances only propagate along downstream running characteristics we can write the velocity potential for the upper and lower surfaces as

$$\begin{aligned}\phi(x, y) &= F(x - \beta y) & y > 0 \\ \phi(x, y) &= G(x + \beta y) & y < 0.\end{aligned}\tag{14.29}$$

Let $y = f(x)$ define the coordinates of the upper surface of the wing and $y = g(x)$ define the lower surface. The full nonlinear boundary condition on the upper surface is

$$\frac{v}{U} \Big|_{y=f} = \frac{df}{dx}.\tag{14.30}$$

In the spirit of the thin airfoil approximation this boundary condition can be approximated by the linearized form

$$\frac{v}{U} \Big|_{y=0} = \frac{df}{dx}\tag{14.31}$$

which we can write as

$$\frac{\partial \phi(x, y)}{\partial y} \Big|_{y=0} = U_\infty \frac{df}{dx} \quad (14.32)$$

or

$$F'(x) = -\frac{U_\infty}{\beta} \frac{df}{dx}. \quad (14.33)$$

On the lower surface the boundary condition is

$$G'(x) = \frac{U_\infty}{\beta} \frac{dg}{dx}. \quad (14.34)$$

In the thin airfoil approximation the airfoil itself is, in effect, collapsed to a line along the x -axis, the velocity potential is extended to the line $y = 0$ and the surface boundary condition is applied at $y = 0$ instead of at the physical airfoil surface. The entire effect of the airfoil on the flow is accounted for by the vertical velocity perturbation generated by the local slope of the wing. The linearized boundary condition is valid on 2-D thin wings and on 3-D wings of that are of "thin planar form".

Recall that (14.26) is only valid for subsonic and supersonic flow and not for transonic flow where $1 - M_\infty^2 \ll 1$.

14.1.4 The pressure coefficient

Let's work out the linearized pressure coefficient. The pressure coefficient is

$$C_P = \frac{P - P_\infty}{\frac{1}{2} \rho_\infty U_\infty^2} = \frac{2}{\gamma M_\infty^2} \left(\frac{P}{P_\infty} - 1 \right). \quad (14.35)$$

The stagnation enthalpy is constant throughout the flow. Thus

$$\frac{T}{T_\infty} = 1 + \frac{1}{2C_p T_\infty} (U_\infty^2 - (U^2 + v^2 + w^2)). \quad (14.36)$$

Similarly the entropy is constant and so the pressure and temperature are related by

$$\frac{P}{P_\infty} = \left(1 + \frac{1}{2C_p T_\infty} (U_\infty^2 - (U^2 + v^2 + w^2)) \right)^{\frac{\gamma}{\gamma-1}}. \quad (14.37)$$

The pressure coefficient is

$$C_P = \frac{2}{\gamma M_\infty^2} \left(\left(1 + \frac{1}{2C_p T_\infty} (U_\infty^2 - (U^2 + v^2 + w^2)) \right)^{\frac{\gamma}{\gamma-1}} - 1 \right). \quad (14.38)$$

The velocity term in (14.37) is small.

$$U_\infty^2 - (U^2 + v^2 + w^2) = - (2uU_\infty + u^2 + v^2 + w^2) \quad (14.39)$$

Now use the binomial expansion $(1 - \varepsilon)^n \cong 1 - n\varepsilon + n(n-1)\varepsilon^2/2$ to expand the term in parentheses in (14.39). Note that the expansion has to be carried out to second order. The pressure coefficient is approximately

$$C_P \cong - \left(\frac{2u}{U_\infty} + (1 - M_\infty^2) \frac{u^2}{U_\infty^2} + \frac{v^2 + w^2}{U_\infty^2} \right). \quad (14.40)$$

Equation (14.40) is a valid approximation for small perturbations in subsonic or supersonic flow.

For 2-D flows over planar bodies it is sufficient to retain only the first term in (14.40) and we use the expression

$$C_P \cong -2 \frac{u}{U_\infty}. \quad (14.41)$$

For 3-D flows over slender approximately axisymmetric, bodies we must retain the last term so

$$C_P \cong - \left(\frac{2u}{U_\infty} + \frac{v^2 + w^2}{U_\infty^2} \right). \quad (14.42)$$

As was discussed above, if the airfoil is a 2-D shape defined by the function $y = f(x)$ the boundary condition at the surface is

$$\frac{df}{dx} = \frac{v}{U_\infty + u} = \tan(\theta) \quad (14.43)$$

where θ is the angle between the airfoil surface and the horizontal. For a thin airfoil this is accurately approximated by

$$\frac{df}{dx} \cong \frac{\phi_y}{U_\infty} \cong \theta. \quad (14.44)$$

For a thin airfoil in *supersonic flow* the wall pressure coefficient is

$$C_{P_{wall}} = \frac{2}{(M_\infty^2 - 1)^{1/2}} \left(\frac{df}{dx} \right) \quad (14.45)$$

where $dU^2/U^2 = - \left(2/\sqrt{M_\infty^2 - 1} \right) d\theta$, which is valid for $M_\infty \geq 1$ has been used. In the thin airfoil approximation in supersonic flow the local pressure coefficient is determined by the local slope of the wing. Figure 14.3 schematically shows the wall pressure coefficient on a thin, symmetric biconvex wing.

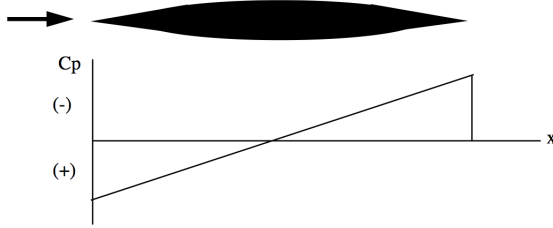


Figure 14.3: Pressure distribution on a thin symmetric airfoil.

This airfoil will have shock waves at the leading and trailing edges and at first sight this would seem to violate the isentropic assumption. But for small disturbances the shocks are weak and the entropy changes are negligible.

14.1.5 Drag coefficient of a thin symmetric airfoil

A thin, 2-D, symmetric airfoil is situated in a supersonic stream at Mach number M_∞ and zero angle of attack. The y-coordinate of the upper surface of the airfoil is given by the function

$$y(x) = A \sin \left(\frac{\pi x}{C} \right) \quad (14.46)$$

where C is the airfoil chord. The airfoil thickness to chord ratio is small, $2A/C \ll 1$. Determine the drag coefficient of the airfoil.

Solution

The drag integral is

$$D = 2 \int_0^C (P - P_\infty) \sin(\alpha) dx. \quad (14.47)$$

where the factor of 2 accounts for the drag of both the upper and lower surfaces and α is the local angle formed by the upper surface tangent to the airfoil and the x -axis. Since the airfoil is thin the angle is small and we can write the drag coefficient as

$$C_D = \frac{D}{\frac{1}{2} \rho_\infty U_\infty^2 C} = 2 \int_0^1 \left(\frac{P - P_\infty}{\frac{1}{2} \rho_\infty U_\infty^2} \right) (\alpha) d\left(\frac{x}{C}\right). \quad (14.48)$$

The local tangent is determined by the local slope of the airfoil therefore $\tan(\alpha) = dy/dx$ and for small angles $\alpha = dy/dx$. Now the drag coefficient is

$$C_D = \frac{D}{\frac{1}{2} \rho_\infty U_\infty^2 C} = 2 \int_0^1 \left(\frac{P - P_\infty}{\frac{1}{2} \rho_\infty U_\infty^2} \right) \left(\frac{dy}{dx} \right) d\left(\frac{x}{C}\right). \quad (14.49)$$

The pressure coefficient on the airfoil is given by thin airfoil theory (14.45) as

$$C_P = \frac{P - P_\infty}{\frac{1}{2} \rho_\infty U_\infty^2} = \frac{2}{\sqrt{M_\infty^2 - 1}} \left(\frac{dy}{dx} \right) \quad (14.50)$$

and so the drag coefficient becomes

$$C_D = \frac{4}{\sqrt{M_\infty^2 - 1}} \int_0^1 \left(\frac{dy}{dx} \right)^2 d\left(\frac{x}{C}\right) = \frac{4A^2 \pi}{C^2 \sqrt{M_\infty^2 - 1}} \int_0^1 \cos^2 \left(\frac{\pi x}{C} \right) d\left(\frac{\pi x}{C}\right) = \frac{2A^2 \pi^2}{C^2 \sqrt{M_\infty^2 - 1}}. \quad (14.51)$$

The drag coefficient is proportional to the square of the wing thickness-to-chord ratio.

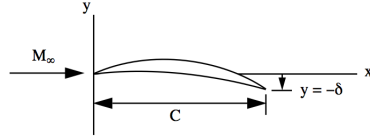


Figure 14.4: Thin cambered 2-D airfoil.

14.1.6 Thin airfoil with lift and camber at a small angle of attack

A thin, cambered, 2-D, airfoil is situated in a supersonic stream at Mach number M_∞ and a small angle of attack as shown in Figure 14.4.

The y -coordinate of the upper surface of the airfoil is given by the function

$$f\left(\frac{x}{C}\right) = A\tau\left(\frac{x}{C}\right) + B\sigma\left(\frac{x}{C}\right) - \frac{\delta x}{C} \quad (14.52)$$

and the y -coordinate of the lower surface is

$$g\left(\frac{x}{C}\right) = -A\tau\left(\frac{x}{C}\right) + B\sigma\left(\frac{x}{C}\right) - \frac{\delta x}{C} \quad (14.53)$$

where $2A/C \ll 1$ and $\delta/C \ll 1$. The airfoil surface is defined by a dimensionless thickness function

$$\begin{aligned} \tau\left(\frac{x}{C}\right) \\ \tau(0) = \tau(1) = 0 \end{aligned} \quad (14.54)$$

a dimensionless camber function

$$\begin{aligned} \sigma\left(\frac{x}{C}\right) \\ \sigma(0) = \sigma(1) = 0 \end{aligned} \quad (14.55)$$

and the angle of attack

$$\tan(\alpha) = -\frac{\delta}{C}. \quad (14.56)$$

Determine the lift and drag coefficients of the airfoil. Let

$$\xi = \frac{x}{C}. \quad (14.57)$$

Solution

The lift integral is

$$L = \int_0^C (P_{lower} - P_\infty) \cos(\alpha_{lower}) dx - \int_0^C (P_{upper} - P_\infty) \cos(\alpha_{upper}) dx. \quad (14.58)$$

where α is the local angle formed by the tangent to the surface of the airfoil and the x -axis. Since the angle is everywhere small we can use $\cos(\alpha) = 1$. The lift coefficient is

$$C_L = \frac{D}{\frac{1}{2} \rho_\infty U_\infty^2 C} = \int_0^1 C_{P_{lower}} d\xi - \int_0^1 C_{P_{upper}} d\xi. \quad (14.59)$$

The pressure coefficient on the upper surface is given by thin airfoil theory as

$$C_{P_{upper}} = \frac{2}{C \sqrt{M_\infty^2 - 1}} \left(\frac{df}{d\xi} \right) = \frac{2}{C \sqrt{M_\infty^2 - 1}} \left(A \frac{d\tau}{d\xi} + B \frac{d\sigma}{d\xi} - \delta \right). \quad (14.60)$$

On the lower surface the pressure coefficient is

$$C_{P_{lower}} = -\frac{2}{C \sqrt{M_\infty^2 - 1}} \left(\frac{dg}{d\xi} \right) = -\frac{2}{C \sqrt{M_\infty^2 - 1}} \left(-A \frac{d\tau}{d\xi} + B \frac{d\sigma}{d\xi} - \delta \right). \quad (14.61)$$

Substitute into the lift integral

$$C_L = \frac{-2}{C \sqrt{M_\infty^2 - 1}} \left(\int_0^1 \frac{df}{d\xi} d\xi + \int_0^1 \frac{dg}{d\xi} d\xi \right) = \frac{-2}{C \sqrt{M_\infty^2 - 1}} \left(\int_0^{-\delta} df + \int_0^{-\delta} dg \right). \quad (14.62)$$

In the thin airfoil approximation, the lift is independent of the airfoil thickness.

$$C_L = \frac{4}{\sqrt{M_\infty^2 - 1}} \left(\frac{\delta}{C} \right) \quad (14.63)$$

The drag integral is

$$D = \int_0^C (P_{upper} - P_\infty) \sin(\alpha_{upper}) dx + \int_0^C (P_{lower} - P_\infty) \sin(-\alpha_{lower}) dx. \quad (14.64)$$

Since the airfoil is thin the angle is small, and we can write the drag coefficient as

$$C_D = \frac{D}{\frac{1}{2}\rho_\infty U_\infty^2 C} \cong \int_0^1 \left(\frac{P_{upper} - P_\infty}{\frac{1}{2}\rho_\infty U_\infty^2} \right) (\alpha_{upper}) d\xi + \int_0^1 \left(\frac{P_{lower} - P_\infty}{\frac{1}{2}\rho_\infty U_\infty^2} \right) (-\alpha_{lower}) d\xi. \quad (14.65)$$

The local tangent is determined by the local slope of the airfoil therefore $\tan(\alpha) = dy/dx$ and for small angles $\alpha = dy/dx$. Now the drag coefficient is

$$C_D = \frac{D}{\frac{1}{2}\rho_\infty U_\infty^2 C} \cong \frac{1}{C} \int_0^1 C_{P_{upper}} \left(\frac{dy_{upper}}{d\xi} \right) d\xi + \frac{1}{C} \int_0^1 C_{P_{lower}} \left(-\frac{dy_{lower}}{d\xi} \right) d\xi. \quad (14.66)$$

The drag coefficient becomes

$$C_D \cong \frac{2}{C^2 \sqrt{M_\infty^2 - 1}} \left(\int_0^1 \left(A \frac{d\tau}{d\xi} + B \frac{d\sigma}{d\xi} - \delta \right)^2 d\xi + \int_0^1 \left(-A \frac{d\tau}{d\xi} + B \frac{d\sigma}{d\xi} - \delta \right)^2 d\xi \right). \quad (14.67)$$

Note that most of the cross terms cancel. The drag coefficient breaks into several terms.

$$C_D \cong \frac{4}{\sqrt{M_\infty^2 - 1}} \times \\ \left(\left(\frac{A}{C} \right)^2 \int_0^1 \left(\frac{d\tau}{d\xi} \right)^2 d\xi + \left(\frac{B}{C} \right)^2 \int_0^1 \left(\frac{d\sigma}{d\xi} \right)^2 d\xi - \left(\frac{B}{C} \right) \left(\frac{\delta}{C} \right) \int_0^1 \left(\frac{d\sigma}{d\xi} \right) d\xi + \left(\frac{\delta}{C} \right)^2 \int_0^1 d\xi \right) \quad (14.68)$$

The third term in (14.68) is

$$\left(\frac{B}{C} \right) \left(\frac{\delta}{C} \right) \int_0^1 \left(\frac{d\sigma}{d\xi} \right) d\xi = \left(\frac{B}{C} \right) \left(\frac{\delta}{C} \right) \int_0^1 d\sigma = \left(\frac{B}{C} \right) \left(\frac{\delta}{C} \right) (\sigma(1) - \sigma(0)) = 0. \quad (14.69)$$

Finally

$$C_D \cong \frac{4}{\sqrt{M_\infty^2 - 1}} \left(\left(\frac{A}{C} \right)^2 \int_0^1 \left(\frac{d\tau}{d\xi} \right)^2 d\xi + \left(\frac{B}{C} \right)^2 \int_0^1 \left(\frac{d\sigma}{d\xi} \right)^2 d\xi + \left(\frac{\delta}{C} \right)^2 \int_0^1 d\xi \right). \quad (14.70)$$

In the thin airfoil approximation, the drag is a sum of the drag due to thickness, drag due to camber, and drag due to lift.

14.2 Similarity rules for high speed flight

The Figure below shows the flow past a thin symmetric airfoil at zero angle of attack. The fluid is assumed to be inviscid and the flow Mach number, $U_{\infty 1}/a_\infty$ where $a_\infty^2 = \gamma P_\infty / \rho_\infty$ is the speed of sound, is assumed to be much less than one. The airfoil chord is c and the maximum thickness is t_1 . The subscript one is applied in anticipation of the fact that we will shortly scale the airfoil to a new shape with subscript 2 and the same chord.

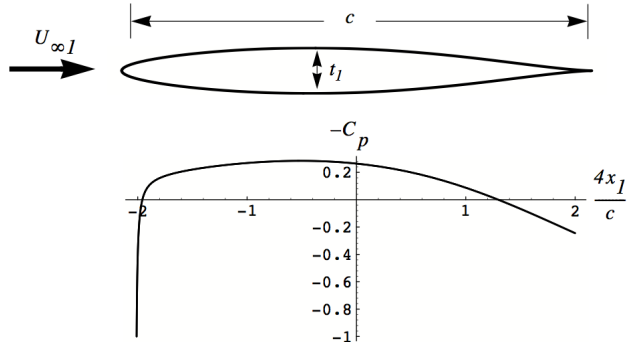


Figure 14.5: Pressure variation over a thin symmetric airfoil in low speed flow.

The surface pressure distribution is shown below the wing, expressed in terms of the pressure coefficient.

$$C_{P_1} = \frac{P_s - P_\infty}{\frac{1}{2} \rho_\infty U_{\infty 1}^2} \quad (14.71)$$

The pressure and flow speed throughout the flow satisfy the Bernoulli relation. Near the

airfoil surface

$$P_\infty + \frac{1}{2} \rho_\infty U_{\infty_1}^2 = P_{s_1} + \frac{1}{2} \rho_\infty U_{s_1}^2. \quad (14.72)$$

The pressure is high at the leading edge where the flow stagnates, then as the flow accelerates about the body, the pressure falls rapidly at first, then more slowly reaching a minimum at the point of maximum thickness. From there the surface velocity decreases and the pressure increases continuously to the trailing edge. In the absence of viscosity, the flow is irrotational.

$$\nabla \times u_1 = 0 \quad (14.73)$$

This permits the velocity to be described by a potential function.

$$u_1 = \nabla \phi_1 \quad (14.74)$$

When this is combined with the condition of incompressibility, $\nabla \cdot \bar{u}_1 = 0$, the result is Laplace's equation.

$$\frac{\partial^2 \phi_1}{\partial x_1^2} + \frac{\partial^2 \phi_1}{\partial y_1^2} = 0 \quad (14.75)$$

Let the shape of the airfoil surface in (x_1, y_1) be given by

$$\frac{y_1}{c} = \tau_1 g\left(\frac{x_1}{c}\right). \quad (14.76)$$

where $\tau_1 = t_1/c$ is the thickness to chord ratio of the airfoil. The boundary conditions that the velocity potential must satisfy are

$$\begin{aligned} \left(\frac{\partial \phi_1}{\partial y_1} \right)_{y_1=c\tau_1 g\left(\frac{x_1}{c}\right)} &= U_{\infty_1} \left(\frac{dy_1}{dx_1} \right)_{body} = U_\infty \tau_1 \frac{dg(x_1/c)}{d(x_1/c)} \\ \left(\frac{\partial \phi_1}{\partial x_1} \right)_\infty &\rightarrow U_{\infty_1}. \end{aligned} \quad (14.77)$$

Any number of methods of solving for the velocity potential are available including the use of complex variables. In the following we are going to restrict the airfoil to be thin,

$\tau_1 \ll 1$. In this context we will take the velocity potential to be a perturbation potential so that

$$\begin{aligned} u_1 &= U_{\infty_1} + u_1' \\ v_1 &= v_1' \end{aligned} \tag{14.78}$$

or

$$\begin{aligned} u_1 &= U_{\infty_1} + \frac{\partial \phi_1}{\partial x_1} \\ v_1 &= \frac{\partial \phi_1}{\partial y_1}. \end{aligned} \tag{14.79}$$

The boundary conditions on the perturbation potential in the thin airfoil approximation are

$$\begin{aligned} \left(\frac{\partial \phi_1}{\partial y_1} \right)_{y_1=0} &= U_{\infty_1} \left(\frac{dy_1}{dx_1} \right)_{body} = U_{\infty_1} \tau_1 \frac{dg(x_1/c)}{d(x_1/c)} \\ \left(\frac{\partial \phi_1}{\partial x_1} \right)_{\infty} &\rightarrow 0. \end{aligned} \tag{14.80}$$

The surface pressure coefficient in the thin airfoil approximation is

$$C_{P_1} = -\frac{2}{U_{\infty_1}} \left(\frac{\partial \phi_1}{\partial x_1} \right)_{y_1=0}. \tag{14.81}$$

Note that the boundary condition on the vertical velocity is now applied on the line $y_1 = 0$. In effect the airfoil has been replaced with a line of volume sources whose strength is proportional to the local slope of the actual airfoil. This sort of approximation is really unnecessary in the low Mach number limit but it is essential when the Mach number is increased and compressibility effects come in to play. Equally, it is essential in this example where we will map a compressible flow to the incompressible case.

14.2.1 Subsonic flow $M_{\infty} < 1$

Now imagine a second flow at a free-stream velocity, U_{∞_2} in a new space (x_2, y_2) over a new airfoil of the same shape (defined by the function $g(x/c)$) but with a new thickness ratio

$\tau_2 = t_2/c \ll 1$. Part of what we need to do is to determine how τ_1 and τ_1 are related to one another. The boundary conditions that the new perturbation velocity potential must satisfy are

$$\begin{aligned} \left(\frac{\partial \phi_2}{\partial y_2} \right)_{y_2=0} &= U_{\infty_2} \left(\frac{dy_2}{dx_2} \right)_{body} = U_{\infty_2} \tau_2 \frac{dg(x_2/c)}{d(x_2/c)} \\ \left(\frac{\partial \phi_2}{\partial x_2} \right)_{\infty} &\rightarrow 0. \end{aligned} \quad (14.82)$$

In this second flow the Mach number has been increased to the point where compressibility effects begin to occur: the density begins to vary significantly and the pressure distribution begins to deviate from the incompressible case. As long as the Mach number is not too large and shock waves do not form, the flow will be nearly isentropic. In this instance the 2-D steady compressible flow equations are

$$\begin{aligned} u_2 \frac{\partial u_2}{\partial x_2} + v_2 \frac{\partial u_2}{\partial y_2} + \frac{1}{\rho} \frac{\partial P}{\partial x_2} &= 0 \\ u_2 \frac{\partial v_2}{\partial x_2} + v_2 \frac{\partial v_2}{\partial y_2} + \frac{1}{\rho} \frac{\partial P}{\partial y_2} &= 0 \\ u_2 \frac{\partial \rho}{\partial x_2} + v_2 \frac{\partial \rho}{\partial y_2} + \rho \frac{\partial u_2}{\partial x_2} + \rho \frac{\partial v_2}{\partial y_2} &= 0 \\ \frac{P}{P_{\infty}} &= \left(\frac{\rho}{\rho_{\infty}} \right)^{\gamma}. \end{aligned} \quad (14.83)$$

Let

$$\begin{aligned} u_2 &= U_{\infty_2} + u'_2 \\ v_2 &= v_2 \\ \rho &= \rho_{\infty} + \rho' \\ P &= P_{\infty} + P' \end{aligned} \quad (14.84)$$

where the primed quantities are assumed to be small compared to the free stream conditions. When quadratic terms in the equations of motion are neglected the equations (14.83)

reduce to

$$\left(1 - \frac{\rho_\infty U_{\infty_2}^2}{\gamma P_\infty}\right) \frac{\partial u_2'}{\partial x_2} + \frac{\partial v_2'}{\partial y_2} = 0. \quad (14.85)$$

Introduce the perturbation velocity potential.

$$\begin{aligned} u_2' &= \frac{\partial \phi_2}{\partial x_2} \\ v_2 &= \frac{\partial \phi_2}{\partial y_2} \end{aligned} \quad (14.86)$$

The equation governing the disturbance flow becomes

$$(1 - M_{\infty_2}^2) \frac{\partial^2 \phi_2}{\partial x_2^2} + \frac{\partial^2 \phi_2}{\partial y_2^2} = 0. \quad (14.87)$$

Notice that (14.87) is valid for both sub and supersonic flow in the thin airfoil approximation. Since the flow is isentropic, the pressure and velocity disturbances are related to lowest order by

$$P' + \rho_\infty U_{\infty_2} u_2' = 0 \quad (14.88)$$

and the surface pressure coefficient retains the same basic form as in the incompressible case.

$$C_{P_2} = -\frac{2}{U_{\infty_2}} \left(\frac{\partial \phi_2}{\partial x_2} \right)_{y_2=0} \quad (14.89)$$

Since we are at a finite Mach number, this last relation is valid only within the thin airfoil, small disturbance approximation and therefore may be expected to be invalid near the leading edge of the airfoil where the velocity change is of the order of the free stream velocity. For example for the "thin" airfoil depicted in Figure 14.5 which is actually not all that thin, the pressure coefficient is within $-0.2 < C_p < 0.2$ except over a very narrow portion of the chord near the leading edge.

Equation (14.87) can be transformed to Laplace's equation, (14.75) using the following change of variables

$$x_2 = x_1$$

$$\begin{aligned} y_2 &= \frac{1}{\sqrt{1 - M_{\infty_2}^2}} y_1 \\ \phi_2 &= \frac{1}{A} \left(\frac{U_{\infty_2}}{U_{\infty_1}} \right) \phi_1 \end{aligned} \quad (14.90)$$

where, at the moment, A is an arbitrary constant. The velocity potentials are related by

$$\phi_2(x_2, y_2) = \frac{1}{A} \left(\frac{U_{\infty_2}}{U_{\infty_1}} \right) \phi_1(x_1, y_1) \quad (14.91)$$

or

$$\phi_1(x_1, y_1) = A \left(\frac{U_{\infty_1}}{U_{\infty_2}} \right) \phi_2 \left(x_1, \frac{1}{\sqrt{1 - M_{\infty_2}^2}} y_1 \right) \quad (14.92)$$

and the boundary conditions transform as

$$\begin{aligned} \left(\frac{\partial \phi_1}{\partial y_1} \right)_{y_1=0} &= U_{\infty_1} \left(\frac{A \tau_2}{\sqrt{1 - M_{\infty_2}^2}} \right) \frac{dg(x_1/c)}{d(x_1/c)} \\ \left(\frac{\partial \phi_1}{\partial x_1} \right)_\infty &\rightarrow 0 \\ \left(\frac{\partial \phi_2}{\partial x_2} \right)_\infty &\rightarrow 0. \end{aligned} \quad (14.93)$$

The transformation between flows one and two is completed by the correspondence

$$\tau_1 = \frac{A}{\sqrt{1 - M_{\infty_2}^2}} \tau_2 \quad (14.94)$$

or

$$\frac{t_1}{c} = \frac{A}{\sqrt{1 - M_{\infty_2}^2}} \left(\frac{t_2}{c} \right). \quad (14.95)$$

Finally the transformed pressure coefficient is

$$C_{P_1} = AC_{P_2}. \quad (14.96)$$

These results may be stated as follows. The solution for incompressible flow over a thin airfoil with shape $g(x_1/c)$ and thickness ratio, t_1/c at velocity U_1 is identical to the subsonic compressible flow at velocity, U_2 and Mach number M_2 over an airfoil with a similar shape but with the thickness ratio

$$\frac{t_2}{c} = \frac{\sqrt{1 - M_{\infty_2}^2}}{A} \left(\frac{t_1}{c} \right). \quad (14.97)$$

The pressure coefficient for the compressible case is derived by adjusting the incompressible coefficient using $C_{P_2} = C_{P_1}/A$. This result comprises several different similarity rules that can be found in the aeronautical literature depending on the choice of the free constant A . Perhaps the one of greatest interest is the Prandtl-Glauert rule that describes the variation of pressure coefficient with Mach number for a body of a given shape and thickness ratio. In this case we select

$$A = \sqrt{1 - M_{\infty_2}^2} \quad (14.98)$$

so that the two bodies being compared in (14.97) have the same shape and thickness ratio. The pressure coefficient for the compressible flow is

$$C_{P_2} = \frac{C_{P_1}}{\sqrt{1 - M_{\infty_2}^2}}. \quad (14.99)$$

Several scaled profiles are shown in Figure 14.6. Keep in mind the lack of validity of (14.99) near the leading edge where the pressure coefficient is scaled to inaccurate values.

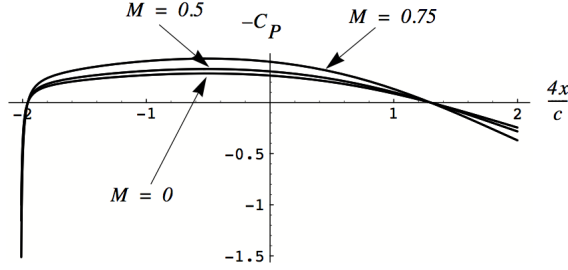


Figure 14.6: Pressure coefficient over the airfoil in Figure 14.5 at several Mach numbers as estimated using the Prandtl-Glauert rule (14.99).

14.2.2 Supersonic similarity $M_\infty > 1$

All the theory developed in the previous section can be extended to the supersonic case by simply replacing $1 - M_\infty^2$ with $M_\infty^2 - 1$. In this instance the mapping is between the equation

$$(M_\infty^2 - 1) \frac{\partial^2 \phi_2}{\partial x_2^2} - \frac{\partial^2 \phi_2}{\partial y_2^2} = 0 \quad (14.100)$$

and the simple wave equation

$$\frac{\partial^2 \phi_1}{\partial x_1^2} - \frac{\partial^2 \phi_1}{\partial y_1^2} = 0. \quad (14.101)$$

A generalized form of the pressure coefficient valid for subsonic and supersonic flow is

$$\frac{C_P}{A} = F \left(\frac{\tau}{A \sqrt{|1 - M_\infty^2|}} \right) \quad (14.102)$$

where A is taken to be a function of $|1 - M_\infty^2|$.

14.2.3 Transonic similarity $M_\infty \approx 1$

When the Mach number is close to one, the simple linearization used to obtain (14.87) from (14.83) loses accuracy. In this case the equations (14.83) reduce to the nonlinear

equation

$$(1 - M_{\infty_1}^2) \frac{\partial u_1'}{\partial x_1} + \frac{\partial v_1'}{\partial y_1} - \frac{(\gamma_1 + 1) M_{\infty_1}^2}{U_{\infty_1}} u_1' \frac{\partial u_1'}{\partial x_1} = 0. \quad (14.103)$$

In terms of the perturbation potential

$$(1 - M_{\infty_1}^2) \frac{\partial^2 \phi_1}{\partial x_1^2} + \frac{\partial^2 \phi_1}{\partial y_1^2} - \frac{(\gamma_1 + 1) M_{\infty_1}^2}{U_{\infty_1}} \frac{\partial \phi_1}{\partial x_1} \frac{\partial^2 \phi_1}{\partial x_1^2} = 0. \quad (14.104)$$

This equation is invariant under the change of variables

$$x_2 = x_1$$

$$y_2 = \frac{\sqrt{1 - M_{\infty_1}^2}}{\sqrt{1 - M_{\infty_2}^2}} y_1 \quad (14.105)$$

$$\phi_2 = \frac{1}{A} \left(\frac{U_{\infty_2}}{U_{\infty_1}} \right) \phi_1$$

where

$$A = \left(\frac{1 + \gamma_2}{1 + \gamma_1} \right) \left(\frac{1 - M_{\infty_1}^2}{1 - M_{\infty_2}^2} \right) \left(\frac{M_{\infty_2}^2}{M_{\infty_1}^2} \right). \quad (14.106)$$

Notice that, due to the nonlinearity of the transonic equation (14.104) the constant A is no longer arbitrary. The pressure coefficient becomes

$$C_{P_1} = \left(\frac{1 + \gamma_2}{1 + \gamma_1} \right) \left(\frac{1 - M_{\infty_1}^2}{1 - M_{\infty_2}^2} \right) \left(\frac{M_{\infty_2}^2}{M_{\infty_1}^2} \right) C_{P_2} \quad (14.107)$$

and the thickness ratios are related by

$$\frac{t_2}{c} = \left(\frac{1 + \gamma_1}{1 + \gamma_2} \right) \left(\frac{1 - M_{\infty_2}^2}{1 - M_{\infty_1}^2} \right)^{\frac{3}{2}} \left(\frac{M_{\infty_1}^2}{M_{\infty_2}^2} \right) \frac{t_1}{c}. \quad (14.108)$$

In the transonic case, it is not possible to compare the same body at different Mach numbers or bodies with different thickness ratios at the same Mach number except by selecting gases

with different γ . For a given gas it is only possible to map the pressure distribution for one airfoil to an airfoil with a different thickness ratio at a different Mach number. A generalized form of (14.102) valid from subsonic to sonic to supersonic Mach numbers is

$$\frac{C_P((\gamma + 1) M_\infty^2)^{\frac{1}{3}}}{\tau^{\frac{2}{3}}} = F \left(\frac{1 - M_\infty^2}{(\tau(\gamma + 1) M_\infty^2)^{\frac{2}{3}}} \right). \quad (14.109)$$

Prior to the advent of supercomputers capable of solving the equations of high speed flow, similarity methods and wind tunnel correlations were the only tools available to the aircraft designer and these methods played a key role in the early development of transonic and supersonic flight.

14.3 Problems

Problem 1 - A thin, 2-D, airfoil is situated in a supersonic stream at Mach number M_∞ and a small angle of attack as shown in Figure 14.7.

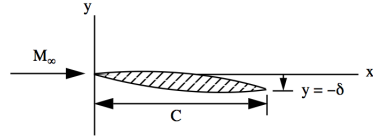


Figure 14.7: Bi-convex airfoil at angle of attack

The y -coordinate of the upper surface of the airfoil is given by the function

$$f(x) = A \frac{x}{C} \left(1 - \frac{x}{C}\right) - \delta \frac{x}{C} \quad (14.110)$$

and the y -coordinate of the lower surface is

$$g(x) = -A \frac{x}{C} \left(1 - \frac{x}{C}\right) - \delta \frac{x}{C} \quad (14.111)$$

where $2A/C \ll 1$ and $\delta/C \ll 1$. Determine the lift and drag coefficients of the airfoil.

Appendix A

Some results from the kinetic theory of gases

A.1 Distribution of molecular velocities in a gas

A.1.1 The distribution derived from the barometric formula

In Chapter 2 the variation of gas density in the atmosphere was derived. In the upper atmosphere where the gas temperature is approximately constant

$$\frac{\rho(z+h)}{\rho(z)} = e^{-\frac{\gamma gh}{a_0^2}}. \quad (\text{A.1})$$

Rewrite (A.1) in terms of molecular parameters

$$\frac{n(z+h)}{n(z)} = e^{-\frac{mgh}{kT}} \quad (\text{A.2})$$

where $n(z)$ is the number of molecules per unit volume at the height z , $m = M_w/N$, is the mass of each molecule (or the average mass in the case of a mixture like air). The Boltzmann's constant

$$k = 1.38 \times 10^{-23} \text{ Joules/K} \quad (\text{A.3})$$

is related to the gas constant and Avagadros number N by

$$k = \frac{R_u}{N}. \quad (\text{A.4})$$

Equation (A.2) expresses the distribution of molecules in any system at constant temperature subject to a body force. The fraction of molecules per unit area above a given altitude $z + h$ is also given by the distribution (A.2). That is

$$\frac{\int_{z+h}^{\infty} n(z) dz}{\int_z^{\infty} n(z) dz} = e^{-\frac{mgh}{kT}} \quad (\text{A.5})$$

which is a basic property of an exponential distribution. The distribution of molecules under the downward pull of gravity given by (A.5) can be used to infer how the velocities of gas molecules are distributed. Consider molecules that pass through some reference height z on their way to height $z + h$.

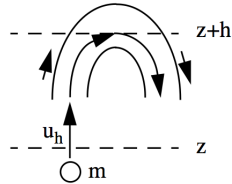


Figure A.1: *Trajectory of an upward moving molecule*

The upward velocity component u_h of a molecule whose kinetic energy at z is equal to its potential energy when it arrives at $z + h$ satisfies

$$mgh = \frac{1}{2}mu_h^2. \quad (\text{A.6})$$

This is the minimum positive velocity needed for a molecule starting at z to reach the height $z + h$.

Let $J_{u>u_h}(z)$ be the flux of molecules (number of molecules/area-sec) passing through the plane z that possess a vertical velocity component greater than u_h and let $J_{u>0}(z)$ be the flux of molecules passing through the plane z with any positive upward velocity. The fraction of molecules passing upward through z with the requisite velocity is $J_{u>u_h}(z) / J_{u>0}(z)$.

This ratio should be the same as the fraction of molecules above the height $z+h$. Therefore one can infer the equality

$$\frac{J_{u>u_h}(z)}{J_{u>0}(z)} = \frac{\int_{z+h}^{\infty} n(z) dz}{\int_z^{\infty} n(z) dz}. \quad (\text{A.7})$$

Using (A.5) we deduce that

$$\frac{J_{u>u_h}(z)}{J_{u>0}(z)} = e^{-\frac{mgh}{kT}} = e^{-\frac{mu_h^2}{2kT}} \quad (\text{A.8})$$

which is plotted in Figure A.2.

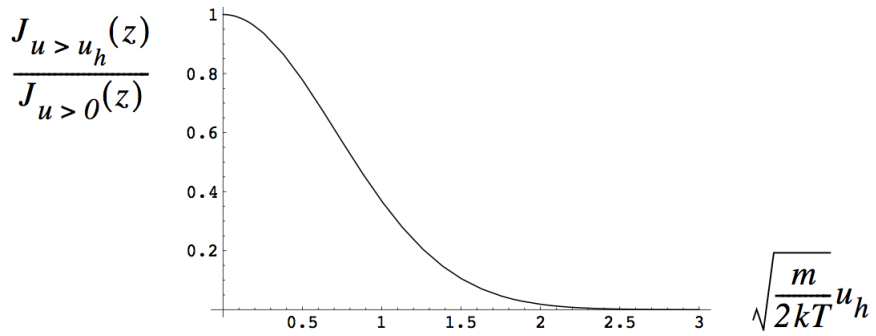


Figure A.2: *Fraction of molecules at any reference height with positive vertical velocity component exceeding u_h .*

Now use (A.7) to generate a probability density function (pdf) $g(u_h)$ for the velocities. The pdf is defined such that, at any height z , $g(u_h) du_h$ equals the fraction of molecules per unit volume with velocity between u_h and $u_h + du_h$. The pdf we are seeking would look something like Figure A.3.

The desired pdf is normalized so that

$$\int_{-\infty}^{\infty} g(u_h) du_h = 1. \quad (\text{A.9})$$

Note that $\int_{-\infty}^{\infty} e^{-x^2} dx = \sqrt{\pi}$.

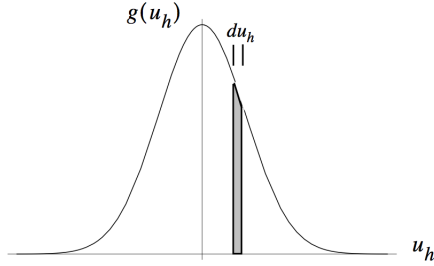


Figure A.3: *Probability density function of one velocity component. The shaded area divided by the whole area (which is one) is the fraction of molecules with velocity between u_h and $u_h + du_h$.*

The number of molecules that pass through a unit area of the plane z in unit time (the flux of molecules) with vertical velocity component u_h is $u_h g(u_h) du_h$. In terms of the velocity pdf

$$\frac{J_{u>u_h}(z)}{J_{u>0}(z)} = \int_{u_h}^{\infty} u_h g(u_h) du_h = e^{-\frac{mu_h^2}{2kT}}. \quad (\text{A.10})$$

Differentiate both sides of (A.10).

$$-u_h g(u_h) = -\frac{mu_h}{kT} e^{-\frac{mu_h^2}{2kT}} \quad (\text{A.11})$$

Thus far

$$g(u_h) = -\frac{m}{kT} e^{-\frac{mu_h^2}{2kT}}. \quad (\text{A.12})$$

Apply the normalization condition (A.9) to (A.12).

$$\int_{-\infty}^{\infty} \frac{m}{kT} e^{-\frac{mu_h^2}{2kT}} du_h = \left(\frac{2\pi m}{kT} \right)^{1/2} \quad (\text{A.13})$$

Finally, the normalized 1-dimensional velocity pdf is

$$g(u_h) = \left(\frac{m}{2\pi kT} \right)^{1/2} e^{-\frac{mu_h^2}{2kT}}. \quad (\text{A.14})$$

We arrived at this result using a model of particles with random vertical velocity components moving in a gravitational field. In a gas in thermodynamic equilibrium at a temperature T , the molecules constantly undergo collisions leading to chaotic motion with a wide range of molecular velocities in all three directions. The randomness is so strong that at any point no one direction is actually preferred over another and one can expect that the probability density function for a velocity component in any direction at a given height z will have the same form as (A.14).

A.1.2 The Maxwell velocity distribution function

We can use a slightly different, more general, argument to arrive at the velocity distribution function in three dimensions. The randomness produced by multiple collisions leads to a molecular motion that is completely independent in all three coordinate directions and so the probability of occurrence of a particular triad of velocities (u_x, u_y, u_z) is equal to the product of three one-dimensional probability distributions.

$$f(u_x, u_y, u_z) = g(u_x) g(u_y) g(u_z) \quad (\text{A.15})$$

In addition, since no direction in velocity space (u_x, u_y, u_z) is preferred over any other, then the three dimensional velocity probability distribution function must be invariant under any rotation of axes in velocity space. This means $f(u_x, u_y, u_z)$ can only depend on the radius in velocity space.

$$f(u_x, u_y, u_z) = f(u_x^2 + u_y^2 + u_z^2) \quad (\text{A.16})$$

The only smooth function that satisfies both (A.15) and (A.16) and the requirement that the probability goes to zero at infinity is the decaying exponential.

$$f(u_x, u_y, u_z) = A e^{-B(u_x^2 + u_y^2 + u_z^2)} \quad (\text{A.17})$$

In a homogeneous gas the number density of molecules with a given velocity is accurately described by the Maxwellian velocity distribution function

$$f(u_1, u_2, u_3) = \left(\frac{m}{2\pi kT} \right)^{3/2} e^{-\frac{m}{2kT}(u_1^2 + u_2^2 + u_3^2)} \quad (\text{A.18})$$

where the correspondence $(u_x, u_y, u_z) \rightarrow (u_1, u_2, u_3)$ is used. The result (A.18) is consistent with the use of (A.14) in all three directions. The dimensions of f are sec^3/m^3 . The pdf (A.18) is shown in figure A.4.

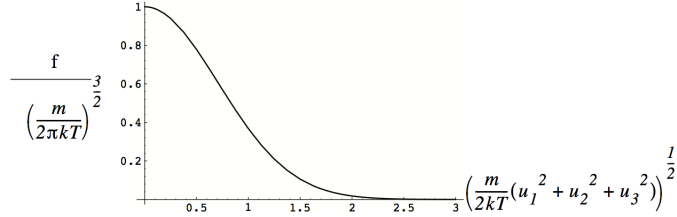


Figure A.4: *Maxwellian probability density function of molecular velocities.*

As with the 1-D pdf, the 3-D pdf is normalized so that the total probability over all velocity components is one.

$$\int_{-\infty}^{\infty} \int_{-\infty}^{\infty} \int_{-\infty}^{\infty} f du_1 du_2 du_3 = 1 \quad (\text{A.19})$$

To understand the distribution (A.18) imagine a volume of gas molecules at some temperature T .

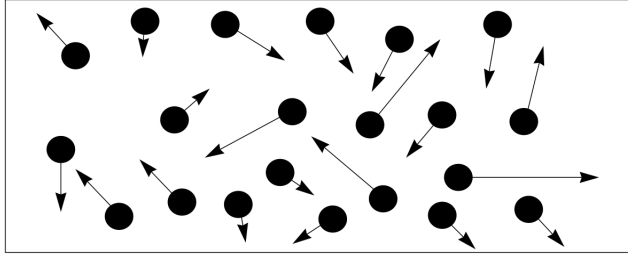


Figure A.5: *Colliding molecules in a box.*

At a certain instant a snapshot of the motion is made and the velocity vector of every molecule in the gas sample is measured as indicated in the sketch above. The velocity components of each molecule define a point in the space of velocity coordinates. When data for all the molecules is plotted, the result is a scatter plot with the densest distribution of points occurring near the origin in velocity space as shown in figure A.6.

The probability density function (A.18) can be thought of as the density of points in figure A.4. The highest density occurs near the origin and falls off exponentially at large distances from the origin. If the gas is at rest or moving with a uniform velocity the distribution is spherically symmetric since no one velocity direction is preferred over another.

The one-dimensional probability distribution is generated by integrating the Maxwellian

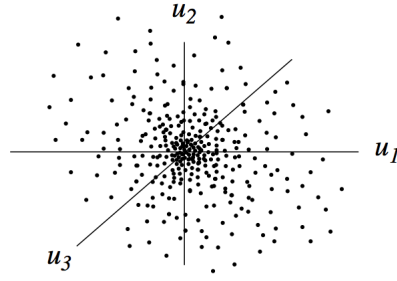


Figure A.6: Schematic of coordinates of a set of colliding molecules in velocity space.

in two of the three velocities.

$$f_{1D} = \int_{-\infty}^{\infty} \int_{-\infty}^{\infty} \left(\frac{m}{2\pi kT} \right)^{3/2} e^{-\frac{m}{2kT}(u_1^2 + u_2^2 + u_3^2)} du_2 du_3 \quad (\text{A.20})$$

which can be rearranged to read

$$f_{1D} = \left(\frac{m}{2\pi kT} \right)^{3/2} e^{-\frac{mu_1^2}{2kT}} \int_{-\infty}^{\infty} e^{-\frac{mu_2^2}{2kT}} du_2 \int_{-\infty}^{\infty} e^{-\frac{mu_3^2}{2kT}} du_3. \quad (\text{A.21})$$

Carrying out the integration in (A.21) the 1-D pdf is

$$f_{1D} = \left(\frac{m}{2\pi kT} \right)^{1/2} e^{-\frac{mu_1^2}{2kT}} \quad (\text{A.22})$$

which is identical to (A.14).

A.2 Mean molecular velocity

Any statistical property of the gas can be determined by taking the appropriate moment of the Maxwellian distribution. The mean velocity of molecules moving in the plus x_1 direction is

$$\hat{u}_1 = \int_{-\infty}^{\infty} \int_{-\infty}^{\infty} \int_0^{\infty} u_1 \left(\frac{m}{2\pi kT} \right)^{3/2} e^{-\frac{m}{2kT}(u_1^2 + u_2^2 + u_3^2)} du_1 du_2 du_3. \quad (\text{A.23})$$

Note that the integration extends only over velocities in the plus x direction. When the integral is evaluated the result is

$$\hat{u}_1 = \left(\frac{kT}{2\pi m} \right)^{1/2}. \quad (\text{A.24})$$

Let's work out the flux in the 1-direction of molecules crossing an imaginary surface in the fluid shown schematically in Figure A.7. This is the number of molecules passing through a surface of unit area in unit time.

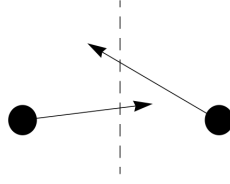


Figure A.7: *Molecules moving through an imaginary surface normal to the x_1 -direction.*

The flux is simply

$$J_1 = n\hat{u}_1 = n \left(\frac{kT}{2\pi m} \right)^{1/2}. \quad (\text{A.25})$$

At equilibrium, the number of molecules crossing per second in either direction is the same. Note that the molecular flux through a surface is the same regardless of the orientation of the surface.

The *mean square molecular speed* is defined as the average of the squared speed over all molecules.

$$\widehat{(u^2)} = (u_1^2 + u_2^2 + u_3^2) \quad (\text{A.26})$$

From the Maxwellian

$$\widehat{u^2} = \int_{-\infty}^{\infty} \int_{-\infty}^{\infty} \int_{-\infty}^{\infty} (u_1^2 + u_2^2 + u_3^2) \left(\frac{m}{2\pi kT} \right)^{3/2} e^{-\frac{m}{2kT}(u_1^2 + u_2^2 + u_3^2)} du_1 du_2 du_3 = \frac{3kT}{m} \quad (\text{A.27})$$

where the integration is from minus infinity to plus infinity in all three directions. The root-mean-square speed is

$$u_{rms} = \sqrt{\widehat{u^2}} = \sqrt{\frac{3kT}{m}}. \quad (\text{A.28})$$

This result is consistent with the famous law of equipartition which states that, for a gas of monatomic molecules, the mean kinetic energy per molecule (the energy of the translational degrees of freedom) is

$$E = \frac{1}{2}mu^2 = \frac{3}{2}kT. \quad (\text{A.29})$$

A.3 Distribution of molecular speeds

The Maxwellian distribution of molecular speed is generated from the full distribution by determining the number of molecules with speed in a differential spherical shell of thickness du and radius u in velocity space. The volume of the shell is $dV_u = 4\pi u^2 du$ and so the number of molecules in the shell is $f dV_u = 4\pi u^2 f du$ where $u^2 = u_1^2 + u_2^2 + u_3^2$. The Maxwellian probability distribution for the molecular speed is therefore

$$f_u = 4\pi u^2 f = 4\pi \left(\frac{m}{2\pi kT} \right)^{3/2} u^2 e^{-\frac{mu^2}{2kT}} \quad (\text{A.30})$$

shown in Figure A.8.

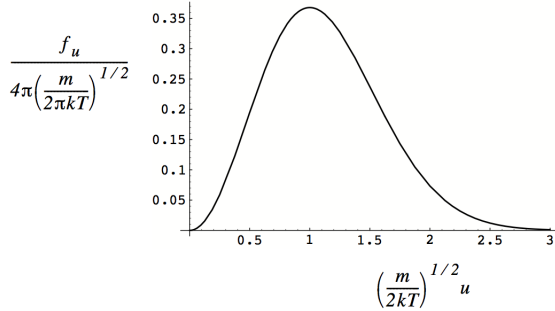


Figure A.8: *Maxwell distribution of molecular speeds.*

The mean molecular speed is

$$\hat{u} = \int_0^\infty u f_u du = \int_0^\infty 4\pi \left(\frac{m}{2\pi kT}\right)^{3/2} u^3 e^{-\frac{mu^2}{2kT}} du = \sqrt{\frac{8kT}{\pi m}}. \quad (\text{A.31})$$

In summary, the three relevant molecular speeds are

$$\begin{aligned} \hat{u}_1 &= \sqrt{\frac{kT}{2\pi m}} \\ \hat{u}_{rms} &= \sqrt{\frac{3kT}{m}} \\ \hat{u} &= \sqrt{\frac{8kT}{\pi m}}. \end{aligned} \quad (\text{A.32})$$

A.4 Pressure

A.4.1 Kinetic model of pressure

Before we use the Maxwellian distribution to relate the gas pressure to temperature it is instructive to derive this relation using intuitive arguments. Consider a gas molecule confined to a perfectly rigid box. The molecule is moving randomly and collides and rebounds from the wall of the container preserving its momentum in the direction normal to the wall. In doing so the molecule undergoes the change in momentum

$$\Delta p = -2mu_1 \quad (\text{A.33})$$

and imparts to the wall A_1 the momentum $2mu_1$. Suppose the molecule reaches the opposite wall without colliding with any other molecules. The time it takes for the molecule to bounce off A_2 and return to collide again with A_1 is $2L/u_1$ and so the number of collisions per second with A_1 is $u_1/2L$.

The momentum per unit time that the molecule transfers to A_1 is

$$\text{Force on wall by one molecule} = \frac{mu_1^2}{L}. \quad (\text{A.34})$$

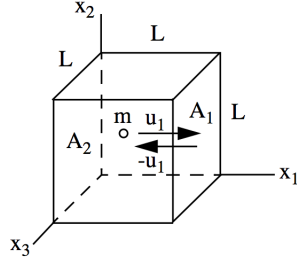


Figure A.9: A rigid box containing an ideal gas.

Let N_p be the number of molecules in the box. The total force on A_1 is the pressure of the gas times the area and is equal to the sum of forces by the individual molecules

$$PL^2 = \frac{1}{L} \sum_{i=1}^{N_p} m_i u_{1i}^2 \quad (\text{A.35})$$

where the index i refer to the i th molecule. If the molecules all have the same mass

$$P = \frac{Nm}{V} \left(\frac{1}{N_p} \sum_{i=1}^{N_p} u_{1i}^2 \right). \quad (\text{A.36})$$

The first factor in (A.36) is the gas density $\rho = N_p m / V$. No one direction is preferred over another and so we would expect the average of the squares in all three directions to be the same.

$$\frac{1}{N_p} \sum_{i=1}^{N_p} u_{1i}^2 = \frac{1}{N_p} \sum_{i=1}^{N_p} u_{2i}^2 = \frac{1}{N_p} \sum_{i=1}^{N_p} u_{3i}^2 \quad (\text{A.37})$$

The pressure is now written

$$P = \frac{\rho u_{rms}^2}{3} \quad (\text{A.38})$$

where

$${u_{rms}}^2 = \frac{1}{N_p} \left(\sum_{i=1}^{N_p} {u_{1i}}^2 + \sum_{i=1}^{N_p} {u_{2i}}^2 + \sum_{i=1}^{N_p} {u_{3i}}^2 \right). \quad (\text{A.39})$$

The root-mean-square velocity defined by a discrete sum in (A.39) is the same as that derived by integrating the Maxwellian pdf in (A.28). Using (A.28) and (A.38) the pressure and temperature are related by

$$P = \frac{\rho}{3} \left(\frac{3kT}{m} \right) = \rho RT. \quad (\text{A.40})$$

We arrived at this result using a model that ignored collisions between molecules. The model is really just a convenience for calculation. It works for two reasons; the time spent during collisions is negligible compared to the time spent between collisions and, in a purely elastic exchange of momentum between a very large number of molecules in statistical equilibrium, there will always be a molecule colliding with A_2 with momentum $-mu_1$ while a molecule leaves A_1 with the same momentum.

A.4.2 Pressure directly from the Maxwellian pdf

The momentum flux at any point is

$$\Pi_{ij} = \int_{-\infty}^{\infty} \int_{-\infty}^{\infty} \int_{-\infty}^{\infty} nm u_i u_j \left(\frac{m}{2\pi kT} \right)^{3/2} e^{-\frac{m}{2kT}(u_1^2 + u_2^2 + u_3^2)} du_1 du_2 du_3. \quad (\text{A.41})$$

For $i \neq j$ the integral vanishes since the integrand is an odd function. For $i = j$ the integral becomes

$$\Pi_{11} = \frac{mn}{\pi^{3/2}} \left(\frac{2kT}{m} \right) \int_{-\infty}^{\infty} {u_1}^2 e^{-\frac{mu_1^2}{2kT}} du_1 \int_{-\infty}^{\infty} e^{-\frac{mu_2^2}{2kT}} du_2 \int_{-\infty}^{\infty} e^{-\frac{mu_3^2}{2kT}} du_3 = nkT \quad (\text{A.42})$$

similarly $\Pi_{22} = nkT$ and $\Pi_{33} = nkT$. The fluid density is

$$\rho = nm \quad (\text{A.43})$$

and the gas constant is

$$k = \frac{R_u}{N} = \frac{M_w}{N} \frac{R_u}{M_w} = mR \quad (\text{A.44})$$

where N is Avogadro's number.

$$N = 6.023 \times 10^{26} \frac{\text{molecules}}{\text{kilogram} - \text{mole}}. \quad (\text{A.45})$$

The force per unit area produced by molecular collisions is

$$\Pi_{11} = \Pi_{22} = \Pi_{33} = nkT = \left(\frac{\rho}{m}\right) mRT = \rho RT = P. \quad (\text{A.46})$$

The normal stress derived by integrating the Maxwellian distribution over the molecular flux of momentum is just the thermodynamic pressure.

$$\Pi_{ij} = P\delta_{ij} = \begin{bmatrix} P & 0 & 0 \\ 0 & P & 0 \\ 0 & 0 & P \end{bmatrix} \quad (\text{A.47})$$

Recall the mean molecular speed $\hat{u} = \sqrt{8kT/\pi m}$. The speed of sound for a gas is $a^2 = \gamma P/\rho$. Accordingly, the speed of sound is directly proportional to the mean molecular speed.

$$a = \left(\frac{\gamma P}{\rho}\right)^{1/2} = \left(\frac{\gamma nkT}{nm}\right)^{1/2} = \left(\frac{\gamma\pi}{8}\right)^{1/2} \hat{u} \quad (\text{A.48})$$

A.5 The mean free path

A molecule of effective diameter σ sweeps out a collision path which is of diameter 2σ . The collision volume swept out per second is $\pi\sigma^2\hat{u}$. With the number of molecules per unit volume equal to n , the number of collisions per second experienced by a given molecule is $\nu_c = n\pi\sigma^2\sqrt{8kT/\pi m}$. The average distance that a molecule moves between collisions is

$$\lambda = \frac{\hat{u}_{rel}}{\nu_c} = \frac{\hat{u}_{rel}}{n\pi\sigma^2\hat{u}} \quad (\text{A.49})$$

where the mean relative velocity between molecules is used. This accounts for the fact that the other molecules in the volume are not static; they are in motion. When this motion is taken into account, the mean free path is estimated as

$$\lambda = \frac{1}{\sqrt{2}n\pi\sigma^2}. \quad (\text{A.50})$$

Typical values for the mean free path of a gas at room temperature and one atmosphere are on the order of 50 nanometers (roughly 10 times the mean molecular spacing).

A.6 Viscosity

Consider the flux of momentum associated with the net particle flux across the plane $y = y_0$ depicted in figure A.10.

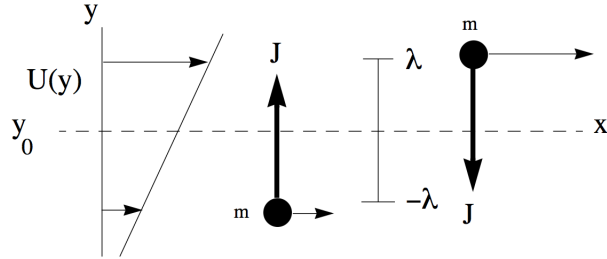


Figure A.10: *Momentum exchange in a shear flow.*

On the average, a particle passing through y_0 in the positive or negative direction had its last collision at $y = y_0 - \lambda$ or $y = y_0 + \lambda$, where λ is the mean free path. Through the collision process, the particle tends to acquire the mean velocity at that position. The particle flux across y_0 in either direction is $J = n(kT/2\pi m)^{1/2}$. The net flux of x_1 -momentum in the x_2 -direction is

$$\Pi_{12} = mJU(y_0 - \lambda) - mJU(y_0 + \lambda) \cong -2mJ\lambda \frac{dU}{dy}. \quad (\text{A.51})$$

The viscosity derived from this model is

$$\mu = 2mJ\lambda = 2\rho\lambda \left(\frac{kT}{2\pi m} \right)^{1/2}. \quad (\text{A.52})$$

In terms of the mean molecular speed this can be written as

$$\mu = \frac{1}{2} \rho \lambda \left(\frac{8kT}{\pi m} \right)^{1/2} = \frac{1}{2} \rho \hat{u} \lambda. \quad (\text{A.53})$$

The viscosity can be expressed in terms of the speed of sound as follows.

$$\mu = \frac{1}{2} \rho \lambda \left(\frac{8nkT}{\pi nm} \right)^{1/2} = \left(\frac{2}{\pi \gamma} \right)^{1/2} \rho a \lambda \quad (\text{A.54})$$

This result can be used to relate the Reynolds number and Mach number of a flow

$$R_e = \frac{\rho U L}{\mu} \cong \frac{U L}{a \lambda} = M \left(\frac{L}{\lambda} \right) \quad (\text{A.55})$$

where L is a characteristic length of the flow and the factor $(2/\pi\gamma)^{1/2}$ has been dropped. The ratio of mean free path to characteristic length is called the Knudsen number of the flow.

$$K_n = \frac{\lambda}{L} \quad (\text{A.56})$$

A.7 Heat conductivity

The same heuristic model can be used to crudely estimate the net flux of internal energy (per molecular mass) across y_0 .

$$Q_2 = m J C_v T (y_0 - \lambda) - m J C_v T (y_0 + \lambda) = -2m J C_v \lambda \frac{dT}{dy} \quad (\text{A.57})$$

The heat conductivity derived from this model is

$$\kappa = \frac{1}{2} \rho \hat{u} \lambda C_v. \quad (\text{A.58})$$

The model indicates that the Prandtl number for a gas should be proportional to the ratio of specific heats.

$$P_r = \frac{\mu C_p}{\kappa} = \frac{C_p}{C_v} = \gamma \quad (\text{A.59})$$

A more precise theory gives

$$P_r = \frac{4\gamma}{9\gamma - 5} \quad (\text{A.60})$$

which puts the Prandtl number for gases in the range $2/3 \leq P_r < 1$ depending on the number of degrees of freedom of the molecular system.

Notice that we got to these results using an imprecise model and without using the Maxwellian distribution function. In fact, a rigorous theory of the transport coefficients in a gas must consider small deviations from the Maxwellian distribution that occur when gradients of temperature or velocity are present. This is the so-called Chapman-Enskog theory of transport coefficients in gases.

A.8 Specific heats, the law of equipartition

Classical statistical mechanics leads to a simple expression for C_p and C_v in terms of β , the number of degrees of freedom of the appropriate molecular model.

$$\begin{aligned} C_p &= \frac{\beta + 2}{2} R \\ C_p &= \frac{\beta}{2} R \\ \gamma &= \frac{\beta + 2}{\beta} \end{aligned} \quad (\text{A.61})$$

For a mass point, m , with three translational degrees of freedom, $\beta = 3$, the energy of the particle is

$$E = \frac{1}{2}mu^2 + \frac{1}{2}mv^2 + \frac{1}{2}mw^2 \quad (\text{A.62})$$

where (u, v, w) are the velocities in the three coordinate directions. The law of equipartition of energy says that any term in E that is quadratic (proportional to a square) in either the position or velocity contributes $(1/2)kT$ to the thermal energy of a large collection of such mass points. Thus the thermal energy (internal energy) per molecule of a gas composed of a large collection of mass points is

$$\tilde{e} = \frac{3}{2}kT. \quad (\text{A.63})$$

For one mole of gas

$$N\tilde{e} = \frac{3}{2}R_u T \quad (\text{A.64})$$

where $R_u = Nk$ is the universal gas constant. On a per unit mass of gas basis the internal energy is

$$e = \frac{3}{2}RT \quad (\text{A.65})$$

where

$$R = \frac{R_u}{\text{molecular weight}}. \quad (\text{A.66})$$

This is a good model of monatomic gases such as Helium, Argon, etc. Over a very wide range of temperatures

$$\begin{aligned} C_p &= \frac{5}{2}R \\ C_v &= \frac{3}{2}R \end{aligned} \quad (\text{A.67})$$

from near condensation to ionization.

A.9 Diatomic gases

A.9.1 Rotational degrees of freedom

The simplest classical model for a diatomic molecule is a rigid dumb bell such as that shown in figure A.11. In the classical theory for a solid object of this shape there is one rotational degree of freedom about each coordinate axis shown in the figure.

The energy of the rotating body is

$$E_{\text{solid dumbbell}} = \frac{1}{2}I_1\omega_1^2 + \frac{1}{2}I_2\omega_2^2 + \frac{1}{2}I_3\omega_3^2. \quad (\text{A.68})$$

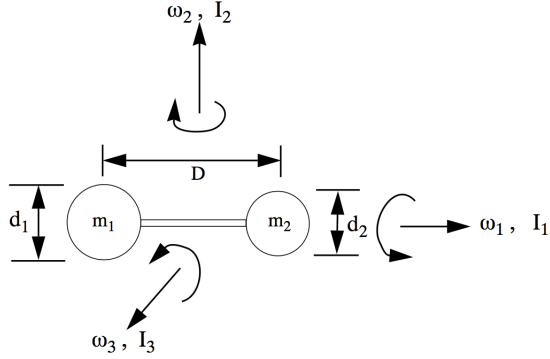


Figure A.11: Rigid dumb bell model of a diatomic molecule.

The moment of inertia about the 2 or the 3 axis is

$$I_2 = I_3 = m_r D^2 \quad (\text{A.69})$$

where

$$m_r = \frac{m_1 m_2}{m_1 + m_2} \quad (\text{A.70})$$

is the *reduced mass*. The moment of inertia of the connecting shaft is neglected in (A.69) where it is assumed that \$d_{1,2} \ll D\$ so that the masses of the spheres can be assumed to be concentrated at the center of each sphere. In classical theory, the energy (A.68) is a continuous function of the three angular frequencies. But in the quantum world of a diatomic molecule the energies in each rotational degree of freedom are discrete. As in the classical case the energy varies inversely with the moment of inertia of the molecule about a given axis. When the Schrödinger equation is solved for a rotating diatomic molecule the energy in the two coordinate directions perpendicular to the internuclear axis is

$$E_{2,3 \text{ diatomic molecule}} = \left(\frac{h}{2\pi} \right)^2 \frac{K(K+1)}{2I_{2,3}} = \left(\frac{h}{2\pi} \right)^2 \frac{K(K+1)}{2(m_r D^2)} \quad (\text{A.71})$$

where \$h\$ is Planck's constant

$$h = 6.626 \times 10^{-34} \text{ J - sec.} \quad (\text{A.72})$$

The atomic masses are assumed to be concentrated at the two atomic centers. The rotational quantum number K is a positive integer greater than or equal to zero, ($K = 0, 1, 2, 3, \dots$). The law of equipartition can be used with (A.71) to roughly equate the rotational energy with an associated gas temperature. Let

$$\frac{1}{2}k\theta_r \cong E_{2,3 \text{ diatomic molecule}}. \quad (\text{A.73})$$

Equation (A.73) defines the characteristic temperature

$$\theta_r = \left(\frac{h}{2\pi} \right)^2 \frac{2}{k(m_r D^2)} \quad (\text{A.74})$$

for the onset of rotational excitation in the two degrees of freedom associated with the 2 and 3 coordinate axes. In terms of the characteristic temperature, the rotational energy is

$$E_{2,3 \text{ diatomic molecule}} = K(K+1)k\theta_r/4. \quad (\text{A.75})$$

Rotational parameters for several common diatomic species are given in figure A.12.

| | $m_r \times 10^{27} \text{ kg}$ | $D \times 10^{10} \text{ M}$ | $\theta_r \text{ } ^\circ\text{K}$ |
|----------------|---------------------------------|------------------------------|------------------------------------|
| H ₂ | 0.8393 | 0.74166 | 349.12 |
| N ₂ | 11.629 | 1.094 | 11.56 |
| O ₂ | 13.284 | 1.207 | 8.32 |
| CO | 11.392 | 1.13 | 11.08 |

Figure A.12: Rotational constants for several diatomic gases.

The characteristic rotational excitation temperatures for common diatomic molecules are all cryogenic and, except for hydrogen (see below), fall below the temperatures at which the materials would liquefy. Thus for all practical purposes, with the exception of hydrogen at low temperature, diatomic molecules in the gas phase have both rotational degrees of freedom fully excited.

A.9.2 Why are only two rotational degrees of freedom excited?

Addition of energy to the degree of freedom associated with rotation about the internuclear axis is quantum mechanically forbidden because of the perfect rotational symmetry about this axis. This is outside of the theory described above, although consistent with it. To demonstrate this, assume that this degree of freedom could be excited. Its discretized energy would be

$$E_{1\text{ diatomic molecule}} = \left(\frac{h}{2\pi}\right)^2 \frac{K(K+1)}{2I_1} \quad (\text{A.76})$$

and the characteristic excitation temperature would be

$$\theta_{r1} = \left(\frac{h}{2\pi}\right)^2 \frac{2}{kI_1} \quad (\text{A.77})$$

Almost all the mass of an atom is concentrated in the nucleus. This would suggest that the appropriate length scale, d , to use in (A.76) might be some measure of the nucleus diameter. Consider a solid sphere model for the two nuclear masses. For a homo-nuclear molecule the characteristic rotational excitation temperature for the 1-axis degree of freedom is

$$\theta_{r1\text{solid nuclear sphere}} = \left(\frac{h}{2\pi}\right)^2 \frac{2}{k(md^2/5)} \quad (\text{A.78})$$

The diameter of the nucleus is on the order of $10^{-14} m$ four orders of magnitude smaller than the diameter of an atom. From this model, one would expect

$$\theta_{r1\text{solid nuclear sphere}} \simeq 10^8 \theta_r. \quad (\text{A.79})$$

This is an astronomically high temperature that would never be reached in a practical situation other than at the center of a star.

Another approach is to ignore the nuclear contribution to the moment of inertia along the 1-axis but include only the moment of inertia of the electron cloud. If we take all of the mass of the electron cloud and concentrate it in a thin shell at the atomic diameter the characteristic rotational temperature is

$$\theta_{r1\text{electron cloud hollow sphere}} = \left(\frac{h}{2\pi}\right)^2 \frac{2}{k((1/3)m_{\text{electron cloud hollow sphere}}d_{\text{atom}}^2)}. \quad (\text{A.80})$$

Most atoms are on the order of $10^{-10} m$ in diameter which is comparable to the internuclear distances shown in figure A.12. But the mass of the proton is 1835 times larger than the electron. So the mass of the nucleus of a typical atom with the same number of neutrons

and protons is roughly 3670 times the mass of the electron cloud. In this model we would expect

$$\theta_{r1_{\text{electron cloud hollow sphere}}} \cong 3670\theta_r \quad (\text{A.81})$$

This would put the rotational excitation temperature along the 1-axis at least into the range $5 \times 10^4 K$ to $3 \times 10^5 K$ or above. In that temperature range, collision energies, $(3/2) kT$, are on the order of 2 to 20 electron volts ($1ev = 1.6 \times 10^{-19} J$). This is comparable to the bond energies of N_2 and O_2 . For example, the dissociation/bond energy of Nitrogen is about 9 electron volts. Moreover, its ionization energy is 14.5 electron volts. So at temperatures where deviation from axi-symmetry along the axis joining the two atoms might occur, additional degrees of freedom due to dissociation and ionization are also coming into play making the energy associated with the third rotational degree of freedom impossible to distinguish. The upshot of all this is that only two of the rotational degrees of freedom are excited in the range of temperatures one is likely to encounter.

The energy of a diatomic molecule at modest temperatures is

$$\begin{aligned} E &= E_T + E_R \\ E_T &= \frac{1}{2}mu^2 + \frac{1}{2}mv^2 + \frac{1}{2}mw^2 \\ E_R &= \frac{1}{2}I_2\omega_2^2 + \frac{1}{2}I_3\omega_3^2. \end{aligned} \quad (\text{A.82})$$

At room temperature

$$\begin{aligned} C_p &= \frac{7}{2}R \\ C_v &= \frac{5}{2}R. \end{aligned} \quad (\text{A.83})$$

From the quantum mechanical description of a diatomic molecule presented above we learn that C_p can show some decrease below $(7/2) R$ at low temperatures. This is because of the tendency of the rotational degrees of freedom to freeze out as the molecular kinetic energy becomes comparable to the first excited rotational mode. This effect can really only be seen in Hydrogen which has the highest rotational excitation temperature. Figure A.13 shows the transition of the constant volume heat capacity of hydrogen from purely translational excited states at low temperature to translational and rotational excited states at room temperature.

Nitrogen and Oxygen liquify at temperatures well above their rotational excitation temperature. More complex molecules with three-dimensional structure can have all three rotational degrees of freedom excited and so one might expect $n = 6$ for a complex molecule at room temperature.

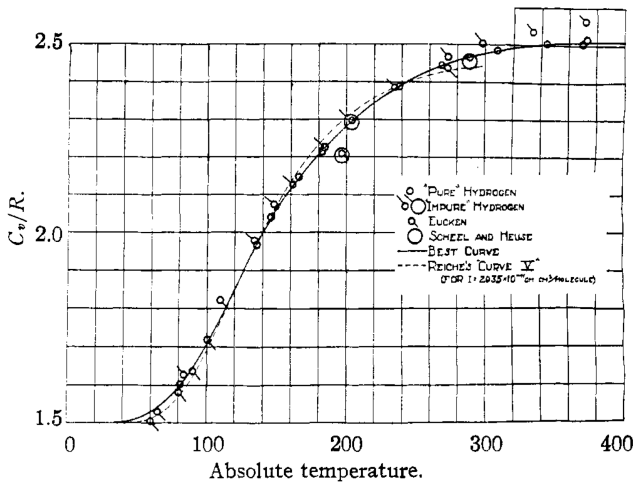


Fig. 3.—Specific heat of hydrogen.

Figure A.13: From: "The specific heat of hydrogen gas at low temperatures from the velocity of sound", paper by Cornish and Eastman, *Journal of the American Chemical Society*, 1928, 50, 3, 627-652

A.9.3 Vibrational degrees of freedom

At high temperatures C_p can increase above $(7/2)R$ because the atoms are not rigidly bound but can vibrate around the mean internuclear distance much like two masses held together by a spring as indicated in figure A.14.

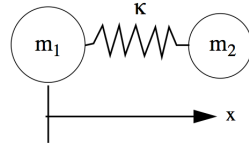


Figure A.14: Diatomic molecule as a spring-mass system.

The energy of a classical harmonic oscillator is

$$E_{\text{spring-mass}} = \frac{1}{2}m_r \dot{x}^2 + \frac{1}{2}\kappa x^2 \quad (\text{A.84})$$

where m_r is the reduced mass, κ is the spring constant and x is the distance between the mass centers.

In the microscopic world of a molecular oscillator the vibrational energy is quantized according to

$$E_V = \left(\frac{h}{2\pi} \right) \omega_0 \left(j + \frac{1}{2} \right) \quad (\text{A.85})$$

where ω_0 is the natural frequency of the oscillator and the quantum number $j = 0, 1, 2, 3, \dots$. The natural frequency is related to the masses and effective spring constant by

$$\omega_0 = \sqrt{\frac{\kappa}{m_r}}. \quad (\text{A.86})$$

For a molecule, the spring constant is called the bond strength. Notice that the vibrational energy of a diatomic molecule can never be zero even at absolute zero temperature.

A characteristic vibrational temperature can be defined using the law of equipartition just as was done earlier for rotation. Let

$$\frac{1}{2}k\theta_v \cong E_V. \quad (\text{A.87})$$

Define

$$\theta_v = \left(\frac{h}{2\pi} \right) \frac{\omega_0}{k} = \left(\frac{h}{2\pi} \right) \frac{1}{k} \sqrt{\frac{\kappa}{m_r}}. \quad (\text{A.88})$$

Vibrational parameters for several common diatomic species are given in Figure A.15.

| | $m_r \times 10^{27} \text{ kg}$ | $\kappa(N/M)$ | $\theta_v \text{ } ^\circ\text{K}$ |
|----------------|---------------------------------|---------------|------------------------------------|
| H ₂ | 0.8393 | 570 | 6297 |
| N ₂ | 11.629 | 2240 | 3354 |
| O ₂ | 13.284 | 1140 | 2238 |
| CO | 11.392 | 1860 | 3087 |

Figure A.15: Vibrational constants for several diatomic gases.

The characteristic vibrational excitation temperatures for common diatomic molecules are all at high combustion temperatures. At high temperature seven degrees of freedom are

excited and the energy of a diatomic molecule is

$$\begin{aligned} E &= E_T + E_R + E_V \\ E_T &= \frac{1}{2}mu^2 + \frac{1}{2}mv^2 + \frac{1}{2}mw^2 \\ E_R &= \frac{1}{2}I_2\omega_2^2 + \frac{1}{2}I_3\omega_3^2 \\ E_V &= \frac{1}{2}m_r\dot{x}^2 + \frac{1}{2}\kappa x^2 \end{aligned} \tag{A.89}$$

where the various energies are quantized as discussed above. At high temperatures the heat capacities approach

$$\begin{aligned} C_p &= \frac{9}{2}R \\ C_v &= \frac{7}{2}R. \end{aligned} \tag{A.90}$$

Quantum statistical mechanics can be used to develop a useful theory for the onset of vibrational excitation. The specific heat of a diatomic gas over a wide range of temperatures is accurately predicted to be

$$\frac{C_p}{R} = \frac{7}{2} + \left(\frac{\theta_v/2T}{\text{Sinh}(\theta_v/2T)} \right)^2. \tag{A.91}$$

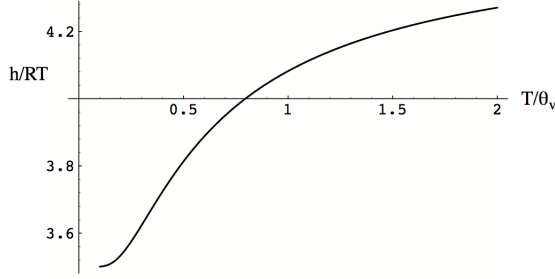
The enthalpy change of a diatomic gas at and above temperatures where the rotational degrees of freedom are fully excited is

$$h(T) - h(T_1) = \int_{T_1}^T C_p dT = R \int_{T_1}^T \left(\frac{7}{2} + \left(\frac{\theta_v/2T}{\text{Sinh}(\theta_v/2T)} \right)^2 \right) dT. \tag{A.92}$$

With T_1 set (somewhat artificially) to zero, this integrates to

$$\frac{h(T)}{RT} = \frac{7}{2} + \frac{\theta_v/T}{e^{\theta_v/T} - 1} \tag{A.93}$$

plotted in figure A.16.

Figure A.16: *Enthalpy of a diatomic gas.*

A.10 Energy levels in a box

We discussed the quantization of rotational and vibrational energy levels but what about translation? The energies for a particle in translational motion are quantized when the particle is confined to a potential well. The wave function for a single atom of mass m contained inside a box satisfies the Schroedinger equation

$$\frac{ih}{2\pi} \frac{\partial \Psi(\bar{x}, t)}{\partial t} + \frac{h^2}{8\pi^2 m} \nabla^2 \Psi(\bar{x}, t) - V(x) \Psi(\bar{x}, t) = 0 \quad (\text{A.94})$$

where $h = 6.626068 \times 10^{-34} m^2 kg / sec$ is Planck's constant defined in equation (A.72). Solutions for a particle in a 1-D and 2-D box are shown in figure A.17. The potential for a 3-D box with sides L_x, L_y, L_z is

$$\begin{aligned} V(\bar{x}) &= 0 & 0 < x < L_x, 0 < y < L_y, 0 < z < L_z \\ V(\bar{x}) &= \infty & \text{on and outside the box.} \end{aligned} \quad (\text{A.95})$$

The solution must satisfy the condition $\Psi = 0$ on and outside the walls of the box. For this potential (A.94) is solved by a system of standing waves.

$$\Psi(x, y, z, t) = \left(\frac{8}{L_x L_y L_z} \right)^{1/2} e^{-i\left(\frac{2\pi E |\bar{k}|}{h}\right)t} \sin\left(\frac{n_x \pi x}{L_x}\right) \sin\left(\frac{n_y \pi y}{L_y}\right) \sin\left(\frac{n_z \pi z}{L_z}\right) \quad (\text{A.96})$$

The quantized energy corresponding to the wave vector

$$\bar{k} = \left(\frac{n_x \pi}{L_x}, \frac{n_y \pi}{L_y}, \frac{n_z \pi}{L_z} \right) \quad (\text{A.97})$$

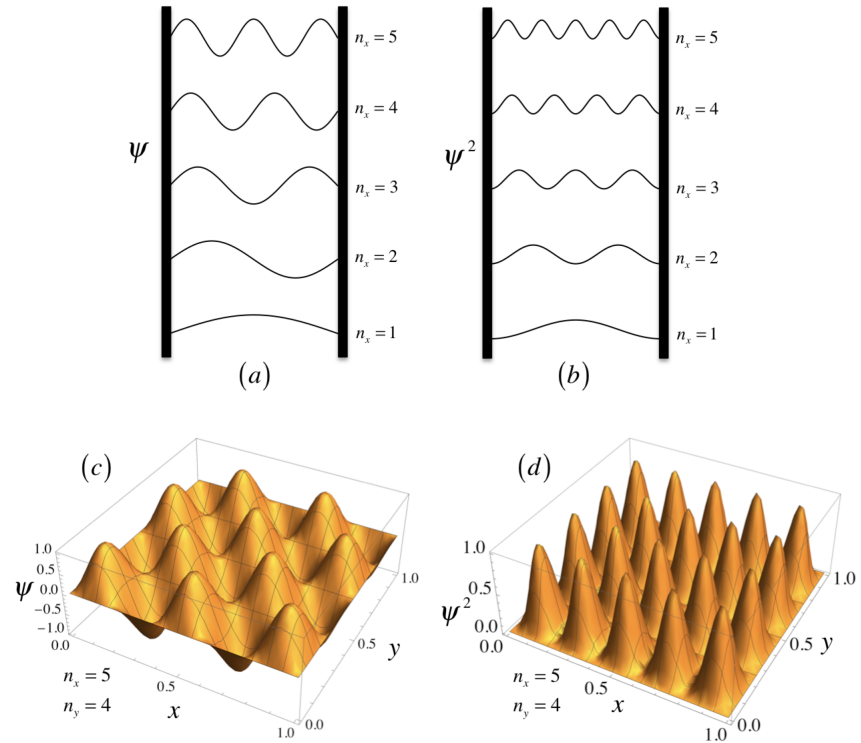


Figure A.17: Figure (a), first five wave functions for a particle in a 1-D box, (b), squared wave functions; proportional to the probability density function that a particle would be found at a particular position in the box. Figure (c), one wave function for a particle in a 2-D box, (d), squared wave function indicating the probable position of the particle in the 2-D box.

is

$$E_{|\bar{k}|} = \frac{h^2}{8\pi^2 m} (k_x^2 + k_y^2 + k_z^2) = \frac{h^2}{8m} \left(\frac{n_x^2}{L_x^2} + \frac{n_y^2}{L_y^2} + \frac{n_z^2}{L_z^2} \right). \quad (\text{A.98})$$

The volume of the box is $V = L_x L_y L_z$. The wave function is zero everywhere outside the box and must satisfy the normalization condition

$$\int_0^{L_x} \int_0^{L_y} \int_0^{L_z} \Psi(\bar{x}, t) \Psi^*(\bar{x}, t) dx dy dz = 1. \quad (\text{A.99})$$

on the total probability that the particle is inside the box. The implication of (A.99) and the condition $\Psi = 0$ on the walls of the box, is that the quantum numbers (n_x, n_y, n_z) must be integers greater than zero. The energy of the particle in the box cannot be zero similar to the case of the harmonic oscillator. For a box of reasonable size, the energy levels are very closely spaced. A characteristic excitation temperature can be defined for translational motion at the lowest possible energy. Let

$$\frac{1}{2} k \theta_T \equiv E_T \quad (\text{A.100})$$

where

$$E_T = \frac{3h^2}{8mV^{2/3}}. \quad (\text{A.101})$$

The translational excitation temperature is

$$\theta_T = \frac{3h^2}{4mkV^{2/3}}. \quad (\text{A.102})$$

Take monatomic helium gas for example. The characteristic translational excitation temperature is

$$\theta_{T_{He}} = \frac{3h^2}{4m_{He}kV^{2/3}} = \frac{3(6.626 \times 10^{-34})^2}{4(6.643 \times 10^{-27}) 1.38 \times 10^{-23} V^{2/3}} = \frac{3.57 \times 10^{-14}}{V^{2/3}} K. \quad (\text{A.103})$$

In general, the characteristic translational temperature is far below any temperature at which a material will solidify. Clearly translational degrees of freedom are fully excited for essentially all temperatures of a gas in a box of reasonable size.

A.10.1 Counting energy states

For simplicity let $L_x = L_y = L_z = L$. In this case, the energy of a quantum state is

$$E_{|\bar{k}|} = \frac{h^2}{8mV^{2/3}} (n_x^2 + n_y^2 + n_z^2). \quad (\text{A.104})$$

Working out the number of possible states with translational energy of the monatomic gas less than some value E amounts to counting all possible values of the quantum numbers, n_x , n_y and n_z that generate $E_{|\bar{k}|} < E$. Imagine a set of coordinate axes in the n_x , n_y and n_z directions. According to (A.98) a surface of constant energy is approximately a sphere (with a stair-stepped surface) with its center at the origin of the n_x , n_y and n_z coordinates. The number of possible states with energy less than the radius of the sphere is directly related to the volume of the sphere. Actually only 1/8th of the sphere is involved corresponding to the positive values of the quantum numbers. Figure A.18 illustrates the idea.

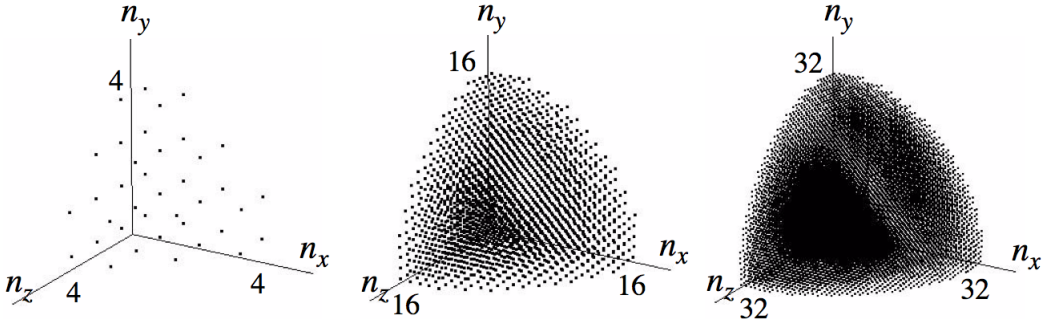


Figure A.18: Points represent quantum states in a box for energies that satisfy $8EmV^{2/3}/h^2 \leq n_x^2 + n_y^2 + n_z^2$. Three cases are shown where the maximum value of the quantum numbers are 4, 16 and 32.

Following Boltzmanns notation, let W be the number of states of the gas with energy less than E .

$$W_{oneatom}(E, V) = \frac{1}{8} \left(\frac{4\pi}{3} (n_x^2 + n_y^2 + n_z^2)^{3/2} \right) = \frac{\pi}{6} (n_x^2 + n_y^2 + n_z^2)^{3/2} \quad (\text{A.105})$$

In terms of the volume of the box and the gas kinetic energy the number of states with

energy $E_{|k|} < E$ is, according to (A.104) and (A.105)

$$W_{oneatom}(E, V) = \frac{\pi}{6} \left(\frac{8m}{h^2} \right)^{3/2} V E^{3/2}. \quad (\text{A.106})$$

Equation (A.106) gives the number of possible energy states with energy less than E for a single atom. If we add a second atom to the box then the number of possible states lies within the positive region of a six dimensional sphere of radius $R = \sqrt{8mV^{2/3}E/h^2}$.

$$\frac{8mV^{2/3}E}{h^2} = (n_{1x}^2 + n_{1y}^2 + n_{1z}^2 + n_{2x}^2 + n_{2y}^2 + n_{2z}^2) \quad (\text{A.107})$$

The volume of a sphere in six dimensions is $(\pi^3/6) R^6$. For a box with N molecules the total number of possible energy states of the system lies within a sphere of $3N$ dimensions with volume

$$\frac{\pi^{3N/2} R^{3N}}{\left(\frac{3N}{2}\right)!}. \quad (\text{A.108})$$

The volume of the positive region of this $3N$ dimensional sphere is

$$\frac{\pi^{3N/2}}{\left(\frac{3N}{2}\right)!} \left(\frac{R}{2}\right)^{3N}. \quad (\text{A.109})$$

In terms of the energy, the number of distinct states with energy less than E is

$$W(E, V, N) = \frac{\pi^{3N/2}}{N! \left(\frac{3N}{2}\right)!} \left(\frac{2m}{h^2}\right)^{3N/2} V^N E^{3N/2}. \quad (\text{A.110})$$

States with the same energy must not be counted more than once. Since the atoms are indistinguishable, the additional factor of $N!$ in the denominator is needed to account for states that are repeated or degenerate. Figure A.19 shows the number of states, $W(E, V, N)$, for the case of N atoms of helium in a box $10^{-7} m$ on a side at $10K$.

If the number of molecules in the volume V is more than a few tens or so, the number of states can be represented using the Stirling approximation for the factorial.

$$\alpha! \cong \alpha^\alpha e^{-\alpha} \quad (\text{A.111})$$

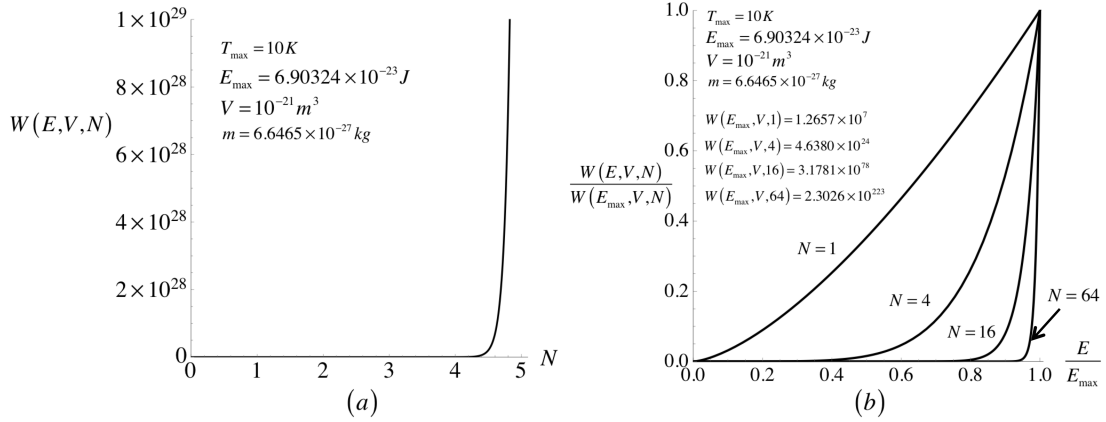


Figure A.19: Number of states of helium gas (A.110) at 10K with energy less than E as a function of both, (a) the number of atoms N , and (b) the energy E for several values of N .

Now

$$W(E, V, N) = \pi^{3N/2} e^{5N/2} \left(\frac{V}{N} \right)^N \left(\frac{4mE}{3h^2 N} \right)^{3N/2}. \quad (\text{A.112})$$

The result (A.112) is presented in Becker's Theory of Heat, page 135, equation 35.4. A more accurate version of the Stirling approximation is

$$\alpha! \cong (2\pi\alpha)^{1/2} \alpha^\alpha e^{-\alpha}$$

which would give

$$W(E, V, N) = \frac{\pi^{3N/2} e^{5N/2}}{\sqrt{6\pi N}} \left(\frac{V}{N} \right)^N \left(\frac{4mE}{3h^2 N} \right)^{3N/2}. \quad (\text{A.113})$$

Note that for values of N greater than a few hundred the number of states with energy less than E is virtually the same as the number of states with energy equal to E because of the extremely steep dependence of (A.113) on N . All of the energy states are concentrated within a membrane thin spherical shell at the energy E .

A.10.2 Entropy of a monatomic gas in terms of the number of states

According to the Law of Equipartition and the development in the early part of this

appendix, the internal energy of a monatomic gas is

$$E = \frac{1}{2}mN\widehat{u^2} = \frac{3}{2}kNT. \quad (\text{A.114})$$

The number of states can be expressed in terms of the temperature as

$$W(T, V, N) = \pi^{3N/2} e^{5N/2} \left(\frac{V}{N}\right)^N \left(\frac{2mkT}{h^2}\right)^{3N/2}. \quad (\text{A.115})$$

Take the logarithm of (A.115).

$$\log(W(T, V, N)) = N \left(\log\left(\frac{V}{N}\right) + \frac{3}{2}\log(T) + \frac{3}{2}\log\left(\frac{2\pi mk}{h^2}\right) + \frac{5}{2} \right) \quad (\text{A.116})$$

Differentiate (A.116) and multiply both sides by Boltzmanns constant, k .

$$k \frac{dW}{W} = \frac{3kN}{2} \frac{dT}{T} + kN \frac{d(V/N)}{V/N} \quad (\text{A.117})$$

Recall $R_u = kN_a$ where N_a is Avogadros number. Equation (A.117) now becomes

$$k \frac{dW}{W} = \frac{3}{2}nR_u \frac{dT}{T} + nR_u \frac{d(V/N)}{V/N}. \quad (\text{A.118})$$

where the number of moles of gas in the box is $n = N/N_a$.

The model we are considering is that of a monatomic gas with only three degrees of freedom. For such a gas the constant volume molar heat capacity is $C_v = 3R_u/2$. Equation (A.118) now reads

$$k \frac{dW}{W} = nC_v \frac{dT}{T} + nR_u \frac{d(V/n)}{V/n}. \quad (\text{A.119})$$

Recall the Gibbs equation

$$dS = \frac{dE}{T} + \frac{P}{T} dV. \quad (\text{A.120})$$

For an ideal gas with the equation of state $PV = nR_uT$ the Gibbs equation becomes

$$dS = nC_v \frac{dT}{T} + nR_u \frac{dV}{V}. \quad (\text{A.121})$$

Comparing (A.121) with (A.119) leads to the conclusion that

$$dS = k \frac{dW}{W}. \quad (\text{A.122})$$

Integrating (A.122) leads to the famous Boltzmann relation for the entropy

$$S = k \log(W) + \alpha. \quad (\text{A.123})$$

Substutute (A.112) into (A.123). The entropy of the gas is

$$S = kN \left(\log \left(\frac{V}{N} \left(\frac{E}{N} \right)^{3/2} \right) + \frac{5}{2} + \frac{3}{2} \log \left(\frac{4\pi m}{3h^2} \right) \right). \quad (\text{A.124})$$

The relation (A.124) is known as the Sackur-Tetrode equation after its discoverers in the early 1900s. It can be used to derive the various equations that govern a gas. In terms of the temperature, the entropy expression is equation (A.116) multiplied by k

$$S = kN \left(\log \left(\frac{V}{N} (T)^{3/2} \right) + \frac{5}{2} + \frac{3}{2} \log \left(\frac{2\pi mk}{h^2} \right) \right) \quad (\text{A.125})$$

which agrees with equation 35.8 in Beckers *Theory of Heat*, page 136.

The additive constant in (A.125) is not in disagreement with the third law nor is the fact that (A.125) becomes singular at $T = 0$. The theory just developed is for a Boltzmann gas that necessarily implies temperatures well above absolute zero where the material is not in a condensed state and Boltzmann statistics apply. The constant is needed for the theory of condensation. The Sackur-Tetrode equation provides a remarkably accurate value of the entropy for monatomic gases. As an example, select helium at a pressure of $10^5 N/m^2$ and temperature of $298.15 K$. At these conditions $V/N = 4.11641 \times 10^{-26} m^3/molecule$. The mass of the helium atom is $m = 6.64648 \times 10^{-27} kg$ using these values the entropy evaluated from (A.125) is

$$\frac{S}{kN} = \log \left(e^{5/2} \left(\frac{V}{N} \right) \left(\frac{2\pi mkT}{h^2} \right)^{3/2} \right) = 15.1727 \quad (\text{A.126})$$

The value provided in tabulations of helium properties is 15.17271576. Similar results can be determined for other monatomic gases.

According to the third law $\alpha = 0$ and

$$S = k \log (W) \quad (\text{A.127})$$

is the absolute entropy of the system. Consider the state of a single atom contained in a box in the limit $T \rightarrow 0$. From the solution to the Schrödinger equation, (A.98), the least energy that the atom can have is

$$E_{111} = \frac{3\hbar^2}{8mV^{2/3}}. \quad (\text{A.128})$$

This is a tiny but finite number. In this model of a single atom gas, as the temperature goes to zero the atom in the box falls into the lowest quantum state and the entropy is $S = k \log (1) = 0$.

We derived (A.127) using the energy states in an ideal monatomic gas rather than follow the more general proof of Boltzmann. The remarkable thing about (A.127) is that it applies to a wide range of systems other than ideal gases including solids and liquids.

Appendix B

Equations in cylindrical and spherical coords

B.1 Coordinate systems

B.1.1 Cylindrical coordinates

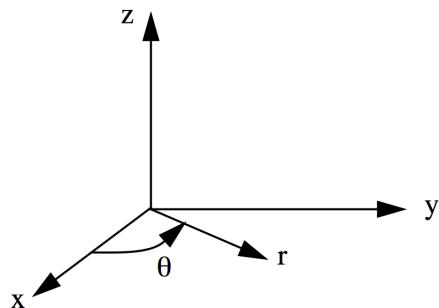


Figure B.1: *right-handed cylindrical coordinate system*

$$x = r \cos(\theta)$$

$$y = r \sin(\theta)$$

$$z = z \quad (B.1)$$

$$r = (x^2 + y^2)^{1/2}$$

$$\theta = \text{ArcTan}(y/x)$$

B.1.2 Spherical polar coordinates

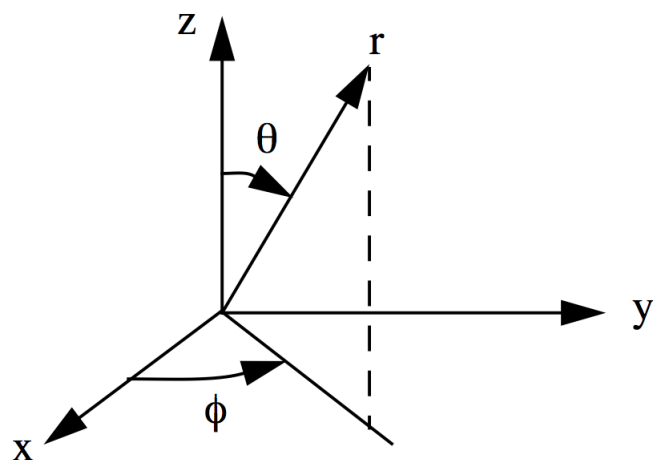


Figure B.2: Right handed spherical polar coordinate system.

$$\begin{aligned}
x &= r \sin(\theta) \cos(\phi) \\
y &= r \sin(\theta) \sin(\phi) \\
z &= r \cos(\theta) \\
r &= (x^2 + y^2 + z^2)^{1/2} \\
\theta &= \text{ArcTan}\left((x^2 + y^2)^{1/2} / z\right) \\
\phi &= \text{ArcTan}(y/x)
\end{aligned} \tag{B.2}$$

B.2 Transformation of vector components

Basic trigonometry can be used to show that the Cartesian and curvilinear components are related as follows.

B.2.1 Cylindrical coordinates

$$\begin{aligned}
U_r &= U_x \cos(\theta) + U_y \sin(\theta) \\
U_\theta &= -U_x \sin(\theta) + U_y \cos(\theta) \\
U_z &= U_z \\
U_x &= U_r \cos(\theta) - U_\theta \sin(\theta) \\
U_y &= U_r \sin(\theta) + U_\theta \cos(\theta) \\
U_z &= U_z
\end{aligned} \tag{B.3}$$

B.2.2 Spherical polar coordinates

$$\begin{aligned}
U_r &= U_x \sin(\theta) \cos(\phi) + U_y \sin(\theta) \sin(\phi) + U_z \cos(\theta) \\
U_\theta &= U_x \cos(\theta) \cos(\phi) + U_y \cos(\theta) \sin(\phi) - U_z \sin(\theta) \\
U_\phi &= -U_x \sin(\phi) + U_y \cos(\phi) \\
U_x &= U_r \sin(\theta) \cos(\phi) + U_\theta \cos(\theta) \cos(\phi) - U_\phi \sin(\phi) \\
U_y &= U_r \sin(\theta) \sin(\phi) + U_\theta \cos(\theta) \sin(\phi) + U_\phi \cos(\phi) \\
U_z &= U_r \cos(\theta) - U_\theta \sin(\theta)
\end{aligned} \tag{B.4}$$

B.3 Summary of differential operations

B.3.1 Cylindrical coordinates

$$\nabla \cdot \bar{U} = \frac{1}{r} \frac{\partial}{\partial r} (r U_r) + \frac{1}{r} \frac{\partial U_\theta}{\partial \theta} + \frac{\partial U_z}{\partial z} \tag{B.5}$$

$$\nabla^2 \rho = \frac{1}{r} \frac{\partial}{\partial r} \left(r \frac{\partial \rho}{\partial r} \right) + \frac{1}{r^2} \frac{\partial^2 \rho}{\partial \theta^2} + \frac{\partial^2 \rho}{\partial z^2} \tag{B.6}$$

$$\begin{aligned}
\bar{\tau} : \nabla \bar{U} &= \tau_{rr} \left(\frac{\partial U_r}{\partial r} \right) + \tau_{\theta\theta} \left(\frac{1}{r} \frac{\partial U_\theta}{\partial \theta} + \frac{U_r}{r} \right) + \tau_{zz} \left(\frac{\partial U_z}{\partial z} \right) + \\
&\tau_{r\theta} \left(r \frac{\partial}{\partial r} \left(\frac{U_\theta}{r} \right) + \frac{1}{r} \frac{\partial U_r}{\partial \theta} \right) + \tau_{\theta z} \left(\frac{1}{r} \frac{\partial U_z}{\partial \theta} + \frac{\partial U_\theta}{\partial z} \right) + \tau_{rz} \left(\frac{\partial U_z}{\partial r} + \frac{\partial U_r}{\partial z} \right)
\end{aligned} \tag{B.7}$$

$$\begin{aligned}
\nabla \rho|_r &= \frac{\partial \rho}{\partial r} \\
\nabla \rho|_\theta &= \frac{1}{r} \frac{\partial \rho}{\partial r} \\
\nabla \rho|_z &= \frac{\partial \rho}{\partial z}
\end{aligned} \tag{B.8}$$

$$\begin{aligned}\nabla \times \bar{U}|_r &= \frac{1}{r} \frac{\partial U_z}{\partial \theta} - \frac{\partial U_\theta}{\partial z} \\ \nabla \times \bar{U}|_\theta &= \frac{\partial U_r}{\partial z} - \frac{\partial U_z}{\partial r} \end{aligned}\quad (\text{B.9})$$

$$\begin{aligned}\nabla \cdot \bar{\tau}|_r &= \frac{1}{r} \frac{\partial}{\partial r} (r \tau_{rr}) + \frac{1}{r} \frac{\partial \tau_{r\theta}}{\partial \theta} - \frac{\tau_{\theta\theta}}{r} + \frac{\partial \tau_{rz}}{\partial z} \\ \nabla \cdot \bar{\tau}|_\theta &= \frac{1}{r} \frac{\partial \tau_{\theta\theta}}{\partial \theta} + \frac{1}{r^2} \frac{\partial}{\partial r} (r^2 \tau_{r\theta}) + \frac{\partial \tau_{\theta z}}{\partial z} \\ \nabla \cdot \bar{\tau}|_z &= \frac{1}{r} \frac{\partial}{\partial r} (r \tau_{rz}) + \frac{1}{r} \frac{\partial \tau_{\theta z}}{\partial \theta} + \frac{\partial \tau_{zz}}{\partial z} \end{aligned}\quad (\text{B.10})$$

$$\begin{aligned}\nabla^2 \bar{U}|_r &= \nabla^2 U_r - \frac{2}{r^2} \frac{\partial U_\theta}{\partial \theta} - \frac{U_r}{r^2} \\ \nabla^2 \bar{U}|_\theta &= \nabla^2 U_\theta + \frac{2}{r^2} \frac{\partial U_r}{\partial \theta} - \frac{U_\theta}{r^2} \\ \nabla^2 \bar{U}|_z &= \nabla^2 U_z \end{aligned}\quad (\text{B.11})$$

where

$$\nabla^2 () = \frac{1}{r} \frac{\partial}{\partial r} \left(r \frac{\partial ()}{\partial r} \right) + \frac{1}{r^2} \frac{\partial^2 ()}{\partial \theta^2} + \frac{\partial^2 ()}{\partial z^2} \quad (\text{B.12})$$

$$\begin{aligned}\bar{U} \cdot \nabla \bar{U}|_r &= U_r \frac{\partial U_r}{\partial r} + \frac{U_\theta}{r} \frac{\partial U_r}{\partial \theta} - \frac{U_\theta^2}{r} + U_z \frac{\partial U_r}{\partial z} \\ \bar{U} \cdot \nabla \bar{U}|_\theta &= U_r \frac{\partial U_\theta}{\partial r} + \frac{U_\theta}{r} \frac{\partial U_\theta}{\partial \theta} + \frac{U_r U_\theta}{r} + U_z \frac{\partial U_\theta}{\partial z} \\ \bar{U} \cdot \nabla \bar{U}|_z &= U_r \frac{\partial U_z}{\partial r} + \frac{U_\theta}{r} \frac{\partial U_z}{\partial \theta} + U_z \frac{\partial U_z}{\partial z} \end{aligned}\quad (\text{B.13})$$

B.3.2 Spherical polar coordinates

$$\nabla \cdot \bar{U} = \frac{1}{r^2} \frac{\partial}{\partial r} (r^2 U_r) + \frac{1}{r \sin(\theta)} \frac{\partial}{\partial \theta} (\sin(\theta) U_\theta) + \frac{1}{r \sin(\theta)} \frac{\partial U_\phi}{\partial \phi} \quad (\text{B.14})$$

$$\nabla^2 \rho = \frac{1}{r^2} \frac{\partial}{\partial r} \left(r^2 \frac{\partial \rho}{\partial r} \right) + \frac{1}{r^2 \sin(\theta)} \frac{\partial}{\partial \theta} \left(\sin(\theta) \frac{\partial \rho}{\partial \theta} \right) + \frac{1}{r^2 \sin(\theta)} \frac{\partial^2 \rho}{\partial \phi^2} \quad (\text{B.15})$$

$$\begin{aligned} \bar{\tau} : \nabla \bar{U} &= \tau_{rr} \left(\frac{\partial U_r}{\partial r} \right) + \tau_{\theta\theta} \left(\frac{1}{r} \frac{\partial U_\theta}{\partial \theta} + \frac{U_r}{r} \right) + \tau_{\phi\phi} \left(\frac{1}{r \sin(\theta)} \frac{\partial U_\phi}{\partial \phi} + \frac{U_r}{r} + \frac{U_\theta \cot(\theta)}{r} \right) + \\ &\tau_{r\theta} \left(r \frac{\partial}{\partial r} \left(\frac{U_\theta}{r} \right) + \frac{1}{r} \frac{\partial U_r}{\partial \theta} \right) + \tau_{r\phi} \left(\frac{\partial U_\phi}{\partial r} + \frac{1}{r \sin(\theta)} \frac{\partial U_r}{\partial \phi} - \frac{U_\phi}{r} \right) + \\ &\tau_{\theta\phi} \left(\frac{1}{r} \frac{\partial U_\phi}{\partial \theta} + \frac{1}{r \sin(\theta)} \frac{\partial U_\theta}{\partial \phi} - \frac{U_\phi \cot(\theta)}{r} \right) \end{aligned} \quad (\text{B.16})$$

$$\begin{aligned} \nabla \rho|_r &= \frac{\partial \rho}{\partial r} \\ \nabla \rho|_\theta &= \frac{1}{r} \frac{\partial \rho}{\partial \theta} \\ \nabla \rho|_\phi &= \frac{1}{r \sin(\theta)} \frac{\partial \rho}{\partial \phi} \end{aligned} \quad (\text{B.17})$$

$$\begin{aligned} \nabla \times \bar{U}|_r &= \frac{1}{r \sin(\theta)} \frac{\partial}{\partial \theta} (\sin(\theta) U_\phi) - \frac{1}{r \sin(\theta)} \frac{\partial U_\theta}{\partial \phi} \\ \nabla \times \bar{U}|_\theta &= \frac{1}{r \sin(\theta)} \frac{\partial U_r}{\partial \phi} - \frac{1}{r} \frac{\partial}{\partial r} (r U_\phi) \\ \nabla \times \bar{U}|_\phi &= \frac{1}{r} \frac{\partial}{\partial r} (r U_\theta) - \frac{1}{r} \frac{\partial U_r}{\partial \theta} \end{aligned} \quad (\text{B.18})$$

$$\begin{aligned}
\nabla \cdot \bar{\tau}|_r &= \frac{1}{r^2} \frac{\partial}{\partial r} (r^2 \tau_{rr}) + \frac{1}{r \sin(\theta)} \frac{\partial}{\partial \theta} (\sin(\theta) \tau_{r\theta}) + \frac{1}{r \sin(\theta)} \frac{\partial \tau_{r\phi}}{\partial \phi} - \left(\frac{\tau_{\theta\theta} + \tau_{\phi\phi}}{r} \right) \\
\nabla \cdot \bar{\tau}|_\theta &= \frac{1}{r^2} \frac{\partial}{\partial r} (r^2 \tau_{r\theta}) + \frac{1}{r \sin(\theta)} \frac{\partial}{\partial \theta} (\sin(\theta) \tau_{\theta\theta}) + \frac{1}{r \sin(\theta)} \frac{\partial \tau_{\theta\phi}}{\partial \phi} + \frac{\tau_{r\theta}}{r} - \frac{\cot(\theta)}{r} \tau_{\phi\phi} \\
\nabla \cdot \bar{\tau}|_\phi &= \frac{1}{r^2} \frac{\partial}{\partial r} (r^2 \tau_{r\phi}) + \frac{1}{r} \frac{\partial \tau_{\theta\phi}}{\partial \theta} + \frac{1}{r \sin(\theta)} \frac{\partial \tau_{\phi\phi}}{\partial \phi} + \frac{\tau_{r\phi}}{r} + \frac{2 \cot(\theta)}{r} \tau_{\theta\phi}
\end{aligned} \tag{B.19}$$

$$\begin{aligned}
\nabla^2 \bar{U}|_r &= \nabla^2 U_r - \frac{2}{r^2} \frac{\partial U_\theta}{\partial \theta} - \frac{2 U_\theta \cot(\theta)}{r^2} - \frac{2}{r^2 \sin(\theta)} \frac{\partial U_\phi}{\partial \phi} - \frac{2 U_r}{r^2} \\
\nabla^2 \bar{U}|_\theta &= \nabla^2 U_\theta + \frac{2}{r^2} \frac{\partial U_r}{\partial \theta} - \frac{U_\theta}{r^2 \sin^2(\theta)} - \frac{2 \cos(\theta)}{r^2 \sin^2(\theta)} \frac{\partial U_\phi}{\partial \phi} \\
\nabla^2 \bar{U}|_\phi &= \nabla^2 U_\phi - \frac{U_\phi}{r^2 \sin^2(\theta)} + \frac{2}{r^2 \sin(\theta)} \frac{\partial U_r}{\partial \phi} + \frac{2 \cos(\theta)}{r^2 \sin^2(\theta)} \frac{\partial U_\theta}{\partial \phi}
\end{aligned} \tag{B.20}$$

$$\nabla^2 () = \frac{1}{r^2} \frac{\partial}{\partial r} \left(r^2 \frac{\partial ()}{\partial r} \right) + \frac{1}{r^2 \sin(\theta)} \frac{\partial}{\partial \theta} \left(\sin(\theta) \frac{\partial ()}{\partial \theta} \right) + \frac{1}{r^2 \sin^2(\theta)} \frac{\partial^2 ()}{\partial \phi^2} \tag{B.21}$$

where

$$\begin{aligned}
\bar{U} \cdot \nabla \bar{U}|_r &= U_r \frac{\partial U_r}{\partial r} + \frac{U_\theta}{r} \frac{\partial U_r}{\partial \theta} + \frac{U_\phi}{r \sin(\theta)} \frac{\partial U_r}{\partial \phi} - \left(\frac{U_\theta^2 + U_\phi^2}{r} \right) \\
\bar{U} \cdot \nabla \bar{U}|_\theta &= U_r \frac{\partial U_\theta}{\partial r} + \frac{U_\theta}{r} \frac{\partial U_\theta}{\partial \theta} + \frac{U_\phi}{r \sin(\theta)} \frac{\partial U_\theta}{\partial \phi} + \frac{U_r U_\theta}{r} - \frac{U_\phi^2 \cot(\theta)}{r} \\
\bar{U} \cdot \nabla \bar{U}|_\phi &= U_r \frac{\partial U_\phi}{\partial r} + \frac{U_\theta}{r} \frac{\partial U_\phi}{\partial \theta} + \frac{U_\phi}{r \sin(\theta)} \frac{\partial U_\phi}{\partial \phi} + \frac{U_r U_\phi}{r} + \frac{U_\theta U_\phi \cot(\theta)}{r}
\end{aligned} \tag{B.22}$$

B.4 Continuity

B.4.1 Cylindrical coordinates

$$\frac{\partial \rho}{\partial t} + \frac{1}{r} \frac{\partial}{\partial r} (\rho r U_r) + \frac{1}{r} \frac{\partial}{\partial \theta} (\rho U_\theta) + \frac{\partial}{\partial z} (\rho U_z) = 0 \tag{B.23}$$

B.4.2 Spherical polar coordinates

$$\frac{\partial \rho}{\partial t} + \frac{1}{r^2} \frac{\partial}{\partial r} (\rho r^2 U_r) + \frac{1}{r \sin(\theta)} \frac{\partial}{\partial \theta} (\sin(\theta) \rho U_\theta) + \frac{1}{r \sin(\theta)} \frac{\partial}{\partial \phi} (\rho U_\phi) = 0 \quad (\text{B.24})$$

B.5 Momentum

B.5.1 Cylindrical coordinates

r – component

$$\begin{aligned} \rho \left(\frac{\partial U_r}{\partial t} + U_r \frac{\partial U_r}{\partial r} + \frac{U_\theta}{r} \frac{\partial U_r}{\partial \theta} - \frac{U_\theta^2}{r} + U_z \frac{\partial U_r}{\partial z} \right) + \frac{\partial P}{\partial r} = \\ \frac{1}{r} \frac{\partial}{\partial r} (r \tau_{rr}) + \frac{1}{r} \frac{\partial \tau_{r\theta}}{\partial \theta} - \frac{\tau_{\theta\theta}}{r} + \frac{\partial \tau_{rz}}{\partial z} + \rho g_r \end{aligned}$$

θ – component

$$\begin{aligned} \rho \left(\frac{\partial U_\theta}{\partial t} + U_r \frac{\partial U_\theta}{\partial r} + \frac{U_\theta}{r} \frac{\partial U_\theta}{\partial \theta} + \frac{U_r U_\theta}{r} + U_z \frac{\partial U_\theta}{\partial z} \right) + \frac{1}{r} \frac{\partial P}{\partial \theta} = \\ \frac{1}{r} \frac{\partial \tau_{\theta\theta}}{\partial \theta} + \frac{1}{r^2} \frac{\partial}{\partial r} (r^2 \tau_{r\theta}) + \frac{\partial \tau_{\theta z}}{\partial z} + \rho g_\theta \end{aligned} \quad (\text{B.25})$$

z – component

$$\begin{aligned} \rho \left(\frac{\partial U_z}{\partial t} + U_r \frac{\partial U_z}{\partial r} + \frac{U_\theta}{r} \frac{\partial U_z}{\partial \theta} + U_z \frac{\partial U_z}{\partial z} \right) + \frac{\partial P}{\partial z} = \\ \frac{1}{r} \frac{\partial}{\partial r} (r \tau_{rz}) + \frac{1}{r} \frac{\partial \tau_{\theta z}}{\partial \theta} + \frac{\partial \tau_{zz}}{\partial z} + \rho g_z \end{aligned}$$

B.5.2 Spherical polar coordinates

r – component

$$\begin{aligned} \rho \left(\frac{\partial U_r}{\partial t} + U_r \frac{\partial U_r}{\partial r} + \frac{U_\theta}{r} \frac{\partial U_r}{\partial \theta} + \frac{U_\phi}{r \sin(\theta)} \frac{\partial U_r}{\partial \phi} - \left(\frac{U_\theta^2 + U_\phi^2}{r} \right) \right) + \frac{\partial P}{\partial r} = \\ \frac{1}{r^2} \frac{\partial}{\partial r} (r^2 \tau_{rr}) + \frac{1}{r \sin(\theta)} \frac{\partial}{\partial \theta} (\sin(\theta) \tau_{r\theta}) + \frac{1}{r \sin(\theta)} \frac{\partial \tau_{r\phi}}{\partial \phi} - \left(\frac{\tau_{\theta\theta} + \tau_{\phi\phi}}{r} \right) + \rho g_r \end{aligned}$$

θ – component

$$\begin{aligned} \rho \left(\frac{\partial U_\theta}{\partial t} + U_r \frac{\partial U_\theta}{\partial r} + \frac{U_\theta}{r} \frac{\partial U_\theta}{\partial \theta} + \frac{U_\phi}{r \sin(\theta)} \frac{\partial U_\theta}{\partial \phi} + \frac{U_r U_\theta}{r} - \frac{U_\phi^2 \cot(\theta)}{r} \right) + \frac{1}{r} \frac{\partial P}{\partial \theta} = \\ \frac{1}{r^2} \frac{\partial}{\partial r} (r^2 \tau_{r\theta}) + \frac{1}{r \sin(\theta)} \frac{\partial}{\partial \theta} (\sin(\theta) \tau_{\theta\theta}) + \frac{1}{r \sin(\theta)} \frac{\partial \tau_{\theta\phi}}{\partial \phi} + \frac{\tau_{r\theta}}{r} - \frac{\cot(\theta)}{r} \tau_{\phi\phi} + \rho g_\theta \end{aligned}$$

ϕ – component

$$\begin{aligned} \rho \left(\frac{\partial U_\phi}{\partial t} + U_r \frac{\partial U_\phi}{\partial r} + \frac{U_\theta}{r} \frac{\partial U_\phi}{\partial \theta} + \frac{U_\phi}{r \sin(\theta)} \frac{\partial U_\phi}{\partial \phi} + \frac{U_r U_\phi}{r} + \frac{U_\theta U_\phi \cot(\theta)}{r} \right) + \frac{1}{r \sin(\theta)} \frac{\partial P}{\partial \phi} = \\ \frac{1}{r^2} \frac{\partial}{\partial r} (r^2 \tau_{r\phi}) + \frac{1}{r} \frac{\partial \tau_{\theta\phi}}{\partial \theta} + \frac{1}{r \sin(\theta)} \frac{\partial \tau_{\phi\phi}}{\partial \phi} + \frac{\tau_{r\phi}}{r} + \frac{2 \cot(\theta)}{r} \tau_{\theta\phi} + \rho g_\phi \end{aligned} \tag{B.26}$$

B.6 Energy equation

Recall that the stagnation enthalpy is

$$h_t = e + \frac{P}{\rho} + k. \tag{B.27}$$

B.6.1 Cylindrical coordinates

$$\begin{aligned}
& \frac{\partial}{\partial t} (\rho(e + k)) + \frac{1}{r} \frac{\partial}{\partial r} (r \rho h_t U_r) + \frac{1}{r} \frac{\partial}{\partial \theta} (\rho h_t U_\theta) + \frac{\partial}{\partial z} (\rho h_t U_z) + \\
& \left(\frac{1}{r} \frac{\partial}{\partial r} (r Q_r) + \frac{1}{r} \frac{\partial Q_\theta}{\partial \theta} + \frac{\partial Q_z}{\partial z} \right) - \left(\tau_{rr} \frac{\partial U_r}{\partial r} + \tau_{\theta\theta} \left(\frac{1}{r} \frac{\partial U_\theta}{\partial \theta} + \frac{U_r}{r} \right) + \tau_{zz} \frac{\partial U_z}{\partial z} \right) - \\
& \left(\tau_{r\theta} \left(r \frac{\partial}{\partial r} \left(\frac{U_\theta}{r} \right) + \frac{1}{r} \frac{\partial U_r}{\partial \theta} \right) + \tau_{rz} \left(\frac{\partial U_z}{\partial r} + \frac{\partial U_r}{\partial z} \right) + \tau_{\theta z} \left(\frac{1}{r} \frac{\partial U_z}{\partial \theta} + \frac{\partial U_\theta}{\partial z} \right) \right) - \\
& U_r \left(\frac{1}{r} \frac{\partial}{\partial r} (r \tau_{rr}) + \frac{1}{r} \frac{\partial \tau_{r\theta}}{\partial \theta} - \frac{\tau_{\theta\theta}}{r} + \frac{\partial \tau_{rz}}{\partial z} \right) - \\
& U_\theta \left(\frac{1}{r} \frac{\partial \tau_{\theta\theta}}{\partial \theta} + \frac{1}{r^2} \frac{\partial}{\partial r} (r^2 \tau_{r\theta}) + \frac{\partial \tau_{\theta z}}{\partial z} \right) - \\
& U_z \left(\frac{1}{r} \frac{\partial}{\partial \theta} (r \tau_{rz}) + \frac{1}{r} \frac{\partial \tau_{\theta z}}{\partial r} + \frac{\partial \tau_{zz}}{\partial z} \right) = \{power sources\}
\end{aligned} \tag{B.28}$$

B.6.2 Spherical polar coordinates

$$\begin{aligned}
& \frac{\partial}{\partial t} (\rho(e + k)) + \\
& \frac{1}{r^2} \frac{\partial}{\partial r} (r^2 \rho h_t U_r) + \frac{1}{r \sin(\theta)} \frac{\partial}{\partial \theta} (\rho h_t \sin(\theta) U_\theta) + \frac{1}{r \sin(\theta)} \frac{\partial}{\partial \phi} (\rho h_t U_\phi) + \\
& \left(\frac{1}{r^2} \frac{\partial}{\partial r} (r^2 Q_r) + \frac{1}{r \sin(\theta)} \frac{\partial}{\partial \theta} (\sin(\theta) Q_\theta) + \frac{1}{r \sin(\theta)} \frac{\partial Q_\phi}{\partial \phi} \right) - \\
& \left(\tau_{rr} \frac{\partial U_r}{\partial r} + \tau_{\theta\theta} \left(\frac{1}{r} \frac{\partial U_\theta}{\partial \theta} + \frac{U_r}{r} \right) + \tau_{\phi\phi} \left(\frac{1}{r \sin(\theta)} \frac{\partial U_\phi}{\partial \phi} + \frac{U_r}{r} + \frac{\cot(\theta) U_\theta}{r} \right) \right) - \\
& \tau_{r\theta} \left(r \frac{\partial}{\partial r} \left(\frac{U_\theta}{r} \right) + \frac{1}{r} \frac{\partial U_r}{\partial \theta} \right) - \tau_{r\phi} \left(\frac{\partial U_\phi}{\partial r} + \frac{1}{r \sin(\theta)} \frac{\partial U_r}{\partial \phi} - \frac{U_\phi}{r} \right) - \\
& \tau_{\theta\phi} \left(\frac{1}{r} \frac{\partial U_\phi}{\partial \theta} + \frac{1}{r \sin(\theta)} \frac{\partial U_\theta}{\partial \phi} - \frac{\cot(\theta) U_\phi}{r} \right) - \\
& U_r \left(\frac{1}{r^2} \frac{\partial}{\partial r} (r^2 \tau_{rr}) + \frac{1}{r \sin(\theta)} \frac{\partial}{\partial \theta} (\sin(\theta) \tau_{r\theta}) + \frac{1}{r \sin(\theta)} \frac{\partial \tau_{r\phi}}{\partial \phi} - \left(\frac{\tau_{\theta\theta} + \tau_{\phi\phi}}{r} \right) \right) - \\
& U_\theta \left(\frac{1}{r^2} \frac{\partial}{\partial r} (r^2 \tau_{r\theta}) + \frac{1}{r \sin(\theta)} \frac{\partial}{\partial \theta} (\sin(\theta) \tau_{\theta\theta}) + \frac{1}{r \sin(\theta)} \frac{\partial \tau_{\theta\phi}}{\partial \phi} + \frac{\tau_{r\theta}}{r} - \frac{\cot(\theta) \tau_{\phi\phi}}{r} \right) - \\
& U_\phi \left(\frac{1}{r^2} \frac{\partial}{\partial r} (r^2 \tau_{r\phi}) + \frac{1}{r} \frac{\partial \tau_{\theta\phi}}{\partial \theta} + \frac{1}{r \sin(\theta)} \frac{\partial \tau_{\phi\phi}}{\partial \phi} + \frac{\tau_{r\phi}}{r} + \frac{2 \cot(\theta) \tau_{\theta\phi}}{r} \right) = \\
& \{power sources\}
\end{aligned} \tag{B.29}$$

B.7 Components of the stress tensor

B.7.1 Cylindrical coordinates

$$\begin{aligned}
 \tau_{rr} &= 2\mu \frac{\partial U_r}{\partial r} - \left(\frac{2}{3}\mu - \mu_v \right) \nabla \cdot \bar{U} \\
 \tau_{\theta\theta} &= 2\mu \left(\frac{1}{r} \frac{\partial U_\theta}{\partial \theta} + \frac{U_r}{r} \right) - \left(\frac{2}{3}\mu - \mu_v \right) \nabla \cdot \bar{U} \\
 \tau_{zz} &= 2\mu \frac{\partial U_z}{\partial z} - \left(\frac{2}{3}\mu - \mu_v \right) \nabla \cdot \bar{U} \\
 \tau_{r\theta} &= \mu \left(r \frac{\partial}{\partial r} \left(\frac{U_\theta}{r} \right) + \frac{1}{r} \frac{\partial U_r}{\partial \theta} \right) \\
 \tau_{rz} &= \mu \left(\frac{\partial U_r}{\partial z} + \frac{\partial U_z}{\partial r} \right) \\
 \tau_{\theta z} &= \mu \left(\frac{\partial U_\theta}{\partial z} + \frac{1}{r} \frac{\partial U_z}{\partial \theta} \right)
 \end{aligned} \tag{B.30}$$

B.7.2 Spherical polar coordinates

$$\begin{aligned}
 \tau_{rr} &= 2\mu \frac{\partial U_r}{\partial r} - \left(\frac{2}{3}\mu - \mu_v \right) \nabla \cdot \bar{U} \\
 \tau_{\theta\theta} &= 2\mu \left(\frac{1}{r} \frac{\partial U_\theta}{\partial \theta} + \frac{U_r}{r} \right) - \left(\frac{2}{3}\mu - \mu_v \right) \nabla \cdot \bar{U} \\
 \tau_{\phi\phi} &= 2\mu \left(\frac{1}{r \sin(\theta)} \frac{\partial U_\phi}{\partial \phi} + \frac{U_r}{r} + \frac{\cot(\theta) U_\theta}{r} \right) - \left(\frac{2}{3}\mu - \mu_v \right) \nabla \cdot \bar{U} \\
 \tau_{r\theta} &= \mu \left(r \frac{\partial}{\partial r} \left(\frac{U_\theta}{r} \right) + \frac{1}{r} \frac{\partial U_r}{\partial \theta} \right) \\
 \tau_{r\phi} &= \mu \left(\frac{1}{r \sin(\theta)} \frac{\partial U_r}{\partial \phi} + r \frac{\partial}{\partial r} \left(\frac{U_\phi}{r} \right) \right) \\
 \tau_{\theta\phi} &= \mu \left(\frac{\sin(\theta)}{r} \frac{\partial}{\partial \theta} \left(\frac{U_\phi}{\sin(\theta)} \right) + \frac{1}{r \sin(\theta)} \frac{\partial U_\theta}{\partial \phi} \right)
 \end{aligned} \tag{B.31}$$

B.8 Energy dissipation function Φ

B.8.1 Cylindrical coordinates

$$\begin{aligned} \Phi = & 2\mu \left(\left(\frac{\partial U_r}{\partial r} \right)^2 + \left(\frac{1}{r} \frac{\partial U_\theta}{\partial \theta} + \frac{U_r}{r} \right)^2 + \left(\frac{\partial U_z}{\partial z} \right)^2 \right) + \\ & \mu \left(r \frac{\partial}{\partial r} \left(\frac{U_\theta}{r} \right) + \frac{1}{r} \frac{\partial U_r}{\partial \theta} \right)^2 + \\ & \mu \left(\frac{\partial U_r}{\partial z} + \frac{\partial U_z}{\partial r} \right)^2 + \mu \left(\frac{\partial U_\theta}{\partial z} + \frac{1}{r} \frac{\partial U_z}{\partial \theta} \right)^2 - \left(\frac{2}{3}\mu - \mu_\nu \right) (\nabla \cdot \bar{U})^2 \end{aligned} \quad (\text{B.32})$$

B.8.2 Spherical polar coordinates

$$\begin{aligned} \Phi = & 2\mu \left(\left(\frac{\partial U_r}{\partial r} \right)^2 + \left(\frac{1}{r} \frac{\partial U_\theta}{\partial \theta} + \frac{U_r}{r} \right)^2 + \left(\frac{1}{r \sin(\theta)} \frac{\partial U_\phi}{\partial \phi} + \frac{U_r}{r} + \frac{\cot(\theta) U_\theta}{r} \right)^2 \right) + \\ & \mu \left(r \frac{\partial}{\partial r} \left(\frac{U_\theta}{r} \right) + \frac{1}{r} \frac{\partial U_r}{\partial \theta} \right)^2 + \\ & \mu \left(\frac{1}{r \sin(\theta)} \frac{\partial U_r}{\partial \phi} + r \frac{\partial}{\partial r} \left(\frac{U_\phi}{r} \right) \right)^2 + \\ & \mu \left(\frac{\sin(\theta)}{r} \frac{\partial}{\partial \theta} \left(\frac{U_\phi}{\sin(\theta)} \right) + \frac{1}{r \sin(\theta)} \frac{\partial U_\theta}{\partial \phi} \right)^2 - \left(\frac{2}{3}\mu - \mu_\nu \right) (\nabla \cdot \bar{U})^2 \end{aligned} \quad (\text{B.33})$$